Characterisation of Polymers

Volume 2

T.R. Crompton

SMITHERS
iSmithers

Contents

1. Pyrolysis – Gas Chromatography 1

1.1 Discussion of Technique and Equipment 1

Combustion Furnace Pyrolyser 4

Filament Pyrolyser 5

Curie Point Pyrolyser 5

Laser Pyrolysis 9

Random Scission 11

Depolymerisation 14

Side Group Elimination 15

1.2 Applications, Homopolymers 17

1.2.1 Polypropylene 17

1.2.2 Determination of Degree of Cure of Rubber 17

1.2.3 Polybutadiene 19

1.2.4 Polyacrylates and Polymethacrylates 19

1.2.5 Polyethylene Oxide 21

1.2.6 Polysulfides 21

1.2.7 Silicon Containing Polymers 30

1.2.8 Miscellaneous Polymers 30

1.3 Copolymer Applications 30

1.3.1 Determination of Unsaturation in Ethylene-Propylene-Diene Terpolymers 30

1.3.2 Acrylate and Methacrylate Based Copolymers 32

1.3.3 Styrene-based Copolymers 38

1.3.4 Vinyl Chloride-Vinylidene Chloride Copolymers 45

1.3.5 Comonomer Units in Polyhexafluoropropylene-Vinylidiene Chloride Copolymers....46
1.3.6 Acrylonitrile-butadiene....46
1.3.7 Miscellaneous Copolymers....56
References....56

2. Complementary Pyrolysis-Gas Chromatography-FT-IR....63
2.1 Theory....63
2.2 Instrumentation....67
2.3 Applications....67
2.3.1 Copolymers....67
References....74

3. Complementary Pyrolysis – Mass Spectrometry....77
3.1 Applications....77
3.1.1 Polyurethane....78
3.1.2 Polyacrylamide....81
3.1.3 Miscellaneous Polymers....91
References....94

4. Complementary Pyrolysis Gas Chromatography-Mass Spectrometry....99
4.1 Homopolymers....99
4.1.1 Polyacrylates....99
4.1.2 Chlorinated Polyethylene....104
4.1.3 Polyimide Synthesised from (4,4′-Hexafluoroisopropylidene) diphthalic Dianhydride (DTG) and an Unfluorinated Polyamide 4,4′-diamino diphenyl Methane (PIF_1)....108
4.1.4 Polypyrrol....112
4.1.5 Miscellaneous Homopolymers....116
4.2 Copolymers....116
4.2.1 Ethylene – Carbon Monoxide....116
4.2.2 Ethylene-vinyl Cyclohexane....116

4.2.3 Styrene Maleic Anhydride 117
4.2.4 Miscellaneous Copolymers 117
References 117

5. Reaction Gas Chromatography Techniques 125
5.1 Hydrolysis Gas Chromatography 126
5.1.1 Saponification Methods 126
5.1.2 Zeisel Procedures 126
5.2 Alkali Fusion 128
5.2.1 Determination of Alkyl and Aryl Groups 128
5.2.2 Determination of Amide and Imide Groups in Polyamides, Polyimides, and Polyamides/Imides 130
5.3 Simultaneous Pyrolysis Derivatisation 133
5.4 Prepyrolysis Derivatistion 133
References 135

6. Sequencing of Homopolymers 139
6.1 Sequencing in Polyethylene 139
6.2 Sequences in Polypropylene 141
6.3 Sequences in Polyisoprene 148
6.4 Sequences in Polystyrene 151
6.5 Sequencing in Polybutadiene 154
6.6 Sequences in Polyurethanes 163
6.7 Sequences in Polydimethylsiloxane 167
6.8 Sequences in Polypropylene Glycols 170
6.9 Sequences in Polyvinylchloride (PVC) 172
6.10 Sequencing in Miscellaneous Homopolymers 172
References 173

7. Sequencing in Copolymers....179

7.1 Olefinic Copolymers....180

7.1.1 Ethylene Propylene....180

7.1.2 Ethylene-1-butene....190

7.1.3 Ethylene-1-hexene....191

7.1.4 Butene-propylene....194

7.1.5 Ethylene-methyl Acrylate, Ethylene-methylmethacrylate....199

7.1.6 Ethylene-vinyl Chloride....201

7.1.7 Butadiene-propylene....203

7.1.8 Miscellaneous Olefinic Copolymers....205

7.2 Styrene Copolymers....205

7.2.1 Styrene-butadiene....205

7.2.2 Styrene Acrylate and Styrene Acrylic Acid....206

7.2.3 Styrene-methyl Acrylate....211

7.2.4 Styrene-methyl Methacrylate....213

7.2.5 Styrene-*n*-butyl Acrylate....216

7.2.6 Styrene-methacrylate Copolymers....221

7.2.7 Methylmethacrylate – α-trifluoro-methacrylic Acid....222

7.2.8 Styrene-methacrylonitrile....226

7.2.8 Butadiene-methylmethacrylate....229

7.3 Vinyl Acetate Copolymers....230

7.3.1 Ethylene-vinyl Acetate....230

7.3.2 Vinyl Acetate-methyl Acrylate....231

7.4 Acrylonitrile and Methacrylonitrile Containing Copolymers....234

7.4.1 Acrylonitrile-ethylmethacrylate....234

7.4.2 Methacrylonitrile-methyl Methacrylate....234

7.4.3 Acrylonitrile Methyl Acrylate....238

7.4.4 Acrylonitrile-butyl Acrylate....242

7.4.5 Acrylonitrile-methyl Methacrylate....245

7.4.6 Methacrylonitrile-vinylidene Cyanide (MAA-VCN) and Cyano-vinyl Acetate-vinylidene Cyanide (CVA-VCN)....250

7.5 Acrylate and Methacrylate Copolymers 252
7.5.1 Methyl Acrylate – *N*-vinyl Carbazole 252
7.5.2 Ethylmethacrylate - Methyl Methacrylate 255
7.6 Polyacrylamide – Acryloyloxyethyltrimethyl Ammonium Chloride (CMA) and Polyacrylamide - Methacryl - Oyloxyethyltrimethylammonium Chloride (CMM) 255
7.7 Vinyl Chloride – Vinylidene Chloride 262
7.8 Ethylene Oxide Containing Copolymers 266
7.8.1 Polyacetal – Ethylene Oxide 266
7.8.2 Ethylene Oxide – Propylene Oxide 269
7.8.3 Ethylene Oxide – *p*-Phenylene Vinylene 276
7.9 Polybutadiene – Acrylonitrile – Methacrylic Acid Terpolymers 276
7.10 Polydimethyl Siloxane - Urethane 283
7.11 Sequences in Miscellaneous Copolymers 286
References 288

8. Stereoisomerism and Tacticity 305
8.1 Tacticity of Polypropylene 306
8.2 Tacticity of Syndiotactic Polystyrene 320
8.3 Tacticity of Polyvinylchloride 328
8.4 Tacticity of Poly(*n*-butyl Methacrylate) 332
8.5 Tacticity of Poly(1-chloro-1-fluoroethylene) 336
8.5.1 Stereoregularity of Polymethyl Methacrylate 340
8.6 Tacticity of Polypropylene Oxide 346
8.7 Tacticity of Polymethylacrylonitrile 352
8.8 Tacticity of Other Miscellaneous Polymers 353
References 354

9. Regioisomerism 365
9.1 Polypropylene Homopolymer 365
9.2 Polypropylene-1-Ethylene Copolymer 369
9.3 Polybutadiene-1-Ethylene Copolymer 371
9.4 Poly-2,3-dimethyl Butadiene 371
9.5 Polybutadiene 372
9.6 Polyisoprene 372
9.7 Polypropylene Glycols 374
9.8 Polyepichlorohydrin 376
9.9 Other Polymers 379
References 380

10. Branching 381
10.1 Branching in Polyethylene 381
10.1.1 Methyl Branching in Polyethylene 382
10.1.2 Ethyl and Higher Alkyl Groups Branching in Polyethylene 383
10.1.3 Size Exclusion Chromatography and Multiangle Laser Light Scattering (SEC-MALLS) 394
10.2 Branching in Olefin Copolymers 395
10.2.1 Ethylene-propylene Copolymer 395
10.2.2 Branching in Ethylene – Higher Olefin Copolymers 398
10.2.3 Branching in Ethylene-propylene Diene Terpolymers 410
10.3 Branching in 1-polybutene 410
10.4 Branching in Polyisoprene 411
10.5 Branching in Polystyrene 411
10.6 Branching in Polyvinylchloride 411
10.7 Branching in Polyvinyl Fluoride 414
10.8 Branching in Polysaccharide Biopolymers 417

10.9 Branching in Miscellaneous Polymers 418

References 418

11. Block Copolymers 425

References 428

12. Types of Unsaturation 431

12.1 Unsaturation in Homopolymers 431

12.1.1 Polybutadiene Unsaturation 431

12.1.2 Polyisoprene Unsaturation 439

12.1.3 Polyethylene Unsaturation 443

12.1.4 Polypropylene Unsaturation 446

12.2 Unsaturation in Copolymers 449

12.2.1 Styrene-divinyl Benzene 449

12.2.2 Polytrimethylolpropane Tri-methacrylate (TRIM) 452

12.2.3 Miscellaneous Copolymers 453

12.3 Ozonolysis Techniques 454

References 461

13. Determination of End-groups 471

13.1 Polypropylene Oxide 472

13.2 Polystyrene 474

13.3 Polyethylene 480

13.4 Polyethylene Terephthalate 482

13.5 Polyisobuylene 483

13.5.1 Tert-chlorine Terminated Polyisobutylene 483

13.5.2 Olefin-Terminated Polyisobutylene 484

13.5.3 Hydroxyl-Terminated Polyisobutylene 485

13.6 Polymethylmethacrylate 486

13.6.1 MALDI-ToF-MS 499

13.6.2 Dye Partition Methods 499
13.7 Terminal Epoxides 500
13.8 Poly(2,6-dimethyl 1,4 Phenylene Oxide) 501
13.9 Miscellaneous End-groups 504
References 506

Abbreviations 513

Subject Index 519

1 Pyrolysis – Gas Chromatography

1.1 Discussion of Technique and Equipment

Pyrolysis is simply the breaking of large, complex molecules into smaller fragments by the application of heat. When the heat energy applied to a molecule is greater than the energy of specific bonds in that molecule, those bonds will dissociate in a predictable, reproducible way. The smaller molecules generated in this bond-breaking process can be identified by a number of analytical tools, including gas chromatography and mass spectrometry. Once identified, they help in understanding the structure of the original macromolecule. Thus, a copolymer of isoprene and styrene is readily identified by a pyrogram, whose dominant peaks are isoprene, styrene, and dipentene, a dimer of isoprene.

Pyrolysis is an analytical technique whereby complex involatile materials are broken down into smaller volatile constituent molecules by the use of very high temperatures. Polymeric materials lend themselves very readily to analysis by this technique. Providing that the pyrolysis conditions are kept constant, a sample should always degrade into the same constituent molecules. Therefore, if the degradation products are introduced into a gas chromatograph (GC), the resulting chromatogram should always be the same and a fingerprint uniquely characteristic of the original sample should be obtained.

Wampler and Levy [1] have discussed factors reflecting reproducibility in pyrolysis – gas chromatography (Py-GC) such as sample size, sample inhomgeneity and pyrolyser design. There are two broad areas of application of Py-GC. The first is its use as a means of qualitatively identifying unknown polymers, e.g., competitor's products, forensic investigations. This fingerprinting approach, useful as it is, is not perused further in this book.

The second area of application, which is the subject matter of this chapter, is the use of the technique to elucidate microstructural detail in a polymer under investigation, e.g.,different types of unsaturation (Chapter 12) and sequence type in copolymers (Chapters 6 and 7). Various workers [2-4] have published Py-GC databases.

Applications for pyrolysis are vast and include all types of synthetic polymers, rubbers, and plastics, as well as latexes, paints, and varnishes, in fact, almost any

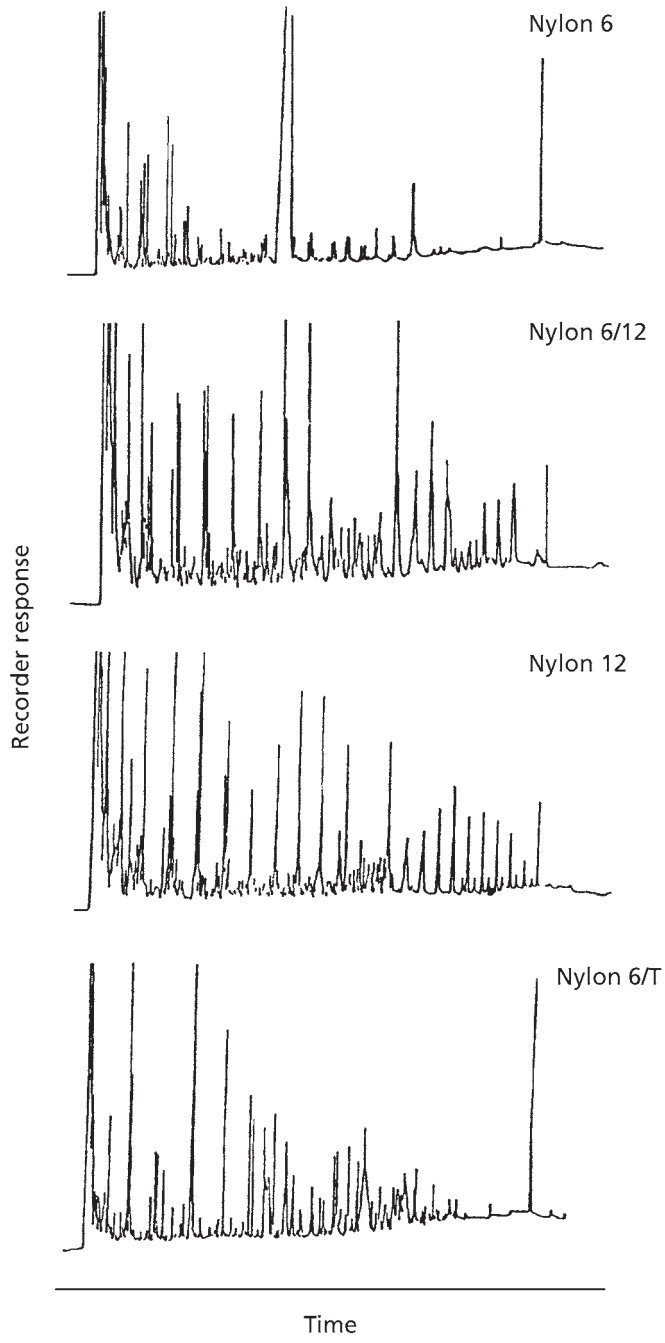

Figure 1.1 Pyrolysis - gas chromatography of Nylon 6, Nylon 6/12, Nylon 12 and Nylon 6/T. (*Source: Author's own files*)

sample that contains involatile organic material that can be contained in a tube or coated onto a platinum ribbon so that it may be pyrolysed. **Figure 1.1** illustrates the difference in the pyrograms obtained for four different Nylons.

The choice of packed or capillary column pyrolysis gas chromatography (cPy-GC) is generally a matter of personal requirements. The type and range of samples to be analysed, the complexity of pyrogram required, and the length of the analysis will all play a significant role in decision making. For the general fingerprinting or analysis of a wide range of routine rubbers or plastics, packed column pyrolysis is more than adequate. However, for comparison of one batch of rubber with another batch of the same rubber, the detail obtained from cPy-GC will probably give the best results because minor details can be compared.

A good pyrolysis instrument must be able to reproducibly heat a sample to a preset temperature at a known rate for a specific amount of time. Inability to control any of these variables will result in a program that cannot be reproduced. If required, the separated pyrolysis products can each be fed into a mass spectrometer to obtain detailed information on pyrolysis product identity (Py-GC-MS) or into a nuclear magnetic resonance (NMR) spectrometer (Py-GC-NMR spectrometry) or into an FT-IR spectrometer.

Instrumentation is discussed next. As examples, the following pyrolyser units, produced by Chemical Data Systems Instruments (CDS) are available.

Pyroprobe 1000. This provides complete choice of thermal processing parameters. Pulse pyrolysis is permitted at rates to 20 °C per second to temperatures as high as 1400 °C. In addition to accuracy and reproducibility, the temperature versatility allows for uninterrupted sequential runs on the same sample under different thermal conditions without removing the sample probe. Two probe designs are available: coil element for solid polymers and ribbon element for polymer film and solvent deposits on polymers.

Pyroprobe 2000. This instrument has independently programmable interface and probe temperatures, and is capable of performing all the functions of the Pyroprobe 1000 and more. It has the ability to program at rates in degrees centigrade per millisecond, second, or minute, as low as 0.01 °C per minute. It can use methods employing up to five independent steps. This flexibility allows complete temperature control of the sample including absorption, volatilisations, and pyrolysis, for pulse or time-resolved experiments. Slow heating rates are ideal for thermal evolution studies and for programmed pyrolysis with continuous analysis by MS or FT-IR spectroscopy.

Pyroprobe 120. In this instrument, the polymer samples are held in a quartz tube that is inserted into the platinum coil. If pyrolyses are to be conducted at slow rates the pyrolyser is interfaced to a sample concentration (Model 320, CDS) which collected the pyrolysates on a Tenax filled trap. In this way polymer samples can be processed for minutes or hours at slow heating rates and the pyrolysates collected for a single GC analysis. When the pyrolysis is complete, the trap is pulse heated and backflushed with the carrier gas. The desorbed pyrolysates are transferred to a gas chromatograph (Model 3700 Varian or equivalent) equipped with a 50 m × 0.25 mm id SE-54 capillary column (Quadrex).

A 6:l split is established at the injection port of the gas chromatograph and the column is programmed from 50 to 280 °C at a rate of 40 °C/min. A flame ionisation detector is used and the area data obtained from a recording integrator.

Wampler and Levy [5] used this apparatus to study the effects of slow heating rates on the products formed during the pyrolysis of polyethylene (PE). They showed that both the pyrolysis temperature and the rate at which that temperature is achieved have significant effects on the formation of pyrolysates from a solid polymer.

Four basic types of pyrolysis have been identified:

a) Combustion furnace pyrolyser

b) Filament pyrolyser

c) Curie point pyrolyser

d) Laser pyrolyser

Various workers [6-10] have discussed modern pyrolyser design.

Combustion Furnace Pyrolyser

In this technique, the sample is heated to a preset temperature in a microfurnace and the pyrolysis products swept as a pulse into the gas chromatograph. Earlier pyrolysis equipmer tended to be somewhat complex in design and operation. Thus, Cox and Ellis [11] described a micro-reactor pyrolyser which they applied to large numbers of polymers. Temperatures increases of 700-1000 °C were used in order to completely pyrolyse 0.1 g samples of the polymers. The pyrolysis products were collected for 15 minutes then swept onto a gas chromatographic column equipped with a flame ionisation detector. This type of equipment has now been displaced by the more recently described equipment as discussed next.

Filament Pyrolyser

A thin film of sample is usually coated onto a Nichrome or platinum spiral or is placed in a small boat so that the weight of the residue remaining after heating can be determined. Although the filament may catalyse the degradation, with 20-30 μg samples the programs obtained with Nichrome, platinum, or gold-plated platinum filaments are identical. The power supply to the filament is generally controlled by a variable transformer and timed by a stopwatch, but exact measurement of the filament temperature is difficult. More elaborate automatic time and voltage controls have been suggested. If desired, the pyrolyser temperature can also be manually programmed to obtain a better equilibrium and to remove the pyrolysis products from the heated zone immediately after they are formed. For quantitative studies of the mechanism and the kinetics of polymer degradation where accurate analysis of the volatile and non-volatile reaction products obtained at a certain temperature and under closely controlled conditions is required, it is preferable to employ preheated tube furnaces than to refine the design of the filament-type pyrolyser. The filament-type pyrolyser does not allow optimum control of degradation conditions.

Samples can be pyrolysed at a series of temperatures between 400 and 1000 °C and the change in degradation behaviour as shown by the (1) 'appearance temperatures' of various peaks and (2) relative abundance of products as a function of temperature noted [12, 13]. Changes of the most characteristic breakdown products *versus* temperature can also be plotted. For homopolymers the temperatures at which degradation products are first obtained may be more distinctive than the retention times of the products.

Figure 1.2(a) and 1.2(b) compares the programs of PVC and polyvinylidene chloride. The high quality of these programs is self-evident and makes it possible to distinguish between the two polymers.

Groton [14] used a platinum filament type pyrolyser and six-way gas sampling valve pyrolyser in conjunction with an isothermal gas chromatograph. The sample was heated on a platinum coil at 950 °C for 26 seconds. For the 150 different polymers investigated, the individual members of a group generally gave pyrograms that allowed unambiguous identification of the original material. The attainment of maximum temperature is quite rapid under all conditions and is fairly insensitive for variations in carrier gas flow rate.

Curie Point Pyrolyser

Giacobbo and Simon [15] have described a very useful pyrolysis unit for microgram samples. The material coated on a small ferromagnetic wire is pushed by means of a

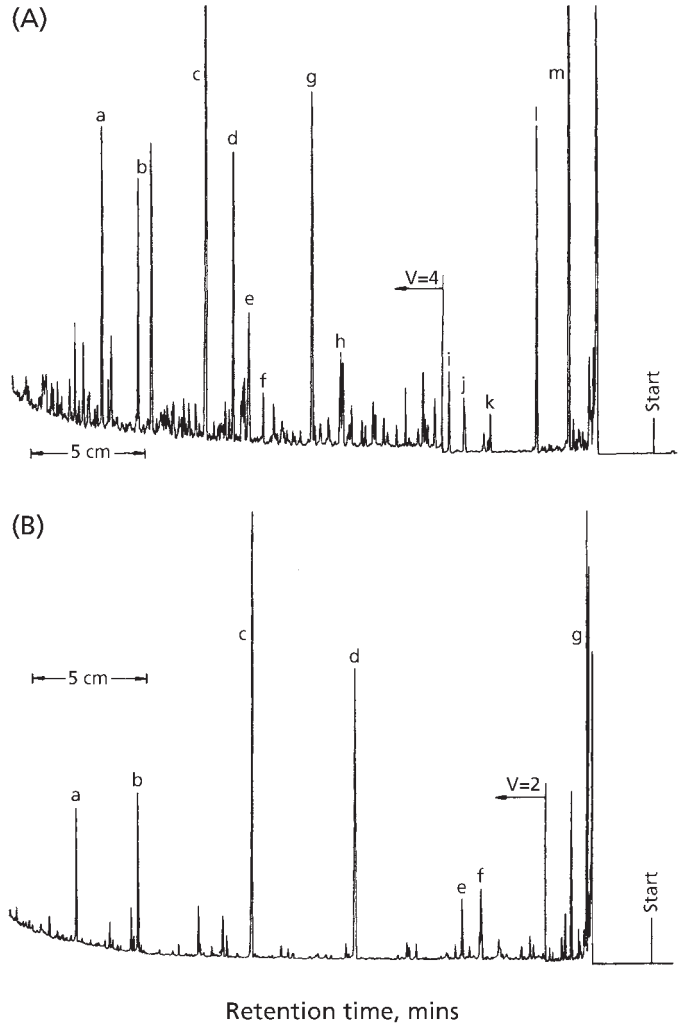

Figure 1.2 (**A**) Filament pyrolysis - gas chromatogram of PVC (a) biphenyl, (b) methyl naphthalene, (c) naphthalene, (d) methylindene, (e) tetralin, (f) methyl indene, (g) indene, (h) indane, (i) styrene, (j) *o*-xylene, (k) ethylbenzene, (l) toluene, (m) benzene. (**B**) Filament pyrolysis - gas chromatography of polyvinylidene chloride, (a) tetra-chlorostyrene, (b) trichlorostyrene, (c) 1,3,5 trichlorobenzene, (d) *m*-dichlorobenzene, (e) trichlorobutadiene, (f) chlorobenzene, (g) vinyldene-chloride. (*Source: Author's own files*)

magnet into the pyrolysis capillary which is surrounded by an induction coil. Using a frequency of 450 kHz the high frequency induction oven will heat an iron wire of 0.6 mm diameter to the Curie temperature in 2×10^{-3} seconds. During the heating time, which can be controlled from 0.06 of a second to several seconds, the temperature of the wire remains at an approximate constant maximum (of a fixed frequency). The pyrolysis temperature can be varied by choosing a ferromagnetic conductor with a suitable Curie point temperature. With a reactor capillary of 0.6 mm and a wire of 0.5 mm diameter and 1 cm length the carrier gas will pass through the reactor in 5×10^{-3} seconds, assuming a flow rate of 10 cm^3/min.

May and co-workers [16] have used this Curie point filament pyrolyser to produce pyrolysis-gas chromatograms for various polymers (see Method 10.1).

Curie point pyrolysis has been used in microstructure studies on styrene-butadiene copolymers [17], polyester containing polyacrylate copolymers [18], vinyl chloride-vinyl acetate copolymer [19] and acrylic emulsions [19].

Method 10.1 – Pyrolysis-Gas chromatography of Polymers. Curie Point Filament Pyrolyser Technique [16]

Summary

This Curie point filament pyrolyser technique enables unknown polymers to be identified.

Apparatus and Conditions

Pyrolyser – Pye Unicam Curie point attached directly to the column, pyrolysis temperature: 610 °C maintained for 10 seconds.

Gas chromatograph – dual columns, twin flame ionisation detectors.

Columns – standard Pye, 1.5 m long × 4 mm id glass (silanised).

Carrier gas – nitrogen with a flow rate of approximately 60 ml/min.

Column packing – Porapak Q, 50 to 80 mesh at 8 °C/min (the temperature was maintained at 200 °C for up to 25 minutes and the programmer started on completion of 10 seconds pyrolysis).

The columns are silanised before being packed by passing a 5% solution of dichlorodimethylsilane in toluene through the columns and then drying at 100 °C.

Packing is facilitated by applying suction from the detector end of the column, accompanied by gentle tapping. The columns are aged by heating at 250 °C for 48 hours, with a nitrogen flow of 60 ml/min. The hydrogen and air flows are adjusted to give approximately the maximum sensitivity.

Method

The pyrolysis wire is prepared in the following way. A 5 to 10 mm length at one end of the wire is flattened until the flattened portion is approximately 1 mm wide. A 'hook' is then made by doubling over about 2 mm of the flattened end. At this stage, the hook end plus a few centimetres of the wire adjacent to it are heated to red heat in a bunsen flame so as to remove contaminants. The sample is placed in the elbow of the hook, care being taken not to touch or otherwise contaminate that end of the wire. The sample is then pressed into close contact with the wire surface by crimping the hook.

Typical Results

In developing a systematic scheme of polymer identification, pyrolysis conditions must be such that all polymers degrade rapidly. However, at temperatures above 1000 °C the pyrograms will also be less suitable for identification, since secondary reactions become predominant, leading to increasing amounts of simple molecules such as carbon dioxide, acetylene, ethylene or benzene which gives less characteristic patterns than those observed for monomers or primary degradation products. Pyrolysis temperatures between 500 and 800 °C (optimum 610 °C) for 10 seconds are recommended.

In this Curie point filament pyrolysis technique the polymer is pyrolysed at a controlled temperature and the pyrolysis products passed into a gas chromatograph. Relative retention data and peak height ratio data obtained when compared with data obtained from known polymers provide a means of identifying the unknown polymer.

Experimental Procedure

The flow rate required for pyrolysis is determined by injecting through the pyrolyser head 1 µl of headspace gas from a retention time standard comprising methanol - *n*-propanol (50 + 50) with the column temperature at 100 °C and immediately programming at 8 °C/min. The flow rate of nitrogen is adjusted to give retention times of 2.6 and 9.1 minutes for methanol and *n*-propanol, respectively.

After fixing the flow rate of carrier gas, the upper temperature limit is adjusted to give a retention time of 4.2 minutes for benzene or 4.4 minutes for cyclohexane when these compounds are injected at the upper temperature limit. These two compounds have retention times of 13.4 minutes (benzene) and 14.0 minutes (cyclohexane) when injected at 100 °C and the oven is programmed as described.

Laser Pyrolysis

The advantages for this technique include rapid heating and cooling of the sample and relatively simple fragmentation patterns. Folmer and Azarranga [20] and Folmer [21] studied this technique in detail and applied it to a range of polymers.

Folmer [21] studied the effects of different operating conditions and methods of sample preparation on fragmentation patterns. Clear or translucent samples give reproducible results if mixed with carbon. Details are discussed in Method 10.2.

Method 10.2 - Pyrolysis - Gas Chromatography of Polymers. Laser Pyrolysis technique [20, 21]

Summary

This laser pyrolysis gas chromatographic technique is used to identify unknown polymers from the pattern of the breakdown products of their pyrolysis products.

Apparatus

A Gen-a-lite Model 3R laser (General) (Laser Corporation, Natick, MA, USA) and a Focuscope (General) Laser Corporation, focussing device. The laser is a 8.3 cm ruby rod with a maximum energy output of 2 joules with a pulse length of 600 microseconds. The instruments are mounted on an optical rail so that the focused beam entered a box containing a sample holder and a peak-diverting prism. The prism is mounted so that the beam can be moved in two directions and can thus be aimed at any desired portion of the sample. The sample holder is a borosilicate glass tube 6 mm od by 25 mm in length. It is clamped between two Teflon (DuPont) gaskets so that carrier gas can sweep through the tube in to the chromatograph. The carrier gas enters the chromamatograph through a 1.6 mm od tube which pierces the injection port septum and extends into the injection port.

Figure 1.3 is a schematic drawing of the apparatus showing the light paths.

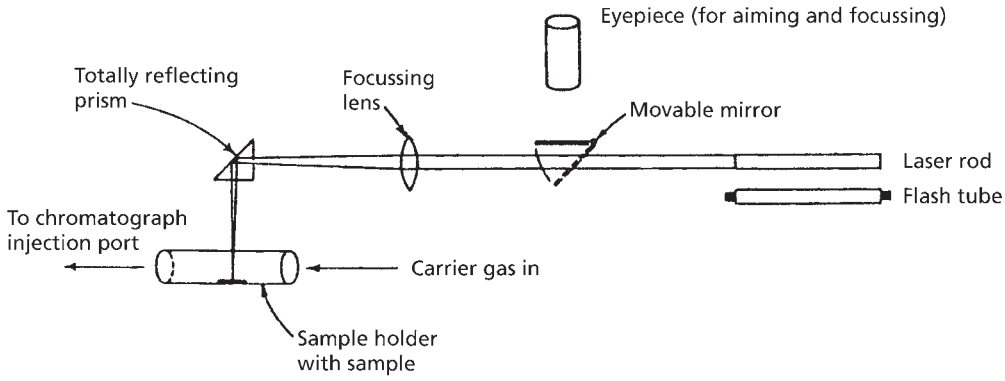

Figure 1.3 Schematic drawing of laser pyrolysis apparatus. (*Reprinted with permission from O.F. Folmer, Jr., Analytical Chemistry, 1971, 43, 8, 1057. ©1971, American Chemical Society [21]*)

The chromatograph used had a pair of flame ionisation detectors. The flame ionisation detectors and the associated duel electrometer were from a Varian Aerograph (Varian Aerograph, Walnut Creek, CA, USA) instrument. The output signal from the electrometer is connected to an Infotronics Digtal Readout Systems Model CRs-104 (Infotronics, Inc., Houston, TX, USA) and the output from this system went into a 10 mV Honeywell (Honeywell, Inc., Philadelphia, PA, USA) strip chart recorder.

Column A. A 223 cm × 0.25 cm id (4.8 mm od) stainless steel column of 70-80 mesh Anakrom ABS coated with 10% UCW-98. This column is operated at room temperature for one minute, then heated to 70 °C at the end of the second minute; its temperature is increased 20 °C/min after a maximum temperature of 210 °C is reached.

This temperature is maintained until all of the components are apparently eluted. Helium is used as a carrier gas at a flow rate of 40-50 ml/min. Hydrogen and air flows are optimised and maintained at those values.

Column B. 476 cm × 0.25 cm id (3.2 mm od) stainless steel column of 70-80 mesh Anakrom ABS coated with 10% UCW-98. It is operated at room temperature for 2 minutes, at 70 °C for another minute, then programmed at 10 °C/min to the end of the analysis or to a temperature of 260 °C which ever came first. Column flow rate is 22 ml/minute. Detector flows are the same as with the other column. Energy output of the laser rod is measured with a Quantromix Model 504 energy meter equipped with a Model 500 energy receiver.

Method

The pyrolysis products produced when the polymer is exposed to laser light are swept into a gas chromatograph. The pattern of the decomposition products is compared with that obtained with known polymers thus facilitating the identification of the unknown polymer.

Experimental Procedure

Three different types of sample preparation were used. All samples were run as solids.

1. None. Small pieces of the sample were run as is.

2. Coated. Sample pieces were coated with graphite by rubbing them with a 6B drawing pencil. Gold coating was accomplished in a vacuum evaporator.

3. Added carbon. Weighed amounts of sample and finely ground permium coke are melted and intimately mixed in a porcelain dish. In some cases the sample was ground and mixed with coke before melting and further mixing.

The polymer is laser pyrolysed using the conditions described under Apparatus.

Folmer [20, 21] studied the effects of different operating conditions and methods of sample preparation on fragmentation patterns. Clear or translucent samples give reproducible results if mixed with carbon. The concentration of carbon is critical; it has a great effect on the fragmentation pattern. Some polymers were run whose pyrolysis chromatograms show great difference in pattern. Others had patterns which were quite similar. To better compare these similar patterns and the patterns arising from different operating conditions, a statistical method was devised. An attempt was made to correlate these comparisons of patterns with some of the known characteristics of the polymers.

During pyrolysis, polymeric materials may degrade via a number of mechanisms that are generally grouped into three classes: random scission, depolymerisation, and side group elimination.

Random Scission

Random Scission results from the production of free radicals along the backbone of the polymer which causes the macromolecule to be fragmented into smaller molecules of varying chain lengths. On chromatographic analysis these fragments reveal a

repeating series of oligomers frequently differing in chain length by the number of carbons in the original monomer:

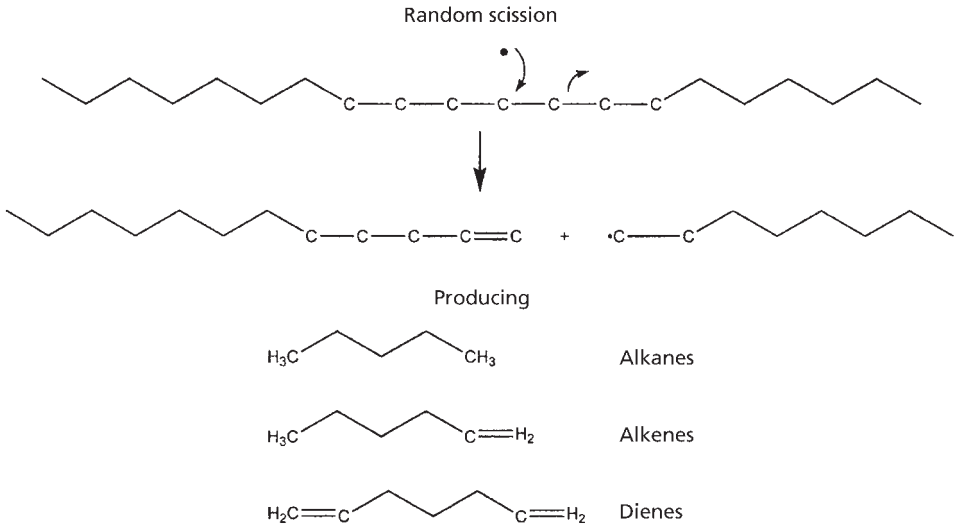

Polyolefins generally degrade through a random scission mechanism, and PE is a good example of this behaviour. When a free radical is formed along the chain of PE, chain scission occurs, producing a molecule with an unsaturated end and another with a terminal free radical. This free radical may abstract a hydrogen from a neighbouring carbon, producing a saturated end and a new radical, or combine with another free radical to form an alkane. Multiple cleavages produce molecules small enough to be volatile, with double bonds at both ends, one end, or neither end. Since the scission is random, molecules are made with a wide variety of chain lengths. These appear in the pyrogram as a series of triplet peaks. Each triplet consists of an alkane, an alkene, and a diene of a specific chain length. The hydrocarbons in each triplet have one more carbon than the molecules in the triplet that eluted just prior to it.

The chromatogram resulting from the pyrolysis of PE at 750 °C shows oligomers containing up to 30 carbons.

An example of the results obtainable by GPC of polyolefins is shown in **Figure 1.4**, which compares the pyrograms of PE, polypropylene (PP), and an ethylene-propylene copolymer. To obtain these results the sample (20 mg), in a platinum dish, was submitted to controlled pyrolysis in a stream of hydrogen as carrier gas. The pyrolysis products were then hydrogenated at 200 °C by passing through a

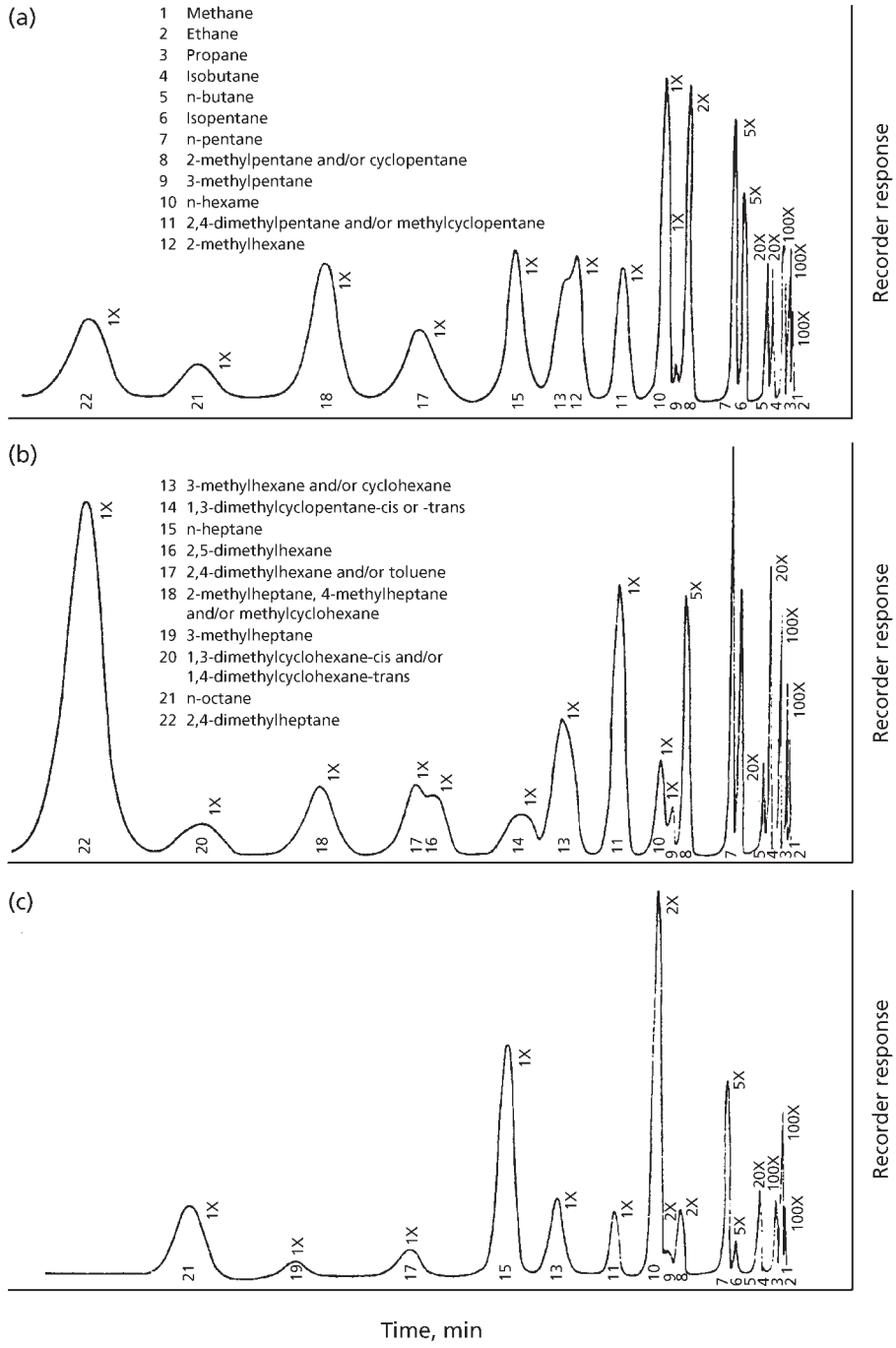

Figure 1.4 Gas chromatograms of (a) PE, (b) polypropylene and (c) ethylene-propylene copolymer. (*Source: Author's own files*)

small hydrogenation section containing 0.75% platinum on 30/50 mesh aluminium oxide. The hydrogenated pyrolysis products were then separated on a squalane on fireback column, and the separated compounds detected by a katharometer. Under the experimental conditions used in this work only alkanes up to C_9 could be detected.

It can be seen that major differences occur between the pyrograms of these three similar polymers. PE produces major amounts of normal C_2 to C_8 alkanes and minor amounts of 2-methyl and 3-methyl compounds such as isopentane and 3-methylpentane, indicative of short-chain branching on the polymer backbone. For PP, branched alkanes predominate, these peaks occurring in regular patterns, e.g., 2-methyl, 3-ethyl, and 2,4-dimethylpentane and 2,4-dimethylheptane, which are almost absent in the PE pyrolysate. Minor components obtained from PP are normal paraffins present in decreasing amounts up to *n*-hexane. This is to be contrasted with the pyrogram of PE, where *n*-alkanes predominate. The ethylene-propylene copolymer, as might be expected, produces both normal and branched alkanes. The concentrations of 2,4-dimethylpentane and 2,4-dimethylheptane are lower than those that occur in PP.

Depolymerisation

Depolymerisation is a free radical mechanism in which the polymer essentially reverts to a monomer or monomers. Unlike random scission, which produces fragments of a variety of chain lengths, depolymerisation generates a simple chromatogram consisting of large peaks for the monomers from which the polymer or copolymer was produced.

Several types of polymers degrade primarily by a free radical depolymerisation including polystyrene and polymethacrylates. When a free radical is produced in the backbone of polyethylemethacrylate, for example, the molecule undergoes scission to produce an unsaturated small molecule (ethylmethacrylate) and another terminal free radical. This radical will also cleave to form ethyl methacrylate and propagate a free radical. The net effect is often referred to as 'unzipping' the polymer.

Polyethyl methacrylate unzips extensively when heated to 600 °C for ten seconds. Copolymers of two or more methacrylate monomers will undergo the same degradation mechanism, producing a peak for each of the monomers used in the original polymerisation.

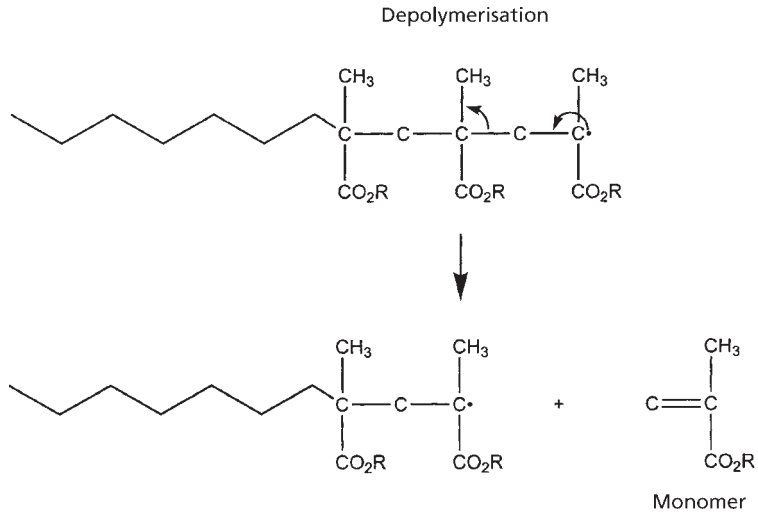

Side Group Elimination

Side group elimination is usually a two-stage process in which the polymer chain is first stripped of atoms or molecules attached to the backbone of the polymer, leaving an unsaturated chain. This polyene then undergoes further reactions, including scission, aromatisation, and char formation:

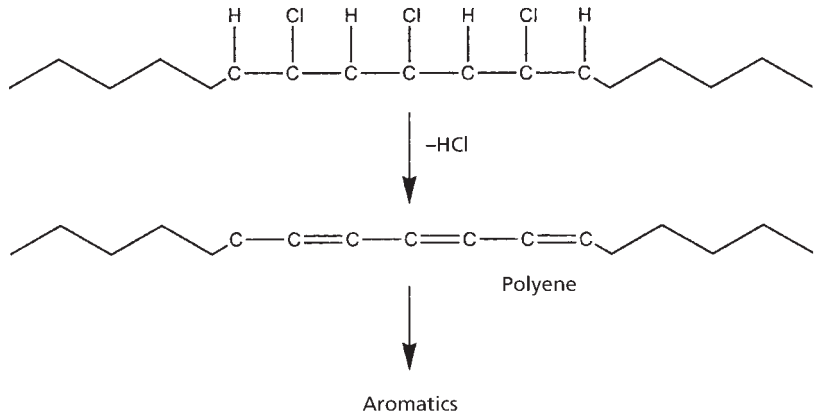

A good example of a material that pyrolyses by unzipping is PVC. PVC first undergoes a loss of hydrogen chloride to form a conjugated polyene backbone. This unsaturated

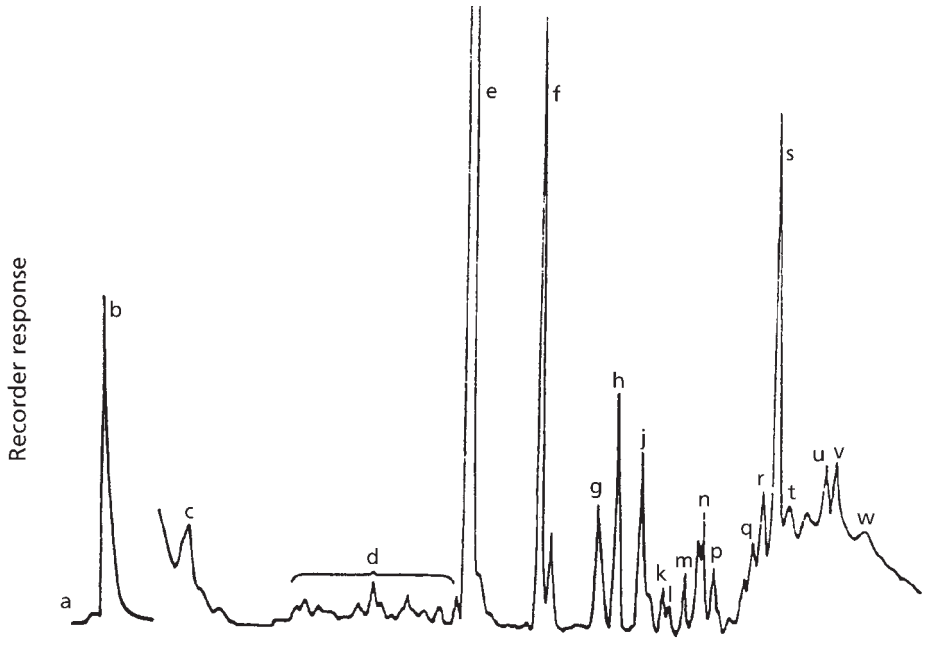

Peak identification	Components
a	CH_4 * CH, * CO_2 *, C_2H_4, * C_2H_6 *
b	HCl, C_3H_6, * C_3H_8 *
c	Butane[a], butene[a], butadiene[a], diacetylene[a]
d	C_5 and C^6 aliphatic and olephinic hydrocarbons
e	Benzene
f	Toluene
g	Chlorobenzene
h	Xylene
j	Allylbenzene
k	C_9H_{12}
l	C_9H_{12}
m	Indane
n	Indene, ethyltoluene
p	Methylindane
r	Methylindanes
s	Naphthalene
t	Dimethylindane
u	Methylnaphthalene
v	Methylnaphthalene, acenaphthalene
w	Dimethylnaphthalene

**Separated and identified on an 8 ft. Poropak QS, HCl ~ 58.3%, ash 3-4%*

Figure 1.5 Programs of PVC resin from 6 m × 4.8 mm in 10% SE32 on 80/100 CRW chromatographic column. Lettered peaks refer to identification below. (*Reprinted with permission from M.M. O'Mara, Journal of Polymer Science Part A-1: Polymer Chemistry, 1970, 8, 7, 1887. © 1970, John Wiley and Sons [6]*)

chain is further degraded, mostly to form aromatics, as well as some smaller, unsaturated hydrocarbon fragments. The principal pyrolysis products produced from PVC (in addition to hydrogen chloride) are benzene, toluene, and naphthalene. Small amounts of chlorinated aromatics may also be produced, which indicate that some chlorine is still attached to the polymer chain during aromatisation. This results from defects in the PVC which place two chlorine atoms either on the same carbon or on neighbouring carbons, so that one remains after hydrogen chloride is eliminated from the original polymer.

O'Mara [6] carried out pyrolysis of PVC (Geon 1-3, CI = 57.5%) by two general techniques. The first method involved heating the resin in the heated (325 °C) inlet of a mass spectrometer in order to obtain a mass spectrum of the total pyrolysate. The second more detailed, method consisted of degrading the resin in a Py-GC interfaced with a MS through a molecule enricher. Samples of PVC and plastisols were pyrolysed at 600 °C in a helium carrier gas flow. Since a stoichiometric amount of hydrogen chloride is released (58.3%) from PVC when heated at 600 °C, over half of the degradation products, by weight, is hydrogen chloride. A typical pyrogram of a PVC resin obtained by this method using an SE32 column is shown in **Figure 1.5**. The major components resulting from the pyrolysis of PVC are benzene, hydrogen chloride, naphthalene and toluene. In addition to these major products, a homologous series of aliphatic and olefinic hydrocarbons ranging from C_1 to C_4 are formed. O'Mara [6] obtained a linear correlation between weight of PVC pyrolysed and weight of hydrogen chloride obtained by GC.

1.2 Applications, Homopolymers

1.2.1 Polypropylene

Sugimura and co-workers [22] used pyrolysis-hydrogenation-glass capillary gas chromatography to obtain high-resolution pyrograms of isotactic, syndiotactic, and atatic polypropylene. They interpreted assigned characteristic peaks in the pyrograms in terms of the stereoregularity and degree of chemical inversion of the monomer units along the polymer chains. This method can be used for the routine characterisation of PP.

1.2.2 Determination of Degree of Cure of Rubber

Py-GC can be used to determine the degree of cure of natural rubber. **Figures 1.6 (a)-(c)** are pyrograms of three samples of natural rubber cured for successively longer intervals. Most of the chromatographic peaks produced by pyrolysis of rubber are insensitive to

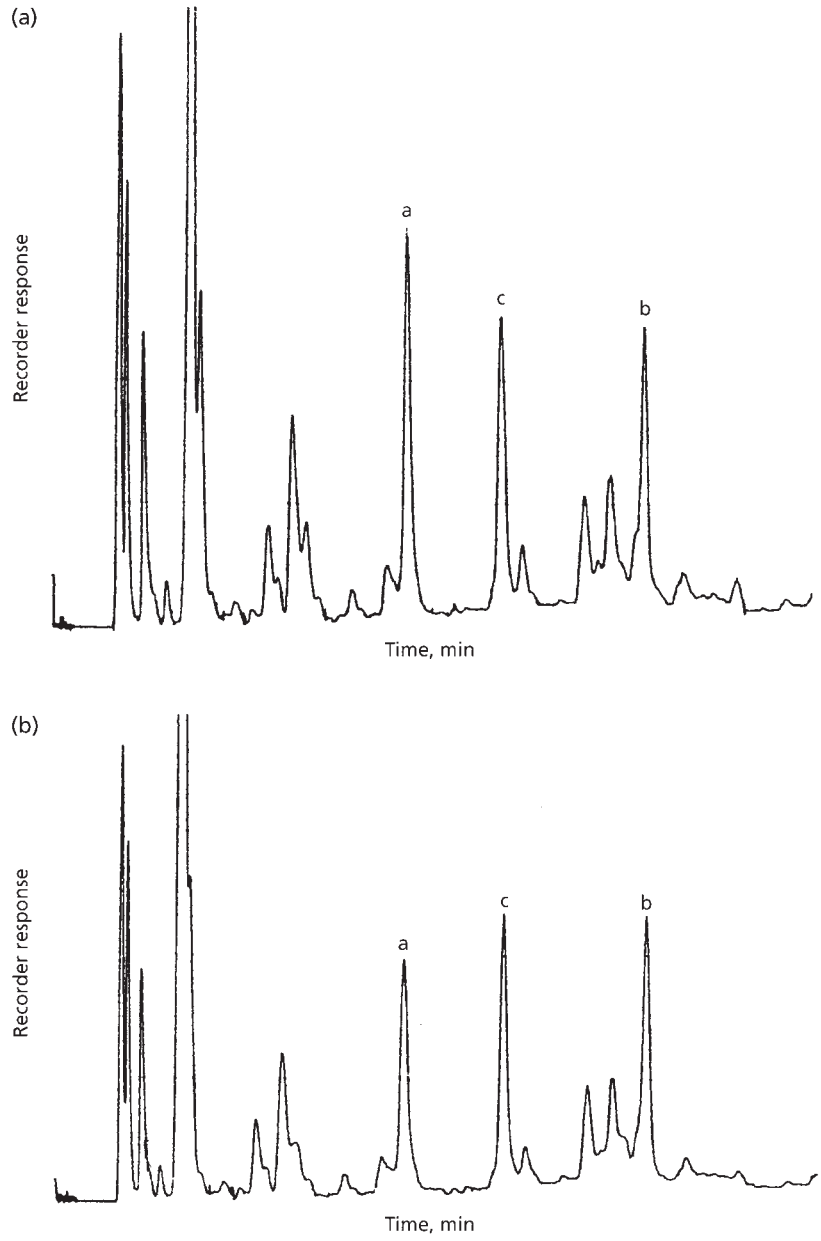

Figure 1.6 Pyrogram of (a) under cured rubber 30 µg; (b) optimally cured rubber 20 µg; (c) over cured rubber 20 µg. (*Source: Author's own files*)

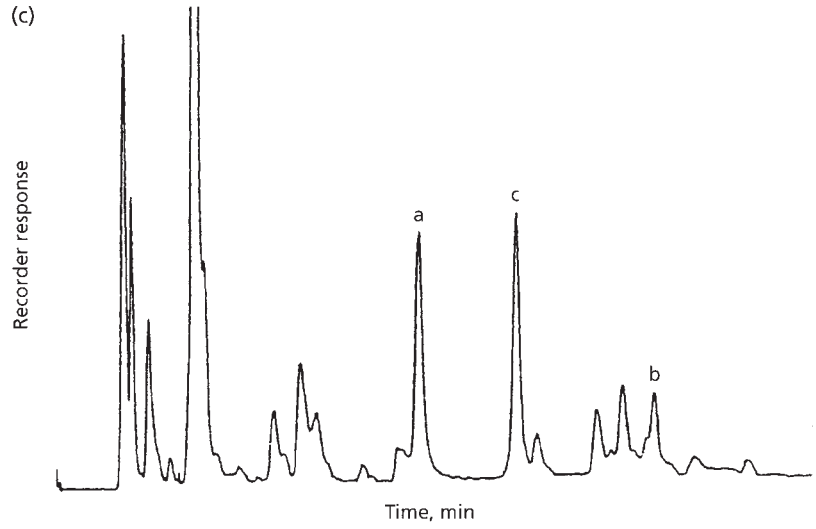

Figure 1.6 *Continued*

the degree of cure. The peaks labelled A and B in **Figures 1.6** (**a**)-(**c**) are sensitive to the degree of cure and are affected oppositely by pyrolysis temperature: peak A increases with increasing temperature and peak B decreases with increasing temperature. The ratio of the areas of peak B to peak A is a measure of the degree of cure.

1.2.3 Polybutadiene

Grimbley and Lehrle [23] studied the thermal degradation mechanism of polybutadiene. This polymer was shown to degrade through parallel degradation with random scission plus secondary deprobagation of oligomers formed by random scission. Only a small contribution was made by the transfer process. Beck has also studied the pyrolysis of polybutadiene [24].

1.2.4 Polyacrylates and Polymethacrylates

Lehmann and Brauer [25] and Brauer [26] investigated the Py-GC of polymethylmethacrylate (PMMA) at temperatures between 400 °C and 1100 °C utilising for the pyrolysis a silica boat surrounded by a platinum heating coil.

Chromatograms obtained from pyrolysing PMMA at 425 °C and 1025 °C using a dinonyl phthalate column are shown in **Figure 1.7**. Monomer is formed nearly

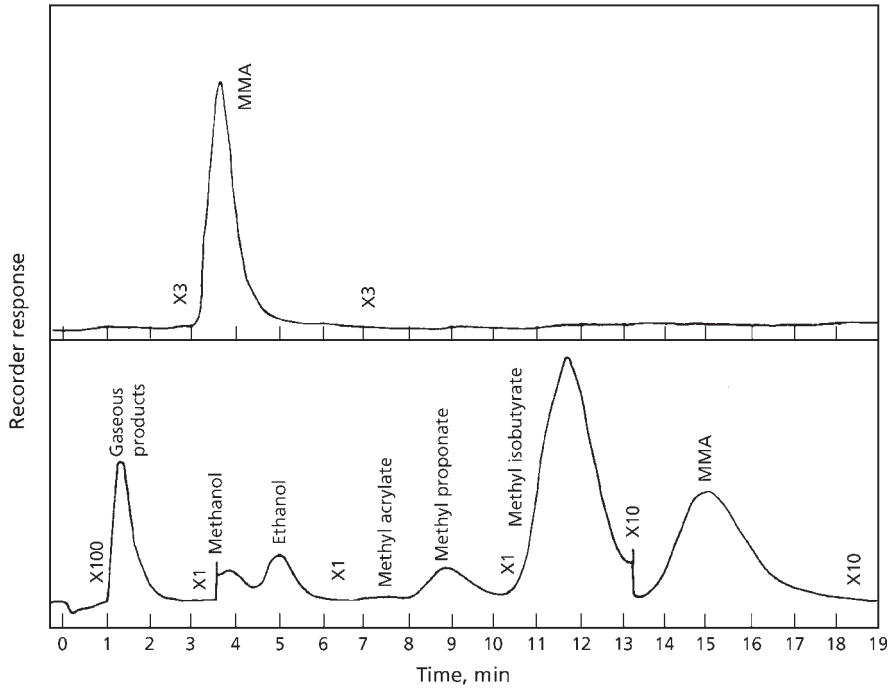

Figure 1.7 Chromatograms of pyrolysis products of polymethylmethacrylate; column, dinoyl phthalate: (a) top pyrolysis temperature: 425 °C; column temperature: 128 °C; the flow rate: 60 ml/min. (b) bottom pyrolysis temperature: 1025 °C; column temperature: 100 °C; the flow rate: 20 ml/min (MMA-methyl methyacrylate monomer). (*Reprinted with permission from F.A. Lehmann and G.M. Brauer, Analytical Chemistry, 1961, 33, 6, 673. ©1961, American Chemical Society [25]*)

exclusively (99.4%) at 425 °C reducing to 20% at 879 °C, whereas a number of additional compounds are detected at 1025 °C. Non-volatile products are retained in the column. In view of these findings regarding the effect of pyrolysis temperature on product composition it is always desirable to investigate temperature effects at an early stage and, indeed, studies performed at different pyrolysis temperatures might provide additional information in polymer microstructure studies.

Wang and co-workers [27] used Py-GC with solvent trapping to quantitatively identify and determine low levels of acrylic and methacrylic acids in polymer chains.

Mukundan and Kishore [28] showed that low temperature pyrolysis of PMMA peroxide gave methylpyruvate and formaldehyde as primary pyrolysis products. Above 350 °C secondary pyrolysis products appear.

1.2.5 Polyethylene Oxide

Fares and co-workers [29] used pyrolysis to characterise degradation products of polyethylene oxide. Both C-O and C-C bond scission of polymer backbone occured upon pyrolytic heating whereas the evolution of small molecules such as diethyl ether and acetaldehyde resulted from controlled thermal degradation of the polymer.

1.2.6 Polysulfides

The characterisation of crosslinked and cured polymers is hindered by their intractability and insolubility, and, in recent years, examination of the thermal degradation behaviour of such polymers is widely recognized to provide characterising information [30, 31]. The nature and composition of the degradation species is a function of the chemical composition and molecular order in the substrate as well as the degradation conditions.

Thiol-terminated liquid polysulfide polymers of the general formula $HS(RS_2)_nRSH$ (R = —$CH_2CH_2OCH_2OCH_2CH_2$—) are employed as the base polymers in the formulations of adhesives and sealants widely used in the aerospace industry [32]. The curing reaction in the formulations involves the oxidation of the mercaptan to a disulfide. Different oxidising agents like lead dioxide, manganese dioxide, dichromates, and so on, are employed as the oxidising agents. The cured polymers are completely insoluble and are difficult to characterise. They contain metal ions in their reduced state and also may contain mercaptide bonds as was shown to be the case for PbO_2-cured polymer [33]. Also, the transition metal ions may form coordinated bonds with the heteroatoms in the polymer backbone. These factors are likely to affect the nature and composition of the thermal degradation products and may provide characterising information. The mechanism and kinetics of thermal decomposition of liquid and ammonium dichromate cured polysulfide polymers from furnace Py-GC and thermogravimetric studies have been reported in earlier studies [34, 35]. Radhakrishnan and Rao [36] have described the pyrolytic behavior of the polysulfide polymers obtained by curing the liquid polymer with three different types of curing agents; namely, an organic oxidising agent, *p*-quinone dioxime, an inorganic peroxide, PbO_2, and a transition metal peroxide, MnO_2. Py-GC and dynamic thermogravimetric data are shown to provide partial characterisation of the substrates. The overall activation energies for thermal decomposition of the cured polymers were evaluated.

As stated previously, the curing of thiol-terminated liquid polysulfide polymers involves the oxidation of the mercaptan to disulfide using higher valency metal oxides or *p*-quinonedioxime. Consequently, the cured polymers will contain reduced forms of the metal ions or *p*-phenylenediamine heterogeneously dispersed in them.

These products may have an effect on the nature and composition of the thermal degradation products of the polymers. In addition, other reagents used in the curing formulations may also affect the product distribution. Hence, a systematic study on the effect of various salts on the thermal degradation of liquid polysulfide polymer was undertaken first.

Twenty percent (*w/w*) of the salt was mixed thoroughly with the liquid polymer, and the resultant mixture was pyrolysed at 420 °C. The nature and composition of the pyrolysates obtained are given in **Table 1.1**. As was shown in earlier studies [34], the major components of the four peaks are: peak 1: 1,3-oxathiolane (I); peak 2: 2-mercaptomethyl oxirane (II); peak 3: 1,3-dioxa-6-thiocane(III), and peak 4: 1,3-dioxa-6,7-dithionane (IV).

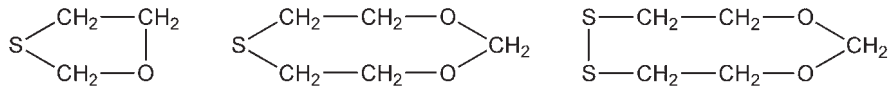

These results show that salts like KCl, K_2SO_4, and $BaCl_2$ and components like DMF, DPG, PPD, etc., have no effect on the nature and composition of the pyrolysates. Salts like $PbCl_2$, $MnSO_4$, $ZnSO_4$, and $K_2Cr_2(SO_4)_4$, which are likely to form mercaptide bonds, greatly influence the composition, but not the nature of the pyrolysates. Thus in the presence of $PbCl_2$, the formation of the cyclic monomer 1,3-dioxa-6,7-dithionane is increased to as much as 50% compared to ~19% when no salt is present (**Figure 1.8**, **Table 1.1**). This was further confirmed by the product analysis at varying concentrations of $MnSO_4$ from 1 to 30%. A plot of the percentage of 1,3-dioxa-6,7-dithionane *versus* the salt content is given in **Figure 1.9**. The concentration of about 42% steadily increases with increase in salt content and finally reaches a limiting value. These observations can be rationalised on the basis of ionic [34, 37] and radical mechanism [34, 38] proposed earlier, for the degradation of thiol-terminated liquid polysulfide polymers. The ionic mechanism involves the nucleophilic attack of the mercaptide ions on the disulfide (—SS—) bond leading to decyclopolymerisation and formation of the cyclic monomer 1,3-dioxa-6,7-dithionane:

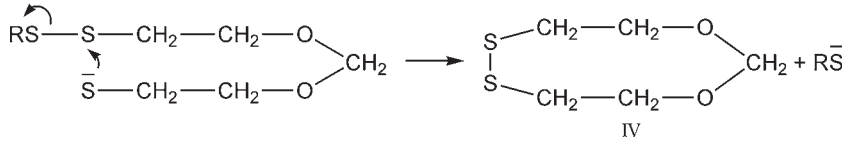

IV

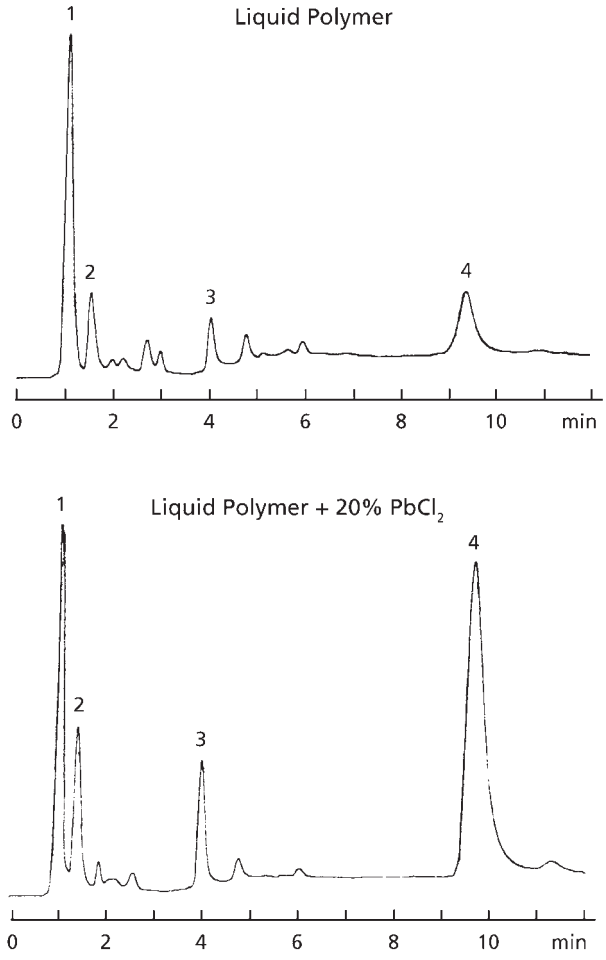

Figure 1.8 Pyrograms of liquid polymers and liquid polymer mixed with 20% $PbCl_2$ at 420 °C with a squalene column; column temperature: 60-120 °C, 15 °C/min; flow rate: 40 ml/min. (*Reprinted with permission from T.S. Radhakrishnan and M.R. Rao, Journal of Applied Polymer Science, 1987, 34, 5, 1985. © 1987, John Wiley and Sons [36]*)

Table 1.1 Effect of Various Salts on the Composition of Major Pyrolysates of Liquid Polysulfide, Pyrolysis Temperature 420 °C

Sample no.	Salt added	Monomer peak area (%)			
		1	2	3	4
1	-	42.6	11.4	7.2	18.7
2	KCl	42.4	11.3	7.3	18.1
3	K_2SO_4	47.3	11.0	6.2	17.9
4	$BaCl_2$	49.3	11.3	5.7	17.2
5	$PbCl_2$	22.1	10.7	7.5	50.7
6	$ZnSO_4$	29.7	9.9	7.9	44.0
7	$MnSO_4$	29.1	11.2	5.2	41.6
8	$K_2Cr_2(SO_4)_4$	33.1	12.0	4.4	32.8
9	PPD	42.3	11.6	7.0	18.4
10	DPG	45.7	10.6	9.4	17.2
11	DMF	46.8	10.5	8.1	17.1
12	ZnO	36.4	11.6	10.3	22.6

Monomer 1: 1,3 oxathiolone
Monomer 2: 2,2 mercapto methyl oxirane
Monomer 3: 1,3 dioxa 6, thiocane
Monomer 4: 1,3 dioxa 6,7 dithionane

*Reprinted with permission from T.S. Radhakrishnan and M.R. Rao, Journal of Applied Polymer Science, 1987, **34**, 5, 1985. ©1985, John Wiley and Sons [36]*

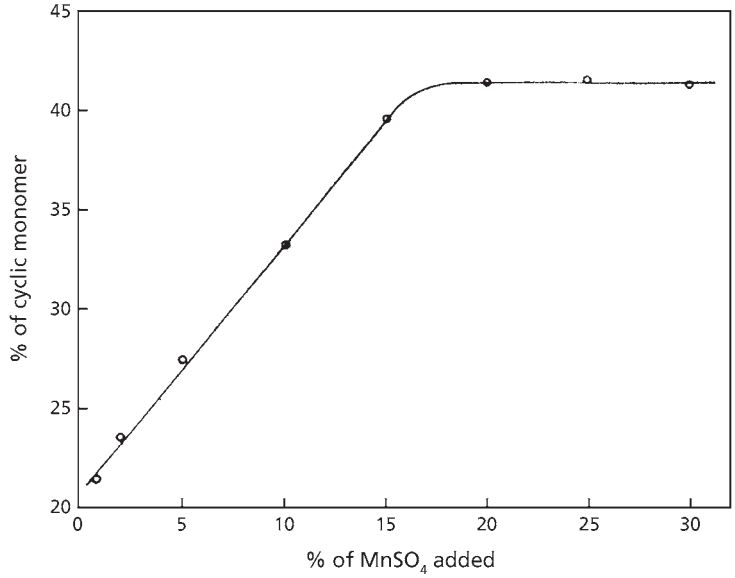

Figure 1.9 Plot of concentration of cyclic monomer, l,3-dioxa-6,7-dithionane (IV) *versus* amount of $MnSO_4$ added. (*Reprinted with permission from T.S. Radhakrishnan and M.R. Rao, Journal of Applied Polymer Science, 1987, 34, 5, 1985. © 1987, John Wiley and Sons [37]*)

The radical mechanism involves the preferential cleavage of the formal bond and formation of 1,3-oxathiolane, as well as the cyclic monomer 1,3-dioxa-6,7-dithionane as the main products:

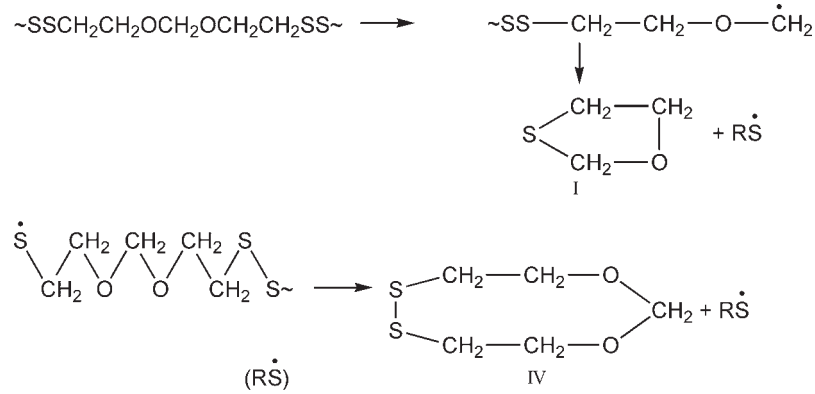

Table 1.2 Composition of Major Pyrolysates from Liquid and Cured Polysulfide Polymers.

Sample	Monomer peak area (%)			
	1	**2**	**3**	**4**
Pyrolysis temperature 420 °C				
Liquid polymer	42.6	11.4	7.2	18.7
Polymer 1	29.2	11.2	9.8	36.8
Polymer 2	34.6	13.8	9.0	22.8
Polymer 3	45.6	10.1	15.4	9.8
Polysulfide latex	18.4	11.0	4.9	59.4
Pyrolysis temperature 470 °C				
Liquid polymer	53.4	9.6	4.3	10.2
Polymer 1	54.0	12.8	2.6	15.9
Polymer 2	55.7	12.5	3.8	11.4
Polymer 3	60.7	10.5	6.8	5.0
Polysulfide latex	37.4	10.2	2.0	379

Monomer 1: 1,3 oxathiolone
Monomer 2: 2,2 mercapto methyl oxirane
Monomer 3: 1,3 dioxa 6, thiocane
Monomer 4: 1,3 dioxa 6,7 dithionane

*Reprinted with permission from T.S. Radhakrishnan and M.R. Rao, Journal of Applied Polymer Science, 1987, **34**, 5, 1985. ©1985, John Wiley and Sons [36]*

In the presence of salts which are likely to increase the concentration of the mercaptide ions, the ionic mechanism dominates resulting in an increase in the concentration of 1,3-dioxa-6,7-dithionane and a decrease in the concentration of 1,3-oxathiolane. The concentration of 1,3-dioxa-6,7-dithionane goes on increasing till the mercaptide ion reaches an equilibrium-limiting value.

The cured liquid polysulfide polymer samples 1, 2, and 3 obtained by curing the liquid polymer using PQD, PbO_2, and MnO_2, respectively, were pyrolysed at 420 and 470 °C. The product composition of the pyrolysates is given in **Table 1.2** and the pyrograms are shown in **Figure 1.10.** Although the nature of the products formed are essentially the same in all cases, distinct differences are observed in their relative concentrations.

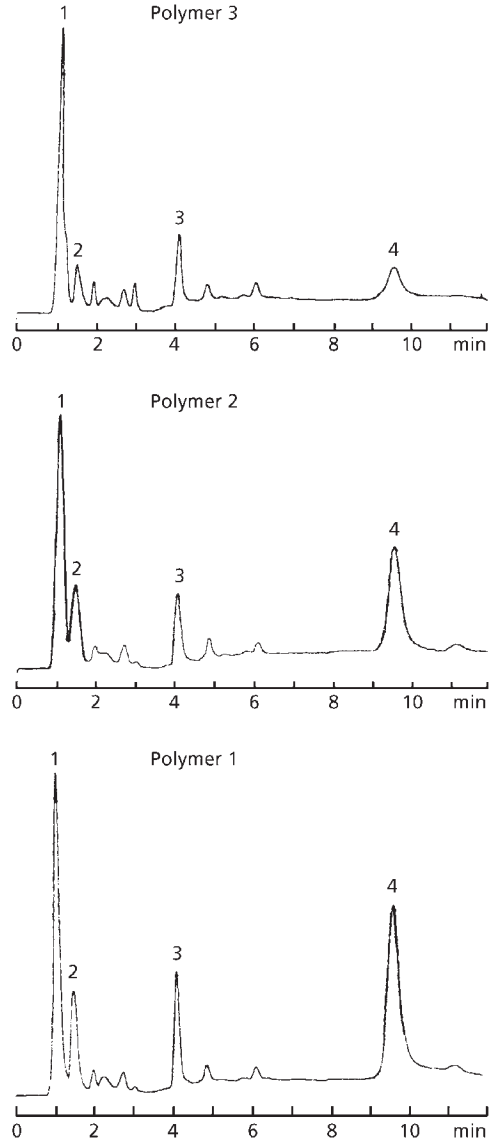

Figure 1.10 Pyrograms of cured polysulfide polymers at 420 °C with a squalene column; column; Column temperature: 60-120 °C, 15 °C/min; flow rate 40 ml/min. (*Reprinted with permission from T.S. Radhakrishnan and M.R. Rao, Journal of Applied Polymer Science, 1987, **34**, 5, 1985. © 1987, John Wiley and Sons [36]*)

Thus, polymer 1 gives the highest concentration of the cyclic monomer, 1,3-dioxa-6,7-dithionane, whereas polymer 3 gives the least amount of this compound, but the highest amount of 1,3-dioxathionane. An interpretation of these results requires an understanding of the factors which influence the formation of the products.

The cyclic monomer, 1,3-dioxa-6,7-dithionane is formed by cyclodepolymerisation through both ionic and radical mechanisms, as pointed out earlier. The extent of depolymerisation, and consequently, the concentration of 1,3-dioxa-6,7-dithionane in the pyrolysates depend on the zip length, defined as the average number of monomer molecules formed between initiation and termination. A measure of zip length relative to chain length can be ascertained by pyrolysing high molecular weight polymer. Hence, a polysulfide polymer latex from which the liquid polymer is obtained by degradation was subjected to pyrolysis. The results in **Table 1.2** show that the concentration of 1,3-dioxa-6,7-dithionane in the pyrolysates is about 60% compared to about 19% in the case of the liquid polymer. These results clearly show that the zip length is quite large, and depolymerisation is limited by the chain length. The depolymerisation process would continue till an impediment occurs along the chain. Such impediments occur either at the crosslinking points or due to the presence of mercaptide bonds (~S—M—S~).

In general the concentration of monomer 4 (1,3-dioxa-6,7-dithionane) in the pyrolysate varied considerably from polymer to polymer. Polymer 1 gives the highest concentration of the cyclic monomer 1,3-dioxa-6,7-dithionane (36.4%, **Table 1.2**) among all the cured polymers. Good mechanical properties and high crosslink density of the polymer suggest almost complete curing. Ozawa's plots show no change in activation energy E_d with the extent of degradation, α, indicating a single mechanism for the entire decomposition process. The value of 122 kJ/mol for the activation energy E_d suggests a radical mechanism for decomposition and rules out the presence of any mercaptide bonds. Therefore, the structure of metal-free polymer 1 should be quite similar to the structure of the polymer latex and may be represented as:

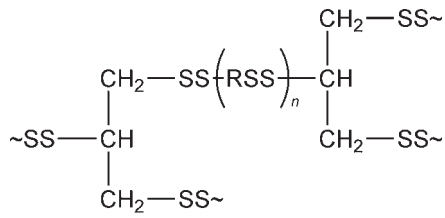

Polymer 1

Polymer 2, obtained by curing the liquid polymer with PbO_2, shows a smaller concentration of the cyclic monomer 1,3-dioxa-6,7-dithionane (22.8%) relative to

polymer 1, indicating greater impediments along the chain either due to crosslinking points or presence of mercaptide (~ S—Pb—S ~) bonds. However, the measured crosslink density of polymer 2 is less than that of polymer 1. Furthermore, thermogravimetric data indicate a change in the mechanism of decomposition with the extent of degradation, α as shown by the change in activation energy E_d with α. The lower value of E_d (< 100~kJ/mol) in the initial stages of decomposition (α < 0.2) clearly proves the simultaneous occurrence of ionic and radical mechanisms and, therefore, the presence of ~-S — Pb — S~ bonds. Thus, the extent of curing of this polymer is incomplete. The inferior mechanical properties of polymer 2 compared to those of polymer 1 also support this conclusion. Based on these considerations, the structure of polymer 2 may be shown as:

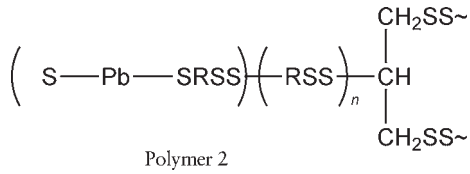

Polymer 2

Polymer 3, obtained by curing with MnO_2, shows the least concentration of 1,3-dioxa-6,7-dithionane indicating larger number of crosslinking points and greater extent of curing than polymers 1 and 2. However, the observed crosslink density of polymer 3 is less than that of polymer 1. In addition, thermogravimetric data indicate the presence of mercaptide (~S-Mn-S~) bonds as shown by the change in mechanism with the extent of degradation, α and low values of the activation energy E_d. These apparently contradicting results can be reconciled if it is assumed that Mn is in the form of a coordinated complex in the cured polymer with S acting as electron pair donors. A plausible structure for the coordinated complex may be represented as:

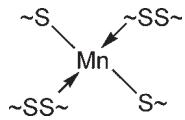

The important conclusions that can be drawn from the work of Radhakrishnan and Rao [36], are: (i) the concentration of the cyclic monmer, 1,3-dioxa-6,7-dithionane formed in the flash pyrolysis of cured polysulfide polymers reflects the structure of the cured polymer; (ii) thermogravimetric data could be used to find the presence of mercaptide bonds in the cured polymers; (iii) Py-GC and thermogravimetric techniques can be used to characterise insoluble polymers, which is clearly brought out in the case of MnO_2-cured polymer.

This work illustrates the way in which carefully planned and conducted studies can provide considerable information on polymer structure.

1.2.7 Silicon Containing Polymers

Blazsó [39] has discussed the pyrolysis conditions suitable for the degradation of polydialkylsilylenes in order to provide structural information. He showed that degradation started at 200 °C and proceeded through the formation of cyclic oligomers at 300 °C. Copolymers containing dimethylysilylene units produced tetra and penta cyclic compounds while copolymers containing ethyl and higher alkyl units produced tetracyclic compounds.

Fujimoto and co-workers [40] studied the pyrolysis products of polysiloxane including their stereo and structural isomers. Separation was achieved by gas chromatography on a fused silica capillary column. Mass fragmentation data was obtained on pyrolysis products formed at 600 °C.

Chu and co-workers [41] carried out pyrolysis of the refractory polymer polyborosilazane under nitrogen at temperatures between 1250 and 1800 °C. The boron content of the pyrolysis product increased with increased thermal exposure time whereas the C:Si ratio remained constant.

1.2.8 Miscellaneous Polymers

Py-GC studies aimed at providing structural information have been conducted on a wide range of other homopolymers in recent years (see **Table 1.3**).

1.3 Copolymer Applications

1.3.1 Determination of Unsaturation in Ethylene-Propylene-Diene Terpolymers

Py-GC has been used to determine the overall composition of ethylene-propylene-diene terpolymers [51]. In attempting to determine the third component in these materials, difficulties might be anticipated, since this component is normally present in amounts around 5 wt%. However, dicyclopentadiene was identified in ethylene-propylene-diene terpolymers even when the amount incorporated was very low.

Table 1.3 Pyrolysis – gas chromatography of homopolymers

Homopolymer	Pyrolysis conditions	Pyrolysis temperature (°C)	Pyrolysis products	Comments	Ref.
Polysulfones, polyphenylene sulfone	Filament pyrolysis with MS flame ionisation GC detection	Varied	SO_2	Kinetics of SO_2 production on sequential pyrolysis	[42]
Polyurethanes based on glycols or amines	-	600	Polyglycols	-	[43]
Polyacrylamide	Flash pyrolysis	500	Methyl cyanide, acrylonitrile, ethyl cyanide, methacrylonitrile, isopropylcyanide	-	[18]
Polyalkylene phthalates	Pyrolysis in vacuum, capillary with MS detection	440	Phthalic anhydride, diols	-	[44]
Linear and cyclic perfluoroalkanes, perfluoropentane, perfluorohexane	-	900	Perfluoro-isobutylene	-	[45]
Polyvinyl pyrrolidine	-	-	-	-	[46]
Aromatic polycyanurates	Laser pyrolysis	-	-	Study of polymer linkages and networks	[47]
Epoxy acrylics based on phenol and *p*-alkyl substituted phenols	-	60-800	Phenol, *p*-cresol, ethylene, acetone, acrylic acid, anisole, higher phenols	-	[48]
Chloromethylated polystyrene	-	-	Styrene monomer	Polymer characterisation, monomer yield decreased with increasing chlorine content of polymer	[49]
Fluoropolymers	-	-	-	Discussion of pyrolysis technique	[50]

Source: Author's own files

Van Schooten and Evenhuis [52, 53] applied their pyrolysis (500 °C)-hydrogenation-gas chromatography technique to unsaturated ethylene-propylene copolymers, i.e., ethylene-propylene-dicyclopentadiene and ethylene-propylene-norbornene terpolymers. The pyrograms show that very large cyclic peaks are obtained from unsaturated rings: methylcyclopentane is found when methylnorbornadiene is incorporated; cyclopentane when dicyclopentadiene is incorporated; methylcyclohexane and 1,2-dimethylcyclohexane when the addition compounds of norbornadiene with isoprene and dimethylbutadiene, respectively, are incorporated; and methylcyclopentane when the dimer of methylcyclopentadiene is incorporated. The saturated cyclopentane rings present in the same ring system in equal concentrations, however, give rise to peaks that are an order of magnitude smaller. Obviously, therefore, the peaks from the terpolymer could be used to determine its content if a suitable calibration procedure could be found.

Yamada and co-workers [54] studied the pyrolysis of vulcanised ethylene, ethylidene norbornene-propylene copolymers at 650 °C.

1.3.2 Acrylate and Methacrylate Based Copolymers

Polethylene Acrylate and Polyethylene-Vinyl Acetate

Barrall and co-workers [55] have described a Py-GC procedure for the analysis of PE-ethyl acrylate and PE-vinyl acetate copolymers and physical mixtures thereof. The pyrolysis chromatogram of PE-vinyl acetate contains two principal peaks. The first is methane and the second is acetic acid:

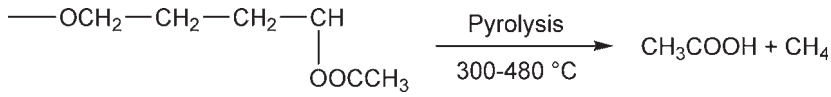

The pyrolysis chromatogram of polyethylene-ethyl acrylate at 475 °C shows one principal peak due to ethanol. No variation in peak areas is noted in the temperature range 300-480 °C. **Table 1.4** shows the analysis of 0.05 g samples of polyethylene-ethyl acrylate and polyethylene-vinyl acetate obtained at a pyrolysis temperature of 475 °C.

Wang and co-workers [27] developed a technique involving solvent trapping of pyrolysates followed by GC or liquid chromatography for the identification of 2-10% of acrylic acid and methacrylic acids in emulsion polymers.

Table 1.4 Pyrolysis at 475 °C results on physical mixtures of polyethylene-ethyl acrylate and polyethylene-vinyl acetate

Mixture	Acetic acid found	Wt.% calculated	Ethylene found	Wt.% calculated[a]	Oxygen found	Wt.% calculated[a]
50% PEEA-1 and 50% PEVA-2	9.10	9.05	2.65	2.62	7.88	8.25
33.3% PEEA-2 and 66.6% PEEA-3	12.15	12.33	0.75	0.70	7.33	7.49

[a] *Calculated from results from acetic acid and ethylene content for individual samples on weight per cent basis*

PEEA = Polyethylene ethylacrylate

PEVA = Polyethylene vinyl acetate

*Reprinted with permission from E.M. Barrall II, R.S. Porter and J.F. Johnson, Analytical Chemistry, 1963, **35**, 1, 73. ©1963, ACS [55]*

Here workers developed a technique that combines pyrolysis of a polymer with trapping of the pyrolysis products in a solvent (0.01 N sulfuric acid:methanol or methylene chloride) followed by analysis of the solvent by gas chromatography or liquid chromatography has been developed. Two vinyl acids (acrylic acid and methacrylic acid) as low-level additives polymerised into polymer chains were qualitatively identified in latex particles using this technique and compared to results obtained for direct Py-GC of the polymer. Although the percentage conversion to the acid monomers through pyrolysis of the acids contained in the emulsion polymers was low, detectable signals and well-resolved peaks were obtained when solvent trapping of the pyrolysis products was applied. The advantages and disadvantages of the trapping technique are discussed.

The pyrolysis-liquid trapping system used in this work is illustrated in **Figure 1.11**.

Trapping pyrolysis products into a solvent has five major advantages over conventional direct Py-GC. They are:

(1) the capability of studying higher boiling pyrolysis products which were not suitable for the GC conditions;

(2) the pyrolysis products are getting preselected/separated through the selection of the trapping solvent as long as the analyte under consideration is trapped (dissolved) with a high efficiency;

(3) the flexibility of further separations and identification techniques, such as GC, LC, SFC;

(4) the flexibility to adjust sample intensities by dilution to reduce the trapping solution concentration or by multiple pyrolysis to increase the concentration in the trapping solution; and

(5) pyrolysis and separation discerned as two events, providing an easily manageable experimental time and design.

Figures 1.12 and 1.13 show the pyrograms for the direct Py-GC of latex solid A and B.

Latex solid A 44.8% solid comprising 50% styrene, 47% butadiene, 3% acrylic acid

Latex solid B 56.3% solid comprising 68% styrene, 25% 2-ethylhexyl acrylate, 7% methacrylic acid

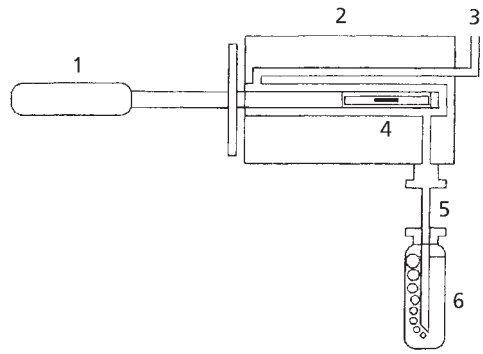

Figure 1.11 Setup of pyrolysis-liquid-trapped system: (1) pyroprobe, (2) pyroprobe interface, (3) helium carrier gas inlet, (4) latex sample, (5) output needle, and (6) liquid collection vial. (*Reprinted with permission from F.C-Y. Wang, B. Gerhart and C.G. Smith, Analytical Chemistry, 1995, 67, 20, 3681. ©1995, American Chemical Society [27]*)

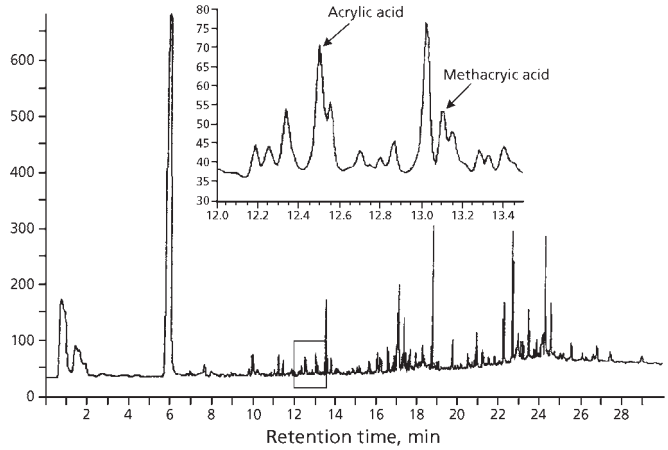

Figure 1.12 Pyrogram from direct Py-GC of latex A (containing acrylic acid). The inset shows the retention time between 12.0 and 13.5 min. The acrylic acid retention is 12.45 min, and the methacrylic acid is 13.02 min. (*Reprinted with permission from F.C-Y. Wang, B. Gerhart and C.G. Smith, Analytical Chemistry, 1995, **67**, 20, 3681. ©1995, American Chemical Society [27]*)

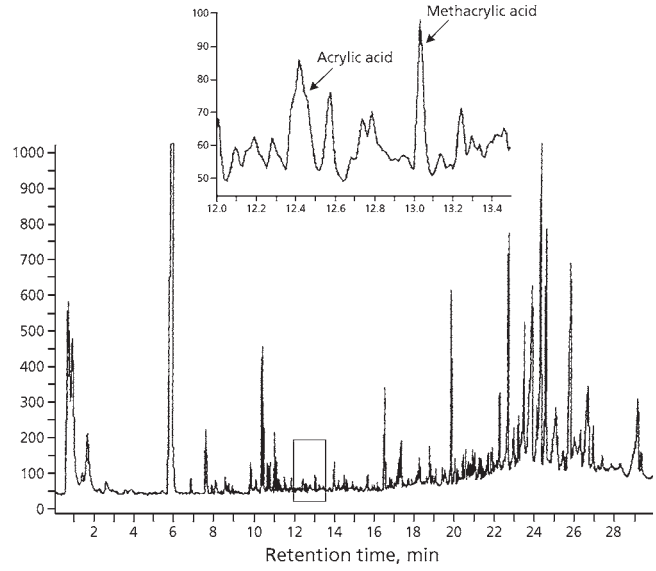

Figure 1.13 Pyrogram from direct Py-GC of latex B (containing methacrylic acid). The inset shows the retention time between 12.0 and 13.5 min. The acrylic acid retention is 12.45 min, and the methacrylic acid is 13.02 min. (*Reprinted with permission from F.C-Y. Wang, B. Gerhart and C.G. Smith, Analytical Chemistry, 1995, **67**, 20, 3681. ©1995, American Chemical Society [27]*)

In these figures the portion of the pyrograms containing the acrylic acid and methacrylic acid peaks, are amplified and placed into an inset frame. Based on chromatography of the standard acid mixture injected into the chromatograph, the retention time of acrylic acid was 12.40 ± 0.05 min and the retention time of methacrylic acid was 13.02 ± 0.05 min. Because the FFAP is a column suitable for separation of relatively polar components, some peaks exhibited poor peak shape since all components produced in the pyrolysis flow through the chromatography column, the separation of acrylic acid and methacrylic acid was not base-line resolved. The qualitative identification of acrylic acid or methacrylic acid was not possible. Owing to interferences from other components in the pyrogram, the peak area of acrylic acid and methacrylic acid could not be measured without further separation or specific detection such as GC-MS.

Figures 1.14 and 1.15 show the gas chromatograms of pyrolysis products trapped in 0.01 N H_2SO_4 solution, for acrylic acid containing latex A and methacrylic acid containing latex B, respectively. In the latex A case (**Figures 1.14, 1.15**), the 0.01 N H_2SO_4 solution-trapped products revealed a significant reduction in complexity of peaks and the acrylic acid and methacrylic acid peaks are better resolved from other pyrolysis products. This is a direct result of the low solubility of the nonpolar pyrolysis products in the polar solution. In contrast, the methanol and methylene chloride-trapped products exhibit gas chromatograms of about the same complexity as direct Py-GC pyrograms. This indicates that the selection of 0.01 N H_2-SO_4 solution as the trapping solvent can properly separate the acrylic acid or methacrylic acid from an abundance of other components

The separation of acrylic acid and methacrylic acid in 0.1 N sulfuric acid trap solutions can also be achived by liquid chromatography. Thus, **Figure 1.16** shows the pyrolysis – 0.01 N sulfuric acid solution trapped in the case of latex A containing acrylic acid.

Mao and co-workers [56] applied Py-GC to acrylic resins including ethyl acrylate – butyl methacarylate copolymer and ethyl acrylate – styrene –ethylmethacrylate terpolymer.

Characteristic peaks of pyrolysates were almost completely separated on the program. The relative molar amounts of the most characteristic pyrolysis products from low boiling hydrocarbons to pentamers were calculated from their peak intensities and interpreted in terms of components of the copolymer and terpolymer.

Py-GC has also been applied to structural studies on uncured polyesters containing acrylate [18], ethyl acrylate – methylmethacrylate copolymers [57] and 2-hydroxy methacrylate – butyl acrylate – ethyl methacrylate terpolymers [58].

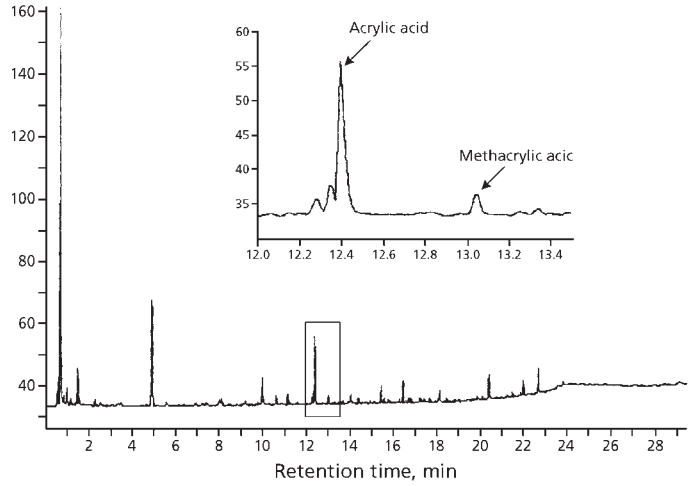

Figure 1.14 Chromatogram of pyrolysis of 0.01 N H_2SO_4 solution-trapped GC of latex A (contains acrylic acid). The inset shows the retention time between 12.0 and 13.5 min. The acrylic acid retention is 12.40 min, and the methacrylic acid is 13.02 min. (*Reprinted with permission from F.C-Y. Wang, B. Gerhart and C.G. Smith, Analytical Chemistry, 1995, 67, 20, 3681. ©1995, American Chemical Society [27]*)

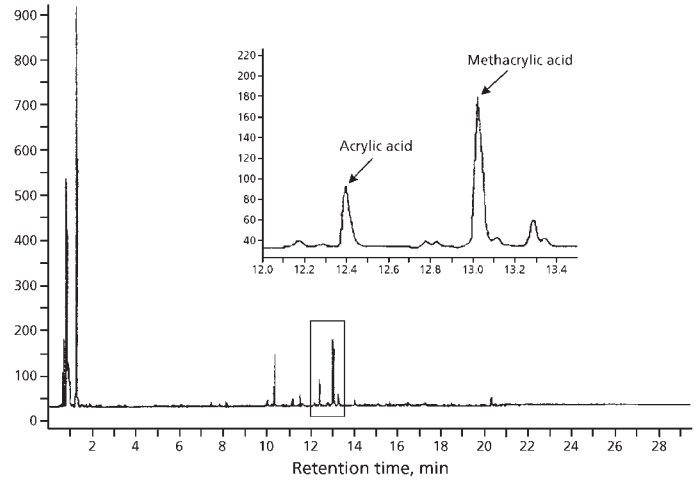

Figure 1.15 Chromatogram of pyrolysis of 0.01 N H_2SO_4 solution-trapped GC of latex B (contains methacrylic acid). The inset shows the retention time between 12.0 and 13.5 min. The acrylic acid retention is 12.40 min, and the methacrylic acid is 13.02 min. (*Reprinted with permission from F.C-Y. Wang, B. Gerhart and C.G. Smith, Analytical Chemistry, 1995, 67, 20, 3681. ©1995, American Chemical Society [27]*)

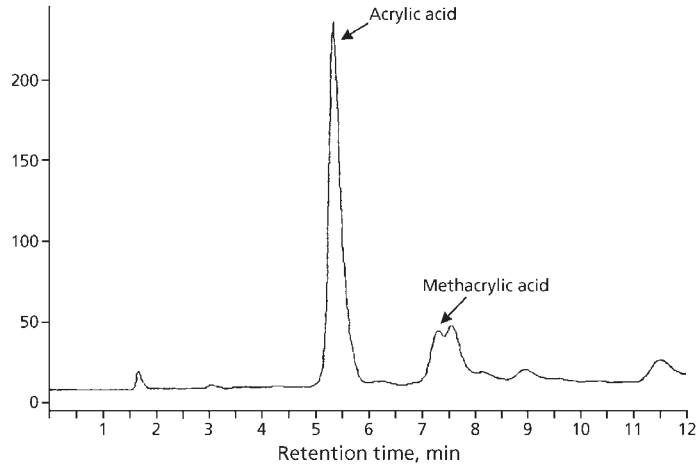

Figure 1.16 Chromatogram of pyrolysis of 0.01 N $HaSO_4$ solution trapped LC of latex A (contains acrylic acid). The acrylic acid retention is 5.34 min, and the methacrylic acid is 7.28 min. (*Reprinted with permission from F.C-Y. Wang, B. Gerhart and C.G. Smith, Analytical Chemistry, 1995, 67, 20, 3681. ©1995, American Chemical Society [27]*)

1.3.3 Styrene-based Copolymers

Styrene-n-Butyl Acrylate Copolymers

Wang and co-workers [59] carried out structure determinations of styrene-*n*-butyl acrylate copolymers. They established the 'degree of structure', i.e., the number average sequence length for styrene and *n*-butyl acrylate repeat units, and compared the results with those obtained from a homogenous (i.e., non-structured) random copolymer. Number average sequence lengths were calculated using formulae that incorporated pure trimer peak intensities and hybrid trimer peak intensities.

Styrene-Methyl Methacrylate Copolymers

Wang and Smith [60] applied Py-GC to determine the composition and microstructure of styrene-MMA copolymers. The composition of these copolymers was quantified by monomer peak intensities obtained from pyrolysis. Because of the poor stability of MMA oligomers, neither MMA dimers nor trimers were detected under normal pyrolysis conditions. The number average sequence length for styrene was determined from pure and hybrid styrene trimer peak intensities. The number average sequence

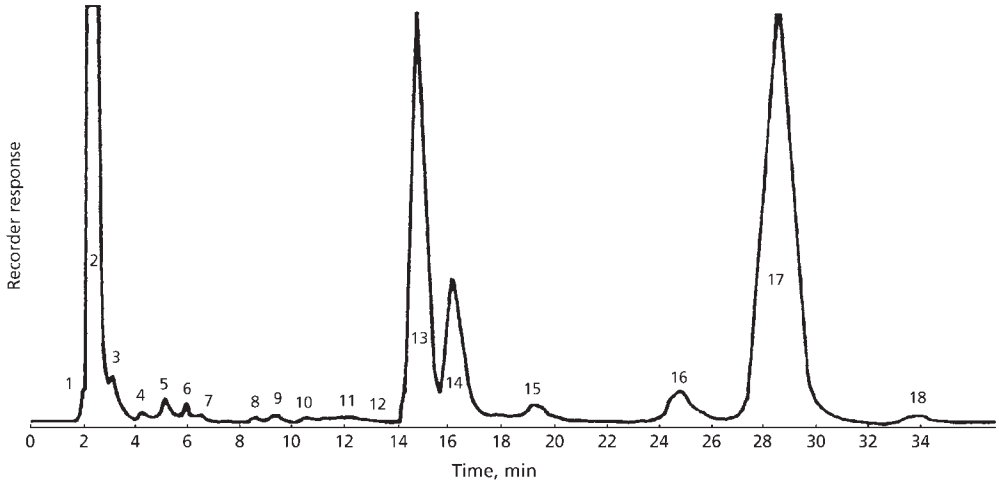

Figure 1.17 Pyrograms of isoprene-styrene copolymer at 600 °C, 10 s duration. (*Reprinted with permission from M.T. Jackson, Jr., and J.Q. Walker, Analytical Chemistry, 1971, 43, 1, 74. ©1971, American Chemical Society [63]*)

length for MMA was determined using formulae that incorporate the composition and number average sequence length of styrene.

Bate and Lehrle [61] and Ishida and co-workers [62] have also studied the pyrolysis of styrene methacrylate copolymers. Jackson and Walker [63] studied the applicability of pyrolysis combined with capillary column GC to the examination of phenyl polymers (e.g., styrene-isoprene copolymer) and phenyl ethers {e.g., bis[*m*-(*m*-phenoxy phenoxy) phenyl]ether}. In the procedure the polymer sample is dissolved in benzene. The pyrolysis Curie point temperature wire is dipped 6 mm into the polymer solution. The polymer-coated wires are then placed in a vacuum oven at 75-80 °C for 30 minutes to remove the solvent. **Figure 1.17** shows a characteristic pyrogram of the copolymer (isoprene-styrene) resulting from a 10 second pyrolysis at 601 °C. When the polyisoprene is pyrolysed, C_2, C_3, C_4, isoprene, and $C_{10}H_{16}$ dimers are produced. When PS is pyrolysed, styrene and aromatic hydrocarbons are the products. **Figure 1.17** shows that the copolymer product distribution and relative area basis resemble the two individual polymer product distributions.

Chloromethylated Polystyrene

Chloromethyl-substituted polystyrene gels usually crosslinked with divinylbenzene (DVB) are widely used as key intermediates for ion-exchange resins, supports for solid-

phase peptide synthesis and polymer-bound organic synthesis. Chloromethyl groups have been introduced into the gel polymers most often by Friedel-Crafts alkylation with chloromethyl methyl ether. Alternatively, chloromethyl groups can be introduced by copolymerisation of styrene, chloromethylstyrene, and DVB. Also, chloromethyl groups can be conveniently introduced by radical chlorination of *p*-methylstyrene-DVB copolymers by reaction with free chlorine. The properties of the resulting copolymers vary depending on the methods of introduction of the chloromethyl groups as well as the degree of chloromethyl substitution.

Methods for obtaining structural information on those chloromethyl substituted polystyrenes are discussed next.

Past work has been limited to infrared and NMR spectroscopy. Ford and Yacoub [64] characterised styrene – DVB (ST-DVB) and styrene – chloromethylstyrene – DVB copolymers by high resolution ^{13}C-NMR. These copolymers were differentiated by the line widths of the backbone methine and chloromethyl carbon peaks [64]. Dependence of the line widths and detected peak areas on DVB content and isomeric distribution of the chloromethyl groups has been discussed [65, 66].

Various workers have shown that shown that Py-GC and Py-MS methodologies are both capable of obtaining information on the chemical structure of insoluble PS networks [67-70]. In particular, high resolution Py-MS is a powerful technique for the characteriastion of copolymers with crosslinked structures [71, 49], and have provided information on structural differences between anionically and radically prepared styrene-DVB copolymers [70].

Nakagawa and co-workers [49] applied Py-GC to a structural study of various chloromethyl substituted PS copolymers prepared by different methods and they applied thermogravimetric analysis to the dihydrochlorination and thermal degradation behaviour of these copolymers. Typical programs of styrene-DVB, styrene-chloromethyl styrene-DVB and chlorinated *p*-methyl styrene-DVB copolymers are shown in **Figures 1.18 - 1.20**, respectively.

In the programs of chloromethylated ST-DVB copolymers (**Figure 1.18**), styrene monomer, dimmer, and dimer characteristics of styrene sequences are commonly observed, and their peak intensities decrease as the chlorine content increases. Additionally, decreases in the peak intensities of the *meta* and *para* isomers of DVB and ethylstyrene (EST) as a function of chlorine content indicate that Friedel-Crafts chloromethylation also occurs on the DVB and EST moieties in the copolymer. The greater decreases in the peak intensities of the *meta* isomers than those of the *para* isomers suggest that the Friedel-Crafts chloromethylation occurs more selectively on the meta isomers of DVB and EST units. *p*-Methyl styrene and its dimer characteristic

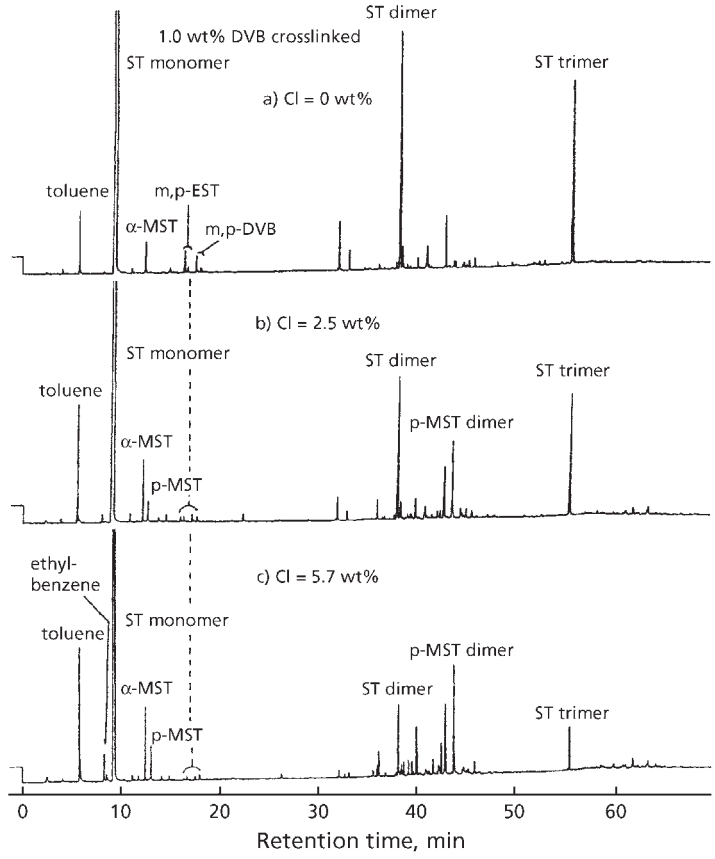

Figure 1.18 High-resolution programs of chloromethylated ST-DVB copolymers. (*Reprinted with permission from H. Nakagawa, S. Tsuge, S. Mohanraj and W.T. Ford, Macromolecules, 1988,* ***21****, 4, 930. © 1988, American Chemical Society [49]*)

of chloromethylated ST units are observed in the pyrograms of chloromethylated samples since the Friedel-Crafts chloromethylation occurs mostly on the *para* position of the styrene units [66].

Similarly, styrene monomer, dimer, and trimer peaks and peaks related to EST and DVB isomers are observed in the programs of ST-chloromethylstyrene-DVB copolymers (**Figure 1.19**). Although the intensities of ST monomer, dimer and trimer decreases as the chlorine content rises, the peak intensities of EST and DVB isomers remain almost constant regardless of the chlorine content, since constant amounts of DVB and EST are introduced by copolymerisation. Here *meta* and *para* isomers are observed for methylstyrene and chloromethylstyrene, since these isomers are contained in the

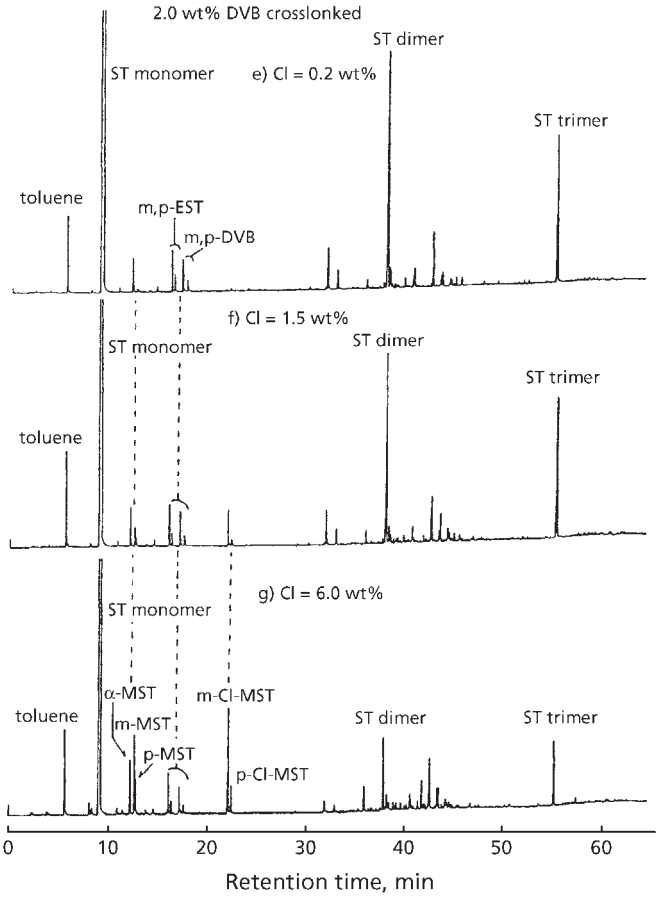

Figure 1.19 High-resolution pyrograms of ST-Cl-MSt-DVB copolymers. (*Reprinted with permission from H. Nakagawa, S. Tsuge, S. Mohanraj and W.T. Ford, Macromolecules, 1988, **21**, 4, 930. © 1988, American Chemical Society [49]*)

chloromethylstyrene used for the copolymerisation and their intensities increase as a function of the chlorine content. Therefore, the chloromethylated ST-DVB copolymers and ST- chloromethylstyrene-DVB copolymers could readily be distinguished by comparing their programs.

In the pyrograms of chlorinated *p*-methyl styrene-DVB copolymers (**Figure 1.20**), peak intensities due to *p*-methyl styrene monomer, dimer, and trimer decrease as the chlorine content increases. As expected, the intensities of *p*-methyl styrene peaks, characteristic of chlorinated *p*-methyl styrene units, increase as the degree of

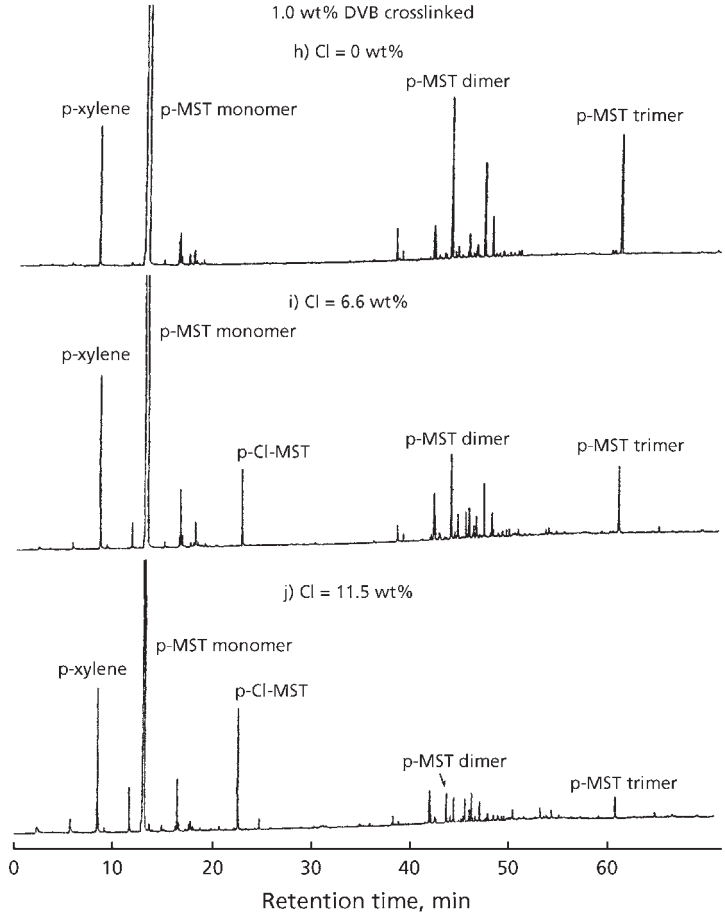

Figure 1.20 High-resolution pyrograms of chlorinated *p*-MST-DVB copolymers. (*Reprinted with permission from H. Nakagawa, S. Tsuge, S. Mohanraj and W.T. Ford, Macromolecules, 1988, 21, 4, 930. © 1988, American Chemical Society [49]*)

chlorination increases. Consequently, chlorinated *p*-methyl styrene-DVB copolymers can be readily distinguished from the other twotypes of chloromethylated PS.

Relationships between chlorine content and peak intensities of the characteristic pyrolysates for the chloromethylated ST-DVB copolymers are shown in **Figures 1.21(a)-(c)**. As shown in **Figure 1.21(a)**, peak intensities of styrene monomer decrease almost linearly with the rise in the chlorine content for the chloromethylated ST-DVB copolymers. Generally, similar relationships are observed between chlorine content and peak intensities of the characteristic products for the other copolymers. Consequently,

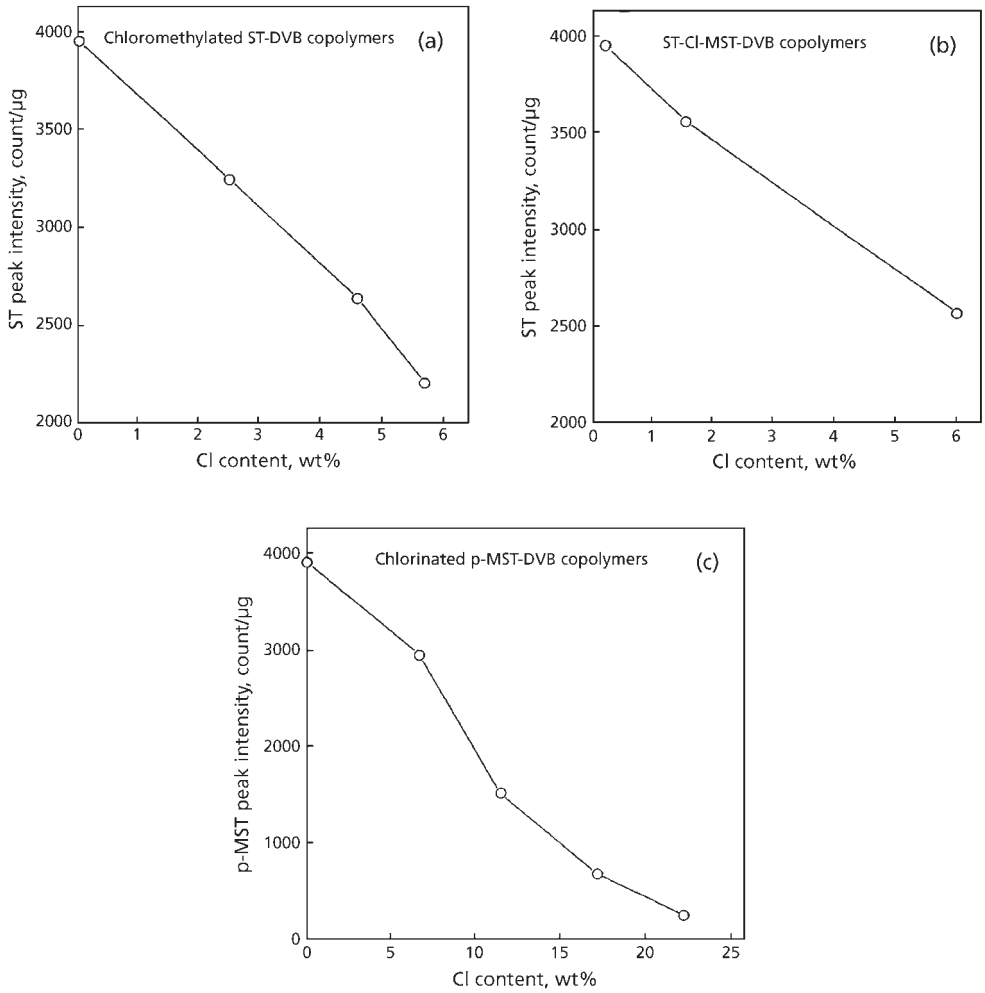

Figure 1.21 Relationships between chlorine content and peak intensities of the characteristic pyrolysates for the three types of chloromethyl-substituted polystyrenes. ST-DVB copolymers. (*Reprinted with permission from H. Nakagawa, S. Tsuge, S. Mohanraj and W.T. Ford, Macromolecules, 1988,* **21**, *4, 930. © 1988, American Chemical Society [49]*)

these relationships could be used as calibration curves for determining the degree of chloromethyl substitution for corresponding copolymer systems.

Typical TGA weight loss curves of the chloromethylated ST-DVB copolymers are shown in **Figure 1.22**. Generally, the weight loss occurs stepwise. The first weight

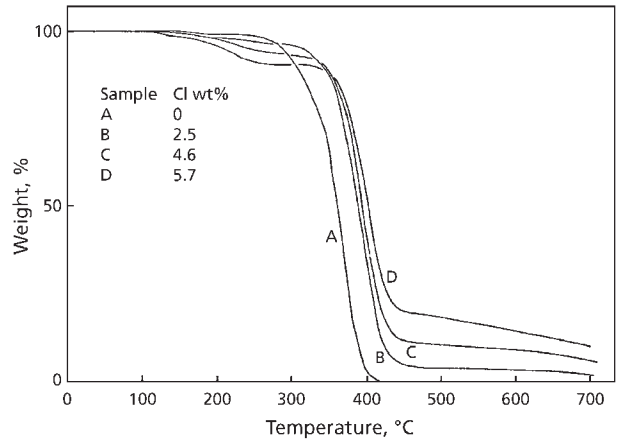

Figure 1.22 Relationships between chlorine content and peak intensities of the characteristic pyrolysates for the three types of chloromethyl-substituted polystyrenes. ST-DVB copolymers. (*Reprinted with permission from H. Nakagawa, S. Tsuge, S. Mohanraj and W.T. Ford, Macromolecules, 1988,* ***21****, 4, 930. © 1988, American Chemical Society [49]*)

loss, occurring around 200 °C, increases as the degree of chloromethylation increases. The main degradation, occurring around 400 °C, shifts to higher temperature, and the amounts of residue increase as the decrease of chloromethylation increases, even though the degree of DVB crosslinking, which primarily affects the thermal stability of the network, is essentially the same. These phenomena suggest that dehydrochlorination occurs around 200 °C, and the residue with a methylene crosslinked structure undergoes further degradation around 400 °C. In connection with this, chlorine-containing pyrolysates observed by Py-GC for either copolymer system in are relatively small, considering the chlorine contents of the original copolymers and the recovery rates in Py-GC decreased as the chlorine content increased.

Other styrene-based polymers which have been studied include styrene-butadiene [49, 72, 73], styrene-acrylonitrile [74, 75], styrene-maleic anhydride [72, 76, 77], styrene-divinyl benzene [71] and styrene-dimethylsiloxane [78].

1.3.4 Vinyl Chloride-Vinylidene Chloride Copolymers

Wang and Smith [79] used Py-GC to carry out compositional and structural studies of these copolymers. Composition and number average sequence lengths (which

reflects monomer arrangements) in the copolymers were calculated using formulae that incorporate pure trimer and hybrid trimer peak intensities.

Because of the differences in reactivity between vinyl chloride and vinylidene chloride monomers, the structure of the copolymer was further investigated on the basis of the percentage of grouped monomers (i.e., the number average sequence length for vinyl chloride and vinylidene chloride repeat units). The results obtained were in excellent agreement with those obtained by PMR spectroscopy.

For this method 2.5 mg of polymer was placed in a quartz tube, which had been equilibrated for 5 minutes at 180 °C. The sample was then pyrolysed for 20 seconds at 700 °C using a pyroprobe CDS 190 with a platinum coil. Gas chromatography was conducted using a flame ionisation or a GC-MS system.

1.3.5 Comonomer Units in Polyhexafluoropropylene-Vinylidiene Chloride Copolymers

Curie point pyrolysis has been used to carry out quantitative analysis of monomer units in polyhexafluorpropylene-vinylidene fluoride [80]. The polymer composition is calculated from the relative amounts of monomer regenerated and the trifuoromethane produced during pyrolysis. A calibration curve is obtained using samples whose compositions are measured by ^{19}F-NMR as standards and a least squares fit calculated. The reproducibility of the pyrolysis step achieved by the Curie point pyrolyser permitted the monomer composition to be determined with a reproducibility of ±1%.

1.3.6 Acrylonitrile-butadiene

Acrylonitrile-butadiene rubbers (NBR) are used for various purposes because of their oil-resistant characteristics. However, NBR do not have enough heat stability due to the presence of double bonds derived from butadiene (BD) units in the main chain. Hydrogenated NBR has been developed [81-83] to improve the thermal stability. During the hydrogenation reactions of NBR, a small number of double bonds are kept unhydrogenated for the subsequent sulfur vulcanisation, and all the cyano groups have to be kept unhydrogenated to retain oil resistance. Since the amount and the distribution of the remaining double bonds influence the properties of the hydrogenated NBR, it is important to characterise their microstructures and the hydrogenation mechanisms. Spectroscopic methods such as IR and NMR have obviously been extensively used to investigate polymer microstructures. Owing to the recent development of excellent pyrolysers and highly efficient fused silica capillary columns, Py-GC has now become an additional powerful tool to give unique information about microstructures of high polymers such as these [84, 85].

Kondo and co-workers [86] investigated the microstructures of hydrogenated NBR with various degrees of hydrogenation by microfurnace Py-GC and infrared and NMR spectroscopy. Characteristic peaks on the pyrograms by Py-GC, specific absorption bands in the IR spectra, and resonance peaks in the ^{1}H-NMR spectra were interpreted in terms of the microstructures of the hydrogenated NBR. Characteristic peaks in ^{13}C-NMR spectra were interpreted in terms of the sequence distribution and hydrogenation mechanisms. Py-GC and ^{13}C-NMR also supplied good complementary information about longer sequence along the chains and the mechanisms of the hydrogenation reaction. This example is discussed in detail as it is an extremely good case of the application of complementary techniques to the solution of a microstructure determination.

Infrared Spectroscopy

Figure 1.23 shows the IR spectra of NBR samples both before and after intermediate hydrogenation.

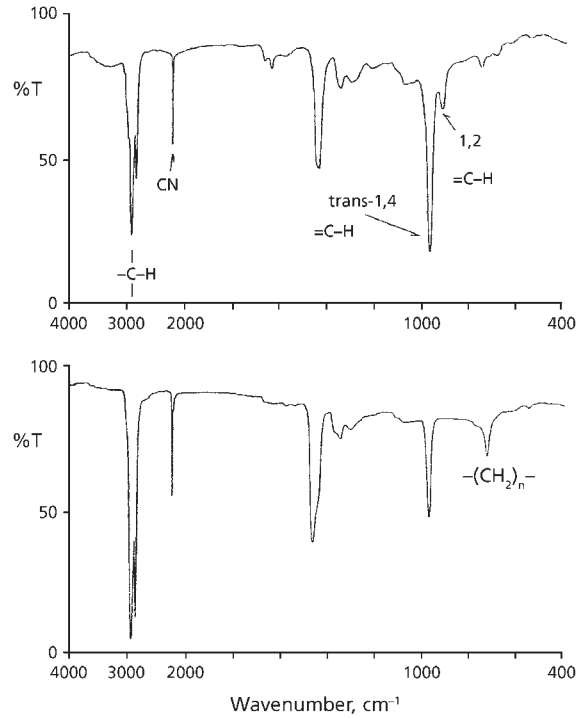

Figure 1.23 IR spectra of NBR before and after intermediate hydrogenation: (a) 37% acrylonitrile, 0% hydrogenation, (b) 37% acrylonitrile, 65% hydrogenation. (*Reprinted with permission from A. Kondo, H. Ohtani, Y. Kosugi, S. Tsuge, Y. Kubo, N. Asada, H. Inaki and A. Yoshioka, Macromolecules, 1988, **21**, 10, 2918. © 1988, American Chemical Society [86]*)

The absorption by aliphatic C-H stretching (3000-2800 cm^{-1}) and newly appeared -$(CH_2)_n$- rocking absorption at about 720 cm^{-1} arising from hydrogenated 1,4-BD units increased with the progress of hydrogenation reaction. In contrast, olefinic C-H out-of-plane deformation absorption of *trans*-1,4-BD units at 970 cm^{-1} and those of vinyls (1,2-BD units) at 910 cm^{-1} showed an opposite tendency. The latter almost disappeared at 65% hydrogenation. This fact suggests that pendent vinyl groups are hydrogenated in preference to 1,4-BD units in the polymer main chain. On the other hand, the fact that the absorption of C=N stretching at about 2240 cm^{-1} little changed in intensity with hydrogenation shows that C≡N groups were hardly reduced under given hydrogenation conditions.

Figure 1.24 shows the relationship between the degree of hydrogenation estimated from the iodine value (see Chapter 3) and that calculated from the relative IR absorbance ratio $[1 - (A_{970}/A_{2240})_h/(A_{970}/A_{2240})_0]$, where A_{970} and A_{2240} are absorbances at 970 and 2240 cm^{-1}, respectively, and the subscripts 0 and h represent NBR samples before and after hydrogenation, respectively. Although on the whole there exists a fairly good linear correlation between them, the plot in an intermediate hydrogenation slightly shifts to a lower value probably because the absorption of 1,2-BD units, which are preferentially hydrogenated, was not taken into account. Furthermore, the absorption

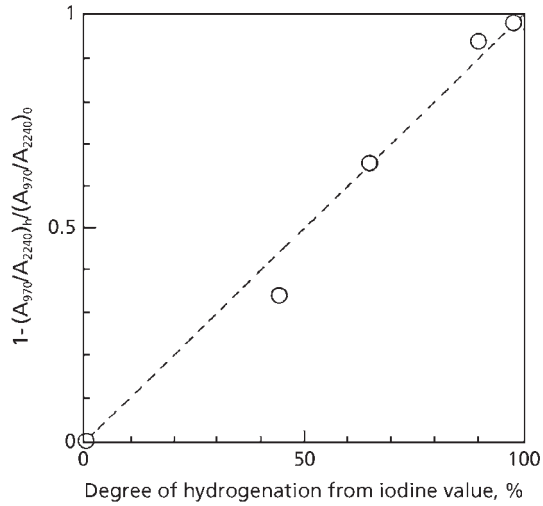

Figure 1.24 Relationship between observed 1- $[(A_{970}/A_{224o})_h/(A_{970}/A_{2240})_0]$ and degree of hydrogenation for hydrogenated NBR. (*Reprinted with permission from A. Kondo, H. Ohtani, Y. Kosugi, S. Tsuge, Y. Kubo, N. Asada, H. Inaki and A. Yoshioka, Macromolecules, 1988,* ***21****, 10, 2918. © 1988, American Chemical Society [86]*)

at 970 cm^{-1} becomes too weak at more than 90% hydrogenation to determine the degree of hydrogenation accurately at higher regions where hydrogenated NBR are expected to be used practically.

NMR Spectroscopy

Figure 1.25 shows ^{1}H-NMR spectra of NBR samples containing 37% acrylonitrile both before (a) N-37, and after 65% hydrogenation (b) N-37 (65). Major peaks are observed in the aliphatic (1-3 ppm) and olefinic regions (5-6 ppm). The peak intensity of the former region increased with the progress of hydrogenation while that in the latter region steeply decreased. The degree of hydrogenation can be calculated from the relative intensities of these paeks . Although the composition of the 1,4- and 1,2-units also affects the peak intensity because the ratios of aliphatic and olefinic protons are different in those units, 2:1 for $–CH_2H=CHCH_2-$ and 1:1 for $–CH_2CH(CH=CH_2)–$, here it is assumed only 1,4 type of double bonds remain even at 44% hydrogenation because 1,2-units are preferentially hydrogenated in an earlier stage of the reaction.

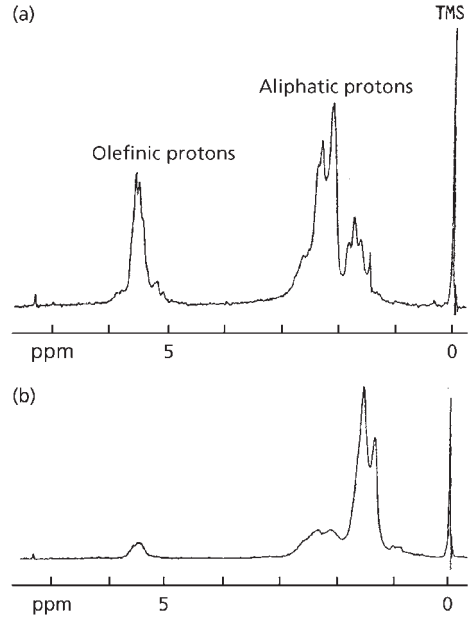

Figure 1.25 ^{1}H-NMR spectra of NBR before and after intermediate hydrogenation: (a) 37% acrylonitrile, 0% hydrogenation, (b) 37% acrylonitrile, 65% hydrogenation. (*Reprinted with permission from A. Kondo, H. Ohtani, Y. Kosugi, S. Tsuge, Y. Kubo, N. Asada, H. Inaki and A. Yoshioka, Macromolecules, 1988, **21**, 10, 2918. © 1988, American Chemical Society [86]*)

Iodine values obtained by ^{1}H-NMR are always slightly higher than those calculated from iodine values.

Pyrolysis-Gas Chromatography

Figure 1.26 shows the programs of NBR samples at 550 °C before and after hydrogenation of a polymer containing 37% acrylonitrile (a) zero hydrogenated, (b) 44% hydrogenation and (c) 98% hydrogenation by using the fused silica capillary column with polydimethylsiloxane stationary phase. **Table 1.5** summarises the characteristic thermal degradation products observed on the pyrograms of NBR

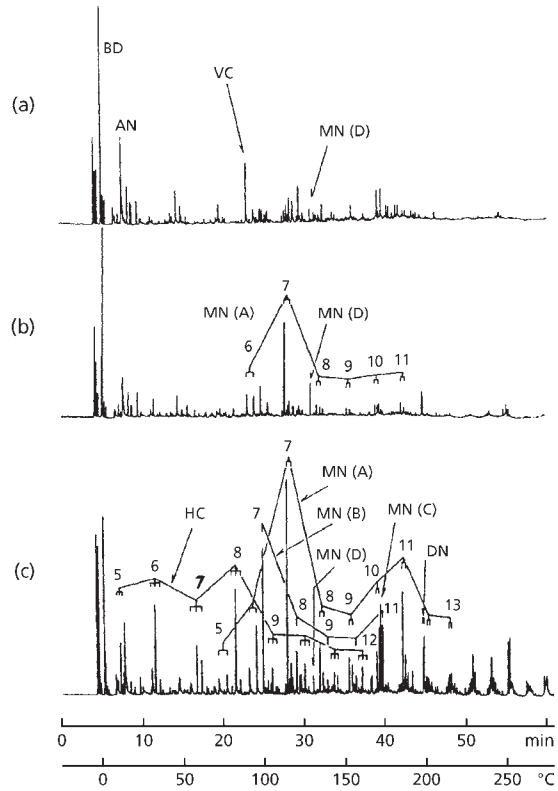

Figure 1.26 Pyrograms of NBRs before and after hydrogenation at 550 °C of a polymer containing 70% acrylonitrile (a) zero hydrogenated, (b) 44% hydrogenated, (c) 98% hydrogenated. A polydimethylsiloxane column: (a) N-37(0); (b) N-37(44); (c) N-37(98). (*Reprinted with permission from A. Kondo, H. Ohtani, Y. Kosugi, S. Tsuge, Y. Kubo, N. Asada, H. Inaki and A. Yoshioka, Macromolecules, 1988,* ***21****, 10, 2918. © 1988, American Chemical Society [86]*)

Table 1.5 Characteristic Degradation Product on pyrolysis of from Hydrogenated NBR			
Compound class	**Abbreviation[a]**	**Structure**	**Sequence[b]**
Butadiene	BD	CH_2=CH-CH=CH_2	B
Butadiene dimer (4-vinylcyclohexene)	VC	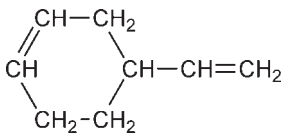	BB
Acrylonitrile hydrocarbons	AN	CH_2=CHCN	A
Hydrocarbons	HC	$CH_3(CH_2)_{n-2}CH_3$ $CH_3(CH_2)_{n-3}CH$=CH_2 CH_2=$CH(CH_2)_{n-4}CH$=CH_2	EE ($n \leq 9$) EEE ($n < 13$)
Mononitriles	MN(A)	$CH_3(CH_2)_{n-2}C\equiv N$ CH_2=$CH(CH_2)_{n-3}C\equiv N$	EA ($n \leq 7$) EEEA ($n \leq 15$)
	MN(B)	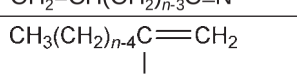	EA ($n \leq 8$) EEA ($n \leq 12$)
	MN(C)	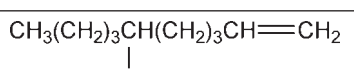	EAE
	MN(D)	CH_2=CHCH=$CHCH_2CH_2C\equiv N$ or CH_3CH_2CH=CHCH=CHC=N	BA
Dinitriles	DN	$N\equiv C(CH_2)_7C\equiv N$ 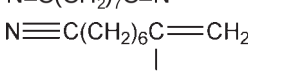	AEA AEA

[a]*Abbreviations correspond to those in Figures 1.26.* [b]*B = 1,4-butadiene unit; A = acrylonitrile; E = hydrogenated 1,4-butadiene unit.*

*Reprinted with permission from A. Kondo, H. Ohtani, Y. Kosugi, S. Tsuge, Y. Kubo, N. Asada, H. Inaki and A. Yoshioka, Macromolecules, 1988, **21**, 10, 2918. ©1988, American Chemical Society [86]*

Table 1.6 Typical Mass Spectral Data of Characteristic Degradation Products produced on pyrolysis of Hydrogenated NBR

Notation	MW[a]	Major ion by EI[b]	Structure
C_7-MN(A) (unsaturated)	109	41 (100), 55 (30), 54 (20), 68 (14), 69 (14), 80 (14)	$CH_2=CH(CH_2)_4C\equiv N$
C_{11}-MN(A) (unsaturated)	165	41 (100), 55 (86), 122 (38), 39 (34), 136 (30), 69 (28)	$CH_2=CH(CH_2)_8C\equiv N$
C_{10}-MN(A) (saturated)	153	41 (100), 43 (74), 96 (59), 82 (54), 110 (54), 55 (45)	$CH_3(CH_2)_8C\equiv N$
C_7-MN(B)	109	68 (100), 43 (80), 41 (70), 67 (57), 42 (42), 39 (34)	$CH_3(CH_2)_3C(C\equiv N)=CH_2$
C_{11}-MN(B)	165	41 (100), 43 (82), 57 (47), 108 (45), 94 (35), 122 (35)	$CH_3(CH_2)_7C(C\equiv N)=CH_2$
C_{11}-MN(C)	165	41 (100), 94 (60), 109 (55), 108 (38), 55 (35), 54 (33)	$CH_3(CH_2)_3C(C\equiv N)(CH_2)_3CH=CH_2$
C_7-MN(D)	107	41 (100), 92 (55), 79 (49), 80 (49), 107 (49), 52 (43)	$CH_2=CHCH=CHCH_2CH_2C\equiv N$ or $CH_3CH_2CH=CHCH=CHC\equiv N$
C_9-DN	150	41 (100), 92 (55), 79 (49), 80 (49), 107 (49), 52 (43)	$N\equiv C(CH_2)_7C\equiv N$
C_{10}-DN	162	41 (100), 55 (99), 94 (55), 39 (47), 54 (37), 68 (36)	$N\equiv C(CH_2)_6C(C\equiv N)=CH_2$

[a]Determined by CI mass spectra. [b] The relative intensities of major peaks in the mass spectra are given in parentheses.

*Reprinted with permission from A. Kondo, H. Ohtani, Y. Kosugi, S. Tsuge, Y. Kubo, N. Asada, H. Inaki and A. Yoshioka, Macromolecules, 1988, **21**, 10, 2918. ©1988, American Chemical Society [86]*

and hydrogenated NBR. Typical mass spectral data of the characteristic degradation products are shown in **Table 1.6**.

Characteristic peaks in the pyrogram of N-37(0) (i.e., polymer containing 37% acrylonitrile, zero hydrogenation) are BD monomer, BD dimmer, and acrylonitrile (AN) monomer, whereas those of hydrogenated NBR consist of a series of linear mononitriles (MN(A)) up to C_{12}, each of which consists of a doublet corresponding to an α-olefinic MN(A) (the former) and a saturated MN(A) (the latter) [88]. Another series of mononitrile positional isomers (MN(B)) are also observed. In addition, C_{11} mononitrile (MN(C)) and C_9 and C_{10} dinitriles (DN), which reflect the alternate arrangement of AN and hydrogenated BD units (BD-AN-BD and AN-BD-AN, respectively), are also observed. Moreover, a series of peaks of hydrocarbons are observed, which reflect the methylene chains produced by hydrogenation. Hydrocarbon peaks of each carbon number consist of a triplet corresponding to an α,ω-di-olefin, an α-olefin, and a *n*-alkane. The fact that up to C_{12}-hydrocarbon peaks are observed suggests that at least a hydrogenated BD-BD-BD sequence exists in the polymer chain.

These results suggests that the number of unhydrogenated 1,4-BD diads in the polymer chain becomes negligible before 44% hydrogenation.

Among a series of MN(A), C_7-MN(A) becomes predominant probably through the following degradation mechanism:

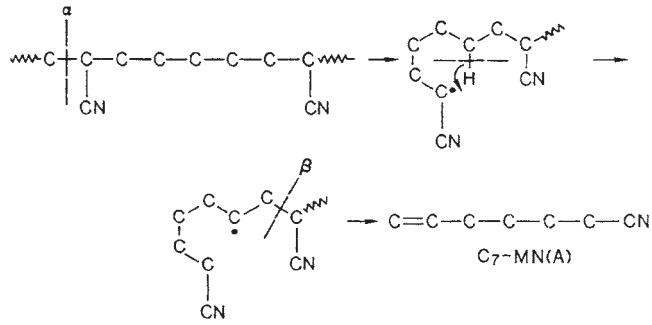

The C-C bond of the α-position of methine carbon is preferentially cleaved, and then the specific intramolecular radical transfer (back-biting) followed by β-scission yields C_7-MN(A) [89], which is likely to occur in a hydrogenated AN-BD-AN sequence. Similarly C_{11}-MN(A) is formed when a hydrogenated AN-BD-BD-AN sequence is subjected to the double back-biting radical transfer followed by β-scission. In fact, the C_{11}-MN(A) peak is the second largest among the peaks of MN(A).

Figure 1.27 shows the relationships between the degree of hydrogenation determined by the iodine value method and the peak area of C_7-MN(A) and C_{11}-MN(A) normalised

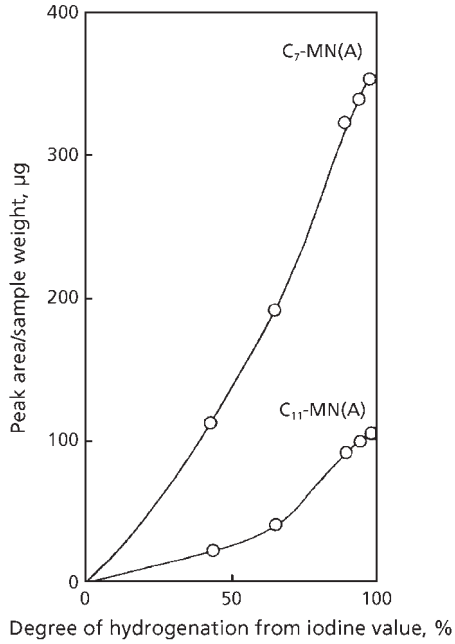

Figure 1.27 Relationships between observed peak intensities of C_7 mononitrile(A) (C_7-MN(A)) and C_{11} mononitrile(A) (C_{11}-MN- (A)) and degree of hydrogenation for hydrogenated NBR. (*Reprinted with permission from A. Kondo, H. Ohtani, Y. Kosugi, S. Tsuge, Y. Kubo, N. Asada, H. Inaki and A. Yoshioka, Macromolecules, 1988, **21**, 10, 2918. © 1988, American Chemical Society [86]*)

with the sample weight (micrograms). Both curves clearly represent monotonously increasing correlation even for the highly hydrogenated samples that are practically used. Among these two curves, that for C_7-MN(A) could be better used as a practical calibration curve since the increments of the peak intensity at the higher hydrogenation region are much larger than those for C_{11}-MN(A).

On the other hand, the formation of MN(B) are associated with the cleavage at the β-position of methane carbon:

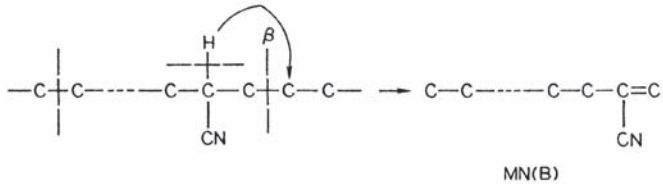

Among these MN(B), the predominant C_7MN(B) may also be given through the following back-biting mechanism on the hydrogenated AN-BD-AN sequence:

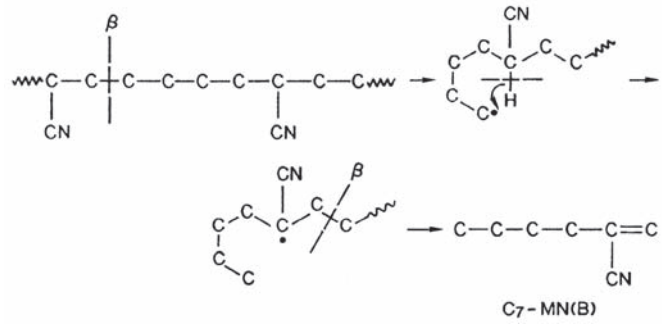

Furthermore, C_{11}-MN(B) are also formed through the double back-biting mechanism on the hydrogenated AN-BD-BD-AN sequence. The formations of MN(C) and DN are interpreted in terms of the cleavages in a hydrogenated sequence with alternating AN and BD units as follows:

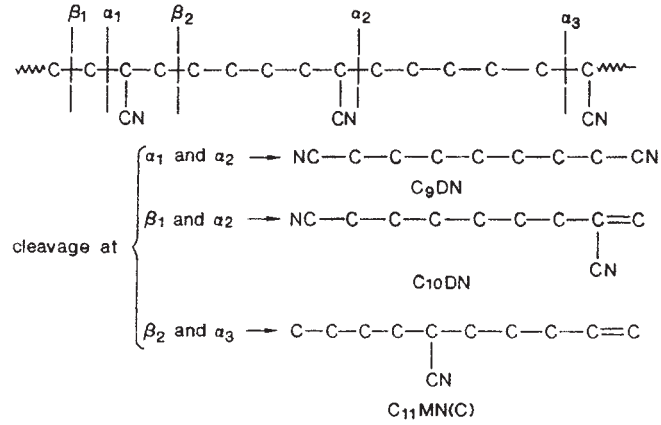

The conclusion reached by Kondo and co-workers [86] as a result of their very detailed study was that specific absorption bands in the IR spectra, resonance peaks in the ^{1}H-NMR spectra, and characteristic peaks on the pyrograms by Py-GC are a good method for tracing the degree of hydrogenation reaction. Among these, the peak intensity of C_7-MN(A) by Py-GC provided a practical calibration curve applicable even to highly hydrogenated NBR. On the other hand, the IR spectra of various hydrogenated NBR suggested a preferential hydrogenation reaction of 1,2-BD units over 1,4-units. Py-GC and ^{13}C-NMR also supplied complementary information

about longer sequences along the chains and the mechanisms of the hydrogenation reaction. The ^{13}C-NMR spectra suggested that the BD units next to the AN units in the polymer chain were more likely to be hydrogenated than those next to the same units (BD).

1.3.7 Miscellaneous Copolymers

Other applications of Py-GC include studies on polyesterurethane [87], ethylene-propylene [90, 91], natural rubber and styrene butadiene rubbers [92, 93], styrene-divinyl benzene [94], polyhexafluoropropylene-vinylidene fluoride [95], acrylic and methacrylic acid [96], PE-ethyl acrylate and PE-vinyl acetate [55] and MMA-ethyl acrylate copolymers [97].

References

1. T.P. Wampler and E.J. Levy, *Journal of Applied Pyrolysis*, 1987, **12**, 2, 75.

2. C.G. Smith, *Journal of Analytical and Applied Pyrolysis*, 1989, **15**, 3, 209.

3. M.J. Matheson, T.P. Wampler, L. Johnson, L. Atherly and L. Smucker, *American Laboratory*, 1997, **5**, 24C.

4. S. Tsuge and H. Ohtani, *Pyrolysis Gas Chromatography of High Polymers Fundamental and Data Compilation*, Techno Systems, Tokyo, Japan, 1989.

5. T.P. Wampler and E.J. Levy, *Analyst*, 1986, **111**, 9, 1065.

6. M.M. O'Mara, *Journal of Polymer Science Part A-1: Polymer Chemistry*, 1970, **8, 7**, 1887.

7. M.H.P.M. Van Lieshout, H-G. Janssen, C.A. Cramers, M.J.J. Hetem and H.J.P. Schalk, *Journal of High Resolution Chromatography*, 1996, **19**, 4, 193.

8. F.C-Y. Wang, *Journal of Chromatography A*, 1997, **753**, 1, 101.

9. J. Helper and M. Sobera, *Journal of Chromatography*, 1997, **776**, 2, 337.

10. S.G. Roussis and J.W. Fedora, *Rapid Communications in Mass Spectrometry*, 1996, **10**, 1, 82.

11. B.C. Cox and B. Ellis, *Analytical Chemistry*, 1964, **36**, 1, 90.

12. C.A. Johnson and M.A. Leonard, *Analyst*, 1961, **86**, 1019, 101.

13. T. Yoshizaki, *Analytical Chemistry*, 1963, **35**, 13, 2177.

14. B. Groten, *Analytical Chemistry*, 1964, **36**, 7, 1206.

15. H. Giacobbo and W. Simon, *Pharmaceutica Acta Helvetiae*, 1964, **39**, 162.

16. R.W. May, E.F. Pearson, J. Porter and M.D. Scothern, *Analyst*, 1973, **98**, 1166, 364.

17. P. Kunch, *Chemia Analityczna*, 1996, **41**, 241.

18. N. Oguri, A. Onishi, S. Uchino, K. Nakahashi and X. Jin, *Analytical Sciences*, 1992, **8**, 1, 57.

19. Y. Tanaka and T. Morikawa, *Koygu Kagaku (Osaka)*, 1974, **48**, 387. [*Chemical Abstracts*, 82, 98702W]

20. O.F. Folmer, Jr., and L.V. Azarraga, *Journal of Chromatographic Science*, 1969, **7**, 665.

21. O.F. Folmer, Jr., *Analytical Chemistry*, 1971, **43**, 8, 1057.

22. Y. Sugimura, T. Nagaya, S. Tsuge, T. Murata and T. Takeda, *Macromolecules*, 1980, **13**, 4, 928.

23. M.R. Grimbley and R.S. Lehrle, *Polymer Degradation and Stability*, 1995, **48**, 3, 441.

24. W.H. Beck, *Combustion and Flame*, 1987, **70**, 2, 171.

25. F.A. Lehmann and G.M. Brauer, *Analytical Chemistry*, 1961, **33**, 6, 673.

26. G.M. Brauer, *Journal of Polymer Science Part A-1: Polymer Chemistry*, 1965, **8**, 3.

27. F.C-Y. Wang, B. Gerhart and C.G. Smith, *Analytical Chemistry*, 1995, **67**, 20, 3681.

28. T. Mukundan and K. Kishore, *Macromolecules*, 1987, **20**, 10, 2382.

29. M.M. Fares, J. Hacaloglu and S. Suzer, *European Polymer Journal*, 1994, **30**, 7, 845.

30. R.J. Gritter, E. Gipstein, and G.E. Adams, *Journal of Polymer Science Part 1: Polymer Chemistry Edition*, 1979, **17**, 12, 3959.

31. *Analytical Pyrolysis*, Eds., C.E.R. Jones and C.A. Cramer, Elsevier, Amsterdam, The Netherlands, 1977.

32. *Polyethers, Volume III*, Ed., N.G. Gaylord, Wiley-Interscience, New York, NY, USA, 1962.

33. P.C. Colodny and A.V. Tobolsky, *Journal of Applied Polymer Science*, 1959, **2**, 4, 39.

34. M.R. Rao and T.S. Radhakrishnan, *Journal of Applied Polymer Science*, 1985, **30**, 2, 855.

35. T.S. Radhakrishnan and M.R. Rao, *Journal of Analytical and Applied Pyrolysis*, 1986, **9**, 4, 309.

36. T.S. Radhakrishnan and M.R. Rao, *Journal of Applied Polymer Science*, 1987, **34**, 5, 1985.

37. M.B. Berenbaum in *The Princeton Conference on the Chemistry of Sulfides*, Ed., A.V. Tobolsky, Wiley-Interscience, New York, NY, USA, 1968.

38. N.A. Rosenthal and M.B. Berenbaum in *Proceedings of the 131st Meeting of the American Chemical Society*, Miami, FL, USA, 1957, Paper No. 1.

39. M. Blazsó, *Journal of Chromatography A*, 1994, **683**, 1, 115.

40. S. Fujimoto, H. Ohtani and S. Tsuge, *Fresenius' Zeitschrift für Analytische Chemie*, 1988, **331**, 3-4, 342.

41. Z-Y. Chu, C-X. Feng, Y-C. Song, X-D. Li and J-Y. Xiao, *Journal of Applied Polymer Science*, 2004, **94**, 1, 105.

42. P. Almén and I. Ericsson, *Polymer Degradation and Stability*, 1995, **50**, 2, 223.

43. M. Furukawa, N. Yoshitake and T. Yokoyama, *Journal of Chromatography A*, 1988, **435**, 1, 219.

44. C.T. Vijayakumar, J.K. Fink and K. Lederer, *European Polymer Journal*, 1987, **23**, 11, 861.

45. T.K.P. O'Mohony, A.P. Cox and D.J. Roberts, *Analytical Proceedings*, 1993, **30**, 6, 242.

46. I. Ericsson and L. Ljunggren, *Journal of Analytical and Applied Pyrolysis*, 1990, **17**, 3, 251.

47. R.F. Cozzens, P. Walter and A.W. Snow, *Polymer Preprints*, 1987, **28**, 1, 35.

48. C.N. Cascaval, D. Rosu and I. Agherghinei, *Polymer Degradation and Stability*, 1996, **52**, 3, 253.

49. H. Nakagawa, S. Tsuge, S. Mohanraj and W.T. Ford, *Macromolecules*, 1988, **21**, 4, 930.

50. V.M. Ryabilkova, T.L. Ivanova, A.N. Zigel, L.N. Pirozhnaya and G.S. Popova, *Zhurnal Analiticheskoi Khimii*, 1988, **43**, 1093.

51. R. Hank, *Rubber Chemistry and Technology*, 1969, **40**, 3, 936.

52. J. van Schooten and J.K. Evenhuis, *Polymer*, 1965, **6**, 11, 561.

53. J. van Schooten and J. K. Evenhuis, *Polymer*, 1965, **6**, 7, 343.

54. T. Yamada, T. Okumoto, H. Ohtani and S. Tsuge, *Rubber Chemistry and Technology*, 1991, **64**, 5, 708.

55. E.M. Barrall II, R.S. Porter and J.F. Johnson, *Analytical Chemistry*, 1963, **35**, 1, 73.

56. S. Mao, H. Ohtani and S. Tsuge, *Journal of Analytical and Applied Pyrolysis*, 1995, **33**, 4, 181.

57. J.J. Shen and E. Woo, *Liquid Chromatography-Gas Chromatography*, 1988, **6**, 1020.

58. S. Yamaguchi, J. Hirano and Y. Isoda, *Journal of Analytical and Applied Pyrolysis*, 1987, **12**, 3-4, 293.

59. F.C-Y. Wang, B.B. Gerhart and P.B. Smith, *Analytical Chemistry*, 1995, **67**, 19, 3536.

60. F.C-Y. Wang and P.B. Smith, *Analytical Chemistry*, 1996, **68**, 17, 3033.

61. D.M. Bate and R.S. Lehrle, *Polymer Degradation and Stability*, 1996, **53**, 1, 39.

62. Y. Ishida, H. Ohtani, S. Tsuge and T. Yano, *Analytical Chemistry*, 1994, **66**, 9, 1444.

63. M.T. Jackson, Jr., and J.Q. Walker, *Analytical Chemistry*, 1971, **43**, 1, 74.

64. W.T. Ford and S.A. Yacoub, *Journal of Organic Chemistry*, 1981, **46**, 4, 819.

65. W.T. Ford and T. Balakrishnan, *Macromolecules*, 1981, **14**, 2, 284.

66. S. Mohanraj and W.T. Ford, *Macromolecules*, 1985, **18**, 3, 351.

67. G. Oehme, H. Baudisch and H. Mix, *Makromolekulare Chemie*, 1976, **177**, 9, 2657.

68. N.J. Coville and C.P. Nicolaides, *Journal of Organometallic Chemistry*, 1981, **219**, 3, 371.

69. C.P. Nicolaides and N.J. Coville, *Journal of Molecular Catalysis*, 1984, **23**, 1, 35.

70. H. Nakagawa and S. Tsuge, *Macromolecules*, 1985, **18**, 10, 2068.

71. H. Nakagawa, Y. Matsushita and S. Tsuge, *Polymer*, 1987, **28**, 9, 1512.

72. N. Kurashima, T. Furnhasly and S. Sato, *Kanzei Chuo Bunsekishoho*, 1996, **35**, 1.

73. D.S. Huh, J.S. Kim, K. Kim, B.K. Ahn and S.K. Suh, *Hanu Hakhoechi*, 1987, **22**, 314.

74. H.J. Cortes, G.L. Jewett, C.D. Pfeiffer, S. Martin and C. Smith, *Analytical Chemistry*, 1989, **61**, 9, 961.

75. N.E. Shadrina, A.V. Dmitrenko, V.F. Pavlova and S.S. Ivanchev, *Journal of Chromatography A*, 1987, **404**, 1, 183.

76. S. Yamaguchi, J. Hirano and Y. Isoda, *Journal of Analytical and Applied Pyrolysis*, 1989, **16**, 2, 159.

77. F.C-Y. Wang, *Journal of Chromatography A*, 1997, **765**, 2, 279.

78. H. Liu, R. Fu, P. Zhu, M. Ye and L. Shi, *Journal of Analytical and Applied Pyrolysis*, 1990, **18**, 1, 79.

79. F.C-Y. Wang and P.B. Smith, *Analytical Chemistry*, 1996, **68**, 3, 425.

80. J.T. Blackwell, *Analytical Chemistry*, 1976, **48**, 13, 1883.

81. A.H. Weinstein, *Rubber Chemistry and Technology*, 1984, **57**, 1, 203.

82. N.A. Mohammadi and G.L. Rempel, *Macromolecules*, 1987, **20**, 10, 2362.

83. Y. Kubo, K. Hashimoto and N. Watanabe, *Kautschuk und Gummi Kunststoffe*, 1987, **40**, 21, 118.

84. S. Tsuge and H. Ohtani in *Applied Polymer Analysis and Characterisation:Recent developments in Techniques, Instrumentation, Problem Solving,* Ed., J. Mitchell, Jr., Hanser Verlag, Munich, Germany, 1986, p.217.

85. S. Tsuge, *Chromatography Forum*, 1986, **4**, 44.

86. A. Kondo, H. Ohtani, Y. Kosugi, S. Tsuge, Y. Kubo, N. Asada, H. Inaki and A. Yoshioka, *Macromolecules*, 1988, **21**, 10, 2918.

87. D. Weber, G. Fülöp and D.O. Hummel, *Die Makromolekulare Chemie – Macromolecular Symposia*, 1990, **52**, 151, 191.

88. H. Ohtani, T. Nagaya, Y. Sugimura and S. Tsuge, *Journal of Analytical and Applied Pyrolysis*, 1982, **4**, 2, 117.

89. H. Ohtani, S. Tsuge, T. Ogawa and H.G. Elias, *Macromolecules*, 1984, **17**, 3, 465.

90. H. Boer and E.C. Kooyman, *Analytica Chimica Acta*, 1951, **5**, 550.

91. J.E. Brown, M. Tryon and J. Manel, *Analytical Chemistry*, 1963, **35**, 13, 2173.

92. N. Tyron, S. Horowicz and E. Mondel, *Journal of Research of the National Bureau of Standards*, 1955, **55**, 219.

93. C.G. Smith and R. Beaver, *TAPPI*, 1980, **63**, 8, 93.

94. N. Svob and F. Flajsnman, *Croatica Chemica Acta*, 1970, **42**, 417.

95. J.T. Blackwell, *Analytical Chemistry*, 1976, **48**, 13, 1883.

96. J. L. Sharp and G. Paterson, *Analyst*, 1980, **1250,** 517.

97. S. Paul, *Journal of Coatings Technology*, 1980, **52**, 661, 47.

2 Complementary Pyrolysis-Gas Chromatography-FT-IR

Whilst pyrolysis-gas chromatography (Py-GC) is a very important analytical tool for the elucidation of polymer structure, the technique becomes even more useful when it is coupled with complementary techniques such as infrared (IR) spectroscopy and more recently mass spectroscopy (MS) (see Chapter 3). These techniques, particularly MS can be used to provide unequivocal identification of volatile pyrolysis products produced on pyrolysis or of individual pyrolysis products separated by GC.

This technique has many applications in qualitative and quantitive thermal analysis degradation studies and polymer microstructure studies [1-3].

The possibilities for polymer characterisation using a dispersive spectrometer have recently been developed [4]. The technique is similar to the thermal volatilisation analysis (TVA) of NcNeill [5], in that the gases evolved from a heated sample are monitored continuously (EGA), and an evolution profile of a suitable parameter is constructed in terms of time or temperature. In Py-EGA-IR, the sample is heated in a stream of gas (inert or reactive) and eluant is monitored by IR spectroscopy as the gas passes through a suitable cell. Spectra of the evolved gases are recorded continuously, so that components may be identified and their concentration determined as they are evolved. The evolution profile is of absorbance against time or temperature, and the areas under the profiles are a quantitative measure of each component. Under controlled conditions, the profiles are reproducible, and can be used for sample identification and comparison purposes.

2.1 Theory

This technique has been studied by Washall and Wampler [6]. Pyrolysis of polymer samples enables IR spectra to be obtained from the vapourised polymer. Many polymers are difficult to analyse by more conventional Fourier transform infrared (FT-IR) sampling techniques due to additives that cause scattering. Carbon-filled rubbers are examples of this type of problem. By dissociating the bonds of the polymer backbone, polymer functionality and structure can be determined much like Py-GC.

Using direct pyrolysis FT-IR in conjunction with other techniques gives a broad picture of the polymer structure and degradation mechanism. The latter is easily investigated using time-resolved pyrolysis in which the sample is heated at a slow rate over a long period of time. In this way degradation products can be monitored as they evolve from the sample.

While the coupling of pyrolysis with IR spectroscopy is not a new technique for analysing polymer samples, the interface is new. The traditional steps of condensing the pyrolysates on IR transmitting window materials and transferring the windows to the sample compartment are eliminated.

This is a complementary technique which provides more detailed information on the structure of polymers than does Py-GC alone. As an example of the application of this technique, Leibman and co-workers [7] applied it to a study of short-chain branching in polyethylene and polyvinylchloride (PVC). The nature and relative quantities of the short branches along the polymer chains were determined, providing detailed microstructural information. Down to 0.1 methyl, ethyl, or *n*-butyl branches per 1000 methylene groups can be determined by this procedure. Other structural defects can be determined, providing significant information on polymer microstructure that is not otherwise readily obtained.

Julian and Domingo [8] have pointed out that the coupling of spectroscopic instruments to liquid chromatography instruments has not been as rapidly developed or successful as techniques such as GC-MS and GC-IR spectroscopy. A new liquid chromatography-infrared spectroscopy interface is described which promises to be a successful marriage of these techniques. Although it does not provide a real-time analysis, it has the advantages of total solvent removal before infrared analysis, analysis of the total liquid chromatography eluant as opposed to incremental fractions, and the ability to produce infrared spectra at high signal-to-noise ratios.

Some pyrolysis FT-IR spectra obtained by FT-IR are shown in **Figure 2.1**. Direct pyrolysis FT-IR of polystyrene (**Figure 2.1**) reveals a spectrum that is almost identical to that of the styrene monomer. Absorption bands indicating vinyl stretch (910 and 1000 cm^{-1}) and aromatic ring stretching at 1496 cm^{-1} are very evident. **Figure 2.1(b)** shows a comparison of Nylon 6,6 and Nylon 6,12 both pyrolysed at 750 °C. The difference between Nylon 6,6 and Nylon 6,12 lies in the length of the hydrocarbon chain. A relative measure of the CH_2 group content to the amide group should be a good indication of the differences. The primary identifier is the intensity of the CH_2 stretching band compared to the amide stretch at 1650 cm^{-1}. This ratio gives a qualitative differentiation between the two polymers. Similar distinctions can be made for other Nylon samples.

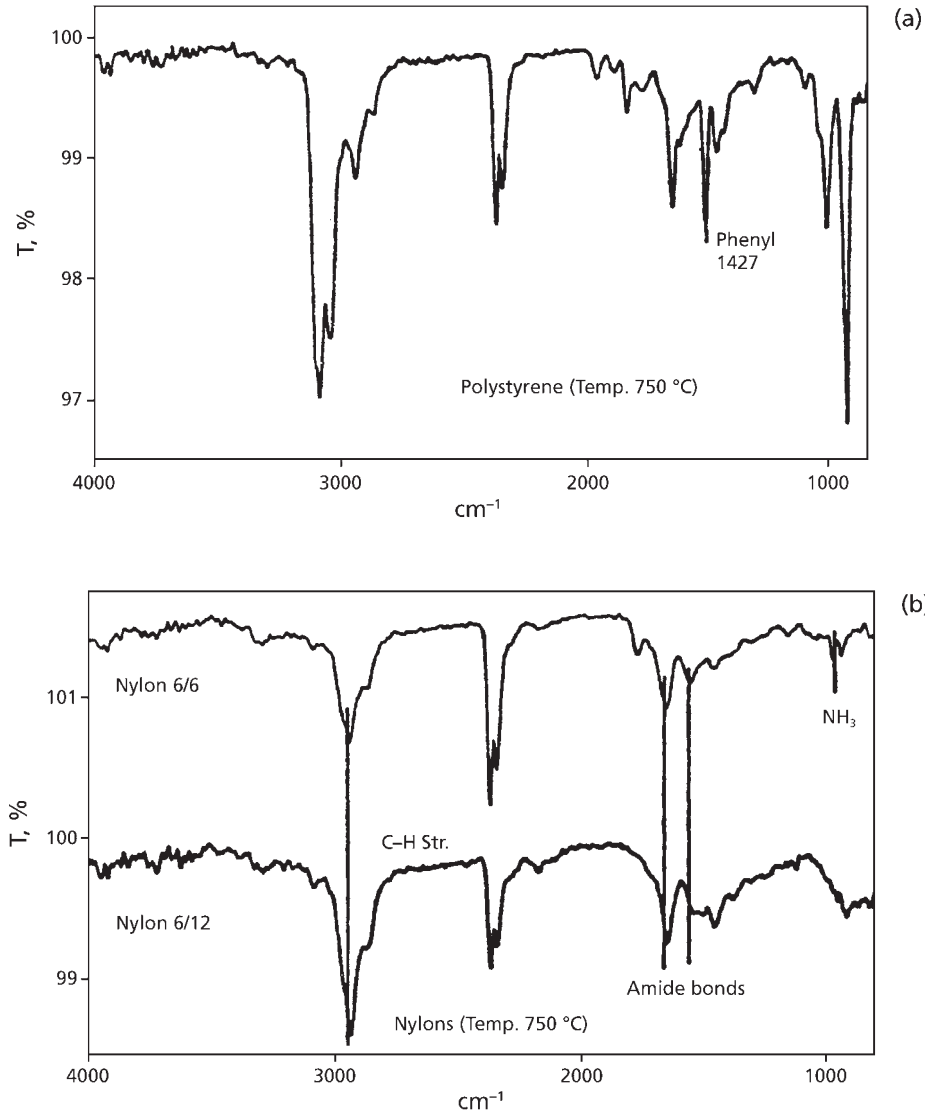

Figure 2.1 Pyrolysis FT-IR spectra of (a) polystyrene, (b) Nylons (*Source: Author's own files*)

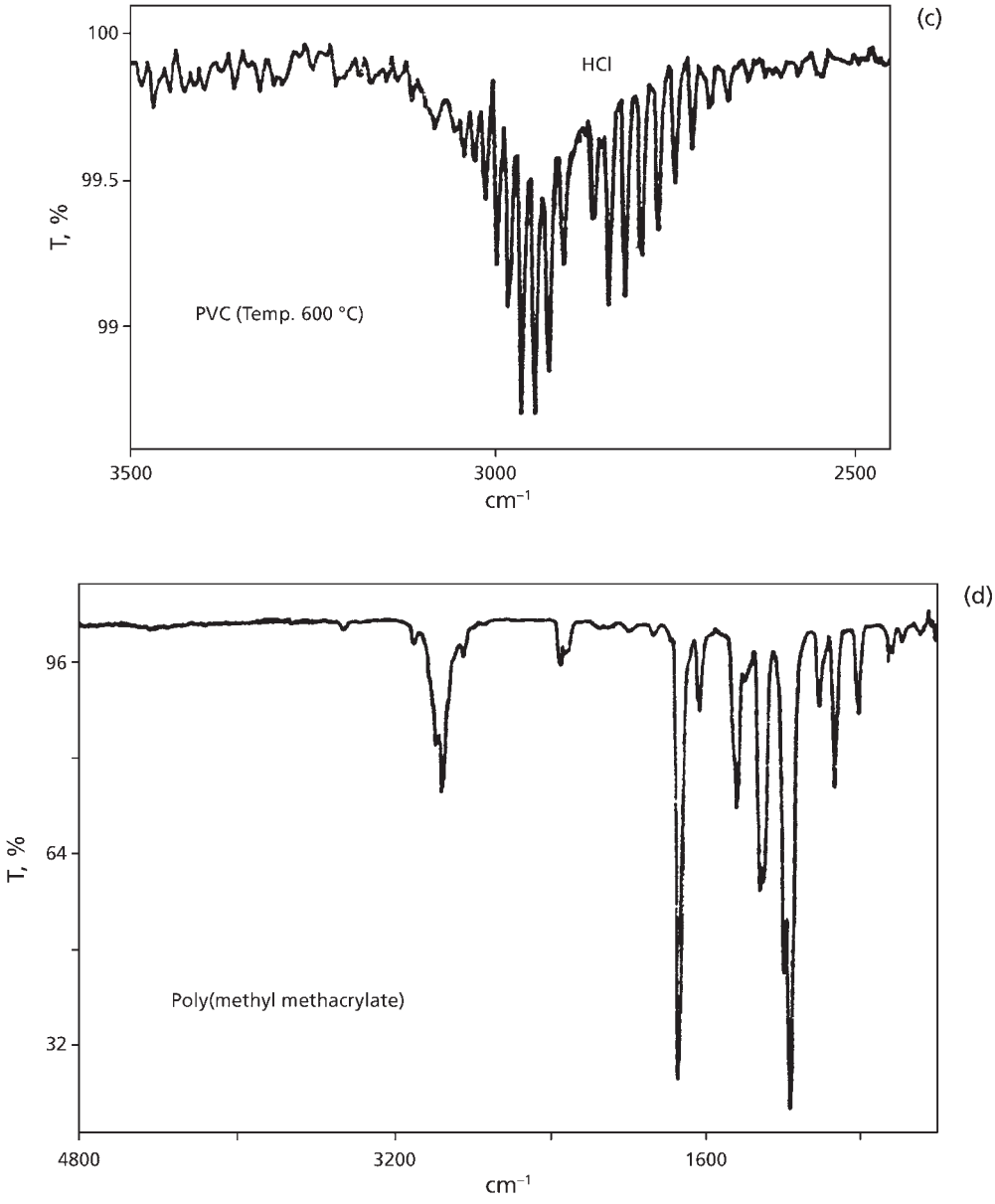

Figure 2.1 *Continued*. (c) PVC and (d) polymethylmethacrylate. (*Source: Author's own files*)

A classic example of the verification of degradation mechanisms is the pyrolysis of PVC. This polymer undergoes side group elimination of hydrogen chloride in the initial step. The resulting polymer chain is a polyene. This polyene then undergoes several scission steps to produce aromatics. Of the aromatics produced, the more prevalent are benzene, toluene, and naphthalene. Since hydrogen chloride is strongly active in the IR region, pyrolysis FT-IR of PVC produces a spectrum of hydrogen chloride as well as some minor absorption bands indicating some aliphatic side products. **Figure 2.1(c)** shows the spectrum of PVC at 600 °C in the 3500-2400 cm^{-1} region. The unmistakable pattern of hydrogen chloride is present.

Figure 2.1(d) shows the spectrum of pyrolysed polymethylmethacrylate (PMMA). A carbonyl stretching bands is clearly present at 1745 cm^{-1}. Also evident is an ester CH_3-O stretch at 1018 cm^{-1}. The spectrum obtained in the pyrolysis experiment can be directly compared to a reference spectrum of methyl methacrylate (MMA).

2.2 Instrumentation

The instrumentation is discussed in Appendix 1 in Volume 1.

The system applied in the study mentioned previously consisted of a CDS model 122 Pyroprobe with a ribbon filament as the heating surface. This pyrolyser heats by varying the resistance of the platinum element. Temperature rise times for flash pyrolysis are typically of the order of milliseconds. IR spectra were obtained with an FT-IR bench system equipped with a CDS pyrolysis/FT-IR interface. The data were collected at 8 cm^{-1} with a deuterated triglycine sulfate detector. The interface is cylindrical in shape with two potassium bromide windows for the IR beam to pass through.

When the beam enters the pyrolysis cell, it is focused directly above the platinum filament of the pyrolyser. The spectra were baseline corrected using a polynomial baseline correction routine. Sample sizes ranged from 100 to 500 μm.

2.3 Applications

2.3.1 Copolymers

Weber and co-workers [9] used pyrolysis FT-IR to characterise polyesterurethane elastomers, a polyester diol, a short chain diol and a diisocyanate.

Copolymers of PMMA are widely used as glazing materials. The commercial 'homopolymer' usually contains a small amount of comonomer such as methyl

acrylate which is included to reduce the number of thermally unstable end groups and to act as a block to thermally or photochemically induced depropagation. Comonomers which can form crosslinks confer increased toughness and solvent resistance on the copolymer. These materials may craze and crack in service, and it useful to be able to identify the general type of comonomer to assist in studies of crazing susceptibility, and to distinguish between different samples of the same material type. It has been suggested that Py-EGA-IR could be a useful method for characterisation of PMMA copolymers.

Davidson [10] analysed a range of commercial PMMA copolymers by linear temperature programmed Py-EGA-IR to determine whether the evolution profiles of various pyrolysis gases against temperature were sufficiently distinctive to allow reliable identification of different types, and to distinguish between different batches of the same type. The results show that, with one exception, the different types and batches can be reliably identified, and reactions to account for some of the compounds evolved were presented. The potential value of Py-EGA-IR analysis of PMMA polymers for both production control and research is demonstrated.

MMA monomer, methanol, and carbon dioxide were detected in the pyrolysis gases. The profiles of rate of evolution against temperature were used to identify the presence of occluded monomer and thermally unstable end groups such as unsaturation. The evolution profiles for MMA and methanol were found to be characteristic for each type of crosslink. Evolution of methanol between 250 °C and 300 °C, and between 300 °C and 350 °C has been attributed to condensation reactions of carboxylic acid and primary amide groups, respectively, with adjacent ester groups. The evolution profiles were used to distinguish between samples from different manufacturers, and to identify material [5].

The pyrolysis system used by Davidson [10] comprised a 20 cm × 1.25 cm quartz tube (1 mm wall) wound with Nichrome tape (0.25 × 1.5 mm) with a total resistance of 7 ohms. The windings were encapsulated in a silicate cement and insulated with several layers of asbestos tape. This unit was then inserted into 3.75 cm diameter stainless steel tube and retained by heat-resistant discs at both ends. At 400 °C in the central 5 cm zone, temperature variation was 2 °C and the maximum temperature gradient was 1 °C/cm.

A pyrex tube, 5 mm id, 30 cm long, was used for pyrolysis. Samples (4-5 mg) were placed in aluminum pans as used for differential scanning calorimetry, folded to fit inside the tube, and located centrally by 3 mm diameter pyrex glass rods of appropriate length either side of the sample pan. Teflon plugs with 1.5 mm diameter stainless steel inlet and outlet tubes conducted the dry nitrogen carrier gas (50 ml/min) through the system to the gas cell. A temperature ramp of 5 °C/min from ambient to 500 °C was

used for all analyses. A chromel-alumel control thermocouple was placed between the pyrolysis tube and the wall of the furnace, adjacent to the sample.

Evolution profiles were constructed as plots of net IR absorbance against temperature for selected absorption bands which were known to be free from interferences. Procedures used for data reduction and calculation of temperatures appropriate to absorption bands of interest were as described previously [4], except that absorbances were normalised to 10 mg sample mass to allow direct comparison of profiles.

Evolution profiles for MMA monomer were of similar form for all samples, consisting of a major evolution event and several minor events. The peak rate temperatures represented by the temperature at maximum absorbance and major event profiles were characteristic for each material, though some batch variation was observed. Most samples yielded (copolymer triazine) carbon dioxide, usually as a single event near 400 °C, and methanol in one or more events between 250 and 450 °C. Duplicate determinations showed that the profiles were superimposable within 1 °C as shown in **Figures 2.2(a)** and 2.2(b) for MMA and methanol for one sample. MMA profiles are shown in **Figure 2.3**, methanol in **Figure 2.4** and carbon dioxide in **Figure 2.5**. Samples in which the copolymer was COOH, and methacrylamide (b), *N*-hydroxylmethyl-methacrylamide and methacrylamide (c) and *N*-methoxymethyl-methacrylamide (d) yielded small amounts of complex carbonyl compounds at high temperatures, usually starting at about the peak rate temperature.

The carbonyl region spectra of these compounds were enhanced by subtracting out that of MMA. Liquid condensates also collected in the cooler parts of the pyrolysis tube. Representative spectra are shown in **Figure 2.6(a) and (b)**. Further examination of the spectra suggested that a second component was present with MMA evolved below 200 °C in samples (the copolymers *N*-hydroxylmethyl-methacrylamide and methacrylamide). Subtraction of MMA carbonyl bands in the 1600-1800 cm^{-1} range revealed the characteristic spectrum of formaldehyde. The evolution profile was similar to that previously observed for occluded methanol [10].

Detailed examination of the pyrolysis products such as methacrylate, methanol and carbon dioxide and formaldehyde provides much structural information on these polymers and enabled distinctions to be made between copolymers containing very low levels of the comonomer.

On the basis that the area under the evolution profile is proportional to the total concentration of component in the gas stream, the reproducibility of the technique [11, 12] is good enough to consider its use for quantitative analysis.

Minor components such as occluded material and thermally unstable end groups can be readily estimated by using a more sensitive absorption band such as that near 1170 cm^{-1}.

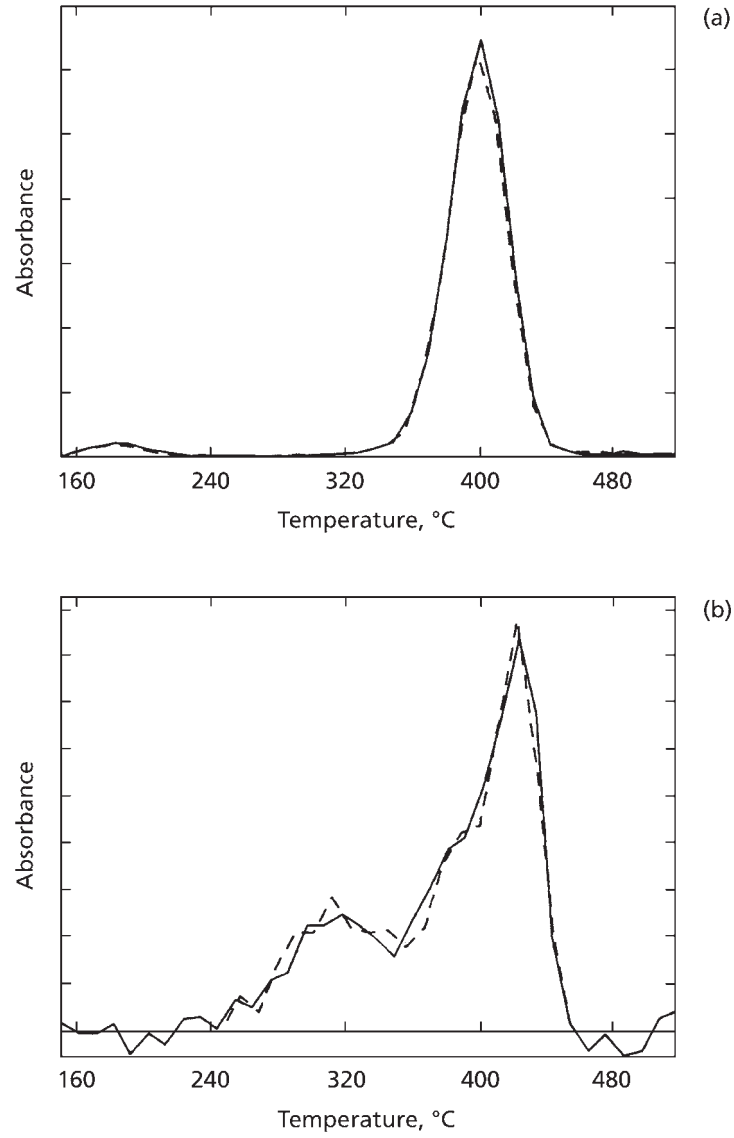

Figure 2.2 (a) Methyl methacrylate evolution from type C copolymer, duplicate analyses, 1310 cm^{-1}, (b) Methanol evolution from type C copolymer, duplicate analysis, 1050 cm^{-1}. (*Reprinted with permission from R.G. Davidson, Journal of Applied Polmer Science, 1987,* ***34****, 4, 1631. ©1987, John Wiley [10]*)

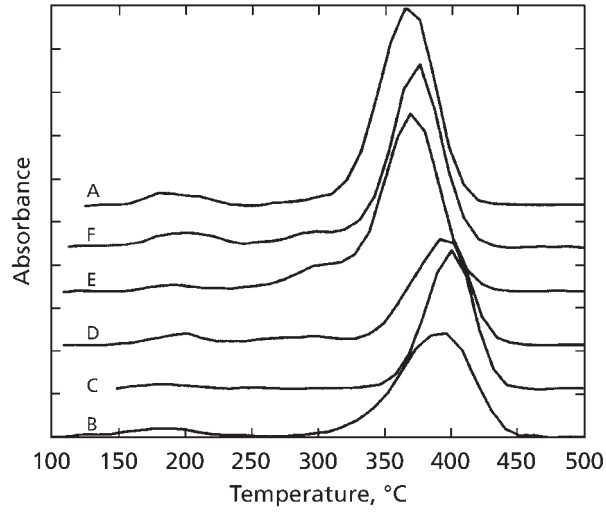

Figure 2.3 Methyl methacrylate evolution profile from PMMA copolymers; letters refer to table in Figure 2.4; 1310 cm^{-1}. Displaced vertically for clarity. (*Reprinted with permission from R.G. Davidson, Journal of Applied Polmer Science, 1987, **34**, 4, 1631. ©1987, John Wiley [10]*)

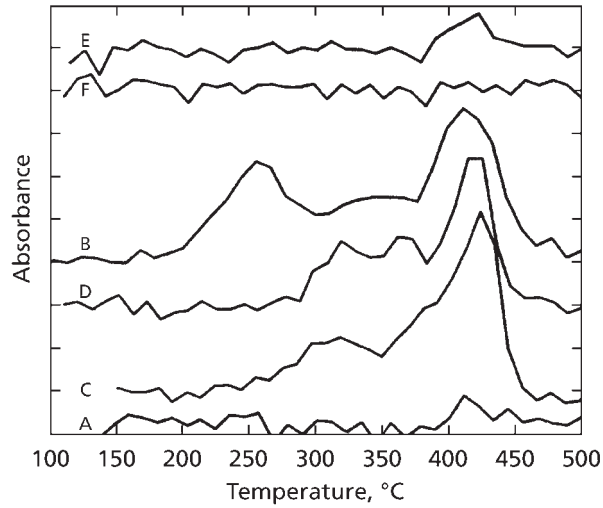

Figure 2.4 Methanol evolution from PMMA copolymers; letters refer to table on next page. Displaced vertically for clarity. 1050 cm^{-1} (*Reprinted with permission from R.G. Davidson, Journal of Applied Polmer Science, 1987, **34**, 4, 1631. ©1987, John Wiley [10]*)

Sample	**Comonomer***
Linear 'homopolymers' A1, A2, A3 (Plex 201, Röhm GmbH)	-
Copolymer B1, B2 (P-76 Polycast)	-COOH, methacrylamide
Copolymer C1, C2 (S-350 Swedlow Inc.)	*N*-hydroxymethyl methacrylamide methacrylamide
Copolymer D1, D2, D3 (Plex 55, Röhm & Haas)	*N*-hydroxymethyl methacrylamide
Copolymer E1, E2 (S-708 Swedlow Inc.)	2,2 Dimethyl 1,3 propanediol dimethacrylate
Copolymer F1, F2 (Plex 249, Röhm GmbH)	2,4,6-*tris*(allyoxy) trizine
*Identified by solvent extraction, chemical and spectroscopic analysis *Reprinted with permission from R.G. Davidson, Journal of Applied Polymer Science, 1987, **34**, 4, 1631. ©1987, John Wiley [10]*	

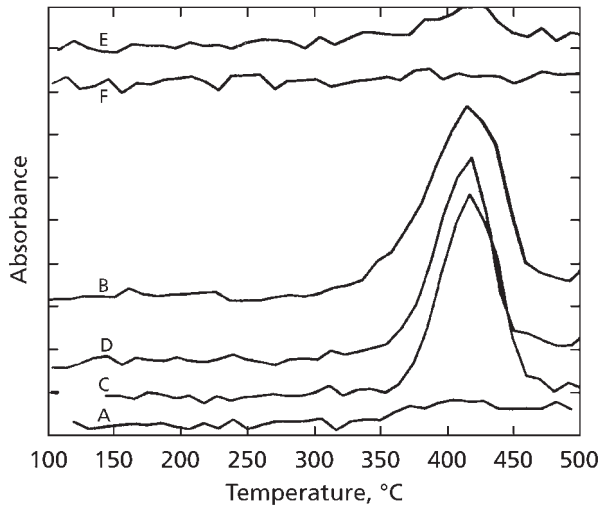

Figure 2.5 Carbon dioxide evolution from PMMA copolymers; letters refer to table in **Figure 2.4**. Displaced vertically for clarity. (*Reprinted with permission from R.G. Davidson, Journal of Applied Polymer Science, 1987, **34**, 4, 1631. ©1987, John Wiley [10]*)

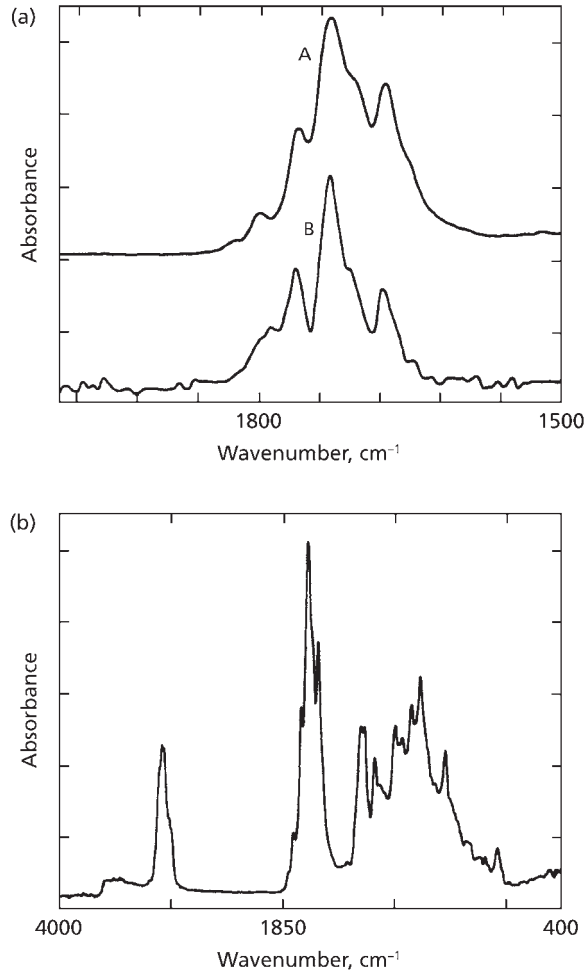

Figure 2.6 (a) Type D copolymer A Liquid pyrolysate; B aerosol at 430 °C, corrected for MMA carbonyl. (b) Type D copolymer, liquid pyrolysate. (*Reprinted with permission from R.G. Davidson, Journal of Applied Polymer Science, 1987, **34**, 4, 1631. ©1987, John Wiley [10]*)

The area under the curve yields the total polymer associated with such groups, and the peak rate temperature may be related to zip length as indicated earlier, so that the number of thermally unstable groups can be estimated.

The methanol profiles are promising. Events peaking near 260 °C and 320 °C give a reasonable estimation of free carboxylic acid and primary amide, even at the low S/N of the present system. The remaining events below 400 °C are not well enough

separated for quantitative work, and the final event does not appear to be correlated with monomer. Better resolution of the profiles with a small volume cell or light pipe, and more frequent sampling, as with FT-IR, might yield more useful results.

Detection of MMA originating from occluded material and from thermal weak links could find application in characterisation of both homopolymers and copolymers. Py-EGA-IR could be used to distinguish between polymers of different molecular weight, and made by different processes, in the same way that McNeill [11] used TVA. The advantage of simultaneous identification and estimation of volatile components by IR may be balanced by the lower sensitivity and inability to detect infrared inactive species such as hydrogen compared with TVA. Changes in composition with degree of polymerisation could thus be monitored; the efficiency of polymerisation processes designed to yield specialty polymers could be assessed; the progress and effectiveness of crosslinking processes using amide type systems could also be checked as, for example, in the determination of residual free acid or amide groups.

Kondo and co-workers [12] studied the microstructure of hydrogenated polyacrylonitrile-butadiene rubbers using Py-GC IR spectroscopy and Py-GC-NMR spectroscopy.

Oguchi and co-workers [13] separated pyrolysis products of MMA-butadiene-styrene terpolymer and identified them by FT-IR, MS and atomic emission spectrometry.

References

1. S.A. Liebman, D.H. Ahlstrom and P.R. Griffiths, *Applied Spectroscopy*, 1976, **30**, 3, 355.

2. J.O. Lephardt, *Applied Spectroscopy Reviews*, 1982, **18**, 2, 265.

3. J.O. Lephardt in *Analytical Pyrolysis: Techniques and Applications*, Ed., K.J. Voorhees, Butterworths, London, UK, 1984, p.95-120.

4. R.G. Davidson and G.I. Mathys, *Analytical Chemistry*, 1986, **58**, 4, 837.

5. I.C. McNeill, *Journal of Polymer Science Part A1: Polymer Chemistry*, 1966, **4**, 10, 2479.

6. J.W. Washall and T.P. Wampler, *A Pyrolysis/FT-IR System for Polymer Quality Control – A Feasibility Study*, Chemical Data Systems, Oxford, PA, USA, 1988.

7. S.A. Liebman, D.H. Ahlstrom, W.H. Starnes and F.C. Schilling, *Journal of Macromolecular Science Part A: Pure and Applied Chemistry*, 1982, **17**, 6, 935.

8. J.M. Julian and R.C. Domingo in *Proceedings of RadTech '96*, Nashville, TN, USA, 1996, Volume 1, p.423.

9. D. Weber, G. Fülöp and P.O. Hummel, *Die Makromolekulare Chemie - Macromolecular Symposia*, 1991, **52**, 151.

10. R.G. Davidson, *Journal of Applied Polymer Science*, 1987, **34**, 4, 1631.

11. I.C. McNeill, *European Polymer Journal*, 1968, **4**, 1, 21.

12. A. Kondo, H. Ohtani, Y. Kosugi, S. Tsuge, Y. Kubo, N. Asada, H. Inaki and A. Yoshioka, *Macromolecules*, 1988, **21**, 10, 2918.

13. R. Oguchi, A. Shimizu, S. Yamashita, K. Yamaguchi and P. Wylie, *Journal of High Resolution Chromaography*, 1991, **14**, 6, 412.

3 Complementary Pyrolysis – Mass Spectrometry

The time has long since passed when one could rely on gas chromatographic data alone to identify unknown compounds in gas chromatograms (GC). The sheer number of compounds that could be present would invalidate reliance on the use of such techniques. The practice nowadays is to link a mass spectrometer (MS) or nuclear magnetic resonance (NMR) or Fourier transform infrared (FT-IR) spectrometers, see following sections) to the outlet of the GC or directly to the pyrolysis unit, so that a mass spectrum is obtained for each chromatographic peak as it emerges from the separation column. If the peak contains a simple substance then computerised library searching facilities attached to the MS will rapidly identify substance. If the emerging peak contains several substances, then the mass spectrum will provide information on the substances present. Alternatively, different GC columns can be tried that will resolve the mixture of substances in question.

The use of GC-MS grew rapidly during the early 1970s as discussed by Shackleford and McGuire [1].

3.1 Applications

Hughes and co-workers [25] and Meuzelaar and co-workers [26] have shown that pyrolysis mass spectrometry (Py-MS) has considerable potential for the characterisation and discrimination of natural and synthetic polymers. Their equipment combined a Curie point pyrolyser and quadruple mass spectrometer operated in an optimum geometric arrangement. The pyrolysate was passed through an empty glass chromatograph column and jet separator before entering the MS. Forty or more sequential mass spectral scans were integrated by computer processing to give a composite mass pyrogram. The system was used to study a wide range of polymeric materials. The sensitivity is sufficiently high to allow samples of 5 μg or less to give adequate electron impact spectra, but in the chemical ionisation mode larger samples are necessary. Mass pyrograms are usually characteristic of the sample type and frequently allow discrimination between samples of similar composition.

The advantages of Py-MS over pyrolysis-gas chromatography (Py-GC) for generating information about polymeric materials are its speed, sensitivity, ease of producing data

that can be, processed by a computer, and the elimination of the variables associated with GC. A major disadvantage of Py-MS is that a complex mixture is produced by a combination of pyrolysis and electron impact fragmentation, which makes a mass pyrogram more difficult to interpret than the chromatogram produced in Py-GC, in which only a pyrolytic breakdown is involved.

3.1.1 Polyurethane [27]

Cyclic adipate oligomers are nonpolymerisable residuals from the polyol used to manufacture the urethane. The chemical ionisation (CI) mass spectrum (**Figure 3.1**) indicates that this is a polyester composed of adipic acid (AA), 1,4-butanediol (BDO), and 1,6-hexanediol (HDO). **Figure 3.2** is a product ion scan for the MH^+ 229 component. The ion at *m/z* 147 is the protonated adipic acid ion, and the ions at *m/z* 129 and 111 are water-loss fragments. The ions at *m/z* 101 ($HO\text{-}C_6H_{12+}$), *m/z* 83 (C_6H_{11+}), and *m/z* 55 (C_4H_{7+}) are from the 1,6-hexanediol moiety. The structure of the MW 228 species is thus $\text{-O-}C_6H_{12}\text{-O-CO-}C_4H_8\text{-CO-}$, which may be abbreviated as HDO-AA-. The MW 200 species in **Figure 3.1** is the corresponding –BDO-AA cyclic monomer.

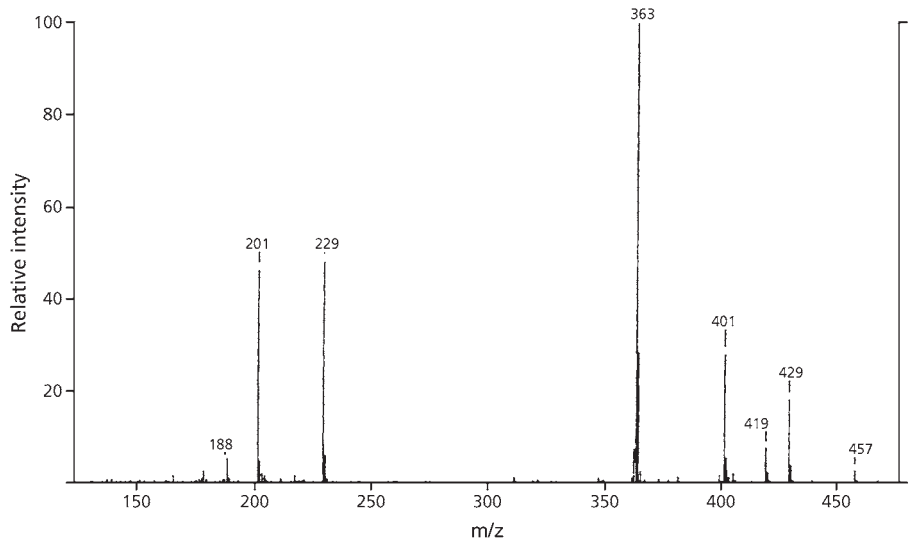

Figure 3.1 CI-MS survey scan of polyurethane (PU; thermal desorption region, 20-200 °C). (*Reprinted with permission from R.P. Lattimer, Rubber Chemistry and Technology, 1995, **68**, 783. ©1995, ACS Rubber Division [27]*)

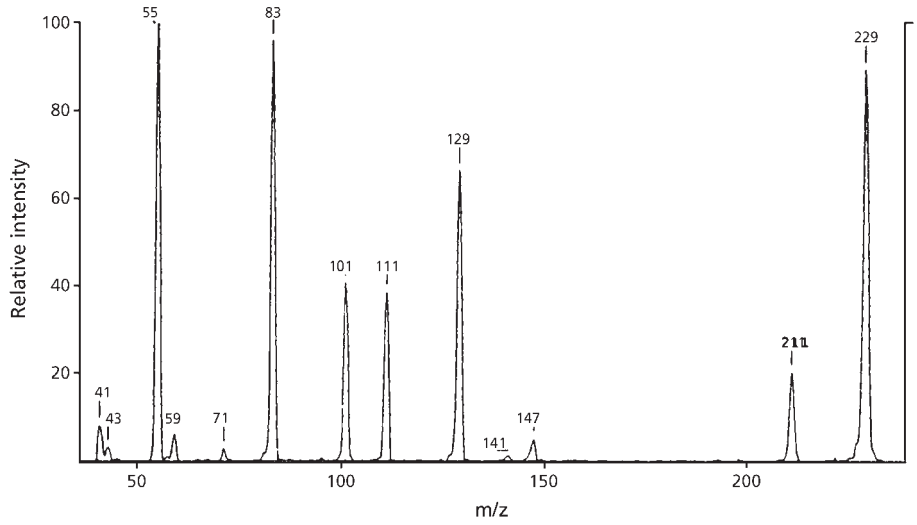

Figure 3.2 Product ion scan (CI-MS/MS) of MH^+ 229 from polyurethane. (*Reprinted with permission from R.P. Lattimer, Rubber Chemistry and Technology, 1995, **68**, 783. ©1995, ACS Rubber Division [27]*)

Figure 3.3 is a product ion scan for the MH^+ 429 component. Product ions include the protonated –BDO-AA- (*m/z* 201) and -HDO-AA- (*m/z* 229) units. The residual cyclic ester oligomers observed via CI-MS (**Figure 3.1**) may be identified as follows:

MW 200 -BDO-AA-
MW 228 -HDO-AA-
MW 400 -BDO-AA-BDO-AA-
MW 428 -BDO-AA-HDO-AA-
MW 456 -HDO-AA-HDO-AA-

Figure 3.4 is a composite CI-MS survey scan showing the initial volatile products from urethane pyrolysis (sample heating range ~200-300 °C). The diisocyanate is readily identified as 4,4´-methylene-bis(phenyl isocyanate) (MDI; MW 250): OCN-ø-CH_2-ø-NCO. The ion at *m/z* 225 is MH^+ for the 'amine-isocyanate' pyrolysis product: OCN-ø-CH_2-NH_2. Fragment ions from MDI include *m/z* 132 (OCN-ø-CH^+_2) and *m/z* 106 (H_2N-ø-CH^+_2). The chain extender is shown to be BDO, which gives intense MH^+ and $(MH - H_2O)^+$ ions at *m/z* 91 and 73, respectively. The 1:1 adduct of MDI and BDO is prominent at MH^+ 341. MH^+ 269 is the adduct of MDI and water. Cyclic polyester pyrolysates in **Figure 3.4** include MH^+ 201, 229, 401, 429 and 457.

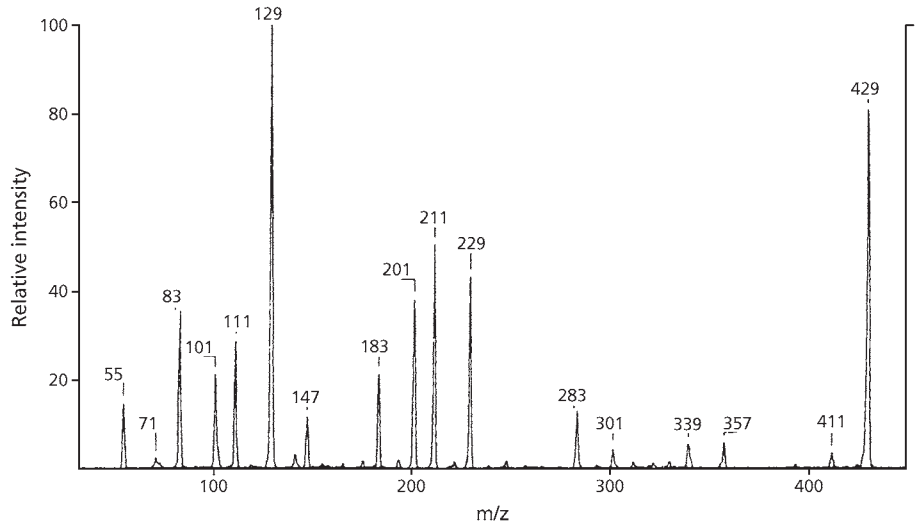

Figure 3.3 Product ion scan (CI-MS/MS) of MH^+ 429 from polyurethane. (*Reprinted with permission from R.P. Lattimer, Rubber Chemistry and Technology, 1995, **68**, 5, 783. ©1995, ACS Rubber Division [27]*)

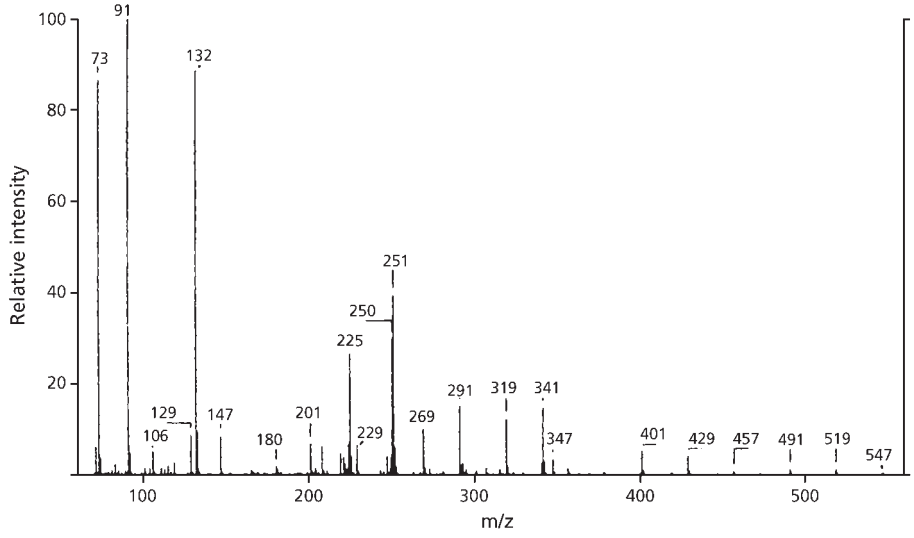

Figure 3.4 CI-MS survey scan of polyurethane (pyrolysis region, 200-300 °C). (*Reprinted with permission from R.P. Lattimer, Rubber Chemistry and Technology, 1995, **68**, 783. ©1995, ACS Rubber Division [27]*)

Several linear (dihydroxyl-terminated) polyester pyrolysates are also observed:

MW 290 HO-BDO-AA-BDO-H
MW 318 HO-BDO-AA-HDO-H
MW 346 HO-HDO-AA-HDO-H
MW 490 HO-BDO-AA-BDO-AA-BDO-H
MW 518 HO-BDO-AA-BDO-AA-HDO-H
MW 546 HO-BDO-AA-HDO-AA-HDO-H

Where:

BDO = 1,4 butanediol
AA = adipic acid
HDO = 1,6 hexanediol

In summary, the competitive thermoplastic PU was found to be composed of MDI, BDO chain extender, and a mixed AA/BDO/HDO polyester. The only volatile chemicals found were the stabiliser Stabaxol P and some residual cyclic ester oligomers.

3.1.2 Polyacrylamide

It is generally known that polyacrylamide (PAM) decomposes in three stages, corresponding to loss of water, ammonia, and tar and volatiles, as temperature increases. However, the chemistry involved in the degradation has not been well defined. Leung and co-workers [28] carried out a study of the thermal degradation behaviour of PAM and PAM-*co*-sodium polyacrylate copolymer (PAANA) characterised by thermal analysis techniques [thermogravimetric analysis (TGA) and differential scanning calorimetry (DSC)] and the chemical changes at various temperatures were followed by gas chromatography-mass spectrometry (GC-MS) and solid state carbon-13 cross polarisation/magic angle spinning nuclear magnetic resonance. They discuss degradation mechanisms based on the results obtained in this work.

The TGA weight loss curves of various samples are plotted in **Figure 3.5** to facilitate comparison. All curves show significant moisture loss as soon as heating is started. The evolution of moisture is essentially completed at about 200 °C. As the temperature increases further, decomposition of the polymers begins. The thermograms clearly show that there are two decomposition regions for poylacrylamide and sodium polyactylate and three for the copolymer-polyacrylamide-*co*-sodium polyarylamide (**Table 3.1**). The thermal degradation behaviour of polyacrylamide and sodium polyarylate is relatively simple. Polyarylamide starts to decompose at 220 °C. The colour of the sample turns yellow at the beginning. As the temperature increases the sample fuses together and expands. At 335 °C, the second decomposition region begins. The rate of weight loss in this region is much higher than that in the first region.

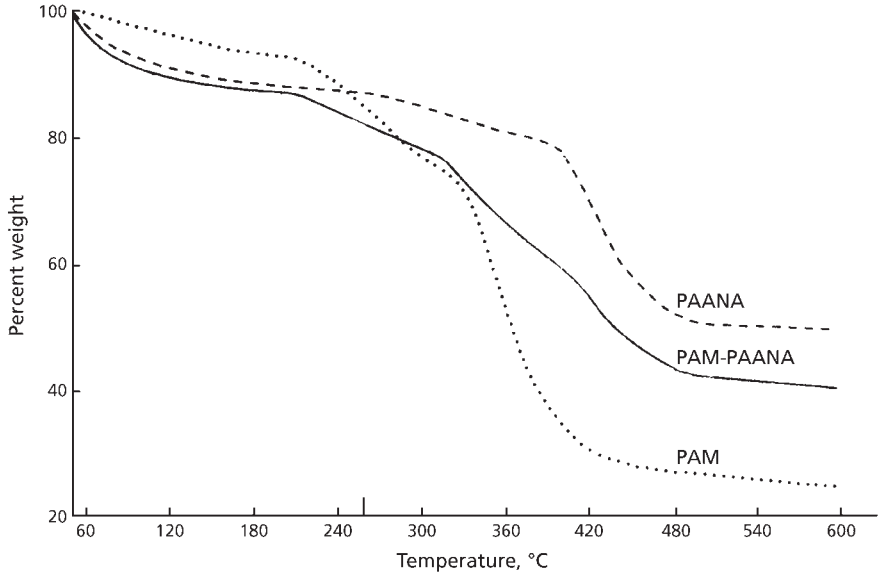

Figure 3.5 TG weight loss curves for PAM, PAANA, and PAM-PAANA. (*Reprinted from W.M. Leung, D.E. Axelson and J.D. Van Dyke, Journal of Polymer Science, Part A: Polymer Chemistry, 1987, **25**, 7, 1825. ©1987, John Wiley and Sons [28]*)

Table 3.1 Thermal Decomposition Behaviour of PAM, PAANA, and PAM-PAANA

Sample	Decomposition region	Temperature range (°C)	Percentage weight change	
			With moisture	Moisture free
PAM	I	220-335	21.3	23.2
	II	335-400	44.7	48.6
PAANA	I	260-400	9.2	10.5
	II	400-480	27.4	31.2
PAM-PAANA	I	220-320	10.4	11.9
	II	320-400	16.0	18.3
	III	400-480	19.3	22.0

*Reprinted from W.M. Leung, D.E. Axelson and J.D. Van Dyke, Journal of Polymer Science, Part A: Polymer Chemistry, 1987, **25**, 7, 1825. ©1987, John Wiley and Sons [28]*

The DTG curve in this region indicates that the decomposition rate reaches its maximum at about 370 °C. At about 500 °C the weight of the sample becomes constant, and a char-like material remains.

The first weight loss region is generally interpreted as the release of ammonia due to the imidisation reaction between the amide groups of the monomer units [29, 30]. The second weight loss region is attributed to the breakdown of the polymer backbone and the imides formed in the first decomposition region. Assuming that imidisation is the sole reaction and that the polymer becomes 100% imidised in the first decomposition region, the moles of ammonia released will be equal to one half of the moles of the repeating unit. The weight loss shown by the TGA studies, however, is approximately twice the calculated quantity. Thus, reactions other than imidisation must take place simultaneously in this region.

PAANA begins to degrade at a higher temperature (260 °C). As the temperature increases to about 400 °C, the second decomposition process occurs. It reaches the maximum decomposition rate at about 425 °C, as indicated by the DTG curve. At 500 °C a plateau is observed in the DTG curve, as *dw/dt* is zero. It is reasonable to assume that the first decomposition of PAANA is due to the decomposition of the carboxylate group, and the second decomposition region is due to the degradation of the backbone of the polymer.

The behaviour of the copolymer is a hybrid of the parent homopolymers. The decomposition occurs in three regions, the first being at 220 °C (decomposition of amide groups), the second at 320-400 °C (decomposition of carboxylate groups) and the third at 400-480 °C (decomposition of polymer backbone). Gas evolution studies of polyacrylamide, sodium polyacrylate and polyarylamide-*co*-sodium polyacrylate were generally conducted at single temperatures lying within each of the distinct decomposition regions determined from DSC and TGA analyses. The temperatures at which the polymers were decomposed are given in **Table 3.2** along with suggested decomposition products from mass spectral analysis. Typical mass spectra for each polymer and decomposition region are shown in **Figure 3.6**.

Ammonia gas (*m/e* 17) is evolved in the first decomposition temperature range for polyacrylamide (represented by the 300 °C mass spectrum in **Figure 3.6.** Other peaks corresponding to *m/e* 18, 28, 32, 40, 42, 44, 54 and 58 indicate the possibility that H_2O, CO, N_2, CO_2, $CONH_2$ and other species may be released at this temperature. The evolution of NH_3 supports the theory that imidisation between neighbouring amide groups in polyacrylamide constitutes one of the major decomposition reactions in this region.

In the second decomposition region for PAM, represented by the 387 °C mass spectrum in **Figure 3.6**, carbon dioxide gas is released. It is suggested that this

Table 3.2 Gas Evolution Studies and Microanalysis Data on Residues						
Polymer	**Decomposition range**	**Decomposition temperature (°C)**	**Gases released**	**Microanalysis data on residues**		
				%C	**%H**	**%N**
PAM	I	271	H_2O, NH_3, N_2, CO, CO_2 and others	52.37	5.33	12.99
	I	300	Same as above	54.09	5.02	13.38
	II	387	CO_2	55.11	3.82	12.05
PAANA	I	351	CO_2	41.28	4.37	Nil
PAM-PAANA	I	271	H_2O, NH_3, CO, N_2, CO_2 and others	39.99	4.17	7.40
	I	300	Same as above	39.22	3.72	6.81
	II	340	CO_2	40.32	6.30	4.16
	III	450	CO_2	17.30	1.21	2.79
*Reprinted from W.M. Leung, D.E. Axelson and J.D. Van Dyke, Journal of Polymer Science, Part A: Polymer Chemistry, 1987, **25**, 7, 1825. ©1987, John Wiley and Sons [28]*						

results from the breakdown of imide units to form nitrile units. Any remaining amide groups may release $CONH_2$ (*m/e* 44) or CO (*m/e* 28) and NH_2 (*m/e* 16) units, which appear in minor amounts.

Direct evidence for the presence of nitrile groups in the residue of a PAM sample heated to 250 °C and held for 1.5 hours is obtained by FT-IR, which shows the characteristic C≡N absorption at 2239 cm^{-1}. The spectrum also shows the presence of isocyanide groups (2168 cm^{-1}) as well as either inorganic cyanide or diazo (2052 cm^{-1}). In addition one can see evidence of amide groups (3340, 3211, 1686, and 1620 cm^{-1}) and imide groups (C=O absorption above 1700 cm^{-1}).

In the PAM-PAANA copolymer (**Figure 3.7**) ammonia is also released in the first decomposition region (271 °C), indicating that imidisation is one of the decomposition

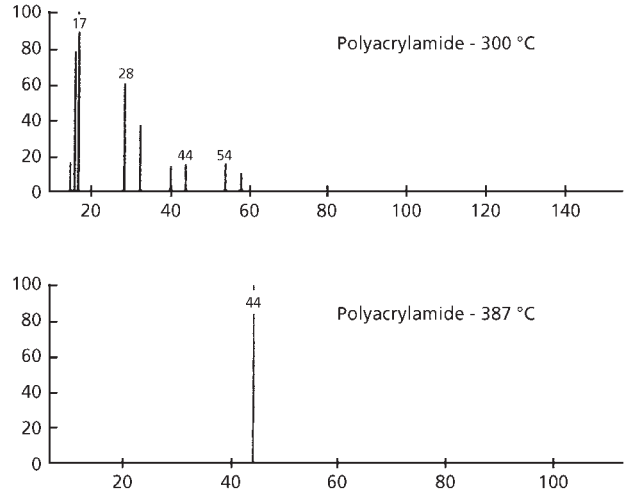

Figure 3.6 Mass spectral data for the decomposition of PAM at two different temperatures. (*Reprinted from W.M. Leung, D.E. Axelson and J.D. Van Dyke, Journal of Polymer Science, Part A: Polymer Chemistry, 1987, **25**, 7, 1825. ©1987, John Wiley and Sons [28]*)

mechanisms in this polymer as well. The amount of ammonia released is reduced in comparison to PAM since there are fewer amide groups to begin with, and imidisation can only occur between neighbouring amide groups. The large peak at *m/e* 44 in **Figure 3.7** may result from the breakdown of imide groups to form nitrile groups with a release of carbon dioxide. It may also result from the decomposition of acrylate with the release of carbon dioxide or decomposition of amide with the release of $CONH_2$. A significant peak at *m/e* 18 indicates a loss of water from isolated amide units to form nitrile groups.

In the second decomposition region for PAM-PAANA (340 °C, **Figure 3.7**), carbon dioxide is released as a result of further breakdown of imide units. Acrylate groups also will begin to decarboxylate as in PAANA, which also releases carbon dioxide at this temperature (**Figure 3.8**).

The third decomposition region (450 °C, **Figure 3.7**) is rather high in temperature and represents the final breakdown of the polymer. Significant charring is observed in the residue, and the gas released is primarily carbon dioxide. Decarboxylation of the acrylate carboxyl groups is completed in this region. The microanalytical data show a high carbon/hydrogen ratio in the residues, as expected when charring takes place. The low overall carbon and hydrogen contents in the residues of the copolymer

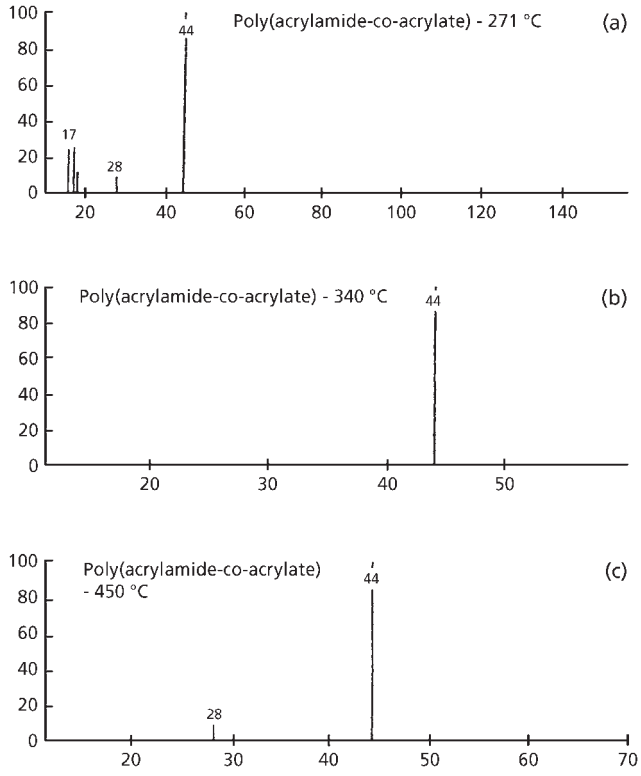

Figure 3.7 Mass spectral data for the decomposition of PAM-PAANA at various temperatures. (*Reprinted from W.M. Leung, D.E. Axelson and J.D. Van Dyke, Journal of Polymer Science, Part A: Polymer Chemistry, 1987,* ***25****, 7, 1825. ©1987, John Wiley and Sons [28]*)

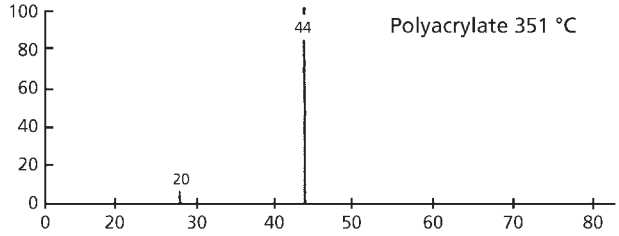

Figure 3.8 Mass spectral data for PAM-PAANA at 340°C. (*Reprinted from W.M. Leung, D.E. Axelson and J.D. Van Dyke, Journal of Polymer Science, Part A: Polymer Chemistry, 1987,* ***25****, 7, 1825. ©1987, John Wiley and Sons [28]*)

suggest significant quantities of inorganic salts, as expected under these conditions. The low nitrogen content in the residue suggests that the nitrile groups formed in the second region have been decomposed. The small peak at *m/e* 28 (possible N_2) may be due to this reaction.

Figure 3.9 illustrates the mass spectral data for a sample of polyacrylamide heated at increasing temperature up to 280 °C in the heating probe of the GC-MS instrument. A high degree of detail can be seen in all of the mass spectral traces in this experiment, including volatile and less volatile decomposition products due to the close proximity of the heated sample to the ionisation chamber of the mass spectrometer. At 115.6 °C the appearance of peaks corresponding to water (*m/e* 18) and acrylamide (*m/e* 71) are evident, along with several larger peaks ranging between them. At this temperature

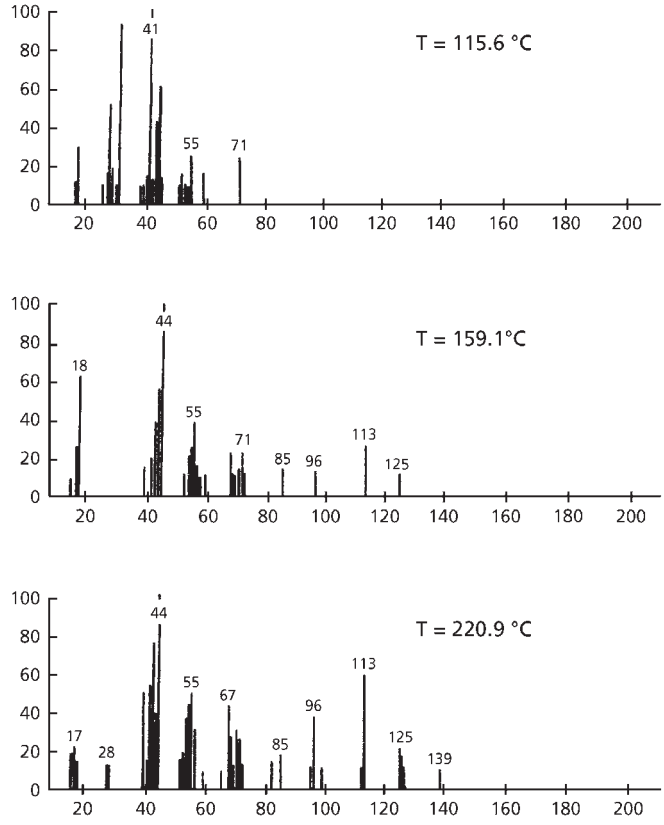

Figure 3.9 Mass spectral data as a function of temperature for PAM. (*Reprinted from W.M. Leung, D.E. Axelson and J.D. Van Dyke, Journal of Polymer Science, Part A: Polymer Chemistry, 1987,* ***25****, 7, 1825. ©1987, John Wiley and Sons [28]*)

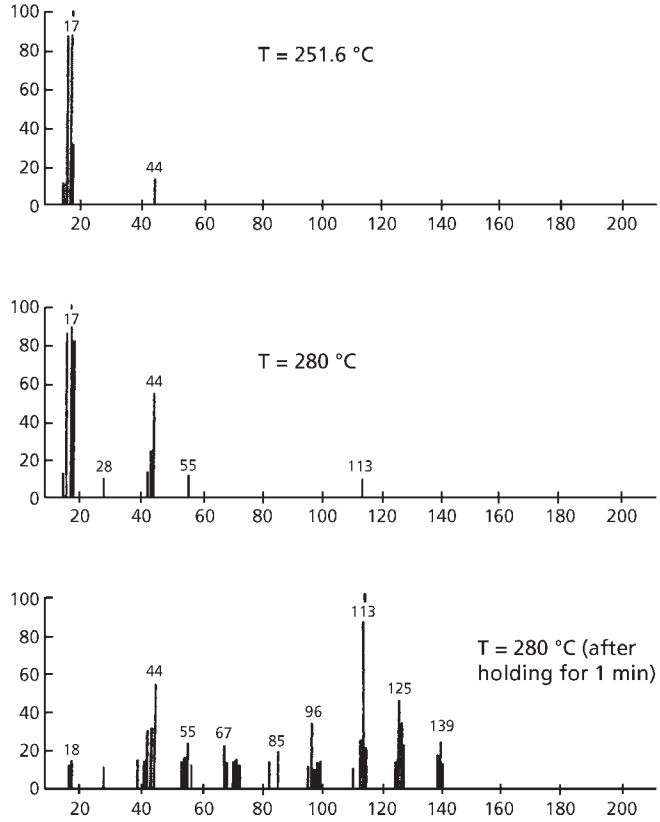

Figure 3.9 *Continued*

some unzipping of the polymer may be occurring, with subsequent breakdown of the monomer units. At 159.1 °C the water and acrylamide peaks are still evident, but a significant peak corresponding to carbon dioxide or $CONH_2$ (*m/e* 44) appears. Evidence is also seen for unzipping of larger units. Although decomposition appears significant, the overall loss in mass at this point is small as seen by TGA.

At 220.9 °C the temperature has reached the onset of endothermic decomposition as determined by TGA. Here the first evidence of ammonia in the evolved gases is seen. At a higher temperature in this region (251.5 °C), the gas released becomes almost exclusively ammonia. A peak for water (*m/e* 18) can also be seen, corresponding to dehydration of amide groups to form nitrile. At 280 °C the ammonia and water peaks are dominant, but carbon dioxide formation becomes significant, resulting from the breakdown of imide groups to form nitrile. Finally, as the temperature is held at 280 °C, the imidisation and dehydration reactions become complete, as noted

by the reduction in ammonia and water release, but carbon dioxide continues to be released as imide groups are broken down. Also significant is the release of units at *m/e* 113, 125, and 139, corresponding to units of:

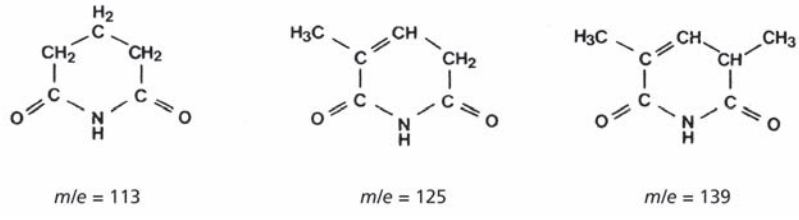

which are obtained by breakdown of imide groups in the polymer.

As a result of this very detailed study, Leung and co-workers [28] were able to elucidate the various decomposition pathways and their relative importance. **Table 3.3** and **Figure 3.10** illustrate these pathways.

Table 3.3 Summary of the Degradation Reactions for PAM and PAM-PAANA at Different Temperature Ranges

	Temperature Range (°C)	Reactions
I PAM	220-335	Major reactions: imidisation followed by nitrile formation; minor reaction: dehydration; formation of imide, nitrile, C=C, and imine.
	> 335	Major reactions: breakdown of imide and amide groups, breakdown of polymer backbone; formation of nitriles, long chain hydrocarbon $-(CH_2)-_n$, n>4.
II PAM:PAANA	220-320	Major reactions: imidisation and dehydration of amide groups; formation of imide, nitrile, isocyanide, aliphatic chains, and carboxyl carbonyl and amide carbonyl group still exists.
	320-400	Major reactions: decarboxylation of acrylate, breakdown of imide and amide groups; formation of longer aliphatic chain, amide carbonyl disappeared, carboxyl carbonyls still exist.
	> 400	Major reactions: final decarboxylation of acrylate, breakdown of polymer backbone; formation of paraffinic-type materials.

*Reprinted from W.M. Leung, D.E. Axelson and J.D. Van Dyke, Journal of Polymer Science, Part A: Polymer Chemistry, 1987, **25**, 7, 1825. ©1987, John Wiley and Sons [28]*

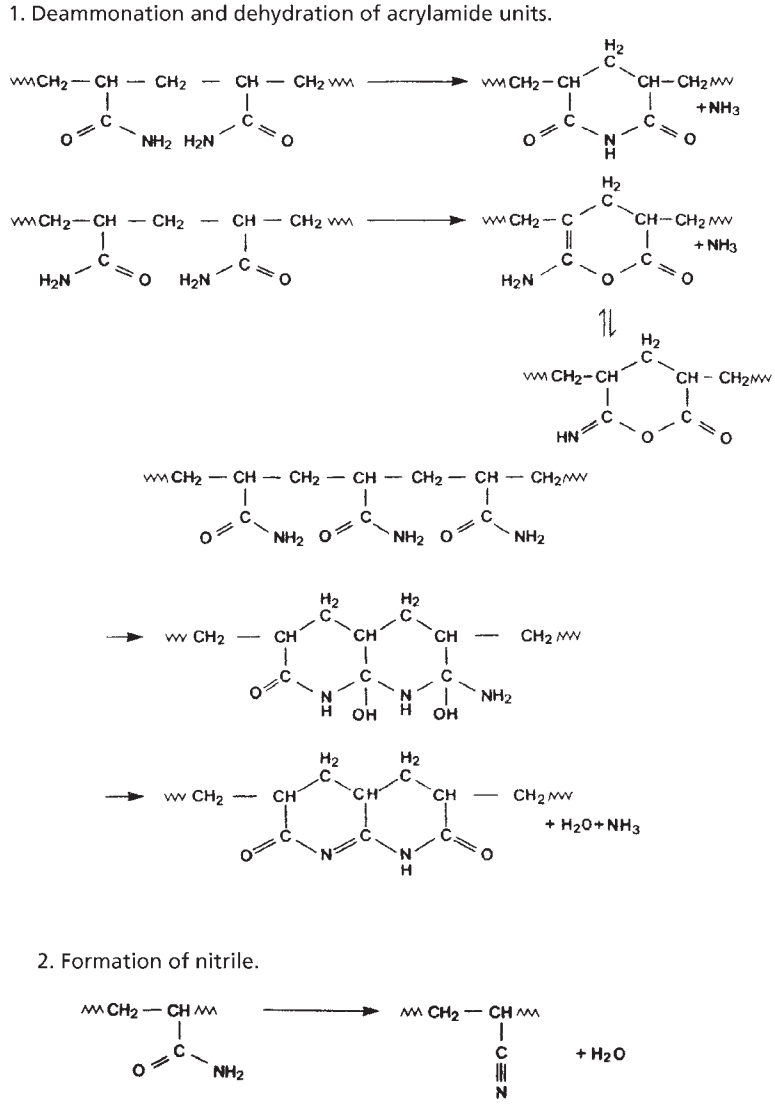

Figure 3.10 Reaction mechanisms in the thermal degradation of PAM and PAM-PAANA. (*Reprinted from W.M. Leung, D.E. Axelson and J.D. Van Dyke, Journal of Polymer Science, Part A: Polymer Chemistry, 1987,* ***25****, 7, 1825. ©1987, John Wiley and Sons [28]*)

3. Formation of saturated and unsaturated aliphetic compounds.

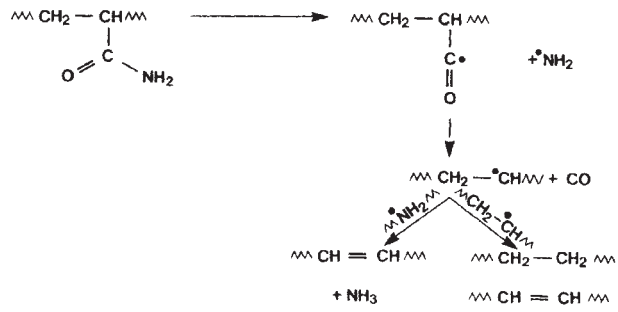

4. Breakdown of imide.

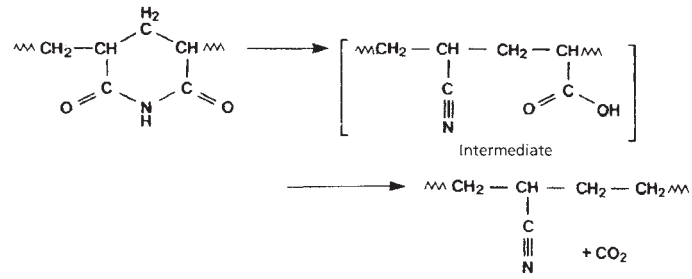

Figure 3.10 *Continued*

3.1.3 Miscellaneous Polymers

Kase and co-workers [31] investigated an isocyanate prepolymer composition using high-performance liquid chromatography and field desorption MS.

Sandra and co-workers [32] present an overview of the use of MS as a detection system for liquid chromatography. Enjalbal and co-workers [33] characterised soluble polymer-supported organic compounds by liquid chromatography/electroscopy ionisation mass spectrometry.

In the mass spectra of products of the nickel chloride-catalysed Py-GC of cellulose, compounds from benzofuran (peak 1) to trimethylxanthone (peak 33) were identified.

Qian and co-workers [34] used in source direct Py-MS to identify 150 different polymers and copolymers. Library searching facilities were included to enable positive polymer identifications to be carried out.

Table 3.4 Characterisation of polymers by pyrolysis-mass spectrometry					
Polymer	**Pyrolysis procedure**	**Pyrolysis temperature (°C)**	**Pyrolysis products**	**Comments**	**Ref.**
Natural rubber, butadiene styrene rubber, styrene-isoprene-styrene elastomers	-	30-450	-	Structure elucidation by study of variation of ion ratio as a function of temperature	[37]
Epoxy resins of diglycidyl ether of bisphenol A and of the tetraglycidyl ether of tetrakis(hydroxyphenyl)ethane	Direct Py-MS	-	Molecular ions with up to 3 bisphenol A units	Field ionisation MS	[38]
Triacrloyloxyethyl phosphate, diacryloyl-oxyethyl phosphate	Direct Py-MS	-	Pyrolysis of acrylate side chains	Characteristic decomposition regions	[39]
Polyethylene oxalate	-	-	Cyclic oligomers	Study of primary thermal decomposition mechanism	[40]
Aromatic and aliphatic polyhydrazides and polyoxamides	Chemical ionisation and electron impact MS	-	-	Study of thermal decomposition process of polymers containing –CO-, -NR-NR-, linkages strongly influenced by structural features	[41]
Polystyrene disulfide	Direct pyrolysis and flash pyrolysis MS	-	Styrene, cyclic styrene sulfides, diphenylthiophen	-	[42]

4-aliphatic polysulfides	-		Cyclic sulfides or disulfides	A back-biting process starting at SH ends	[43]
Acrylic copolymers with long aromatic chains	Temperature resolved pyrolysis, field ionisation MS	-	Phenol, olefins	*Cis* elimination of acrylic ester bonds	[44]
Poly(tetrafluoroethylene), PMMA, rubber hydrochloride, polyepichlorohydrin fluorinated ethylene-propylene copolymer, polyvinyl fluoride, polyvinylidene fluoride styrene butadiene copolymer	Temperature programmed, pyrolysis MS	-	-	-	[45]
Polyurethane	Pyrolysis tandem MS	-	Methylene diisocyanate, 1,4-butane diol, 1,4-cyclohexane dimethanol, low molecular weight oligomers of hydroxyl terminated tetramethylene glycol adipate	Cleavage of urethane link via NH transfer resulting in these products	[36]
Source: Author's own files					

In this procedure the unknown polymer was pyrolysed within the ion source of a mass spectrometer by a coiled filament designed for desorption chemical ionisation/ desorption electron ionisation applications. Pyrolysis products ionised by 70 eV electron impact yielded highly reproducible mass spectra which were characteristic of the polymer.

Mattern and co-workers [35] carried out laser mass spectrometry on polytetrafluoroethylenes. They found that a fragmentation mechanism common to each fluoropolymer yields structurally relevant ions indicative of the orientation of monomer units within the polymer chain. A unique set of structural fragments distinguished the positive ion spectra of each homopolymer, allowing identification.

Various other applications of Py-MS to the characterisation of polymers are reviewed in **Table 3.4**.

References

1. W.W. Shackleford and J.M. McGuire, *Spectroscopy*, 1986, **10**, 17.

2. P.E. Kelly, *Ion Trap Detector Literature Reference List*, Finnegan MAT, IDT Publication No.21.

3. P.E. Kelly, *New Advances in the Operation of the Ion Trap Mass Spectrometer*, Finnegan MAT, IDT Publication No.10.

4. C. Campbell, *Ion Trap Detector Gas Chromatography Technology*, Finnegan MAT, IDT Publication No.15.

5. G.C. Stafford, *Recent Improvements in Analytical Applications of Advanced Trap Technology*, Finnegan MAT IDT Publication No.16

6. G.C. Stafford, *Advanced Ion Trap Technology in an Economical Detector for GC*, Finnegan MAT IDT Publication No.20.

7. G.C. Stafford, *The Finnegan MAT Ion Trap Mass Spectrometer (ITMS) – New Developments with Ion Technology*, Finnegan MAT IDT Publication No.24.

8. B.F. Rordorf, *An Automated Flow Tube Kinetics Instrument with Integrated GC – ITD Analysis*, Finnegan MAT IDT Publication No.13.

9. J.E.P. Syka, *Positive Ion Chemical lonization with an Ion Trap Mass Spectrometer,* Finnegan MAT IDT Publication No.19.

10. R.A. Yost, N. McClennan and H.L.C. Menzzelaan, *Enhanced Full Scale Sensitivity and Dynamic Range in Finnigan MAT Ion Trap Detector with New Automatic Gain Control Software,* Finnegan MAT IDT Publication No.22.

11. C. Camp, *Ion Trap Advancements, Higher Sensitivity and Greater Dynamic Range with Automatic Gain Control Software,* Finnegan MAT IDT Publication No. 23.

12. J.M. Richards and M.C. Bradford, *Development of a Cure Point Pyrolyser Inlet for the Finnigan MAT Ion-Trap Detector,* Finnegan MAT IDT Publication No.25.

13. P. Bishop, *The Ion-Trap Detector, Universal and Specific Detection in One Detector,* Finnegan MAT IDT Publication No.28.

14. P. Bishop, *The Use of an IDT 50 GLC Ion-Trap Detector Combination,* Finnegan MAT IDT Publication No.36.

15. P. Bishop, *Low Cost Mass Spectrometer for* GC, Finnegan MAT IDT Publication No.42.

16. C. Campbell and S. Evans, *The Ion-Trap Detector - The Techniques and its Application,* Finnegan MAT IDT Publication No.29.

17. E. Olsen, *Serially Interfaced Gas Chromatography Fourier Transform Infrared Spectrometer Ion-Trap Mass Spectrometer,* Finnegan MAT IDT Publication No.35.

18. J. Allison, *The Hows and Whys of Ion Trapping,* Finnegan MAT IDT Publication No.41.

19. J. Todd, C. Mylchreest, T. Berry and D. Graves, *Supercritical Chromatography Mass Spectroscopy with an Ion-Trap Detector,* Finnegan MAT IDT Publication No.46.

20. J.W. Eichelberger and W.L. Budd, *Studies in Mass Spectroscopy with an Ion-Trap Detector*, Finnegan MAT IDT Publication No.47.

21. J.W Eichelberger and L.E. Slivan, *Existence of Self-Chemical lonization in the Ion-Trap Detector*, Finnegan MAT IDT Publication No.48.

22. E. Genin, *Le Detecteur a Plegeage D'jous de Chromatographic en Phase Gazeuse Technologic et Applications,* Finnegan MAT IDT Publication No.53.

23. M. Le Leir, *The Use of the IDT - a Low Cost GC/MS System for the Identification of Trace Compounds,* Finnegan MAT IDT Publication No.51.

24. J.M. Richards, W.H. McClennan, J.A. Burger and H.H.C. Menza, *Pyrolysis-Short Column GC/MS Using the IDT and ITMS*, Finnegan MAT IDT Publication No.56.

25. J.C. Hughes, B.B. Wheals and M.J. Whitehouse, *Analyst*, 1977, **102**, 1211, 143.

26. H.L.C. Meuzelaar, M.A. Posthumus, P.G. Kistemaker and J. Kistemaker, *Analytical Chemistry*, 1973, **45**, 8, 1546.

27. R.P. Lattimer, *Rubber Chemistry and Technology*, 1995, **68**, 5, 783.

28. W.M. Leung, D.E. Axelson and J.D. Van Dyke, *Journal of Polymer Science, Part A: Polymer Chemistry*, 1987, **25**, 7, 1825.

29. J. Zurakowska-Orszagh, W. Buse and K. Soerjosoeharto, *Bulletin de l'Academie, Polonaise des Science, Serie des Science Chimiques*, 1977, **11**, 845.

30. H.D. Burrows, H.A. Ellis and S.I. Utah, *Polymer*, 1981, **22**, 12, 1740.

31. M. Kase, K. Kurihara and Y. Tachikawa, *Kobunshi Ronbunshu*, 1999, **56**, 1, 8.

32. P. Sandra, G. Vanhoenacker, F. Lynen, L. Li and M. Schelfaut, *LCGC Europe*, 2001, **14**, 81.

33. C. Enjalbal, F. Lamaty, P. Sanchez, E. Suberchicot, P. Ribière, S. Varray, R. Lazaro, N. Yadav-Bhatnagar, J. Martinez and J-L. Aubagnac, *Analytical Chemistry*, 2003, **75**, 2, 175.

34. K. Qian, W.E. Killinger, M. Casey and G.R. Nicol, *Analytical Chemistry*, 1996, **68**, 6, 1019.

35. D.E. Mattern, F.T. Lin and D.M. Hercules, *Analytical Chemistry*, 1984, **56**, 14, 2762.

36. R.P. Lattimer, H. Muenster and H. Budzikiewicz, *Journal of Analytical Applied Pyrolysis*, 1990, **17**, 3, 237.

37. M. Erdogan, T. Yalçin, T. Tinçer and S. Süzer, *European Polymer Journal*, 1991, **27**, 4-5, 413.

38. B. Plage and H-R. Schulten, *Macromolecules*, 1988, **21**, 7, 2018.

39. H. Liang and W. Shi, *Polymer Degradation and Stability*, 2004, **84**, 3, 525.

40. A. Ballistreri, D. Garozzo, M. Giuffrida, G. Impallomeni and G. Montaudo, *Polymer Degradation and Stability*, 1988, **21**, 4, 311.

41. A. Ballistreri, D. Garozzo, G. Montaudo, A. Pollicino and M. Giuffrida, *Polymer*, 1987, **28**, 1, 139.

42. G. Montaudo, C. Puglisi, M. Blazò, K. Kishore and K. Ganesh, *Journal of Analytical Applied Pyrolysis*, 1994, **29**, 2, 207.

43. G. Montaudo, E. Scamporrino, C. Puglisi and D. Vitalini, *Polymer*, 1987, **28**, 3, 477.

44. B. Plage and H-R. Schulten, *Journal of Analytical Applied Pyrolysis*, 1991, **19**, 283.

45. W.A. Westall and A.J. Pidduck, *Journal of Analytical Applied Pyrolysis*, 1987, **11**, 3.

4 Complementary Pyrolysis Gas Chromatography-Mass Spectrometry

The incorporation of a gas chromatography (GC) stage between pyrolysis (Py) and mass spectrometry (MS) has the obvious advantage of refining the detail that can be achieved in structural analysis and rendering MS identification of pyrolysis products more certain. The application of Py-GC-MS to the identification of complex mixtures of volatile compounds produced under high temperature conditions has been reviewed by Chang and Tackett [1].

4.1 Homopolymers

4.1.1 Polyacrylates

4.1.1.1 Polypropylacrylate and Polybutylacrylate

Polyisopropyl acrylate degradation has been examined by Grassie and Speakman [2] using a bulk technique with low temperature heating at 265 °C. The major products were reported to be carbon dioxide and propylene with small amounts of carbon monoxide and isopropylene. It was reported that no chain fragment fraction as experienced with other primary esters were produced.

The branched chain polytertiary butyl acrylate has been considered by several workers [3-5] at low temperatures. Schaefgen and Sarasohn [3] have studied this degradation at several low temperatures. At 160 °C isobutylene was lost quantitatively while above 180 °C approximately half of the weight of the polymer was lost after 12 hours of heating with the gaseous products being 36% isobutylene, 11% water, and 3% carbon dioxide. Elemental analysis of the pyrolysis residue corresponded approximately to polyacrylic anhydride ($C_6H_6O_3$).

Grant and Grassie [4] and Grassie and Weir [5] have discussed the degradation of polytertiary butyl acrylate in terms of the work of Schaefgen and Sarasohn [3] and all observed autocatalytic behaviour in the elimination of olefin from the polymeric ester.

This work shows, contrary to earlier research conducted at low temperatures, that substantial yields of liquid products are obtained on the high temperature degradation of the isomeric polypropylacrylates and polybutylacrylates. The products of the degradation reactions are identified and a comparison is possible with the results of studies of the polymers of the normal esters, i.e., methyl to butyl, the branched chain propyl, and the three branched butyl esters, all of the polymers having been examined under the same conditions.

A mechanism involving random homolytic scission of the chain followed by a series of inter and intramolecular transfer reactions has previously been shown to be applicable to the simple *n*-alkyl polyacrylates and is suggested to be generally applicable to the lower branched chain esters.

Table 4.1 Degradation Products and Yields of Poly-*n*-Propyl Acrylate and Polyisopropyl Acrylate

n-Propyl acrylate	Retention time (min)	Relative abundance (%)	Reference
Propane	0.8	4.25	
n-Propanol	1.4	7.09	[8]
n-Propyl acrylate	3.3	17.08	
n-Propyl methacrylate	4.6	1.00	
Saturated dimer	14.8	26.1	
Saturated dimer	15.2	5.10	
Unsaturated dimer	15.5	34.04	
Unsaturated dimer	16.1	5.27	
Isopropylene	0.8	16.05	[2]
Isopropanol	1.1	5.56	[2]
Isopropyl acrylate	2.7	6.03	
Saturated dimer	12.5	8.44	
Unsaturated dimer	13.1	25.24	
Saturated trimer	17.5	38.67	
Unsaturated trimer			

*Reprinted with permission from J. K. Haken and L. Tan, Journal of Polymer Science: Polymer Chemistry Edition, 1987, **25**, 5, 1451. ©1987, Wiley Interscience [7]*

While the degradation of the lower *n*-alkyl polyacrylates by a Py-GC-MS technique [6] has been studied it was not until the work of Haken and Tan [7] that the Curie point pyrolysis at 80 °C of isomeric polypropylacrylates and polybutylacrylates were investigated.

From **Table 4.1** it is apparent that the same pattern of products occur with degradation of the polymer of isopropyl as with that of the primary *n*-propyl ester, the saturated and unsaturated dimers being observed together with a higher molecular weight product indicated to be a mixture of saturated and unsaturated trimers.

While Grassie and co-workers [8] identified propylene as a low temperature degradation product of poly(*n*-propyl acrylate) it was not found with the higher temperatures but *n*-propane was identified. The formation may be explained as a simple dealkulation of the ester as shown in Equation (4.1):

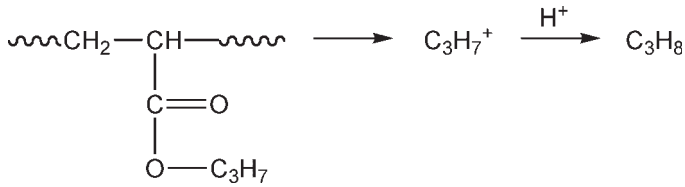

With poly-*n*-propyl acrylate a greater amount of monomer was produced than with the polyisopropyl ester and as expected from the mechanism proposed the proportion of propane was much lower with the polymeric normal ester compared with amounts of polypropylene (PP) from the polymeric isoester.

The predominant products resulting from degradation of the polyisopropyl acrylate were considered to be a mixture of saturated and unsaturated trimer as prominent appropriate peaks indicative of ion fragments were found and were directly comparable with similar fragments of other esters studied.

Tables 4.2 and 4.3 show the degradation products of the polymeric isomeric butyl esters. It is apparent with the products of poly-*n*-butylacrylate that the identification of *n*-butyl formate, *n*-butyl acetate, the saturated and unsaturated dimers extends the earlier reports of Grassie and co-workers [8]. The formation of *n*-butyl acetate is consistent with that of methyl acetate formation and is simple scission at the chain end and hydrogen addition.

With polyisobutyl acrylate the formation of isobutylene monomer and oligomers occurs.

The reaction mechanism for isobutylene formation is derived from the general mechanism of Grassie and co-workers [8]. Polyisobutyl acrylate degradation produces more simple saturated esters than the other homologous polymeric esters.

Table 4.2 Degradation Products of Isomeric Polybutylacrylates			
Poly-*n*-butyl acrylate)	**Polyisobutyl acrylate**	**Poly-*sec*-butyl acrylate**	**Poly-*tert*-butyl acrylate**
Carbon dioxide			Carbon dioxide
1-Butene	Isobutylene Acrylic acid	Isobutylene	Isobutylene
n-Butyl formate		*Sec*- butanol	
n-Butyl acetate	Isobutyl acetate α-Methyl-isobutyl propionate		
n-Butyl acrylate	Isobutyl acrylate	*Sec*-butyl acrylate	*Tert*-butyl acrylate
n-Butyl methacrylate	Isobutyl methacrylate Isobutyl ethacrylate α, α-Dimethyl-isobutyl propionate		
Saturated dimer	Saturated dimer	Saturated dimer	Saturated dimer
Unsaturated dimer	Unsaturated dimer		
Saturated trimer	Unsaturated dimer	Unsaturated dimer	
*Reprinted with permission from J. K. Haken and L. Tan, Journal of Polymer Science: Polymer Chemistry Edition, 1987, **25**, 5, 1451. ©1987, Wiley Interscience [7]*			

Table 4.3 Pyrolysis Yields of Polybutylacrylates			
Product name	**Retention time (min)**	**Relative abundance**	**Reference**
Poly(*n*-butyl acrylate)			
Carbon dioxide	0.4	4.63	[11]
1-Butene	1.1	10.64	[11]
n-Butyl formate	2.1	2.90	
n-Butanol	2.8	18.97	[11]
n-Butyl acetate	4.1	3.92	

Table 4.3 *Continued*			
n-Butyl acrylate	5.1	35.85	[11]
n-Butyl methacrylate	5.7	0.98	[11]
Saturated dimer	15.3	6.89	
Unsaturated dimer	15.8	15.20	
Poly(isobutyl acrylate)			
Isobutylene	0.7	1.09	
Acrylic acid	1.6	1.27	
Isobutyl acetate	3.4	1.50	
Isobutyl acrylate	4.2	37.88	
Isobutyl methacrylate	4.9	0.62	
α-Methyl isobutyl propionate	5.1	0.52	
Isobutyl ethacrylate	6.3	0.78	
α,α-Dimethyl isobutyl propionate	9.9	7.78	
Saturated dimer	14.3	18.79	
Unsaturated dimer	14.9	23.34	
Saturated trimer	17.9	6.25	
Poly(*sec*-butyl acrylate)			
Isobutylene	0.8	44.25	
Sec-butanol	1.6	2.69	
Sec-butyl acrylate	3.8	15.35	
Saturated dimer	12.6	11.59	
Unsaturated dimer	13.2	26.11	
Poly(tert-butyl acrylate)			
Carbon dioxide	1.0	4.50	
Isobutylene	2.3	5.02	[4]
Tert-butyl acrylate	5.2	7.74	
Saturated dimer	16.7	19.23	
Unsaturated dimer	17.3	17.16	
Mixed trimers	25.0	46.33	
*Reprinted with permission from J. K. Haken and L. Tan, Journal of Polymer Science: Polymer Chemistry Edition, 1987, **25**, 5, 1451. ©1987, Wiley Interscience [7]*			

The degradation products of poly-*tertiary*-butyl acrylate are shown in **Table 4.2** and the formation of carbon dioxide, monomer and dimers are consistent with the mechanisms for poly-*n*-butyl acrylate. Isobutylene formation is in agreement with that from the work of Schaefghen and Sarasohn [3], while the presence of carbon dioxide, monomer, and dimers extends their work.

In common with the polymers of the normal alkyl esters and of the isomeric propyl esters steric factors reduce the intramolecular transfer reactions and the yields of monomer and low molecular weight products increase as the alkyl chain length is increased.

4.1.2 Chlorinated Polyethylene

Chlorinated polyethylene (CPE) is a polyethylene that has random chlorine substitution. It has toughness and barrier properties, as well as ignition resistance. Depending on the degree of chlorination, CPE polymers can have elastomeric and thermoplastic forms which have extraordinary compatibility with a range of other materials. This makes CPE readily adaptable to common compounding and curing techniques. CPE polymers can produce end products that are hard and tough or soft and flexible. Most commercial CPE products contain 25-50 wt% chlorine.

CPE is an ignition-resistant polyethylene. It is also used in blends to change the ignition characteristics of other polymers. CPE has no unsaturation in the polymer backbone, giving it excellent ozone and weathering properties. The saturated backbone also results in a temperature stability that allows CPE to perform well continuously at temperatures of 150 °C. CPE can provide satisfactory resistance to most acids, bases, oils, and alcohols.

The chlorination reaction of polyethylene can be expressed as:

where one molecule of chlorine reacts with polyethylene to yield one molecule of hydrogen chloride and one atom of chlorine substituted into the polymer. This chlorination can be achieved by solution (solvent), aqueous suspension, or fluidised bed processes. The distribution of chlorine atoms in the CPE polymer chain and the properties of CPE are greatly affected by the morphology of the polyethylene used and the accessibility of the polyethylene chain to the chlorination. To better control the chlorination processes, understand the chlorine atom distribution, and develop

improved structure/property relationships, it is necessary to have an analytical method that is capable of a quantitative determination of the composition and microstructure in the CPE.

The distribution of chlorine atoms in CPE has been studied by infrared spectroscopy (IR) [9-11]. The CH_2 bending bands in the 1400 to 1475 cm^{-1} range were used to determine the proportion of methylene groups centred in -$CH_2CH_2CH_2$-, -CH_2CH_2CHCl-, and -$CHClCH_2CHC1$- triads [11]. The chlorine atom distribution in CPE has also been intensively investigated by nuclear magnetic resonance spectroscopy (NMR) [12-20].

Various workers [21-28] have applied Py-GC-MS to structural studies on CPE. Wang and Smith [29] used Py-GC and Py-GC-MS to establish the microstructure of four CPE containing between 25%, 36%, 42% and 48% of chlorine.

Pyrolysis products such as benzene, toluene, styrene, and naphthalene were observed. The amount of these aromatic compounds formed directly reflects the concentration of chlorine atoms and their distribution in the CPE. The composition and structure calculations were based on those degraded trimer peak intensities obtained by Py-GC. This Py-GC method can be used to quantitatively determine the chlorine content in CPE. The same method can also explore the microstructure through number-average sequence length (NASL) of ethylene and vinyl chloride monomers. Other structure-related terms, such as the percentage of grouped vinyl chloride monomers, i.e., the percentage of chlorine atoms structured as polyvinyl chloride (PVC)-like structures, can also be calculated.

Figure 4.1 shows the pyrograms of all four CPE samples. The characteristic components of pyrolysed CPE are benzene, toluene, styrene, naphthalene [27, 28] and a series of aliphatic hydrocarbons (sets of dialkenes, alkenes, and alkanes). The aromatic hydrocarbons are the result of chain scission followed by dehydrochlorination of the chlorinated part of the polymer chain. They are also the major pyrolysis products of PVC [28]. The aliphatic hydrocarbons result from the pyrolysis of the polyethylene (PE) portion of the polymer chain. If a CPE pyrogram is displayed together with those of PE and PVC, as in **Figure 4.2**, it is clear that the CPE pyrogram is almost a combination of the PE and PVC pyrograms. The relative intensities of aromatic hydrocarbon peaks and aliphatic hydrocarbon peaks in the CPE pyrogram depend on the degree of chlorination and the distribution of chlorine atoms.

One way to conceive of the distribution of chlorine atoms in the polymer is to view it as the combination of monomers of ethylene, vinyl chloride, 1,2-dichloroethylene, 1,1-dichloethylene, 1,1,2-trichloroethylene, and tetrachlorethylene. When the CPE contains no more than 50 wt% chlorine, the polymer can considered as a copolymer

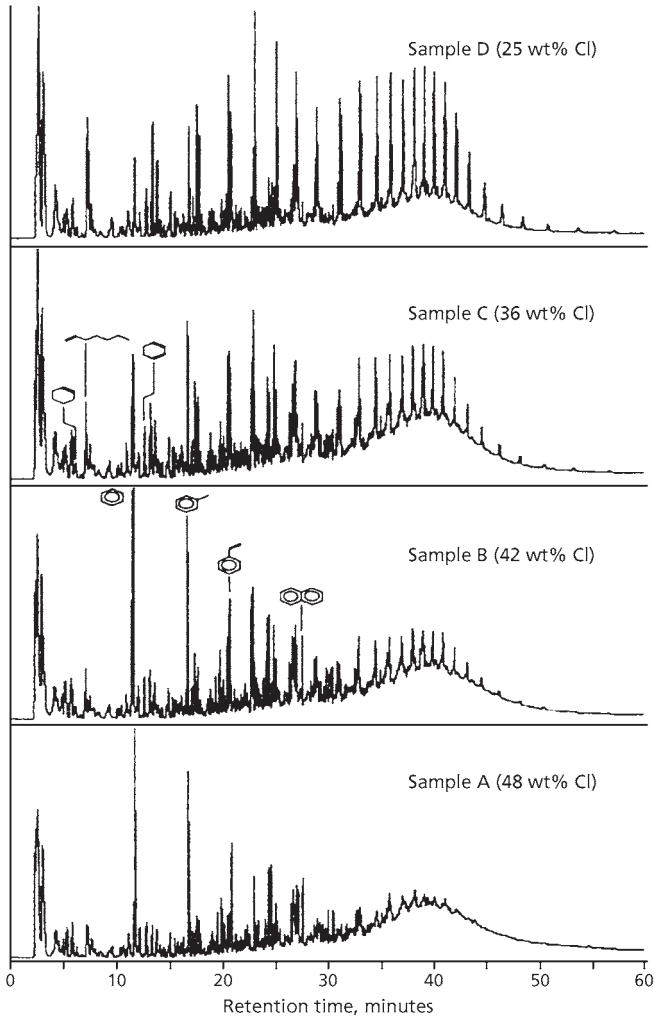

Figure 4.1 Pyrogram of CPE polymers. The pyrogram of the polymer containing 25% chlorine (Cl) (top) possesed considerable PE-like characteristics. As the Cl level increased, the pyrogram gradually acquired more PVC-like characteristics, such as that of the 48% Cl polymer (bottom). (*Reprinted with permission from F.C-Y. Wang and P.B. Smith, Analytical Chemistry, 1997, 69, 4, 618. ©1997, ACS [29]*)

of ethylene and vinyl chloride [27]. A few 1,2-dichloroethylene, 1,1-dichloethylene, and 1,1,2-trichloroethylene monomer-like units may exist in the CPE with 48 wt% of chlorine, but the level is so small that they do not have a significant effect on this assumption.

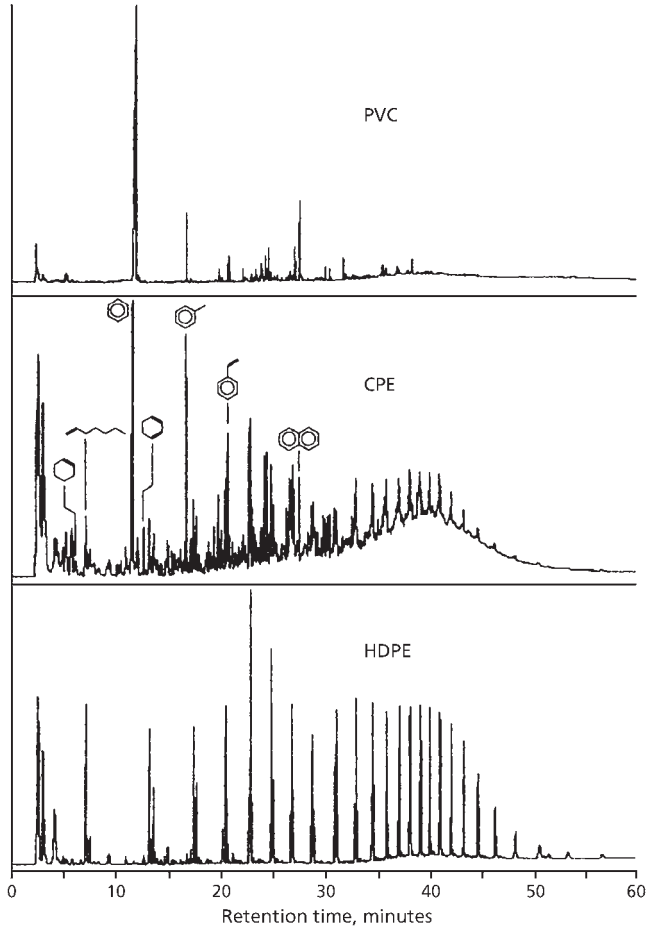

Figure 4.2 Pyrograms of PVC, CPE, and PE. The program of CPE (centre) can be viewed as the combination of the program of PVC (top) and the program of PE (bottom). (*Reprinted with permission from F.C-Y. Wang and P.B. Smith, Analytical Chemistry, 1997, 69, 4, 618. ©1997, ACS [29]*)

The composition and microstructure calculation is based on the triad distribution of CPE pyrolysis fragments. If the CPE is considered as a copolymer of ethylene (E) and vinyl chloride (V), the possible triad combinations of these two monomers are the following six trimers: ethylene triad (labelled EEE), the triad of two ethylene and one vinyl chloride (labelled EEV, VEE, and EVE), the triad of one ethylene and two vinyl chloride (labelled VVE, EVV, and VEV), and the vinyl chloride triad (labeled VVV). The pyrolysis products of these four kinds of triads are 1-hexene, cyclohexene,

1,3-cyclohexadiene, and benzene, respectively. The NASL of both monomers can be calculated on the basis of formulas developed by Wang and Smith [29].

This Py-GC method can be used to determine both the composition and microstructure of CPE. The determination of the composition and structure of CPE is achieved through the detection of the pyrolysis trimers and the application of two critical assumptions for the polymer system. The chlorine contents of all polymers tested are in excellent agreement with NMR measurements and the product composition specification. To distinguish the structural differences of polymers with the same composition, there are several structure-related terms that have been derived to reveal the structural difference, such as the percent of grouped monomers, the NASL of grouped monomers, and the percentage of chlorine atoms in PVC-like structures. The composition and microstructure of CPE is a direct reflection of the CPE preparation method and the degree of chlorination. In other words, the composition and microstructure of CPE can be used to rationalise the physical-mechanical properties obtained from different chlorination processes. This method extends the capabilities of pyrolysis from the quantitative and structural study of copolymer systems into the realm of chemically modified homopolymers.

4.1.3 Polyimide Synthesised from (4,4′-Hexafluoroisopropylidene) diphthalic Dianhydride (DTG) and an Unfluorinated Polyamide 4,4′-diamino diphenyl Methane (PIF_1)

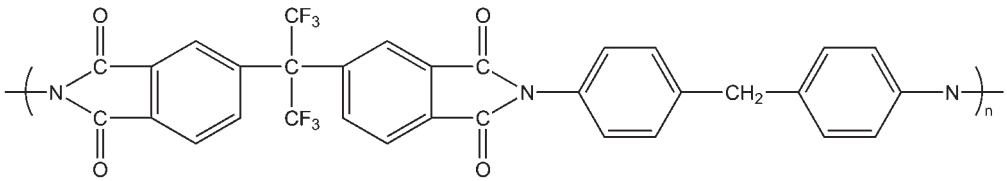

The chemical structures of fluorinated polyimide (PIF_2).

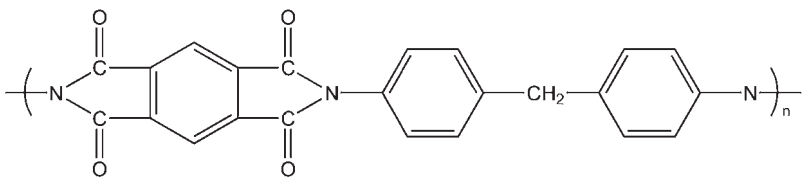

The chemical structures of unfluorinated polyimide (PIF_1).

Ren and co-workers [30] investigated the characterisation of this fluorine containing thermally resistant polymer using high resolution Curie point Py-GC-MS, thermogravimetric analysis and Fourier transform IR (FT-IR) spectroscopy.

Pyrolysis was carried out at 590, 670, 740 and 920 ºC.

The DTG in **Figure 4.3** showed that PIF_2 had two weight-loss peaks, whereas PIF_1 exhibited only one weight-loss peak. They should have different thermal degradation mechanisms. It is believed that the first weight-loss peak in the DTG of PIF_2, which ranges from 485.42 to 621.23 °C, was associated with fluorine. The total ion chromatograms (TIC) of the PIF_1 and PIF_2 pyrolysis at 740 °C are shown in **Figure 4.4**. The chemical structure of each pyrolysate is shown in **Figure 4.5**. The pyrolysates of PIF_2 are different from the pyrolysates of PIF_1. Some pyrolysates such as aniline, *p*-aminotoluene, 9-phenyl-9H-fluorene, and [l,1´-biphenyl]-4,4´-dicarbonitrile could be found in the pyrolysates of PIF_1, while they could not be found in the pyrolysates of PIF_2. It was found that the fluorine-containing pyrolysates were HCF_3 and $C_6H_5CF_3$. In general, there are three classes of pyrolysates. The first class of pyrolysates is low boiling-point products such as CO, CO_2, and HCF_3. The

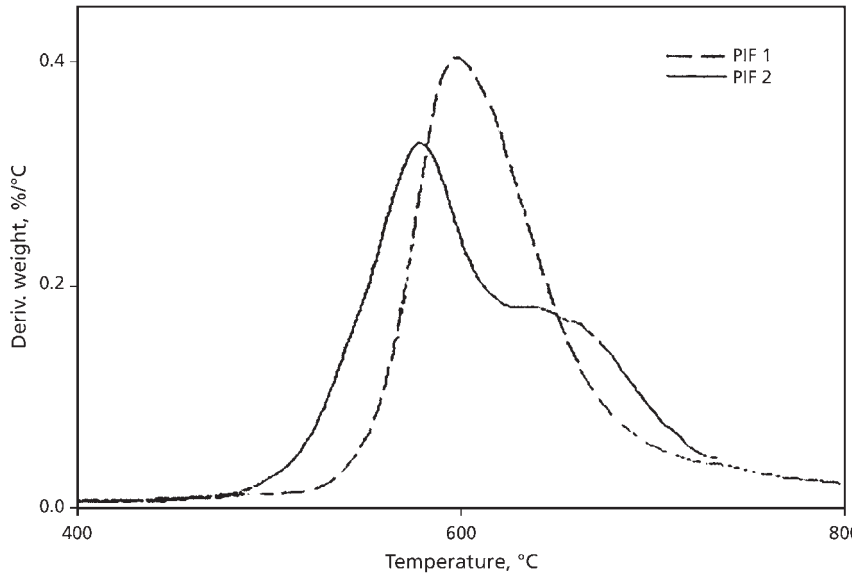

Figure 4.3 Differential thermograms of fluorinated polyimide (PIF_2) and unfluorinated polyimide (PIF_1). (*Reprinted with permission from L. Ren, W. Fu, Y. Luo, H. Lu, D. Jia, J. Shen, B. Pang and T-M. Ko, Journal of Applied Polymer Science, 2004, **91**, 4, 2295. ©2004, Wiley Periodicals [29]*)

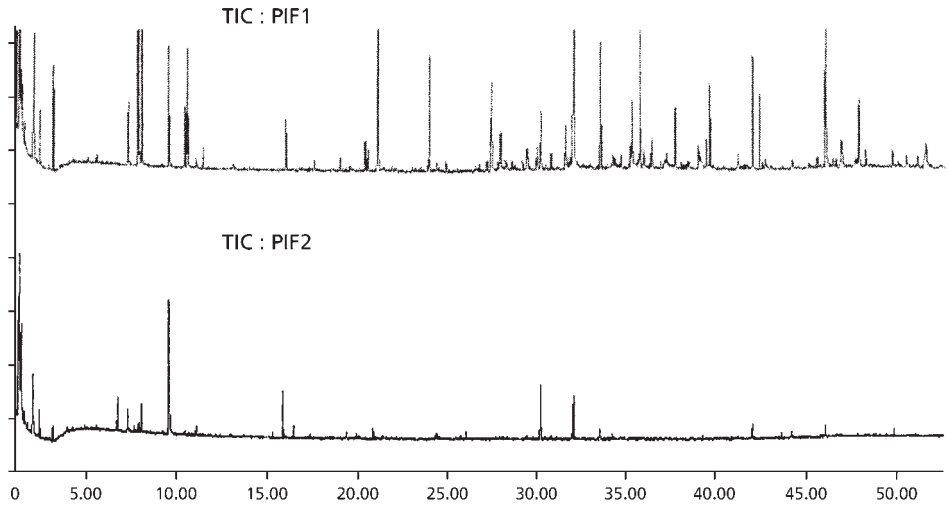

Figure 4.4 Total ion chromatogram (TIC) of fluorinated polyimide (PIF_2) and unfluorinated polyimide (PIF_1) at 740 °C. (*Reprinted with permission from L. Ren, W. Fu, Y. Luo, H. Lu, D. Jia, J. Shen, B. Pang and T-M. Ko, Journal of Applied Polymer Science, 2004,* ***91****, 4, 2295. ©2004, Wiley Periodicals [30]*)

second class of pyrolysates, which is directly formed from the polymer backbone, has the characteristic structure of the main chain, such as compounds 13, 14, 16, and 18 in **Figure 4.5**. The third class is formed through the rearrangement reaction or cyclisation reaction such as compound 15 in **Figure 4.5**. Multistep pyrolysis was used to study the thermal degradation process and the two weight-loss peaks of DTG of PIF_2. The sample was first pyrolysed at 590 °C for 5 s. Subsequently, the residue of the pyrolysis was gathered and pyrolysed at 920 °C for 5 s. Their TIC revealed that HCF_3 and $C_6H_5CF_3$ occured in the first pyrolysis at 590 °C. However, they were not found in the pyrolysis of the residue at 920 °C. It indicates that the C–C bond of the CF_3–C–CF_3 in PIF_2 should be broken in the first pyrolysis. In addition, it was found that the pyrolyses at 670, 740, and 920 °C are the same, although different from the pyrolysis at 590 °C, i.e., the pyrolysis of PIF_2 is dependent on the pyrolysis temperature.

As a consequence of the pyrolysis and the FT-IR studies the proposed thermal degradation mechanism shown in **Figure 4.5** was developed for PIF_2 at 740 °C.

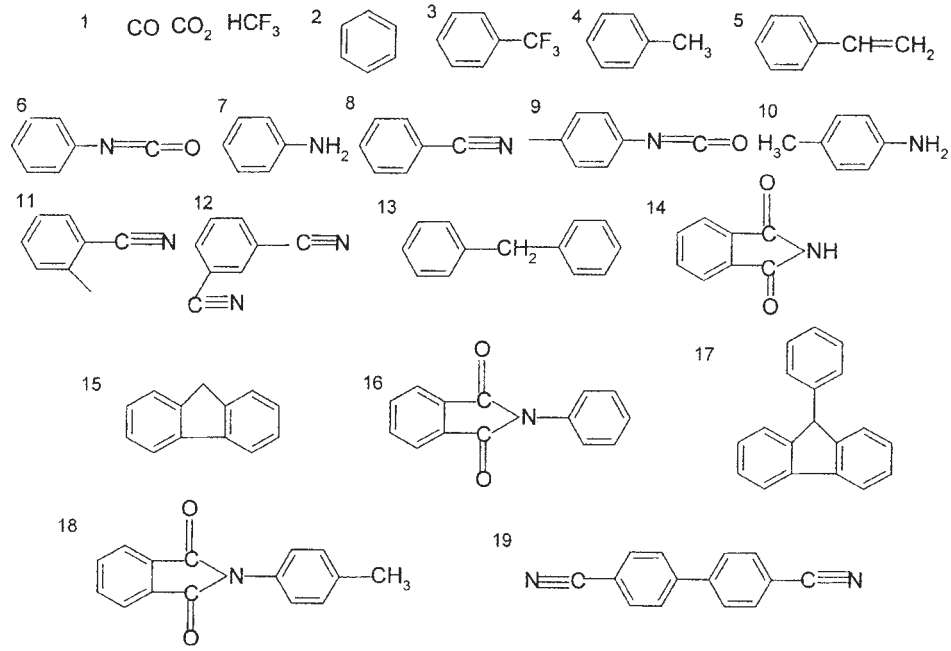

Pyrolysates of PIF1 and PIF2 at 740 °C							
No.	**m/z**	**PIF2**	**PIF1**	**No.**	**m/z**	**PIF2**	**PIF1**
1	28	+	+	11	117	+	+
	44	+	+				
	70	+	–				
2	78	+	+	12	128	+	+
3	146	+	–	13	168	+	+
4	92	+	+	14	147	+	+
5	104	+	+	15	166	+	+
6	119	+	+	16	223	+	+
7	93	–	+	17	242	–	+
8	103	+	+	18	237	+	+
9	133	+	+	19	204	–	+
10	107	–	+				

Figure 4.5 Chemical structure of pyrolysates at 740 °C of fluorinated polyimide (PIF_2) and unfluorinated polyimide (PIF_1). (*Reprinted with permission from L. Ren, W. Fu, Y. Luo, H. Lu, D. Jia, J. Shen, B. Pang and T-M. Ko, Journal of Applied Polymer Science, 2004, **91**, 4, 2295. ©2004, Wiley Periodicals [30]*)

4.1.4 Polypyrrol

Kojima and co-workers [31] applied Py-GC-MS and infrared spectroscopy to a study of the structure and thermal plasma polymerised decomposition of polypyrrole.

Decomposition products identified after pyrolysis at 500 °C are reviewed in **Table 4.4** and **Figure 4.6**. In the IR spectrum of polypyrrole there are bands at 2250 cm^{-1} associated with the pyrrole ring vibration thought to be due to either C≡N stretching and/or to C≡C stretching, and bands at the 1630 cm^{-1} due to either C=N stretching and/or to C=C stretching. The band at the 2950 cm^{-1} range may also be assigned to aliphatic C–H stretching modes. For liquid pyrrole, the N–H stretching, C–H stretching, C–H out-of-plane bending modes occur at 3400, 3100, 768, and 565

Table 4.4 Mass spectrometric assignment of gas chromatographic peaks 5-14

Peak No.	t_R/min	Reference Compound	t_R/min	Δ[a]
5	11.4	Acetonitrile	11.7	2.9 ± 0.1
6	12.5	Acrylonitrile	12.5	3.5 ± 0.2
7	16.2	Propionitrile	15.8	3.7 ± 0.1
8	18.0	Isobutyronitrile	17.8	3.6 ± 0.3
9	19.8	*Cis*-crotononitrile	19.3	3.1 ± 0.2
9	19.8	*Trans*-crotononitrile	22.0	3.1 ± 0.2
9	19.8	Allyl cyanide	22.2	3.2 ± 0.3
10	21.8	*n*-butyronitrile	21.6	3.6 ± 0.3
11	22.6	*Trans*-crotononitrile	22.0	3.4 ± 0.3
11	22.6	Allyl cyanide	22.2	3.4 ± 0.3
12	25.0	Pyrrole	24.8	2.8 ± 0.1
13	30.0	*N*-methylpyrrole	23.8	8.7 ± 0.2
13	30.0	2-Methylpyrrole	29.5	3.4 ± 0.2
14	34.2	2,5-Dimethypyrrole	32.8	12.2 ± 0.2
14	34.2	2-Ethylpyrrole	33.4	3.5 ± 0.2

*Reproduced with permission from T. Kojima, H. Takaku, Y. Urata and K. Gotoh, Journal of Applied Polymer Science, 1993, **48**, 8, 1395. ©1993, Wiley Interscience [31]*

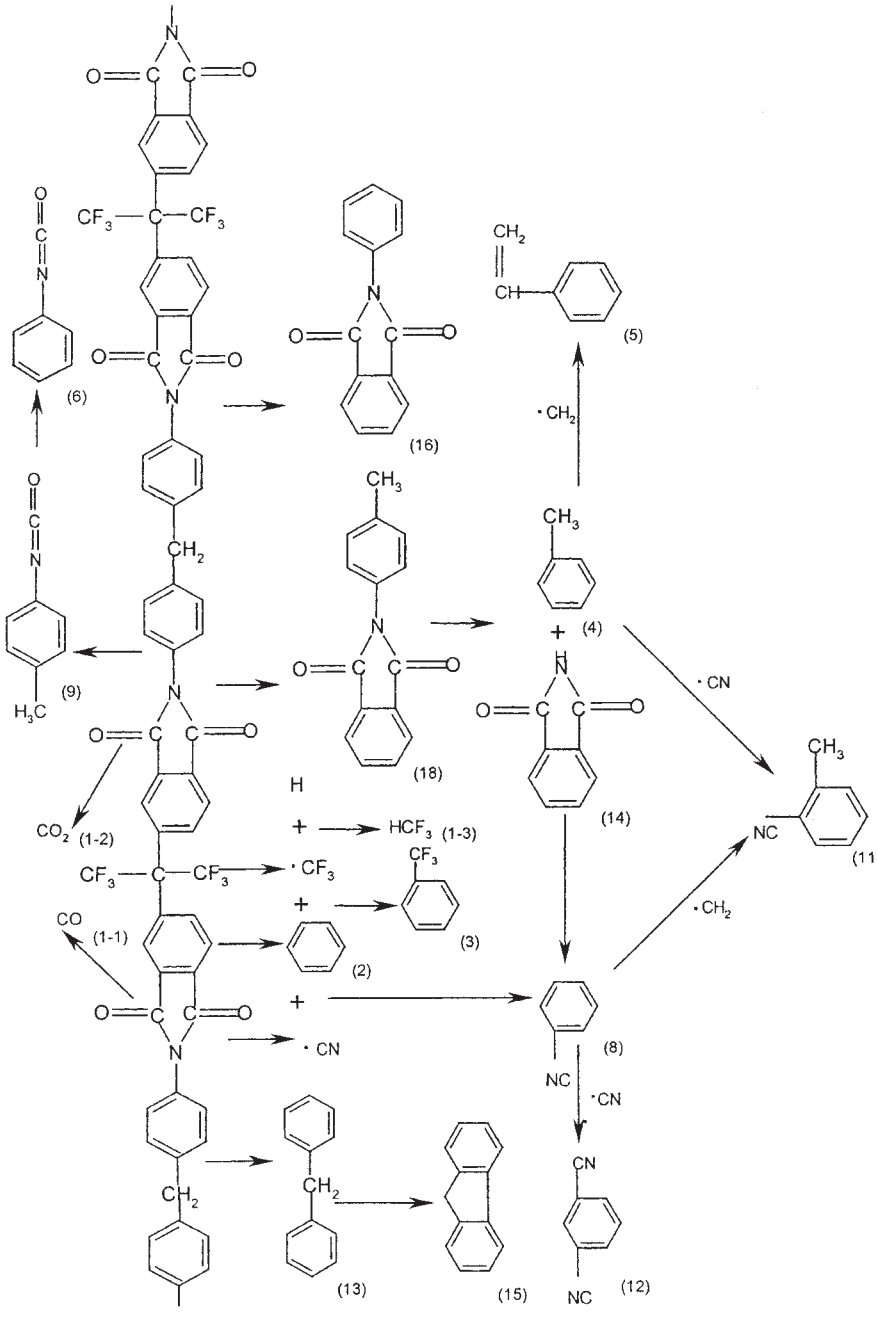

Figure 4.6 Degradation mechanism of polypyrrole and its thermal decomposition products after pyrolysis at 500 °C. (*Reprinted with permission from T. Kojima, H. Takaku, Y. Urata and K. Gotoh, Journal of Applied Polymer Science, 1993, 48, 8, 1395. © 1993, Wiley Periodicals [30]*)

cm^{-1}. Since these frequencies are scarcely influenced by the surrounding atoms, the bands at 3400, 3100, 730 (and/ or 790), 600 cm^{-1}, in the IR spectrum of polypyrrole, may be assigned to the modes mentioned previously, respectively. The bands at 730 and 790 cm^{-1} are similar to the absorptions associated with monosubstituted benzene ring vibration, which appear in the IR spectra of plasma-polymerised benzene, styrene and toluene.

Kojima and co-workers [31] proposed that in a plasma discharge pyrrole is in equilibrium with acetylene and allylleneimine (C_2H_2NH):

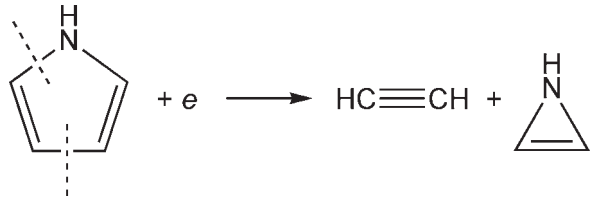

Production of a cation of allylleneimine by electron bombarding is well known in studies of mass spectrometry on pyrrole [32]. A polymer, from a vinyl pyrrole, which is produced from uncleavaged pyrrole and acetylene consists of monosubstituted pyrrole rings. This is made evident by the discrepancy in IR spectra between polypyrrole and poly(pyrrole-2,5-diyl)-like polypyrrole [33], and by the thermal decomposition

products: a relatively large amount of 2-methylpyrrole and 2-ethylpyrrole, and, on the contrary, small amount of 2,5-dimethylpyrrole. The bands at the 2250 cm^{-1} range in the IR spectrum of polypyrrole are considered to be due to the cyanomethyl substituents formed by the addition of acetylenimine to double bonds in the main chain with isomerisation.

It is also considered that imino-1,3-butadiene-4-yl, produced only by the first cleavage of a C–N bond of pyrrole in the discharge, is polymerised by radical coupling. If polypyrroles consists of imino-l,3-butadiene-4-yl units, the evolution of a large amount of pyrrole in the thermal decomposition of polypyrroles is interpreted by a ring-closing depolymerisation of the same sort as poly(ε-caprolactam).

Evolution of large amount of nitriles in the thermal decomposition of polypyrroles is interesting because no nitriles evolve from pyrrole in the general thermal decomposition. Nitriles are thought to evolve from the main chain, including cyano(–C≡N), nitrilo (–N≡), and/or cyanomethyl, the existence of which may be confirmed in the IR spectrum of polypyrroles.

Table 4.5 Characterisation of homopolymers by Pyrolysis -GC-MS					
Polymer	**Pyrolysis procedure**	**Pyrolysis tempertaure**	**Pyrolysis products**	**Comments**	**Ref.**
Polyaryl ether ketone	Flash pyrolysis	Up to 800 °C	Phenol	Wider range of products at high temperatures	[80]
Dicyclic polyimide	-	-	Aliphatic and aromatic products	TGA also applied	[81]
PS, styrene cured polyesters, including chlorinated norbornene dicarboxylic acid, 1,2-propane diol and maleic anhydride	Pyrolysis under nitrogen and *in vacuo*	-	-	-	[82]
Polyurethanes	-	-	Polyol and diisocyanate residues	-	[83]
Polyphenylene sulfide	Flash pyrolysis	550 °C	-	-	[84]
Phenol-formaldehyde resins	Pulsed mode pyrolysis	-	Phenol, methyl-substituted phenols	Cleavage of phenol-methylene bond and subsequent hydrogen abstraction	[85]
Cationic and anionic ion exchange resins	Foil pulse pyrolysis	400-500 °C	Sulfur dioxide, benzene at 500 °C also ethyl benzene, styrene, hydrogen sulfide, toluene at higher temperatures. Anionic resins: trimethylamine methyl chloride at 400 °C, and styrene, *p*-methyl styrene, *p*-ethyl styrene at 400-900 °C.	-	[86]
TGA: thermogravimetric analysis					

4.1.5 Miscellaneous Homopolymers

Products obtained by pyrolysis of other polymers is reviewed in **Table 4.5**. Some specific applications of the chromatography-MS technique to various types of polymers include the following: PE [34, 35], poly(1-octene) [29], poly(1-decene) [29], poly(1-dodecene) [29], CPE [36], polyolefins [37, 38], acrylic acid-methacrylic acid copolymers [39, 40], polyacrylate [41], nitrile rubber [42], natural rubbers [43, 44], chlorinated natural rubber [45, 46], polychloroprene [47], PVC [48-50], polysilicones [51, 52, 53], polycarbonates [54], styrene-isoprene copolymers [55], substituted olystyrene [56], PP carbonate [57], ethylene-vinyl acetate [58], Nylon 66 [59], polyisopropenyl cyclohexane-α-methyl styrene copolymers [60], cresol-novolac epoxy resins [61], polymeric flame retardants [62], poly(4-*N*-alkyl styrenes) [63], polyvinyl pyrrolidone [64], polybutyl-cyanoacrylate [65], polysulfides [66], poly(diethyl-2-methacryl-oxy) ethyl phosphate [67, 68], polyetherimide [69], bisphenol-A [70], polybutadiene [71], polyacenaphthalene [72], poly(l-lactide) [73], polyesterimide [74], polyphenylene triazine [75], poly-4-*N*-vinyl pyridine [76], diglycidylether-bisphenol-A epoxy resins [77], polyvinylidene chloride [78] and poly-*p*-chloromethyl styrene [79].

4.2 Copolymers

4.2.1 Ethylene – Carbon Monoxide

Kiji and co-workers [87] investigated the composition and microstructure of alternating olefin-carbon monoxide copolymers and their derivatives including ethylene-styrene-carbon monoxide alternating polymer, norbornene-amine copolymer and polymers modified with phosphorus pentasulfide or phosphorus pentoxide or primary amines.

In each pyrolysis, hydrocarbons originating from the corresponding olefin comonomer confirmed that the 1,4 arrangements of the ketonic groups in the alternating copolymers were converted into pyrrole, thiophen and furan containing chains with primary amines, phosphorus pentasulfide and phosphorus pentoxide, respectively. The oxygen containing groups which remained intact during the modification with phosphorus pentasulfide were detected in small amounts in the pyrolysates.

4.2.2 Ethylene-vinyl Cyclohexane

Zaikin and co-workers [88] used Py-GC to examine volatiles produced by pyrolysis of block and random ethylene-vinyl cyclohexane copolymers. Zaikin and co-workers

[89] also examined polyvinylcyclohexane and styrene divinyl benzene copolymers and characterised the diad distribution in these polymers.

4.2.3 Styrene Maleic Anhydride

Billiani and co-workers [90] observed that pyrolysis of styrene-maleic anhydride copolymer and styrene diethyl maleate at 450 °C produced products of toluene, ethyl benzene, styrene monomer from the maleic anhydride and diethyl fumarate copolymers and styrene oligomers from the styrene diethyl maleate copolymers.

Incorporated maleic anhydride units degraded at temperatures 80 °C lower than the degradation temperatures for the polymer backbone.

4.2.4 Miscellaneous Copolymers

Py-GC-MS has been used to characterise elastomers including natural rubber, butyl rubber, polychloroprene and acrylonitrile-butadiene copolymer [91]. Other copolymers that have been investigated include: 1-octene-1-decene-1-dodecane terpolymer [92], acrylic-acid methacrylic acid [39], styrene-butadiene[93-95], styrene-isoprene [54], ethylene-vinyl acetate [96], polyisopropenyl cyclohexane – *n*-methyl styrene [57], vinyl pyrrolidine- methacryloxysilicone [97], ethylene-carbon monoxide [98], acrylic copolymers [99], 1-vinyl-2-pyrrolidine – 1-vinyl-3-methylimidoazolium chloride [100], acrylonitrile-butadiene-styrene [101], acetone-furfural [102] and styrene-acrylonitrile [103].

References

1. C. Chang and J.R. Tackett, *Thermochimica Acta*, 1991, **192**, 181.

2. N. Grassie and J.G. Speakman, *Journal of Polymer Science, A-1:Polymer Chemistry*, 1971, **9**, 4, 949.

3. J.R. Schaefgen and I.M. Sarasohn *Journal of Polymer Science,* 1962, **58**, 166, 1049.

4. D.H. Grant and N. Grassie, *Polymer*, 1962, **1**, 445.

5. N. Grassie and N.A. Weir, unpublished data.

6. L. Gunawan and J.K. Haken, *Journal of Polymer Science: Polymer Chemistry Edition*, 1985, **23**, 9, 2539.

7. J. K. Haken and L. Tan, *Journal of Polymer Science: Polymer Chemistry Edition*, 1987, **25**, 5, 1451.

8. N. Grassie, J.G. Speakman and T.I. Davis, *Journal of Polymer Science, Part A-1:Polymer Chemistry*, 1971, **9**, 4, 931.

9. B-M. Quenum, P. Berticat and G. Vallet, *Polymer Journal*, 1975, **7**, 3, 277.

10. J.J. Lindberg, F. Stenman and I. Laipio, *Journal of Polymer Science: Polymer Symposia*, 1973, **42**, 2, 925.

11. N. Grassie and J.D. Fortune, *Makromolekulare Chemie*, 1973, **168**, 1.

12. B. Hösselbarth, F. Keller and M. Findeisen, *Acta Polymerica*, 1989, **40**, 6, 371.

13. B. H. Chang, R. Zeigler and A. Hiltner, *Polymer and Engineering Science*, 1988, **28**, 18, 1167.

14. W. Busch, F. Kloos and J. Brandrup, *Die Angewandte Makromolekulare Chemie*, 1982, **105**, 187.

15. P. Pinther, F. Keller and M. Hartmann, *Acta Polymerica*, 1980, **31**, 5, 299.

16. F. Keller, M. Michajlov, S. Stoeva, *Acta Polymerica*, 1979, **30**, 11, 694.

17. F. Keller, *Plaste und Kautschuk*, 1979, **26**, 3, 136.

18. F. Keller, *Faserforschung und Textil Technik*, 1978, **29**, 2, 133.

19. I.A. Abu-Isa and M.E. Myers, Jr., *Journal of Polymer Science: Polymer Chemistry Edition*, 1973, **11**, 1, 225.

20. T. Saito, Y. Matsumura and S. Hayashi, *Polymer Journal*, 1970, **1**, 6, 639.

21. J. Kálal, J. Zachoval, J. Kubát and F. Svec, *Journal of Analytical and Applied Pyrolysis*, 1979, **1**, 2, 143.

22. T. Shimono, M. Tanaka and T. Shono, *Journal of Analytical and Applied Pyrolysis*, 1979, **1**, 1, 77.

23. A. Alajbeg, P. Arpino, D. Deur-Siftar and G. Guiochon, *Journal of Analytical and Applied Pyrolysis*, 1980, **1**, 3, 203.

24. F.C-Y. Wang, B.B. Gerhart and P.B. Smith, *Analytical Chemistry*, 1995, **67**, 19, 3536.

25. F.C-Y. Wang and P.B. Smith, *Analytical Chemistry*, 1996, **68**, 3, 425.

26. F.C-Y. Wang and P.B. Smith, *Analytical Chemistry*, 1996, **68**, 17, 3033.

27. S. Tsuge, T. Okumoto and T. Takeuchi, *Macromolecules*, 1969, **2**, 2, 200.

28. S. Tsuge and H. Ohtani, *Pyrolysis Gas Chromatography of High Polymers Fundamentals and Data Compilation*, Techno-Systems, Tokyo, Japan, 1989, p.178.

29. F.C-Y. Wang and P.B. Smith, *Analytical Chemistry*, 1997, **69**, 4, 618.

30. L. Ren, W. Fu, Y. Luo, H. Lu, D. Jia, J. Shen, B. Pang and T-M. Ko, *Journal of Applied Polymer Science*, 2004, **91**, 4, 2295.

31. T. Kojima, H. Takaku, Y. Urata and K. Gotoh, *Journal of Applied Polymer Science*, 1993, **48**, 8, 1345.

32. J.H. Benyon and R.A. Saunders, *The Mass Spectra of Organic Molecules*, Elsevier, Amsterdam, The Netherlands, 1968, p.296.

33. K.K. Kanazawa, A.F. Diaz, M.T. Krounbi and G.B. Street, *Synthetic Metals*, 1981, **4**, 2, 119.

34. D.L. Zoller, F.J. Cox, M.V. Johnston and K. Qian, *Polymer Preprints*, 2000, **41**, 1, 669.

35. *Pyrolysis – GC/MS/IR Analysis of Polyethylene*, Hewlett Packard Application Note, 228971, 1989.

36. R. Yang, G. Li and K. Wang, *Journal of Applied Polymer Science*, 2001, **81**, 2, 359.

37. C. Westphal, C. Perrot and S. Karlsson, *Polymer Degradation and Stability*, 2001, **73**, 2, 281.

38. M. Predel and W. Kaminsky, *Polymer Degradation and Stability*, 2000, **70**, 3, 373.

39. J.L. Sharp and G. Paterson, *Analyst*, 1980, **105**, 1250, 517.

40. O. Chiantore, D. Scalarone and T. Learner, *International Journal of Polymer Analysis and Characterisation*, 2003, **8**, 1, 67.

41. H. Zhang, P.R. Westmoreland, R.J. Farris, E.B. Coughlin, A. Plichta and Z.K. Brzozowski, *Polymer*, 2002, **43**, 20, 5463.

42. M-R.S. Fuh and G-Y. Wang, *Analytica Chimica Acta*, 1998, **371**, 1, 89.

43. *Rubber Technology International*, 1997, p.129.

44. M. Phair and T. Wampler in *Proceedings of the 150th ACS Rubber Division Meeting*, Louisville, KY, USA, Fall 1996, Paper No.69.

45. D. Yang, S-D. Li and D-M. Jia, *China Synthetic Rubber Industry*, 2001, **24**, 375.

46. D. Yang, S-D. Li, W-W. Fu, J-P. Zhong and D-M. Jia, *Journal of Applied Polymer Science*, 2003, **87**, 2, 199

47. R.S. Lehrle, N. Dadvand, I.W. Parsons, M. Rollinson, I.M. Horn and A.R. Skinner, *Polymer Degradation and Stability*, 2000, **70**, 3, 395.

48. R.P. Lattimer and W.J. Kroenke, *Journal of Applied Polymer Science*, 1980, **25**, 1, 101.

49. N. Dadvand, R.S. Lehrle, I.W. Parsons and M. Rollinson, *Polymer Degradation and Stability*, 1999, **66**, 2, 247.

50. D. Fabbri, D. Tartari and C. Trombini, *Analytica Chimica Acta*, 2000, **413**, 1-2, 3.

51. J.C. Kleinert and C.J. Weschler, *Analytical Chemistry,* 1980, **52**, 8, 1245.

52. M. Ezrin and G. Lavigne in *Proceedings of the 60th SPE Annual Technology Conference ANTEC 2002*, San Francisco, CA, USA, 2002, Session W9, Paper No.577.

53. S. Fujimoto, H. Ohtani and S. Tsuge, *Fresenius' Journal of Analytical Chemistry*, 1988, **331**, 3-4, 342.

54. K. Oba, H. Ohtani and S. Tsuge, *Polymer Degradation and Stability*, 2001, **74**, 1, 171.

55. *Pyrolysis GC/MS/IR Analysis of Kraton 1107*, Hewlett Packard Application Note 228-100, 1989.

56. V.V. Zuev, F. Bertini and G. Audisio, *Polymer Degradation and Stability*, 2001, **71**, 2, 213.

57. X.H. Li, Y.Z. Meng, Q. Zhu and S.C. Tjong, *Polymer Degradation and Stability*, 203, **81**, 1, 157.

58. L. Häuβler, G. Pompe, V. Albrecht and D. Voigt, *Journal of Thermal Analysis and Calorimetry*, 1998, **52**, 1, 131.

59. *Pyrolysis GC/MS/IR Analysis of Nylon 6/6*, Hewlett Packard Application Note 228-106, 1989.

60. R.J. Gritter, E. Gipstein and G.E. Adams, *Journal of Polymer Science: Polymer Chemistry Edition*, 1979, **17**, 12, 3959.

61. J.B. Maynard, J.E. Twitchell and J.Q. Walker, *Journal of Chromatographic Science*, 1979, **17**, 82.

62. F.C-Y. Wang, *Analytical Chemistry,* 1999, **71**, 10, 2037.

63. V.V. Zuev, F. Bertini and G. Audisio, *Polymer Degradation and Stability*, 2000, **69**, 2, 169.

64. T.M.H. Cheng and E.G. Malawer, *Analytical Chemistry*, 1999, **71**, 2, 468.

65. A. Hickey, J.J. Leahy and C. Birkinshaw, *Macromolecular Rapid Communications*, 2001, **22**, 14, 1158.

66. S. Sundarrajan, M. Surianarayanan, K.S.V. Srinivasan and K. Kishore, *Macromolecules*, 2002, **35**, 9, 3331.

67. L-H. Perng, *Journal of Polymer Research*, 2000, **7**, 3, 195.

68. L.H. Perng, C.J. Tsai, Y.C. Ling, S.D. Wang and C.Y. Hsu, *Journal of Applied Polymer Science*, 2002, **85**, 4, 821.

69. S. Carroccio, C. Puglisi and G. Montaudo, *Polymer Preprints*, 2000, **41**, 1, 684.

70. Y. Haishima, Y. Hayashi, T. Yagami and A. Nakamura, *Journal of Biomedical Materials Research Part B: Applied Biomaterials*, 2001, **58**, 2, 209.

71. J.A.J. Jansen and W.E. Haas, *Analytica Chimica Acta*, 1987, **196**, 69.

72. T. Hammond and R.S. Lehrle, *European Polymer Journal*, 1987, **23**, 8, 653.

73. Y. Fan, H. Nishida, T. Mori, Y. Shirai and T. Endo, *Polymer*, 2004, **45**, 4, 1197.

74. S-H. Hsiao and W-T. Leu, *High Performance Polymers*, 2004, **16**, 3, 461.

75. Z. Jiang, Y. Luo, X. Jin and F. Lu, *Journal of Analytical and Applied Pyrolysis*, 1993, **26**, 3, 145.

76. G. Audisio and F. Severini, *Journal of Analytical and Applied Pyrolysis*, 1987, **12**, 2, 135.

77. H. Nakagawa, S. Tsuge and T. Koyama, *Journal of Analytical and Applied Pyrolysis*, 1987, **12**, 2, 97.

78. A. Yasuhara and M. Morita, *Environmental Science and Technology*, 1988, **22**, 6, 646.

79. B. Boinon, D. Ainad-Tabet and J.P. Monthéard, *Journal of Analytical and Applied Pyrolysis*, 1988, **13**, 3, 171.

87. J. Kiji, T. Okano, T. Chiyoda, F. Bertini and G. Audisio, *Journal of Analytical and Applied Pyrolysis*, 1997, **40-41**, 331.

80. M. Day, J.D. Cooney and D.M. Wiles, *Journal of Analytical and Applied Pyrolysis*, 1990, **18**, 2, 163.

81. E. Jakab, F. Till, T. Székely, S.S. Kozhabekov and B.A. Zhubanov, *Journal of Analytical and Applied Pyrolysis*, 1992, **23**, 3, 229.

82. G.H. Irzl, C.T. Vijayakumar and K. Lederer, *Journal of Analytical and Applied Pyrolysis*, 1988, **13**, 4, 305.

83. H. Ohtani, T. Kimura, K. Okamoto, S. Tsuge, Y. Nagataki and K. Miyata, *Journal of Analytical and Applied Pyrolysis*, 1987, **12**, 2, 115.

84. D.R. Budgell, M. Day and J.D. Cooney, *Polymer Degradation and Stability*, 1994, **43**, 1, 109.

85. L. Prókai, *Journal of Analytical and Applied Pyrolysis*, 1987, **12**, 3-4, 265.

86. B.G. Brodda, S. Dix and J. Fachinger, *Separation Science Technology*, 1993, **28**, 1-3, 653.

88. V.G. Zaikin, R.G. Mardanov, V.I. Kleiner, B.A. Krentsel and B.N. Bobrov, *Journal of Analytical and Applied Pyrolysis*, 1983, **26**, 3, 185.

89. V.G. Zaikin, R.G. Mardanov, V.I. Kleiner, B.A. Krentsel and N.A. Platé, *Journal of Analytical and Applied Pyrolysis*, 1990, **17**, 4, 291.

90. G.H. Billiani, C.T. Vijayakumar, J.K. Fink and K. Lederer, *Journal of Analytical and Applied Pyrolysis*, 1989, **16**, 3, 221.

91. J.A. Hiltz and T. Foster, *Direct Exposure Probe/Mass Spectrometry and Pyrolysis-Gas Chromatography/Mass Spectrometry Study of the Effect of Gamma Radiation Exposure Thermal Degradation Products of Natural Rubber: Polycaprolactone Mixtures*, Report No. DREA-TM-95/214, Defence R&D, Canada, 1995.

92. R. Yang, G. Li and K. Wang, *Journal of Applied Polymer Science*, 2001, **81**, 2, 359.

93. S.R. Shield, G.N. Ghebremsekel and C. Hendrix in *Proceedings of the 159th ACS Rubber Division Meeting*, Providence, RI, USA, Spring 2001, Paper No.19.

94. G.N. Ghebremsekel and C. Hendrix in *Proceedings of the 152nd ACS Rubber Division Meeting*, Cleveland, OH, USA, Fall 1997, Paper No.72.

95. *Analysis of Polybutadiene by GC/IR/MS and Pyrolysis*, Hewlett Packard Application Brief IRD 87-7, 1987.

96. W.J. Van Ooij, J.M. Kim, S. Luo and S. Borros, in *Proceedings of the 156th ACS Rubber Division Meeting*, Orlando, FL, USA, 1999, Paper No.57.

97. J-C. Kim, M-E. Song, S-K. Park, E-J. Lee, M-J. Rang and H-J. Ahn, *Journal of Applied Polymer Science*, 2002, **85**, 10, 2244.

98. J. Kiji, A. Yamada, F. Bertini and G. Audisio, *Macromolecular Rapid Communications*, 2001, **22**, 8, 598.

99. A.M. Casanovas and X. Rovira, *Journal of Analytical and Applied Pyrolysis*, 1987, **11**, 227.

100. E. Gmahl and W. Ruess, *International Journal of Cosmetic Science*, 1992, **15**, 2, 77.

101. M.M. Shapi and A. Hesso, *Journal of Chromatography A*, 1991, **562**, 681.

102. R. Sánchez, C. Hernández, G. Jalsovszky and G. Czira, *European Polymer Journal*, 1994, **30**, 1, 37.

103. M.M. Shapi and M-L. Riekkola, *Journal of Microcolumn Separations*, 1992, **4**, 35.

5 Reaction Gas Chromatography Techniques

Polymers being solid substances, with a few exceptions, cannot be directly analysed using gas chromatography (GC). However, it is possible by the application of well-controlled chemical reactions to decompose polymers to simpler volatile substances that are amenable GC and thereby one can obtain information concerning the original polymer.

A further special case of reaction gas chromatography (RGC) involves pyrolysis (or photolysis) of the polymer in the absence of oxygen and examination of the volatiles produced by gas chromatography to provide information on the structure of the original polymer.

Further complementary techniques can be applied to obtain even more information. Thus RGC can be coupled with mass spectrometry (MS) or nuclear magnetic resonance spectroscopy.

There are three broad catagories of reaction gas chromatography:

1. Reaction of the polymer with a suitable reagent followed by analysis of the reaction products by, for example, GC, MS or another relevant technique (see Section 5.1.1).

2. Simultaneous pyrolysis-derivatisation: the presence of a suitable reagent followed by immediate analysis by suitable techniques (see Section 5.2).

3. Prepyrolysis/derivatisation in which the functional groups of the polymer are reacted with a suitable reagent to obtain a favourable thermal decomposition pathway followed by examination by pyrolysis and other suitable techniques. The main difference between prepyrolysis derivatisation and postpyrolysis derivatisation is that the polymer backbone should be stable enough to resist the attack from the derivatisation reagent in prepyrolysis derivatisation (see Section 5.3).

5.1 Hydrolysis Gas Chromatography

5.1.1 Saponification Methods

Ester groups occur in a wide range of polymers, e.g., polyethylene terephthlate. The classic chemical method for the determination of ester groups, namely saponification, can be applied to some types of polymer. For example, copolymers of vinyl esters and esters of vinyl esters and esters of acrylic acid can be saponified in a sealed tube with 2 M sodium hydroxide. The free acids from the vinyl esters can then be determined by GC. The alcohols formed by the hydrolysis of the acrylate esters are determined by GC. Polymethyl acrylate can be hydrolysed rapidly and completely under alkaline conditions; however, the monomer units in polymethylmethacrylate (PMMA) prepared and treated similarly are resistant to hydrolysis although their benzoate end-groups react readily. Thus, saponification techniques should be applied with caution to polymeric materials.

5.1.2 Zeisel Procedures

Hydrolysis using hydriodic acid has been used for the determination of the methyl ethyl, propyl, and butyl esters of acrylates, methacrylates, or maleates [1] and the determination of polyethyl esters in methyl methacrylate (MMA) copolymers [2, 3]. First, the total alcohol content is determined using a modified Zeisel hydriodic acid hydrolysis [4]. Second, the various alcohols, after being converted to the corresponding alkyl iodides (see **Table 5.1**), are collected in a cold trap and then separated by GC. Owing to the low volatility of the higher alkyl iodides the hydriodic acid hydrolysis technique is not suitable for the determination of alcohol groups higher than butyl. This technique has also been applied to the determination of alkoxy groups in acrylate esters [1].

Anderson and co-workers [5] used combined Zeisel reaction and GC to analyse acrylic copolymers. Acrylic esters were cleaved with hydriodic acid and gas chromatography was used for analysing the alkyl iodides so formed:

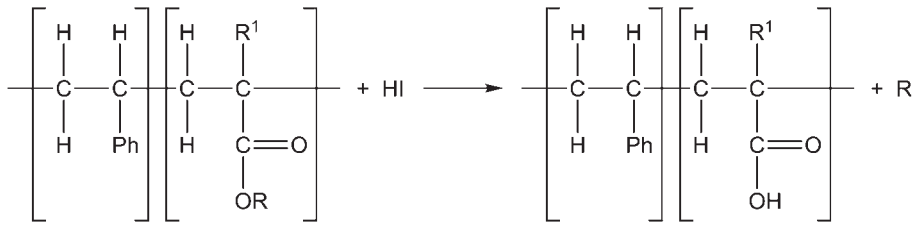

Using this procedure, the recovery of alkyl iodides is greater than 95% for polymers containing between 10 and 90% of the methyl, ethyl, and butyl esters of acrylic and methacrylic acid. In addition, the use of isopropylbenzene as the trapping solvent allows the determination of all C_1 to C_4 alkyl iodides.

Table 5.1 shows some results obtained by applying this method to a range of acrylic polymers. The calculated recoveries are greater than 95% for polymers containing

Table 5.1 Recovery of alkyl iodides from the Zeisel cleavage of acrylic polymers[a]

Polymer	Methyl acrylate %	Methyl methacrylate %	Ethyl acrylate %	Ethyl methacrylate %	Butyl acrylate %	Butyl methacrylate %
1	33.7 (33.3)		33.0 (33.3)		32.7 (33.3)	
2		33.6 (33.3)		33.4 (33.3)		31.9 (33.3)
3			19.5 (20.0)			
4		50.1 (50.0)	30.5 (30.0)			
5		59.9 (60.0)			39.8 (40.0)	
6		29.7 (30.0)			29.8 (30.0)	
7		59.8 (60.0)				9.8 (10.0)
8	19.9 (20.0)		19.8 (20.0)			19.8 (20.0)
9		30.1 (30.0)		30.0 (30.0)	29.8 (30.0)	
10		29.9 (30.0)	29.6 (30.0)		39.7 (40.0)	
11		60.1 (60.0)	30.1 (30.0)			9.5 (10.0)

[a] *All values are the average of at least three determinations and are reported as: % monomer found (% monomer in polymer). Theoretical data in brackets.*

Reprinted with permission from D. G. Anderson, K. E. Isakson, D. L. Snow, D. J. Tessari, and J. T. Vandeberg, Analytical Chemistry, 1971, ***43****, 7, 894. ©1971, ACS [5]*

between 10 and 100% acrylic monomer. The method has a 99% confidence interval of 0.8. The presence of comonomers such as styrene, acrylonitrile, vinyl acetate, acrylamide, or acrylic acid does not change the recovery of acrylate or methacrylate esters. Non-quantitative results are obtained, however, for polymers containing hydroxypropyl methacrylate.

The Ziesel reaction has been used for the determination of alkoxyl groups in cellulosic materials [6-8] and the determination of ether groups in cellulose and polyvinyl ethers [9]. However, hydriodic acid also cleaves any ester linkages on the polymer backbone, giving positive interference.

5.2 Alkali Fusion

5.2.1 Determination of Alkyl and Aryl Groups

The technique of potassium hydroxide fusion–RGC has been applied to the determination of alkyl and aryl groups in polysiloxanes. The method involves the quantitative cleavage of all organic substituents bonded to silicon, producing the corresponding hydrocarbons:

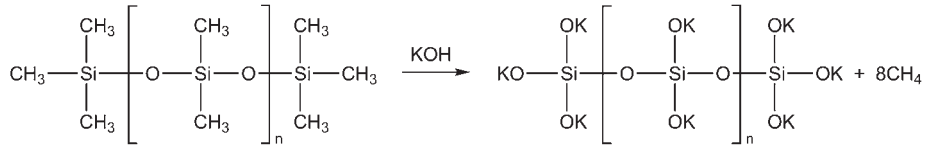

After concentration of the volatile products, they are separated and determined by GC. The percentage relative standard deviation (RSD) of the method is 1.00%; the average deviation between experimental and theoretical results is 0.5% absolute.

Various other reagents have been used for the determination of organic substituents bonded to silicon in organosilicon polymers (**Table 5.2**).

Characterisation of polyester-based and polyether-based urethane rubbers. Haken and co-workers [22, 23] and Vimalasiri and co-workers [24] characterised these rubbers by cleaving the polyurethane chains with alkali and acid fusion reactions followed by column chromatography to identify the fragments produced.

Fusion with alkali and sodium acetate also served to cleave bisphenol A polycarbonate – dimethylsiloxane block copolymer. Bisphenol A diacetate produced was identified by gas chromatography as a polycarbonate fragment and gas-solid chromatography was used to identify methane produced by cleavage of substituted siloxone.

Table 5.2 Reaction methods for the quantitative determination of organic substituents bonded to silicon					
Group determined	**Reagent**	**Reaction conditions**	**Product**	**Analysis**	**Reference**
Phenyl	60% aqueous KOH in DMSO	2 h at 120 °C	Benzene	GC	[10]
Phenyl	Bromine in glacial acetic acid	Boiling solution	Bromobenzene	Titration of excess bromine	[11]
Ethyl and phenyl	Phosphorus pentoxide and water	30-580 °C over 45 min	Ethane and benzene	GC-FID	[12]
Methyl and ethyl	Powdered potassium hydroxide	2 h at 250-270 °C	Methane and ethane	Gas buret	[13]
Methyl	Sulfuric acid	20 min at 280-300 °C	Methane	Gas buret	[14, 15]
Phenyl	Ethylbromide in the presence of aluminium chloride	...	Hexaethyl benzene	Gravimetric	[16]
Vinyl	Phosphorus pentoxide and water	80-600 °C over 40 min	Ethylene	GC-FID	[17]
Vinyl	Phosphorus pentoxide	Ambient to 500 °C	Ethylene	GC-FID	[18]
Vinyl	90% Sulfuric acid	75-250 °C at 10 °C/min and 1 h at 250 °C	Ethylene	GC-TC	[19]
Vinyl	Sodium hydroxide pellets	300 °C for 15 min	Ethylene	Colorimetric	[20]
Vinyl	KOH pellets	Heat with Meker burner	Ethylene	GC-FID	[21]

KOH: Potassium hydroxide
DMSO: Dimethylsulfoxide
GC-FID: GC with flame ionisation detection
GC-TC: GC with thermal conductivity detection
Source: Author's own files

5.2.2 Determination of Amide and Imide Groups in Polyamides, Polyimides, and Polyamides/Imides

Schleuter and Siggia [25-27] and Frankoski and Siggia [28] used the technique of alkali fusion RGC for the analysis of imide monomers and aromatic polyimides, polyamides, and poly(amide-imides). Samples are hydrolysed with a molten potassium hydroxide reagent at elevated temperatures in a flowing inert atmosphere:

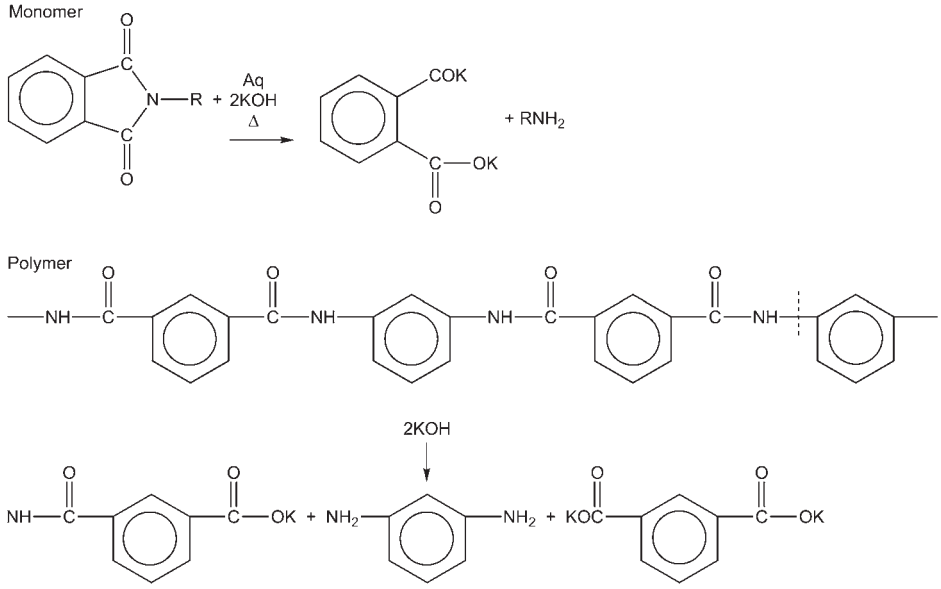

Volatile reaction products are concentrated in a cold trap before separation by GC. The identification of the amine and/or diamine products aids in the characterisation of the monomer or polymer; the amount of each compound generated is used as the basis for quantitative analysis. The average RSD of the method is ±1.0%.

Table 5.3 summarises the chemical structures and sample designations of the polymers studied. **Table 5.4** summarises the diamine recoveries obtained. These data represent the mole percentage of theoretical diamine based on the dry weight of sample and the idealised linear polymer repeat units depicted in **Table 5.4**. Recoveries were, in all cases, between 90% and 101% of theoretical values.

Table 5.3 Structure, water content and decomposition temperature of the polymers studied.

	Structure of repeat unit	Wt.% water	Decomposition temperature, ºC
PI-1	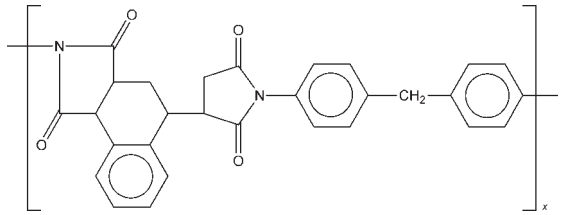	6.5	385
PI-2	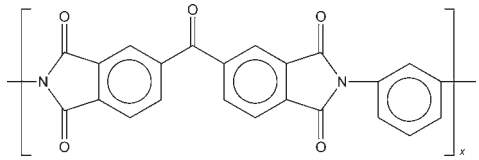	2.2	410
PI-3	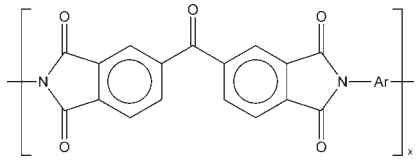	3.4	410
PI-4	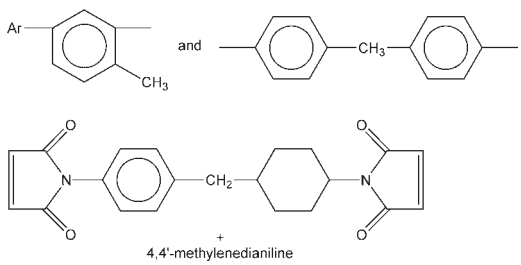 4,4'-methylenedianiline	0.6	310
PA-1	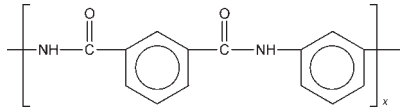	5.8	315
PA-2	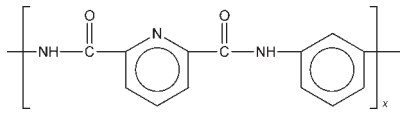	9.7	330
PAI-1	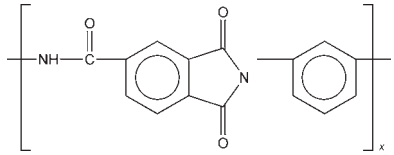	6.2	340

Table 5.3 *Continued*

PAI-2	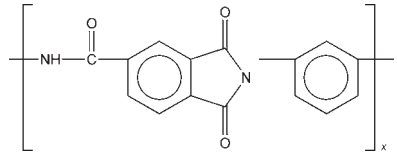	12.6	395
PAI-3	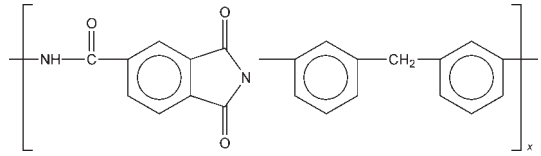	8.9	340

*Reprinted with permission from D.D. Schlueter and S. Siggia, Analytical Chemistry, 1977, **49**, 14, 2343. ©1977, ACS. [25]*

Table 5.4 Analysis of polyimides (PI), polyamides (PA) and poly(amide-imides) (PAI) by alkali fusion RGC

Sample	Diamine produced	Mol% of theoretical[a] ± RSD[b]	
		5 min at 380 °C	30 min from 100 to 390 °C
PI-1	4,4´-Methylenedianiline	98.3 ± 0.8	97.5 ± 0.9
PI-2	*m*-Phenylenediamine	89.1 ± 0.7 91.2 ± 0.9 91.6 ± 1.3	91.0 ± 0.8 91.0 ± 0.7
PI-3	2,4-Toluenediamine	73.1 ± 0.2 97.8 ± 0.5	73.2 ± 1.0 99.1 ± 1.2
	4,4´-Methylenedianiline	24.8 ± 0.3	25.9 ± 0.2
PA-1	*m*-Phenylenediamine	100.7 ±0.6	97.0 ± 1.7 97.7 ±1.7 97.9 ± 1.0 99.6 ± 2.6
PA-2	*m*-Phenylenediamine	95.9 ± 0.6 96.4 ± 1.5	93.1 ± 0.7 93.3 ± 0.5
PAI-1	*m*-Phenylenediamine	93.5 ± 0.9	93.1 ± 0.7 95. 3 ± 0.5

Table 5.4 *Continued*			
PAI-2	*m*-Phenylenediamine	93.5 ± 1.1 94.1 ± 0.6 95.1 ± 1.2	97.4 ±0.9
PAI-3	4,4´-Methylenedianiline	98.0 ± 1.1	98.8 ± 1.1

[a]*These recovery values are based on the structures shown in Table 5.5, which assume that one mole of diamine is produced for each mole of repeat unit*

[b]*The relative standard deviation is based on five or more determinations*

Reprinted with permission from D.D. Schlueter and S. Siggia, Analytical Chemistry, 1977, ***49****, 14, 2349. ©1977, ACS [25]*

5.3 Simultaneous Pyrolysis Derivatisation

Challinor [29] has developed a method involving simultaneous pyrolysis-alkylation-GC and applied it to the characterisation of a range of polyesters, phenolic resins and polymer additives. The technique gives additional information about the composition of carboxylic acids, alcohols and substituted phenolic compounds in the pyrolysis products of these polymer types. The procedure involves methylation or butylation, using tetramethyl- or tetrabutyl-ammonium hydroxide, in the pyrolysis zone of the pyrolyser with analysis by flame ionisation GC or GC-MS. The advantages are greater structural information, minimal sample manipulation and increased sensitivity.

Similarly, Venema and Boom-Van Geest [30] have described an *in situ* hydrolysis/methylation pyrolysis-GC method for the characterisation of polymers. Carboxyl, aromatic amino and hydroxy functional groups in polymers were methylated in this procedure.

5.4 Prepyrolysis Derivatistion

Another recent development in derivatisation technology is of the prepyrolysis type. The purpose of this type of derivatisation is to convert the functional group in the polymer in a design way to obtain a favorable thermal degradation pathway during pyrolysis. These favourable pathways normally utilise a major monomer or monomer-related fragment to allow for easier qualitative and quantitative analysis. The major difference between the prepyrolysis derivatisation and postpyrolysis derivatisation is that the polymer backbone should be stable enough to resist the attack from the

derivatisation reagent in prepyrolysis derivatisation. Pyrolysis is merely the mechanism to decompose the polymer to fragments.

In the prepyrolysis derivatisation, the main considerations of this modification or derivatisation are four-fold:

1. Ease and convenience; the derivatisation reaction takes place without rigorous conditions such as heating the sample to high temperature or reacting in high pressure.

2. Reduced interference from surrounding materials; most derivatisation reagents for primary amines are hydrogen sensitive, which means these reagents cannot be used in aqueous solutions or chemicals with alcohol or acid functional groups.

3. The final product will degrade with a favorable thermal degradation pathway. The derivatisation reaction will produce a stable functional group. Under thermal degradation, this derivatised polymer will depolymerise with either an unzipping pathway or a major fragment-producing pathway.

4. The major monomer or fragment produced either by the unzipping reaction or by monomer-related chain cleavage should be suitable for GC separation and detection. For example, the monomer or fragment should be a nonpolar compound when a nonpolar capillary separation column is used. The elution time of the fragment should not be so fast as to lose the resolution from other pyrolysates in the separation. At the same time, the elution time should not be too long, which would waste analysis time.

A thermal degradation pathway reselection study of polymethacrylic acid through derivatisation [31] demonstrated the value of prepyrolysis derivatisation in Py-GC qualitative and quantitative analysis. The pyrolysis of polymethacrylic acid, produced a number of pyrolysates that reflected the unzipping degradation as well as the random chain scission and recombination. If the polymer has been derivatised by tetramethyl ammonium hydroxide to convert the acid functional group to methyl ester, the thermal degradation of PMMA only produces one major fragment which is the methyl methacrylate monomer. In the same study, several copolymers containing low levels of methacrylic acid were successfully characterised by this prepyrolysis derivatisation technique.

The study of a styrene-butyl acrylate copolymer system [32] demonstrated that the statistical distribution of triads can be correlated to the trimers obtained from Py-GC. If all eight trimers are well resolved in the pyrogram and the peak area can be obtained, the number-average sequence length as well as composition can be calculated from these trimer peak intensities.

In many other polymer cases, because of the stability of the trimer components, they do not always contain all the trimer peaks in the pyrogram. An example is the styrene-MMA copolymer system [33]. The dimers and trimers of methyl methacrylate do not normally exist in the pyrogram under any pyrolysis conditions. However, the structure information can still be obtained by utilising the monomer peak intensity to generate the composition along with the information obtained from other trimers.

The trimers produced from pyrolysis of polymers are not always fragments with the three original monomer units bonded together. Sometimes, the trimers may go through a decomposition to lose certain easy to lose fragments to form more stable compounds. An example is the vinyl chloride—vinylidene chloride copolymer system [34]. The pyrolysis mechanism involves a dehydrohalogenation reaction to form benzene, chlorobenzene, dichlorobenzene, and trichlorobenzene. With the knowledge of monomer reactivities and polymerisation kinetics, a correlation can be made between the triad distribution of the polymer to that detected in the pyrogram. The copolymer structure as well as composition can be elucidated.

Polymeric structure determination does not have to be limited by the copolymer system. Other polymers that are produced by other methods may be treated as a copolymer system consisting of two different types of monomers. Chlorinated polyethylene is a good example [35]. In some circumstances, a chlorinated polyethylene system can be considered as a copolymer system of vinyl chloride and 1,2-dichloroethylene. By examining the appropriate fragments that correspond to the trimer combination of vinyl chloride and 1,2-dichloroethylene, one can utilise a statistical formula to calculate the number-average sequence length and composition. One can also explore the chlorine content as well as the arrangement of chlorine atoms in the polyethylene chain.

References

1. D.L. Miller, E.P. Samsel and J.G. Cobler, *Analytical Chemistry*, 1961, **33**, 6, 677.

2. J. Haslam, J.B. Hamilton and A.R. Jeffs, *Analyst*, 1958, **83**, 983, 66.

3. J. Haslam and A.R. Jeffs, *Journal of Analytical Chemistry*, 1957, **7**, 24.

4. E.P. Samsel and J.A. McHard, *Industrial and Engineering Chemistry Analytical Edition*, 1942, **14**, 9, 750.

5. D. G. Anderson, K. E. Isakson, D. L. Snow, D. J. Tessari, and J. T. Vandeberg, *Analytical Chemistry*, 1971, **43**, 7, 894.

6. R. Fritz, *Fresenius' Zeitschrift für Analytical Chemistry,* 1960, **176**, 421.

7. A. Steyermark, *Journal of the Association of Official Agricultural Chemists*, 1955, **38**, 367.

8. S. Ehrlich-Rogozinski and A. Patchornik, *Analytical Chemistry*, 1964, **36**, 4, 840.

9. F. Viebock and C. Brechner, *Berichte der Deutschen Chemischen Gesellschaft*, 1930, **63**, 3207.

10. R.D. Parker, Dow Corning Corporation, Barry, UK, unpublished procedure.

11. G. Gritz and H. Hurcht, *Zeitschrift fur Anorganische und Allgemeine Chemie*, 1962, **317**, 35.

12. V.M. Krasikova, A.N. Kaganova and V.D. Lobtov, *Journal of Analytical Chemistry USSR*, 1971, **28**, 1458. [English translation]

13. M.G. Voronlov and V.T. Shemyatenkova, *Bulletin of the USSR Academy of Sciences, Division of Chemical Science*, 1961, 178. [*Chemical Abstracts*, 1961, **55**, 16285b.]

14. J. Franc and K. Placek, *Collection of Czechoslovak Chemical Communications*, 1973, **38**, 513.

15. J. Franc, *Chemical Abstracts*, 1975, **82**, 67923q.

16. A.P. Kreshkov, V.T. Shemyatenkova, S.V. Syavtsillo and N.A. Palarmarchuck, *Journal of Analytical Chemistry USSR*, 1960, **15**, 727. [English translation]

17. G.W. Heylmun, R.L. Bujalski and H.B. Bradley, *Journal of Gas Chromatography*, 1964, **2**, 300.

18. V.M. Krasikova and A.N. Kaganova, *Journal of Analytical Chemistry USSR*, 1970, **25**, 1212. [English translation]

19. E.R. Bissell and D.B. Fields, *Journal of Chromatographic Science*, 1972, **10**, 164.

20. J. Franc and K. Placek, *Mikrochimica Acta*, 1975, **64**, 1, 31.

21. C.L. Hanson and R.C. Smith, *Analytical Chemistry*, 1972, **44**, 9, 1571.

22. J.K. Haken, P.A.D.T. Vimalasiri and R.P. Burford, *Journal of Chromatography*, 1984, **399**, 1, 295.

23. J.K. Haken, *Trends in Analytical Chemistry*, 1990, **9**, 1, 14.

24. P.A.D.T. Vimalasiri, R.P. Burford and J.K. Haken, *Rubber Chemistry and Technology*, 1987, **60**, 3, 555.

25. D.D. Schlueter and S. Siggia, *Analytical Chemistry*, 1977, **49**, 14, 2343.

26. D.D. Schlueter and S. Siggia, *Analytical Chemistry*, 1977, **49**, 14, 2349.

27. D.D. Schlueter, *Applications of Alkali Fusion Reaction Gas Chromatography to Organic Functional Group Analysis*, University of Massachusetts, 1976 [Ph.D. Thesis].

28. S.P. Frankoski and S. Siggia, *Analytical Chemistry*, 1972, **44**, 3, 507.

29. J.M. Challinor, *Journal of Analytical Applied Pyrolysis*, 1989, **16**, 4, 323.

30. A. Venema and R.C.A. Boom-Van Geest, *Journal of Microcolumn Separations*, 1995, **7**, 4, 337.

31. F.C-Y. Wang, *Analytical Chemistry*, 1998, **70**, 17, 3642.

32. F.C-Y. Wang, B.B. Gerhart and P.B. Smith, *Analytical Chemistry*, 1995, **67**, 19, 3536.

33. F.C-Y. Wang and P.B. Smith, *Analytical Chemistry*, 1996, **68**, 17, 3033.

34. F.C-Y. Wang and P.B. Smith, *Analytical Chemistry*, 1996, **68**, 3, 425.

35. F.C-Y. Wang and P.B. Smith, *Analytical Chemistry*, 1997, **69**, 4, 618.

6 Sequencing of Homopolymers

This chapter is concerned with the precise sequence in which monomer units exist in a homopolymer. This information is quite different from that covered in methods for the determination of the ratio in which monomer units occur. Sequencing in copolymers is more complicated and is dealt with separately in Chapter 7.

6.1 Sequencing in Polyethylene

Voigt [1] states that the formation of decomposition products of polyethylene (PE) is a result of a primary step in a statistical thermal breaking down of a chain:

$$–CH_2–CH_2–CH_2–CH_2– \rightarrow –CH_2–CH_2^{\bullet} – {}^{\bullet}CH_2–CH–$$

in which the free radicals formed can react further either by depolymerisation (unzipping) or by the transfer of hydrogen atoms. The first type of reaction leads to the corresponding monomers, while the latter competes with continuing decomposition of the chains to form a spectrum of hydrocarbons with different chain lengths. This spectrum contains, apart from saturated hydrocarbons and diolefins, olefins which, in their structure and quantitative distribution, are dependent in characteristic manner on the nature of the initial polymers, as might well be expected. The very marked depolymerisation which takes place with other polymers - such as polymethacrylates, polystyrene (PS), and the like - does not appear to play any major role in the cases of polyethylene or other polyolefins, since the corresponding monomers do not exist in any considerable excess as compared with the other decomposition products. As is to be expected, only unbranched fractions arising from statistical decomposition arise in the case of polyethylene, which breaks down with reactions of the following type:

$$CH_2–CH_2–CH_2^{\bullet} + {}^{\bullet}CH_2–CH_2 \rightarrow –CH_2–CH{=}CH_2 + CH_3–CH_2–$$

$$–CH_2–CH_2–CH_2– + {}^{\bullet}CH_2–CH_2– \rightarrow - CH_2–CH–CH_2– + CH_3–CH_2–$$

$$–CH_2–CH_2–CH_2–CH_2–CH_2– \rightarrow –CH_2–CH{=}CH_2 + {}^{\bullet}CH_2–CH_2– \qquad (6.1)$$

The very small amounts of branched molecules which are present even in low-pressure polyethylenes do not make themselves noticeable on the gas chromatogram under the conditions employed by Voigt [1]. Branched molecules are, however, found under other more searching gas chromatographic conditions. In this connection, it should be pointed out that high-pressure polyethylenes produced completely identical gas chromatograms.

According to Wall and co-workers [2] the pyrolysis of polyethylene proceeds by a radical chain mechanism. The products formed result from the process of random-chain cleavage, followed by intermolecular or intramolecular hydrogen abstraction. Hydrogen abstraction occurs preferentially at tertiary carbon atoms, and product formation results from homolysis of the carbon-carbon bond at the beta position relative to the radical site. The major products formed are the *n*-alkanes and alpha-omega-diolefins. The peaks between the triplets result from chain branching.

From an examination of the products formed from the pyrolysis of high-density polyethylene and polymethylene, Tsuchiya and Sumi [3, 4] proposed that the major hydrogen-abstraction reaction is due to an intramolecular cyclisation. They proposed that, following initial radical formation at C_1, successive intramolecular hydrogen abstractions occur along the chain resulting in the formation of new radicals at C_5, C_9 and C_{13} as shown in Equations 6.2 to 6.5.

$$R\text{–}R \rightarrow 2\ R \tag{6.2}$$

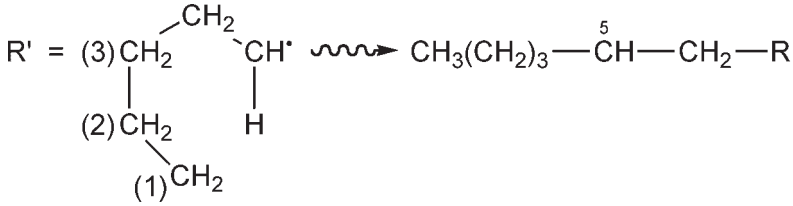

(6.3)

$$CH_3\text{–}(CH_2)_3\text{–}CH\text{–}CH_2\text{–}R \rightarrow CH_3\text{–}(CH_2)_6\text{–}CH_2\text{–}\overset{9}{C}H\text{–}CH_2R \tag{6.4}$$

$$CH_3\text{–}(CH_2)_6\text{–}CH_2\text{–}\overset{9}{C}H\text{–}CH_2\text{–}R \rightarrow CH_3\text{–}(CH_2)_{11}\text{–}\overset{11}{C}H\text{–}CH_2\text{–}R \tag{6.5}$$

Cleavage of the carbon-carbon bonds at the beta position to these macroradicals, results in the formation of increased amounts of C_6, C_{10} and C_{14} α-olefins and C_3, C_7 and C_{11} *n*-alkanes over that which could be predicted from statistical-chain cleavage.

6.2 Sequences in Polypropylene

The studies of Wall and Straus [5] indicate that pyrolysis of polypropylene proceeds, principally by random cleavage of the polymer chain. Voigt observed no straight-chain decomposition products of polypropylene with a chain length greater than C_5, a fact that is in agreement with the prediction readily deduced from the head-to-tail structures of the polymer. The larger decomposition products all contain methyl branches, and the multiple-branched chains contain the expected 2,4-branching.

Van Schooten and Evenhuis [6] and van Schooten and Mostert [7] found identical pyrolysis patterns for various polypropylene samples. Depolymerisation is much more important for polypropylene whose pyrogram can be interpreted as originating from intramolecular hydrogen transfer with the fifth carbon atom of the secondary radical:

1,*n*-pentane + 1, 1,2,4 dimethyl heptane (6.6)

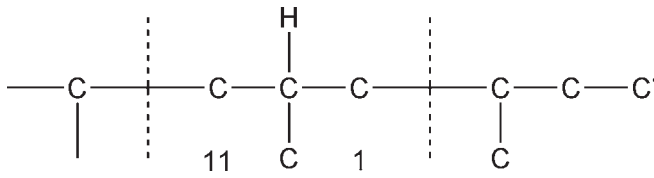

(6.7)

The primary radical gives it this way:

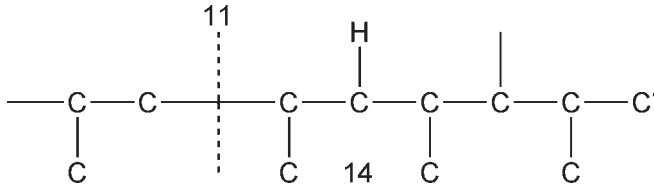

(6.8)

The isobutane and especially the methane peaks are rather small, indicating that this reaction is not very frequent for the primary radical. For this radical, hydrogen transfer with the sixth carbon atom might be more important, as the 2-methylpentane peak could be explained in this way. Another possibility is that this peak has to be ascribed to intramolecular hydrogen transfer reactions (i.e., formation of 2-methylpentadiene). **Table 6.1** lists the products expected from intramolecular hydrogen transfer during the pyrolysis of polypropylene.

Inoue and co-workers [8], Zambelli and co-workers [9] and Randall [10] have shown that ^{13}C-NMR is an informative technique for measuring stereochemical sequence distributions in polypropylene. These workers reported chemical shift sensitivities to configurational tetrad, pentad and hexad placements for this polymer.

Table 6.1 Products expected from intramolecular hydrogen transfer during pyrolysis of polypropylene (main peaks found in program are underlined)

	Number of the hydrogen-donating carbon				
	5	**6**	**7**	**8**	**9**
Secondary radical 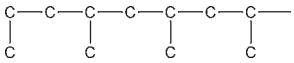	<u>nC_5</u> <u>2.4MC</u>	CH_4 <u>$2MC_5$</u> $4MC_7$* $4.6MC_9$	$4MC_7$ $2.4.6MC_9$	CH_4 $2.4MC_7$ $4.6MC_9$* $4.6.8MC_{11}$	$4.6MC_9$ $2.4.6.8MC_{11}$
Primary radical 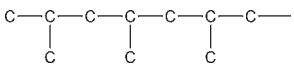	$1C_4$ <u>$2MC_5$</u> <u>$2.4MC_7$</u> CH_4	<u>$2MC_5$</u> $2.4.6MC_7$	CH_4 $2.4MC_5$ $2.4MC_7$ $2.4.6MC_9$	$2.4MC_7$ $2.4.6.8MC_9$	CH_4 $2.4.6MC_7$ $2.4.6MC_9$ $2.4.6.8MC_{11}$

**Formed by hydrogen exchange with a methyl group.*

nC_5 = n-pentane, $4MC_7$ = 4-methyl heptane, $4.6MC_9$ = 4,6-dimethylnonane, $2MC_5$ = 2-methyl pentane, $2.4MC_7$ = 2,4-dimethyl heptane, $2.4.6MC_7$ = 2,4,6-trimethylnonane.

Reprinted with permission from J. van Schooten and J.K. Evenhuis, Polymer, 1965, 6, 11, 561. ©1965, Elsevier [6]

The sequence lengths of stereochemical additions in amorphous and semicrystalline polypropylene were accurately measured using ^{13}C-NMR [11]. The method has some limitations for addition polymers having predominantly isotactic sequences.

Randall [12] has described work on the application of quantitative ^{13}C-NMR to measurements of average sequence length of like stereochemical additions in polypropylene. He describes sequence lengths of stereochemical addition in vinyl polymers in terms of the number-average lengths of like configurational placements. Under these circumstances a pure syndiotactic polymer has a number-average sequence length of 1.0; a polymer with 50:50 meso-racemic additions has a number-average sequence length of 2.0 and polymers with more meso than racemic additions have number-average sequence lengths greater than 2.0. Amorphous and crystalline polypropylenes were examined using ^{13}C-NMR, as examples of the applicability of the average sequence length method. The results appear to be accurate for amorphous and semi-crystalline polymers but limitations are present when this method is applied to highly stereoregular vinyl polymers containing predominantly isotactic sequences [12]. Randall has measured the ^{13}C-NMR spin lattice relaxation times of isotactic and syndiotactic sequences in amorphous polypropylene. Spin-lattice relaxation times for methyl, methylene, and methine carbons in an amorphous polypropylene

were measured as a function of temperature from 46 to 138 °C. The carbons from isotactic sequences characteristically exhibited the longest spin relaxation times of those observed. The spin relaxation time differences increased with temperature with the largest differences occurring for methine carbons, where a 32% difference was observed. Randall determined activation energies for the motional processes affecting spin relaxation times for isotactic and syndiotactic sequences. Essentially no dependence upon configuration was noted. High-resolution NMR spectra of isotactic and syndiotactic polypropylene have been used by Cavelli [13] to provide conformational information.

It is known [14, 15] that, on the surface of the heterogeneous Ziegler-Natta catalysts promoting the isotactic polymerisation of propene, active centres are also present which may give rise to the formation of significant amounts of '*r*-rich' sequences (syndiotactic or 'syndiotactoid'). As a matter of fact, syndiotactic polypropene was isolated for the first time as an 'impurity' from samples of isotactic polypropene prepared in the presence of catalyst systems such as, for example, α- or γ -$TiCl_3$ in combination with $Al(C_2H_5)_2F$ or LiC_4H_9 [16].

The fraction of *r*-rich sequences is higher in polypropene samples obtained with $MgCl_2$-supported 'high-yield' catalysts, particularly when suitable Lewis bases are added to the Al-alkyl cocatalyst [17-20]. High-yield catalyst systems have been disclosed which are able to produce polypropene samples containing up to one-third by weight of such sequences [19].

The ^{13}C-NMR spectroscopic characterisation of propene homopolymers and copolymers with low amounts of [1-^{13}C]-ethene obtained with the above catalysts allowed Busico and co-workers [18, 21] to prove that this type of (predominantly) syndiotactic chain propagation proceeds via 1,2 (primary) propene insertion (as already known for the isotactic propagation), under the steric control of the monomeric unit added last.

In these polymers, the fractions which are extractable with low-boiling solvents (e.g., diethyl ether, pentane, hexane) may be conceived, from the microstructural viewpoint, as mixtures of enantiomorphic-site controlled isotactoid sequences and of chain-end controlled syndiotactoid sequences.

In fact, the experimental distributions of the steric pentads, as evaluated from routine ^{13}C-NMR spectra, can be reasonably reproduced within a simple 'two site' statistical model (see, for example references [18, 22, 23]), with three adjustable parameters: σ (probability of formation of a *R-(S-)* unit at a *R-(S-)* preferring isospecific centre), P_r (probability of formation of an *r* diad at a syndiospecific centre), and *w* (weight fraction of the polymer formed at the isospecific centres).

However, some mismatch is usually observed in the region of the *mr*-centred, pentads; this has been proposed to result from the presence of steric pentads arising from chemical junctions between isotactoid and syndiotactoid sequences (blocks) [21, 23].

The pentad distribution, with (a maximum of) only nine independent data, is not an adequate basis for more sophisticated statistical calculations. On the other hand, with the availability of ^{13}C-NMR spectrometers operating at very high magnetic fields, it is now possible to expand the microstructural determination on propene polymers to the heptad level at least.

Busico and co-workers [24] presents the main results of a 150 MHz ^{13}C-NMR characterisation of polypropene fractions containing high amounts of syndiotactoid sequences, and of the statistical analysis of the spectroscopic data in terms of a Coleman-Fox type [25] 'two-site' model taking into account the hypothesis of junctions between isotactoid and syndiotactoid sequences.

The results provide additional evidence in favour of this hypothesis, namely, the copresence of *m*-rich and *r*-rich sequences (stereoblocks) in single polypropene molecules. This indicates the ability of isospecific and syndiospecific active centres to interconvert reversibly in times which are shorter than the average growth times of the polymer chains.

As representative examples Busico selected two different fractions (fraction A, diethyl ether-soluble; fraction B, hexane-soluble/pentane-insoluble) of a polypropene sample prepared in the presence of the catalyst system $MgCl_2/TiCl_4$-TMP/$Al(C_2H_5)_3$ (TMP = 2,2,6,6-tetramethylpiperidine).

The methyl region of the 150 MHz ^{13}C-NMR spectrum of fraction B is shown in **Figure 6.1**.

When not assigned in the literature [26, 27] the resonances were attributed on the basis of chemical shift calculations according to the γ-gauche effect [27] and by comparative analysis with the 150 MHz ^{13}C-NMR spectra of samples of isotactic and syndiotactic polypropene prepared with homogeneous group IV metallocene-based catalysts [28].

A complete resolution was achieved for the resonances arising from the *mmmm*-centred and *rr*-centred heptads, the latter showing a fine structure reaching the nonad or even the undecad level.

In the first column of **Tables 6.2 and 6.3**, Busico and co-workers [24] report the experimental stereosequence distributions of the two fractions, as evaluated from the spectral integration.

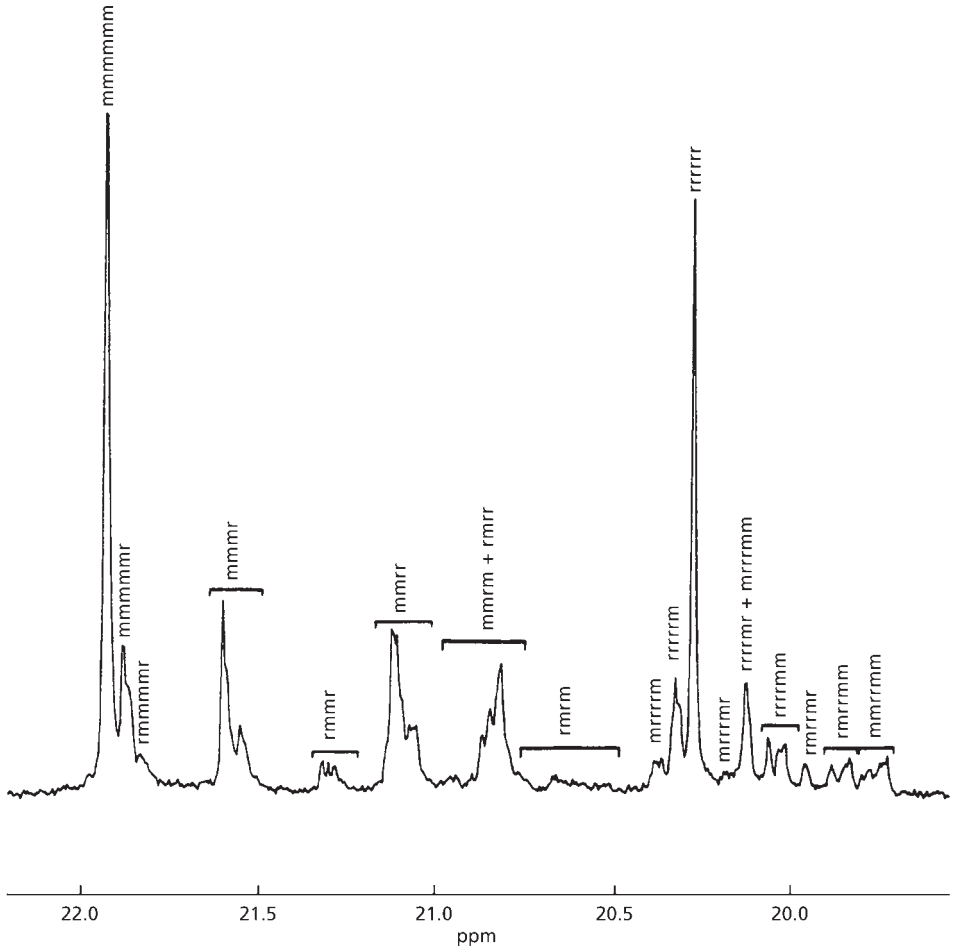

Figure 6.1 Methyl region of the 150 MHz ^{13}C-NMR spectrum of fraction B (δ scale in ppm downfield from TMP). (*Reprinted with permission from V. Busico, P. Corradini, R. De Biasio, L. Landriani and A.L. Segre, Macromolecules, 1994, **27**, 16, 4521. ©1994, ACS, USA [24]*)

Table 6.2 Experimental Stereosequence Distribution for Fraction A and Best-Fitting Distributions Calculated According to the Two Statistical Models

Stereosequence	% (experimental)	% (calculated, 'two-site')	% (calculated, 'Coleman-Fox two-site')
mmmmmm	8.8	10.2	8.4
mmmmmr + rmmmmr	6.6	7.5	7.4
mmmr	11.0	11.7	12.1
rmmr	3.6	3.0	3.0
mmrr	15.1	12.8	14.1
mmrm + rmrr + rmrm	19.5	21.5	19.4
rrrrrr	8.6	8.9	8.5
rrrrrm + mrrrrm	7.4	6.3	7.8
mrrrmr	1.5	1.8	1.8
rrrrmr + mrrrmm	5.6	5.9	5.7
rmrrmr	1.2	1.8	1.6
rmrrmm	3.2	2.3	2.4
mmrrmm	2.8	3.3	2.7
		$\sigma = 0.76$ $P_r = 0.81$ $w = 0.69$	$\sigma = 0.80$ $P_r = 0.86$ $w = 0.65$ $p_{i/s} = 0.088$ $(p_{s/i} = 0.17)$
		$10^3\Sigma^a = 2.1$ $10^4\Omega^b = 1.9$	$10^3\Sigma^a = 0.48$ $10^4\Omega^b = 0.48$

[a] $\Sigma = \Sigma(y_i - y_i^\circ)^2$, [b] $\Omega = \Omega(y_i - y_i^\circ)^2/(n\text{-}m)$ *(where n (= 14) is the number of independent experimental data and m is the number of adjustable parameters.*

Reprinted with permission from V. Busico, P. Corradini, R. De Biasio, L. Landriani and A.L. Segre, Macromolecules, 1994, 27, 16, 4521. ©1994, ACS [24]

Table 6.3 Experimental Stereosequence Distribution for Fraction B and Best-Fitting Distributions Calculated According to the Two Statistical Models

Stereosequence	% (experimental)	% (calculated, 'two-site')	% (calculated, 'Coleman-Fox two-site')
mmmmmm	17.9	18.1	17.6
mmmmmr + rmmmmr	8.3	8.6	8.5
mmmr	10.0	11.5	11.5
rmmr	2.4	1.8	1.7
mmrr	13.6	12.0	12.4
mmrm + rmrr + rmrm	13.6	14.3	13.1
rrrrrr	14.1	14.1	14.0
rrrrrm + mrrrrm	5.3	5.3	6.3
mrrrmr	0.7	0.9	0.9
rrrrmr + mrrrmm	4.1	4.7	4.6
rrrrmm	4.3	2.2	3.5
rmrrmr	1.0	0.9	0.8
rmrrmm	1.5	1.7	1.7
mmrrmm	3.2	3.9	3.4
		$\sigma = 0.82$ $P_r = 0.88$ $w = 0.70$	$\sigma = 0.84$ $P_r = 0.90$ $w = 0.67$ $p_{i/s} = 0.028$ $(p_{s/i} = 0.057)$
		$10^3\Sigma^a = 1.1$ $10^4\Omega^b = 1.0$	$10^3\Sigma^a = 0.67$ $10^4\Omega^b = 0.67$

[a] $\Sigma = \Sigma(y_i - y_i^\circ)^2$, [b] $\Omega = \Omega(y_i - y_i^\circ)^2/(n\text{-}m)$ *(where n (= 14) is the number of independent experimental data and m is the number of adjustable parameters.*

Reprinted with permission from V. Busico, P. Corradini, R. De Biasio, L. Landriani and A.L. Segre, Macromolecules, 1994, **27**, *16, 4521. ©1994, ACS [24]*

6.3 Sequences in Polyisoprene

Polyisoprene (hydrogenated natural rubber) is a completely alternating ethylene propylene copolymer (i.e., has not ethylene or propylene blocking) and is therefore an interesting substance for pyrolysis gas chromatography (Py-GC) studies. The surface area of the main peaks up to C_{13} obtained by Van Schooten and Evenhuis [6, 29] indicate that the unzipping reaction which would yield equal amounts of ethylene and propylene in the hydrogenated pyrolysate, evidently takes place to some extent, but is less important than the hydrogen transfer reactions:

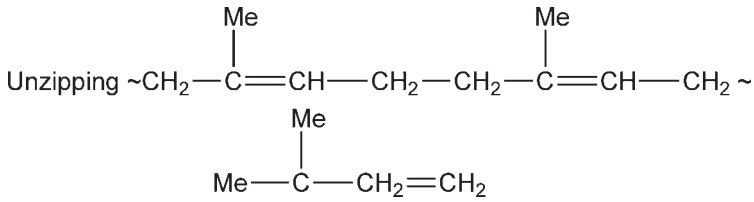

(6.9)

The large numbered peaks produced upon Py-GC reflect the many possible transfer reactions for this polymer some of which are illustrated next. Hydrogen transfer reactions which occur from the fifth carbon atom predominate as indicated by the large butane, 3-methyl hexane and 2-methyl heptane peaks:

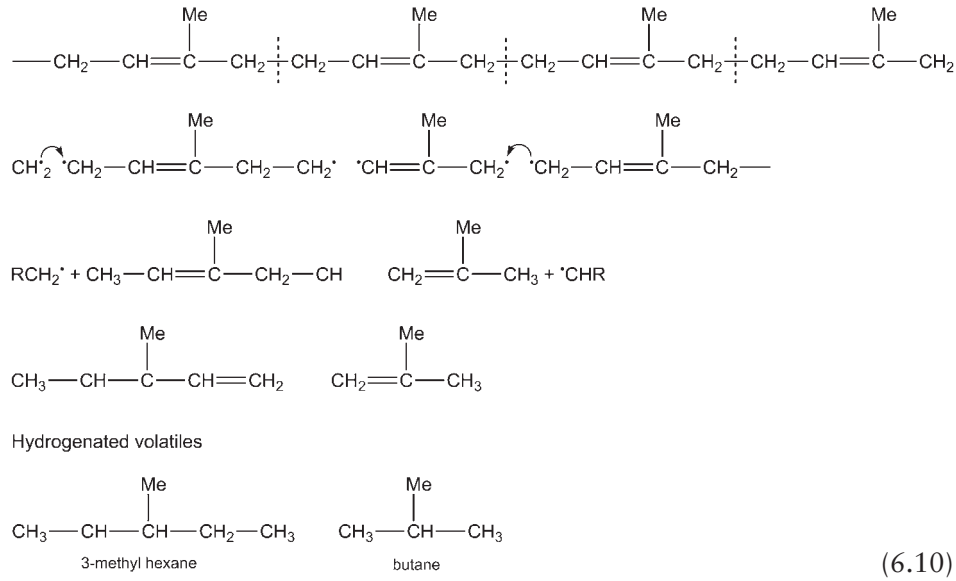

(6.10)

Hydrogen transfer also from the ninth carbon atom, which is shown by the size of the 3-methyl nonane, 3,7-dimethyldecane and the 2,6-dimethylundecane peaks:

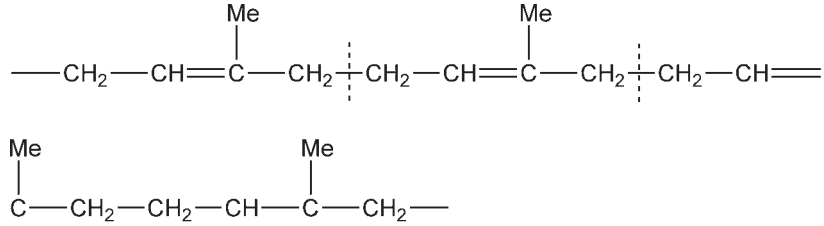

Products after hydrogenation

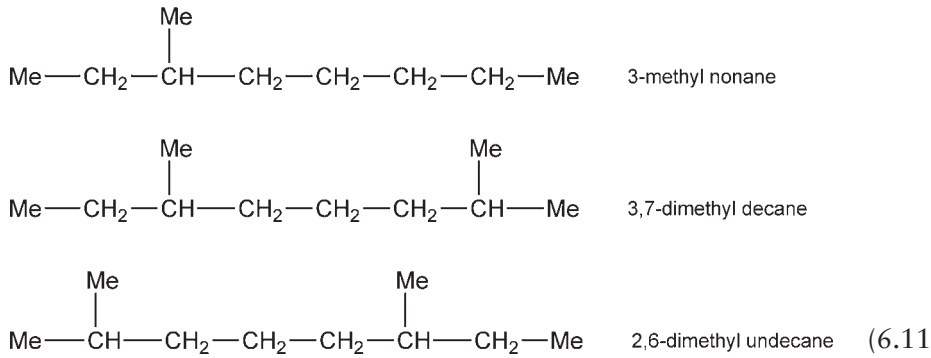

(6.11)

Ozonozation

The technique has been applied to various unsaturated polymers. Thus, polyisoprene, having nearly equal 1,4 and 3,4 structures, produced large amounts of laevulinaldehyde, succinaldehyde and 2,5 hexanedione, indicating blocks of 1,4 structures in head-tail, tail-tail and head-head configurations.

Thus the ozonide of the tail-to-tail 1,4 configuration upon ozonisation and hydrolysis yields succinaldehyde (CHO-CH_2-CH_2-CHO). Similarly, the ozonides of the head-to-tail and head-to-head configurations yield laevulinaldehyde (CHO-CH_2-CH_2-CO-CH_3) and 2,5-hexane dione (-CH_3-CO-CH_2-CH_2-CO-CH_3), respectively.

Boochathum and co-workers [30] applied ozonisation-gel permeation chromatography (GPC) to a study of the structure of solution grown *trans* 1,4-poyisoprene crystals.

Crystallisation of synthetic *trans*-l,4-polyisoprene (TPI) at -20 °C in hexane and amylacetate solutions gave chain-folded α-type crystals with 53% and 57% crystallinity, respectively. Selective ozonolysis degradation of the isoprene units in the surface folds associated with high-resolution GPC measurement was used to determine the crystalline stem length, stem length distribution and fold surface structure of the TPI crystals.

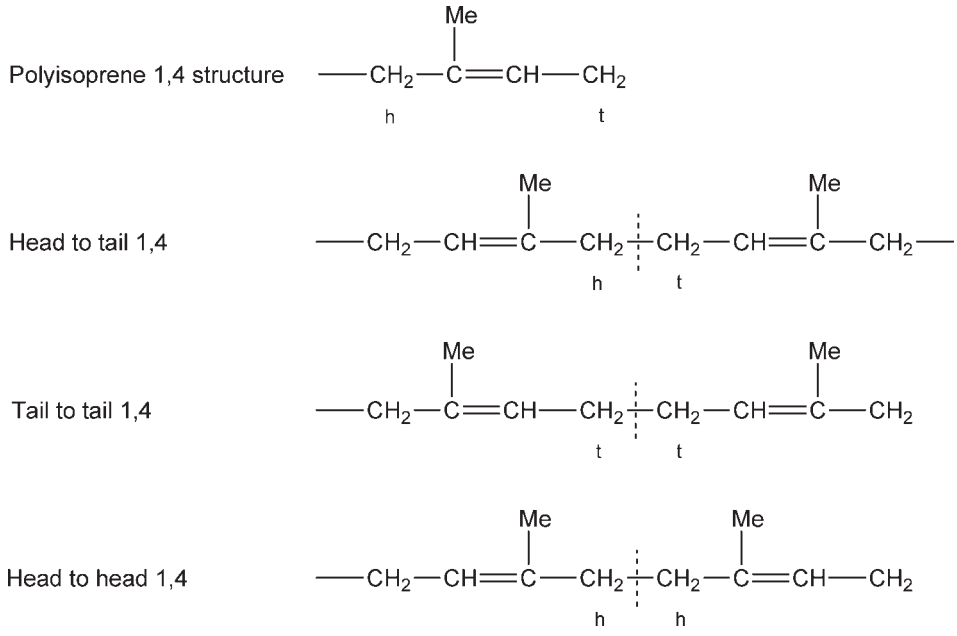

(6.12)

The oligomer fraction, obtained by ozonolysis of solution grown TPI crystals grown in hexane followed by reduction with lithium aluminium hydride was found by ^{1}H- and ^{13}C-NMR measurements to comprise a series of homologues of the *trans*-1,4-isoprenoid compounds of the following structure:

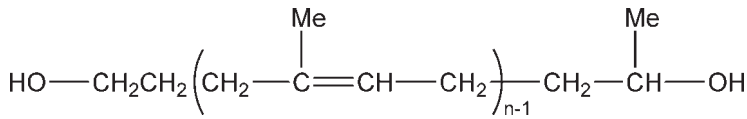

(6.13)

The whole products obtained was composed of high-molecular weight fractions, which are assumed to come from the piled-up lamellae, and also oligomer parts of single traverses and double traverses, which are assumed to come from monolayers and bilayers, respectively. The purified oligomer fractions of single traverses were subjected to high-resolution GPC in order to determine the molecular weight of each fraction via the standard calibration curve.

As ozone uptake increased, the isoprene units of the main fraction of oligomer products were found to decrease from 13, reaching a constant value at 11 for hexane and 12 for amylacetate. The polydipersity of the oligomer fractions was found to be in the range of 1.01-1.02. These findings suggested that the chain fold structure might be tight folding with slightly irregular folds, with a stem length of 11 monomers and a dispersion of 2.3 for lamellae grown from hexane, and 12 monomers with dispersion of 2.3 for those grown from amylacetate.

6.4 Sequences in Polystyrene

Static secondary ion mass spectrometry (SIMS) [31] has been applied to structural characterisation [32-35] and surface analysis of polymers [36, 37]. Polymers can be identified from fingerprint spectra or from fragments characteristic of the backbone and pendant groups. Liquid matrix SIMS-FAB-MS has provided only approximate oligomer distribution.

SIMS spectra of polymers have been confined to the low-mass range *(m/z* ≤ 500) mainly due to the mass analysers used (e.g., quadrupole). With the advent of high-transmission time-of-flight mass analysers coupled to sensitive detection systems (e.g., post-acceleration and single ion counting), primary ion dosages have been reduced considerably, minimising fragmentation; detection of high mass ions (up to *m/z* ~5000) has been dramatically increased [38]. A series of aliphatic polyamides (Nylons) was studied by time-of-flight SIMS (TOF-SIMS) [39]. Cationisation of the repeat unit with Ag^+ and Na^+ produced high-mass ions characteristic of the type of Nylon and the repeat unit sequence in the polymer chain. Polymer fragments cationised with Ag^+ and Na^+, containing as many as 24 repeat units (Nylon 6) and as high as *m/z* ~3500 [Nylon 66(α6)], were detected.

Bletsos and co-workers [38] present SIMS spectra of diverse polymers: including polystyrene. The spectra were obtained by TOF-SIMS equipment, equipped with a mass-selected pulsed primary ion source, an angle- and time-focusing time-of-flight analyser, and a single-ion-counting detector. Fragmentation in the low-mass range provided some structural information about the repeat unit. Fragmentation patterns were unique for polymers having different repeat units but of equal mass; distinguishing between such polymers was possible. Oligomer distributions obtained from mass spectra compared well with distributions determined by other techniques (e.g., GPC) for the same polymers.

Several polystyrenes (PS) having various substituent groups at different positions on the hydrocarbon backbone or the benzene ring were studied. Part of the TOF-SIMS spectrum of PS is shown in **Figure 6.2** as a typical example. PS fragments cationised with Ag^+, $(nR + Ag)^+$ (R = amu), produce the most intense peaks in the spectrum above *m/z* = 500; the spacing between them corresponds to the repeat unit of the polymer. The pattern of fragment ion peaks within the spacing of one repeat unit is consistent throughout the spectrum and is characteristic of the repeat unit and its various substituent groups. For example, the peaks of the $(nR + Ag)^+$ series due to fragments containing 10 repeat units (*n* = 10) for poly(*p-tert*-butylstyrene) (R = 160 amu) and poly(4-methoxystyrene) (R = 134 amu) appear at *m/z* 1707 and 1447. The spacing between the $(nR + Ag)^+$ peaks for *poly(p-tert*-butylstyrene) is 160 amu and between the poly(4-methoxystyrene) is 134 amu. Therefore, from the peak position and the spacing between peaks the repeat units of polymers can be determined.

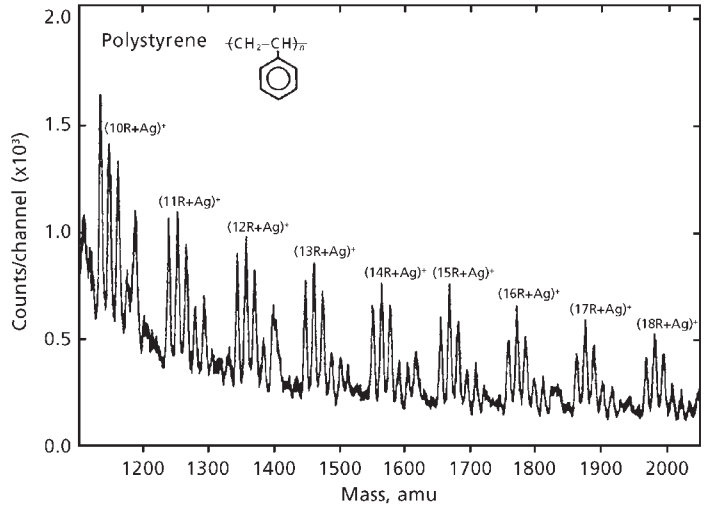

Figure 6.2 TOF-SIMS spectrum of PS in the range *m/z* 1100-2050. Peaks due to PS fragments containing an integral number of repeat units and cationised with Ag^+ are identified. The fragmentation pattern within each repeat unit spacing is repeated throughout the spectrum. (*Reprinted with permission from I.V. Bletsos, D.M. Hercules, D. Van Leyen and A. Benninghoven, Macromolecules, 1987,* ***20****, 2, 407. ©1987, ACS, USA [38]*)

Poly(α-methylstyrene) (P(α-MS)) and poly(4-methyl-styrene) (P(4-MS)) were studied to establish the effect of location of a substituent group on the TOF-SIMS spectrum. Specifically, it was sought to determine the effect of substituting a methyl group on a phenyl group and on the chain backbone. The repeat units of (P(α-MS)) and (P(4-MS)) have equal masses, R = 118 amu; the most prominent peaks, due to Ag^+ cationised fragments $(nR + Ag)^+$, for both (P(α-MS)) and (P(4-MS)) appear at exactly the same *m/z* values. Therefore, it is not possible to distinguish between (P(α-MS)) and (P(4-MS)) by the positions and the spacings of these peaks. The $(nR + Ag)^+$ however, are surrounded by a series of peaks of varying intensity spaced at $\pm n'\Delta m$, where $n' = 1, 2, 3$, and 4 and Δm = 14-16 mass units. Data are shown for the two polymers in **Table 6.4**. The positions of the smaller peaks and their relative intensities are different in the two spectra, permitting one to distinguish readily between (P(4-MS)) and (P(α-MS)).

The differences in fragmentation are due to the different positions of the $-CH_3$ substituent group in the two PS. It was generally observed that substituent groups at different locations in the backbone or the benzene ring produce different fragmentation patterns for the polystyrenes. Bond cleavage seems to occur statistically, and the chemical stability of the fragments produced is reflected by the peak intensities.

Table 6.4 Relative Intensities of Cluster Peaks for (P(α-MS)) and (P(4-MS)) Appearing at ± *n′*Δ*m* of the (*n*R + Ag)⁺ Series									
Polymer	**-4Δ*m***	**-3Δ*m***	**-2Δ*m***	**-Δ*m***	**(*n*R + Ag)⁺**	**+Δ*m***	**+2Δ*m***	**+3Δ*m***	**+4Δ*m***
(P(α-MS))	34	91	87	80	100	19	16	13	13
(P(4-MS))	50			100	91	67	51	48	42
*Reprinted with permission from I.V. Bletsos, D.M. Hercules, D. Van Leyen and A. Benninghoven, Macromolecules, 1987, **20**, 2, 407. ©1987, ACS, USA [38]*									

Mass spectrometry (MS) is also a useful technique for the determination of molecular weight distributions of low molecular weight polymers and can provide information about the structure of the repeat unit and the number of repeat units for individual oligomers. In contrast, classical techniques used for determining molecular weights (e.g., GPC, vapour pressure osmometry, light scattering, NMR) measure average properties of an oligomer mixture and do not yield information on different types of oligomers present.

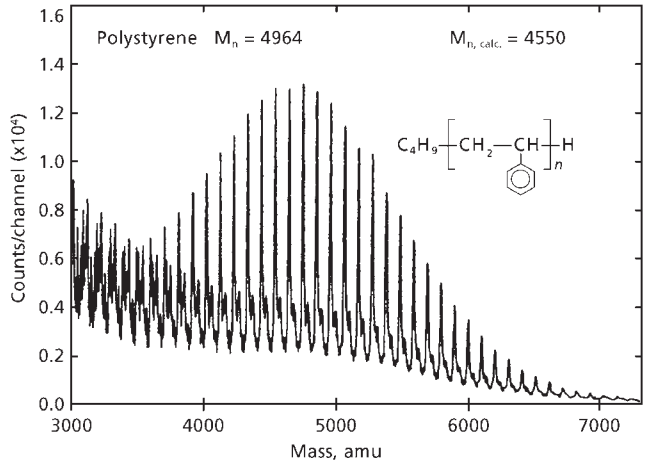

Figure 6.3 TOF-SIMS spectrum of PS standard in the range *m/z* 3000-7200, showing the distribution of PS oligomers cationised with Ag^+. The number average molecular weight determined by TOF-SIMS, $M_{n,calcd}$ = 4550, is within 8% of the value determined by GPC. M_n = 4964. (*Reprinted with permission from I.V. Bletsos, D.M. Hercules, D. Van Leyen and A. Benninghoven, Macromolecules, 1987, 20, 2, 407. ©1987, ACS, USA [38]*)

Molecular weight distributions obtained from TOF-SIMS spectra were evaluated by Bletsos and co-workers [38] by using polymer standards having known molecular weight distributions. A TOF-SIMS spectrum of a PS standard with a number average molecular weight (M_n) = 4964 (determined by GPC) is shown in **Figure 6.3**. Below *m/z* 3500, the most intense peaks are due to Ag^+ cationised polymer fragments corresponding to the series $(nR + Ag)^+$. In the range *m/z* 3500-7000, intact oligomers are detected giving rise to the $(nR + C_4H_9 + H + Ag)^+$ series. These peaks are the most intense in this range, and their intensity distribution reflects the number average molecular weight distribution of the PS standard. Loss of a terminal $-C_4H_9$ group results in the $(nR + Ag)^+$ series, having lower intensity than $(nR + C_4H_9 + H + Ag)^+$. The higher intensity of the $(nR + C_4H_9 + H + Ag)^+$ series indicates that even if some fragmentation occurs, the dominant process in the *m/z* 3500-7000 range is desorption of intact polymer molecules cationised with Ag^+. The value, M_n = 4550 was calculated from peak intensities without istopic abundance corrections. The calculated M_n value = 4550 is within 8% of M_n = 4964 determined by GPC.

6.5 Sequencing in Polybutadiene

Polybutadiene is regarded as a copolymer consisting of three isomeric units, *cis* 1,4-, *trans* 1,4- and 1,2-.

cis 1,4

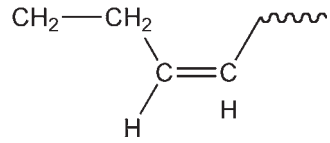

trans 1,4

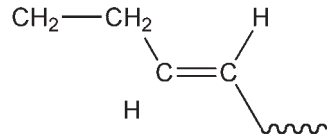

1,2

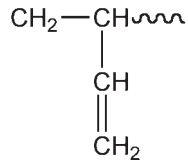

(14)

The variety of sequence distributions of these isomeric units and the tacticities of 1,2 units are governed by the initiator and polymerisation solvent. The control of these structural factors is significantly important for getting a good performance of

rubber properties. Several approaches have been used for the determination of the average sequence length and tacticity of 1,2 units by using either a spectroscopic or chromatographic method. ^{13}C-NMR studies on hydrogenated polybutadiene provided the information that syndiotactic 1,2 sequences were allowed to crystallise with longer than 3.7 racemic succession of 1,2 units [40]. The GC measurements of ozonolysis products or metathesis products from polybutadiene were applied to the analysis of some diad and triad sequences of 1,2 units [41, 42]. However, the structural information thus obtained was restricted in principle only to short sequences, i.e., diad, triad, and so on. If the alignment of 1,2 units is characterised as a distribution from short to long sequences including the tacticity, it will provide definitive evidence on the relationship between the microstructure and physical properties, as well as that of the polymerisation conditions and microstructure.

With this in mind, Tanaka and co-workers [43] proposed a new method for the characterisation of the sequence distribution of styrene units in styrene-butadiene copolymers by a combination of selective ozonolysis of the double bonds in butadiene units and GPC measurements of the resulting products. His method is based upon high resolution GPC analysis of the alcohols corresponding to styrene sequences obtained by scission of all the carbon-carbon double bonds of butadiene units. The ozonolysis-GPC method has already been proven to be a very powerful tool to characterise the sequence distribution of styrene units and the tacticity in random, partially blocked, and triblock styrene-butadiene copolymers [39, 44-48] in this study a new analytical method of the sequence distribution of 1,2 units in polybutadiene was investigated on the basis of the ozonolysis-GPC method.

In this method ozonisation was carried out by blowing an equimolar amount of ozonated oxygen (1.3%) to carbon-carbon double bonds into a 0.4% *w/v* chloroform solution of the polybutadiene at -30 °C. Reductive degradation of the resulting ozonide was performed by the addition of a small amount of water, after the ozonide had reacted with 4 mol of lithium aluminum hydride in ethyl ether. After reductive degradation, neutralisation was carried out by adding 1.5 mol of trifluoroacetic acid into the resulting LiOH and $Al(OH)_3$. The resulting product was distilled off at atmospheric pressure followed by distillation at reduced pressure. Trifluoroacetates for GPC were prepared by allowing the reductive degraded products suspended in dry chloroform to react with *5* mol of trifluoroacetic anhydride (TFAA) In the presence of a catalyst mixture consisting of 1 mol% 4-(dimethylamino)pyridine and an equimolar amount of triethylamine based on hydroxyl groups at 38 °C for 14 hours. Upon the completion of the reaction, the precipitate was filtered. Trifluoroacetates were obtained after chloroform had been removed at atmospheric pressure.

The following ozonisation reactions occur at 1,2- and 1,4-butadiene units:

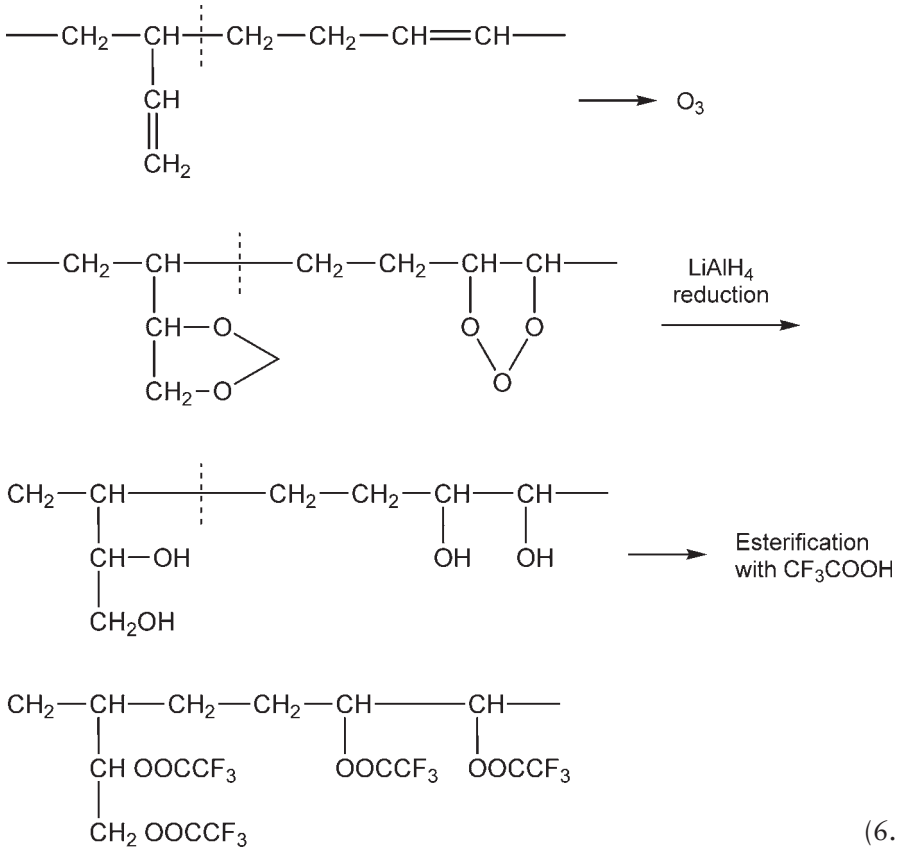

(6.15)

Polyols corresponding to 1,4-$(1,2)_n$-1,4, n = 0-3 and so on, sequences are the products obtained by reductive degradation of polybutadiene ozonide with lithium aluminium hydride ($LiALH_4$).

The polyols were converted into chloroform-soluble trifluoroacetates via esterification with TFAA. **Figure 6.4** shows a high-resolution GPC curve of the trifluoroacetates obtained from the ozonolysis products of polybutadiene.

Accordingly, a model compound corresponding to the 1,4-1,2-1,4 sequence was prepared by ozonolysis of 4-vinyl-1-cyclohexene, followed by esterification with TFAA. The GPC elution volume of this model compound was found to be 171 ml. Therefore, the corresponding peak observed in **Figure 6.4** is assignable to the 1,4-1.2-1.4 sequence. The peak appearing at the elution volume 187 ml is assigned to the 1,4-1,4 sequence because it has the same elution volume as trifluoroacetate derived from 1,4-butanediol as a model compound corresponding to the 1,4-1,4 sequence.

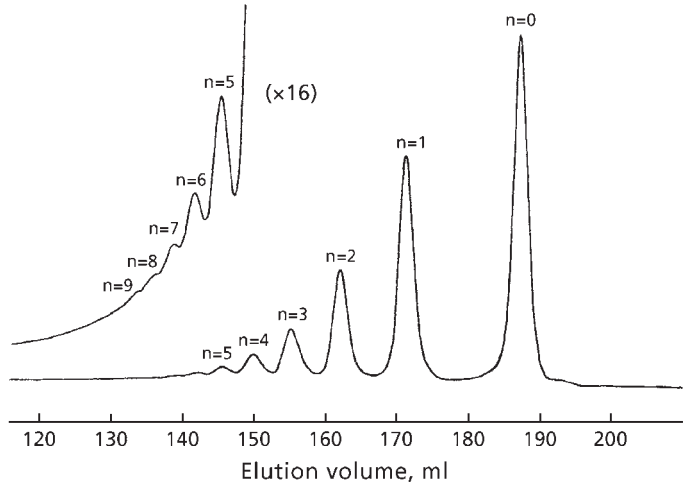

Figure 6.4 High-resolution GPC curve for the trifluoroacetates of ozonolysis products from polybutadiene. Peak *n* indicates the number of 1,2 units in 1,4-$(1,2)_n$-1,4 sequences. (*Reprinted with permission from Y. Tanaka, S. Kawahara, T. Ikeda and H. Tamai, Macromolecules, 1993,* **26***, 19, 5253. ©1993, ACS, USA [43]*)

The other peaks that appeared in the order of decreasing elution volume in **Figure 6.4** are presumed to be n = 2-9, respectively. A plot of log M_w of n = 0-9 *versus* elution volume gave a straight line. This shows that the structural assignment is valid.

Parts a and b of **Figure 6.5** show the ^{13}C-NMR spectra of the compounds corresponding to n = 1 and 2, respectively. The former was prepared by the ozonolysis of 4-vinyl-1-cyclohexene, and the latter was obtained by GPC fractionation of the ozonolysis product of polybutadiene. It is clear that all the hydroxyl groups have been esterified with TFAA.

The trifluoroacetates in a chloroform solution were found to have a maximum absorption wavelength of 270 nm as measured by a multichannel ultraviolet (UV)-vis detector. Therefore, the above GPC measurements can also be performed with a UV detector.

Acetate derivatives prepared with acetic anhydride were also found to be soluble in chloroform. **Figure 6.6** shows the GPC curve of acetate derivatives obtained from the ozonolysis product of polybutadiene in a way similar to the case of TFAA. In this chromatogram, the peak of the 1,4-1,2-1,4 sequence appeared at an elution volume of 164 ml. Other peaks corresponding to the products of the 1,4-$(1,2)_n$-1,4 sequence of n = 2-9 were also observed.

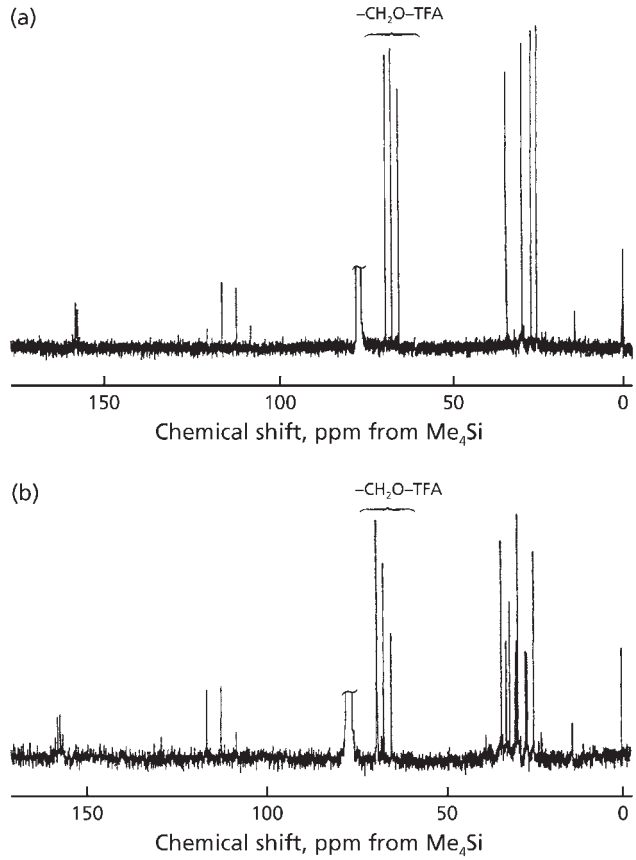

Figure 6.5 ^{13}C-NMR spectra of trifluoroacetates corresponding to the 1,4-1,2-1,4 sequence from the ozonolysis product of 4-vinyl-1-cyclohexene (a) and the GPC fraction corresponding to the 1,4-$(1,2)_n$-1,4 sequence (b). (*Reprinted with permission from Y. Tanaka, S. Kawahara, T. Ikeda and H. Tamai, Macromolecules, 1993,* ***26****, 19, 5253. ©1993, ACS, USA [43]*)

However, the peak of the 1,4-1,4 sequence was not detected because it overlapped with an intense impurity peak. A small shoulder observed at the peak of 164 ml is presumed to arise from unreacted hydroxyl groups that partially remained in the acetate derivatives. Therefore, the reactivity of acetic anhydride toward polyols is lower than that of TFAA. The GPC chromatogram of acetate derivatives of the ozonolysis products from polybutadiene showed a poorer separation than that of TFAA derivatives due to the smaller molecular weight of acetate groups. In contrast with trifluoroacetates, acetate derivatives in a chloroform solution were found to have no maximum absorption in the UV region as shown by a multichannel detector.

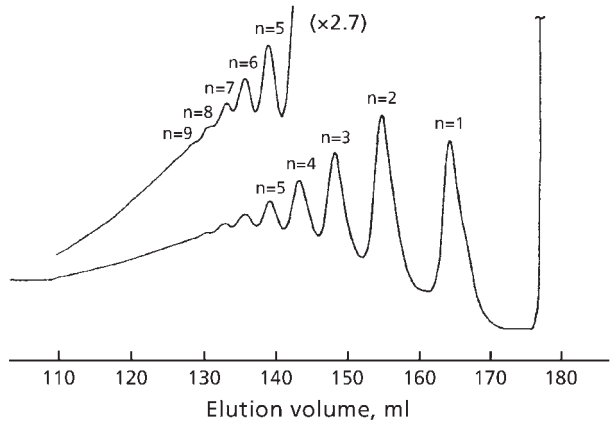

Figure 6.6 High resolution GPC curve for the acetate derivatives of the ozonolysis products from polybutadiene. Peak *n* shows the number of 1,2 units in 1,4-$(1,2)_n$-1,4 sequences. (*Reprinted with permission from Y. Tanaka, S. Kawahara, T. Ikeda and H. Tamai, Macromolecules, 1993, 26, 19, 5253. ©1993, ACS, USA [43]*)

The findings clearly indicate that the ozonolysis-GPC method can also be applied to the analysis of the sequence distribution of 1,2 units in polybutadiene by successive derivation of polyols to trifluoroacetates. It is remarkable that the peak corresponding to the 1,4-1,4 sequence is clearly observed in this measurement in addition to 1,4-$(1,2)_n$-1,4 sequences. On the basis of the relative intensity of each peak, the quantitative measurement of the sequence distribution can be made by compensation with an appropriate correction factor for the refractive index or UV absorptivity of each fraction.

The oxidation of double bonds in polymers in a non-aqueous solvent leads to the formation of ozonides which, when acted upon by water, are hydrolysed to carbonyl compounds:

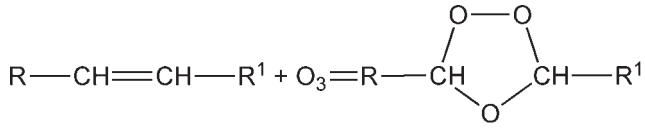

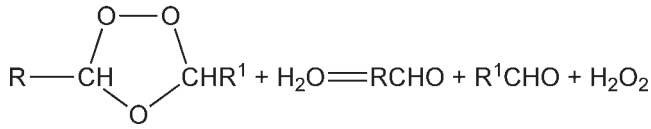

(6.16)

Triphenyl phosphine is frequently used to assist this reaction. Clearly, when applied to complex unsaturated polymers this reaction has great potential for the elucidation of the microstructure of the unsaturation. Examination of the reaction products, for example by conversion of the carbonyl compounds to carboxylates then esters followed by gas chromatography, enables identifications of these products to be made.

An example of the value of the application of this technique to a polymer structural problem is the distinction between polybutadiene made up of consecutive 1,4-1,4 butadiene sequences I, and polybutadiene made up of alternating 1,4 and 1,2 butadiene sequences. II, i.e., 1,4-1,2-1,4:

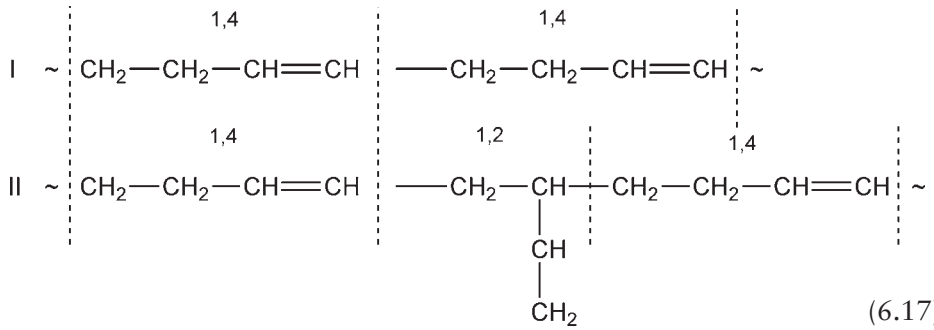

(6.17)

Upon ozonolysis, followed by hydrolysis, these in the case of 1,4-1,4 sequences produce succinaldehyde (CHO—CH_2—CH_2CHO) and in the case of 1,4-1,2-1,4 sequences produce formyl 1,6-hexane-dial and formaldehyde:

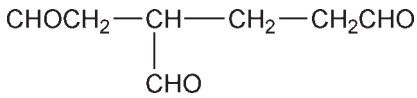

(6.18)

Analysis of the reaction product for concentrations of succinaldehyde and 3-formyl 1,6 –hexanedial shows whether the polymer is 1,4-1,4 or 1,4-1,2-1,4 or whether it contains both types of sequence. The 3-formyl-1,6-hexane dial content is directly proportional to the 1,2(vinyl) content of polymers containing 1,4-1,2-1,4 butadiene sequences. **Table 6.5** shows results obtained in the ozonisation of polymers having 98% *cis*-1,4 structure, 98% *trans*-1,4 structure and a series of polymers containing from 11% to 75% 1,2 structure. The final products obtained from these polymers were succinaldehyde, 3-formyl-1,6 hexanedial, and 4-octene-1,8-dial. Model compounds were ozonised and the products were compared with those from the polymers.

Figures 6.7 and 6.8 show chromatographic separation of the ozonolysis products from polybutadienes having different amounts of 1,2 structure, as measured by infrared or NMR spectroscopy. **Figure 6.9** shows the relationship of 1,2 content to the amount of 3-formyl-1,6 hexane-dial in the ozonolysis products.

Table 6.5 Microozonolysis of polybutadiene						
Sample	*Cis*-1,4	*Trans*-1,4	Area (from GC)%			
			Succinaldehyde*	3-Formyl 1,6-hexanedial**	4-Octene 1,8-dial	1,2 units occurring in 1,4-1,2-1,4 sequences
1	98.0	2	50	1	49	0.5
2	89.1	10.9	30	10	60	5
3	89.0	11.0	43	7	50	3
4	81.0	19.0	34	14	52	6
5	76.2	23.8	36	25	39	11
6	71.8	28.2	33	27	40	11
7	69.7	30.3	48	26	26	10
8	67.7	32.3	36	26	38	9
9	64.2	35.8	38	31	31	10
10	62.8	37.2	45	27	28	8
11	50.5	49.5	26	41	33	12
12	56.0	44.0	30	39	31	11
13	26.0	74.0	33	64	3	5

** Produced by ozonisation hydrolysis of 1,4-1,4 sequences*
*** Produced by ozonisation hydrolysis of 1,4-1,2-1,4 sequences*
Source: Author's own files

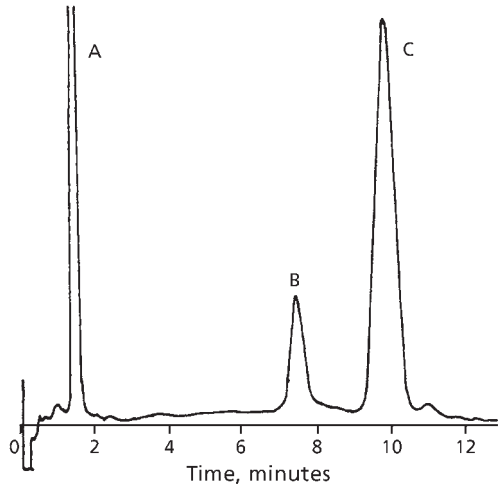

Figure 6.7 Ozonolysis products from polybutadiene containing 11% vinyl structures: (A) succinaldehyde; (B) 3-formyl-l,6-hexanedial; (C) 4 octene-1,8 dial. (*Source: Author's own files*)

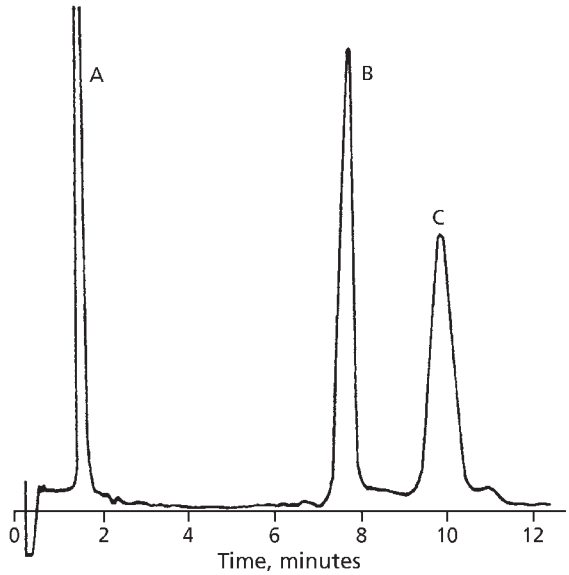

Figure 6.8 Ozonolysis products from polybutadiene containing 37.2% vinyl structure: (A) succinaldehyde; (B) 3-formyl-1,6-hexanedial; (C) 4-octene-1,8-dial. (*Source: Author's own files*)

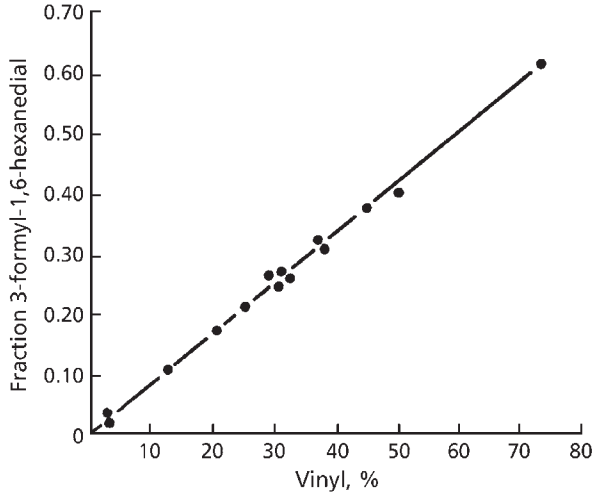

Figure 6.9 Relationship of yield of 3-formyl-1,6-hexanedial from ozonolysis to percentage vinyl structures (from NMR or infrared spectra) in polybutadienes. (*Source: Author's own files*)

The amount of 1,4-1,2-1,4 sequences in polybutadienes can be estimated from the amounts of the different ozonolysis products (**Table 6.5**) if one considers the amount of 1,4 structure not detected, since the ozonolysis technique cleaves the centre of a butadiene monomer unit, one half of a 1,4 unit remains attached to each end of a block of 1,2 units after ozonolysis; these structures do not elute from the GC column. Using random copolymer theory, the maximum amounts of these undetected 1,4 structures can then be calculated. Tanaka and co-workers [49] have also discussed the determination by ozonolysis of 1,2 butadiene units in polybutadiene.

Various other workers have used ozonisation-GPC to analyse 1,2 and 1,4 sequences in polybutadiene [39, 44-47].

6.6 Sequences in Polyurethanes

Pyrolysis coupled to mass spectrometry has been used to characterise polyurethanes (PU), but the degradative nature of the technique has restricted the study of PU to the low-mass range ($m/z \leq 500$) [50]. TOF-SIMS studies of Nylons [51] indicated that the technique might be used succesfully to characterise PU. The primary objective in the characterisation of PU is identification of the R_1, R_2, and R_3 groups in the general PU formula: H-[[OR_1]$_m$$OR_2$OC(=O)N$HR_3$NHC(=O)]$_n$-[$OR_1$]$_m$-$OR_2$OH,

where R_1 = -$[CH_2]_k$-OC(=O)-$[CH_2]_l$-C(=O), R_2 = -$[CH_2]_k$-, and R_3 = 1,4-C_6H_4-CH_2-1,4-C_6H_4, -$[CH_2]_6$-, 1,4-C_6H_{10}-CH_2-1,4-C_6H_{10}, or 1,3-$C_6H_3CH_3$.

Bletsos and co-workers [38] were the first to report the observation of high-mass fragments in PU by ToF-MS.

In general, fragments characteristic of the PU back-bone, the R_1 R_2, and R_3 groups, carbon clusters, and Ag^+ clusters dominate the PU TOF-SIMS spectra in the low-mass range (*m/z* <400).

A section of the TOF-SIMS spectrum of a PU in the range *m/z* 650-1650 is shown in **Figure 6.10**. The formula of the PU used in this example are given next. Bond cleavage produces four different kinds of fragments (labelled A to D) cationised with Ag^+ or Na^+ and observed in the range *m/z* 400-3000. The highest *m/z* peak in the spectrum was observed at *m/z* 3052:

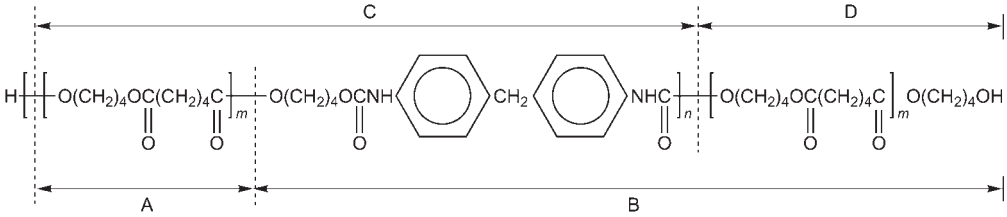

(6.19)

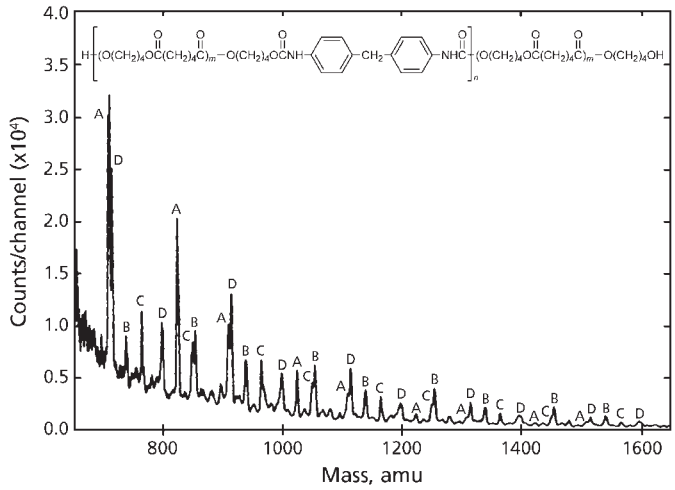

Figure 6.10 TOF-SIMS spectrum of a polyurethane in the range *m/z* 650-1650. The peaks are identified by the letter of the series to which they correspond, i.e., (A) (xA + M)$^+$, (B) (xB + M)$^+$, (C) (xC + M)$^+$, and (D) (xD + M)$^+$, where M = Ag, Na and x = 1, 2, 3. (*Reprinted with permission from I.V. Bletsos, D.M. Hercules, D. Van Leyen and A. Benninghoven, Macromolecules, 1987, 20, 2, 407. ©1987, ACS, USA [38]*)

Table 6.6 Fragments observed for PU in the range *m/z* 600-1700[a]

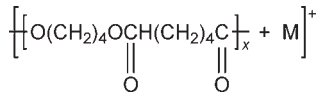

x	M = Ag	M = Na	x	M = Ag	M = Na
3	707 (30309), 709 (21227)[b]	623 (80367)	6	1307 (1308)	1223 (1630)
4	907 (10170)	823 (20341)	7	1507 (795)	1423 (832)
5	1107 (3531)	1023 (5886)	8	1707 (451)	1623 (559)
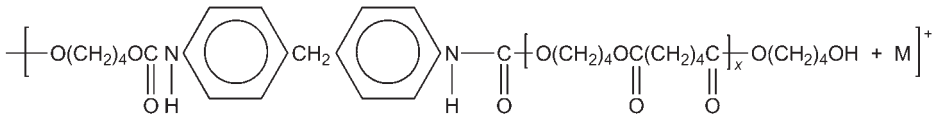					
1	736 (9184), 738 (8266)[b]	652 (17450)	4	1336 (2378)	1252 (4161)
2	936 (6683)	852 (9589)	5	1536 (1505)	1452 (2378)
3	1136 (4075)	1052 (6339)	6	1736 (870)	1652 (1397)
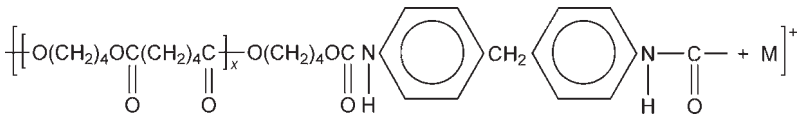					
1	647 (14287), 649 (14300)[b]	563 (16073)	4	1247 (2556)	1163 (3357)
2	847 (8719)	763 (11021)	5	1447 (1367)	1363 (1783)
3	1047 (4618)	963 (6683)	6	1647 (752)	1563 (903)

Table 6.6 ***Continued***

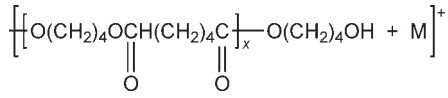

2	596 (21431), 598 (21500)[b]	512 (48220)	5	1196 (2626)	1112 (5977)
3	796 (10563), 798 (9643)[b]	712 (24798)	6	1396 (1486)	1312 (2734)
4	996 (5521)	912 (13076)	7	1596 (753)	1512 (1333)

[a] *Peaks due to the silver doublet are seen only in the low mass range because of spectrometer resolution.*

[b] *Peak intensities are given in parentheses (counts/channel).*

Reprinted with permission from I.V. Bletsos, D.M. Hercules, D. Van Leyen and A. Benninghoven, Macromolecules, 1987, ***20****, 2, 407. ©1987, ACS, USA [38]*

Fragmentation patterns are consistent throughout the detectable mass range and correspond to four well-defined series of peaks: $(A + M)^+$, $(B + M)^+$, $(C + M)^+$, and $(D + M)^+$, where M = Ag, Na. The peaks in the spectrum of **Figure 6.10** are identified by the letter of the series to which they correspond. All peaks observed for PU are given in **Table 6.6**. From the position of a peak and the spacing between consecutive peaks of the same series, the structures of the PU repeat unit and terminal groups can be determined. For example, the peaks at *m/z* 707, 709 correspond to $-[[O(CH_2)_4OC(=O)(CH_2)_4C(=O)]_3- + Ag]^+$, and the peak at *m/z* 852 corresponds to $-[O(CH_2)_4OC(=O)NH\text{-}1,4\text{-}C_6H_4\text{-}CH_2\text{-}1,4\text{-}C_6H_4\text{-}NHC(=O)\text{-}[O(CH_2)_4OC(=O)(CH_2)_4C(=O)]_2\text{-}O(CH_2)_4OH + Na]^+$.

The major fragments of the PU under Ar^+ bombardment can be generalised as follows: fragment A, $-[[OR_1]_x + M]^+$; fragment B, $(H)\text{-}[OR_2OC(=O)NHR_3NHC(=O)\text{-}[OR_1]_x\text{-}OR_2OH + M]^+$; fragment C, $-[[OR_1]x\text{-}OR_2OC(=O)\text{-}NHR_3NHC(=O)- + M]^+$; fragment D, $-[[OR_2]_x\text{-}OR_3OH + m]^+$. Peaks corresponding to the B series are reported here as cationised polymer fragments, but they could also be due to desorption of cationised PU oligomers. The difference between the two possible structures is one hydrogen;

the resolution of the instrument used *(m/Δm* ~ 1000) was not sufficient to distinguish between the two possible structures.

The difference in mass between an A fragment, i.e., -$[(OR_1)_x$ - + M]$^+$, and a C fragment, i.e., -$[[OR_1]_x$ -$OR_2OC(=O)NHR_3NHC(=O)$- + M]$^+$, corresponds to the mass of -$[OR_2OC(=O)NHR_3NHC(=O)]$. Specifically for the PU of **Figure 6.10**, the difference between the peaks at *m/z* 1163 due to -$[(O(CH_2)_4OC(=O)(CH_2)_4C(=O))_4O$-$(CH_2)_4OC(=O)$NH-1,4-$C_6H_4$-$CH_2$-1,4-$C_6H_4$-NHC(=O) + Na]$^+$ and *m/z* 823 due to -$[(O(CH_2)_4OC(=O)(CH_2)_4C(=O))_4$ + Na]$^+$ is *m/z* 340, which is the mass of -$[O$-$(CH_2)_4OC(=O)$NH-1,4-C_6H_4-CH_2-1,4-C_6H_4-NHC(=O)]-. From such well-defined fragmentation patterns the structures of the diols, esters, and isocyanates used in the synthesis of PU can be identified and their sequence in the repeat unit and terminal groups can be determined.

6.7 Sequences in Polydimethylsiloxane

A TOF-SIMS spectrum of polydimethylsiloxane (PDMSO) is shown in **Figure 6.11**. The distribution of peak intensities observed by Bletsos and co-workers [38] in the range *m/z* 500-9300 reflects the oligomer distribution of PDMSO. The spacing between consecutive peaks is equal to the repeat unit (R) of PDMSO (R = 74 amu) from which the polymer can be identified. The peaks observed in the spectrum are due to polymer fragments and polymer molecules cationised with Ag^+. In SIMS the impact of primary ions desorbs molecules and fragments and generates Ag^+ ions by sputtering the substrate [44, 52]. Cationisation of molecules and fragments can be accounted for by this mechanism.

Generally, cationisation stabilises molecular and fragment ions [53]. Cationisation with silver is commonly observed in SIMS experiments when Ag foils are used as substrates. Silver ions sputtered from the substrate are usually the most abundant cations observed in the mass spectrum.

In the mass range *m/z* 500-9600 the TOF-SIMS spectrum of PDMSO results from a convolution of two processes occurring during the SIMS experiment. First, desorption of intact polymer chains generates the most intense series of peaks in the high-mass range of the spectrum *(m/z* 500-9600). Desorption of intact polymer chains yields a series of peaks corresponding to (nR + CH_3 + H + Ag)$^+$, where n = 8, 9, 10, ..., 128. The ions detected in this series have mass values corresponding to the presence of a terminal methyl group, indicating that desorption of polymer molecules occurs without fragmentation. The intensity distribution of the peaks of this series reflects the oligomer distribution of the PDMSO studied. Second, fragmentation of polymer chains is evident from peaks on the low-mass side of the main peaks, as shown in

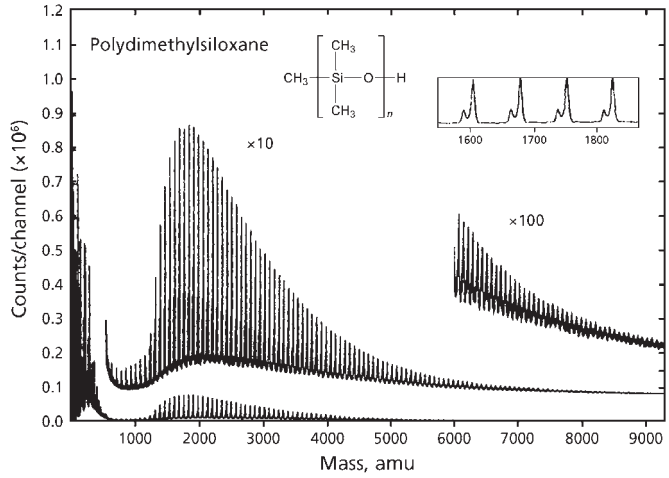

Figure 6.11 TOF-SIMS spectrum of PDMSOin the range *m/z* 0-9300. The most intense peaks are due to desorption of intact polymer molecules cationised with Ag^+ (nR + CH_3 + H + Ag)$^+$. The peaks appearing in the inset on the low *m/z* side of the most intense peaks are due to fragments of PDMSO cationised with Ag^+ and containing a large number of repeat units (nR + Ag)$^+$. The oligomer distribution of this polymer is not known. (*Reprinted with permission from I.V. Bletsos, D.M. Hercules, D. Van Leyen and A. Benninghoven, Macromolecules, 1987,* ***20****, 2, 407. ©1987, ACS, USA [38]*)

the inset of **Figure 6.11**; the same fragment ion peaks appear as the shaded region of lower intensity in the spectrum of **Figure 6.11** due to the extended mass scale used in the spectrum. This second series of peaks corresponds to (nR + Ag)$^+$, where n = 7, 8, 9, ..., 70. These peaks result from fragments produced by cleavage of the -Si-O- bond along the polymer backbone.

Further fragmentation within a repeat unit is not observed; i.e., no fragment ions of the type (nR - O + Ag)$^+$, (nR–$m$$CH_3$ + Ag)$^+$, or [nR - $Si(CH_3)_2$ + Ag]$^+$ were detected.

The spacing between consecutive peaks in both the desorption, (nR + CH_3 + H + Ag)$^+$, and fragmentation, (nR + Ag)$^+$, series corresponds to the mass of the polymer repeat unit (R = 74 amu). Peaks for both series are tabulated for the range *m/z* 800-2500 in **Table 6.7**. The intensity maximum of the (nR + CH_3 + H + Ag)$^+$ series occurs at *m/z* 1825, n = 23; after n = 23, the intensity decreases approximately exponentially as a function of *m/z*. The intensity maximum of the (nR + Ag)$^+$ series occurs at *m/z* 1735, n = 22. Up to *m/z* 1143, n = 14, the (nR + Ag)$^+$ series is more intense than (nR + CH_3 + H + Ag)$^+$. A transition in intensity occurs at n = 15.

Table 6.7 Ions Observed for PDMSO in the Range *m/z* 800-2500		
n	**(nR + CH_3 + H + Ag)$^+$**	**(nR + Ag)$^+$**
10	863 (2601)[a]	847 (5853), 849 (6243)[b]
11	937 (2862)	921 (7154)
12	1011 (3428)	995 (7382)
13	1085 (3559)	1069 (8831)
14	1159 (5800)	1143 (9227)
15	1233 (15093)	1217 (10875)
16	1307(30714)	1291 (13595)
17	1381 (45567)	1365 (17371)
18	1455 (55889)	1439 (19 133)
19	1529 (62434)	1513 (20 140)
20	1603 (67302)	1587(20761)
21	1677 (69013)	1661 (20875)
22	1751 (68634)	1735 (20990)
23	1825 (69355)	1809(19961)
24	1899(68923)	1883 (19046)
25	1973(65182)	1957 (17571)
26	2047(63936)	2031 (16324)
27	2121 (63028)	2105(15983)
28	2195 (59288)	2179(15505)
29	2269(56907)	2253(15432)
30	2343 (54013)	2327(14950)
31	2417 (49190)	2401 (13599)
32	2491 (49262)	2475 (12538)

[a] *Peaks due to silver isotopes not resolved.*

[b] *m/z of ions; intensity in parentheses (counts/channel).*

Reprinted with permission from I.V. Bletsos, D.M. Hercules, D. Van Leyen and A. Benninghoven, Macromolecules, 1987, ***20****, 2, 407. ©1987, ACS, USA [38]*

Fragments containing an integral number of repeat unit and a terminal $Si(CH_3)_3$ group, [nR + $Si(CH_3)_3$]$^+$, n = 0, 1, 2, ..., 5, give rise to ions having the same *m/z* as the (nR - H)$^+$ series. Ions resulting from the loss of one methyl group constitute the (nR - CH_3)$^+$ series, n = 1, 2, 3, ..., 7. Loss of two methyl groups from fragments consisting of an integral number of repeat units corresponds to the (nR - $2CH_3$)$^+$ series, n = 2, 3, 4. Ions resulting from the loss of one hydroxyl group correspond to the (nR - OH)$^+$ series, n = 1, 2, 3, ..., 7. Loss of one methoxy group produces a series of ions having the formula (nR - CH_3O)$^+$, n = 1, 2, 3, ..., 7. Addition of a proton is observed for ions up to the tetramer (nR + H)$^+$, n = 1, 2, 3, 4 *(m/z* 75, 149, 223, 297). The ions at *m/z* 74, 148, and 222 are the monomer and cyclic dimethylsiloxanes, nR$^+$, n = 2, 3. This series of cyclic dimethylsiloxanes might have been produced during the synthesis of PDMSO by termination of the linear chain growth by cyclisation at early chain growth stages [54]. The ions at *m/z* 193, 267, 341, and 415 probably are cyclic species with a bridging oxygen atom formed by decomposition of cyclic dimethylsiloxanes [55].

Two major processes that a polymer undergoes during the SIMS experiment are seen in the PDMSO spectrum. Desorption of whole polymer molecules generates the oligomer distribution for the polymer. Fragmentation produces large chain fragments composed of many repeat units. Extensive degradation of the polymer, which produces structurally significant fragments, is evident at *m/z* <500. The highest mass ion detected was at approximately *m/z* 9600 and is cationised with a single silver ion; it has a terminal methyl group and consists of 128 repeat units of PDMSO. It is possible that ions of even higher mass *(m/z* $\geq 10^4$) were produced. The mass registration of the spectrum, however, ended at *m/z* 9600 due to settings of the extraction voltage (5 kV) and the postacceleration (15 kV).

6.8 Sequences in Polypropylene Glycols

Extensive ozonisation followed by $LiALH_4$ reduction of oxyalkylene groups in polypropylene glycols produces monomeric diglycols as shown opposite (6.20-6.22).

Figure 6.12 is an example of a gas chromatogram of the ozonolysis product of polypropylene glycol showing the presence of all three types of breakdown products mentioned above, including the two optical isomers of dipropylene glycol (1a and 1b) (Equation 6.23).

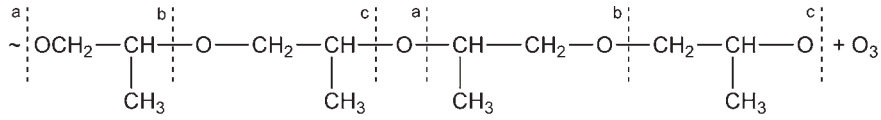

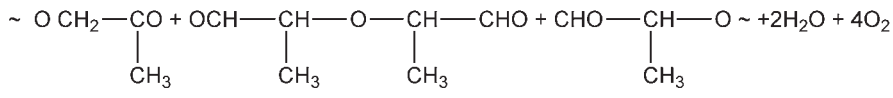

t h h t Head to head

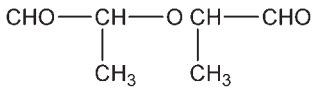

Which on reduction yields:

diprimary propylene glycol 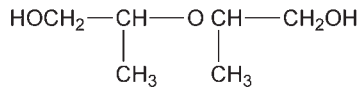 (6.20)

or 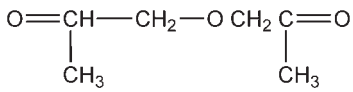 Tail to tail

Which on reduction yields disecondary propylene glycol:

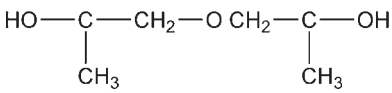 (6.21)

or 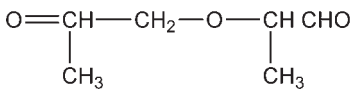 Head to tail

Which on reduction yields primary secondary propylene glycol:

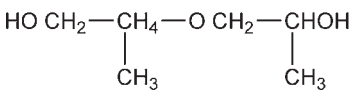 (6.22)

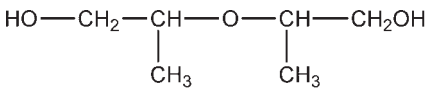

1a 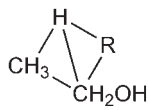 1b 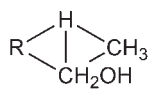 R is 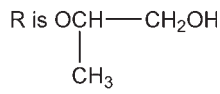 (6.23)

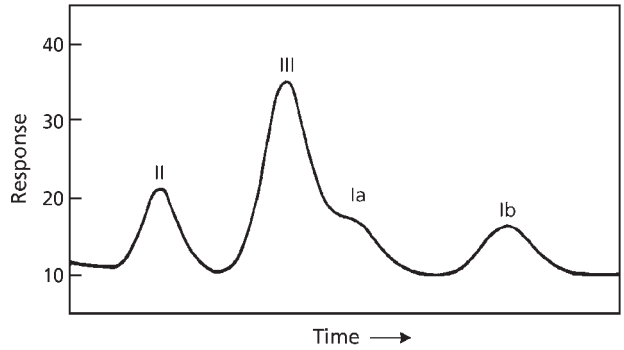

Figure 6.12 Gas liquid chromatogram of dipropylene glycol from amorphous polypropylene glycol, $ZnEt_2.H_2O$ catalyst. (*Source: Author's own files*)

6.9 Sequences in Polyvinylchloride (PVC)

Guo and co-workers [56] showed that dihydrochlorinated PVC had high concentrations of long polyene sequences. Bowley and co-workers [57] have demonstrated by Raman spectroscopy the effect of stretching prior to dehydrochlorination on the length of polyene sequences in PVC. Increased stretching increased the length of sequences.

6.10 Sequencing in Miscellaneous Homopolymers

This is reviewed in **Table 6.8**.

Table 6.8 Sequencing homopolymers and polymers		
Polymer	**Comments**	**Reference**
PVC	Pentad and hexad placements	[13, 16, 58-66]
Polychloroprene	Diad and traid sequences	[50, 67]
Chlorinated PE	Methylene sequences	[51, 52, 68, 69]
PS	Stereochemical sequence distribution of tetrad, pentad and hexad placements	[69-74]
Polypropylene oxide	Average sequence length	[75]
Chlorosulfonated PE	-	[76]
Glycidyl acrylate	-	[77]
Polytetrafluoroethylene	Head-to-tail, head-to-head and tail-to-tail placements	[78]
Polyethers	-	[79]
Polyacetals	-	[59, 60]
Polymethylmethacrylate	Length of stereoregular sequences	[73, 74]
Poly(4-vinylpyridine)	Sequencing	[80]
Butadiene-propylene	Sequencing	[81]
Polyamides	Sequence distribution	[82]
O-amino phenylene diamine 4,2-bis(2-amino-phenoxy) benzene	Determination of 2-10 catenated phenylenes, structural repeat units	[83]
Source: Author's own files		

References

1. J. Voigt, *Kunststoffe*, 1964, **54**, 2.

2. L.A. Wall, S.L. Madorsky, D.W. Brown, S. Straus and R. Simha, *Journal of the American Chemical Society*, 1954, **76**, 13, 3430.

3. Y. Tsuchiya and K. Sumi, *Journal of Polymer Science Part B: Polymer Letters*, 1968, **6**, 5, 357.

4. Y. Tsuchiya and K. Sumi, *Journal of Polymer Science Part A-1: Polymer Chemistry*, 1968, **6**, 2, 2415.

5. L.A. Wall and S. Straus, *Journal of Polymer Science*, 1960, **44**, 144, 313.

6. J. van Schooten and J.K. Evenhuis, *Polymer*, 1965, **6**, 11, 561.

7. J. van Schooten and S. Mostert, *Polymer*, 1963, **4**, 135.

8. Y. Inoue, A. Nishioka and R. Chûjô, Die *Makromoleculare Chemie*, 1972, **152**, 1, 15.

9. A. Zambelli, D.E. Dorman, A.I.R. Brewster and F.A. Bovey, *Macromolecules*, 1973, **6**, 6, 925.

10. J.C. Randall, *Journal of Polymer Science: Polymer Physics Edition*, 1974, **12**, 4, 703.

11. J.C. Randall, *Journal of Polymer Science: Polymer Physics Edition*, 1976, **14**, 11, 2083.

12. J.C. Randall, *Journal of Polymer Science: Polymer Physics Edition*, 1976, **14**, 9, 1693.

13. L. Cavalli, G.C. Borsini, G. Carraro and G. Confalonieri, *Journal of Polymer Science Part A-1: Polymer Chemistry*, 1970, **8**, 4, 801.

14. P. Corradini, V. Busico and G. Guerra in *Comprehensive Polymer Science*, Volume 4, Pergamon Press, Oxford, UK, 1988, p.29-50.

15. P. Pino, U. Giannini and L. Porri in *Encyclopedia of Polymer Science and Engineering*, Volume 8, 2nd Edition,, John Wiley and Sons, New York, NY, USA, 1987, p.147-220.

16. E. Schroeder and M. Byrdy, *Plaste und Kautschuk*, 1977, **24**, 11, 757.

17. G. Natta, I. Pasquon, P.Corradini, M. Peraldo, M. Pegoraro and A. Zambelli, *Rendiconti Lincei Scienze Fisichi e Naturali*, 1960, **28**, 539.

18. V. Busico, P. Corradini, L. De Martino, F. Graziano and A. Iadicicco, *Die Makromolekulare Chemie*, 1991, **192**, 1, 49.

19. R.C. Job, inventor; Shell Oil Company, assignee; WO 9012816, 1990.

20. R. Ohnishi, M. Tsuruoka, H. Funabashi and A. Tanaka, *Polymer Bulletin*, 1992, **29**, 1-2, 199.

21. V. Busico, P. Corradini and L. De Martino, *Die Makromolekulare Chemie, Rapid Communications*, 1990, **11**, 2, 49.

22. M.W. van der Burg, J.C. Chadwick, O. Sudmeijer and H.J.A.F. Tulleken, *Die Makromolekulare Chemie, Theory and Simulations*, 1993, **2**, 3, 399.

23. Y. Doi, *Die Makromolekulare Chemie, Rapid Communications*, 1982, **3**, 9, 635.

24. V. Busico, P. Corradini, R. De Biasio, L. Landriani and A.L. Segre, *Macromolecules*, 1994, **27**, 16, 4521.

25. B.D. Coleman and T.G. Fox, *Journal of Chemical Physics*, 1963, **38**, 5, 1065.

26. G. Di Silvestro, P. Sozzani, B. Savare and M. Farina, *Macromolecules*, 1985, **18**, 5, 928.

27. T. Hayashi, Y. Inoue, R. Chûjô and Y. Doi, *Polymer*, 1989, **30**, 9, 1714.

28. J.A. Ewen, M.J. Elder, R.L. Jones, L. Hasperslagh, J.L. Attwood, S.G. Bott and K. Robinson, *Die Makromolekulare Chemie - Macromolecular Symposia*, 1991, **48-49**, 253.

29. J. van Schooten and J.K. Evenhuis, *Polymer*, 1965, **6**, 7, 343.

30. P. Boochathum, M. Shimizu, K. Mita and Y. Tanaka, *Polymer*, 1993, **34**, 12, 2564.

31. A. Benninghoven and W.K. Sichtermann, *Analytical Chemistry*, 1978, **50**, 8, 1180.

32. J.A. Gardella and D.M. Hercules, *Analytical Chemistry*, 1980, **52**, 2, 226.

33. J.E. Campana, J.J. De Corpo and R.J. Colton, *Applications of Applied Surface Science*, 1981, **8**, 3, 337.

34. D. Briggs, *Surface and Interface Analysis*, 1982, **4**, 4, 151.

35. D. Briggs, M.J. Hearn and B.D. Ratner, *Surface and Interface Analysis*, 1984, **6**, 4, 185.

36. J.A. Gardella and D.M. Hercules, *Analytical Chemistry*, 1981, **53**, 12, 1879.

37. D.E. Mattern and D.M. Hercules, *Analytical Chemistry*, 1985, **57**, 11, 2041.

38. I.V. Bletsos, D.M. Hercules, D. Van Leyen and A. Benninghoven, *Macromolecules*, 1987, **20**, 2, 407.

39. Y. Tanaka, H. Sato and Y. Nakafutami, *Polymer*, 1981, **22**, 12, 1721.

40. K. Makino, M. Ikeyama, Y. Takeuchi and Y. Tanaka, *Polymer*, 1982, **23**, 3, 413.

41. J. Furukawa, K. Haga, E. Kobayashi, Y. Iseda, T. Yoshimoto and K. Sakamoto, *Polymer Journal*, 1971, **2**, 3, 371.

42. H. Abendroth and E. Caryi, *Makromolekulare Chemie*, 1975, **176**, 3, 775. Fran to check

43. Y. Tanaka, S. Kawahara, T. Ikeda and H. Tamai, *Macromolecules*, 1993, **26**, 19, 5253.

44. Y. Tanaka, H. Sato, Y. Nakafutami and Y. Kashiwazaki, *Macromolecules*, 1983, **16**, 12, 1925.

45. Y. Tanaka, H. Sato and J. Adachi, *Rubber Chemistry and Technology*, 1986, **59**, 1, 16.

46. Y. Tanaka, H. Sato and J. Adachi, *Rubber Chemistry and Technology*, 1987, **60**, 1, 25.

47. Y. Tanaka, Y. Nakafutami, Y. Kashiwazaki, J. Adachi and K. Tadokoro, *Rubber Chemistry and Technology*, 1987, **60**, 2, 207.

48. Y. Tanaka in *Handbook of Polymer Science and Technology, Synthesis and Properties*, Volume 1, Ed., N.P. Cheremisinoff, Marcel Dekker, Inc., New York, NY, USA, 1989, p.677.

49. Y. Tanaka, S. Kawahara, T. Ikeda and H. Tamai, *Macromolecules*, 1993, **26**, 19, 5253.

50. S.L. Marshall, *European Polymer Journal*, 1983, **31**, 1, 1.

51. I.V. Bletsos, D.M. Hercules, D. Greifendorf and A. Benninghoven, *Analytical Chemistry*, 1985, **57**, 12, 2384.

52. H. Grade and R.G. Cooks, *Journal of the American Chemical Society*, 1978, **100**, 18, 5615.

53. F.W. Röllgen, F. Borchers, U. Giessmann and K. Levsen, *Organic Mass Spectrometry*, 1977, **12**, 9, 541.

54. M.J. Hunter, J.F. Hyde, E.L. Warrick and H.J. Fletcher, *Journal of the American Chemical Society*, 1946, **68**, 4, 667.

55. J.C. Kleinert and C.J. Weschler, *Analytical Chemistry*, 1980, **52**, 8, 1245.

56. L. Guo, G. Shi and Y. Liang, *Polymer*, 2001, **42**, 13, 5581.

57. H.J. Bowley, D.L. Gerrard and W.F. Maddams, *Die Makromolekulare Chemie*, 1987, **188**, 4, 899.

58. C.J. Carman, A.R. Tarpley, Jr., and J.H. Goldstein, *Macromolecules*, 1971, **4**, 4, 445.

59. C.J. Carman, *Macromolecules*, 1973, **6**, 5, 725.

60. F.A. Bovey, E.W. Anderson, D.C. Douglas and J.A. Manson, *Journal of Chemical Physics*, 1963, **39**, 5, 1199.

61. K.C. Ramey, *Journal of Physical Chemistry*, 1966, **70**, 8, 2525.

62. F. Heatley and F.A. Bovey, *Macromolecules*, 1969, **2**, 3, 241.

63. N. Sütterlin and G. Meyerhoff, *Makromolekulare Chemie*, 1973, **165**, 223.

64. J.L. Millan and J.L. De La Pena, *Revista de Plasticos Modernos*, 1973, **26**, 206, 232.

65. T. Kelen, G. Galambos, F. Tüdos and G. Bálint, *European Polymer Journal*, 1969, **5**, 5, 617.

66. E. Bezdadea, D. Braun, E. Buruiana, A. Caraculacu and G. Istrate-Robil, *Angewandte Makromolkulare Chemie*, 1974, **37**, 1, 35.

67. T. Okada and T. Ikushige, *Journal of Polymer Science: Polymer Chemistry Edition*, 1976, **14**, 8, 2059.

68. I.A. Abu-Isa, *Journal of Polymer Science Part A-1: Polymer Chemistry Edition*, 1972, **10**, 3, 881.

69. I.A. Abu-Isa and M.E. Myers, Jr., *Journal of Polymer Science: Polymer Chemistry Edition*, 1973, **11**, 1, 225.

70. Y. Inoue, A. Nishioka and R. Chûjô, *Die Makromolekulare Chemie*, 1972, **156**, 1, 207.

71. B. Jasse, F. Laupretre and L. Monnerie, *Makromolekulare Chemie*, 1977, **178**, 1987.

72. T. Nagamura and A.E. Woodward, *Journal of Polymer Science: Polymer Physics Edition*, 1976, **14**, 2, 275.

73. S. Tsuge and H. Ohtani, *Polymer Degradation and Stability*, 1997, **58**, 1-2, 109.

74. J. K. Haken, *Journal of Chromatography A*, 1998, **825**, 171.

75. Z. Mencik and D.R. Fitchmun, *Journal of Polymer Science*, 1973, **11**, 5, 973.

76. E.G. Brame, Jr., *Journal of Polymer Science Part A-1: Polymer Chemistry Edition*, 1971, **9**, 7, 2051.

77. F. Keller, C. Fuhrmann, H. Roth, G. Findeisen and M. Rätzsch, *Plaste Kautsch*, 1977, **24**, 9, 626.

78. D.E. Mattern, F.T. Lin and D.M. Hercules, *Analytical Chemistry*, 1984, **56**, 14, 2762.

79. B.T. Chait, J. Shpungin and F.H. Field, *International Journal of Mass Spectrometry and Ion Processes*, 1984, **58**, 121.

80. G. Audisio and F. Severini, *Journal of Analytical and Applied Pyrolysis*, 1987, **12**, 2, 135.

81. C.J. Carman, *Macromolecules*, 1974, **7**, 6, 789.

82. C. Vu and J. Cabestany, *Journal of Applied Polymer Science*, 1991, **42**, 11, 2857.

83. G.C. Eastmond and J. Paprotny, *Polymer*, 2004, **45**, 4, 1073.

7 Sequencing in Copolymers

The sequencing of monomer units in a copolymer has important consequences for physical properties such as tacticity and stereochemistry and chemical properties of the copolymer.

Mechanical and physical properties are an important aspect of the use of polymers and can be governed by not only the composition but also by the structure of the polymeric molecules and the existence of homopolymer domains. Thus, the understanding of the relationship between mechanical, physical, and chemical properties becomes critically important. The polymer structure has a direct effect on such properties as modulus, glass transition temperature, film porosity, and minimum film formation temperature. By varying the monomer feed rates, initiator concentration, and chain transfer agent concentration, such properties as monomer sequence, molecular weight distribution, and particle size distribution can be affected. By knowing the monomer sequence in the final product, the emulsion polymer chemist will have a powerful tool for understanding to what degree an experimental parameter affects the polymer structure.

Sequences can occur in either of two ways:

(a) Copolymerisation of two or more different monomer units, e.g., styrene-butadiene

(b) Different arrangements of one monomer, namely, head-to-head, tail-to-head or head-to-tail.

For example: Tail-to-head polypropylene

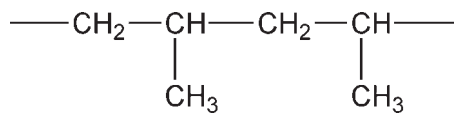

or

Tail-to-tail polypropylene

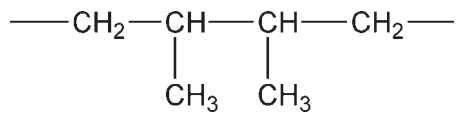

Sequencing in different types of copolymers is now discussed in detail.

7.1 Olefinic Copolymers

7.1.1 Ethylene Propylene

A good example of a polymer in which sequences of different monomer units occur is ethylene-propylene, and this will be discussed here in some detail. Processes for the manufacture of this polymer can produce several types of polymer which, although they may contain similar proportions of the two monomer units, differ appreciably in their physical properties. The differences in these properties lie not only in the ratio of the two monomers present but also, and very importantly, in the detailed microstructure of the two monomer units in the polymer molecule. Ethylene-propylene copolymers might consist of mixtures of the following types of polymer:

i) Physical mixture of ethylene homopolymer and propylene copolymer:

E-E-E-E-E-P-P-P-P

ii) Copolymers in which the propylene is blocked, for example:

E-E-P-P-P-P-P-E-E-E-E-E-E-P-P-P-

iii) Copolymers in which the propylene is randomly distributed, for example:

-E-P-E-P-E-P-E-P- (alternating, e.g., pure *cis*-1,4 polyisoprene),
or -E-E-E-P-E-E-E-E-E-P-E-E-E-E

iv) Copolymers containing random (or alternating) segments together with blocks along the chains, i.e., mixtures of (iii) and (ii) (random and block) or (iv) and (ii) (alternating and block), for example:

-E-P-E-P-E-P-

v) Copolymers containing tail-to-tail propylene units in propylene blocks:

i.e., head-to-head and tail-to-tail addition giving even-numbered sequences of methylene groups:

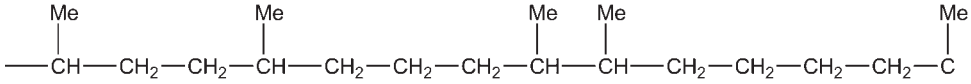

vi) Graft copolymers

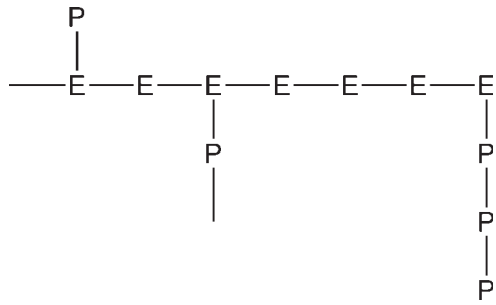

Various methods are available for determining the percentage of ethylene and propylene, the ethylene:propylene ratio and the type of ethylene and propylene unit sequencing in these polymers, and these methods are discussed in further detail in this section.

In fact the problem is somewhat more subtle than expressed previously, the types of measurements that are commonly required are:

a) determination of total percentage of propylene in the polymers, regardless of the manner in which the propylene is bound;

b) determination of total percentage of ethylene in the polymers, regardless of the manner in which the ethylene is bound;

c) determination of proportion of total propylene content of polymer which is blocked and that which is randomly distributed along the polymer chain.

Several possible techniques are available for carrying out these analyses, and these are now discussed:

- Pyrolysis of sample followed by gas-liquid chromatography (GLC) of pyrolysis products.

- Direct (IR) infrared spectroscopy of polymer, either at room temperature or at elevated temperatures.

- Pyrolysis of sample followed by infrared spectroscopy.

- Nuclear magnetic resonance spectroscopy and proton magnetic resonance spectroscopy.

Pyrolysis-gas Chromatography

Pyrolysis-gas chromatography (Py-GC) can be used to obtain fine detail regarding minor, but often very important detail, concerning polymer structure such as monomer sequences and, also, branching, crosslinking copolymer structure and the nature of the end-groups, and can also be used to elucidate polymer structure between adjacent monomer units in copolymers and to determine monomer ratios in copolymers.

Major differences occur between the pyrograms of three similar polymers. Polyethylene produces major amounts of normal C_2 to C_8 alkanes and minor amounts of 2-methyl and 3-methyl compounds such as isopentane and 3-methylpentane, which are indicative of short chain branching on the polymer backbone. For polypropylene, branched alkanes predominate, these peaks occurring in regular patterns, e.g., 2-methyl, 3-ethyl and 2,4-dimethylpentane and 2,4-dimethylheptane which are almost absent in the polyethylene pyrolysate. Minor components obtained from polypropylene are normal paraffins present in decreasing amounts up to normal hexane.

This is to be contrasted with the pyrogram of polyethylene, where *n*-alkanes predominate. The ethylene-propylene copolymer, on the other hand as might be expected, produces both normal and branched alkanes. 2,4-Dimethylpentane and 2,4-dimethylheptane concentrations are lower than occur in polypropylene.

Van Schooten [1] prepared gas chromatograms of hydrogenated pyrolysis products of polyethylene, polypropylene, ethylene-propylene copolymers and polyisoprene (hydrogenated natural rubber). These indicate a high degree of alternation in the ethylene-propylene copolymers. They identified most peaks in the chromatograms and ascribed them to a single component (**Figure 7.1(a)**), some to two or three different iso-alkanes or cycloalkanes (**Figure 7.1(b)**). A survey of the relative concentrations of the pyrolysis products is presented in **Figure 7.1 (a) and (b)** where peak areas have been given for the pyrolysis products of polyethylene, polypropylene, polyisoprene and for a copolymer containing about 50% methylene. A cursory examination of these figures shows that, apart from a few minor differences, the pyrolysis spectra of the ethylene-propylene rubber and polyisoprene are very similar. This would indicate a high degree of alternation in the ethylene-propylene copolymer, because presumably the spectrum of a C_2/C_3 copolymer, having poor alternation, resembles that of a 1:1 mixture of polyethylene and polypropylene. The same conclusion was drawn from the size of the 2,4-dimethylheptane peak.

The main feature of the pyrolysis spectra of polyethylene, polypropylene and isoprene can be interpreted on the basis of simultaneous breakage of carbon-carbon bonds in the main polymer chain. For a more detailed interpretation of the pyrolysis spectrum it is necessary to assume a series of radical-chain reactions in which intramolecular hydrogen abstraction plays an important role.

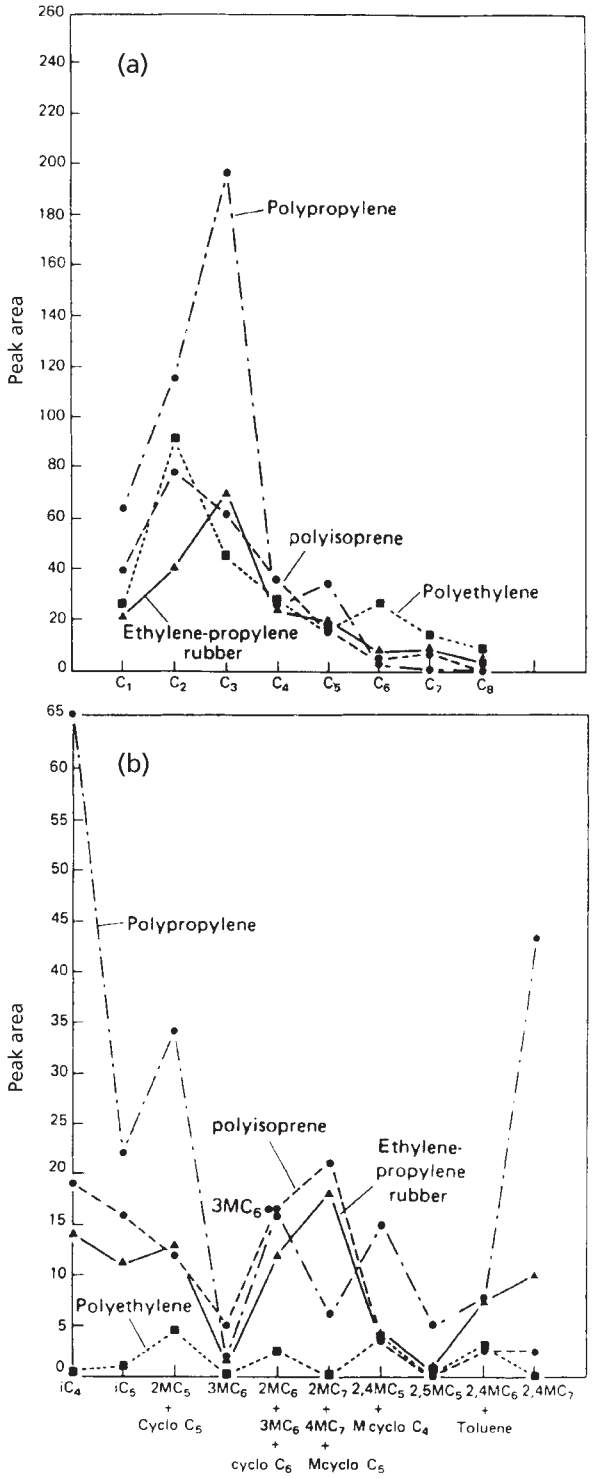

Figure 7.1 Peak areas obtained after pyrolysis of polyolefins; (a) normal alkanes; (b) iso-alkanes. (*Reprinted with permission from J. van Schooten, E.W. Duck and R. Berkenbosch, Polymer, 1961, 2, 357. ©1961, Elsevier [1]*)

High-vacuum pyrolysis at 40 °C of ethylene-propylene coolymers carried out by Van Schooten and co-workers [1] followed by trapping of released volatiles in dry ice-acetone, produced a mixture of olefins and alpha-olefins. The most volatile fractions, collected in dry ice-acetone, were hydrogenated to saturated hydrocarbons, which were analysed by GLC. For samples of copolymer prepared using either titanium trichloride or vanadium oxychloride catalysts the chromatogram of this fraction showed peaks of 2,4-dimethylheptane, 2-methylheptane, 4-methylheptane, 2,4-dimethylhexane, 3-methylhexane and 2-methylhexane, but only in the chromatogram of the volatile fraction from the copolymer produced using vanadium was a peak of 2,5-dimethylhexane found. This is an indication that polymers prepared with a catalyst containing vanadium oxychloride contain methylene sequences of two units between branches. Van Schooten and co-workers [1] conclude that ethylene-propylene copolymers prepared with vanadium-containing catalysts, especially those with $VOCI_3$ or $VO(OR)_3$, have methylene sequences of two and four units.

Infrared Spectroscopy

The infrared absorption of ethylene copolymers in the 14.28-11.76 μm region can provide information about their sequence distributions. Studies on model hydrocarbons by workers various [1-4] have shown that the absorption of methylene groups in this region is dependent on the size of methylene sequences in the compounds. Methylene absorptions observed in this region, and their relation to structures occurring in ethylene copolymers, are shown in **Table 7.1**. The absorptions at 13.81 and 13.68 μm of several ethylene-propylene copolymers have been assigned [5] to

Table 7.1 Methylene absorption and copolymer structure responsible for absorption in ethylene copolymers

$-(CH_2)_n-$	cm^{-1}	μm	Sequence	Structure number
$-(CH_2)_1$	815	11.76	~CH_2 $CHRCH_2$ $CHRCH_2CHR$~	(2)
$-(CH_2)_2$	751	13.31	~CH_2 $CHRCH_2CH_2CHRCH_2$~ or $CHRCHRCH_2CH_2CHRCHR$~	(3a) (3b)
$-(CH_2)_3$	733	13.64	~$CH_2CHRCH_2CH_2CH_2CHR$~	(4)
$-(CH_2)_4$	726	13.77	~$CH_2CHR(CH_2CH_2)_2CHRCH_2$~ or ~$CHRCHR(CH_2CH_2)_2CHRCHR$~	(5) (5b)
$-(CH_2)_5$	722	13.85	~$CH_2CHR(CH_2CH_2)_nCH_2CHR$~	(6)

Source: Author's own files

structures (6) and (4), respectively, (**Table 7.1**). The relative intensities observed were qualitatively consistent with sequence distributions calculated for the copolymers, assuming reactivity ratios of 7.08 and 0.088 for ethylene and propylene, respectively. Veerkamp and Veermans [6] developed a technique to measure the intensities of these absorptions accurately. By assuming similar extinction coefficients for the two bands, the ratio of methylene units in $(CH_2)_3$ and larger methylene sequences in a number of copolymers was determined. The results agreed reasonably well with theoretical values. The presence of $(CH_2)_2$ sequences in ethylene-propylene copolymers has been considered in studies of their structure [7]. Such sequences could result from tail-head incorporation of propylene units into the copolymers (structure (3a), **Table 7.1**).

Bucci and Simonazzi [3] also investigated the assignment of infrared bands of ethylene-propylene copolymers in the spectral region 11.11-15.38 μm. They calculated absorbances at various frequencies and attempted a numerical evaluation of the distribution of monomeric units in the copolymer. The spectra of ethylene-propylene copolymers in this frequency range show peaks or shoulders at 12.27, 13.30, 13.64 and 13.85 μm, whose intensity changes with composition. For the assignment of these bands they examined spectra of several model compounds which contain $(\text{-}CH_2\text{-})_n$ sequences with different values of *n* and compared these with values from the literature [1, 2, 5, 7, 8]. On the basis of this comparison they assigned bands at 12.27, 13.30, 13.34 and 13.85 μm to the $(\text{-}CH_2\text{-})$ sequences with n = 1, 2, 3, and 5 or more, respectively.

This assignment does not agree with that proposed by Van Schooten and Morstert [7], who assign bands at approximately these wavelengths to $(\text{-}CH_2\text{-})$ sequences with n = 1, 2, 3, and 4.

Bucci and Simonazzi [3] think that the difference lies in the fact that these authors assigned the band at 13.64 μm to the sequence $(\text{-}CH_2\text{-})_4$. Bucci and Simonazzi were not able to detect in ethylene-propylene copolymer any absorption at 13.79 μm where the sequence $(\text{-}CH_2)_4$ should occur. They recorded the spectrum of squalane compensated with 2,6,10,14-tetramethylpentadecane, and did find a band due to $(\text{-}CH_2)_4$ at 13.77 μm.

Natta and co-workers [5] determined the degree of alternation of ethylene and propylene units in ethylene-propylene copolymers from the infrared spectrum, using peaks at 13.35, 13.70 and 13.83 μm, the one at 13.70 μm being attributed to a sequence of three methylene groups between branch points, presumably due to the insertion of one ethylene between two similarly oriented propylene molecules:

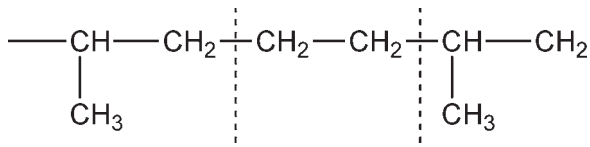

To check the correctness of this interpretation von Schooten and co-workers [7] examined the IR spectrum between 13 and 14 μm of ethylene-propylene copolymers prepared with various catalyst systems and compared them with the spectra of some model compounds, namely 2,5-dimethylhexane, 2,7-dimethyloctane, 4-methylpentadecane, 4-*n*-propyltridecane, polypropylene, polyethylene, polybutene-1 and hydrogenated polyisoprene, the last being considered as an ideally alternating ethylene-propylene copolymer.

The infrared absorption bands between 14.28 and 12.99 μm of various samples are given in **Figure 7.2**. These bands are due to rocking modes of the CH_2 groups, and their frequency depends on the length of the CH_2 sequences. In 2,5-dimethylhexane, hydrogenated polyisoprene and 2,7-dimethyloctane there are two, three and four CH_2 groups between branches, respectively, corresponding to peaks in the infrared spectra at 13.28 μm (ε spec = 0.0231 g cm), 13.53 μm (ε spec = 0.0581 g cm) and 13.75 μm (ε spec = 0.0421 g cm). Amorphous and crystalline polypropylene do not show any absorption at all in this region, whereas crystalline polyethylene shows two peaks at 13.65 and 13.85 μm. The latter peak is also found in liquid low molecular weight hydrocarbons [2] and in amorphous polymers containing long sequences of CH_2 groups [2]; the 13.62 μm peak is a crystalline band, attributed to the CH_2 rocking in the polyethylene crystal [2, 3, 8-11]. From the spectra of an amorphous polybutene-1 it was concluded that ethyl side-groups give rise to a peak at around 13.1 μm and from the spectra of 4-methylpentadecane and 4-*n*-propyltridecane that *n*-propyl groups absorb at 13.53 μm, proving that the shoulder at 13.3 μm found in some polymers is not due to ethyl or *n*-propyl end-groups.

In the spectra of all copolymers, except sample 6 (**Table 7.1**), they found a sharp peak at 13.80-13.85 μm, which must be ascribed to sequences of CH_2 groups longer than four, i.e., sequences of more than two ethylene units.

Significant differences are, however observed between the various spectra in the wavelength region from 13.0 to 13.7 μm. None of the copolymer spectra shows a clear shoulder at 13.53 μm where hydrogenated polyisoprene shows maximum absorption.

This means that in all the samples the content of $(CH_2)_3$ sequences is low. There are, however, several samples showing a pronounced shoulder at around 13.3 μm, which should probably be assigned to sequences of two CH_2 groups between branch points (*cf*. spectrum of 2,5-dimethylhexane). Of these samples two have been prepared with a $VOCl_3$-containing catalyst and one with a $VO(O\text{-}t\text{-}Bu)_3$-containing catalyst. Only a few of the samples prepared with a catalyst containing VCL_3, showed the shoulder at 13.3 μm. This shoulder was always observed in samples which had been prepared with a catalyst obtained from $VOCl_3$ or $VO(OR)_3$. It might well be that this band

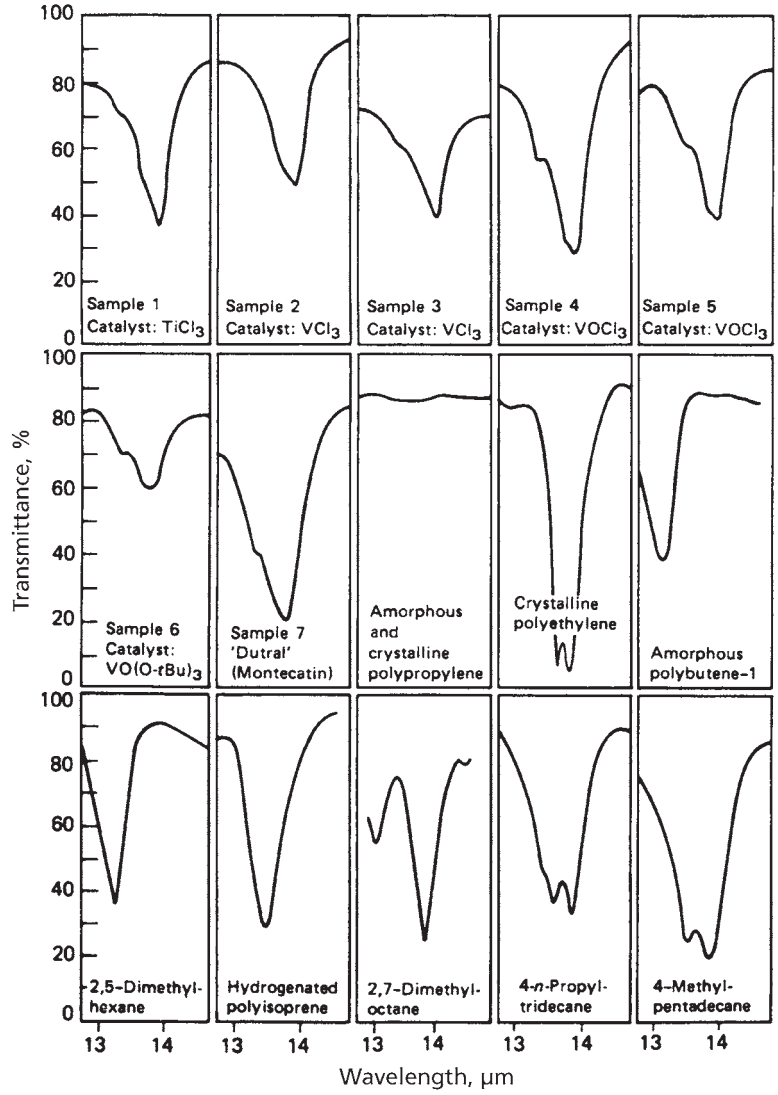

Figure 7.2 Infrared spectra between 700 and 770 cm^{-1} (13-14 μm) C_1-C_2 copolymers and model compounds. (*Reprinted with permission from J. van Schooten and S. Mostert, Polymer, 1963, 4, 135. ©1963, Elsevier [7]*)

arises from the presence of $(CH_2)_4$ sequences. This holds for samples which were prepared wlth catalysts containing $VO(O\text{-}t\text{-}Bu)_3$ or $VOCl_3$ and which, as we have seen also display absorption bands that indicate the presence of C_2 sequences. None of the copolymer spectra obtained thus far indicate the presence of the structure:

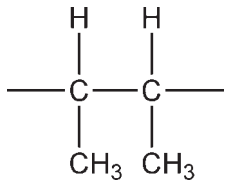

Which would give rise to absorption at 8.9 μm. This means that head-to-head orientation of propylene occurs only after addition of an ethylene unit.

Van Schooten and co-workers [1] have shown that ethylene-propylene copolymers prepared with $VOCl_3$ or $VO(OR)_3$-containing catalysts not only contain odd-numbered methylene sequences, as was expected, but also sequences to two units. Some indications for the presence of methylene sequences of four units were found. Tanaka and Hatada [12] also investigated copolymers with much lower ethylene contents and pure polypropylenes prepared with catalysts consisting of $VOCl_3$ or $VO(OR)_3$ and alkylaluminium sesquichloride.

The IR spectra of the ethylene-propylene copolymers containing 15 to 30 mole% of ethylene show little or no absorption above 13.70 μm. This means that very few methylene sequences of four or more units are present. The absorption peaks at 13.30 and 13.60 μm reveal the presence of sequences of two and three units, respectively. Thus these copolymers contained nearly all of the ethylene in isolated monomer units.

Veerkamp and Veermans [6] have reported on the differential measurement of $(CH_2)_2$ and $(CH_2)_3$ units at 13.42 and 15.87 μm, respectively, in ethylene-propylene copolymers. The band at 13.89 μm was assigned to units of 5 or more CH_2 units. Thus, the absorbance ratio A13.42/A13.89 μm provides a measure of the number of isolated ethylene units, and when corrected for the effect of composition (by multiplying by the ratio mole% C_3/mole% C_2) is related to the inverse of the ratio A10.33 μm/A8.69 μm times the ratio mole/C_2/mole%C_3. The more random the copolymer, as indicated by the absorbance ratio A13.42 μm/A13.89 μm for the relative number of isolated ethylene units, the more diffuse the 10.33 μm band becomes.

In summary, the appearance of contiguous *versus* isolated monomer units may be studied by the spectral characteristics of the methyl and methylene group rocking and wagging bands.

Liang and co-workers [13] on the basis of frequencies, relative intensities, polarisation properties, and effects on deuteration of polypropylene, have tentatively assigned the 10.33 μm band in polypropylene to the methyl rocking mode mixed with CH_2 and CH rocking vibrations. From this assignment, perhaps it is a change in the magnitude of the mixing with the CH_2 and CH modes in the case of the isolated propylene units in the copolymer which gives rise to a more diffuse absorption band at 10.33 μm. In this connection, Liang and co-workers [13] prepared non-stereospecific polypropylene in which 10.33 and 8.69 μm bands are either missing or very weak. Also, the occurrence of head-to-head arrangements of contiguous propylene units would be expected to influence the behaviour of the methyl rocking mode and any mixing which may be involved.

For the purpose of polymer characterisation the ratio of absorbances at 10.33 and 8.69 μm should provide a measure of the degree of randomness with respect to the introduction of propylene units into the copolymer. On the basis of the observation, the ratio A10.33 μm/A8.69 μm should decrease as the randomness increases. In addition, an increase in ethylene content is expected to increase the probability of producing propylene units isolated by ethylene units. For comparison of the 10.33 to 8.69 absorbance ratio with other data, correction for the effect of composition is made by multiplying by the ratio mole% CH_2 mole%CH_3, the molar ratio of ethylene to propylene in the copolymer. Relationships have been found between this modified absorbance ratio and other established physical or spectral properties indicative of randomness (or conversely, block polymer).

Rausch and co-workers [14] applied IR spectroscopy to the examination of methylene sequences in ethylene-propylene copolymers.

Nuclear magnetic resonance spectroscopy. Ethylene-propylene copolymers can contain up to four types of sequence distribution of monomeric units. These are propylene to propylene (head-to-tail and head-to-head), ethylene-propylene and ethylene to ethylene. These four types of sequences and the average sequence lengths of both monomer units, i.e., the value of *n*, below can be measured by the Tanaka and Hatada [15] method.

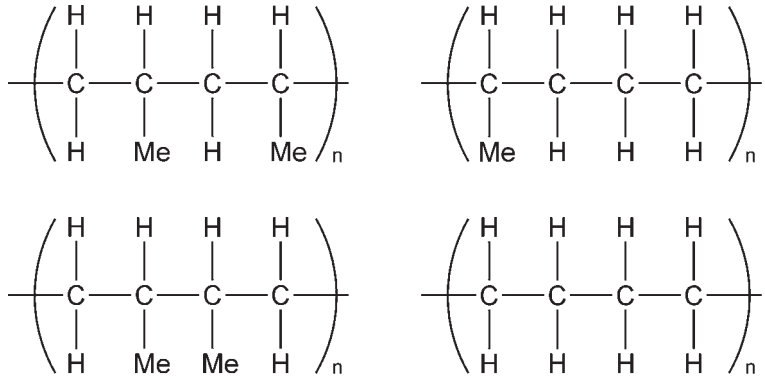

Measurements were made at 15.1 MHz. Assignments of the signals carried out using the method of Grant and Paul and also by comparing the spectra with those of squalane, hydrogenated natural rubber (isoprene), polyethylene and atactic polypropylene. The accuracy and precision of intensity measurements were acceptable at 12% maximum.

Tanaka and Hatada [12] studied the accuracy and precision of such intensity measurements in ^{13}C-NMR spectra and elucidated the distribution of monomeric units in ethylene-propylene copolymers. These analyses are particularly straightforward if one of the monomer units is present at a level of 95% or greater, because the other monomer will then occur primarily as an isolated unit.

The investigation of the chain structure of copolymers by ^{13}C-NMR has several advantages because of the large chemical shift involved. Crain and co-workers [16] and Cannon and Wilkes [17] have demonstrated this for the determination of the sequence distribution in ethylene-propylene copolymers. In these studies the assignments of the signals were deduced by using model components and the empirical equation derived by Grant and Paul for low molecular weight linear and branched alkanes.

Ray and co-workers [18] determined comonomer content in isotactic ethylene-propylene copolymers, complete diad and triad content as well as partial tetrad and pentad distributions using ^{13}C-NMR.

Proton magnetic resonance spectroscopy has been used to characterise ethylene-propylene block copolymers, containing from zero to 40% ethylene, either as homopolymer or copolymer blocks [19]. The test is independent of tacticity and provides qualitative information on copolymer sequencing and propylene chain structures. The analysis was developed using a series of standard reference polymers synthesised to contain various ratios of ^{14}C-tagged ethylene and propylene. All measurements were made on 10% polymer solutions in diphenyl ether. Analyses are accurate to about ±10% at higher ethylene concentrations.

Various other workers have discussed the application of NMR spectroscopy to sequencing studies on ethylene-propylene copolymers [19-32].

7.1.2 Ethylene-1-butene

Cheng [33] carried out a ^{13}C-NMR study of the triad distribution in fractionated ethylene-1-butene copolymers prepared with catalyst systems containing more than one active site. Analysis of the triad sequence distributions indicate that the data is compatible with the occurrence of three discrete active sites.

Information attained by Cheng [32] on these fractions included:

1) the minimum number of active sites that fits the data
2) the reaction probabilities of comonomers at each active site,
3) the contribution of each active site to the amount of copolymers being made.

Kuroda and co-workers [34] fractionated ethylene-1-butene copolymers by successively extracting it with diisopropyl ether at 20 °C (Fraction 1), *n*-hexane at 20 °C [Fraction 2), *n*-hexane at its boiling point (Fraction 3), and cyclohexane at its boiling point (Fraction 4). The residual polymer (cyclohexane insolubles) is designated Fraction 5. The whole (unfractionated) polymer is called W. The ^{13}C-NMR triad distribution data reported by Kuroda and co-workers are summarised in **Table 7.2**.

Table 7.2 ^{13}C-NMR Comonomer Triad Sequence Distribution in Ethylene/1-Butene Copolymer

	Wt%	Sequence					
		(BBB)	(BBE)	(EBE)	(BEB)	(EEB)	(BEE)
F1	18.4	0.047	0.090	0.163	0.075	0.267	0.358
F2	7.0	0.014	0.043	0.141	0.040	0.245	0.517
F3	13.6	0.003	0.020	0.103	0.019	0.188	0.667
F4	32.0	0.000	0.005	0.058	0.004	0.113	0.820
F5	29.0	0.000	0.002	0.030	0.002	0.059	0.907
W	100.0	0.001	0.022	0.080	0.021	0.141	0.735

E = ethylene unit
B = butene-1 unit

*Reprinted with permission from N. Kuroda, Y. Nishikitani, K. Matsuura and M. Miyoshi, Die Makromolekulare Chemie, 1987, **188**, 8, 1897. ©1987, John Wiley and Sons [34]*

7.1.3 Ethylene-1-hexene

Cheng [15] also determined the comonomer sequence distribution in ethylene-1-hexene copolymers. These copolymers have attracted increasing attention because of their use in linear low-density polyethylene. The microstructure of this copolymer has been previously studied by ^{13}C-NMR [35, 36]. FIorin-Michel and co-workers [35], made

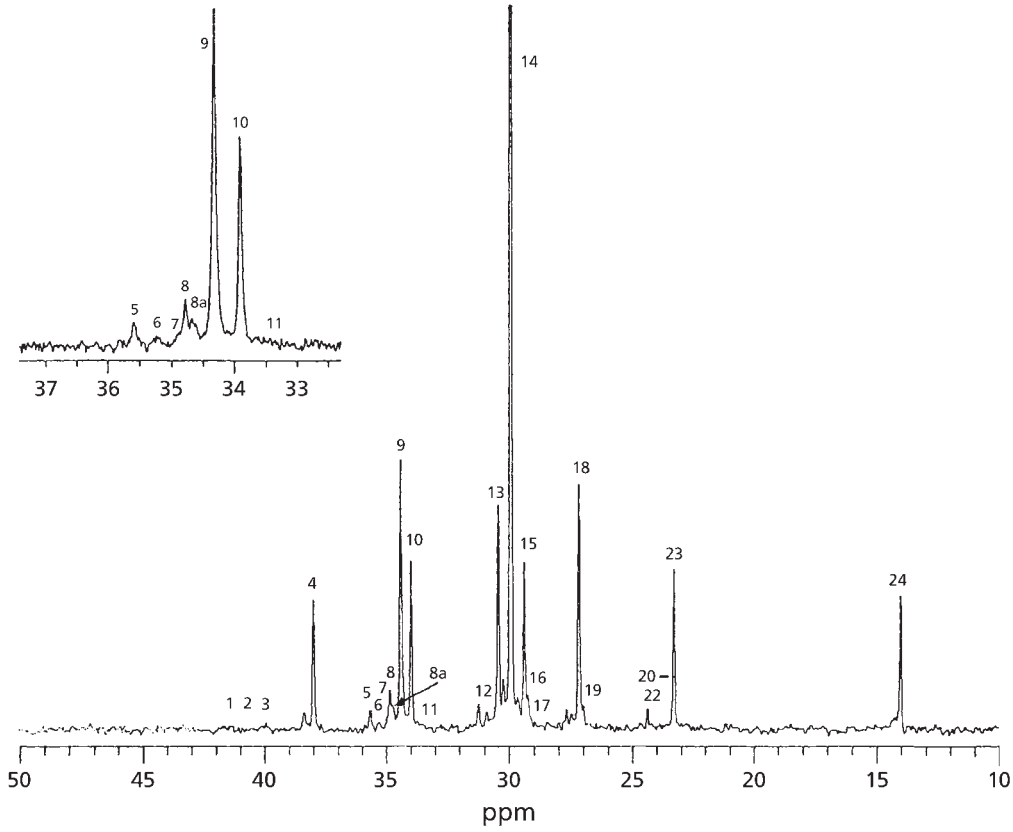

Figure 7.3 ^{13}C-NMR spectrum of EH copolymer (E/H = 82/18). The vertical scale has been enlarged to show the smaller resonances; as a result, line 14 has been truncated. The line numbers and assignments are given in **Table 7.3**. The inset shows the expanded region for lines 5-11. (*Reprinted with permission from K. Soga, T. Uozumi, and J.R. Park, Die Makromolekulare Chemie, 1990, 191, 12, 2853. ©1990, John Wiley and Sons. [26]*)

the first attempt to assign the ^{13}C-NMR spectra of ethylene-1-hexene copolymers. Hsieh and Randall [36] subsequently gave revised assignments and also provided a computational framework for the determination of comonomer sequence distribution. Recently, Soga and co-workers [37] (see **Figure 7.3**) and De Pooter and coworkers [38], reported the ^{13}C-NMR data of a number of these copolymers.

In this work, the NMR assignments of ethylene-1-hexene copolymers are reexamined, and improvements in the assignments obtained. A computerised analytical methodology is also developed to obtain accurate comonomer sequence distribution.

Table 7.3 ^{13}C-NMR Assignments and First-Order Markovian Probabilities of Ethylene/1-Hexene Copolymers

Line	Shift	Sequence	Markovian Probability (Fi)a
1	41.6	$S_{\alpha\alpha}$ HHHH	$P_{hh}^2 P_{eh}$
2	41.0	$S_{\alpha\alpha}$ HHHE	$2P_{hh}^2 P_{eh} P_{he}$
3	40.1	$S_{\alpha\alpha}$ EHHE	$P_{hh} P_{eh} P_{he}^2$
4	38.1	$T_{\delta\delta}$ EHE	$P_{he}^2 P_{eh}$
5	35.7	$T_{\beta\delta}$ HHE	$2 P_{he} P_{hh} P_{eh}$
6	35.4	$S_{\alpha\gamma}$ HHEH	$2 P_{he} P_{eh}^2 P_{hh}$
7+8+8a	35.1 34.9 34.8	B4 HHHHH $S_{\alpha\gamma}$ EHEH B4 HHHHE $S_{\alpha\delta}$ HHEE B4 EHHHE	$P_{hh}^4 P_{eh}$ $2 P_{he} P_{eh} P_{hh}$ $P_{hh}^3 P_{he} P_{eh}$ $2 P_{he} P_{ee} P_{hh} P_{eh}$ $P_{he}^2 P_{hh}^2 P_{eh}$
9	34.5	$S_{\alpha\delta}$ EHEE B4 HHHEX B4 EHHEX	$2P_{he}^2 P_{ee} P_{eh}$ $2P_{hh}^2 P_{he} P_{eh}$ $2P_{he}^2 P_{hh} P_{eh}$
10	34.0	B4 EHE	$P_{he}^2 P_{eh}$
11	33.5	$T_{\beta\beta}$ HHH	$P_{hh}^2 P_{eh}$
12	31.0	$S_{\gamma\gamma}$ HEEH	$P_{he}P_{ee} P_{eh}^2$
13	30.5	$S_{\gamma\delta}$ HEEEH	$2P_{he}P_{eh} P_{ee}^2$
14	30.0	$S_{\delta\delta}$ $HE_{n>3}H$	$2P_{he} P_{ee}^2 - P_{he} P_{eh} P_{ee}^2$
15+16+17	29.2-29.5	B3 H	P_{eh}
18+19	27.1-27.3	$S_{\beta\delta}$ XHEE	$2 P_{he} P_{eh} P_{ee}$
20+21+22	24.2-24.4	$S_{\beta\beta}$ HEH	$P_{he} P_{eh}^2$
23	23.4	B2 H	P_{eh}
24	14.1	B1 H	P_{eh}
	Sum	2E + 6H	$2 P_{he} + 6P_{eh}$

[a] For Bernoullian probabilities, set $P_{bh} = P_{eh} = P_h = P_{he} = P_{ee} = P_e$, where P_h and P_e are the probabilities of 1-hexene and ethylene, respectively. For two component (B/B) probabilities, set $F_{total} = w_1F_1 + w_2F_2$ where w_i and F_i are the weight fraction and the Bernoullian expression for component i.

*Reproduced with permission from K. Soga, T. Uozumi, and J.R. Park, Die Makromolekulare Chemie, 1990, **191**, 12, 2853. ©1990, John Wiley and Sons [37]*

Assignments are found in the 34.0-35.5 ppm region. In this region (lines 6-10), three types of carbons overlap: C_4, $S_{\alpha\gamma}$, and $S_{\alpha\delta}$. In this work, six resonances can be distinguished (including line 8a). By analogy to ethylene/propylene [39-41] and ethylene/1-butene [42, 43] copolymers, $S_{\delta\gamma}$ and $S_{\alpha\delta}$ are assigned to four resonances. Intensity considerations indicate that the C_4 carbon is split by comonomer sequence effect into pentads.

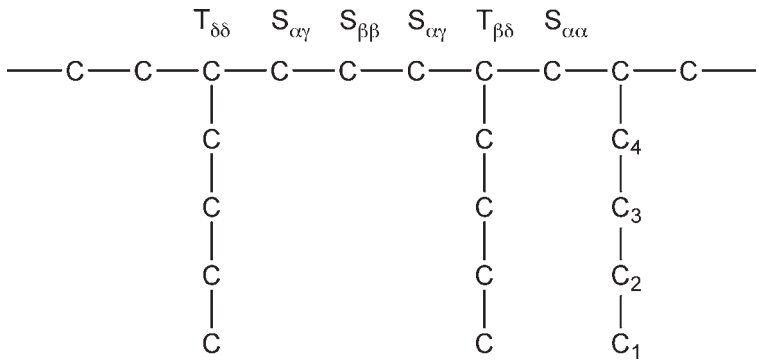

S and T indicate secondary and tertiary backbone carbons, and C_i corresponds to the ith carbon from the branch chain end. The Greek subscripts provide a measure of the distance of neighbouring butyl branches. Assignments are listed in **Table 7.3**.

7.1.4 Butene-propylene

A number of peaks arising from different pentad and hexad comonomer sequences have been observed in the ^{13}C-NMR spectrum of stereoregular 1-butene-propylene copolymers due to recent improvements in sensitivity and resolution [44]. ^{13}C-NMR chemical shift assignments of triad and tetrad sequences were obtained from chemical shift calculation using empirical rules [45, 46] and from comparison of the spectra of copolymers with different compositions [45]. In addition, the pentad and hexad assignments have been proposed from the quantitative analysis of the spectrum by a reaction probability model [44].

The chemical shift calculation (γ-effect method) based on the γ-effect of the ^{13}C chemical shift and the rotational isomeric state model (RIS model) has been developed as a reliable method for predicting chemical shift differences among pentad, hexad, and heptad sequences in various polyolefins [47-49, 14, 50, 51]. ^{13}C chemical shift assignments of tactic pentad and heptad sequences in polypropylene have been provided by this method [47-49]. Hayashi and co-workers [45, 46] confirmed that the chemical shift due to the γ-effect is also sensitive to different comonomer sequences in ethylene-propylene copolymers. Asakura and co-workers [52] have demonstrated that

the γ-effect method is applicable to the chemical shift prediction of tactic sequences in poly(1-butene) by considering the dominant conformation of the side chain.

In previous work, Aoki [53] has applied the γ-effect method to predict chemical shift differences among propylene (P)-centred pentad comonomer sequences in a stereoregular 1-butene (B)-propylene copolymer. The calculation predicts that resonances of BPB-, BPP-, and PPP-centred pentads appear as the respective groups of the split peaks. This result agrees well with the profile of the splittings in the observed spectrum, although the calculated chemical shift differences are overestimated. P-centred pentad assignments by this method agree well with previous assignments by Cheng [54].

^{13}C 2D-INADEQUATE NMR has been developed as a reliable method to determine the connectivity of carbon atoms [55-57]. By using this method, Hikichi and co-workers [44] confirmed the validity of the ^{13}C chemical shift assignments of various types of carbons in a stereoirregular ethylene-propylene (E-P) copolymer proposed by Randall [40]. The pentad comonomer sequence assignments of methane carbon resonances in stereoregular E-P copolymer have been provided from the connectivities between methane and methyl carbons [57].

Aoki and co-workers [46] established ^{13}C-NMR chemical shift assignments of comonomer sequences in a stereoregular 1-butene-propylene copolymer from the 2D-INADEQUATE spectrum and from the chemical shift data calculated on the basis of ^{13}C-NMR γ-effect. By tracing the carbon-carbon connectivities in the 2D-INADEQUATE spectrum, the validity of previous assignments [54] of triad and tetrad sequences was confirmed. Referring to these assignments, the chemical shift differences among pentad and hexad sequences are predicted by the chemical shift calculation via the γ-effect. Aoki and co-workers [46] modified Mark's [47] RIS model by considering the side-chain conformation in a 1-butene unit and used it for matrix multiplication. Thus, the conformational state of the side chain is also examined from the chemical shift calculation.

The paper by Aoki [46] demonstrated that the analytical method based on the 2D-INADEQUATE spectrum and the chemical shift calculation via the γ-effect is very powerful for the assignment of ^{13}C-NMR spectra of higher α-olefin copolymers. A stereoregular 1-butene-propylene copolymer is a suitable example, since reliable assignments have been proposed by a reaction probability model [54].

Aoki and co-workers [46] confirmed previous assignments of triad and tetrad sequences in this copolymer. Referring to the confirmed assignments, the chemical shift differences among comonomer sequences longer than pentad were predicted by the chemical shift calculation (the γ-effect method) based on the γ-effect of the ^{13}C chemical shift and Mark's rotational isomeric state model modified by considering the side-chain conformation in a 1-butene unit. Assignments provided in this study

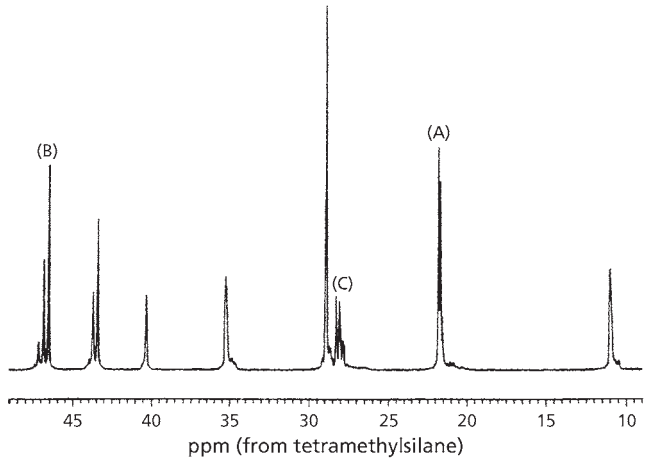

Figure 7.4 ^{13}C-NMR spectrum of a stereoregular 1-butene-propylene copolymer. (*Reprinted with permission from A. Aoki, T. Hayashi and T. Asakura, Macromolecules, 1992, **25**, 1, 155. ©1992, ACS [46]*)

agree well with Cheng's assignments [54] by a reaction probability model. Further, the conformational probability of the side chain in a 1-butene unit was evaluated through the chemical shift calculation.

Figure 7.4 shows the ^{13}C-NMR spectrum of a stereoregular 1-butene-propylene copolymer. On the basis of previous assignments [58], complicated peaks arising from different comonomer sequences longer than pentad are observed in the resonance regions of the methyl carbon of propylene (A), the central methylene carbon of a PP diad (B), and the side-chain methylene carbons of 1-butene (C) among propylene units.

In the region of the methyl carbon in the propylene unit (from 21.4 to 22.0 ppm), the side-chain methylene carbon in the 1-butene unit (from 27.5 to 28.5 ppm), and the central methylene carbon of the PP diad (from 46.5 to 47.5 ppm), the peaks arising from different comonomer sequences longer than pentad are observed. In order to provide assignments of these peaks, the chemical shift differences among pentad and hexad comonomer sequences were calculated by the γ-effect method. **Table 7.4** shows the calculated chemical shift differences in the resonance regions of methyl and methylene carbons in 1-butene-propylene copolymer are shown below:

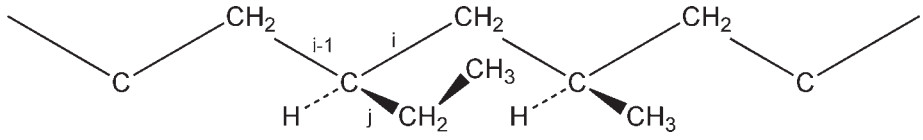

Table 7.4 Calculated ^{13}C-NMR Chemical Shift Differences in the Resonance Regions of Methyl and Methylene Carbons of a 1-Butene-Propylene Copolymer		
Carbon[a]	**Comonomer sequences[a]**	**Chemical shift differences[b], ppm**
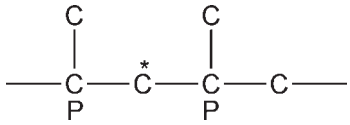	BBPPBB	0.000
	BBPPBP	-0.048
	PBPPBP	-0.096
	BBPPPB	-0.185
	BBPPPP	-0.222
	PBPPPB	-0.233
	PBPPPP	-0.273
	BPPPPB	-0.370
	BPPPPP	-0.410
	PPPPPP	-0.451
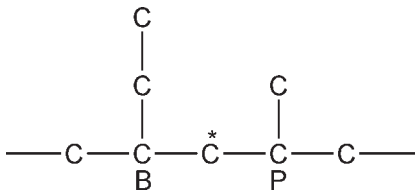	BBPB	0.000
	PBPB	-0.087
	BBPP	-0.183
	PBPP	-0.270
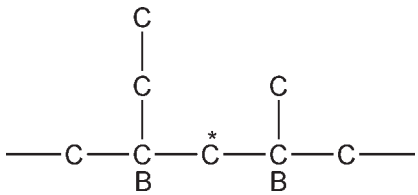	BBBB	0.000
	BBBP	-0.096
	PBBP	-0.203
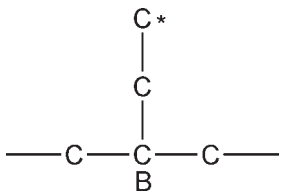	PPBPP	0.000
	BPBPP	-0.032
	BPBPB	-0.064
	PBBPP	-0.133
	BBBPP	-0.170
	PBBPB	-0.170
	BBBPB	-0.201
	PBBBP	-0.265
	BBBBP	-0.313
	BBBBB	-0.350

Table 7.4 *Continued*		
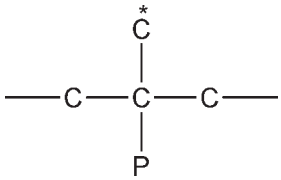	PPPPP	0.000
	BPPPP	-0.032
	BPPPB	-0.074
	PBPPP	-0.154
	PBPPB	-0.191
	BBPPP	-0.196
	BBPPB	-0.239
	PBPBP	-0.318
	BBPBP	-0.360
	BBPBB	-0.403
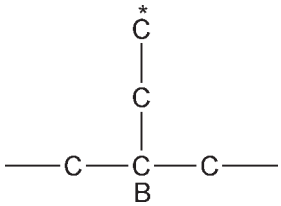	PBP	0.000
	BBP	-0.026
	BBB	-0.052

[a] *C, P and B denote the carbon atom, the propylene unit, and the 1-butene unit, respectively.*

[b] *Chemical shift differences are expressed by ppm relative to thyose of the peaks appearing at the lowest field, set to be 0.000 ppm.*

*Reprinted with permission from A. Aoki, T. Hayashi and T. Asakura, Macromolecules, 1992, **25**, 1, 155. ©1992, ACS, USA. [46]*

Planar zig-zag conformation of 1-butene-propylene copolymer methane resonance regions were excluded because of their low spectral resolution.

Aoki and co-workers [46] demonstrated that spectral analysis based on the 2D-INADEQUATE spectrum and the ^{13}C chemical shift calculation via the γ-effect is very useful for ^{13}C-NMR chemical shift assignments of higher α-olefin copolymers. The successful result of this spectral analysis for a stereoregular 1-butene-propylene copolymer confirms the reliability of this method. Further, the conformational states of the side chain in the 1-butene unit is evaluated through the chemical shift calculation by considering the side-chain conformation. Therefore, this method is applicable to the analysis of the ^{13}C-NMR spectrum and of the side-chain conformation in various olefin homo- and co-polymers.

7.1.5 Ethylene-methyl Acrylate, Ethylene-methylmethacrylate

Sigimura and co-workers [48] investigated sequencing in ethylene-methylmethacrylate (MMA) copolymers by Py-GC techniques.

In these copolymers the methacrylate units can be either unbranched (1) or branched (2):

(1) Unbranched

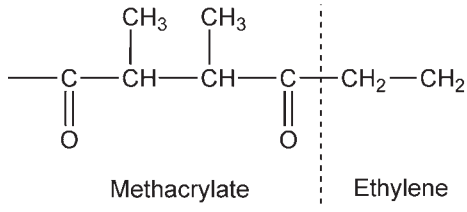

(2) Branched

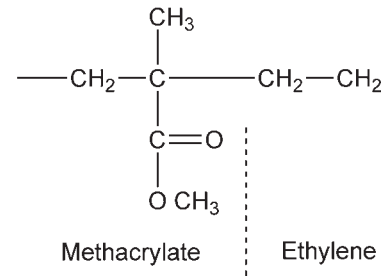

Upon pyrolysis at 400 °C, the branched copolymer produces butadiene (CH_2=CH-CH=CH_2) and the branched polymer produces 1-butene (CH=CH-CH_2-CH_3).

It was observed that the higher the MMA content of the copolymer the higher the amount of butadiene produced, i.e., the higher the degree of branching, relative to the amount of 1-butene. Typically, when the MMA content is about 16%, relative to 1-butene, then butadiene production is about 24% higher than occurs in a copolymer containing 8% MMA. Such polymer units containing fairly long chains of ethylenene.

In a pyrogram of an ethylene-methylacrlate copolymer we obtain, besides the two C_4 hydrocarbons due to methacrylate units, amounts of C_{10} to C_{35} mono-olefins with a terminal double bond.

Ethylene-MMA carbon monoxide terpolymer and ethylene-carbon monoxide and ethylene-methylacrylate (EMA-CO) copolymers.

Bruch and Payne [49] applied homonuclear two-dimensional correlated NMR spectroscopy (COSY), 2-dimensional ^{13}C and ^{1}H correlated and ^{13}C distorsionless ^{1}H correlated and ^{13}C enhancement by polorisation transfer spectroscopy (DEPT) to line assignment in the ^{1}H and ^{13}C spectra of a terpolymer containing ethylene, methyl acrylate and carbon monoxide.

The unique coupling patterns and chemical shifts observed for many sequences enabled the proton monomer sequence assignments to be made unambiguously at

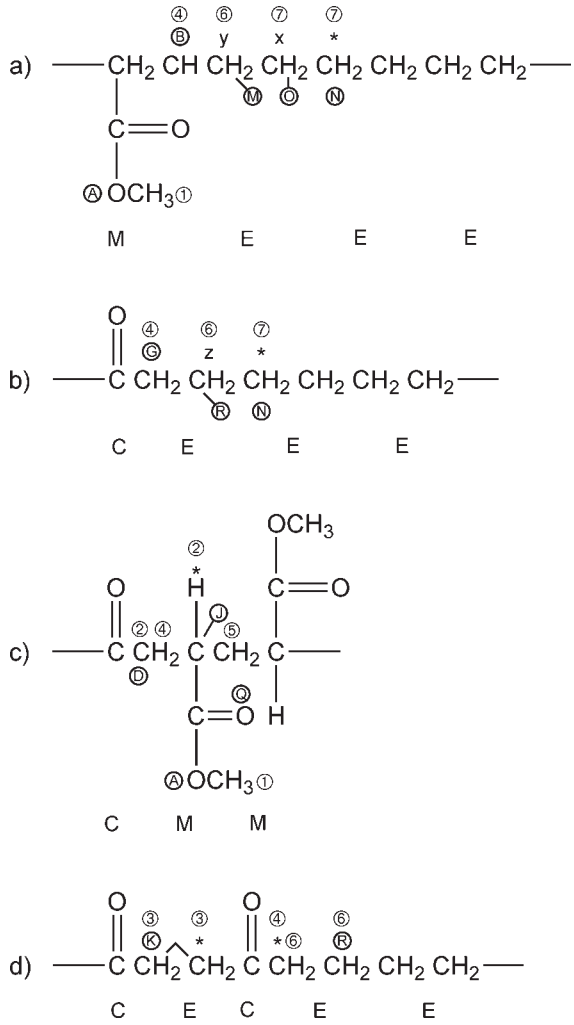

Figure 7.5 Structure of several monomer sequences in E/MA/CO terpolymer. (a) Structure of MEEE tetrad. The indicated methylenes at the centre of an EEE triad are coupled to neighboring x methylenes, and these x. methylenes are coupled to neighbouring y methylenes in MEE triads. (b) Structure of CEEE tetrad. The indicated EEE methylenes are coupled to neighboring z methylenes in CEE triads. (c) Structure of CMM triad. The central methine is coupled to the methylenes on either side in MM and CM diads. (d) Structure of CECEE pentad. There is weak four-band coupling between indicated α methylenes in CEC and CEE triads. E = ethylene segment, M = methylmethacrylate segment, C = carbon monoxide segment. (*Reprinted with permission from M.D. Bruch and W.G. Payne, Macromolecules, 1986, 19, 11, 2712. ©1986, ACS, USA. [49]*)

the triad level from the 2D COSY spectrum of this complex terpolymer (EMA-CO). In addition, end groups corresponding to terminal EE, ME, and CE were observed and assigned in the COSY spectrum. The coupling patterns observed in the COSY spectra of both EMA and EMA-CO indicate that predominantly racemic MM diads are formed in these polymers. This is in excellent agreement with previous results on other acrylate-containing polymers made by free radical initiators.

The ^{13}C line assignments were made from the combination of DEPT and 2D ^{13}C-^{1}H correlated spectroscopy despite the complexity of the conventional ^{13}C spectrum. DEPT spectroscopy allowed the multiplicity of each resonance to be determined unambiguously. Hence, ^{13}C assignments were made easily from the 2D ^{13}C-^{1}H correlated spectrum even in situations where overlap of methine and methylene signals occurs in the proton spectrum. Furthermore, equivalent and nonequivalent methylenes were distinguished in the 2D ^{13}C-^{1}H correlated spectrum, and this allowed ^{13}C assignments to be made despite spectral overlap of proton resonances. Proton chemical shifts were determined more accurately from the ^{13}C-^{1}H correlated spectrum because of the greater dispersion in the ^{13}C spectrum. All ^{1}H and ^{13}C assignments were confirmed by looking at the ^{13}C spectra of the copolymers EMA and E-CO.

The combination of several techniques proved more powerful than any one alone in assigning the ^{1}H and ^{13}C spectra of this complex terpolymer. Despite spectral overlap, detailed line assignments were made in both the ^{1}H and ^{13}C spectra. These techniques show tremendous potential for interpretation to NMR spectra of similar polymers.

Figure 7.5 illustrates the type of information on sequencing that can be obtained by this technique.

7.1.6 Ethylene-vinyl Chloride

Detailed IR investigations [50, 51, 59-61] of secondary chlorides, including the dimer and trimer model compounds of polyvinyl chloride (PVC), coupled with normal coordinate calculations [60-62] of their expected vibrational frequencies, have led to the correlation of C–Cl stretching frequencies with the local conformations in PVC. This correlation is depicted in **Figure 7.6** where the nomenclature of Mizushima and co-workers [63] is adopted. As an example, S_{CH} denotes a secondary chloride that is *trans* to C across one and *trans* to H across the other CHCl–CH_2 backbone bond. The correlation between C–Cl stretching frequencies and local conformation can also be applied to the analysis of the C–Cl stretching region of the IR spectra of ethylene-vinyl chloride (E-V) copolymers, which were recently reported [64].

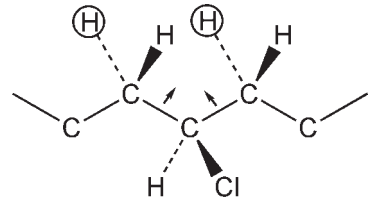

S_{HH} (606-614 cm^{-1})

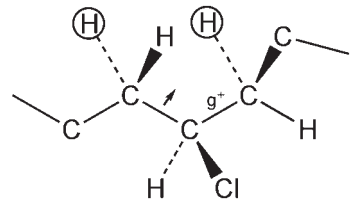

$S_{HH'}$ (627-638 cm^{-1})

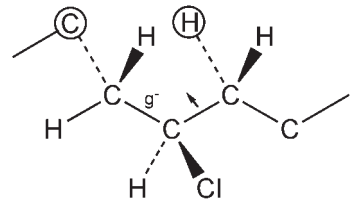

S_{CH} (665-693 cm^{-1})

Figure 7.6 Illustration of the SHH, SHH´ and SCH conformers around a –CHCl- unit, where the circled atoms (H or C) are trans to Cl. t, g+, g- denote *trans*, gauche+ and gauche- bond conformations. (*Source: Author's own files.*)

Based on the IR spectra of PVC and its model compounds and the IR spectrum of 4-chlorooctane, it would be expected that all three V-centred E-V triad structures (EVE, EVV, VVV) contributed intensity to the S_{HH} and S_{CH} C–Cl vibrations at 606-614 and 665-693 cm^{-1}, respectively. On the other hand, only the VVV and the racemic EVV[EVV(r)] triads should have $S_{HH'}$, C–Cl vibrations in the frequency range 627-638 cm^{-1} (see **Table 7.5**). Knowledge of the E-V triad distributions should permit an analysis of the C–Cl stretching region of the IR spectra of E-V copolymers.

Tonelli and Bowmer [65] studied the C-H stretching vibrations in the IR spectra of ethylene-vinyl chloride copolymers and investigated the correlation between conformations, microstructure, conformation possibilities and IR intensities (**Table 7.5**).

Table 7.5 Correlation between conformation, microstructure and C-Cl stretching frequence in E-V copolymers		
Conformer	**E-V triad**	**C-Cl (cm^{-1})**
SHH	EVE, EVV, VVV	606-614
SHH′	EVV(r), VVV	627-638
SCH	EVE, EVV, VVV	665-693
*Reprinted with permission from A.E. Tonelli and T.N. Bowmer, Journal of Polymer Science: Polymer Physics Edition, 1987, **25**, 5, 1153. ©1987, John Wiley and Sons [65]*		

7.1.7 Butadiene-propylene

The ozonolysis technique has been applied to a study of sequencing in butadiene-propylene copolymers [66-68]. Samples of highly alternating copolymers of butadiene and propylene yielded large amounts of 3-methyl-1,6-hexane-dial when submitted to ozonolysis. The ozonolysis product from 4-methyl-cyclohexane-1 was used as a model compound for this structure. Ozonolysis of these polymers occurs as shown next:

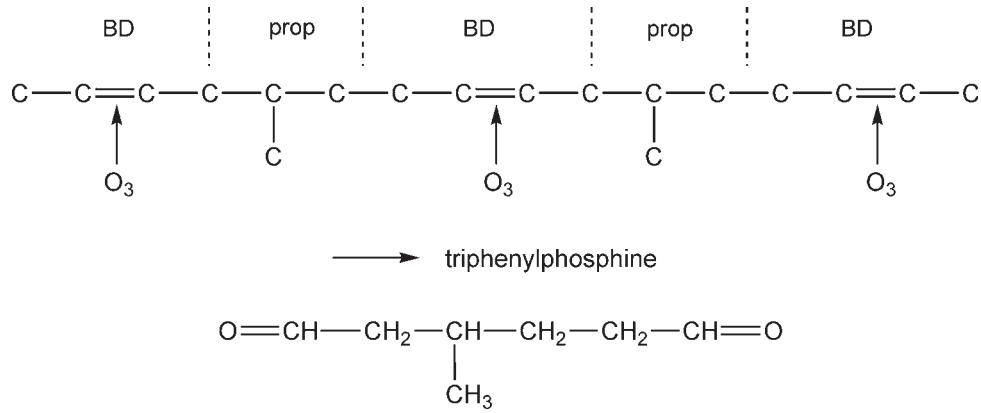

The amount of alternation in these polymers can be determined if the amounts of 1,4- and 1,2-polybutadiene structure and total propylene have been determined by IR or NMR spectroscopy. **Table 7.6** shows results obtained for several butadiene-propylene copolymers having more or less alternating structure. Similar polymers have been analysed by Kawasaki [67] by use of conventional ozonolysis methods with esters as the final products.

Table 7.6 Microzonolysis of butadiene-propylene copolymers								
	1,4 (%)	1,2 (%)	Propylene (mole%)	Area (from gas chromatography) %				
				Succinaldehyde*	3-methyl-1,6-hexanedial**	3-Formyl 1,6-hexanedial	4-Octene-1,8-dial	Alternating BD/Pr (%)
A	45	5.7	49.3	5	92	1	2	77
B	47.8	2.2	50	11.5	85	0.5	3	71
C	53.1	3.2	43.7	25	61	6	8	48
D	-	-	30	49	38	1	12	33

**Produced upon ozonisation/hydrolysis of 1,4-1,4 butadiene units.*

***Produced upon ozonisation/hydrolysis of 1,4-1,2-1,4 butadiene units.*

Source: Author's own files

7.1.8 Miscellaneous Olefinic Copolymers

Sequencing studies have also been conducted on the following olefin copolymers: ethylene terephthalate [69-72], ethylene-α-olefin [73], ethylene-α-methylstyrene [74], ethylene-decene-1 [75], ethylene-butene [33], ethylene-propylene diene [76], miscellaneous ethylene copolymers [49] and ethylene-acrylonitrile [77].

7.2 Styrene Copolymers

7.2.1 Styrene-butadiene

Ozonisation followed by gel permeation chromatography (GPC) has been used by Tanaka and co-workers [78, 79] to study sequencing of vulcanised styrene copolymers. Tanaka and co-workers [78, 79] carried out the ozonolysis in methylene dichloride and examined the fractions obtained following GPC by ^{1}H-NMR. These workers found nonad, diad and triad styrene sequences flanked by 1,4-butadiene units and long styrene sequences:

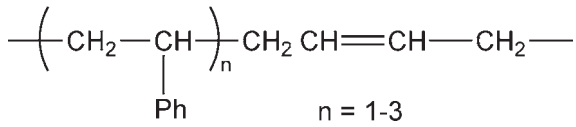

In further work configurational sequences were determined in styrene units and the arrangement of styrene and 1,2-butadiene units in styrene-butadiene rubber. Tanaka and co-workers [79] carried out ^{1}H- and ^{13}C-NMR spectroscopy on products obtained by ozonisation – GPC and ozonisation – high-performance liquid chromatography (HPLC). Ozonides were produced from diad and triad styrene sequences and from the 1,4-butadiene sequences which flanked them. The chromatograms showed 2 or 3 peaks corresponding to styrene diad and triad. Ozonolysis products obtained from styrene and 1,2- butadiene sequences were separated in up to three fractions by HPLC. The first and second of these peaks in these fractions were assigned to 1,4- and 1,2-butadiene units and the peaks in the third fraction were assigned to meso and racemic forms of 1,4-styrene, 1,4-butadiene sequence structure. Tanaka [80], again using the ozonolysis-GPC technique showed that the ozonolysis products obtained from styrene-butadiene and styrene isoprene copolymers indicated the presence of 77 to 99% styrene block sequences in linear copolymers. A linear copolymer could be distinguished from star copolymer by comparing the molecular weight and chemical composition of the main peak and shoulder peaks by GPC and also by comparing the molecular weight of the block styrene sequences determined by ozonisation – GPC.

Pattuelli [81] also used ozonolysis – HPLC in sequencing studies on styrene-butadiene copolymers.

7.2.2 Styrene Acrylate and Styrene Acrylic Acid

NMR techniques have been widely used to study copolymer composition and monomer sequence distribution. In the 1960s, Bovey used a statistical method to assign the sequence distribution of methyl methacrylate - styrene (MMA-S) and MMA-α-methylstyrene (MMA-α-MS) copolymers from ^{1}H-NMR data [82]. Ito and co-workers studied the coisotacticity of MMA-S [83], MMA-α-MS [84], MMA-methyl acrylate (MMA-MA) [85] and vinylidene chloride – vinyl acetate (VC-VA) [86] copolymers by ^{1}H-NMR.

In the 1970s and 1980s, ^{13}C-NMR was used to investigate a number of polymer systems with generally excellent results. The large chemical shift range in ^{13}C-NMR permits the study of more complex copolymer systems and the elucidation of detailed structural information [87-93]. Uebel and co-workers for example, reassigned the sequence distribution of MMA-S copolymer and determined the reactivity ratios of butylstyrene-MMA copolymerisation [94, 95]. Brar and co-workers assigned the sequence distribution of MMA-ethyl methacrylate (MMA-EMA), MMA-S, MMA-*n*-butyl methacrylate (MMA-*n*-BuMA), and acrylic acid - MMA (AA-MMA) copolymers by ^{13}C-NMR [97-100]. Tacx and co-workers investigated solution and emulsion copolymers of S-EMA and S-MA and proposed a microstructure model for high conversion copolymerisation [101, 102] and Van Doremaelel [103]. The monomer sequence distributions of chlorotrifluoroethylene-vinyl acetate (CTFE-VA) and CTFE-vinyl propionate emulsion copolymers has been determined [104]. The development of two-dimensional NMR spectroscopy permits easier assignment of complex copolymer spectra peaks [105].

A question posed by Wong and Poehlein [105] regarding the monomer system of styrene acrylic acid is whether sequence distribution information can be determined in NMR spectra. In this work, ^{1}H- and ^{13}C-NMR spectra of S-AA copolymers were examined to determine the resonances that are sensitive to the copolymer microstructure. The compositions of the copolymers were measured by NMR and the reactivity ratios calculated. The triad sequences were assigned by experiments and the Alfrey-Mayo statistics-kinetics model.

Figure 7.7 shows a typical 400 MHz ^{1}H-NMR spectra of low-conversion S-AA bulk copolymer dissolved in DMSO-D_6 and in DMSO-D_6-$CDCl_3$ at 50 ºC. The chemical shift of different protons are: 1-2 ppm for all methine protons and the methlene proton of the styrene units in the copolymer chain; 2.3 ppm for the methlene proton

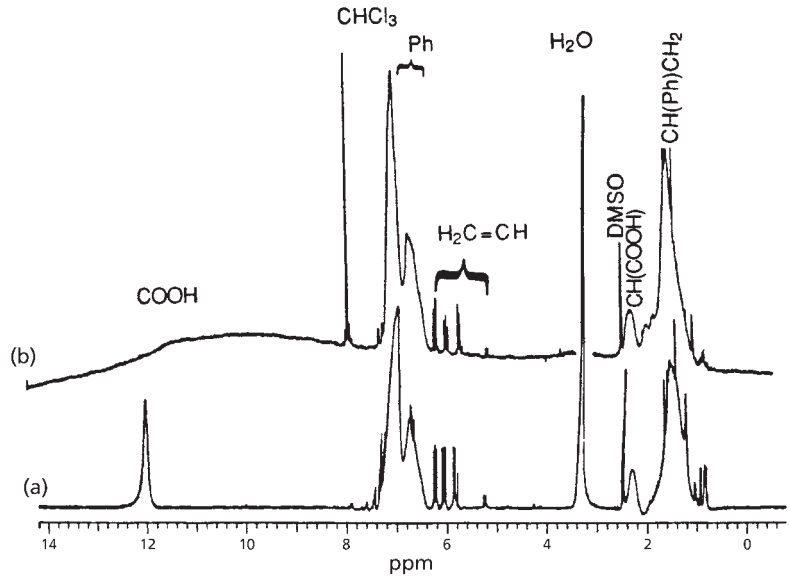

Figure 7.7 ^{1}H-NMR spectra of bulk styrene-acrylic acid copolymer, SA-40, DMSO as solvent at 90 °C. (*Reprinted with permission from S. Wong and G.W. Poehlein, Journal of Applied Polymer Science, 1993, 49, 6, 991. ©1993 John Wiley and Sons [105]*)

of the acrylic acid unit in the copolymer chain; 3.3 ppm for water in DMSO-D_6, 5.2-6.4 ppm multipeaks for the end groups of the copolymer chains that may be double bonds and isobutylnitrile; 6.4-7.4 ppm for aromatic protons; and 12.1 for the proton of the carboxyl group on the copolymer chain.

The resonance behaviour of the carboxyl proton is heavily affected by the solvent used. A clear single resonance peak appears in the ^{1}H-NMR spectra if DMSO-D_6 is used and the baseline is straight. This sharp peak disappears, however, when a DMSO-D_6-$CDCl_3$ solvent mixture is used. Such behaviour may result from dissociation of the carboxyl proton ion (or carboxylate ion pair) or from the formation of hydrogen bonds with the chlorides in chloroform.

Figure 7.8 is an example of the 100 MHz ^{13}C-NMR spectrum of S-AA bulk copolymer in DMSO-D_6 at 90 °C. The resonance peak at 44 ppm is produced by the methylene carbon of the acrylic acid unit in the copolymer chain. All other carbons in the copolymer chain in the 36-42 ppm range were overlapped by DMSO. The C_2-C_5 carbons of phenyl have peaks at 125-130 ppm, the C_1 carbon of phenyl at 143-144.5 ppm (tripeaks), and the carboxyl carbon at 175-177.5 ppm (tripeaks). Two tripeaks

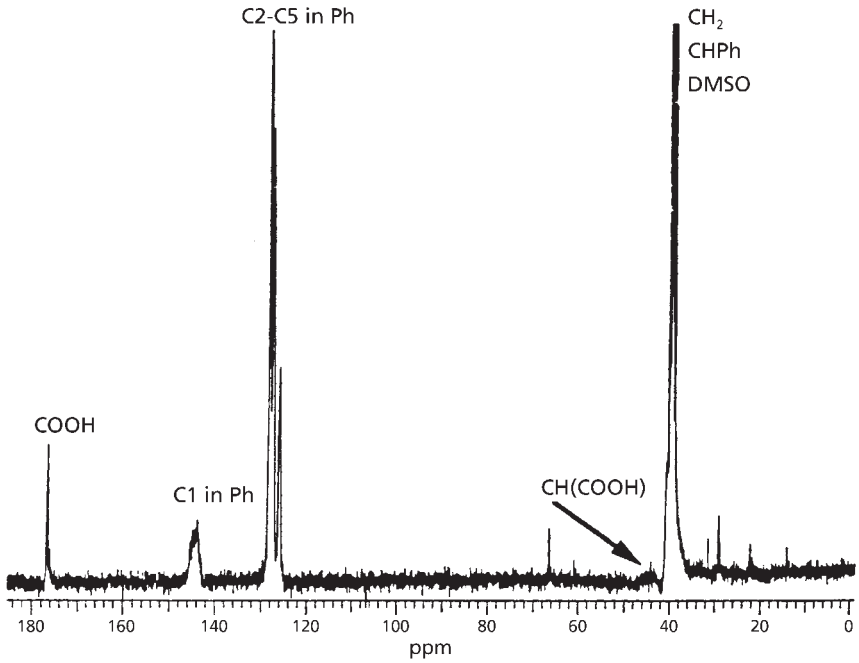

Figure 7.8 ^{13}C-NMR spectra of styrene-acrylic acid copolymer, SA-40, DMSO as solvent at 90 °C. (*Reprinted with permission from S. Wong and G.W. Poehlein, Journal of Applied Polymer Science, 1993,* ***49****, 6, 991. ©1993 John Wiley and Sons [105]*)

caused by carboxyl carbon and C_1 in phenyl may contain the information on the monomer sequence distribution. This will be discussed later.

The smaller peaks are the most interesting part of **Figure 7.8**. Higher concentration samples (> 10%) were used in order to facilitate quantitative analysis. In addition to determining monomer composition in the range 30-85% styrene in copolymer, this method has been used in sequencing distribution studies.

Figure 7.9 and Figure 7.10 show the expanded ^{13}C-NMR spectra of the carboxyl carbon and the C_1 carbon of phenyl in the copolymer, respectively. The split resonance peaks for one kind of carbon make it possible to investigate the monomer sequence distribution. The triads were assigned as shown in **Figures 7.9 and 7.10**.

With emulsion copolymers the mole fractions of styrene triplets (F_{SSS}) is much smaller and the mole fraction of acrylate-styrene-acrylate units (F_{ASA}) is much higher than the corresponding F_{SSS} and F_{ASA} values for bulk copolymers.

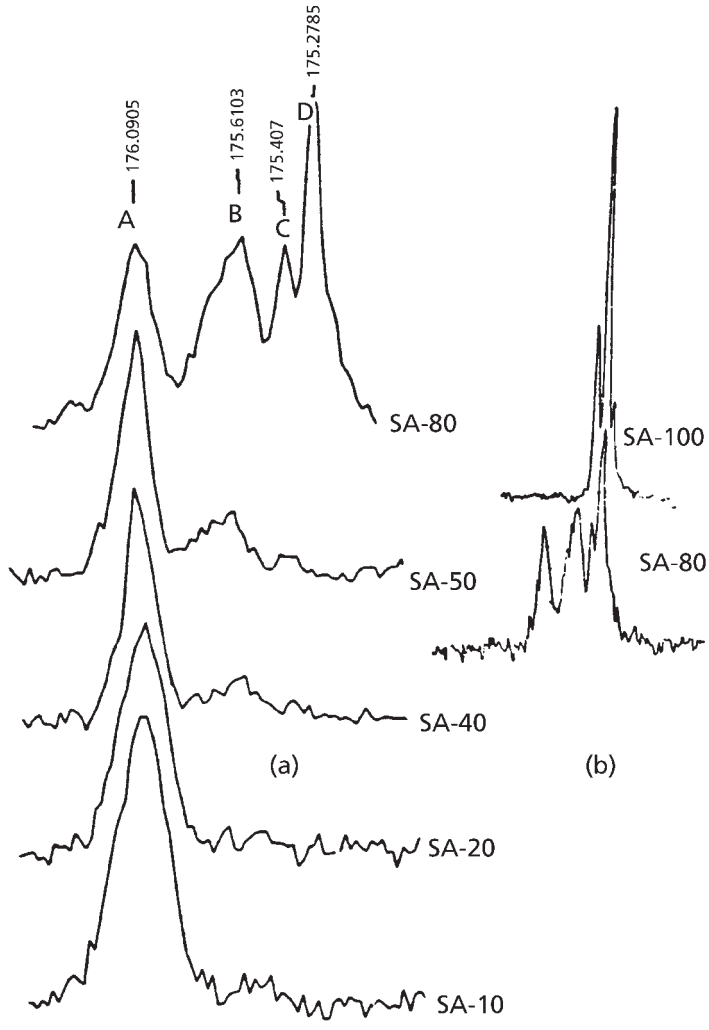

Figure 7.9 Expanded ^{13}C-NMR spectra of carboxyl carbon on S-AA copolymer. Peak: (A) SAS, (B) AAS, (C) AAA, (D) AAA. (*Reprinted with permission from S. Wong and G.W. Poehlein, Journal of Applied Polymer Science, 1993, **49**, 6, 991. ©1993 John Wiley and Sons [105]*)

Wong and Poelhlein [105] concluded that the distribution of styrene-acrylic acid copolymers can be measured by ^{13}C-NMR of the carboxyl carbon and the C_1, carbon of phenyl in S-AA copolymers. Low-conversion copolymer composition data obtained by NMR at different initial monomer ratios were used with the Kelen-Todos plot method to determine the reactivity ratios of r_a = 0.13 and r_s = 0.38. The resonance peaks split by triads were assigned and confirmed by comparing experimental triad

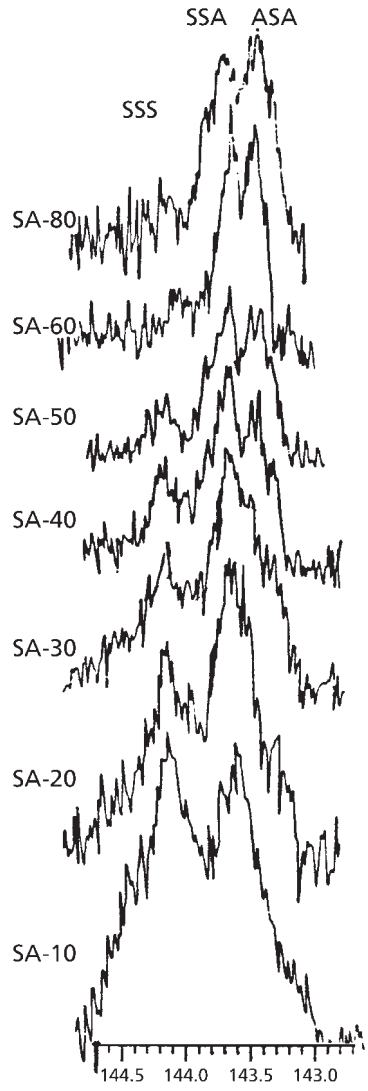

Figure 7.10 Expanded ^{13}C-NMR spectra of C_1 carbon of phenyl on S-AA copolymers. (*Reprinted with permission from S. Wong and G.W. Poehlein, Journal of Applied Polymer Science, 1993, **49**, 6, 991. ©1993 John Wiley and Sons [105]*)

values with those calculated from the Alfrey-Mayo statistics-kinetics model. The triad distribution of S-AA emulsion copolymers were measured to obtain information about emulsion copolymerisation mechanisms when hydrophilic/hydrophobic monomers are used.

7.2.3 Styrene-methyl Acrylate

Determination of the intramolecular (triad distribution, tacticity) and intermolecular (chemical composition and molar mass distribution) copolymer microstructure is generally recognised as a prerequisite, since revealing the molecular microstructure may supply information about the monomer addition process, e.g., about the preference of monomers to add in a (co)iso- or cosyndiotactic configuration [106-108]. Moreover, knowledge about the inter- and intra-molecular structures is of paramount importance for the understanding of relations between molecular structure and polymer properties [109-111]. Furthermore, the microstructure depends upon the polymerisation process and provides information on the reaction mechanisms occurring during polymerisation [112, 113]. NMR methods provide information on the average copolymer composition as well as on the intramolecular structure [106-108]. However, the majority of publications concerning the elucidation of intramolecular microstructure of copolymers deal with well-defined low-conversion (< 15%) bulk or solution copolymers. Several examples in the field of styrene-methacrylate copolymers can be found in the literature [83-84, 96, 114, 115]. Far less attention however, has been paid to the determination of the microstructure of copolymers obtained by high-conversion solution processes [102, 116] or high-conversion emulsion processes [117-119] even though high conversion is of great technological importance. In the case of high-conversion solution copolymerisation of styrene (S) and MMA, it has also been shown that the inter- and intra-molecular structure could be successfully predicted, on the basis of the integrated Alfrey-Mayo model, by using kinetic parameters obtained for low-conversion data [120-122]. Similar results were obtained by Tacx and co-workers [107] on the S-EMA system [96, 116]. However, due to the overlap of OCH_3 or OCH_2 resonances (in the S-MMA and S-EMA, respectively), and the methine main-chain backbone resonances in the ^{1}H-NMR spectra of the previously-mentioned systems [96, 115] as already put forward by Harwood [108], still problems may occur with the correct quantitative analysis of the sequence assignment of the acrylate-centred triads; see Kale and co-workers [95].

With this consideration in mind, van Doremaele and co-workers [103] studied S-MMA system, because (i) no overlap occurs between the OCH_3 resonances and the other main-chain resonances [123], (ii) mixed configurational and compositional sequence effects are reported to occur for the OCH_3 ^{1}H-NMR resonances [124-126], and (iii) the polymer statistics can be rigorously tested via an analysis of the ^{13}C carbonyl carbons [127, 128]. Contrary to S-MMA or S-EMA systems, [126, 129, 130] the ^{13}C chemical shifts of these carbons in the S-MMA system are only influenced by compositional sequence effects [130]. For low-conversion (< 20%) solution S-MMA copolymers, van Doremaele and co-workers [103] measured the reactivity ratios, and the set of reactivity ratio r values, together with the assumed Alfrey Mayo model, which were used to test the validity of this model (via an interpretation of the ^{13}C-NMR data). Moreover, they tried to distinguish between on the one hand

Ito's earlier peak assignment [123] (tentatively based on the same assignment order for S-MMA copolymers [83, 85]), which results in an extremely high coisotacticity (σ_{MS} = 0.8-0.9), and on the other hand an alternative assignment [131] apparently resulting in a much lower σ_{MS}.

In attempt to achieve this goal, 2D NMR COLOC experiments [132] were performed on three well-defined homogeneous low-conversion copolymers, thus trying to correlate the ^{1}H-NMR OCH_3 region and the ^{13}C-NMR carbonyl region. Related 2D-NMR techniques have been performed very recently on the alternating S-MMA system [133]. On the basis of triads only (with the influence of pentads neglected), the quantitative NMR results of the alternating S-MMA copolymers were approximately consistent with the I-Y assignment. However, no expansion was given of the 2D spectrum in the methoxy region of the random copolymer.

Van Doremaele and co-workers [103] also analysed the microstructure of some high-conversion solution S-MMA copolymers and compared it to model calculations using the integrated Alfrey Mayo model [102]. Even more challenging is the microstructure of high-conversion emulsion copolymers, because emulsion copolymerisation is a heterogeneous process. Therefore, models describing the emulsion copolymer microstructure are necessarily more complex. The model used by these workers for S-M copolymers takes into account this heterogeneity by calculating the monomer partitioning between the three phases [118-134]. With use of the Alfrey Mayo equations in combination with local monomer concentrations, together with numerical integration over conversion, the sequence distribution of the emulsion copolymer has been calculated and a comparison is made between the experimentally determined and the calculated triad fractions.

Van Doremaele and co-workers [103] concluded that the composition and sequence distribution of solution S-MMA copolymers can be described according to the integrated Alfrey-Mayo model. The experimental sequence distribution, in terms of triad fractions of emulsion S-MMA copolymers determined by means of ^{13}C-NMR, confirms the validity of the model calculations used.

Moreover, a comparison between the ^{1}H-NMR spectra of the emulsion copolymers and the model calculations of the triad fractions, demonstrates that, under the described experimental conditions, the coisotacticity parameter of S-MMA copolymers is independent of the polymerisation process used (i.e., solution or emulsion polymerisation); i.e., σ_{MS} = 0.9, provided the I-Y assignment is correct or σ_{MS} = 0.3 provided the alternative assignment is correct.

Brar and Sunita [135] used ^{13}C-NMR to determine sequence distributions in styrene-ethyl acrylate copolymers.

7.2.4 Styrene-methyl Methacrylate

An important system of interest in copolymerisation studies is the S-MMA copolymer. These copolymers have been extensively studied by proton NMR [136]. The result of these studies is that the analysis of sequence distribution is possible, although rather complicated due to sensitivity toward pentad sequences in the methoxy region. Another possibility for analysing sequence distributions is ^{13}C-NMR. The carbon NMR spectra of statistical copolymers of S-MMA were investigated by Katritzky and co-workers [137] and by Kato and co-workers [138]. It was shown that in carbon NMR a splitting not only occurs in the carbonyl, quaternary, methoxy, and α-methyl carbons in the MMA-centred unit, but also in the aromatic C_1 and methine carbons in the S-centred unit. Therefore, carbon NMR made it possible to determine simultaneously MMA-centred and S-centred stereosequences [101, 137, 138]. Katritzky and Kato independently developed an assignment for the aromatic C_1 resonance and the α-methyl main-chain carbon resonance [137, 138]. The assignments of the aromatic C_1 and α-methyl carbon resonances by Katritzky [137] and Kato [138] are, however, reversed. Hirai and co-workers [120] pointed out this problem and confirmed that the Kato assignment (e.g., of the aromatic C_1) is the correct one. Hirai showed that the assignments pertaining to the alternating structural parts in the carbon NMR spectra of the statistical S-MMA copolymers [139] are in agreement with the carbon NMR spectra of fully alternating S-MMA copolymers. The triplet peaks in the NMR spectra of the alternating copolymer of the styrene-methacrylate-styrene (SMS; methoxy protons) or methacrylate-styrene-methacrylate (MSM; C_1 carbon) triads were assigned as cosyndiotactic, coheterotactic, and coisotactic configuration in order of increasing shielding. This assignment was substantiated by comparison of the NMR peak areas of several carbons with the peak areas of the methoxy proton NMR signals of several alternating copolymers made with different kinds of Lewis acids [120, 139] and by the combined use of partly relaxed NMR signals and selective decoupling NMR techniques. Another ambiguity also exists in the literature: the tacticity splitting of the SMS triad of the α-methyl carbon resonance in the alternating S-MMA copolymer seems to have the same order of shielding as the aromatic C_1 [131], but in the proton NMR assignment then reverse situation has been suggested [124]. Although these assignments in the proton NMR spectra are seemingly confirmed by calculations, [121] the 2D NOESY (two-dimensional nuclear Overhauser effect spectroscopy) experiments of Heffner [133] showed that this is impossible: a cross peak exists between the α-methyl and the aromatic proton signals at lower field. Notwithstanding these contradictions in the assignments, up to now the assignments and the conclusions of Katritzky and co-workers [137] and of Hirai and co-workers [120] are both used in the literature indiscriminately [131, 140].

To further develop views on sequencing in S-MMA, Aerdts and co-workers [141] discuss the α-methyl resonances in both the CH and the ^{13}C-NMR spectra of alternating copolymers, and secondly the carbon resonances of the aromatic C_1

and α-methyl carbon of the statistical copolymers which they assigned in terms of configurational and triad sequences. The basic structure of S-MMA-S sequence is:

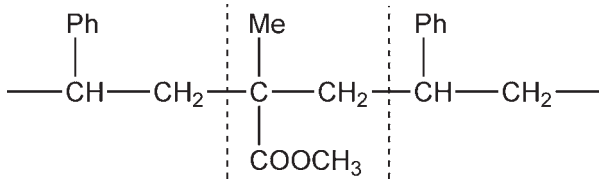

Alternating and statistical copolymers were considered as shown in **Figure 7.11,** the methoxy protons in alternating copolymers are split into three peaks: X (3.5-3.2 ppm, syndiotactic), Y (3.3-2.8 ppm, heterotactic) and Z (2.7-2.2 ppm, isotactic). In **Figure 7.12** the three different configurations are shown.

Whereas in the alternating S-MMA copolymers, there exist only three different configurations of the SMS triad and three different configurations of the MSM triad the number of sequences in statistical S-MMA copolymers clearly exceeds that in alternating copolymers.

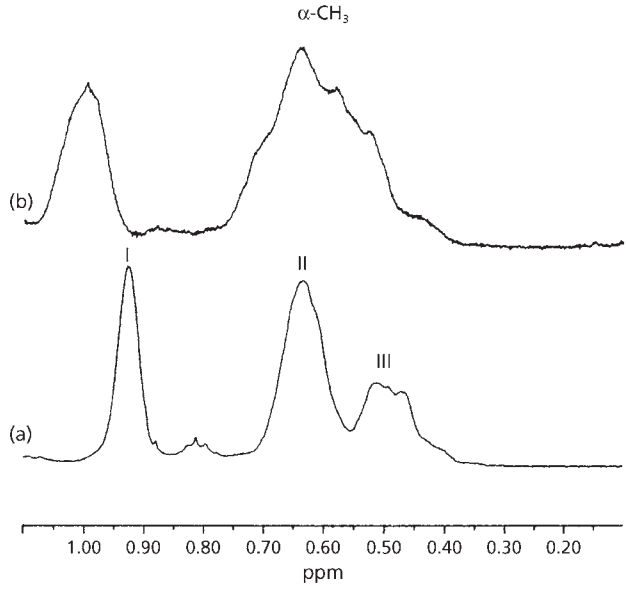

Figure 7.11 Expanded proton NMR spectra of the α-methy resonances of the alternating copolymer (a) in hexachloro-1,3-butadiene and (b) in $CDCl_3$. (*Reprinted with permission from A.M. Aerdts, J.W. de Haan and A.L. German, Macromolecules, 1993,* **26***, 8, 1965. ©1993, ACS [141]*)

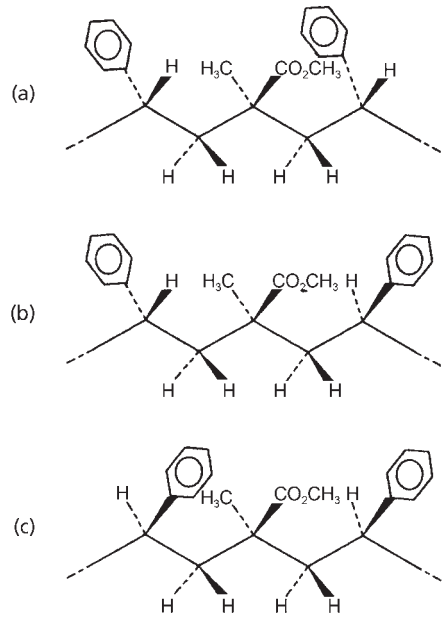

Figure 7.12 Various configurations of the SMS triad: (a) syndiotactic, (b) heterotactic, (c) isotactic. (*Reprinted with permission from A.M. Aerdts, J.W. de Haan and A.L. German, Macromolecules, 1993, **26**, 8, 1965. ©1993, ACS [141]*)

In statistical copolymers a total of 20 configurational sequences occur; i.e., for the MMA-centred triads, the following 10 tacticity coefficients and sequences are possible: $\sigma_{mm}{}^2 F_{mmm}$, $2\ \sigma_{mm}\ (1 - \sigma_{mm})\ F_{mmm}$, and $(1 - \sigma_{mm})^2\ F_{mmm}$ for the MMM sequence, $\sigma_{mm}\ \sigma_{ms}\ F_{mms}$, $(1 - \sigma_{mm})\ \sigma_{sm}\ F_{mms}$, $\sigma_{mm}\ (1 - \sigma_{sm})\ F_{mms}$, and $(1 - \sigma_{mm})\ (1 - \sigma_{sm})\ F_{mms}$, for the MMS or SMM sequences, and $\sigma_{sm}{}^2\ F_{sms}$, $2\ \sigma_{sm}\ (1 - \sigma_{sm})\ F_{sms}$, and $(1 - \sigma_{sm})^2\ F_{sms}$ for the SMS sequences.

Here σ is the probability that two adjacent monomeric units have a meso configuration (isotactic). Similar configurational sequences are present for the S-centred triads. The coisotacticity σ_{sm} is calculated from the methoxy region in the proton NMR spectrum to be 0.44 [136, 95]. The other tacticities σ_{mm} and σ_{ss} are taken from the carbon NMR spectra of the homopolymers: 0.23 [142] and 0.29, respectively [121].

Aerdts and co-workers [141] conclude that the MMA-centred triads and the styrene-centred triads can be directly calculated from the α-CH_3 and C_1 peak areas in the carbon NMR spectra. This is contrary to the proton NMR spectra of the SMMA copolymers, where the peak splitting of the methoxy protons is so complicated that the peak areas cannot be translated directly to sequences. It is only possible to

theoretically predict M-centred pentads, in which case the peak areas can be calculated and compared with experimental values.

Various other workers have applied high resolution NMR to the measurement of sequences in S-MMA copolymers [122, 143, 124].

7.2.5 Styrene-n-butyl Acrylate

Although as, can be seen from the discussion so far, ^{1}H- and ^{13}C-NMR spectroscopy predominates as a means of establishing sequencing in styrene-acrylate and styrene-methacrylate copolymers other techniques such as Py-GC have been employed.

Wang and Smith [144] have described a Py-GC method to investigate the microstructure of emulsion polymers. The number-average sequence length, which reflects the monomer arrangement in the polymer, was calculated using the formulas that incorporate the pure trimer peak intensities and hybrid trimer peak intensities. In this study, styrene and *n*-butyl acrylate copolymer systems were used to measure 'the degree of structure' (i.e., the number-average sequence length for styrene and *n*-butyl acrylate repeat units) and compared to a homogeneous nonstructured (or random) copolymer. The number-average sequence length information was further extended to calculate the composition. For the emulsion polymers examined in this study, the composition elucidated from the number-average sequence length matched the preparation recipe and/or what was measured by ^{13}C-NMR.

Pyrolysis followed by GC separation is a mechanism utilising thermal energy to break down a polymeric structure to monomers and oligomers and separation of those units for quantitation. Because of the temperature limitations of the common silicone capillary column, only the dimer and trimers of the system studied here can be reliably separated and detected. The major mechanism of producing dimers and trimers with pyrolysis can be attributed to thermal degradation. A relatively small amount of dimers and trimers is formed as a result of a recombination of monomers. This mechanism is demonstrated as follows:

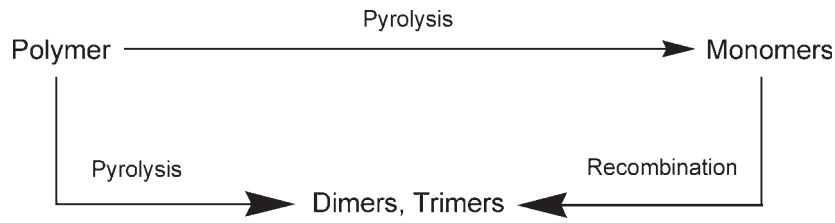

The intensity of the various dimer and trimer peaks in a pyrolysis gas chromatogram will reflect the monomer sequence. Pyrolysis of an emulsion polymer is performed on

the dried film. The liquid emulsion is heated in the pyrolysis chamber at 250 °C for 10 minutes and allowed to coalesce to a solid. A volatility experiment showed there were no detectable materials released during this period.

The response of the flame ionization detector (FID) detector is assumed equal for all three styrene-centred trimers and for all three *n*-butyl acrylate centred trimers in this study. Essentially, FID is a carbon atom counter; any components having the same number of carbon atoms should have the same response. The styrene-centred trimers have 22-24 carbon atoms; the difference in carbon atoms is less than ±5% around those trimers. This fact makes the equal response assumption valid. The same argument also applied to *n*-butyl acrylate-centred trimers.

The 500 °C pyrolysis temperature was chosen to obtain a higher yield of trimer for both styrene and *n*-butyl acrylate. **Figure 7.13** shows the typical pyrogram of a 50%/50% by weight STY/*n*-BA homogeneous emulsion polymer. **Figure 7.14** is an expansion of the trimer area in **Figure 7.13**.

Figure 7.15 shows the pyrogram of the trimer area for five different mole compositions of STY/*n*-BA. The number-average sequence lengths were calculated for all five polymers. The peak areas were normalised on the basis of the summation of N_{SSS}, and

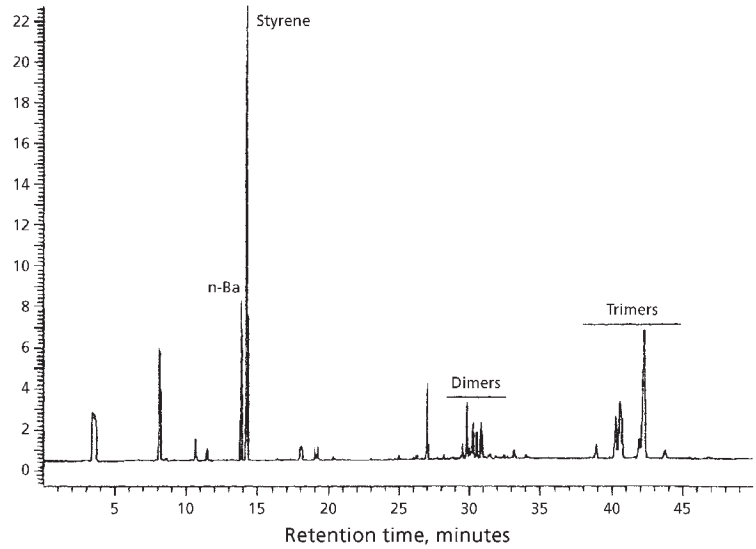

Figure 7.13 Typical pyrogram of a 50%/50% by weight STY/*n*-BA homogeneous emulsion polymer. (*Reprinted with permission from F.C-Y. Wang and P.B. Smith, Analytical Chemistry, 1996, 68, 17, 3033. ©1996, ACS, USA. [144]*)

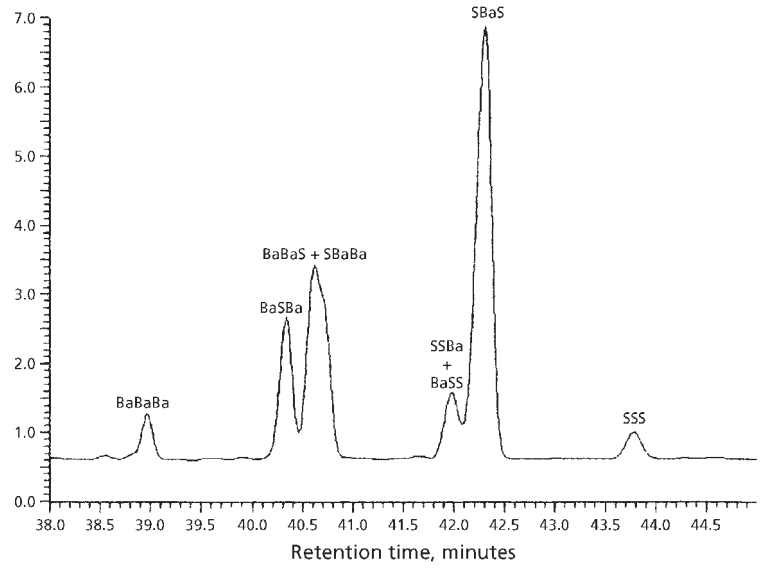

Figure 7.14 Trimer area of 50%/50% STY/*n*-BA homogeneous emulsion polymer with trimer assignments, where Ba = *n*-butyl acrylate and S = styrene. (*Reprinted with permission from F.C-Y. Wang and P.B. Smith, Analytical Chemistry, 1996, 68, 17, 3033. ©1996, ACS, USA. [144]*)

$N_{SSBA + BASS}$, and N_{BaSBa} equalling 1 and the summation of N_{BABABA}, $N_{SBABA + BABAS}$, and N_{BASBA} equalling 1. All normalised peak areas were then used to calculate the number-average sequence length for both styrene and *n*-butyl acrylate (**Table 7.7**).

Wang and Smith [144] concluded that by applying the proper statistical formula and the data obtainable from Py-GC, the number-average sequence length as well as the monomer composition of an emulsion copolymer can be explored. The structure of a copolymer of two monomeric types can be quantified by deriving the percentage of grouped monomers and the number-average length of grouped monomers. This method could be extended to any copolymer system as long as all six trimer peaks can be identified and the peak intensities obtained by assuming that these intensities represent the polymer compositions. This method extends the capabilities of pyrolysis not only in the quantitative study of monomer composition but also in the realm of polymer structure investigation.

In further work Wang and Smith [145] applied Py-GC to the determination of the number average trimer sequence lengths of grouped monomers in styrene-*n*-butyl acrylate copolymers. The method can be applied to any copolymer system as long as all six trimer peaks were identified and peak intensities obtained.

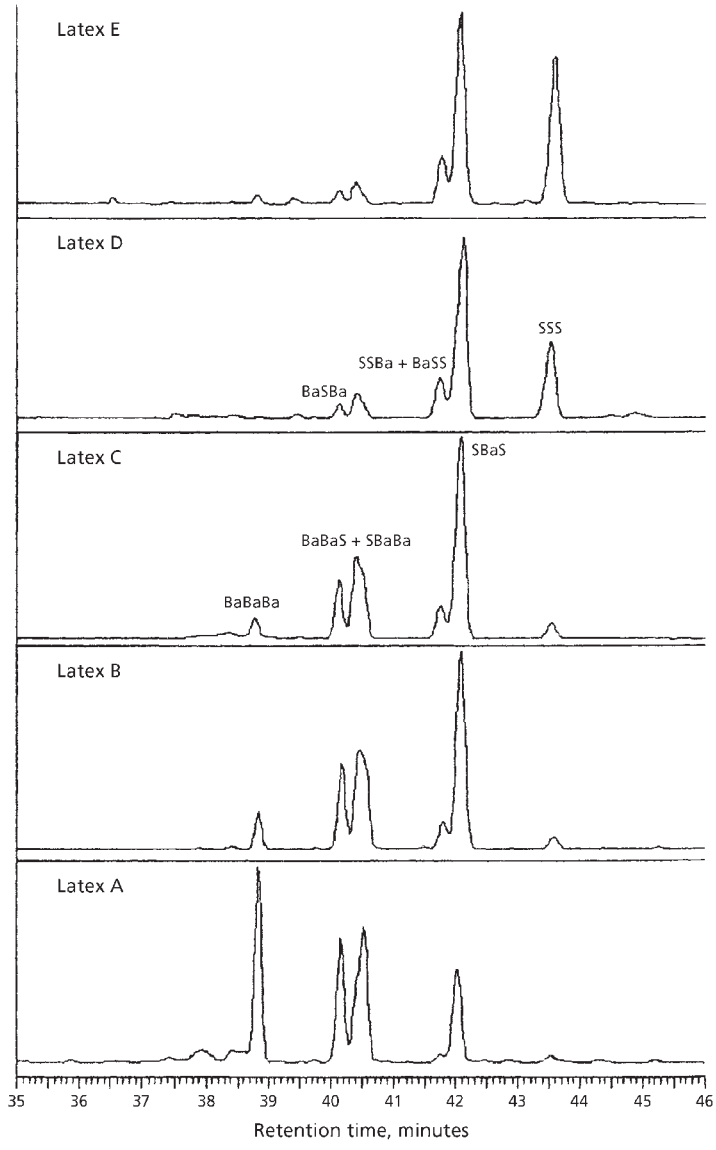

Figure 7.15 Pyrogram of the trimer area for five different compositions of STY/*n*-BA. The pure trimer peaks directly reflect the relative abundance of the monomers, where Ba = *n*-butyl acrylate and S = styrene. (*Reprinted with permission from F.C-Y. Wang and P.B. Smith, Analytical Chemistry, 1996, 68, 17, 3033. ©1996, ACS, USA. [144]*)

Table 7.7 Number-average sequence length for different compositions of homogenous styrene-a-butylacrylate (S-B) emulsion polymers from Py-GC method

Mole% of styrene in co-polymer	A	B	C	D	E
Normalised peak intensity					
SSS	0.069	0.116	0.168	0.610	0.733
SSB + BSS	0.058	0.221	0.322	0.305	0.210
BSB	0.872	0.663	0.511	0.085	0.057
N(S)	1.11	1.29	1.49	4.21	6.17
BBB	0.374	0.076	0.058	0.005	0.031
BBS + SBB	0.401	0.379	0.323	0.123	0.106
SBS	0.224	0.545	0.620	0.872	0.863
N(B)	2.35	1.36	1.28	1.07	1.09
mol %					
S	32	49	54	80	85
B	68	51	46	20	15
Experimental wt%					
S	28	44	49	76	82
B	72	56	51	24	18
Standard wt%					
S	25	43	50	74a	82
B	75	57	50	26a	18
Grouped (%)					
S	13	34	49	91	94
B	78	46	38	13	14
Grouped					
N(S)	4.39	3.05	3.04	3.00	8.98
N(B)	3.86	2.40	2.36	2.08	2.59

A-E: Weight percentage determined by ^{13}C-NMR analysis, for compostitions of A-E SB under mole% above.

*Reprinted with permission from F.C-Y. Wang and P.B. Smith, Analytical Chemistry, 1996, **68**, 17, 3033. ©1996, ACS [144]*

7.2.6 Styrene-methacrylate Copolymers

Styrene Methacrylate

Wang and Smith [144] showed that it is not possible to determine the number-average sequence length of STY/MMA copolymer systems using only the dimer and trimer peak distribution by Py-GC because MMA dimer and MMA trimer fragments are not generated in detectable quantities. By determination of the number-average sequence length of styrene (which was calculated from dimers) and the composition (which is calculated from monomers), the number-average sequence length of MMA was calculated. The structure information was further quantified by deriving the percentage of grouped monomers and the number average length of grouped monomers. This method could be extended to other copolymer systems in which one of the monomers does not produce stable dimer and trimer fragments but gives stable monomer peaks. This class of polymers includes α-methylstyrene and aliphatic methacrylates. This development, extends the structural study of copolymers by Py-GC not only to the well-behaved copolymer system but also to those copolymer systems that produce incomplete dimer and trimer fragments.

Table 7.8 shows some typical results obtained by this procedure for structured. Randomly distributed and blend S-MMA copolymers.

Table 7.8 shows the number-average sequence length (N(S), $N(M)$) and other structure-related terms for these three polymers. The structural differences between these three emulsion polymers can be seen by the large difference in the number-average sequence for both styrene and MMA. The grouped number-average sequence length and the percentage of the grouped monomer strongly indicated that the structured polymer H has a separate domain of polymerised styrene and MMA, but polymer blend J has entirely separate polymeric monomers.

For copolymers containing monomers such as α-methylstyrene and aliphatic methacrylate, there is a unique phenomenon of polymer degradation when a methyl group attaches to one of the vinyl carbons. The monomer is always the most favourable degradation product. In this situation, there is no detectable dimer or trimer available for any structure interpretation for Py-GC. The ultimate way to obtain structure information is to rely on the partially available dimer and trimer peaks and the composition.

The applicationof NMR to sequencing in styrene-methacrylate has also been reported [146, 127].

Table 7.8 Composition and number-average sequence length data for structured (H), randomly distributed (I) and blend (J) styrene-methylmethacrylate polymers from Py-GC method[a]

	Sample ID		
	H	**I**	**J**
Std wt% S	82[b]	82[b]	82[b]
Std wt% M	18[b]	18[b]	18[b]
Wt% S	82.8	82.8	82.8
Wt% M	17.2	17.2	17.2
N(S)	61.25	6.75	1580
N(M)	13.21	1.45	342
%G(S)	99	92	100
%G(M)	97	39	100
GN(S)	889.5	13.0	4190
GN(M)	28.4	5.5	493

[a] N(S), N(M) = number average sequence lengths for styrene and methylmethacrylate units.

%G(S) and GN(M) are % of grouped monomer units.

GN(S) and GN(M) are number average sequence length of grouped monomer units.

[b] Composition data from ^{13}C-NMR results

*Reprinted with permission from F.C-Y. Wang and P.B. Smith, Analytical Chemistry, 1996, **68**, 17, 3033. ©1996, ACS [144]*

7.2.7 Methylmethacrylate – α-trifluoro-methacrylic Acid

It is often the case that both monomer sequence and stereochemical configuration must be taken into account when studying the microstructure of copolymers. In ^{1}H-NMR, the resonances appear to be broad because of a multitude of chemical shifts corresponding to the many possible sequences present. There are too many of these to be individually resolved and assigned. Only those spectra of simple copolymers, e.g., the alternating ST-MMA copolymer, have been assigned without doubt [133]. Isotactic and syndiotactic MA-MMA copolymers have been studied by ^{1}H-NMR in different solvents and the peaks due to the methyl groups were assigned completely [147]. Xu and Frisch [128] have reported the results of the structural study of MMA-α-trifluoromethacrylic acid (TFMA) copolymers using

the methyl resonance of the ^{1}H-NMR spectra where both the monomer sequence and the stereochemical configuration were considered.

MMA-TFMA copolymer shows three broad peaks each with fine splitting (**Figure 7.16**). The splitting is caused by the different triad monomer sequences of the copolymer at each of the triad stereochemical configurations rather than by the pentad stereochemical configuration.

Consideration of the M-centred triad monomer sequences and the stereochemical configurations of the copolymer, lead one to expect to find ten of them: M_rM_rM, M_rM_mM, M_mM_mM, M_rM_rF, M_rM_mF, M_mM_rF, M_mM_mF, F_rM_rF, F_rM_mF, and F_mM_mF which are numbered from 1 to 10, respectively, in **Figures 7.16 and 7.17**. (M = Methyl methacrylate, F = fluoromethacrylic acid). Yet the intensities of each of the finely split peaks would be very hard to determine due to the overlapping of those peaks. Deuterated pyridine was also used to obtain the NMR spectra of PMMA and the copolymer. A different pattern of the ^{1}H-NMR spectrum for the copolymer was obtained (as shown in **Figure 7.17**). By comparing the ^{1}H-NMR spectrum of the copolymer with that of PMMA in pyridine, it was recognised that the copolymer sequences gave rise to the resonance in the methyl region which were not so much overlapped with those peaks due to the stereochemical configurations of the pure PMMA. The spectra show further that the peaks due to the different monomer sequences are shifted by different distances. This is useful for assigning the peaks. Three peaks located at 1.22, 1.33, and 1.48 ppm can be directly assigned to M_rM_rM, M_rM_mM or M_mM_rM and M_mM_mM, respectively,

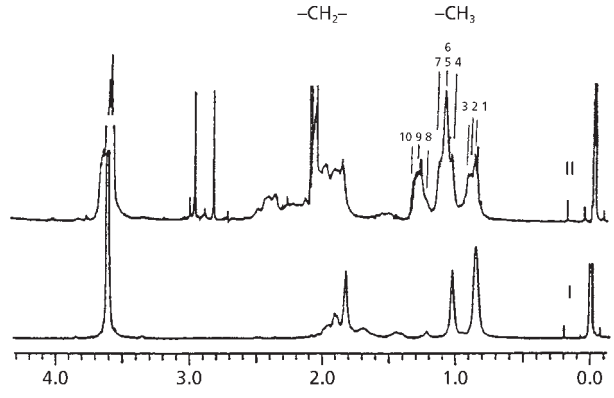

Figure 7.16 1H-NMR spectra of PMMA (I) and MMA-TFMA copolymer (II) with 23% of TFMA in molar percentage in acetone-d6. (*Reprinted with permission from Q. Xu and H.L. Frisch, Journal of Polymer Science Part A: Polymer Chemistry Edition, 1994, 32, 15, 2803. ©1994, John Wiley and Sons [128])*

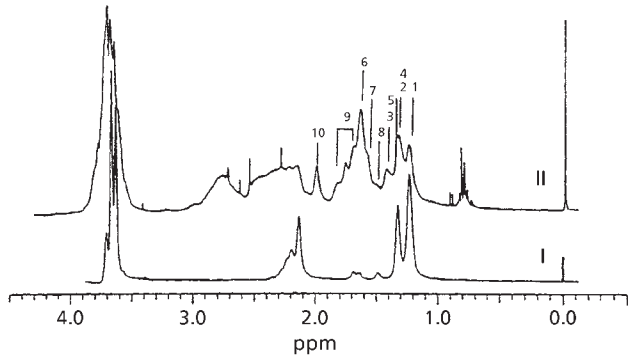

Figure 7.17 ^{1}H-NMR spectra of PMMA (I) and MMA-TFMA copolymer (II) with 23% of TFMA in molar percentage in acetone-d5. (*Reprinted with permission from Q. Xu and H.L. Frisch, Journal of Polymer Science Part A: Polymer Chemistry Edition, 1994, 32, 15, 2803. ©1994, John Wiley and Sons [128]*)

Table 7.9 Triad sequence intensities of methyl resonance in ^{1}H-NMR spectrum of MMA-TFMA copolymer (15% TFMA)

Peak	1	2	3	4	5	6	7	8	9	10
Intensity	160	10	7	115	21	44	22	16	18	2.5
Triad (Stereochemical Configurations)	*rr* (Peak 1 + 2 + 3)			*rm* (Peak 4 + 5 +6 + 7)				*mm* (Peak 8 + 9 + 10)		
Intensity (%)										
In acetone-d6	43			49				9		
In pyridine-d5	43			47				11		
Triad monomer sequence	MMM (Peak 1 + 4 + 8)			MMF (Peak 2 + 5 + 6 + 9)				FMF (Peak 3 + 7 + 10)		
Intensity (%)	70.0			22.4				7.6		
TFMA% (C)[a]										
In molar	15.8									

[a] *C = B/(A + B), A = 70 + 22.4 + 7.6 = 100, B = 22.4/2 + 7.6 = 18.8*

TFMA: MMA-α-trifluoromethacrylic acid

*Reprinted with permission from Q. Xu and H.L. Frisch, Journal of Polymer Science Part A: Polymer Chemistry Edition, 1994, **32**, 15, 2803. ©1994, John Wiley and Sons [128]*

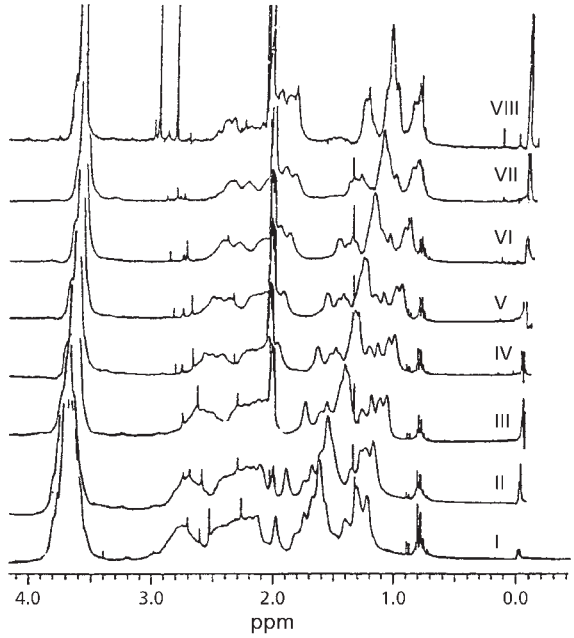

Figure 7.18 ^{1}H-NMR spectra of MMA-TFMA copolymer with 23% of TFMA in molar percentage in solvent mixture of pyridine-d5 and acetone-d6 at the pyridine/acetone volume ratios of (I) 100/0, (II) 85/15, (III) 70/30, (IV) 50/50, (V) 40/60, (VI) 30/70, (VII) 10/90, and (VIII) 0/100. (*Reprinted with permission from Q. Xu and H.L. Frisch, Journal of Polymer Science Part A: Polymer Chemistry Edition, 1994, 32, 15, 2803. ©1994, John Wiley and Sons [128]*)

by comparing the two spectra in **Figure 7.17**. Xu and Frisch [128] observed, in **Figure 7.18**, the peaks shifting as the solvent was changed from acetone to pyridine. One of the two peaks due to sequences M_mM_mF and F_mM_mF shifted to 1.99 ppm. One of the three peaks due to sequences M_mM_rF, M_rM_mF, and F_mM_rF shifted to 1.4 ppm. Two peaks due to sequences M_rM_rF and F_rM_rF shifted to 1.3 and 1.4 ppm, and overlapped with the peaks due to M_mM_rM and M_mM_rF sequences.

The triad sequences found are given in **Table 7.9**. The triad monomer sequences are limited to MMM, MMF, FMF and MFM. There are no such sequences as FFM or FFF.

Sequencing studies have been conducted on other methacrylate and styrene containing copolymers. These include S-MMA [124, 133, 143, 148, 149], styrene-methacrylic acid [150], methacrylic acid-MMA [147], acrylic acid-methacrylic acid [100], methacrylate-

ethyl acetate [151, 152], MMA-tri-*n*-butyl methacrylate, MMA-methylacrylate [153], MMA-ethyl methacrylate [154], methacrylic ester-hydroxy acrylate [155].

7.2.8 Styrene-methacrylonitrile

For vinyl copolymers, NMR studies provide valuable information on the mode of arrangements of different comonomeric units along the polymer chain (comonomer sequence) and the stereochemistry of the placement of these units along the polymer chain (cotacticity). Since the overall physicomechanical properties of the copolymers are dependent on these structural features, the investigation of their microstructures is of fundamental interest. Amongst the large number of copolymer systems investigated, greater attention has been paid to styrene-MMA and styrene-acrylonitrile copolymers for microstructure analysis [137, 145, 156-161].

Whereas intensive ^{1}H and ^{13}C-NMR studies have been pursued for these copolymer systems surprisingly little information is available on another closely related copolymer system, namely styrene-methacrylonitrile copolymer, except for a few ^{1}H-NMR studies by Harwood and co-workers [162-164].

Dhal and Steigel [165] carried out a full microstructural analysis of 2,2′-azobisisobutyronitrile initiated random and alternating styrene-methacrylonitrile copolymers by ^{13}C-NMR.

By carrying out NMR measurements at higher magnetic fields (75 MHz for ^{13}C-NMR) it became possible to obtain highly resolved resonance lines which can be utilised for structural analysis. **Figures 7.19 and 7.20** show, ^{13}C-NMR spectra of random and alternating styrene-methacrylonitrile copolymers, respectively.

A ^{13}C-NMR spectrum of a random copolymer (**Figure 7.19**) reveals several multiple lines for various carbon atoms suggesting their sensitivity to the structural arrangements of the comonomer units along the polymer chain. Of the different carbon atoms, the fine structures exhibited by the backbone quaternary carbon atom due to methacrylonitrile units and the methine carbon atom of the styrene units are particularly significant and have been utilised for comonomer sequence analyses.

For the quaternary carbon atom, unlike a single resonance line observed around 32.5 ppm in the homopolymer spectrum of polymethacrylonitrile, three distinct signals with further finer structures within themselves were observed in the spectra of the copolymers. This is a clear indication of the sensitivity of this carbon atom to comonomer sequence distributions. Assignments of these peaks under three general regions of chemical shifts to different sequential triads were carried out systematically

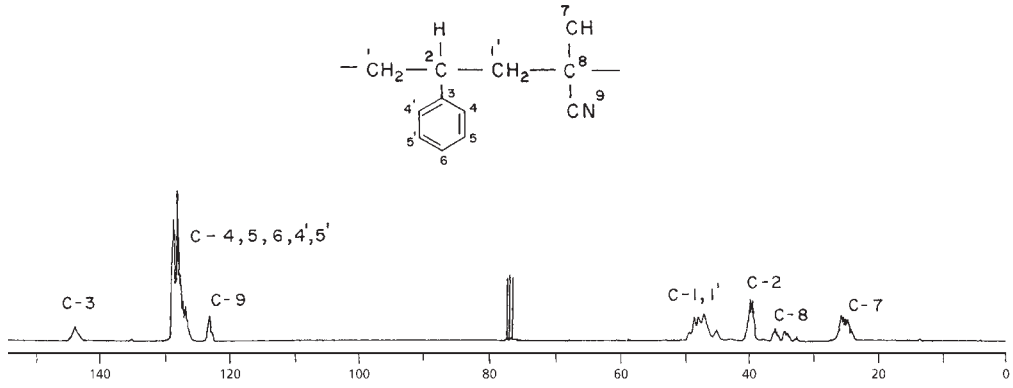

Figure 7.19 Typical ^{13}C-NMR spectrum of a STY:MAN (53:47) copolymer. (*Reprinted with permission from P.K. Dhal and A. Steigel, Polymer, 1991, 32, 4, 721. ©1991, Elsevier [165]*)

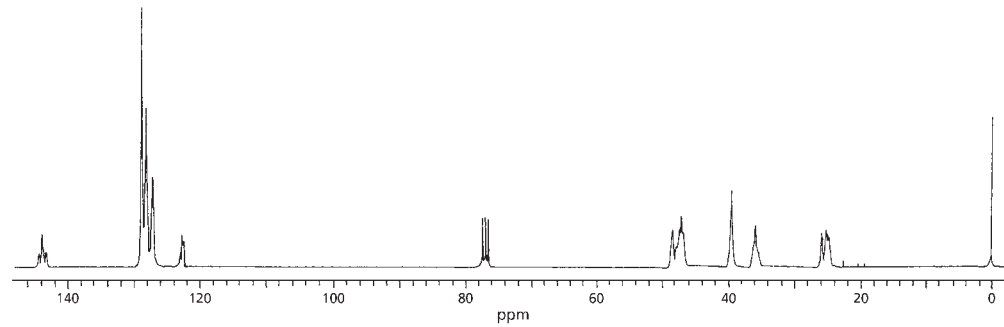

Figure 7.20 ^{13}C-NMR spectrum of alternating STY:MAN copolymer. (*Reprinted with permission from P.K. Dhal and A. Steigel, Polymer, 1991, 32, 4, 721. ©1991, Elsevier [165]*)

in the following manner. The peak appearing at approximately 32.5 ppm corresponds to that of polymethacrylonitrile and hence can be assigned to an MMM type triad. Similarly, the resonance lines at approximately 34.5 ppm and 36.0 ppm have been assigned to MMS + SMM and SMS triads, respectively, (the terms 'M' and 'S' correspond to methacrylonitrile and styrene monomer units, respectively).

After obtaining the sequence distribution information about the methacrylonitrile-centred comonomer triads, Dhal and Steigel [165] proceeded to analyse styrene-

Table 7.10 Chemical shift assignments of styrene centred comonomer triads from the backbone methane carbon resonance in styrene-methacrylonitrile copolymer.

Serial number	Mole fraction of styrene in copolymers	Chemical shift of different triads [a,b]		
		SSS	SSM + MSS	MSM
1	0.24	- -	39.9 (0.24)	39.5 (0.76)
2	0.53	40.8 (0.19)	40.0 (0.42)	39.5 (0.39)
3	0.88	40.8 (0.76)	40.1 (0.21)	39.5 (0.03)

[a] *The chemical shifts reported correspond to the peak maxima*

[b] *The numbers given inside brackets below the chemical shift values correspond to the relative intensities of these triads*

Reprinted from P.K. Dhal and A. Steigel, Polymer, 1991, ***32****, 4, 721.*
©1991, Elsevier [165]

centred comonomer sequence distributions in these copolymers. For this purpose, the resonance lines due to the backbone methine carbon atom belonging to the styrene monomer were used. This carbon atom resonates over the chemical shift range of 39.0-41.0 ppm and is adequately resolved to three signal lines, thus revealing its sensitivity to comonomer sequence effect at triad level.

On the basis of the variation of signal intensities as a function of copolymer composition as well as with the help of the calculated chemical shifts using ν contributions as described above, these workers assigned these three signal lines unambiguously to the three possible triads. The most downfield peak appearing at approximately 41.0 ppm corresponds to the methine carbon resonance of polystyrene and hence can be assigned to be SSS triad. Accordingly, the signals at approximately 40.0 ppm and 39.5 ppm have been ascribed to SSM + MSS and MSM triads, respectively. The information about the chemical shifts of these triads for different copolymer compositions are summarised in **Table 7.10**.

The legitimacy of these assignments of signals to different types of pentad structures is based on the following corelationships [166]:

$$mmmr + 2(rmmr) = mmrm + mmrr$$

$$mrrr + 2(mrrm) = rrmr + mmrr$$

where '*m*' and '*r*' correspond to the meso and racemic placement of comonomer units in a dyad as described earlier. Because these sets of equations are independent of any type of propagation models, such as Bernoullian or Markovian, they serve as an excellent test for verifying the authenticity of signal assignments to different configurational triads. These requirements are met reasonably well for all the three carbon atoms, thereby approving the authenticity of the analysis.

Dong and Hill [167] analysed the FT-IR spectra of a series of random styrene-methacrylonitrile copolymers to determine the dependence of the observed frequencies of the individual spectral peaks on copolymer composition.

The CN bond stretching frequency was shifted to a higher value with an increase in the methacrylonitrile (MAN) content in the copolymers. There was no linear relationship between the CN frequency and the diad fraction of MAN-MAN linkages in the copolymer chain, as reported previously for styrene-acrylonitrile copolymers. Different methods for the copolymer sample preparation can cause differences in the shifts in the CN frequency. This suggests that the polymer morphology plays an important role. A study of blends of polymethacrylonitrile (PMAN) with polystyrene has shown that the CN frequency is shifted to a higher value with an increase of the PMAN composition of the blends.

When the MAN content of the copolymers is above 40 mol%, some MAN units in the copolymer chain would not have an adjacent styrene unit. Then the repulsion between neighbour MAN units would lead to an increase in the CN bond stretching frequency. In addition, if the samples were dissolved in solution or if they were precipitated rapidly, as for the potassium bromide-disk samples, the establishment of the equilibrium conformation to form a specific interaction between the MAN units and their neighbouring styrene units would not be optimised. Therefore, the single, unique value for the CN bond stretching frequency would not be observed for the solution or precipitated samples when the MAN content in the SMAN copolymers is less than 40 mol%.

7.2.8 Butadiene-methylmethacrylate

Upon ozonolysis this copolymer yields succinic acid, succindialdehyde and dicarboxylic acids containing several MMA residues. The percentage of butadiene (9.2%) recovered as succinic acid and succindialdehyde provided a measure of the 1,4-butadiene-1,4-butadiene linkages in the copolymers, and the percentage of MMA units (51%) recovered as trimethyl 2-methyl-butane-1,2,4-tricarboxylate (4) $n = 1$, provided a measure of the MMA units in the middle of butadiene-methacrylate-butadiene triads.

7.3 Vinyl Acetate Copolymers

7.3.1 Ethylene-vinyl Acetate

Beshah [168] has pointed out that conventional techniques involving estimation of chemical shifts of particular species in comonomer sequences from empirical additive rules and estimation of relative intensities assuming Bernoullian or Markovian propagation statistics has some drawback to the universal implementation of the techniques. These reasons include the fact that chemical shifts are mostly dependent on the nature of solvents, temperature, pH, and impurity materials such as paramagnetic species and as a result, it becomes difficult to use literature values for the empirical rules. Also, stereochemical configuration and comonomer sequencing produce similar intensities for many sequence probabilities, hence assignment of comonomer sequences based on the theoretical fit of peak intensities may have some ambiguities.

Table 7.11 ^{13}C Chemical shift assignment of ethylene-vinyl acetate copolymers

Carbon	Moiety	Structure segment	^{13}C Chemical shift (ppm)
CH_3O	P	V	20.9
CH_2	$S_{\beta\beta}$	VEV	21.3
CH_2	$S_{\beta\delta}$	EVEE	25.4
CH_2	$S_{\beta\delta}$	VVEE	25.7
CH_2	$S_{\gamma\delta}$	VEEE	29.9
CH_2	$S_{\delta\delta}$, $S_{\gamma\gamma}$	EEEE, EE	30.1
CH_2	$S_{\alpha\gamma}$	EVEV	34.2
CH_2	$S_{\alpha\delta}$	VVEE	34.5
CH_2	$S_{\alpha\delta}$	EVEE	34.6
CH_2	$S_{\alpha\delta}$[a]		35.3
CH_2	$S_{\alpha\alpha}$	EVVE	39
CH_2	$S_{\alpha\alpha}$	VVVE	39.5
CH	$T_{\beta\beta}$	VVV	69.3 – 69.7
CH	$T_{\beta\delta}$	VV and VVV	70.6 – 71.1
CH	$T_{\delta\delta}$	EVEE	73.4 - 74

[a] *Irregular sequence*

Reprinted with permission from K. Beshah, Macromolecules, 1992, 25, 21, 5597. ©1992, ACS [168]

A summary of the ^{13}C chemical shift assignments together with the structural block segment to which the carbon moiety belongs is summarised in **Table 7.11**.

Beshah [168] has analysed the comonomer sequences of ethylene-vinyl acetate copolymer by a novel approach that utilises two-dimensional heteronuclear single quantum coherence and total correlation spectroscopy (2D HSQC-TOCSY). The combined carbon-proton and proton-proton correlations in a single 2D experiment enables a *direct* correlation among neighbouring species. Hence, it is independent of the estimations of chemical shifts and peak intensities that are requisites of conventional procedures. Moreover, the proton-detected heteronuclear correlation experiment takes advantage of the high resolution of ^{13}C as well as the high sensitivity of ^{1}H-NMR spectroscopy. As a result, it was possible to obtain improved assignments and much more detailed microstructural information.

7.3.2 Vinyl Acetate-methyl Acrylate

Florjanczyk and Skórkiewicz [169] investigated the monomer sequence distribution in vinyl acetate-methyl acrylate copolymers prepared using ethyl aluminium chloride catalysts. They assigned the methyl acrylate centred triads but did not determine the triad sequences quantitatively. Brar and Charan [170] reported the determination by proton magnetic resonance spectroscopy of the comonomer sequence distribution in terms of various V- and M-centred triads using methine resonance signals of V- as well as M-monomeric units. The resonance signals due to the methine carbon of the M-monomeric unit and the methylene carbons of the V-monomeric unit were differentiated using the ^{13}C-NMR DEPT technique.

The experimental values of V- and M-centred triads from ^{13}C $\{^{1}H\}$ triads were compared with the theoretical values from Harwood's [171] statistical model using copolymerisation reactivity ratios. The reactivity ratios for free-radical solution copolymerisation of V with M were calculated using the Kelen-Tudos (KT) [172] and the nonlinear error in variables (EVM) [173] methods using the RREVM [174] program. Homonuclear ^{1}H-2D-COSY and 2D-NOESY NMR of the copolymer sample were recorded for determining the interactions between different protons in the copolymer chain.

The ^{13}C-NMR DEPT spectrum of a vinyl acetate-methyl acrylate copolymer containing 44% vinyl acetate in $CDCl_3$ is shown in **Figure 7.21**. It is seen that the signals due to methine and methylene carbons of methyl acrylate and vinyl acetate monomeric units are differentiated.

The signals at δ 41.3, 40.2, 39.43, 38.3, and 37.6 ppm can be attributed to the methine carbons of the M monomeric unit and the signals at δ 39.02 ppm and at

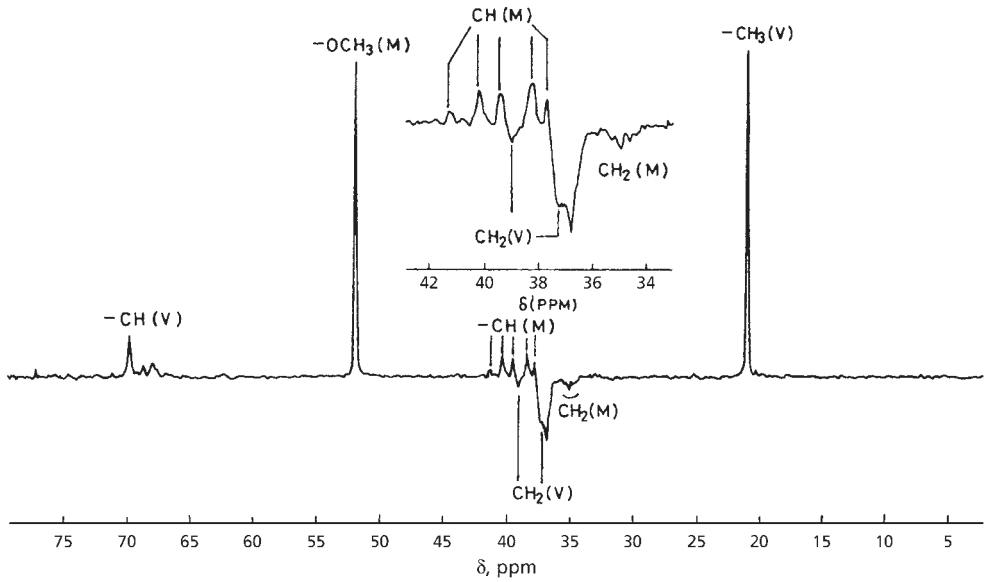

Figure 7.21 (a) ^{13}C-NMR spectrum of V/M (V = 44 mol% in the copolymer). (b) Expanded resonance region δ 36-41.3 ppm. Methylene resonances appear as negative peaks and methine and methyl carbon resonances appear as positive peaks. (*Reprinted with permission from A.S. Brar and S. Charan, Journal of Applied Polymer Science, 1994, **53**, 13, 1813. ©1994, John Wiley and Sons [170]*)

δ 36.8 ppm are attributed to the methylene carbons of the V-monomeric units. These assignments have been used to determine the relative fractions of M-centred triads.

^{13}C{^{1}H}-NMR spectra of the copolymer sample in the region δ 36.0-41.5 ppm show that the signal at δ 41.3 ppm increases in intensity while the signals at δ 38.3 and 37.6 ppm decrease in intensity with increase in concentration of the M unit in the copolymer. By comparison with the ^{13}C{^{1}H}-NMR spectrum of the homopolymer polymethyl acrylate, the signal at δ 41.3 ppm has been assigned to MMM compositional triads, whereas compositional variation in the intensity of the signals at δ 38.30 and 37.6 ppm shows that these signals can be assigned to VMV triad sequences. The signals at δ 40.2 and at 39.4 ppm have been assigned to MMV triad sequences. The relative fractions of MMM, MMV, and VMV triads were measured from peak area measurements under various resonance signals. Experimental values of M-centred triads are in good agreement with theoretical values obtained using r_v = 0.04 and r_M = 7.28 in Harwood's statistical model (**Table 7.12**).

Table 7.12 Experimental and calculated values of M- and V-centred triads vinylacetate (V) – methylacrylate (M) copolymers

Mol fraction of V in the copolymer	Triad	Triad Fractions	
		a	*b*
0.75	VVV	0.48	0.37
	VVM	0.41	0.48
	MVM	0.11	0.15
	MMM	0.02	0.03
	MMV	0.35	0.27
	VMV	0.63	0.70
0.63	VVV	0.22	0.18
	VVM	0.46	0.49
	MVM	0.32	0.33
	MMM	0.02	0.08
	MMV	0.43	0.40
	VMV	0.55	0.52
0.44	VVV	0.07	0.10
	VVM	0.43	0.44
	MVM	0.50	0.46
	MMM	0.13	0.17
	MMV	0.47	0.44
	VMV	0.40	0.39
0.37	VVV	0.03	0.07
	VVM	0.39	0.39
	MVM	0.58	0.55
	MMM	0.18	0.20
	MMV	0.51	0.50
	VMV	0.31	0.30
0.31	VVV	0.01	0.02
	VVM	0.22	0.26
	MVM	0.77	0.72
	MMM	0.31	0.37
	MMV	0.49	0.48
	VMV	0.20	0.15

Samples VM6 and VM7 (V = 23 and V = 16 mol% in the copolymer, respectively), could not be used for triad sequence determination because resolution was not good.

[a] *Triad fractions determined from ^{13}C-NMR spectra of copolymers.*

[b] *Triad fraction calculated using rV = 0.04 and rM = 7.28 in Harwood's statistical model*

Reprinted with permission from A.S. Brar and S. Charan, Journal of Applied Polymer Science, 1994, 53, 13, 1813. ©1994, John Wiley [170]

Other vinyl copolymers that have been the subjects of sequencing studies include: vinyl acetate-acrylic acid [175], vinyl acetate-behenyl acetate [176], vinyl acetate-alkymethacrylate [177] and α-methylstyrene-vinylether [178].

7.4 Acrylonitrile and Methacrylonitrile Containing Copolymers

7.4.1 Acrylonitrile-ethylmethacrylate

Kapur and Brar [179] prepared acrylonitrile-ethyl methacrylate (A/E) copolymers of different monomer concentrations in bulk by free radical initiation. Copolymer composition was determined by nitrogen analysis and the comonomer reactivity ratios were determined by the method of Kelen-Tüdos. ^{13}C-NMR spectra of several A/E copolymers are discussed in terms of their triad monomer sequence and cotacticity. Terminal and penultimate reactivity ratios were calculated using the observed monomer triad sequence distribution determined from ^{I3}C-NMR spectroscopy for individual samples. Triad sequence distribution was used to calculate dyad concentrations, probability parameters, number average sequence lengths, and the comonomer mole fractions in the copolymers. The configurational sequence distributions in terms of all the 10 A-centred and 10 E-centred triad cotactic sequences have been determined and found to be in excellent agreement with those obtained using various cotactic probability parameters.

The populations of all the 20 A- and E-centred tactic monomer sequence triads mentioned previously, in the A/E copolymer samples calculated using the probability parameters and those obtained from ^{13}C-NMR spectra are given in **Table 7.13**. The observed and the calculated tactic triad sequence populations are in fairly good agreement. The – EE – sequence in a EEE and EEA triad has a slightly different value of P_r. Similarly the –AA sequence in AAA and AAE triad has a different value of P_r. The cotacticity of –EA– sequence is random. The tacticities or –EE– and the –AA– diads in the copolymer are identical to tacticities in homopolymers. The cotacticity of the –AE– diad is also random and indicates that E and S monomer unit do not interact sterically during the copolymerisation.

7.4.2 Methacrylonitrile-methyl Methacrylate

San Roman and co-workers [161] studied the microstructure and stereochemical configuration of methacrylonitrile (N), methyl methacrylate (M), copolymers prepared by free-radical polymerisation at 60 °C on the basis of the classical terminal copolymerisation model and with the assumption of Bernoullian statistics for the

Table 7.13 Evaluation of the 10 monomer sequence distribution triads for A-centred and E-centred groups[a] in acrylonitrile (A) – ethyl methacrylate (E) copolymers

	90.0% A acrylonitrile		79.8% A acrylonitrile		70.0% A acrylonitrile	
	Calculated	Observed	Calculated	Observed	Calculated	Observed
$[E_rE_rE]$	0.013	-	0.052	-	0.088	0.084
$[E_mE_rE]$	0.007	-	0.028	-	0.047	0.040
$[E_mE_mE]$	0.000	-	0.004	-	0.006	0.017
$[E_rE_rA]$	0.095	0.088	0.158	0.164	0.170	0.186
$[E_rE_mA]$	0.090	0.090	0.133	0.127	0.187	0.0168
$[E_mE_rA]$	0.025	0.30	0.052	0.050	0.045	0.051
$[E_mE_mA]$	0.024	0.026	0.044	0.046	0.050	0.047
$[A_rE_rA]$	0.197	0.201	0.155	0.158	0.092	0.096
$[A_mE_rA]$	0.373	0.374	0.263	0.254	0.203	0.217
$[A_mE_mA]$	0.176	0.171	0.111	0.117	0.112	0.094
$[E_mA_mE]$	0.038	0.046	0.074	0.077	0.144	0.178
$[E_mA_rE]$	0.080	0.114	0.174	0.173	0.260	0.260
$[E_rA_rE]$	0.041	-	0.103	0.101	0.118	0.084
$[A_mA_mE]$	0.118	0.120	0.114	0.106	0.115	0.144
$[A_mA_rE]$	0.117	0.115	0.124	0.133	0.096	0.102
$[A_rA_mE]$	0.125	0.123	0.135	0.138	0.104	0.077
$[A_rA_rE]$	0.123	0.125	0.105	0.101	0.087	0.078
$[A_mA_mA]$	0.096	0.088	0.046	0.049	0.021	-
$[A_mA_rA]$	0.179	0.185	0.085	0.122	0.038	-
$[A_rA_rA]$	0.082	0.084	0.040	-	0.018	-

[a] *Calculated: calculated fractions using the configurational probabilities*

Observed: Observed fractions from the ^{13}C-NMR spectra

*Reprinted with permission from G.S. Kapur and A.S. Brar, Journal of Polymer Science Part A: Polymer Chemistry, 1991, **29**, 4, 479. ©1991, John Wiley [179]*

distribution of the stereochemical configuration of monomer units. From the analysis of ^{1}H-NMR spectra the reactivity ratios were determined, their values being r_N= 0.883 (methylacrylo-nitrate) and r_M = 0.892 (methyl methacrylate). From the analysis of the ^{13}C-NMR resonance signals assigned to the quaternary carbon and the carbonyl group of M units and the α-CH_3 group of both the M and N units, the statistical parameters σ_{NN} = 0.37, σ_{MM} = 0.24, and σ^* = σ_{NM} = 0.87 were determined. The coisotacticity parameter σ^* is observably higher than the isotacticity parameters of the corresponding homopolymers, σ_{NN} and σ_{MM}, which indicates some strong interactions between the nitrile and carbonyl groups of neighbouring methacrylonitrile and MMA units.

Figure 7.22 shows a schematic preparation of methacrylonitrile (N) centred triads in methacrylonitrile-MMA (M) copolymers.

For a complete description of the monomer sequence distribution and relative stereochemical configuration of monomer sequences, at least in terms of N- and M-centred triads, it is necessary to take into consideration as many as 10 different triads with a central N unit, which may be magnetically distinguishable as is shown in the scheme of **Figure 7.22**. Since both monomeric repeating units have a quaternary pseudoasymmetric carbon, from a stereochemical point of view 10 triads with a central M unit sensitive to tacticity must also be considered. The statistical analysis of the monomer sequence distribution and of the stereochemical configuration of the copolymer sequences was carried under the following assumptions: with respect to the chemical composition of copolymer sequences, it was assumed that

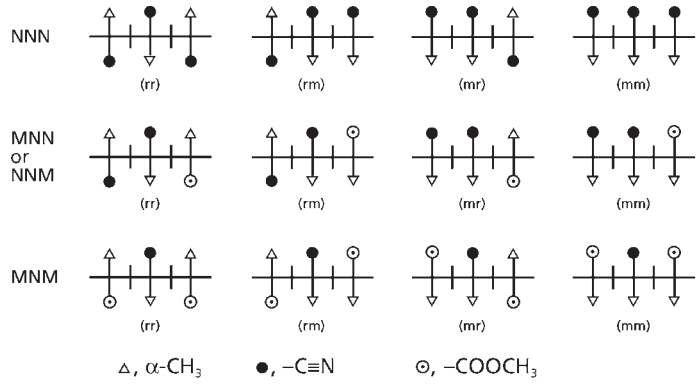

Figure 7.22 Schematic representation of N-centred triads in meth-acrylonitrile-methyl methacrylate copolymers. (*Reprinted with permission from J. San Roman, B. Vazquez, M. Valero and G.M. Guzman, Macromolecules, 1991,* ***24****, 23, 6089. ©1991, ACS, USA. [161]*)

the copolymerisation process is described correctly by the terminal unit model [180, 181]. From a stereochemical point of view, it was assumed that the configurational sequence distribution (tacticity) may be described according to Bernoullian statistics, with the isotacticity and coisotacticity parameters σ_{NN}, σ_{MM}, σ_{NM} and σ_{MN} as defined by Bovey [72, 182] and Coleman [183], where σ_{ij} is the probability of generating a meso diad between an *i*-ended growing radical and the incoming *j* monomer.

The molar fractions of tactic M-centred triads, independent of the chemical structure, M or N, of neighbouring units of copolymer samples with different compositions (N = mole fraction of methyacrylonitrile) are collected in **Table 7.14**.

Table 7.14 Distribution of the stereochemical configuration of M-centred sequences along the copolymer chains, for methacrylonitrile-methylmethacrylate (N-M) copolymers prepared by free-radical copolymerisation[a]

f_N (copolymer)[b]	Tactic sequence	Triad molar fraction	
		Experimental	Calculated
0.11_0	*mm*	0.064	0.096
	mr + rm	0.406	0.428
	mm	0.529	0.475
	mm	0.125	0.143
0.20_9	*mr + rm*	0.440	0.470
	rr	0.434	0.387
	mm	0.288	0.260
0.41_0	*mr + rm*	0.462	0.500
	rr	0.250	0.240
	mm	0.432	0.403
0.59_5	*mr + rm*	0.455	0.463
	rr	0.114	0.133
	mm	0.616	0.572
0.79_1	*mr + rm*	0.315	0.368
	rr	0.068	0.060

[a] *Values calculated have been obtained with the copolymerisation parameters indicated in the text.*

[b] f_N *Mole fraction of methacrylonitrile*

Reprinted with permission from: J. San Roman, B. Vazquez, M. Valero and G.M. Guzman, Macromolecules, 1991, ***24****, 23, 6089. ©1991, ACS [161]*

Experimental values have been determined from the integrated intensities of the three resonance signals (M-centred triads resonance peaks of quaternary carbon of the MMA units), whereas the values quoted in the fourth column have been determined by the sum of the contribution of MMM, MMN, NMM and NMN triads, with the stereochemical configuration of interest according to the scheme of **Figure 7.22**, but using the parameters r_N = 0.883, r_M = 0.892, r = reactivity ration. σ_{NN} = 0.37, σ_{MM} = 0.24, and colsotacticity factor σ^* = 0.87 (σ is probability of the adjacent monomeric limits having a meso configuration (isotactic). The excellent agreement of experimental and calculated values in the whole range of composition analysed makes it clear that this copolymerisation model is useful for the microstructural analysis of this system.

7.4.3 Acrylonitrile Methyl Acrylate

Brar and Sunita [184] have reported the reactivity ratios (r) for the acrylonitrile(A)-methyl acrylate (M) monomer pair using the errors in variables model (EVM) [185, 186] with the use of a computer program written by O'Driscoll and co-workers [187]. The primary structure factors: monomer composition, diad/triad sequence distribution, conditional probabilities, and number-average sequence lengths of acrylonitrile-methyl acrylate copolymers were determined on the basis of $^{13}C\{^1H\}$-NMR analyses and compared with those calculated from reactivity ratios as determined from EVM program. The diad sequence calculated from $^{13}C\{^1H\}$-NMR (proton decoupled ^{13}C-NMR) spectra was correlated with the T_g of A/M copolymers.

The acrylonitrile-methyl acrylate (A/M) copolymers of different monomer compositions were prepared by bulk polymerisation using free radical initiator (benzoyl peroxide). Terminal and penultimate reactivity ratios were calculated using the observed monomer triad sequence distribution.

Proton NMR was not applicable due to signal overlap. **Figure 7.23** Shows $^{13}C\{^1H\}$-NMR spectrum of A/M copolymer containing 57.0% acrylonitrile recorded in a mixture of $CDCl_3$ and dimethylsulfoxide-d6 at ambient temperature signals around δ = 27.3-20.1, 33.49 and 51.6, i.e., $(CH)_A$, $-(CH_2)_A$ and $-(OCH_3)_M$ could not be used due to poor resolution and the fact that $-(CH_2)_M$ and $-(CH)_M$ cartons of methyl acrylate overlapped with the solvent signals. The nitrile carbon of the acrylonitrile unit appeared as a well-resolved multiplet around δ = 121.0-118.7 ppm, showing its sensitivity towards different monomer placement. In the case of the A/M copolymer, a shift occurs in the position of various functional groups of A and M units as compared to that in homopolymers; this is due to the change in the nature of adjacent monomeric units in the copolymer, which changes the chemical shifts of A and M -centred triads.

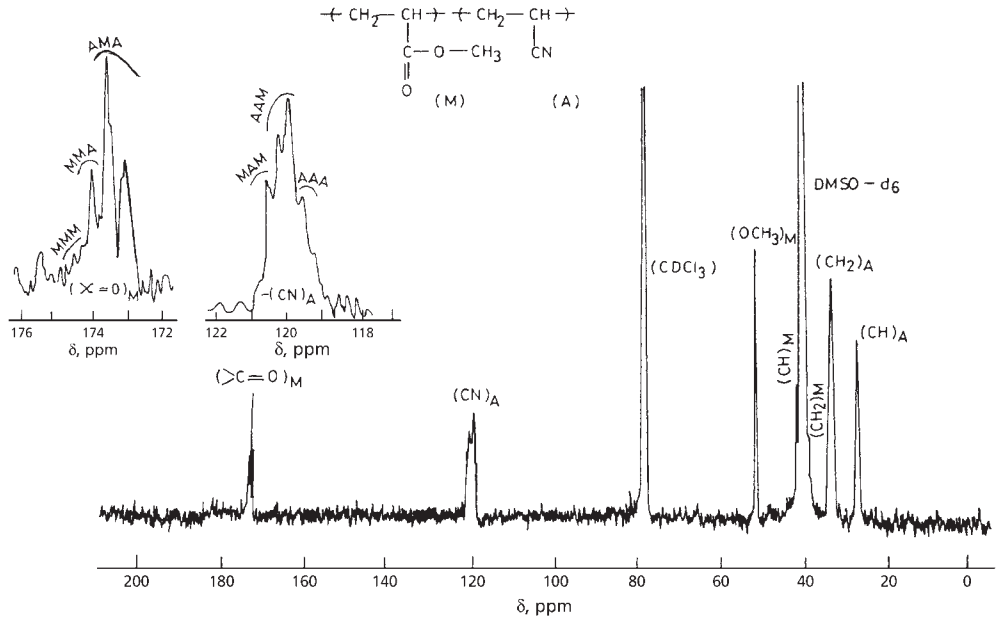

Figure 7.23 $^{13}C[^{1}H]$-NMR spectrum of acrylonitrile-methyl acrylate copolymer (A = 57.0 mol %) along with expanded carbonyl and nitrile carbon resonances in mixture of $CDCl_3$ and DMSO-d6 at room temperature (25 °C). (*Reprinted with permission from A.S. Brar and A. Sunita, Journal of Polymer Science Part A: Polymer Chemistry Edition, 1992, **30**, 12, 2549. ©1992, John Wiley and Sons [184]*)

The carbonyl carbon (>C=O) and nitrile carbon (-CN) expansion of A/M copolymer (A = 57.0 mol%) is shown in **Figure 7.23**. PMMA shows a singlet centred around δ = 174.3 ppm. As the concentration of acrylonitrile in the copolymer increases, signals characteristic of PMMA decrease, whereas a set of signals centred around δ = 173.9 ppm start appearing. These signals with a further increase in the A content increase to a maximum and then decrease, whereas a third new set of resonance signals appeared at around δ = 173.5 ppm. Three sets of signals whose intensities change with copolymer composition can be assigned to the carbonyl carbon of a central M unit in MMM, AMM(MMA), and AMA triad sequences from low to high field. The assignment of signals was done on the basis of electronic interaction. In the case of M centred triads, introduction of an A unit in MMM triads causes the upfield shift in the position of AMM (by ≈ 0.40 ppm) and AMA (by ≈ 0.50 ppm). This may be due to the increase in the electron density at the carbonyl carbon of central M unit which can be due to the di-magnetic effect from the anisotropy of immediate -CN neighbours. Concentrations of various M-centred

Table 7.15 Calculated and observed fractions of acrylonitrile (A-) and methylacrylate (M-) centred triads in A/M co-polymers

Sample No.	A- Mole fraction in copolymer	Triads	Triad concentrations calculated from			Penultimate reactivity ratios (*r*)
			Observed	Alfrey-Mayo model	Harwood penultimate model	
1	0.36	AAA	0.04	0.04	0.03	$r_{AA} = 0.56$ $r_{MA} = 0.61$ $r_{MM} = 0.53$ $r_{AM} = 0.56$
		AAM	0.33	0.31	0.30	
		MAM	0.63	0.65	0.67	
		MMM	0.31	0.29	0.30	
		MMA	0.50	0.50	0.49	
		AMA	0.19	0.21	0.21	
2	0.47	AAA	0.05	0.07	0.07	$r_{AA} = 0.42$ $r_{MA} = 0.46$ $r_{MM} = 0.36$ $r_{AM} = 0.43$
		AAM	0.36	0.39	0.38	
		MAM	0.59	0.54	0.55	
		MMM	0.13	0.19	0.19	
		MMA	0.49	0.49	0.48	
		AMA	0.38	0.32	0.33	
3	0.53	AAA	0.13	0.13	0.12	$r_{AA} = 0.65$ $r_{MA} = 0.43$ $r_{MM} = 0.43$ $r_{AM} = 0.54$
		AAM	0.40	0.46	0.45	
		MAM	0.47	0.41	0.43	
		MMM	0.10	0.11	0.11	
		MMA	0.47	0.45	0.44	
		AMA	0.43	0.44	0.45	
4	0.57	AAA	0.14	0.20	0.19	$r_{AA} = 0.36$ $r_{MA} = 0.51$ $r_{MM} = 0.72$ $r_{AM} = 0.42$
		AAM	0.52	0.50	0.49	
		MAM	0.34	0.30	0.32	
		MMM	0.08	0.07	0.06	
		MMA	0.33	0.37	0.37	
		AMA	0.59	0.56	0.57	
5	0.61	AAA	0.33	0.32	0.30	$r_{AA} = 0.56$ $r_{MA} = 0.63$ $r_{MM} = 0.33$ $r_{AM} = 0.49$
		AAM	0.50	0.49	0.49	
		MAM	0.17	0.19	0.21	
		MMM	0.02	0.03	0.03	
		MMA	0.29	0.29	0.29	
		AMA	0.69	0.67	0.68	

Table 7.15 *Continued*						
6	0.71	AAA	0.50	0.48	0.46	r_{AA} = 0.62 r_{MA} = 0.50 r_{MM} = 0.84 r_{AM} = 0.48
		AAM	0.40	0.42	0.43	
		MAM	0.10	0.10	0.11	
		MMM	0.02	0.01	0.01	
		MMA	0.19	0.20	0.19	
		AMA	0.79	0.79	0.79	
7	0.88	AAA	0.67	0.70	0.68	r_{AA} = 0.53 r_{MA} = 0.31 r_{MM} = 0.00 r_{AM} = 0.73
		AAM	0.28	0.28	0.29	
		MAM	0.05	0.03	0.03	
		MMM	0.00	0.00	0.00	
		MMA	0.14	0.10	0.10	
		AMA	0.86	0.90	0.90	
*Reprinted with permission from A.S. Brar and A. Sunita, Journal of Polymer Science Part A: Polymer Chemistry Edition, 1992, **30**, 12, 2549. ©1992, John Wiley and Sons [184]*						

triads can be calculated from the relative area of the resonance signals. These triad concentrations are normalised areas of the respective signals. **Table 7.15** contains the compositions information the various methyl acrylate centred triads along with calculated values.

Table 7.16 contains the copolymerisation parameters of acrylonitrile-methylacrylate copolymers containing between 0.36 and 0.88 mole fraction of acrylonitrile (i.e., F_A) for various monomer feed ratios and indicate that a knowledge of mole fractions (F) and reactivity ratios (*r*) enables prediction to be made, not only of average mole ratios but also of average number of sequences of monomer units per length of polymer and the average sequence length of each monomer.

Triad sequence distributions were used to calculate diad concentrations, probability parameters, number average sequence lengths and the comonomer mole fractions in the copolymers. The experimental fractions of all the ten A centred and ten M centred triad cotactic sequences were found to be in excellent agreement with those calculated using the probabilities parameters.

Table 7.16 Copolymerisation parameters of acrylonitrile-methylacrylate copolymers determined by ^{13}C-NMR spectroscopy

Sample Number	Acrylonitrile mole fraction (in copolymer)	(η)	$P_{M/A}$	$P_{A/M}$	N_A	N_M	Run number (R)
1	0.36	0.53	0.79	0.44	1.27	2.27	56.49
2	0.47	0.81	0.77	0.62	1.30	1.61	68.73
3	0.53	0.66	0.67	0.66	1.49	1.51	66.67
4	0.57	0.52	0.60	0.75	1.67	1.33	66.67
5	0.61	0.59	0.42	0.83	2.38	1.20	55.86
6	0.71	0.54	0.30	0.88	3.33	1.14	44.74
7	0.88	0.36	0.19	0.93	5.26	1.07	31.59

N_A: Number average sequence length of acrylonitrile monomer

N_M: Number average sequence length of acrylate monomer

$P_{M/A}$: Probability that an A/M unit comes about as a result of an acrylonitrile growing chain adding methyl acrylate

$P_{A/M}$: Probability that an M/A unit comes about as a result of a methyl acrylate growing chain adding acrylonitrile

Reprinted with permission from A.S. Brar and A. Sunita, Journal of Polymer Science Part A: Polymer Chemistry Edition, 1992, 30, 12, 2549. ©1992, John Wiley and Sons [184]

7.4.4 Acrylonitrile-butyl Acrylate

Brar and Sunita [188] have described a method for the analysis of acrylonitrile-butyl acrylate (A/B) copolymers of different monomer compositions. Copolymer compositions were determined by elemental analyses and comonomer reactivity ratios were determined using a non-linear least squares errors-in-variables model. Terminal and penultimate reactivity ratios were calculated using the observed monomer triad sequence distribution determined from ^{13}C{^{1}H}-NMR spectra. The triad sequence distribution was used to calculate diad concentrations, conditional probability parameters, number-average sequence lengths and block character of the copolymers. The observed triad sequence concentrations determined ^{13}C{^{1}H}-NMR spectra agreed well with those calculated from reactivity ratios.

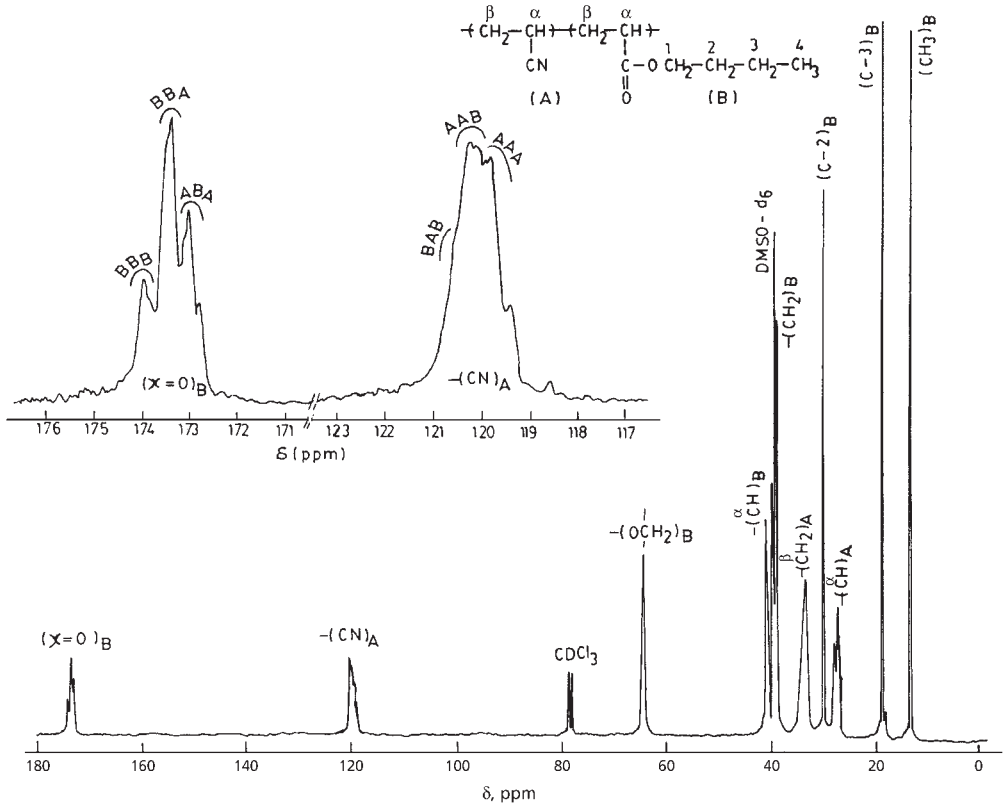

Figure 7.24 $^{13}C[^{1}H]$-NMR spectrum of A/B copolymer (A = 55.0 mol%) along with the expanded carbonyl carbon (>C=O) and nitrile carbon (-CN) in mixture of $CDCl_3$ and DMSO-d6 at room temperature. (*Reprinted with permission from A. S. Brar and A. Sunita, Polymer, 1992, 30, 12, 2549. ©1993, Elsevier [184]*)

The $^{13}C\{^{1}H\}$-NMR spectrum of the A/B copolymer (A = 55.0 mol%) recorded in a mixture of $CDCl_3$ and DMSO-d_6 at room temperature is shown in **Figure 7.24**. The various resonance signals have been assigned by comparing the copolymer spectrum with NMR spectra of homopolymers. In the case of polyacrylonitrile (PAN), $-CH_2$ and -CH carbons appeared around δ = 33.4 ppm and 27.8-28.1 ppm, respectively. The nitrile (-CN) carbon in PAN appeared as a multiplet in the region δ = 118.2-120.8 ppm. Kamide and co-workers [189] have evaluated the pentad tacticity of R-PAN using high-magnetic-field NMR. In the case of polybutylacrylate (PBA), the resonance signals around δ = 64.2 and 174.2 ppm can be assigned to $-OCH_2$ and >C=O carbons, respectively.

The -αCH and -βCH_2 in PBA appeared around δ = 41.3 and 34.4-36.3 ppm. The sharp resonance singlets around δ = 30.5, 18.9 and 13.5 ppm can be attributed to C_2, C_3 and (-CH_3) carbons, respectively. In the A/B copolymer, the resonance signals around δ = 13.4, 18.7, 30.1 and 64.4 ppm can be assigned to $(\text{-CH}_3)_B$, $(C_3)_B$, $(C_2)_B$ and $(\text{O-CH}_2)_B$ carbons of butyl acrylate monomer. The resonance signals around δ = 26.8-28.2 and 33.4-35.1 ppm can be attributed to $(\text{-}\alpha\text{CH})_A$ and $(\text{-}\beta\text{CH}_2)_A$ carbons, respectively, but could not be used for the sequence analysis because of poor resolution. The $(\text{-CH}_2)_B$ and $(\text{-CH})_B$ carbons overlapped with the solvent DMSO-d_6 signals (δ = 38.8-42.0 ppm) and, therefore, could not be used for the analysis of B-centred sequences. The carbonyl carbon in the A/B copolymer appeared as a multiplet around δ = 172.6-174.2 ppm, indicating that the splitting of the >C=O signal is due to its sensitivity towards the compositional sequences. The nitrile carbon of the A unit appeared as a well resolved multiplet around δ = 119.2-121.2 ppm, showing its sensitivity towards different monomer placements. In the case of the A/B copolymer, a shift occurs in the position of various functional groups of A and B units compared to that in homopolymers; this is due to the change in the nature of adjacent monomeric units in the copolymer, which changes the chemical shifts of A- and B-centred triads.

The carbonyl carbon (>C=O) and nitrile carbon (-CN) expansion of the A/B copolymer (A = 55.0 mol%) are shown in **Figure 7.24**. PBA shows a singlet centred around δ = 174.2 ppm. As the concentration of acrylonitrile in the copolymer increases, signals characteristic of PBA decrease, whereas a set of signals centred around δ = 173.5 ppm start appearing. These signals, with a further increase in the acrylonitrile content, increase to a maximum and then decrease, whereas a third new set of resonance signals appears at around δ = 173.0 ppm. The three sets of signals whose intensities change with copolymer composition can be assigned to the carbonyl carbon of a central B unit in BBB, ABB (BBA) and ABA triad sequences from low to high field.

Figure 7.25 shows the plots of normalised acrylonitrile (A) and butylacrylate (B)-centred triad concentrations *versus* the mole fractions of acrylonitrile (fA) and butyl acrylate (fB) in the copolymer.

The increase in the concentration of acrylonitrile in the copolymers increases the fraction of the AAA triad while it decreases the fraction of the BAB triad. The fraction of the AAB triad first increases with the increase in concentration of acrylonitrile, passes through a maximum value and then starts decreasing. The maximum fractions of AAB and BBA triads are obtained at 0.60 and 0.55 mole fractions of the respective monomers.

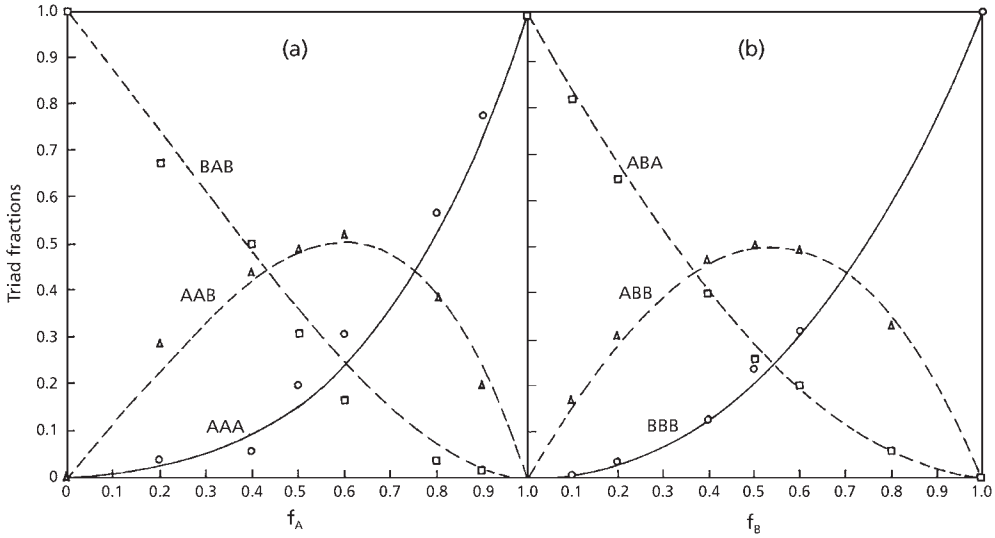

Figure 7.25 Plots of (a) A- and (b) B-centred triad fractions *versus* the feed in mole fractions of A and B monomers, respectively. (*Reprinted with permission from A. S. Brar and A. Sunita, Polymer, 1993, **34**, 16, 3391. ©1993, Elsevier [184]*)

7.4.5 Acrylonitrile-methyl Methacrylate

Gerken and Ritchey [190] reported the ^{13}C-NMR of series of acrylonitrile-methyl methacrylate (A/M) copolymers and determined the copolymer microstructure. They reported the configuration probabilities of A/M copolymers and Bernoullian statistics were found to describe the monomer configuration, a result in conflict with the conclusions of Pham [191]. Gerken and Ritchey [190] assigned the resonance lines of carbonyl and nitrile carbons to different triad cotactic sequences on the assumption that M and A monomer units have the same sensitivity to the tacticity of an adjacent A monomer unit. Also they did not calculate cotactic triad fractions from ^{13}C-NMR spectra and did not compare experimental cotactic triad fractions with those expected from configurational probabilities have been made.

Kapur and Brar [192] report the ^{13}C-NMR spectra of a series of acrylonitrile-methyl methacrylate copolymers. The primary structure, including monomer composition, monomer sequence distribution and triad tacticity of A/M copolymers were determined on the basis of ^{13}C[^{1}H]-NMR analysis and compared with the calculated fractions. The resonance of carbonyl and nitrile carbons were assigned to different cotactic triads by considering the possible electronic interactions between the central monomer unit and its immediate neighbours.

A 25 MHz $^{13}C[^{1}H]$-NMR spectrum of the A/M copolymer (A = 79.0 mol% in feed) recorded in DMSO-d_6 at 120 °C having the various resonances is shown in **Figure 7.26**. The carbonyl (>C=O) carbon expansions of the A/M copolymers are shown in **Figure 7.27**. The three sets of lines whose intensities change with copolymer composition can be assigned to carbonyl centred in MMM, MMA(AMM) and AMA triad sequences from low to high field. The tacticities of the MMM sequence have been identified [193]. The other resonances and shoulders comprising AMM and AMA sequences can be attributed to the four AMM(MMA) cotacticities. Concentrations of various M centred triads can be calculated from the relative area of the resonance peaks. Similar compositional information regarding the A-centred triads can be made using the nitrile (-CN) carbon resonance region. **Figure 7.28** shows the expanded nitrile resonance for the series of AM copolymers. Resonance peaks due to the AAA triad are expected to appear most upfield and that of the MAM triad to be most downfield. Kamide and co-workers [189] evaluated the pentad tacticity of PAN using the -CN carbon peak. **Table 7.17** contains the compositional information concerning the various M-centred and A-centred triads along with the distribution obtained by Harwood's program [171] using the terminal model reactivity ratios (r_A = 0.21 and r_M = 1.42).

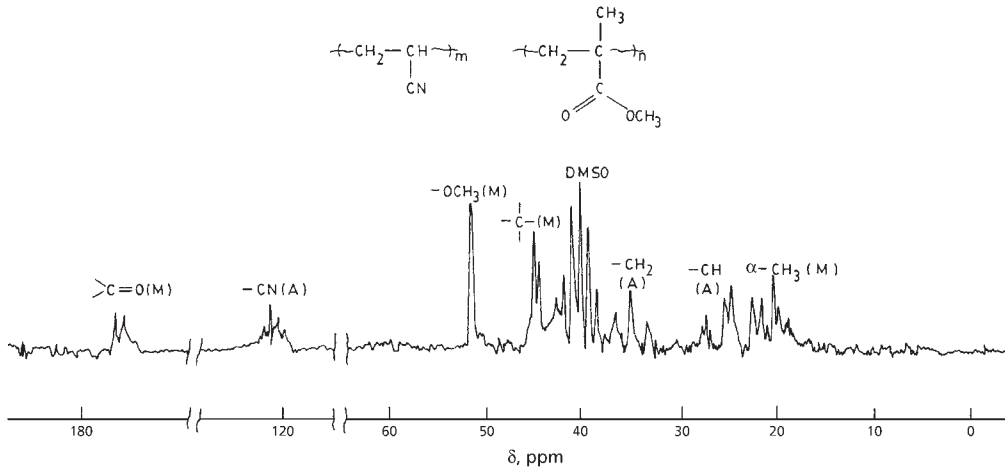

Figure 7.26 25 MHz $^{13}C[^{1}H]$-NMR spectrum of acrylonitrile (A)-methyl methacrylate (M) copolymer (79.0 mol% of A in feed) recorded in DMSO-d_6 solution at 120 °C. (*Reprinted with permission from G.S. Kapur and A.S. Brar, Polymer, 1991, **32**, 6, 1112. ©1991, Elsevier [192]*)

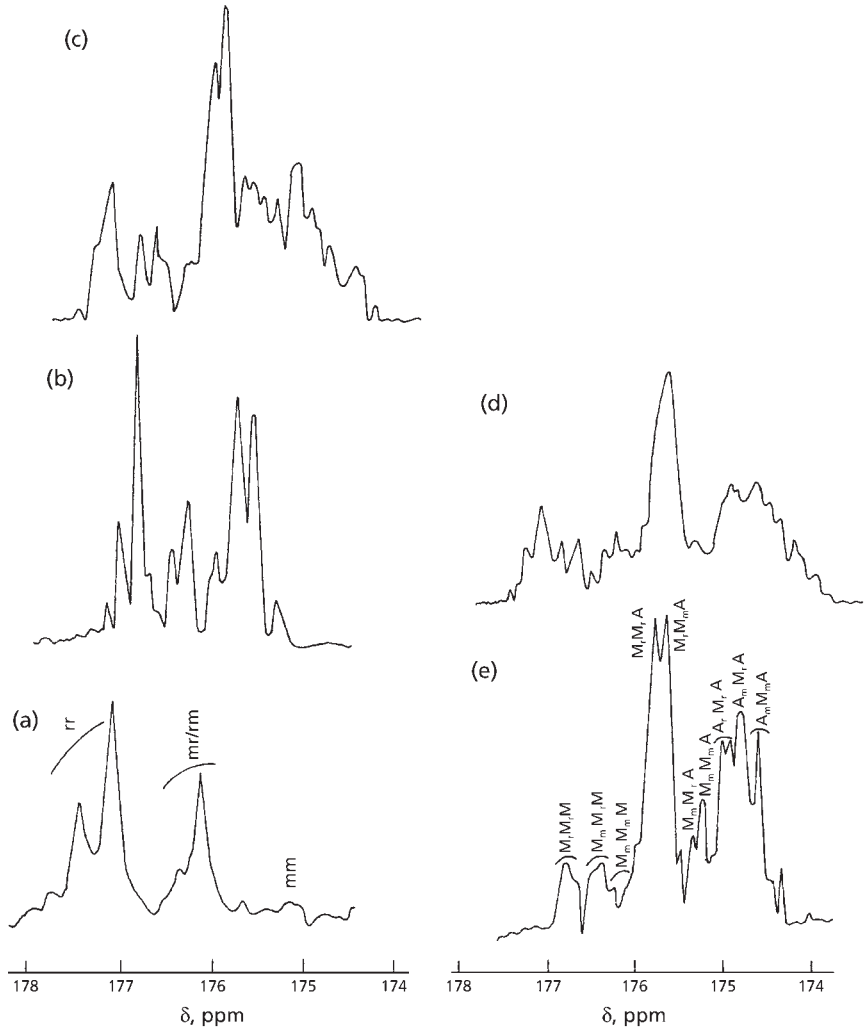

Figure 7.27 Expanded carbonyl (>C=O) carbon resonance spectra for acrylonitrile (A)-methyl methacrylate (M) copolymer; mol% of M in feed is (a) 100%; (b) 60.4%; (c) 40.5%; (d) 30.0%; (e) 21.0%. (*Reprinted with permission from G.S. Kapur and A.S. Brar, Polymer, 1991,* ***32****, 6, 1112. ©1991, Elsevier [192]*)

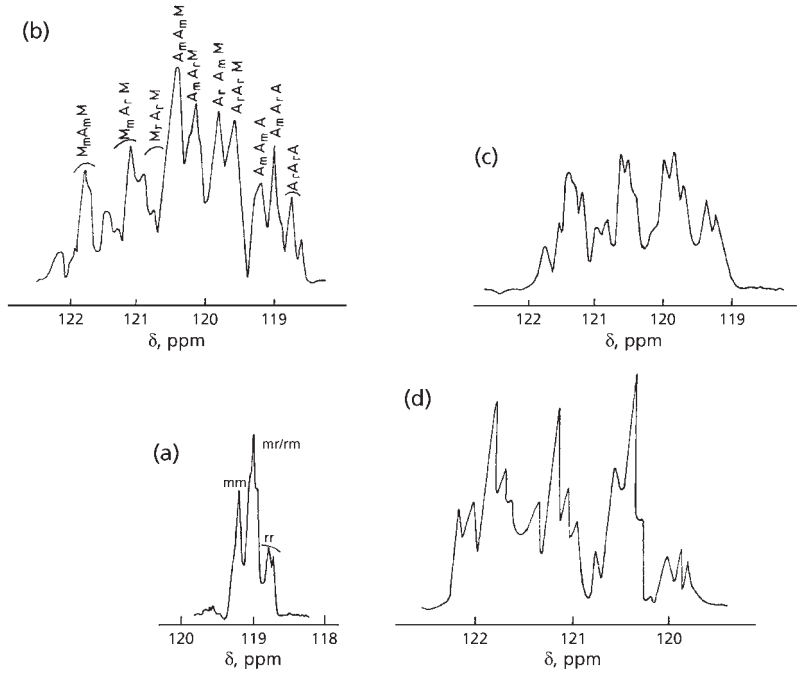

Figure 7.28 Expanded nitrile (-CN) carbon resonance spectra for acrylonitrile (A)-methyl methacrylate (M) copolymer; mol% of A in feed is (a) 100%; (b) 79.0%; (c) 59.5%; (d) 39.6%. (*Reprinted with permission from G.S. Kapur and A.S. Brar, Polymer, 1991,* ***32****, 6, 1112. ©1991, Elsevier [192]*)

Table 7.17 Calculated and observed fractions of A and M centred triads in acrylonitrile (A) – methyl methacrylate (M) copolymers

A mol%	Triad	Observed[a]	Terminal[b]	Penultimate[c]	Penultimate reactivity ratios
79.0	AAA	0.281	0.195	0.278	$r_{AA} = 0.326$, $r_{MA} = 0.187$ $r_{MM} = 1.17$, $r_{AM} = 1.53$
	AAM	0.431	0.493	0.441	
	MAM	0.288	0.312	0.281	
	MMM	0.060	0.075	0.057	
	MMA	0.410	0.398	0.417	
	AMA	0.530	0.527	0.525	
59.5	AAA	0.065	0.056	0.081	$r_{AA} = 0.33$, $r_{MA} = 0.22$ $r_{MM} = 1.13$, $r_{AM} = 1.49$
	AAM	0.346	0.360	0.340	
	MAM	0.589	0.584	0.579	
	MMM	0.201	0.242	0.199	
	MMA	0.531	0.500	0.544	
	AMA	0.268	0.258	0.257	
39.6	AAA	0.023	0.015	0.021	$r_{AA} = 0.324$, $r_{MA} = 0.209$ $r_{MM} = 0.99$, $r_{AM} = 1.72$
	AAM	0.213	0.213	0.203	
	MAM	0.764	0.772	0.776	
	MMM	0.384	0.468	0.405	
	MMA	0.516	0.432	0.492	
	AMA	0.100	0.100	0.103	

[a] By ^{13}C-NMR spectroscopy using the carbonyl carbon amd nitrile carbon resonance for M and A centred triad fractions, respectively.

[b] By terminal model Harwood's program [171]

[c] By penultimate model Harwood's program [171]

7.4.6 Methacrylonitrile-vinylidene Cyanide (MAA-VCN) and Cyano-vinyl Acetate-vinylidene Cyanide (CVA-VCN)

Either of these give alternating copolymers whose mirostructure has been studied using ^{13}C-NMR by Montheard and co-workers [194]. MAA, CVA and VCN all exhibit repulsive effects when adding monomer and copolymer containing high proportions of the same monomers. Their reactivities depend on the electron deficiency of double bond arising from electron-withdrawing characteristics of the attached groups. VCN, MAM and CVA possess a pronounced dipole due to a nitrile group conjugated with a

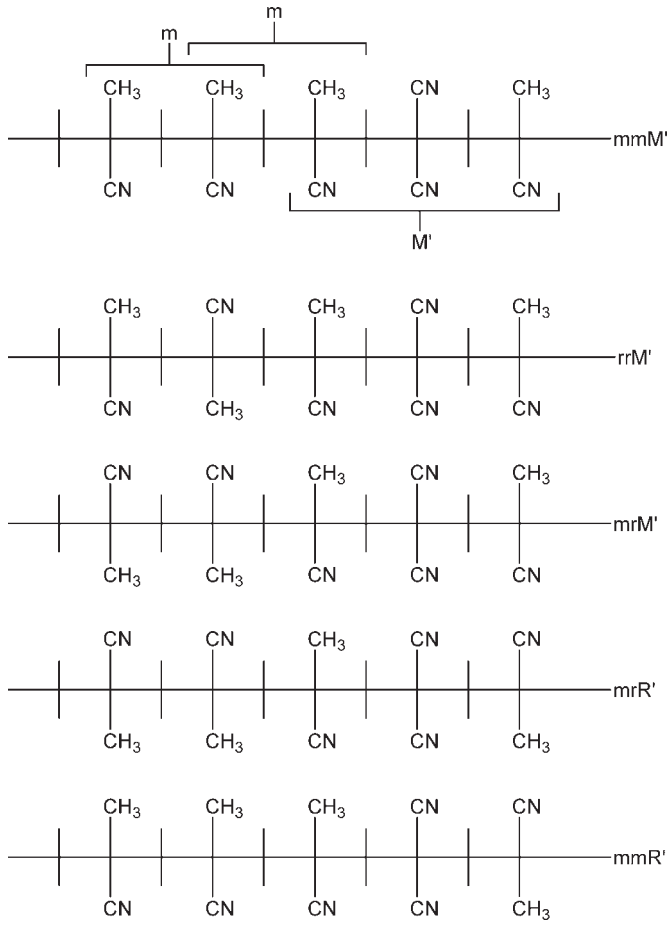

Figure 7.29 Homosequence of MAN linked to an alternating structure. (*Reprinted with permission from J.P. Montheard, J.P. Masli, A. Belfkira, M. Raihane and Q-T. Pham, Macromolecular Reports, 1994, A31, 1. ©1994, Marcel Dekker [194]*)

Table 7.18 Chemical shift assignments of the copolymers *p*-vinyldine cyanide-methacrylonitrile p(VCN-MAN) and *p*-vinylidine cyanide-cyanovinyl acetate p(VCN-CVA), prepared from equimolar mixtures

	p(VCN-MAN)	p(VCN-CVA)
CH_2	43.5-45.0 (MAN)* 46.6-48.2 (VCN)	42.7 (CVA + VCN)
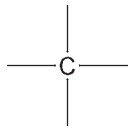	32.3-32.8 (MAN) 29.5-29.8 (VCN)	67.2-68.0 (CVA) 28.4-28.5 (VCN)
CH_3	23.9-24.9 (MAN)	20.2-20.8 (CVA)
CN	119.1-120.9 (MAN) 113.3-114.5 (VCN)	112.7-120.45 (VCN + CVA)
CO		168.16 (CVA)

*Reprinted from J.P. Montheard, A. Mesli, A. Belfkira, M. Raihane and Q-T. Pham, Macromolecular Reports, 1994, **A31**, 1. ©1994, Marcel Dekker [194]*

methylenic double bond and this type of repulsion is not accounted for in the Lewis-Mayo copolymerisation model. Therefore, the penultimate model for electron-deficient monomers can explain the nature of the propagation reaction. The CN groups of polyCVA give three peaks which can be referred to the three configurations of triads denoted *mm*, *mr* or *rm* and *rr* (**Figure 7.29**).

The main chemical shifts of the copolymers p(VCN-MAN) and p(VCN-CVA) are given in **Table 7.18**.

For the two copolymers, the composition can be calculated by measurement of areas of CN groups in p(VCN-MAN) or of areas due to the quaternery carbon of VCN and to the CH_3 of CVA units: the percentages of MAN and CVA incorporated are close to 53% and 54%, respectively.

The lack of chemical shift at 66 ppm due to the CH_2 groups of PVCN suggests a mostly alternating structure of these copolymers. The structure of these products would be alternating and terminated by homosequences of MAN or CVA. The examination of CN groups in p(VCN-MAN) is in good agreement with this proposition: three CN peaks are observed for the MAN units due to the three different pentads denoted M′M′, R′M′ and R′R′. The most important peak is probably due to the R′R′ pentad.

Three groups of three peaks are also observed for the VCN unit, in the range 113.3-114.6 ppm which can be explained by the nine centred VCN heptads denoted M′M′M′M′, M′M′R′M′ or M′R′M′M′, R′M′M′M′ or M′M′M′R′, R′M′R′M′ or M′M′R′M′, R′M′M′R′, M′R′R′M′, R′R′R′M′ or M′R′R′R′. Because of the almost alternate structure and the symmetry of the VCN (n - 1) and (n + 1) units, the chemical shifts of the Cα, CN and CH_3 groups of the central MAN n-unit should only be affected by the spatial orientations of the MAN (n - 2) and (n + 2) units. That is the reason why capital letters M′ (co-meso triad) and R′ (co-racemic triad) are utilised here (small letters m (meso) and r (racemo) are conventionally reserved for classical configurational dyads).

No homopolymer seems to be present in the copolymer p(VCN-MAN): The ^{13}C-NMR spectrum of pMAN shows a single peak at 123.2 ppm for the CN group and five peaks are observed in the range 122.4-122.6 for the CN groups of MAN of the copolymer: the examination of the sequences of MAN units linked to the alternating structure is also in good agreement with this hypothesis. Similar conclusions are observed with p(VCN -CVA). The copolymers of VCN with MAN or CVA are mostly alternating.

Other acrylonitrile and methacrylonitrile containing copolymers that have been subject to sequencing studies include styrene-methacrylonitrile [165], acrylonitrile – *trans* 1,3-pentadiene [195], acrylonitrile-ethyl acrylate [196], acrylonitrile – ethylmethacrylate [179, 197], acrylonitrile – methylmethacrylate [194], acrylonitrile – butyl methacrylate [198], acrylonitrile – vinyl acetate [199], acrylonitrile-methacrylic acid [200], acrylonitrile – butyl acrylate [187, 192], acrylonitrile – butadiene [201], acrylonitrile – methyl acrylate [184], acrylonitrile – alkyl methacrylate [179, 192, 198] and acrylonitrile – ethyl acrylate [196].

7.5 Acrylate and Methacrylate Copolymers

7.5.1 Methyl Acrylate – N-vinyl Carbazole

Crone and Natansohn [202] investigated the microstructure of a series of high conversion copolymers of MA and NVC. Proton and ^{13}C-NMR spectra were assigned by comparison with the homopolymers and by using heteronuclear shift correlation spectroscopy. Experimentally determined sequence distributions were compared with those calculated from reactivity ratios approximated from the copolymer compositions. Agreement was good for low NVC content copolymers. Three signals were particularly useful in providing rapid assessment of the distribution of NVC units within low NVC content copolymers, i.e., proton 1 and carbon 1 of NVC and the carbonyl carbon of MA.

N-vinyl Carbazol

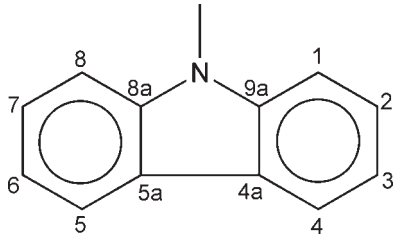

1: aromatic hydrocarbons and aromatic proton
8a: aromatic hydrocarbons

In the series of poly(MA-*co*-NVC) copolymers examined it is possible to discern three peaks in the methoxy region of copolymers 1 and 2. The peaks are labelled A, B, and C in **Figure 7.30**. As the content of NVC increases, the methoxy signal moves upfield to the point that methoxy signals of MA and methine signals of NVC cannot be resolved. The methine signal in pNVC appears between 3.4 and 3.6 ppm and the pMA methoxy appears at 3.7 ppm. When the NVC content reaches 33% in copolymer 3, the methoxy peak has moved upfield to overlap the methine signal, making it impossible to determine the relative intensity of the three methoxy peaks. In copolymer 1 containing 12% NVC, the predominant peak is the one at lowest field (having the same chemical shift as the methoxy signal in the homopolymer), and the smallest is the high field peak. The same relative order is observed in copolymer 2. This suggests that there is a shielding effect in the poly (MA-*co*-NVC) copolymer series similar to that in poly(MA-*co*-styrene).

Visual inspection of the aromatic region of the ^{1}H spectra of pNVC and copolymers 1 and 5, reveals that the eight aromatic protons resonate in three groups and that relative intensities change as the concentration of NVC increases. In addition, a new peak appears at 5.0 ppm when the concentration of NVC is above 44%. This signal, which corresponds to one proton in pNVC, is assigned to shielded proton 1. Integration alone is not sufficient, yet when combined with hetero- and homo-nuclear shift correlation, it becomes possible to identify the components of these peaks.

The good agreement between experimental and predicted sequence distributions suggests that the terminal model applies to the copolymerisation of MA with NVC when NVC contents are relatively low. Lack of correlation between calculated and experimental compositions arising from feeds with high NVC concentrations is not relevant to further investigations since the copolymers studied contain less than 40% NVC.

Throughout the copolymer series, a trend of increased signal width with increased NVC content is observed. This increase in width is a result of closer contact with the shielding cone of NVC units. Shielding moves the signals upfield and various degrees of shielding resulting from a multitude of chain conformations generate increasingly

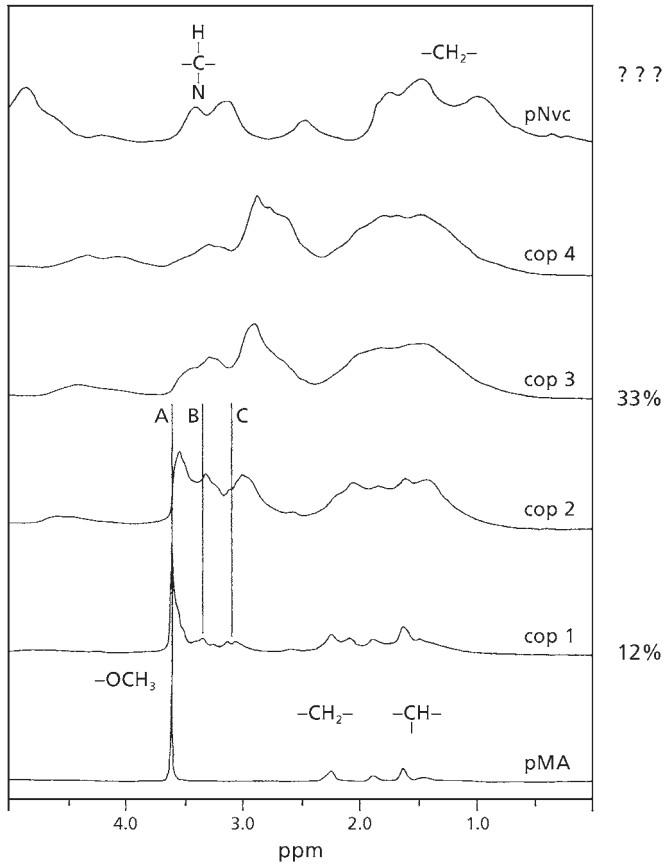

Figure 7.30 Aliphatic region of the proton spectra of pNVC, pMA, and copolymers 1-4. (*Reprinted with permission from G. Crone and A. Natansohn, Journal of Polymer Science Part A: Polymer Chemistry, 1992, **30**, 8, 1655. ©1992, John Wiley and Sons [202]*)

broader signals. The increased signal width and the large upfield shifts associated with proximity to NVC units enable assignment of the spectra. One clearly resolved proton signal, shielded proton 1 at 3.4 to 3.6 ppm in the NVC ring, leads to pentad distribution at high NVC content. Several carbons in the NVC ring were useful in determining sequence distributions. In particular, carbon 8a analysis results in a triad distribution and carbon 1 resonances exhibit pentad sensitivity. The carbonyl carbon signal of MA provides tacticity information in addition to sequence distribution information.

Three of the resonances are particularly suited to assessment of the isolation of NVC in a copolymer: carbon 1 and shielded proton 1 of NVC and the carbonyl carbon of

MA. The upfield resonance of proton 1 at 5.0 ppm serves as an alert to long NVC sequences since its presence indicates that the copolymer contains NVC sequences at least five units long. The low field resonance in the carbon 1 signal is narrow and easily resolved in copolymers with low NVC content. Dominance by this resonance signifies that NVC units are separated from each other by at least two MA units. An assessment of the frequency of NVC groups can be made by examining the intensity of the high field components of the carbonyl resonance. All isolated MA sequences as well as a portion of MA units terminating or commencing a MA sequence resonate above 174.5 ppm. Hence, absence of the high field portion of the carbonyl resonance indicates that MA sequences are largely uninterrupted.

Though sequence distributions calculated from reactivity ratios can effectively describe the distribution and isolation of NVC units in copolymers with low NVC concentrations, analysis of carbon spectra for the three resonances described above provides a more convenient evaluation.

7.5.2 Ethylmethacrylate - Methyl Methacrylate

Kitayama and co-workers [154] described a method based on ^{1}H-NMR spectroscopy for the differentiation of highly isotactic ethylmethacrylate (EMA) - MMA block copolymer, random copolymer and a mixture of the corresponding homopolymers through monomer sequence (and end-group) analysis.

NMR signals due to the monomeric units provide clear indications for distinguishing the block copolymers from the random copolymers. From the chemical shift of the initiator fragment signal it is possible to differentiate adjacent monomer units in PMMA – block poly EMA and poly(EMA)-block PMMA. The main part of the spectrum for a mixture of PMMA and polyEMA is identical to those for block copolymers but the mixture shows two C_4Hg signals at 0.826 and 0.845 ppm arising from both copolymers and this can be distinguished from block copolymers.

7.6 Polyacrylamide – Acryloyloxyethyltrimethyl Ammonium Chloride (CMA) and Polyacrylamide - Methacryl - Oyloxyethyltrimethylammonium Chloride (CMM)

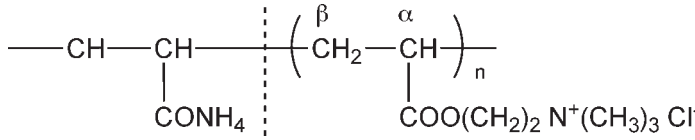

Acrylamide-acryloyloxyethyltrimethyl ammonium chloride (CMA)

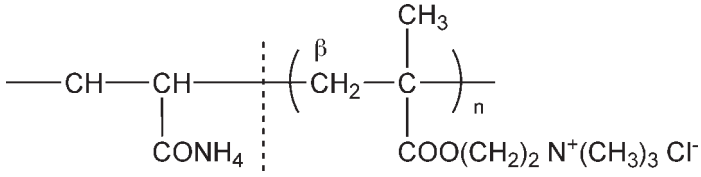

Acrylamide-methacryl-oyloxyethyltrimethyl ammonium chloride (CMM)

Vu and Cabestany [203] examined polymers containing 5, 15, and 30% of the CMA or CMM copolymer in deuterium oxide by ^{13}C- and ^{1}H-NMR. The distribution of monomer sequences were measured by both ^{1}H statistical calculation and by ^{13}C-NMR.

Table 7.19 shows the statistically calculated percentages of the acrylamide (AM), CMA, and CMM centred triads for the polymers CMA 5, 15, 30 and CMM 5, 15, 30 polymerised up to 100% conversion.

^{13}C-NMR spectra of CMA shows that the CO group gives a sharp resonance line, and the CβH$_2$ group, a broad symmetrical resonance pattern, which reflects the low influence of tacticity. The CαH carbon atom, sensitive to triads, gives three well-resolved peaks at 39.1, 40 and 40.8 ppm in the 26/48/26 ratio (**Figure 7.31**). These lines are assigned to the *mm*, *mr* + *rm*, *rr* triads.

Statistical calculations carried out according to Pham [204] show that the propagation of dyads and triads occurs in accordance with Bernoulli's model, (with $P(m) = P(r) = 0.5$). When the probabilities for the two monomers are equal, the configuration of the propagating macroradical is then independent of the *m* or *r* nature of the end dyad. Furthermore, the probability of occurrence of *m* and *r* dyads is equal, and the configuration of the homopolymer is statistical. The chemical shifts of poly(CMA) are summarised in **Tables 7.20 and 7.21** and in poly(CMM) in **Tables 7.22 and 7.23**.

It is possible to determine quantitatively by ^{13}C-NMR each monomeric component either on the basis of the ester/amide CO sequences for both types of polymers (**Figures 7.32 and 7.33**) or on the basis of the ester OCH$_2$ and of the (ester + amide) CβH$_2$ for poly (AM–CMA), and on the basis of the ester OCH$_2$ and of the amide CβH$_2$ sequences for poly(AM-CMM). (AM=acrylamide).

In conclusion Vu and Cabestany [203] have shown that ^{13}C-NMR is a powerful tool for analysing the tacticity of acrylic homopolymers and the cotacticity of acrylamide/acrylate copolymers. The configurational propagation of the dyads and triads follows Bernouilli's statistical model in the case of homopolymers: $P(m) = 0.43$, $P(r) = 0.57$ for poly(AM); $P(m) = P(r) = 0.50$ for poly (CMA) and $P(m) = 0.24$, $P(r) = 0.76$ for poly (CMM). In the case of copolymers obtained by the inverse emulsion polymerisation technique

Table 7.19 Calculated results (simulation, Olakaov's first order statistics), and experimental results (^{13}C-NMR) of the percentage of triads centred around polyacrylamide – methacryl oyloxyethyltrimethyl (CMM) and polyacrylamide acryloyloxyethyltrimethyl ammonium chloride (CMA)

% of centred triads	CMM5		CMM15		CMM30		CMA5		CMA15		CMA30	
	Calculated	^{13}C	Calculated	^{13}C	Calculated	^{13}C	Calculated	^{13}C	Calculated	^{13}C	Calculated	^{13}C
AAA	91	90	75	78.5	56	72	90	a	70	80	41.5	45
AAC + CAA	8.5	10	20	18.2	29	23	9.7	a	27	14.6	45.5	44
CAC	0.6	0	5.7	3.3	15	5	0.3	a	3	5.7	13	11
CCC	0	a	3	7	10	13	0	a	1	a	3	a
CCA + ACC	8	a	24	22	40	34	4	a	12	a	26	a
ACA	92	a	73	71	50	53	96	a	87	a	71	a

[a] *Quantification was not possible because of lack of spectral resolution*

CMM5-CMM30 = 5-30% CMM

CMA5-CMA30 = 5-30% CMA

Reprinted with permission from C. Vu and J. Cabestany, Journal of Applied Polymer Science, 1991, ***42****, 11, 2857. ©1991, Wiley and Sons [203]*

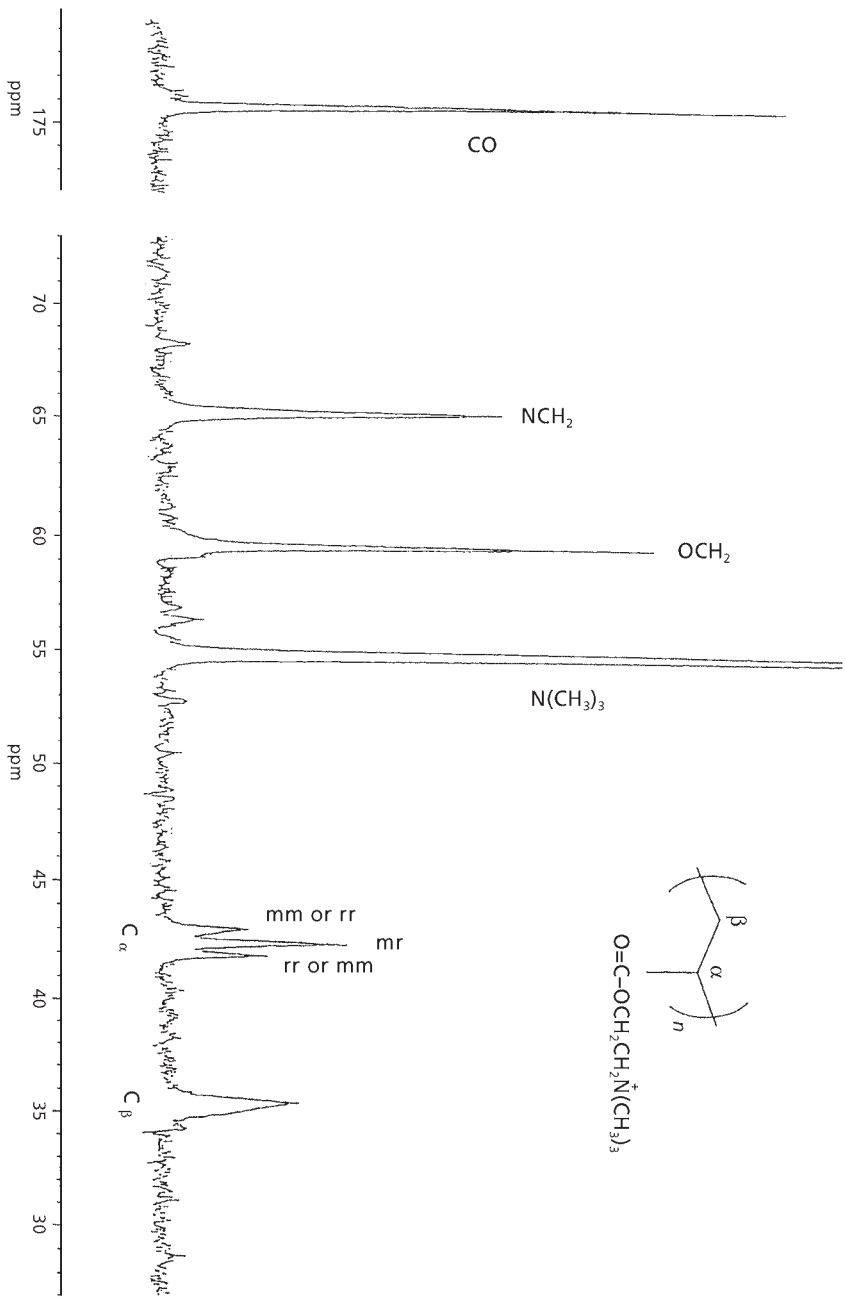

Figure 7.31 ^{13}C-NMR spectrum of poly (CMA). (*Reprinted with permission from C. Vu and J. Cabestany, Journal of Applied Polymer Science, 1991, **42**, 11, 2857. ©1991, John Wiley and Sons [203]*)

Table 7.20 Poly(CMA): Spectral ^{1}H - and ^{13}C-NMR Assignments						
	$C\beta H_2$	$C\alpha H$	NCH_2	OCH_2	$^{+}N(CH_3)_3$	CO
^{1}H (ppm)	1.82	2.47	3.76	4.52	3.29	-
^{13}C (ppm)	33.2	40	64	57.4	52.4	173.6
*Reprinted with permission from C. Vu and J. Cabestany, Journal of Applied Polymer Science, 1991, **42**, 11, 2857. ©1991, Wiley and Sons [203]*						

Table 7.21 ^{1}H - and ^{13}C-NMR Chemical Shifts of Poly(CMM)							
	CH_3	$C\beta H_2$	C	OCH_2	NCH_2	$^{+}N(CH_3)_3$	CO
^{1}H (ppm)	1.25	2.1	-	4.53	3.85	3.25	-
^{13}C (ppm)	19.7	54	45.9	60.1	65	54.9	178
*Reprinted with permission from C. Vu and J. Cabestany, Journal of Applied Polymer Science, 1991, **42**, 11, 2857. ©1991, Wiley and Sons [203]*							

Table 7.22 Poly(CMM) – Identification of Triads around the CαCarbon Atom by ^{13}C-NMR			
Triads	*rr*	(*mr* + *rm*)	*mm*
^{13}C (ppm)	45.98	45.74	45.3
Calculated	0.56	0.39	0.05
Found (^{13}C)	0.60	0.35	0.03
*Reprinted with permission from C. Vu and J. Cabestany, Journal of Applied Polymer Science, 1991, **42**, 11, 2857. ©1991, Wiley and Sons [203]*			

Table 7.23 Poly(CMM) – Identification of the Triads and Pentads around the CO Carbon Atom by ^{13}C-NMR									
Pentads	***mrrm***	***mrrr***	***rrrr***	***mrmm***	***mrmr* + *rrmm***	***rrmr***	***mmmm***	***rmmm***	***rmmm***
^{13}C (ppm)	178.9	178.8	178.6	178.3	178.2	178.0	177.8	177.7	177.6
Calculated	0.03	0.21	0.32	0.02	0.13	0.21	0.01	0.02	0.03
Found (^{13}C)	0.05	0.2	0.3	0.02	0.11	0.25	0.01	0.02	0.03
Triads	*rr* = 0.55			*rm* = 0.38			*mm* = 0.05		
*Reprinted with permission from C. Vu and J. Cabestany, Journal of Applied Polymer Science, 1991, **42**, 11, 2857. ©1991, Wiley and Sons [203]*									

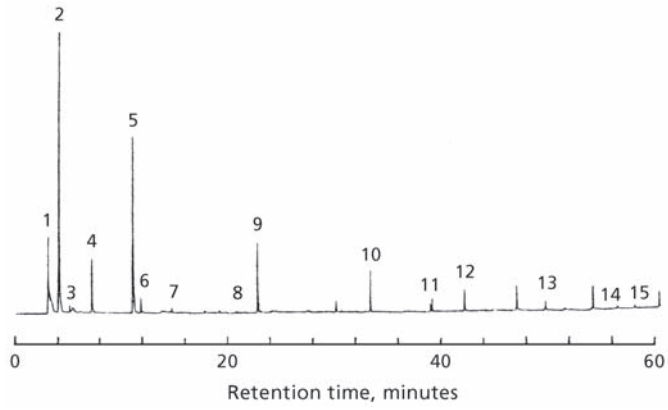

Peak No.	Representation by E and F unit	Structure (name)
1	F	CH_2O (formaldehyde)
2	EF	(1,3-dioxolane)
3	F_3	(1,3,5-trioxane)
4	EF_2	
5	E_2F	(1,3,6-trioxocane)
6	F_4	
7	EF_3	

Peak No.	Representation by E and F unit
8	F_5
9	E_3F
10	E_4F
11	$(E_2F)_2$
12	E_5F
13	E_6F
14	E_7F
15	$(E_2F)_3$

Figure 7.32 Peak no. corresponds to that in the scan at the top of this page. E = ethylene oxide, F = formaldehyde. (*Reprinted with permission from C. Vu, and J. Cabestany, Journal of Applied Polymer Science, 1991,* ***42****, 11, 2857. ©1991, John Wiley and Sons [203]*)

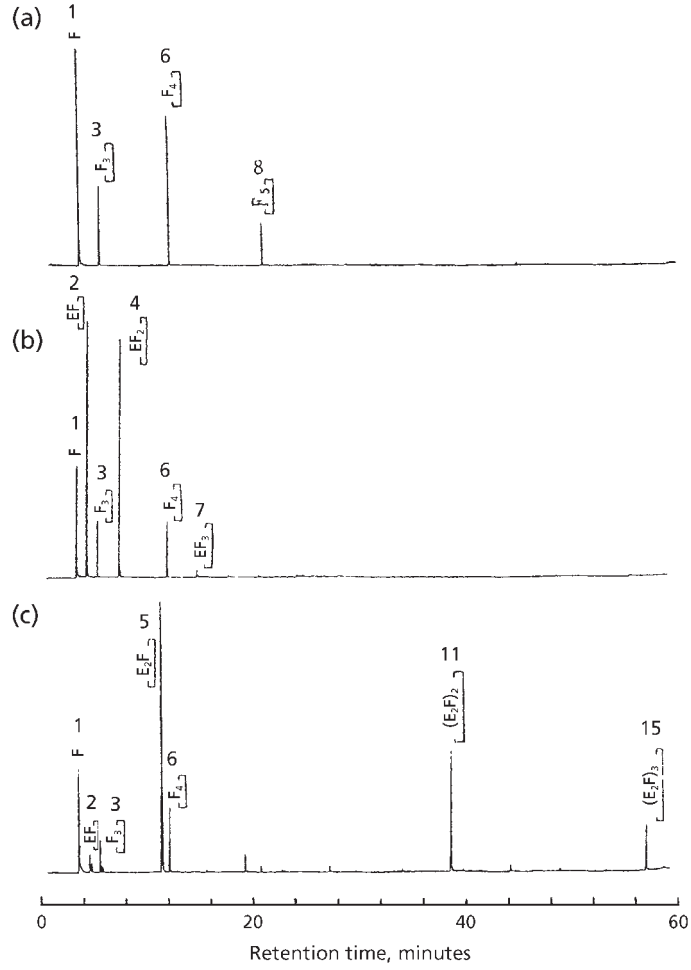

Figure 7.33 Pyrograms of model polymers at 400 °C in the presence of 5 wt% $CoSO_4$: (a) POM homopolymer; (b) POM-DO copolymer; (c) POM-TOC copolymer. Peaks 1-15 are assigned in **Figure 7.32**. (*Reprinted with permission from C. Vu and J. Cabestany, Journal of Applied Polymer Science, 1991,* ***42****, 11, 2857. ©1991, John Wiley and Sons [203]*)

from acrylamide and cationic acrylic monomer (CMA or CMM), the distribution of the monomeric sequences obeys Markov's first-order statistics.

There is good agreement between the calculated chemical sequences distribution and that obtained experimentally by ^{13}C-NMR. Computer simulations are particularly useful for obtaining these results as well as for simulating the copolymerisation of AM/cationic monomer. The chemical composition obtained from spectral analysis was found to be in good agreement with the results obtained by elemental analysis. In addition, it clearly appears that the chemical microstructure of the AM/CMA copolymers indicates a homogenous distribution of the monomer units along the polymer backbone, which is not the case of the copolymers AM/CMM that exhibit a far more heterogeneous microstructure.

7.7 Vinyl Chloride – Vinylidene Chloride

Wang and Smith [145] have developed a technique based on pyrolysis followed by GC for determining up to four monomer units in vinylidene chloride – vinyl chloride – (C/D) copolymers.

The major mechanism of producing oligomers with pyrolysis can be attributed to thermal degradation. The intensity of the various oligomer peaks in a pyrolysis gas chromatogram will reflect the monomeric sequence and polymer structure when the formation of pyrolysis products is proportional to their existence in the copolymer.

Determining composition by pyrolysis normally depends on the monomer production after polymer chain scission. However, vinyl chloride and vinylidene chloride are both gaseous monomers and are not well retained on a capillary GC column under normal conditions. In addition, other gases that result from pyrolysis of this system, such as hydrogen chloride, and butadiene, interfere with the monomer detection. As a result, a composition analysis utilising the monomers of vinyl chloride/vinylidene chloride copolymer through pyrolysis is a poor approach. Wang and Smith [145], therefore, the used trimer peak intensities to achieve the composition quantitative analysis as well as the number average sequence determination for the vinylidene chloride/vinyl chloride copolymer system.

The unique phenomenon in the pyrolysis of vinylidene chloride/vinyl chloride copolymer is the trimer formation. Under pyrolysis conditions, the polymer will directly undergo the thermal dehydrochlorination to form a conjugated polyene [205]. The polymer will then unzip, followed by a radical cyclisation to form benzene, chlorobenzene, dichlorobenzene, and trichlorobenzene. The mechanism can be expressed as:

1. dehydrochlorination

   $-(CH_2-CHCl)- \rightarrow -(CH=CH)-$

   $-(CH_2-CCl_2)- \rightarrow -(CH=CCl)-$

2. unzipping

   CCC

   Polymer chain → CCD, DCC, CDC

   DDC, CDD, DCD
   DDD

4. cyclisation

CCC	benzene
CCD, DCC, CDC	chlorobenzene
DDC, CDD, DCD	dichlorobenzene
DDD	trichlorobenzene

Where C = vinyl chloride monomer
D = vinylidene chloride monomer

Because these chlorinated aromatics are so stable, the trimer formation pathway is the major pyrolysis pathway for the vinyl chloride/vinylidene chloride copolymer.

Two major factors dominate the relationship between triad distribution and trimer production. The first is the pyrolysis efficiency, which represents the probability/efficiency of breakdown of a specific triad configuration to produce the corresponding trimer. The second is the detection efficiency, which results in variable FID responses for the trimers. These two factors cannot be separated in the vinylidene chloride/vinyl chloride copolymer composition and structure determination case. The relationship between trimer production and triad distribution can be expressed as:

$$\text{experimental trimer peak intensity} \times K_n \rightarrow \text{triad distribution in the polymer}$$

where K_n is the combination of pyrolysis efficiency and detection efficiency. Because the trimers CCD, DCC, and CDC all form chlorobenzene, the second assumption needs to be made that K_n is the same for CCD, DCC, and CDC. Additionally, the same assumption needs to be made for dichlorobenzene with the trimers of DDC, CDD, and DCD. The triad distribution in the polymer and the trimer peak intensities from pyrolysis can be written as:

benzene peak intensity × K_1 = CCC distribution in the polymer

chlorobenzene peak intensity × K_2 = CCD, DCC, CDC distribution in the polymer

dichlorobenzene peak intensity × K_3 = CDD, DDC, DCD distribution in the polymer

trichlorobenzene peak intensity × K_4 = DDD distribution in the polymer

The K_1, K_2, K_3 and K_4 values can be calculated by pyrolysing four different known compositions of vinylidene chloride/vinyl chloride copolymer standards. The composition calculation from the trimers will be as follows:

mol % of C =
normalised/corrected benzene peak intensity +
(2/3) normalised/corrected chlorobenzene
peak intensity + (1/3) normalised/corrected dichlorobenzene peak intensity

mol % of D =
normalised corrected benzene peak intensity +
(2/3) normalised/corrected dichlorobenzene
peak intensity + (1/3) normalised/ corrected chlorobenzene peak intensity

The determination of number average sequence lengths for the vinyl chloride and vinylidene chloride is challenging owing to the fact that six of eight trimers are not resolved by Py-GC. As mentioned previously, there is no way to know how much chlorobenzene peak intensity is contributed from triad CCD and DCC or from CDC. The same situation exists for the dichlorobenzene peak from the triad of DDC, CDD, and DCD. To utilise equations listed below, a third assumption needs to be made to obtain all six terms of triad intensities.

Number average sequence length of C and D is as follows:

$$\tilde{n}_{\mathrm{C}} = \frac{N_{\mathrm{CCC}} + N_{\mathrm{CCD+DCC}} + N_{\mathrm{DCD}}}{(1/2)N_{\mathrm{CCD+DCC}} + N_{\mathrm{DCD}}}$$

$$\tilde{n}_{\mathrm{D}} = \frac{N_{\mathrm{DDD}} + N_{\mathrm{CDD+DDC}} + N_{\mathrm{CDC}}}{(1/2)N_{\mathrm{CDD+DDC}} + N_{\mathrm{CDC}}}$$

where n_{C} and n_{D} are the number average sequence lengths of monomers C and D. N_{CCC}, $N_{\mathrm{CCD\,+\,DCC}}$, N_{DCD}, N_{CDC}, $N_{\mathrm{CDD\,+\,DDC}}$ and N_{DDD} are the experimentally derived triad molar fractions or numbers of molecules. From the previous formulas, if all six triad molar fractions or numbers of molecules can be generated, and the number average sequence lengths of monomers C and D can be calculated.

The third assumption results from the known reactivity difference between vinyl chloride and vinylidene chloride monomers in the copolymerisation process. In the polymer molecules formed in the beginning of the polymerisation, vinyl chloride exists in the polymer chain as a single unit among many vinylidene chloride units. In the polymer molecules formed in the latter part of the polymerisation, vinylidene chloride exists in the polymerisation chain as a single unit among many vinyl chloride units. Because of the relative reactivity ratio (r_1, r_2) of vinylidene chloride and vinyl chloride monomers, the probability of forming an alternating monomeric unit in the copolymer molecules is minimal. With this assumption, the polymer molecules have a vinylidene chloride/vinyl chloride distribution as follows:

Beginning part of polymerisation	- - - DDDDDDDCDDDDDD - - -
	- - - DDDDCDDDDCDDDD - - -
	- - - DDDCDDDCDDDCDD - - -
	- - - DDCDDCDDCDDCDD - - -
	- - - CCDCCDCCDCCDCC - - -
	- - - CCCDCCCDCCCDCC - - -
	- - - CCCCDCCCCDCCCC - - -
Latter part of the polymerisation	- - - CCCCCCCDCCCCCC - - -

The triad distribution can be expressed as follows:

N_{CCC} = normalised/corrected benzene peak intensity

$N_{CCD} + N_{DCC}$ = (2/3) normalised/corrected chlorobenzene peak intensity

N_{CDC} = (1/3) normalised/corrected chlorobenzene peak intensity

$N_{CDD} + N_{DDC}$ = (2/3) normalised/corrected dichlorobenzene peak intensity

N_{DCD} (1/3) normalised/corrected dichlorobenzene peak intensity

N_{DDD} = normalised/corrected trichlorobenzene peak intensity

These terms are subsequently used for the number average sequence length determination. **Table 7.24** shows a comparison of Py-GC and NMR values for the number average sequence length calculation of vinylidene chloride/vinyl chloride copolymer samples A–F. The number average sequence lengths for vinyl chloride, *N*(C), and vinylidene chloride, *N* (D), of samples C, D, and E are all within 1 unit difference (1.53 *versus* 1.40, 1.78 *versus* 1.50, and 3.69 *versus* 3.00 for vinyl chloride, 6.17 *versus* 5.70, 5.51 *versus* 5.10, and 2.40 *versus* 2.20 for vinylidene chloride). These values indicate that the results from Py-GC have a very good agreement with ^{1}H-NMR results.

Table 7.24 Composition Results Calculated from Pyrolysis Peak Intensities Compared with the ^{1}H-NMR Results of Five Different Compositions of Vinylidene Chloride/Vinyl Chloride Copolymer

		Samples					
		A	B	C	D	E	F
Corrected normalised peak intensity	CCC	0.115	0.138	0.172	0.253	0.604	
	CCD	0.317	0.330	0.349	0.371	0.250	0.997
	DCD	0.568	0.532	0.479	0.375	0.146	0.002
	DDD	0.748	0.737	0.719	0.697	0.360	0.002
	DDC	0.222	0.228	0.238	0.243	0.448	0.876
	CDC	0.031	0.035	0.043	0.060	0.192	0.100
Py-GC NASL	N(C)	1.38	1.43	1.53	1.78	3.69	0.024
	N(D)	7.06	6.70	6.17	5.51	2.40	392.90
	Wt% C	11.16	12.12	13.79	17.25	49.73	13.53
	Wt% D	88.84	87.88	86.21	82.75	50.27	94.93
^{1}H-NMR NASL	N(C)			1.40	1.50	3.00	5.07
	N(D)			5.70	5.50	2.20	
	Wt% C			13.66	17.95	46.77	
	Wt% D			86.34	85.05	53.23	

NASL: number average sequence length

Reprinted with permission from F.C-Y. Wang and P.B. Smith, Analytical Chemistry, 1996, ***68****, 3, 425. ©1996, ACS [145]*

Various other vinylidene chloride containing copolymers have been studied including vinylidene chloride – styrene [206], vinylidene chloride – MMA [207], vinyl esters [208] and vinylidene chloride – isobutylene [208].

7.8 Ethylene Oxide Containing Copolymers

7.8.1 Polyacetal – Ethylene Oxide

Polyacetals which are mainly comprised of oxymethylene (-OCH_2-) (F) units are among the most popular engineering plastics. The thermal stability of polyacetals is improved

by acetylation of terminal OH groups or by copolymerisation with a small amount of ethylene oxide (-OCH_2CH_2-) (E) because the oxymethylene homopolymer is subject to thermal depolymerisation to formaldehyde at relatively low temperatures, even below 170 °C. In the copolymer polyacetals, it is important to estimate the ethylene oxide content and the distributions of the ethylene oxide units, since these affect various properties of the polymer. A structural investigation of polyacetals, however, is quite difficult, even by spectroscopic methods, because of their insolubility in most solvents at room temperature. So far only a few studies to characterise polyacetal copolymers by means of NMR have been reported [209-212].

Yamashita and co-workers [209] estimated the sequence length of F and E units in copolymers of 1,3-dioxolane and 1,3,5-trioxane by ^{1}H-NMR at 60 MHz using their chlororform solutions at 60 °C. Later Fleischer and co-workers [210] applied ^{13}C-NMR at 25.2 MHz using a lanthanide shift reagent in chloroform solution to study the sequence distribution of such copolymers. In these reports, however, only polyacetal samples containing relatively large amounts (more than 3.5 mol%) of ethylene oxide units were studied because of their solubility in the used solvent. On the other hand, Ogawa and co-workers [212] evaluated the end-groups and the sequence distributions of a copolyacetal with a smaller E content (1.6 mol%) by ^{1}H-NMR at 270 MHz using *o*-dichlorobenzene as a solvent at 150 °C [211]. However, dissolving the polymer in *o*-dichlorobenzene at such an elevated temperature might cause degradation of oxymethylene sequences in the polymer chain depending on the copolymer composition. Recently, Wada and co-workers [211] reported the determination of end groups in polyacetal copolymers by ^{1}H-NMR at 270 MHz using hexafluoro-2-propanol (HFIP) as a solvent at room temperature.

Ishida and co-workers [213] applied reactive pyrolysis in the presence of cobalt sulfate as a catalyst to the evaluation of ethylene oxide sequences up to E_7 in copolymers on the basis of peak intensities of the cyclic ethers containing ethylene oxide units on the program. Pyrolysis gives the pyrogram shown in **Figure 7.32**.

Cyclic ethers containing ethylene oxide (E) and oxymethylene (F) units are predominant. In this case, much larger cyclic ethers are observed up to E_7F and $(E_2F)_3$ by using a capillary column. Here, the peaks of E_2F and F_4 overlapped completely when using a nonpolar column such as polydimethylsiloxane. However, by using mildly polar polymethylphenylsiloxane, they were sufficiently resolved. The distributions of E units as well as the E contents of the polymers can be determined from the intensities of peaks due to these cyclic ethers obtained if the peaks on the pyrogram reflect the chemical structures in the original polymer chain.

The three model polymers were subjected to Py-GC analysis in the presence of cobalt sulfate in order to confirm whether the sequence distributions estimated by the cyclic

ethers on the programs reflect those in the original polymer chain. **Figure 7.33** shows the programs of (a) polyoxymethylene (POM) homopolymer, (b) POM - 1,3-dioxolane (DO) copolymer, and (c) POM – 1,3,6-trioxocane (TOC) copolymer at 400 °C in the presence of 5 wt% cobalt sulfate.

As would be expected from the polymer structure, in the pyrogram of the POM-homopolymer (a), formaldehyde (F) and cyclic compounds comprising only F units are observed while no cyclic ether containing E unit(s) is observed. This result suggests that the formation of E unit(s) from oxymethylene sequences does not occur during the reactive pyrolysis of the POM homopolymer sample.

Similarly, in the pyrogram of POM – (1,3-dioxolane copolymer) oxymethylene, i.e., $-(CH_2O)_n - (CH_2CHO)_n$-(CH_2CHO)-$(CH_2\text{-}CH_2O)_m -$ containing (5.38% ethylene oxide units, and has a sequence length of ethylene oxide units = 1), only cyclic ethers

Table 7.25 Sequence distributions of polyacetal-ethylene oxide copolymers estimated by Py-GC

	POM-EO-1 [98.6/1.4]		POM-EO-2 [95.3/4.7]		POM-EO-3 [91.1/8.9]	
	Py-GC[a]	Hydrolysis[b]	Py-GC[a]	Hydrolysis[b]	Py-GC[a]	Hydrolysis[b]
-FEF-	70.1 (74.5)	79.3	60.0	59.0	44.3	47.1
$-FE_2F-$	25.5 (22.3)	17.2	33.0	1.6	37.1	32.2
$-FE_3F-$	4.4 (3.2)	3.5	5.6	8.7	9.5	14.9
$-FE_4F-$			1.4	0.7	5.2	4.9
$-FE_5E-$					2.7	0.9
$-FE_6E-$					0.9	
$-FE_7F-$					0.3	
Total	100.0	100.0	100.0	100.0	100.0	100.0

[a] Sequence distribution obtained by Py-GC through the reactive pyrolysis at 400 °C in the presence of 5 wt% cobalt sulfate. The values in brackets are obtained in the presence of 1 wt% cobalt sulfate.

[b] Sequence distribution obtained from hydrolysis followed by GC.

EO = Ethylene oxide units, F = oxymethylene units

*Reprinted with permission from Y. Ishida, H. Ohtani, K. Abe, S. Tsuge, K. Yamamoto and K. Katoh, Macromolecules, 1995, **28**, 19, 6528. ©1995, ACS [213]*

reflecting isolated E units such as EF, EF_2, and EF_3 are observed in addition to the cyclic ethers formed from the F sequence. Furthermore in the pyrogram of the POM – TOC copolymer (c) $–(CH_2O)_n – CH_2\text{-}CH_2O\ CH_2\text{-}CH_2O(CH_2O)_m$ (7.4% ethylene oxide units, sequence length of ethylene oxide units = 2), cyclic ethers reflecting EE dyads such as E_2F, $(E_2F)_2$ and $(E_2F)_3$ are characteristically observed. Here, the fact that a small peak of EF is observed suggests that the degradation of the EE dyad in the polymer chain to form EF occurs to some extent. However, since the peak intensity of EF is much smaller than those of cyclic ethers reflecting EE dyads such as E_2F, $(E_2F)_2$, and $(E_2F)_3$, the contribution of the degraded EE dyad could be negligible. These results observed for the model polymers indicate that the sequence distributions of E units in the original polymer chain are almost quantitatively reflected in the cyclic ethers formed through the reactive pyrolysis in the presence of cobalt sulfate.

The method was applied to the determination of ethylene oxide sequences up to 7 units long in copolymers. On the basis of peak intensities of cyclic ethers containing ethylene oxide units in the pyrogram pyrolysis results were in reasonably good agreement with those obtained by hydrolysis – GC (see **Table 7.25**).

7.8.2 Ethylene Oxide – Propylene Oxide

The most powerful method of characterising the chemical structure of these statistical and block copolymers is ^{13}C-NMR, and in early studies of statistical oxyethylene/oxypropylene (EP) copolymers [214, 215], the monomer sequence was elucidated at the diad level. More recently a triad analysis of 25 MHz ^{13}C spectra has been reported [216] but this involved computer decomposition of the intensities of strongly overlapping bands. In view of the advantages in simpilicity and chemical shift resolution to be gained by using higher magnetic fields, Heatley and co-workers [217] studied the application of these techniques. They report an investigation at 75.5 MHz of ^{13}C spectra of statistical and block EP copolymers together with EO and PO homopolymers for comparison. The spectrum interpretation was assisted considerably by the use of the attached proton test (APT) [219-221] pulse sequence to obtain CH and CH_2 subspectra and of the Lorentz-Gaussian transformation technique [221] for resolution enhancement.

The NMR spectrum of propylene oxide – ethylene oxide – propylene oxide – ethylene oxide triblock copolymers are shown in **Figures 7.34 and 7.35**, respectively.

Figure 7.34 shows the terminal CHOH region of spectra of samples with different P block lengths, while **Figure 7.36** shows the main backbone carbon region. From the variation in relative intensities in **Figure 7.34**, it is a straightforward task to identify resonances corresponding to oxyethylene chains terminated by one, two, or

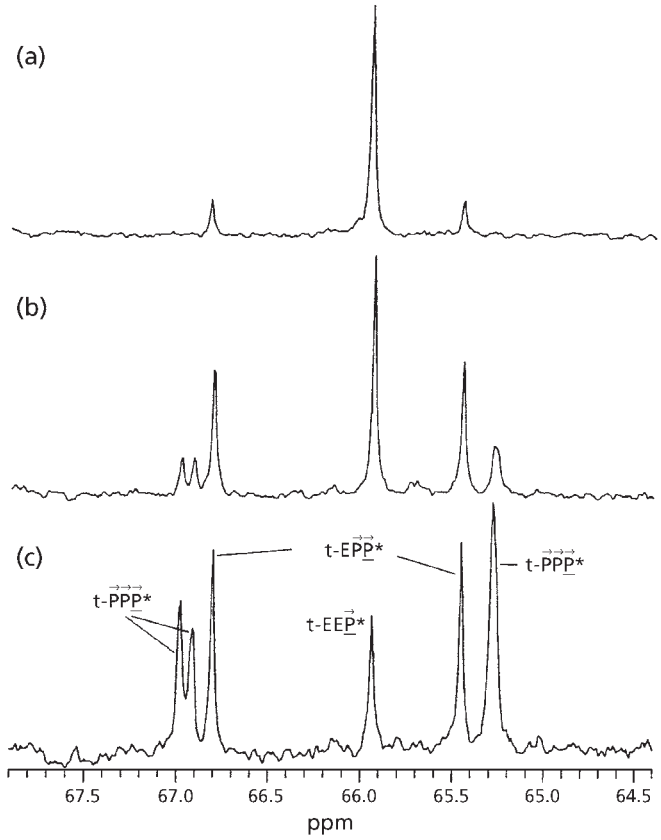

Figure 7.34 CHOH terminal resonances of PEP triblock co-polymers: (a) P1E39P1, (b) P2E39P2, (c) P3E39P3. (*Reprinted with permission from F. Heatley, Y. Luo, J. Ding, R.H. Mobbs and C. Booth, Macromolecules, 1988, **21**, 9, 2713. ©1989, ACS, USA. [217]*)

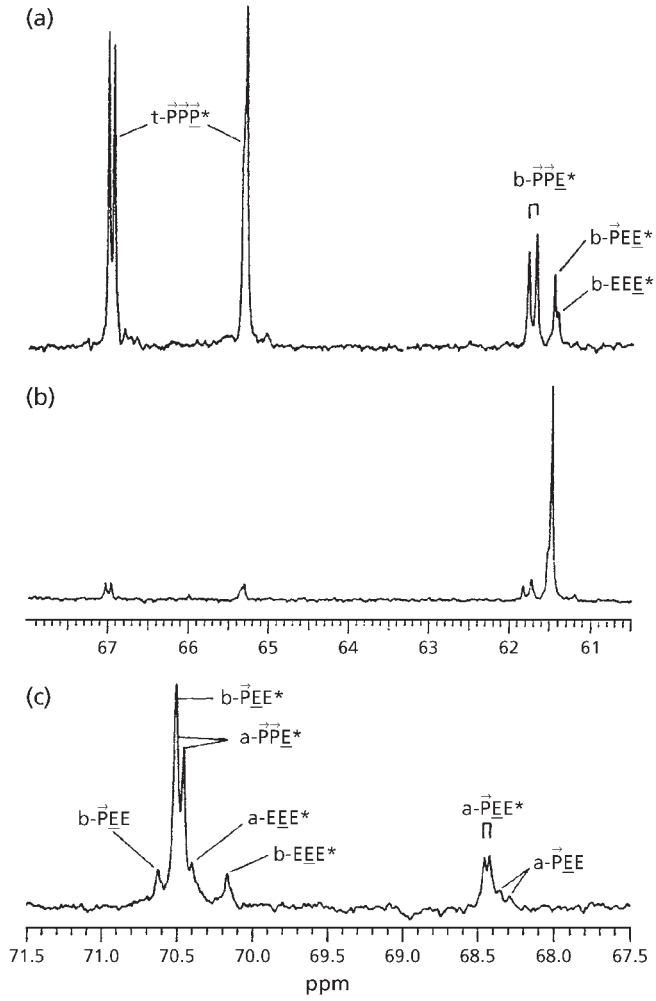

Figure 7.35 ^{13}C spectra of EPE triblock copolymers: (a) terminal resonances of E0.3P16E0.3, (b) terminal resonances of E9P26E9, (c) end-group resonances of E0.3P26E0.3, in vicinity of PEO resonance. (*Reprinted with permission from F. Heatley, Y. Luo, J. Ding, R.H. Mobbs and C. Booth, Macromolecules, 1988, **21**, 9, 2713. ©1989, ACS, USA. [217]*)

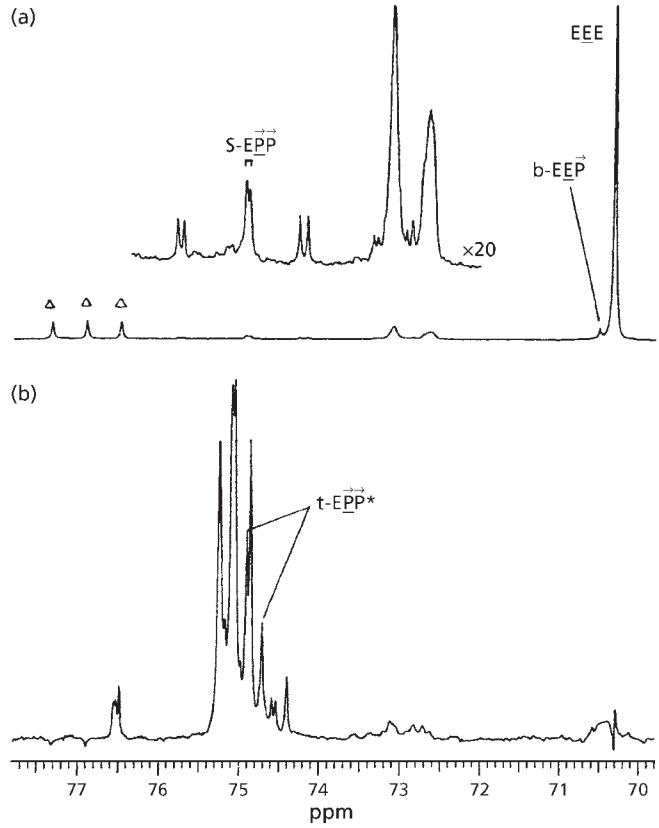

Figure 7.36 (a) CH_2 and (b) CH subspectra of P10E39P10 (Δ, $CDCl_3$ solvent). (*Reprinted with permission from F. Heatley, Y. Luo, J. Ding, R.H. Mobbs and C. Booth, Macromolecules, 1989,* ***21****, 9, 2713. ©1988, ACS, USA. [217]*)

three or more P units. For chains terminated by a single P unit, there is of course no stereochemical splitting, whereas with two P units, there is a large splitting due to *m/r* isomerism of the terminal diad. With three or more P units, the terminal carbon resonance is identical with that of PPO homopolymer. Peaks from penultimate units occur in the vicinity of main-chain carbons and were distinguished in the same way as peaks from the end units. These assignments are given in **Table 7.26**. The exceptional high-frequency shift of the s-EP* carbon is noteworthy.

Figure 7.37(a) shows the terminal carbon region of the spectrum of the low MW EP statistical copolymer CH-EP. Both t-P* and b-E* peaks are observed. Peaks occur at positions found in the spectra of the triblock copolymers and assigned to t-EEP* t-EPP*, t-PPP*, b-EEE*, b-PEE*, and b-PPE* and b-PPE* end triads.

Table 7.26 ^{13}C Chemical Shift Assignments for ethylene oxide – propylene oxide (E/P) polymers in $CDCl_3$ at 22 ºC and concentration of 0.15 g/cm^3	
Carbon	**δC**
EEE, a-EEP	70.33
b-EEP, PEP	70.50
b-PEE	70.60
a-EPEE, a-EPEP	68.29
a-PPEE, a-PPEP	68.29, 68.37
b-PEP	70.74
PEP	68.50
s-PP	72.64, 73.11
t-PPP	74.86, 75.06, 75.10, 75.26
s-PPPP	75.00, 75.03, 75.11
s-PPP	74.5-75.5
t-PPP	72.5-73.8
t-PPE	74.89, 75.06
s-EPP	74.87, 74.91
t-EPP	74.73, 74.94
t-EPP	72.75, 73.12
s-EPE	74.91
t-EPE	74.73
b-EEE	61.46
a-EEE	72.35
b-EEE	70.09
b-PEE	61.48
a-PEE	72.29
b-PEE	70.51
a-PEE	68.42, 68.45
b-EPE	61.72
b-PPE	61.72, 61.83
a-PPE	70.46, 70.51
t-PPP	65.32, 66.95, 67.03

Table 7.26 *Continued*	
Carbon	**δC**
s-PPP	74.6, 74.26, 75.71, 75.79
t-PPP	74.42, 74.56, 74.61, 76.53
s-PPP	72.86, 73.04, 73.32, 73.36
t-EPP	65.48, 66.85
s-EPP	74.28, 75.53
t-EPP	74.24, 75.88
s-EPP	75.01, 75.10
t-PEP, t-EEP	65.98
s-EEP	76.76
Reprinted with permission from F. Heatley, Y. Luo, J. Ding, R.H. Mobbs and C. Booth, Macromolecules, 1989, ***21****, 9, 2713. ©1989, ACS [217]*	

There is a more or less equal distribution of *m* and *r* PP diads. There is no evidence of end groups other than E* or P*, nor of initiation sites other than oxyethylene or oxypropylene. In this polymer two additional end units, EPE* and PEP*, may occur. The resonances of the terminal carbons would be expected to be close to those of b-PP<u>E</u>* and t-EE<u>P</u>*, respectively. In the case of the former, it is noticeable that whereas in the EPE triblock spectra, the b-PP<u>E</u>* signal is a symmetrical doublet at δ_c 61.72 and 61.83, the corresponding peaks in the statistical copolymer are not of equal intensity, that at δ_C 61.72 being more intense. The additional component at this frequency is therefore tentatively assigned to a singlet from the b-EP<u>E</u>* carbon. The t-PE<u>P</u>* and t-EE<u>P</u>* resonances are indistinguishable.

Van Rooji and co-workers [222] have also carried out sequencing studies on ethylene oxide – propylene oxide copolymers. ^{13}C-NMR spectra at 75.5 MHz of ethylene oxide – propylene oxide solutions in deuterochloroform enabled triad sequences to be unequivocally identified including the effects of stereoisomerism and end groups.

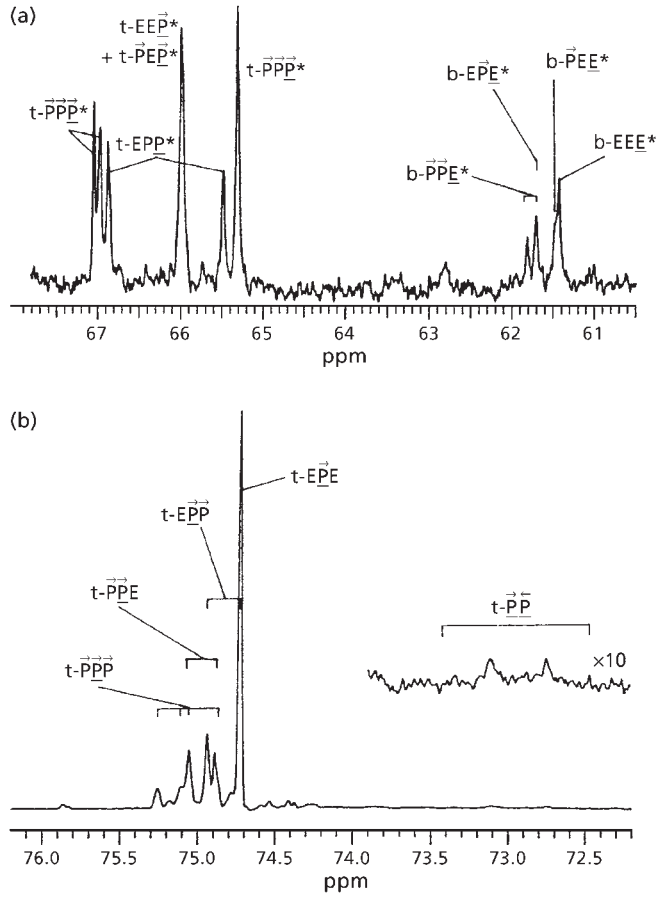

Figure 7.37 Spectra of low MW statistical EP copolymer, CH-EP: (a) terminal resonances, (b) CH subspectrum of main-chain carbons, resolution-enhanced with Te = 0.2 and Tg = 0.3 s. (*Reprinted with permission from F. Heatley, Y. Luo, J. Ding, R.H. Mobbs and C. Booth, Macromolecules, 1988,* ***21****, 9, 2713. ©1989, ACS, USA. [217]*)

7.8.3 Ethylene Oxide – p-Phenylene Vinylene

Poly-*p*-phenylene vinylene and its derivatives are electrically conducting polymers. Yang and co-workers [223] studied microstructure and sequencing in phenylene vinylene - ethylene oxide and methylene - ethylene oxidecopolymers:

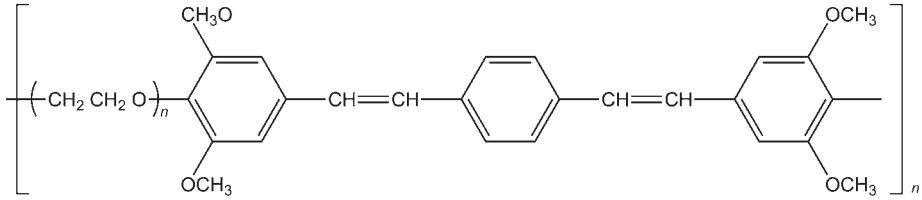

In the IR spectra of these copolymers, the band at 1682-1695 cm^{-1}, which was assigned to the C=O stretching vibration in the dialdehydes, is no longer present, but a new band at 957-959 cm^{-1} has emerged. This new band is attributed to the out-of-plane bending vibration of the *trans* -CH=CH- moieties, which are formed from the C=O. It is noteworthy that the copolymers contain polyvinylene units which are only 2.5 units long. Sequencing studies have also been conducted on polyethylene oxide – 1,2-butylene [224] and ethylene oxide – epichlorohydrin copolymers.

7.9 Polybutadiene – Acrylonitrile – Methacrylic Acid Terpolymers

Rao and co-workers [201] applied Py-GC and ^{13}C-NMR to the determination of sequence distribution of butadiene (B), acrylonitrile (A) – methacrylic acid (M) terpolymers. The sequence distribution was described in terms of six triads: BB, B, ABA, ABB, BBA, MBB and AMB and was found to vary with the mode of addition of methacrylic acid monomer.

The NMR data was found to be in good agreement with a mechanism of polymerisation in which methacrylic acid is preferentially involved in initiation reactions by a thiyl radical arising from the reaction of the chain modifier, 1-dodecanethiol, and cyanoisopropyl radical generated from azobis-isobutyro-nitrile (AIBN) initator. Binders obtained by curing the liquid terpolymers with an epoxy resin showed widely varying mechanical properties with tensile strength varying from 4.3 to 0.6 kg/cm^2 and elongation at break from 130 to 450%. It was found that tensile strength increases and elongation decreases with the number of acrylonitrile units between the methacrylic acid crosslinks. Good correlation was obtained between triad population ratio [ABB + BBA] [BB^{v}B]/[ABA] [MBB] and the mechanical properties of the binders. Py-GC data at 550 and 600 °C confirmed the results obtained from ^{13}C-NMR, and the mole ratio of butadiene to arylonitrile in the pyrolysates showed correlation with the properties of binders.

Rao and co-workers [201] classified into (i) triads containing butadiene (B), (ii) triads containing butadiene (B) and acrylonitrile (A) and (iii) triads containing B, A and M units. These workers discuss under separate headings the following types of triads: BBB, ABA, ABB-BBA, MBM, MBB and BBM under olefinic carbon resonances: BBB, ABA, ABB triads under nitrile carbon resonances.

The main conclusions that can be drawn from the ^{13}C-NMR studies of the terpolymers can be summarised as follows:

(i) The average configuration of the butadiene units is essentially the same in all the polymers.

(ii) The incorporation of l-dodecyl thiyl moiety into the polymer chain is quite considerable for all the polymers.

(iii) The number of butadiene units connected to the methacrylic acid unit is not commensurate with the concentration of the acid when compared to the number of butadiene units connected to acrylonitrile units. The former increases from polymer I to (MW = 4778) acrylonitrile 11.8%) to polymer V (MW 2781, acrylonitrile 11.8%) (See **Table 7.27**).

Table 7.27 Triad Intensity Ratios for polybutadiene (B) – acrylonitrile (A) – methacrylic acid (M) Terpolymers

Sample number	Polymer	[ABB] + [BBA] [ABA]	[BBB][a]/ [MBB]	[BB^{v}B][b]/ [MBB]	[BB^{v}B][b]/ [t-CH_3][c]	[ABB] + [BBA] × [BB^{v}B]/[MBB] [ABA]
2	I	6.2	8.2	5.0	5.1	31.0
2	II	5.7	5.5	2.7	2.2	15.4
3	III	4.7	4.8	2.2	3.1	10.3
4	IV	4.4	4.7	2.3	2.0	10.1
5	V	3.7	4.2	2.1	1.8	7.8

[a] *Calculated from Sp^2 carbon resonances, [BBB] = ttc/t*
[b] *Calculated from Sp^3 carbon resonances*
[c] *t-CH_3 = terminal CH_3*

Reprinted with permission from M.R. Rao, T.V. Sebastian, T.S. Radhakrishnan and P.V. Ravindran, Journal of Applied Polymer Science, 1991, ***42****, 3, 753. © 1991, John Wiley and Sons [201]*

(iv) Polymer I (MW = 4978, 11.8% acrylonitrile) contains triads of the type ABM or BMA.

(v) The fractional population of the triads ABA increases from polymer I (MW = 4978, 11.8% acrylonitrile) to polymer V (MW = 2781, 11.8% acrylonitrile).

(vi) The concentration of the terminal methyl groups varies from polymer I to V.

All these observations can be rationalised by assuming the mechanism of polymerisation to be similar to free radical addition of thiols to olefins as outlined next:

Initiation:

$$NC(CH_3)_2CN{=}NC(CH_3)_2CN \xrightarrow[\text{catalyst}]{\Delta} NC(CH_3)_2\dot{C}$$

$$NC(CH_3)_2\dot{C} + RSH \longrightarrow NC(CH_3)_2CH + R\dot{S}$$

Addition:

$$R\dot{S} + CH_2{=}C(CH_3)COOH \longrightarrow RSCH_2\dot{C}(CH_3)COOH$$

Propagation:

$$RSCH_2\dot{C}(CH_3)COOH + CH_2{=}CH{-}CH{=}CH_2 \longrightarrow {\sim}CH_2CH{=}CH\dot{C}H_2$$

Chain transfer:

$${\sim}CH_2CH{=}CH\dot{C}H_2 + RSH \longrightarrow {\sim}CH_2CH{=}CHCH_3 + R\dot{S}$$

Termination:

$${\sim}CH_2CH{=}CH\dot{C}H_2 \rightarrow \text{chain stopper} \longrightarrow {\sim}CH_2CH{=}CHCH_3$$

In summary, the average microstructure of the terpolymers as established by Rao and co-workers [200] can be represented as:

$$C_{12}H_{25}SM\ (BBB)_a\ (BBA)_b\ (BBM)_c - (BMA)_d\ (ABA)_eCH_2 - CH = CH - CH_3$$

The essential differences between the structures of polymers I and V are:

(i) the number of BBA units between two methacrylic acid units decreases from polymer I to V, as indicated by the decrease in the population ratio of (ABB + BBA) and ABA triads (**Table 7.27**); and

(ii) the fraction of MBB triads increases and consequently the fraction of AMB or BMA triads decreases from polymer I to V as reflected by the decrease in the ratio of $BB^{V}B$ and MBB sequences.

The terpolymer samples (0.6-0.7 mg) were pyrolysed at 550 and 600 °C and typical pyrograms of polymers I and IV are shown in **Figure 7.38**. The results are

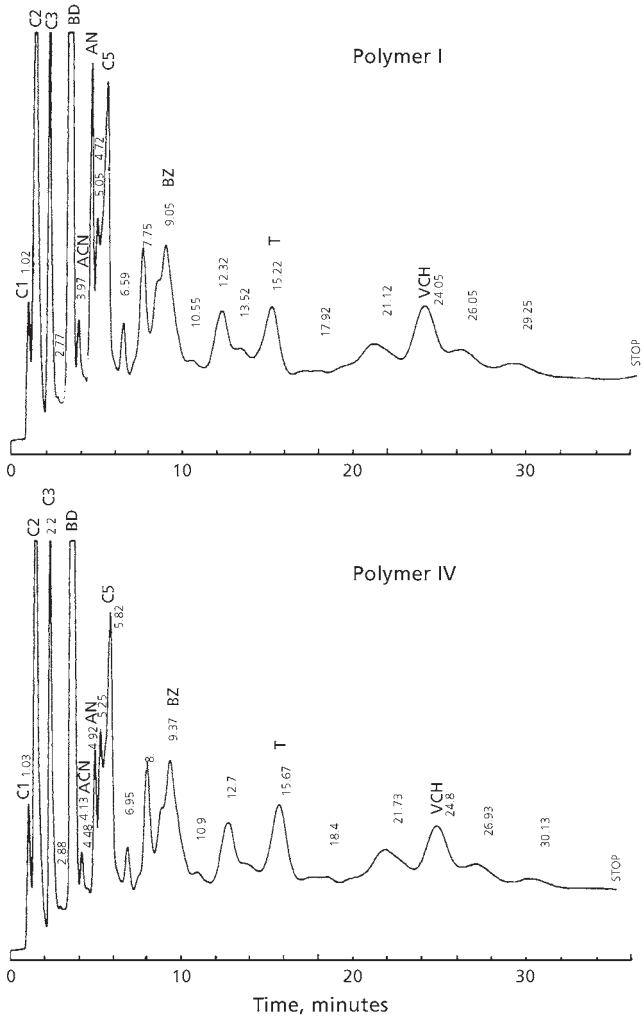

Figure 7.38 Pyrograms of polymers I and IV at 550 °C (see **Table 7.27**). (*Reprinted with permission from M.R. Rao, T.V. Sebastian, T.S. Radhakrishnan and P.V. Ravindran, Journal of Applied Polymer Science, 1991,* **42**, *3, 753. ©1991, John Wiley and Sons [201]*)

Table 7.28 Composition of major pyrolysates of butadiene (B) – acrylonitrile – (A) methyacrylic acid (M) terpolymers

Polymer	Wt %[a]										Mol %	
	C_1 (1.0)	C_2 (1.3)	C_3 (2.2)	B (3.5)	CAN (4.0)	A (4.7)	C_5 (5.6)	BZ (9.1)	T (15.2)	VCH (24.1)	B/A	B/ VCH
Pyrolysis temperature: 550 °C												
I	1.3	7.5	4.7	24.3	0.4	3.6	7.3	9.3	5.4	6.7	6.6 ± 0.2	7.2 ± 0.2
II	1.4	7.3	4.5	23.2	1.1	2.2	7.4	8.5	5.4	5.7	10.3 ± 0.3	8.1 ± 0.2
III	1.4	7.7	4.5	26.2	1.2	2.1	7.4	9.7	5.3	6.2	12.3 ± 0.4	8.5 ± 0.3
IV	1.5	7.4	4.4	25.9	1.2	2.1	7.1	8.6	5.2	6.4	12.1 ± 0.3	8.1 ± 0.2
V	1.5	7.9	5.0	26.5	0.8	1.8	7.1	9.0	6.2	5.8	14.4 ± 0.4	9.1 ± 0.3
VII	1.4	7.4	4.5	25.7	1.1	2.0	7.7	10.3	6.3	6.7	12.6 ± 0.4	7.7 ± 0.2
Pyrolysis temperature: 600 °C												
I	2.4	8.8	5.4	20.9	1.3	3.6	8.1	7.6	6.8	3.5	5.7 ± 0.2	11.9 ± 0.3
II	2.4	8.6	5.6	20.9	1.4	2.6	7.9	7.5	6.9	3.4	7.9 ± 0.2	12.3 ± 0.3
III	2.3	8.2	5.1	20.8	1.1	2.3	7.9	7.3	6.8	3.7	8.9 ± 0.3	11.2 ± 0.3
IV	2.2	8.2	5.2	22.0	1.2	2.5	7.5	7.6	7.0	3.5	8.6 ± 0.3	12.6 ± 0.4
V	2.4	8.6	5.5	23.1	1.0	2.3	7.4	7.3	7.0	3.5	9.9 ± 0.3	13.2 ± 0.4
VII	2.2	7.8	4.8	21.4	1.5	2.5	8.0	8.1	7.2	4.1	8.4 ± 0.2	10.4 ± 0.3

[a] Values in brackets are the retention times in minutes. For interpretation of key – see text.
From butadiene part of molecule:
C_1 – C_3 = ethylene, propylene from butadiene part of molecule
B = butadiene from butadiene part of molecule
BZ = benzene from butadiene part of molecule
T = toluene from butadiene part of molecule
VCH = vinylcylohexone from butadiene part of molecule
From acrylonitrile part of molecule:
A = acrylonitrile from acrylonitrile part of molecule
CAN = acrylnitrile from acrylonitrile part of molecule

given in **Table 7.28**. The major products of pyrolysis were found to be ethylene, propylene, butadiene (B), benzene, toluene, and vinyl cyclohexane (VCH) from the butadiene part and acrylonitrile (AN) and acetonitrile from the acrylonitrile part of the polymers.

The composition of the products of pyrolysis at 550 °C (**Table 7.28**) shows that mole ratios of BD/VCH and BD/AN increases from polymer I to V, although the change in BD/VCH ratio is only marginal. Similar trends are observed at the pyrolysis temperature of 600 °C also (**Table 7.28**), although, the differences narrow down considerably. These ratios are sensitive to the sequence distribution of BD and AN units in the polymer chain. It is recognised that the formation of VCH, a dimer of BD, requires the presence of two butadiene moieties adjacent to each other and, consequently, in copolymers of BD. The VCH/BD) ratio is dependent on the distribution of co-monomer and becomes almost zero for an alternating copolymer. Hence, the marginal increase in BD/VCH ratio from polymer I to V reflects the increasing alternating nature of the placement of acrylonitrile units in the chain. This is consistent with the observation from ^{13}C-NMR studies that the population of ABA triads increase from polymer I to V.

The mechanism of degradation of polybutadiene (PBD), as suggested by Golub and Gargiulo [225], involves main chain scission to give radical ends, which can undergo depolymerisation (to yield mainly BD and VCH) [226] or cyclisation to give cyclised PBD as shown in the scheme on the following page.

For copolymers of BD and AN, the cyclisation will be more facile due to the pendant nitrile group as in the case with polyacrylonitrile (PAN) polymers [227, 228]. The likely cyclisation reactions are shown in the scheme next, and this mechanism of decomposition suggests that the greater the alternating nature of the polymers, the greater will be the extent of cyclisation reactions. The cyclised polymers would undergo further thermal degradation to give various products.

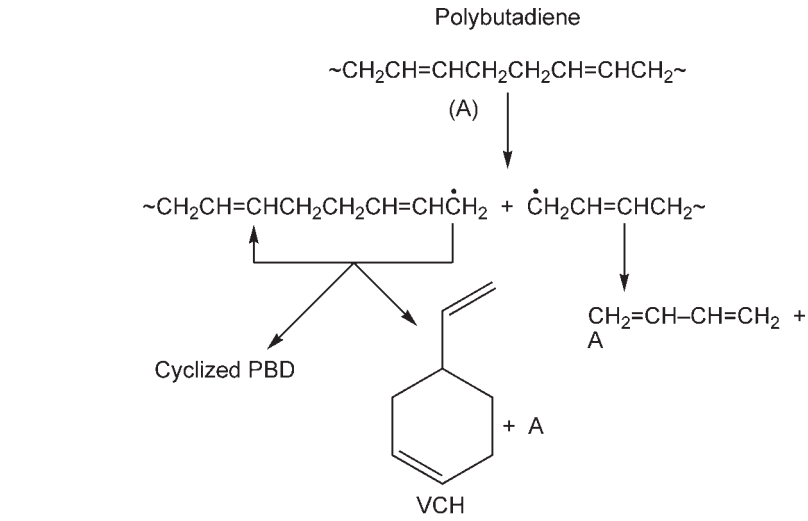
Polybutadiene
~CH2CH=CHCH2CH2CH=CHCH2~
(A)
~CH2CH=CHCH2CH2CH=CHĊH2 + ĊH2CH=CHCH2~
CH2=CH–CH=CH2 +
A
Cyclized PBD
+ A
VCH

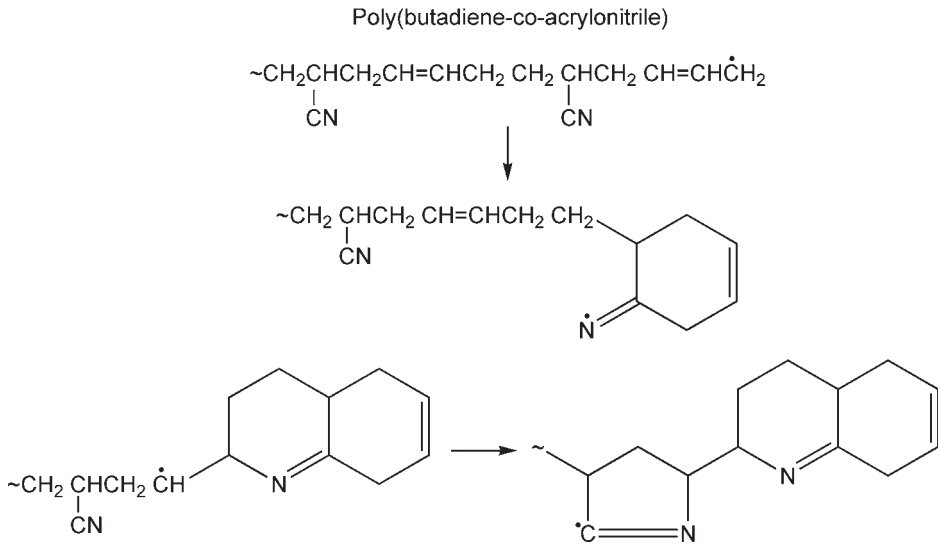
Poly(butadiene-co-acrylonitrile)
~CH2CHCH2CH=CHCH2 CH2 CHCH2 CH=CHĊH2
CN
CN
~CH2 CHCH2 CH=CHCH2 CH2
CN
N
~CH2 CHCH2 ĊH
CN
N
~
N
ĊC
N

7.10 Polydimethyl Siloxane - Urethane

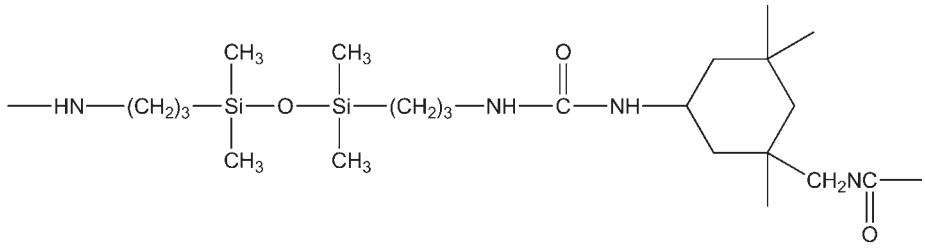

So far in this chapter on sequencing, two techniques have predominated, namely NMR spectroscopy and Py-GC. An exception is the work of Zhuang and co-workers [228] who used time-of-flight secondary ion mass spectrometry (ToF-SIMS) in their study of the distribution of polydimethylsiloxane (PDMSO) segment lengths at the surface of PDMSO – urethane segmented copolymers. Their aim in this work, was to establish whether, at the surface of the copolymer, the distribution of segment or chain lengths is different than in the bulk of the polymer.

SIMS has been emerging as a potential tool, particularly with ToF detection technologies which are able to yield increased resolution, mass range, and transmission.

Prior to the work of Zhuang and co-workers [229] ToF-SIMS had not provided information on segment length distribution at the surface of a multicomponent polymer, particularly in the form of a thick film. The difficulties in accomplishing this are primarily due to (a) lack of structurally well-defined copolymers, (b) charging effects at the surfaces upon ion beam perturbation [230-233], (c) lack of cationising ions, and (d) polymer chain entanglement and interchain and/or intrachain interactions in a polymer. In many cases, however, complete charge compensation for the analysis of an insulating sample can be attained in ToF-SIMS by flooding the surface with low-energy (10 eV) electrons pulsed between ion pulses [234-236].

Figures 7.39(a) and (b) show the positive ToF-SIMS spectra from the thick PU-PDMSO film in the range of *m/z* = 0-300 and 1000-2500. Comparing **Figure 7.39(b) and 7.39(c)**, a remarkable resemblance is seen between the spectrum from the copolymer and that originating from pure PDMSO, except that the peak at *mlz* =116 from the PDMSO end cap is noticeably lower in the PU-PDMSO spectrum (which may arise from the fact that after incorporation in the PU-PDMSO spectrum it requires two bonds to be broken to form the 116 fragment). This is a strong indication that the PDMSO segment compositionally dominates the surface of the thick PU-PDMSO film. The peaks in **Figure 7.39(b)** are separated from each other by 74 Da. According to a 'simple statistical model' for chain scission [237], stating that only main chain scission occurs, the masses of all possible fragments formed by any two chain cleavages

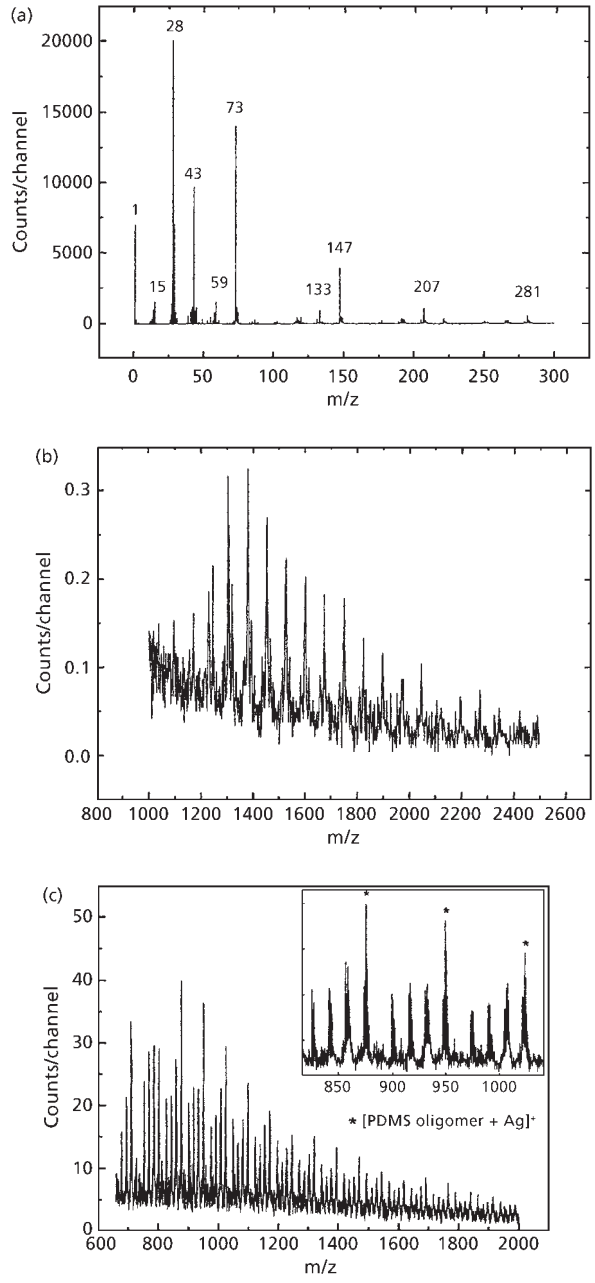

Figure 7.39 (a) Thick film of polydimethylsiloxane-polyurethane on aluminium in the range *m/z* 0-300. (b) Thick film of polydimethylsiloxane-polyurethane in the range *m/z* 1000-2500. (c) Submonolayer thin film of polydimethylsiloxane on silver in the range *m/z* 0-300. (*Reprinted with permission from H. Zhuang, J.A. Gardella, Jr., and D.M. Hercules, Macromolecules, 1997, **30**, 4, 1153. ©1997, ACS [229]*)

along the PU-PDMSO copolymer backbone were calculated and compared to the mass values of the peaks in **Figure 7.39(b)**. Only those fragments having the structure represented in Scheme 1 agree with the series observed in **Figure 7.39(b)**. At this point, it is not known what caused the stability of this particular fragment ion structure, but it is certain that the spectrum observed is not consistent with any other type of fragmentation considered from bond breaking. All other ion structures from bond breaking near or within the urea linkage were rejected because they were not consistent with the repeating mass pattern or the isotopic pattern of the repeating cluster.

Scheme 1. Fragmentation Mechanism of the PU-PDMSO Copolymer in the Form of a Thick film

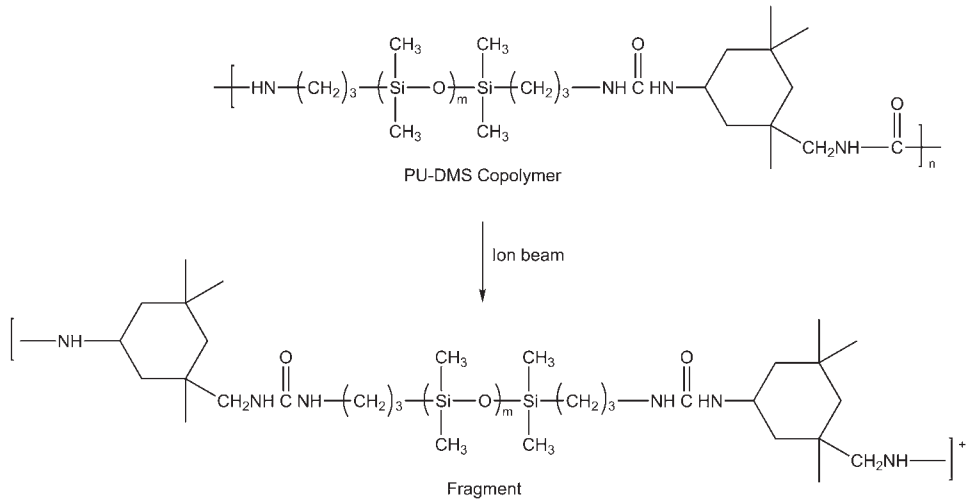

Based on the assigned fragment structure, the length distribution (relative intensities versus *m* values) was constructed. It was calculated that M_n = 1131.3, M_w = 1172.4, and M_w/M_n = 1.1, very close to those values of the pure PDMSO (1K) prepolymers. This result suggests that the PDMSO segment segregated at the surface of the PU-PDMSO copolymer with a PDMSO nominal MW of approximately 1000 Da is basically identical with that in the bulk in terms of PDMSO segment length distribution.

The distribution of PDMSO segment lengths segregated at the surface was nearly identical with that in the bulk for the PU-PDMSO copolymer with PDMSO of a nominal MW of approximately 1000 Da, this accomplishment opens a door to study segment length distributions at the surface of other siloxane copolymers as a function of bulk segment length distribution and polymer processing.

In addition, by comparing the low-mass (m/z = 0–300) spectra from the submonolayer PDMSO prepolymer film on Ag and the thick PU-PDMSO copolymer film on Al, it

was noted that the PDMSO segment compositionally dominated the surface of the thick PU-PDMSO film. This observation agrees well with earlier ESCA results.

Ions detected and assigned to fragments in the low-mass range ($m/z \leq 300$) provided structural information about the repeat units and the end groups. The high mass spectrum of the PDMSO homopolymer yielded a series of ions assigned to Ag+-cationised oligomers; this enabled determination of the molecular weight distribution. In the high-mass (m/z = 800-3500) spectra of thick PU-PDMSO films, the peak series was assigned to a simple fragmentation process. That process would yield ions where the intact PDMSO segment is present, it therefore can be used to evaluate the PDMSO segment length distribution at the surface of the copolymer. It was found that the distribution of PDMSO segment lengths segregated at the surface of the thick film was almost identical with that in the bulk for PU-PDMSO with PDMSO nominal molecular weight of approximately 1000 Da. These results allow the development of an analysis of ion structure and a stepwise procedure for evaluating the segment length distributions in the near-surface region of siloxanes.

Wide angle ESCA has been used to determine the length of PDMSO segments in PDMSO. These results were evaluated using a concentration – depth profile deconvolution programme, and continuous concentration – depth profiles of the hard segment were reported in the near-surface region [238-240]. This yields a more intuitive understanding of the compositional features of PU-PDMSO copolymers. Each aforementioned case showed a PDMSO-rich surface due to the incompatibility of the soft segment and hard segment and the lower surface energy of the soft segment in the segmented copolymers.

7.11 Sequences in Miscellaneous Copolymers

Various other methods including IR spectroscopy, UV spectroscopy, electrical polarisation, and thermochemical methods, crystallinity measurements, entropies of polymerisation, glass transition temperatures and solution property measurements have been used to determine sequence distribution. This has been reviewed by Harwood [156]. Further work on sequence measurement is reviewed in **Table 7.29**.

Table 7.29 Review of Methods used to Determine Sequences			
Polymer	**Technique**	**Sequence measured**	**Reference**
Aromatic ethylene glycol polyesters	NMR	Sequence distribution	[241]
Arylether-sulfone	NMR	Structure and sequencing	[242]
Methylvinylidene cyanide-vinyl acetate	NMR	Sequence distribution	[243]
Vinylidene cyanide-methacrylonitrile-cyanovinyl acetate	NMR	Sequence distribution	[244]
Styrene-vinylidene cyanide	NMR	Sequence distribution	[245]
12-Oxydodecanoyl polyester amides	NMR	Sequence distribution	[246]
Fluorine containing polyarylether sulfones	NMR	Sequence distribution	[247]
General polymers	NMR	Sequence distribution	[248, 249]
Aromatic amide terpolymers	NMR	Sequence distribution	[250]
Miscellaneous polymers	MS	Sequence distribution	[251]
Butadiene-isoprene	Py-GC - MS	Sequence distribution	[252]
Condensation copolymers	Py-MS	Sequencing	[253]
Polyester polyamides	Fast atom bombardment MS	Sequencing	[254]
Ethylene-tetrafluoroethylene, perfluoro butylethylene	Py-GC	Sequence length distribution	[255]
Miscellaneous copolymers	Py-GC	Sequence distribution	[256]
Ethylene oxide-polyacetal	Hydrolysis-methylation Py-GC	Sequence distribution	[213]
Ethylene propylene	IR spectrometry	$-CH_2-CH_2$ sequences	[23-25]
1-Hexane-4-methyl-1-pentene	IR spectrometry	Block structure	[26]

Table 7.29 *Continued*			
Ethylene butylene	IR spectrometry	$-CH_2-CH_2$ sequences	[27]
Acrylonitrile-2-substituted propene	IR spectrometry	$-CH_2-CH_3$ sequences	[28]
Acrylonitrile-styrene	IR spectrometry	Styrene sequences	[29-30]
Styrene-vinyl acetate	IR spectrometry	Sequence distribution	[31]
α-Methyl styrene-methylene block copolymers	IR spectrometry	α-Methyl styrene sequences	[32]
Styrene-methacrolein	IR spectrometry	Sequence length of styrene units	[257]
Styrene maleic anhydride	IR spectrometry	Styrene sequences	[258]
Styrene methylmethacrylate	IR spectrometry	Styrene sequences	[259]
Vinyl chloride-vinylidene chloride	IR spectrometry	Methylene sequences	[213, 260, 261, 262]
Source: Author's own files			

References

1. J. van Schooten, E.W. Duck and R. Berkenbosch, *Polymer*, 1961, **2**, 357.
2. H.L. McMurry and V. Thornton, *Analytical Chemistry*, 1952, **24**, 2, 318.
3. G. Bucci and T. Simonazzi, *Journal of Polymer Science Part C: Polymer Symposia*, 1964, **7**, 1, 203.
4. G. Bucci and T. Simonazzi, *La Chimica e L'Industria*, 1962, **44**, 262.
5. G. Natta, G. Mazzanti, A. Valvassori, G. Sartori and D. Merero, *La Chimica e L'Industria*, 1960, **42**, 125.
6. T.A. Veerkamp and A. Veermans, *Die Makromolekulare Chemie*, 1961, **50**, 1, 147.
7. J. van Schooten and S. Mostert, *Polymer*, 1963, **4**, 135.

8. G. Natta, G. Dall'Asta, G. Mazzanti and F. Ciampelli, *Kolloid-Zeitschrift*, 1962, **182**, 50.

9. N. Sheppard and G.B.B.M. Sutherland, *Nature*, 1947, **159**, 739.

10. F.M. Rugg, J.J. Smith and L.H. Wartman, *Journal of Polymer Science*, 1953, **11**, 1, 1.

11. G.B.B.M. Sutherland, *Discussions of the Faraday Society*, 1950, **9**, 274.

12. Y. Tanaka and K. Hatada, *Journal of Polymer Science: Polymer Chemistry*, 1973, **11**, 8, 2057.

13. C.Y. Liang, M.R. Lytton and C.J. Boone, *Journal of Polymer Science*, 1961, **54**, 160, 523.

14. P.B. Rausch, R. Hannock, J.P. Coates, A. Bunn and H.A. Willis, *Polymer Science and Technology*, 1987, **36**, 261.

15. H.N. Cheng, *Polymer Bulletin*, 1991, **26**, 3, 325.

16. W.O. Crain, Jr., A. Zambelli and J.D. Roberts, *Macromolecules*, 1971, **4**, 3, 330.

17. C. Cannon and C. Wilkes, *Rubber Chemistry and Technology*, 1971, **44**, 3, 781.

18. G.J. Ray, P.E. Johnson and J.R. Knox, *Macromolecules*, 1977, **10**, 4, 773.

19. R.S. Porter, *Journal of Polymer Science Part A-1: Polymer Chemistry*, 1966, **4**, 1, 189.

20. H.N. Cheng and M.A. Bennett, *Die Makromolekulare Chemie*, 1987, **188**, 11, 2665.

21. J.C. Randall, *Polymer Sequence Determination: Carbon-13 Method*, Academic Press, New York, NY, USA, 1977, p.53-58.

22. J.C. Randall, *Polymer Sequence Determination: Carbon-13 Method*, Academic Press, New York, NY, USA, 1977, p.135-138

23. C. Tosi, *Die Makromolekulare Chemie*, 1973, **170**, 1, 231.

24. V.P. Popov and A.P. Duvanova, *Zhurnal Prikladnoi Spektroskopii*, 1973, **18**, 1077.

25. M. Seeger, J. Exner and H.J. Cantow, *Quaderni de 'La Ricerca Scientifica'*, 1973, **84**, 102. [Chemical Abstracts, 1973, **81**, 50225]

26. H. Seno, S. Tsuge and T. Takeuchi, *Die Makromolekulare Chemie*, 1972, **161**, 1, 195.

27. N.G. Bakuyutov, Y.V. Kissin, I. Vavilova and Z.V. Arkhipova, *Vysokomolekulyarnya Soedineniya Seria*, 1975, **13**, 2163.

28. K. Kamide and K. Yamaguchi, *Die Makromolekulare Chemie*, 1972, **162**, 1, 205.

29. P. Simak and E. Ropte, *Die Makromolekulare Chemie*, 1975, **Supplement 1**, 507.

30. N. Oi and K. Moriguchi, *Bunseki Kagaku*, 1974, **23**, 798. [Chemical Abstracts, 1974, **82**, 17308x]

31. N. Oi, K. Myazaki, K. Moriguchi and H. Shimada, *Kobunshi Kagaki*, 1972, **29**, 388.

32. J.R. Ebdon, S.H. Kandil and K.J. Morgan, *Journal of Polymer Science: Polymer Chemistry*, 1979, **17**, 9, 2783.

33. H.N. Cheng, *Polymer Bulletin*, 1990, **23**, 6, 589.

34. N. Kuroda, Y. Nishikitani, K. Matsuura and M. Miyoshi, *Die Makromolekulare Chemie*, 1987, **188**, 8, 1897.

35. B. Florin-Michel, M-F. Llauro, R. Spitz and Q-T. Pham, *European Polymer Journal*, 1979, **15**, 3, 277.

36. E.T. Hsieh and J.C. Randall, *Macromolecules*, 1982, **15**, 5, 1402.

37. K. Soga, T. Uozumi, and J.R. Park, *Die Makromolekulare Chemie*, 1990, **191**, 12, 2853.

38. M. De Pooter, P.B. Smith, K.K. Dohrer, K.F. Bennett, M.D. Meadows, C.G. Smith, H.P. Schouwenaars and R.A. Geerards, *Journal of Applied Polymer Science*, 1991, **42**, 2, 399.

39. G.J. Ray, P.E. Johnson and J.R. Knox, *Macromolecules*, 1977, **10**, 4, 773.

40. J.C. Randall, *Macromolecules*, 1978, **11**, 1, 33.

41. H. N. Cheng, *Analytical Chemistry*, 1982, **54**, 11, 1828.

42. G.J. Ray, J. Spanswick, J.R. Knox and C. Serres, *Macromolecules*, 1981, **14**, 5, 1323.

43. E.T. Hsieh and J.C. Randall, *Macromolecules*, 1982, **15**, 2, 353.

44. K. Hikichi, T. Hiraoki, M. Ikura, K. Higuchi, K. Eguchi and M. Ohuchi, *Polymer Journal (Japan)*, 1987, **19**, 11, 1317.

45. T. Hayashi, Y. Inoue, R. Chujo and T. Asakura, *Polymer Journal (Japan)*, 1988, **20**, 10, 895.

46. A. Aoki, T. Hayashi and T. Asakura, *Macromolecules*, 1992, **25**, 1, 155.

47. J.E. Mark, *Journal of Chemical Physics*, 1972, **57**, 6, 2541.

48. Y. Sugimura, S. Tsuge and T. Takeuchi, *Analytical Chemistry*, 1978, **50**, 8, 1173.

49. M.D. Bruch and W.G. Payne, *Macromolecules*, 1986, **19**, 11, 2712.

50. T. Shimanouchi and M. Tasumi, *Spectrochimica Acta*, 1967, **17**, 7, 755.

51. J.J. Shipman, V.L. Folt and S. Krimm, *Spectrochimica Acta*, 1962, **18**, 12, 1603.

52. T. Asakura, K. Omaki, S.N. Zhu and R. Chujo, *Polymer Journal (Japan)*, 1984, **16**, 9, 717.

53. A. Aoki, *Polymer Communications*, 1990, **31**, 4, 130.

54. H.N. Cheng, *Journal of Polymer Science: Polymer Physics Edition*, 1983, **21**, 573.

55. A. Bax, R. Freeman and T.A. Frenkiel, *Journal of the American Chemical Society*, 1980, **102**, 15, 4898.

56. A. Bax, R. Freeman and T.A. Frenkiel, *Journal of the American Chemical Society*, 1981, **103**, 8, 2102.

57. R. Freeman, T.A. Frenkiel and M.B. Rubin, *Journal of the American Chemical Society*, 1982, **104**, 20, 5545.

58. J.C. Randall, *Macromolecules*, 1978, **11**, 3, 592.

59. D. Doskocilová, J. Stokr, B. Schneider, H. Pivcová, M. Kolinsky, J. Petránek and D. Lím, *Journal of Polymer Science Part C: Polymer Symposia*, 1967, **16**, 1, 215.

60. C.G. Opaskar and S. Krimm, *Spectrochimica Acta Part A: Molecular Spectroscopy*, 1967, **23**, 8, 2261.

61. W.H. Moore and S. Krimm, *Journal of Molecular Spectroscopy*, 1974, **51**, 1, 1.

62. W.H. Moore and S. Krimm, *Die Makromolekulare Chemie*, 1975, Supplement 1, 491.

63. S-I. Mizushima, T. Shimanouchi, K. Nakamura, M. Hayashi and S. Tsuchiya, *Journal of Chemical Physics*, 1957, **26**, 4, 970.

64. T.N. Bowmer and A.E. Tonelli, *Journal of Polymer Science: Polymer Physics Edition*, 1986, **24**, 8, 1631.

65. A.E. Tonelli and T.N. Bowmer, *Journal of Polymer Science: Polymer Physics Edition*, 1987, **25**, 5, 1153.

66. M.J. Hackathorn and M.J. Brock, *Journal of Polymer Science: Polymer Chemistry*, 1975, **13**, 4, 945.

67. A. Kawaski in *Proceedings of the 27th Autumn Meeting of the Japan Chemical Society Preprints*, 1972, **2**, 20.

68. M.J. Hackathorn and M.K. Brock, *Rubber Chemistry and Technology*, 1972, **45**, 5, 1295.

69. N. Yoshie, Y. Inoue, H.Y. Yoo and N. Okui, *Polymer*, 1994, **35**, 9, 1931.

70. H. Jancke, F. Böhme, K. Graßhoff, M. Rätzsch and G. Rafler, *Die Makromolekulare Chemie*, 1989, **190**, 12, 3173.

71. K.R. Amundson, J.A. Reimer and M.M. Denn, *Macromolecules*, 1991, **24**, 11, 3250.

72. D. Garozzo, M. Giuffrida, G. Montaudo and R.W. Lenz, *Journal of Polymer Science Part A: Polymer Chemistry*, 1987, **25**, 1, 271.

73. T.A. Ojala and G. Fink, *Die Makromolekulare Chemie, Rapid Communications*, 1988, **9**, 2, 85.

74. T. Kanezaki, M. Kijima, K. Kume, K. Sato and T. Asakura, *Polymer*, 1994, **35**, 12, 2523.

75. B. Para, J.A. Delgado, E. Pérez and A. Bello, *Die Makromolekulare Chemie*, 1994, **195**, 7, 2457.

76. T. Yamada, T. Okumoto, H. Ohtani, and S. Tsuge, *Rubber Chemistry and Technology*, 1987, **60**, 2, 207.

77. J.C. Randall, C.J. Buff, M. Kelchtermans and B.H. Gregory, *Macromolecules*, 1992, **25**, 10, 2624.

78. Y. Tanaka, K. Nunogaki and J. Adachi, *Rubber Chemistry and Technology*, 1988, **61**, 1, 36.

79. Y. Tanaka, Y. Nakafutami, Y. Kashiwazaki, J. Adachi and K. Tadokoro, *Rubber Chemistry and Technology*, 1987, **60**, 2, 207.

80. Y. Tanaka, H. Sato and J. Adachi, *Rubber Chemistry and Technology*, 1987, **60**, 1, 25.

81. M.E. Pattuelli, A. Montalti, G.T. Viola and A. Zazzetta, *Journal of Chromatography A*, 1994, **665**, 1, 117.

82. F.A. Bovey, *Journal of Polymer Science*, 1962, **62**, 173, 197.

83. K. Ito and Y. Yamashita, *Journal of Polymer Science Part B: Polymer Letters*, 1965, **3**, 8, 625.

84. K. Ito, S. Iwase, K. Umehara and Y. Yamashita, *Journal of Macromolecular Science, Part A: Pure and Applied Science*, 1967, **1**, 5, 891.

85. K. Ito and Y. Yamashita, *Journal of Polymer Science Part B: Polymer Letters*, 1965, **3**, 8, 631.

86. K. Ito and Y. Yamashita, *Journal of Polymer Science Part B: Polymer Letters*, 1968, **6**, 3, 227.

87. A. Simmons, A. Natansohn and A. Eisenberg, *Journal of Polymer Science Part A: Polymer Chemistry*, 1987, **25**, 8, 2221.

88. T. Hayashi, Y. Inoue and R. Chujo, *Macromolecules*, 1988, **21**, 11, 3139.

89. H.N. Cheng and G.H. Lee, *Macromolecules*, 1988, **21**, 11, 3164

90. H. Sato, T. Ishikawa, K. Takebayashi and Y. Tanaka, *Macromolecules*, 1989, **22**, 4, 1748.

91. H. Ketels, J. Beulen and G. Van der Velden, *Macromolecules*, 1988, **21**, 7, 2032.

92. R. Volpe and T.E. Hogen-Esch, *Macromolecules*, 1990, **23**, 19, 4196.

93. F. Heatley, G. Yu, W-B. Sun, E.J. Pywell, R.H. Mobbs and C. Booth, *European Polymer Journal*, 1990, **26**, 5, 583.

94. J.J. Uebel and F.J. Dinan, *Journal of Polymer Science: Polymer Chemistry*, 1983, **21**, 6, 1773.

95. J.J. Uebel and F.J. Dinan, *Journal of Polymer Science: Polymer Chemistry*, 1983, **21**, 8, 2427.

96. L.T. Kale, K.F. O'Driscoll, F.J. Dinan and J.J. Uebel, *Journal of Polymer Science Part A: Polymer Chemistry*, 1986, **24**, 11, 3145.

97. A.S. Brar, and A.K. Saini, *Journal of Applied Polymer Science*, 1986, **32**, 4, 4607.

98. A.S. Brar, G.S. Kapur and S.K. Dubey, *European Polymer Journal*, 1988, **24**, 8, 807.

99. A.S. Brar and G.S. Kapur, *Polymer Journal Japan*, 1988, **20**, 9, 811.

100. A.S. Brar, E. Arunan and G.S. Kapur, *Polymer Journal (Japan)*, 1989, **21**, 9, 689.

101. J.C.J.F. Tacx, G.P.M. Van Der Velden and A.L. German, *Journal of Polymer Science Part A: Polymer Chemistry*, 1988, **26**, 5, 1439.

102. J.C.J.F. Tacx, G.P.M. van der Velden and A.L. German, *Polymer*, 1988, **29**, 9, 1675.

103. G.H.J. van Doremaele, A.L. German N.K. De Vries and G.P.M. van der Valden, *Macromolecules*, 1990, **23**, 19, 4206.

104. D. Murray and I. Piirma, *International Polymer Colloid Group Newsletter*, September 1991.

105. S. Wong and G.W. Poehlein, *Journal of Applied Polymer Science*, 1993, **49**, 6, 991.

106. J.L. Koenig, *Chemical Microstructure of Polymer Chains*, John Wiley and Sons,New York, NY, USA, 1980.

107. J.C. Tacx, *Microstructural investigation of copolymers: a key in revealing relations between polymerization conditions and polymer properties*, University of Eindhoven, The Netherlands, 1986. [PhD Thesis]

108. H.J. Harwood in *NMR Principles and Progress, Volume 4, Natural and Synthetic High Polymers*, Eds., P. Diehl, E.Fluck and R. Kosfeld, Springer Verlag, Berlin, Germany, 1970.

109. C. Pichot, M-F. Llauro and Q-T. Pham, *Journal of Polymer Science: Polymer Chemistry Edition*, 1981, **19**, 10, 2619.

110. V.B.F. Mathot and M.F.J. Pijpers, *Polymer Bulletin*, 1984, **11**, 3, 297.

111. M. Hirooka and T. Kato, *Journal of Polymer Science: Polymer Letters Edition,* 1974, **12,** 1, 31.

112. M. Nomura, U.S. Satpathy, Y. Kouno and K. Fujita, *Journal of Polymer Science Part C: Polymer Letters Edition*, 1988, **26**, 9, 385.

113. G.H.J. van Doremaele, A.M. van Herk, J.L. Ammerdorffer and A.L. German, *Polymer Communications*, 1988, **29**, 10, 299.

114. J. San Román, E.L. Madruga and M.A. Del Puerto, *Angewandte Makromolekulare Chemie*, 1979, **78**, 1, 129.

115. J.C.J.F. Tacx, G.P.M. van der Velden and A.L. German, *Journal of Polymer Science: Polymer Chemistry Edition*, 1988, **26**, 7, 1439.

116. Y. Yamashita and K. Ito, *Applied Polymer Symposium*, 1969, **8**, 245.

117. Emulsion Polymers and Elumsion Polymerisation, Eds., J.E. Johnson, D.R. Bassett and T.B. MacRury, ACS Symposium Series No.165, ACS, Washington, DC, USA, 1981.

118. M.F. Llauro-Darricades, C. Pichot, J. Guillot, L.G. Rios, M.A.E. Cruz and C. Guzman, *Polymer*, 1986, **27**, 6, 889.

119. M-F. Llauro, R. Spitz, C. Pichot and S. Nishida, *Journal of Macromolecular Science Part A: Pure and Applied Chemistry*, 1983, **19**, 6, 881.

120. H. Hirai, H. Koinuma, T. Tanabe and K. Takeuchi, *Journal of Polymer Science: Polymer Chemistry Edition*, 1979, **17**, 5, 1339.

121. Y. Inoue, A. Nishioka and R. Chujo, *Polymer Journal (Japan)*, 1971, 2, 4, 535.

122. Sharon A. Heffner, Frank A. Bovey, Lisa M. Verge, Peter A. Mirau, and A. E. Tonelli, *Macromolecules*, 1986, **19**, 6, 1628.

123. K. Ito and Y. Yamashita *Journal of Polymer Science Part B: Polymer Letters Edition*, 1965, **3**, 8, 637.

124. H. Koinuma, T. Tanabe and H. Hirai, *Die Makromolekulare Chemie*, 1980, **181**, 2, 383.

125. T. Tanabe, H. Koinuma and H. Hirai, *Die Makromolekulare Chemie*, 1980, **181**, 4, 931.

126. T. Tanabe, H. Koinuma and H. Hirai, *Journal of Polymer Science: Polymer Chemistry Edition*, 1981, **19**, 12, 3293.

127. S. Jayanthi and K. Kishore, *Macromolecules*, 1993, **26**, 8, 1985.

128. Q. Xu and H.L. Frisch, *Journal of Polymer Science Part A: Polymer Chemistry Edition*, 1994, **32**, 15, 2803.

129. S.H. Kandil and M.A. El-Gamal, *Journal of Polymer Science Part A: Polymer Chemistry*, 1986, **24**, 11, 2765.

130. H. Koinuma, T. Tanabe and H. Hirai, *Macromolecules*, 1981, **14**, 3, 883.

131. M.K. Niknam, *^{1}H and ^{13}C-NMR) studies of copolymers of aromatic monomers with acrylate and methacrylate esters*, University of Akron, OH, USA, 1985. [PhD Thesis]

132. H. Kessler, C. Griesinger, J. Zarbock and H.R. Loosli, *Journal of Magnetic Resonance*, 1984, **57**, 2, 331.

133. S.A. Heffner, F.A. Bovey, L.M. Verge, P.A. Mirau and A.E. Tonelli, *Macromolecules*, 1986, **19**, 6, 1628.

134. J. Guillot in *Polymer Reacton Engineering*, Eds., K-H. Reichert and W. Geisler, Huthig and Wepf Verlag, Basel, Switzerland, 1989.

135. A.S. Brar and Sunita, *Die Makromolekulare Chemie*, 1993, **194**, 6, 1707.

136. A.M. Aerdts, J.W. De Haan, A.L. German, and G.P.M. Van der Velden, *Macromolecules*, 1991, **24**, 7, 1473.

137. A.R. Katritzky, A. Smith and D.E. Weiss, *Journal of the Chemical Society, Perkin Transactions*, 1974, **2**, 13, 1547.

138. Y.K. Kato, I. Ando and A. Nishioka, *Nippon Kagaku Kaishi*, 1975, 501.

139. H. Hirai, *Journal of Polymer Science: Macromolecular Reviews*, 1976, **11**, 47.

140. A.E. Tonelli in *NMR Spectroscopy and Polymer Microstructure: The Conformational Connection*, VCH Publishers, Inc., New York, NY, USA, 1989.

141. A.M. Aerdts, J.W. de Haan and A.L. German, *Macromolecules*, 1993, **26**, 8, 1965.

142. Y. Inoue, A. Nishioka and R. Chûjô, *Die Makromolekulare Chemie*, 1972, **156**, 1, 207.

143. H.J. Harwood and W.M. Ritchey, *Journal of Polymer Science Part B: Polymer Letters Edition*, 1965, **3**, 5, 419.

144. F.C-Y. Wang and P.B. Smith, *Analytical Chemistry*, 1996, **68**, 17, 3033.

145. F.C-Y. Wang and P.B. Smith, *Analytical Chemistry*, 1996, **68**, 3, 425.

146. H.L. Frisch and Q. Xu, *Macromolecules*, 1992, **25**, 20, 5145.

147. *NMR Principles and Progress*, *Volume 4*, *Natural and Synthetic High Polymers*, Eds., P. Diehl, E. Fluck and R. Kosfeld, Springer, Berlin, Germany, 1971, p.47-69.

148. I. Lüderwold and O. Vogl, *Die Makromolekulare Chemie*, 1979, **180**, 10, 2295.

149. Y. Sugimura, T. Nagaya and S. Tsuge, *Macromolecules*, 1981, **14**, 3, 520.

150. H.L. Frisch and Q. Xu, private communication.

151. J. Kríz, B. Masar and P. Vlcek, *Die Makromolekulare Chemie*, 1993, **194**, 5, 1435.

152. J. San Román and M. Valero, *Polymer*, 1990, **31**, 7, 1216.

153. M.M.C. López-González, M. Fernández-García, J.M. Barrales-Rienda, E.L. Madruga and C. Arias, *Polymer*, 1993, **34**, 14, 3123.

154. T. Kitayama, K. Ute, M. Yamamoto, N. Fujimoto and K. Hatada, *Polymer Bulletin*, 1992, **25**, 6, 683.

155. A. Gallardo and J. San Román, *Polymer*, 1994, **35**, 12, 2501.

156. H.J. Harwood, *Angewandte Chemie International Edition in English*, 1965, **4**, 12, 1051.

157. K. Yokota and T. Hirabayashi, *Journal of Polymer Science: Polymer Chemistry Edition*, 1976, **14**, 1, 57.

158. J. Schaefer, *Macromolecules*, 1971, **4**, 1, 107.

159. E.O. Stejskal and J. Schaefer, *Macromolecules*, 1974, 7, 1, 14.

160. C. Pichot and Q-T. Pham, *Die Makromolekulare Chemie*, 1979, **180**, 10, 2359.

161. J. San Roman, B. Vazquez, M. Valero and G.M. Guzman, *Macromolecules*, 1991, **24**, 23, 6089.

162. R.C. Chang and H.J. Harwood, *Polymer Preprints*, 1973, **14**, 1, 31.

163. R.C. Chang and H.J. Harwood, *Polymer Preprints*, 1973, **12**, 2, 338.

164. M. Murano K. Shimizu and H.J. Harwood, *Polymer Preprints*, 1969, **10**, 193.

165. P.K. Dhal and A. Steigel, *Polymer*, 1991, **32**, 4, 721.

166. Y. Inoue, K. Koyama, R. Chûjô and A. Nishioka, *Journal of Polymer Science: Polymer Letters Edition*, 1973, **11**, 1, 55.

167. L. Dong and D.J.T. Hill, *Polymer Bulletin*, 1995, **34**, 3, 323.

168. K. Beshah, *Macromolecules*, 1992, **25**, 21, 5597.

169. Z. Florjanczyk and B. Skórkiewicz, *Journal of Polymer Science Part A: Polymer Chemistry Edition*, 1989, **27**, 5, 1559.

170. A.S. Brar and S. Charan, *Journal of Applied Polymer Science*, 1994, **53**, 13, 1813.

171. H.J. Harwood, *Journal of Polymer Science Part C: Polymer Symposia,* 1968, **25**, 1, 37.

172. T. Kelen and F. Tüdos, *Journal of Macromolecular Science Chemistry Part A Pure and Applied Chemistry*, 1975, **9**, 1, 1.

173. M.J. Box, *Technometrics*, 1970, **12**, 2, 219.

174. M. Dube, R.A. Sanayei, A. Penlidis, K.F. O'Driscoll and P.M. Reilly, *Journal of Polymer Science Part A: Polymer Chemistry Edition*, 1991, **29**, 5, 703.

175. A.S. Brar and Sunita, *European Polymer Journal*, 1991, **27**, 1, 17.

176. B. Subrahmanyam, S.D. Baruah, M. Rahman, J.N. Baruah and N.N. Dass, *Journal of Polymer Science Part A: Polymer Chemistry Edition*, 1992, **30**, 10, 2273.

177. G.S. Kapur and A.S. Brar, *Die Makromolekulare Chemie*, 1992, **193**, 7, 1773.

178. M. Sawamoto, T. Hasebe, M. Kamigaito and T. Higashimura, *Journal of Macromolecular Science Chemistry Part A: Pure and Applied Chemistry*, 1994, **31**, 8, 937.

179. G.S. Kapur and A.S. Brar, *Journal of Polymer Science Part A: Polymer Chemistry*, 1991, **29**, 4, 479.

180. F.R. Mayo and F.M. Lewis, *Journal of the American Chemical Society*, 1944, **66**, 9, 1594.

181. T. Alfrey, Jr., and G. Goldfinger, *Journal of Chemical Physics*, 1944, **12**, 6, 205.

182. F.A. Bovey and G.V.D. Tiers, *Journal of Polymer Science*, 1969, **44**, 143, 173.

183. B.D. Coleman, *Journal of Polymer Science*, 1958, **31**, 122, 155.

184. A.S. Brar and A. Sunita *Journal of Polymer Science Part A: Polymer Chemistry Edition*, 1992, **30**, 12, 2549.

185. H. Patino-Leal, P.M. Reilly and K.F. O'Driscoll, *Journal of Polymer Science, Polymer Letters Edition*, 1980, **18**, 3, 219.

186. R. Van Der Meer, H.N. Linssen and A.L. German, *Journal of Polymer Science: Polymer Chemistry Edition*, 1978, **16**, 11, 2915.

187. K.F. O'Driscoll, L.T. Kale, L.H. Garcia Rubio and P.M. Reilly, *Journal of Polymer Science: Polymer Chemistry Edition*, 1984, **22**, 11, 2777.

188. A. S. Brar and A. Sunita, *Polymer*, 1993, **34**, 16, 3391.

189. K. Kamide, H. Yamazaki, K. Okajima and K. Hikichi, *Polymer Journal (Japan)*, 1985, **17**, 12, 1233.

190. T.A. Gerken and W.M. Ritchey, *Journal of Applied Polymer Science: Applied Polymer Symposia*, 1978, **34**, 17.

191. Q.T. Pham, *Nuclear Magnetic Resonance*, 1971, **4**, 119.

192. G.S. Kapur and A.S. Brar, *Polymer*, 1991, **32**, 6, 1112.

193. I.R. Peat and W.F. Reynolds, *Tetrahedron Letters*, 1972, **13**, 14, 1359.

194. J.P. Montheard, A. Mesli, A. Belfkira, M. Raihane and Q-T. Pham, *Macromolecular Reports*, 1994, **A31**, 1-2, 1.

195. A. Petit and J. Néel, *Journal of Applied Polymer Science*, 1990, **41**, 1-2, 267.

196. A.S. Brar and A. Sunita, *European Polymer Journal*, 1992, **28**, 7, 803.

197. A.S. Brar and S.K. Dubey, *Industrial Journal of Chemistry, Section A*, 1989, **28A**, 570.

198. G.S. Kapur and A.S. Brar, *Die Makromolekulare Chemie*, 1991, **192**, 11, 2733.

199. A.S. Brar and Sunita in *Polymer Science: Contemporary Themes, Volume II*, Ed., S. Sivaram, Symposium Proceeding of Polymers'91, Pune, India, 1991, p.582.

200. J.D. Barbely, D.J.T. Hill, A.P. Lang and J.H. O'Donnell, *Polymer International*, 1991, **26**, 3, 171.

201. M.R. Rao, T.V. Sebastian, T.S. Radhakrishnan and P.V. Ravindran, *Journal of Applied Polymer Science*, 1991, **42**, 3, 753.

202. G. Crone and A. Natansohn, *Journal of Polymer Science Part A: Polymer Chemistry*, 1992, **30**, 8, 1655.

203. C. Vu and J. Cabestany, *Journal of Applied Polymer Science*, 1991, **42**, 11, 2857.

204. Q.T. Pham, *Ann Composit*, 1985, **49**, 27.

205. S. Eonomoto, *Journal of Polymer Science Part A: Polymer Chemistry*, 1969, **7**, 1, 255.

206. Y. Inoue, K. Kawaguchi, Y. Maruyama, Y.S. Jo, R. Chûjô, I. Seo and M. Kishimoto, *Polymer*, 1989, **30**, 4, 698.

207. Y. Maruyama, Y.S. Jo, Y. Inoue, R. Chûjô, S. Tasaka and S. Miyata, *Polymer*, 1987, **28**, 7, 1087.

208. Y. Inoue, A. Kashiwazaki, Y. Maruyama, Y.S. Jo, R. Chûjô, I. Seo and M. Kishimoto, *Polymer*, 1988, **29**, 1, 144.

209. Y. Yamashita, T. Asakura, M. Okada and K. Ito, *Die Makromolekulare Chemie*, 1969, **129**, 1, 1.

210. D. Fleischer and R.C. Schulz, *Die Makromolekulare Chemie*, 1975, **176**, 3, 677.

211. T. Wada, S. Yahiro and H. Tamura, *Polymer Preprints, Japan*, 1992, **41**, 4310.

212. T. Ogawa, W. Ishitobi and K. Jinta, *Journal of Applied Polymer Science*, 1989, **38**, 1, 87.

213. Y. Ishida, H. Ohtani, K. Abe, S. Tsuge, K. Yamamoto and K. Katoh, *Macromolecules*, 1995, **28**, 19, 6528.

214. E.B. Whipple and P.J. Green, *Macromolecules*, 1973, **6**, 1, 38.

215. X-C. Chen, *Bopoxue Zazhi*, 1984, **1**, 409.

216. F. Halmo, L. Malik and T. Liptai, *Chem Prum*, 1986, **36**, 203.

217. F. Heatley, Y. Luo, J. Ding, R.H. Mobbs and C. Booth, *Macromolecules*, 1989, **21**, 9, 2713.

218. D.L. Rubenstein and T.T. Nakashima, *Analytical Chemistry*, 1979, **51**, 14651A.

219. Christian Le Cocq and Jean-Yves Lallemand, *Journal of the Chemical Society, Chemical Communications*, 1981, 4, 150.

220. S.L. Patt and J.N. Shoolery, *Journal of Magnetic Resonance*, 1982, **46**, 3, 535.

221. A.G. Ferrige and J.C. Lindon, *Journal of Magnetic Resonance*, 1978, **31**, 2, 337.

222. G.J. van Rooij, M.C. Duursma, C.G. de Koster, R.M.A. Heeren, J.J. Boon, P.J.W. Schuyl and E.R.E. van der Hage, *Analytical Chemistry*, 1998, **70**, 5, 843.

223. Z. Yang, F.E. Karasz and H.J. Geise, *Macromolecules*, 1993, **26**, 24, 6570.

224. F. Heatley, G-E. Yu, W-B. Sun, E.J. Pywell, R.H. Mobbs and C. Booth, *European Polymer Journal*, 1990, **26**, 5, 583.

225. M.A. Golub and R.J. Gargiulo, *Journal of Polymer Science*, *Polymer Letters Edition*, 1972, **10**, 1, 41.

226. D.W. Brazier and N.V. Schwartz *Journal of Applied Polymer Science*, 1978, **22**, 1, 113.

227. N. Grassie in *Developments in Polymer Degradation – 1*, Ed., N. Grassie, Applied Science, London, UK, 1977 p.137.

228. N. Grassie and J.N. Hay, *Journal of Polymer Science*, 1962, **56**, 163, 189.

229. H. Zhuang, J.A. Gardella, Jr., and D.M. Hercules, *Macromolecules*, 1997, **30**, 4, 1153.

230. H.W. Werner and A.E. Morgan, *Journal of Applied Physics*, 1976, **47**, 4, 1232.

231. H.W. Werner and N. Warmoltz, *Journal of Vacuum Science and Twchnology A*, 1984, **2**, 2, 726.

232. W. Reuter, M.L. Yu, M.A. Frisch and M.B. Small, *Journal of Applied Physics*, 1980, **51**, 2, 850.

233. D.W. Vance, *Journal of Applied Physics*, 1971, **42**, 13, 5430.

234. J.A. Gardella and D.M. Hercules, *Analytical Chemistry*, 1981, **53**, 12, 1879.

235. J.E. Campana, J.J. De Corpo and R.J. Colton, *Journal of Applied Surface Science*, 1981, **8**, 337.

236. D. Briggs, M.J. Hearn and B.D. Ratner, *SIA Surface Interface Analysis*, 1984, **6**, 4, 184.

237. P.A. Zimmerman, D.M. Hercules and A. Benninghoven, *Analytical Chemistry*, 1993, **65**, 8, 983.

238. X. Chen, J.A. Gardella, T. Ho and K.J. Wynne, *Macromolecules*, 1995, **28**, 5, 1635.

239. J.A. Gardella, T. Ho, K.J. Wynne and H-Z. Zhuang, *Journal of Colloid and Interface Science*, 1995, **176**, 1, 277.

240. T. Ho and K.J. Wynne, *Macromolecules*, 1996, **29**, 11, 3991.

241. R. Po, P. Cioni, L. Abis, E. Occhiello and F. Garbassi, *Polymer Communications*, 1991, **32**, 7, 208.

242. A. Bunn, *British Polymer Journal*, 1988, **20**, 4, 307.

243. J.P. Montheard, B. Boinon, M. Reihane and Q.T. Pham, *Polymer Communications*, 1991, **32**, 18, 567.

244. J.P. Monthéard, B. Boinon, A. Belfkira, M. Raihane and Q.T. Pham, *Die Makromolekulare Chemie*, 1993, **194**, 10, 2839.

245. I. Goodman and M.T. Rodríguez, *Macromolecular Chemistry and Physics*, 1994, **195**, 3, 1075.

246. Z. Wang, T. Chen and J. Xu, *Journal of Applied Polymer Science*, 1994, **51**, 9, 1533.

247. H.N. Cheng, *Macromolecules*, 1997, 30, 14, 4117.

248. H.N. Cheng, *International Journal of Polymer Analysis and Characterisation*, 1997, **4**, 171.

249. P.A. Curnuck and M.E.B. Jones, *British Polymer Journal*, 1973, **5**, 1, 21.

250. G. Montaudo, *Trends in Polymer Sciences*, 1996, **4**, 3, 81.

251. V.G. Zaikin, R.G. Mardanov, V.A. Yakovlev and N.A. Platé, *Journal of Analytical Applied Pyrolysis*, 1992, **23**, 1, 33.

252. G. Montaudo, *Polymer Science Symposium Proc Polymer*, 1991, **2**, 552.

253. G. Montaudo, *Polymer Preprints*, 1989, **30**, 341.

254. T. Isemura, Y. Jitsugiri and S. Yonemori, *Journal of Analytical Applied Pyrolysis,* 1995, **33**, 103.

255. T. Hammond and R.G. Lehrie, *British Polymer Journal*, 1989, **21**, 23.

256. H. Shirakawa, N. Yamagaki and S. Kambara, Personal Communication from Dr N Yamazaki, Tokyo Institute of Technology.

257. J. Kálal, M. Houska, O. Seycek and P. Adámek, *Die Makromolekulare Chemie*, 1973, **164**, 1, 249.

258. T.L. Arg and H.J. Harwood, *Journal of the American Chemical Society, Polymer Preprints*, 1964, **5**, 306.

259. K. Yaragisawa, *Chemistry of High Polymers (Tokyo)*, 1964, **21**, 312.

260. H. Germar, *Die Makromolekulare Chemie*, 1965, **84**, 1, 36.

261. J.J. Uebel and F.J. Dinan, *Journal of Polymer Science Polymer Chemistry*, 1983, **21**, 8, 2427.

262. C. Vu and J. Cabestany, *Journal of Applied Polymer Science*, 1991, **42**, 11, 2857.

8 Stereoisomerism and Tacticity

During polymerisation it is possible to direct the way in which isotactic monomers join on to a growing chain. This means that side-groups (X) may be placed randomly (atactic) or symmetrically along one side of the chain (isotactic) or in a regular alternating pattern along the chain (syndiotactic) as shown next.

Along with chemical composition, molecular weight, molecular weight distribution and type and amount of gel, branching is considered to be one of the fundamental parameters needed to characterise polymers fully, and this latter property, which is a microstructural feature of the polymer, has very important effects on polymer properties. Changes in branching of a given polymer such as polypropylene (PP) lead to changes in its stereochemical configuration and this, in turn, is a fundamental polymer property to formulating both polymer physical characteristics and mechanical behaviour. Technically each methane carbon in a poly(1-olefin) is asymmetric.

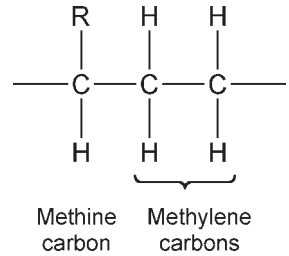

However, this symmetry cannot be observed because two of the attached groups are essentially equivalent for long chains. Thus a specific polymer unit configuration can be converted into its opposite configuration by simple end-to-end rotation and subsequent translation. It is possible, however, to specify relative configurational differences, and Natta introduced the terms 'isotactic' to describe adjacent units with the same configurations, and 'syndiotactic' to describe adjacent units with opposite configurations [1]. Tacticity is defined as the ratio of syndiotactic to isotactic structure. Although originally used to describe diad configurations, 'isotactic' now describes a polymer sequence of any number of like configurations and 'syndiotactic' describes any number of alternating configurations. Diad configurations are called meso if they are alike and racemic if they are unalike [2]. Thus from a configurational standpoint, a poly(1-olefin) can be viewed as a copolymer of meso and reacemic diads.

8.1 Tacticity of Polypropylene

An interesting aspect of the PP chain structure is the existence of distinct configurational isomers resulting from the presence of a *pseudo* asymmetric carbon atom. The actual polymer stereogularity or tacticity, as it is termed, is quite variable, being dependent on the nature of the catalyst, the presence or absence of additives, and other parameters such as temperature or reaction medium. Since the polymer morphology and hence physical properties are crucially dependent on the tacticity of the PP, the measurement of these properties is of considerable importance both in commercial production and fundamental investigations.

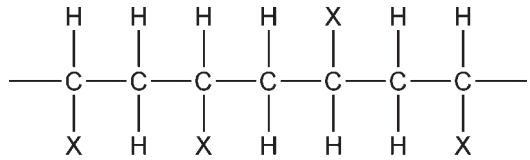

Atactic

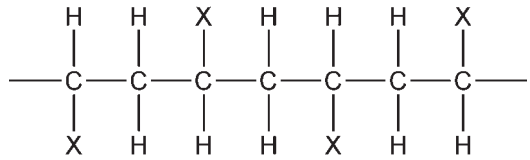

Syndiotactic

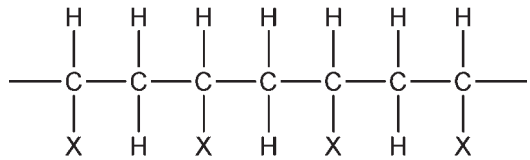

Isotactic

Three-dimensionally, atactic (aPP), and isotactic PP (iPP) may be represented as shown in **Figure 8.1**. Multiple sequences of syndiotactic or isotactic units can exist in PP. Thus diad and triad of iPP would have the structures:

Diad

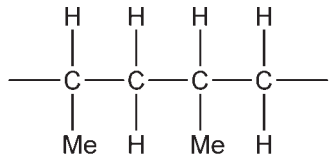

Triad

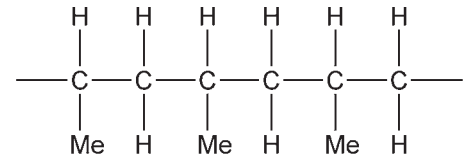

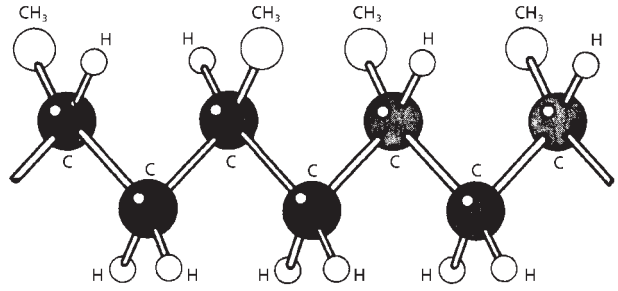

(a) Atactic polypropylene

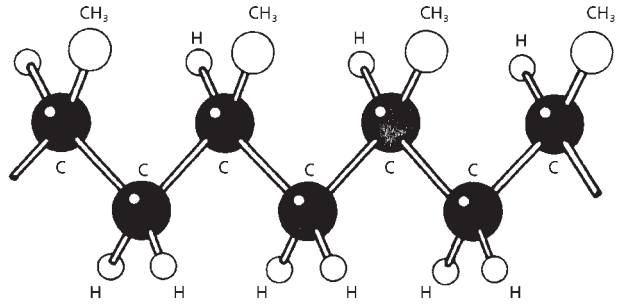

(b) Isotactic polypropylene

Figure 8.1 Polypropylene structures. (*From Author's own files*)

Similarly, a pentad and hexad of syndiotactic PP (sPP) would have the structures:

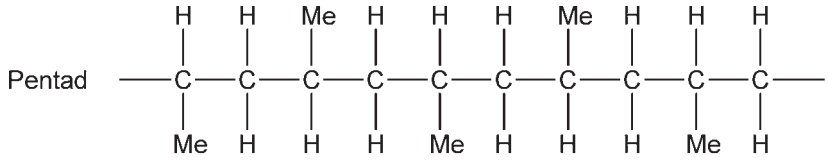

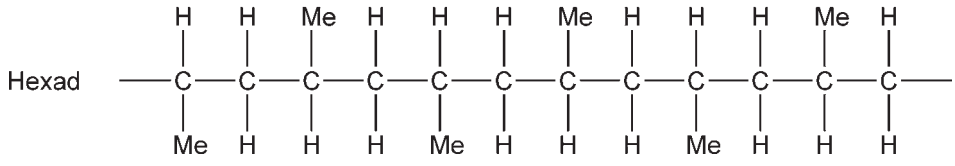

As well as this the monomer units in a polymer can exist in head to head, head to tail and tial to tail configurations as illustrated below in the case of iPP (discussed later under regioisomerism, Chapter 9).

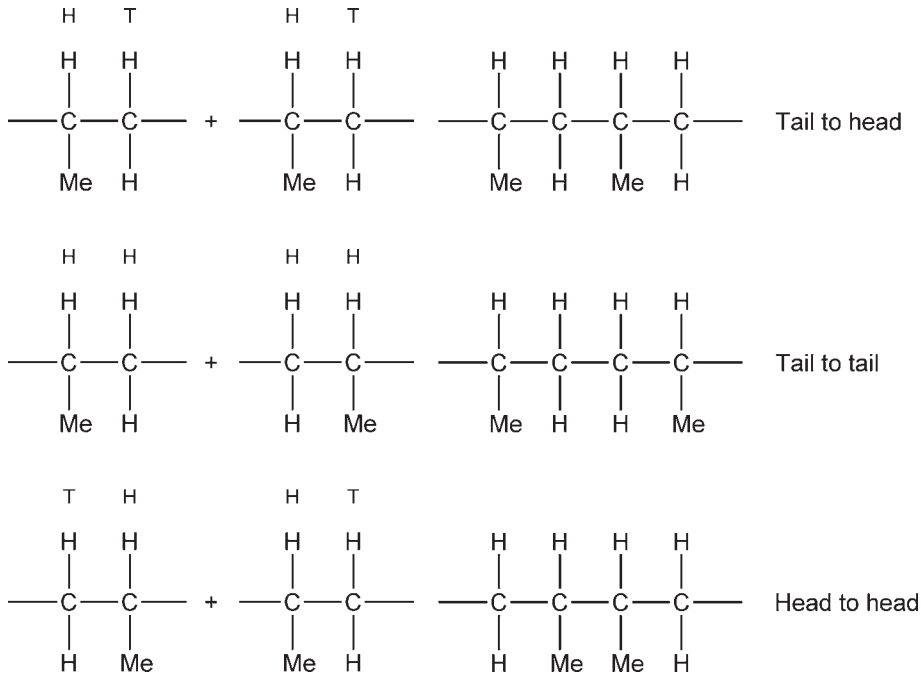

Processes for the manufacture of ethylene-propylene copolymer can produce several distinct types of polymer which, although they may contain similar proportions of the two monomer units, differ appreciably in their physical properties. The differences in these properties lie not only in the ratio of the two monomers present but also, and very importantly, in the detailed microstructure of the two monomer units in the polymer molecule. Ethylene-propylene copolymers might consist of mixtures of the following types of polymer:

(i) Physical mixture of ethylene homopolymer and propylene copolymer:

E-E-E-E-E- P-P-P-P

(ii) Copolymers in which the propylene is blocked, for example:

E-E-P-P-P-P-P-E-E-E-E-E-E-P-P-P-

(iii) Copolymers in which the propylene is randomly distributed, for example:

-E-P-E-P-E-P-E-P (alternating e.g., pure *cis*-1,4-polyisoprene) or

-E-E-E-P-E-E-E-E-E-P-E-E-E-E

(iv) Copolymers containing random (or alternating) segments together with blocks along the chains, i.e., mixtures of (iii) and (ii) (random and block) or (iii) and (ii) (alternating and block), for example:

-E-P-E-P-E-P-

(v) Containing tail-to-tail propylene units in propylene blocks:

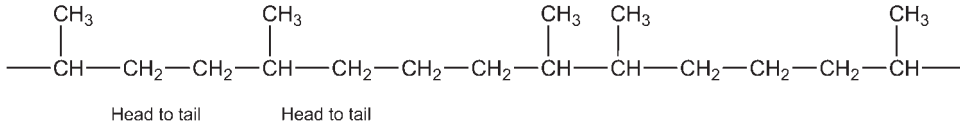

i.e., head-to-head and tail-to-tail addition giving even-numbered sequences of methylene groups.

(vi) Graft copolymers

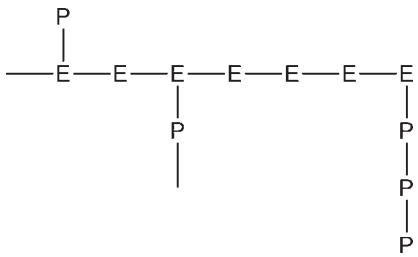

Although molecular symmetry is well understood, until the development of proton NMR (pNMR), and later ^{13}C-NMR, a study of this aspect of polymer structure presented problems.

The advantages of ^{13}C-NMR in measurements of polymer stereochemical configuration arise primarily from a useful chemical shift range which is approximately 20 times that obtained by pNMR. The structural sensitivity is enhanced through an existence of well-separated resonances for different types of carbon atoms. Overlap is generally not a limiting problem. The low natural abundance (<-1%) of ^{13}C nuclei is another favourable contributing factor. Spin-spin interactions among ^{13}C nuclei can be safely neglected, and proton interactions can be eliminated entirely through heteronuclear decoupling. Thus each resonance in a ^{13}C-NMR spectrum represents the carbon chemical shift of a particular polymer moiety. In this respect, ^{13}C-NMR resembles mass spectrometry because each signal represents some fragment of the whole polymer molecule. Finally, carbon chemical shifts are well behaved from an analytical viewpoint because each can be dissected, in a strictly additive manner, into contributions from neighbouring

carbon atoms and constituents. This additive behaviour led to the Grant and Paul rules [3], which have been carefully applied in polymer analyses, for predicting alkane carbon chemical shifts.

The advantages so clearly evident when applying ^{13}C-NMR to polymer configurational analyses are not devoid of difficulties. The sensitivity of ^{13}C-NMR to subtle changes in molecular structure creates a wealth of chemical shift-structural information which must be 'sorted out'. Extensive assignments are required because the chemical shifts relate to sequences from three to seven units in length. Model compounds, which are often used in ^{13}C-NMR analyses, must be very close structurally to the polymer moiety reproduced. For this reason, appropriate model compounds are difficult to obtain. A model compound found useful in PP configurational assignments was heptamethylheptadecane, where the relative configurations were known [4]. To be completely accurate, the model compounds should reproduce the conformational as well as the configurational polymer structure. Thus, reference polymers such as predominantly isotactic and syndiotactic polymers form the best model systems. Even when available, only two assignments are obtained from these particular polymers. Pure reference polymers can be used to generate other assignments [5].

To obtain good quantitative ^{13}C-NMR data one must understand the dynamic characteristics of the polymer being studied. Fourier transform techniques, combined with signal averaging, are normally used to obtain ^{13}C-NMR spectra. Equilibrium conditions must be established during signal averaging to ensure that the experimental conditions have not led to distorted spectral information. The nuclear Overhauser effect (NOE), which arises from ^{1}H, ^{13}C heteronuclear decoupling during data acquisition, must also be considered.

Energy transfer, occurring between the ^{1}H and ^{13}C nuclear energy levels during spin decoupling can lead to enhancements of the ^{13}C resonances by factors between 1 and 3. Thus the spectral relative intensities will only reflect the polymer's moiety concentrations if the differentiated NOE are equal or else taken into consideration. Experience has shown that polymer NOE are generally maximal, and consequently equal, because of a polymer's restricted mobility [6, 7]. To be sure, one should examine the polymers NOE through gated decoupling or paramagnetic quenching, and thereby avoid any misinterpretation of the spectral intensity data.

The ^{13}C configurational sensitivity falls within a range from triad to pentad for most vinyl polymers. In non-crystalline polypropylenes, three distinct regions corresponding to methylene (46 ppm), methine (28 ppm) and methyl (20 ppm) carbons are observed in the ^{13}C-NMR spectrum. (The chemical shifts are reported with respect to an internal tetramethylsilane (TMS) standard.) The ^{13}C spectrum of a 1,2,4-trichlorobenzene solution at 125 °C of a typical amorphous PP is shown in

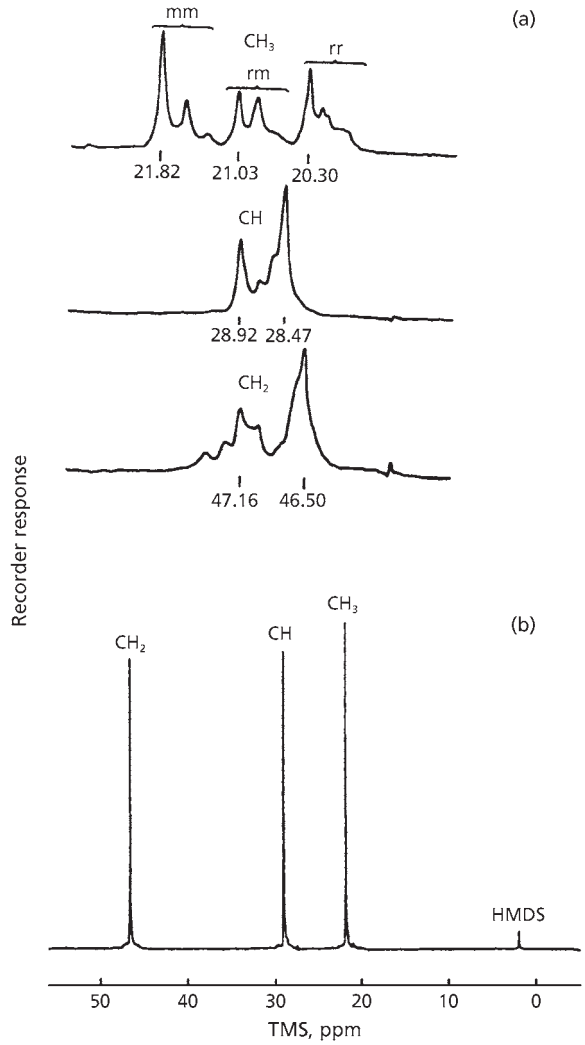

Figure 8.2 ^{13}C-NMR spectroscopy of polypropylene (a) methyl, methine and methylene regions of the ^{13}C-NMR spectrum of (a) non-crystalline polypropylene; (b) ^{13}C-NMR spectrum at 25.2 MHz of crystalline polypropylene. (*Source: Authors own files*)

Figure 8.2(a). Although a configurational sensitivity is shown by all three spectral regions, the methyl region exhibits by far the greatest sensitivity and is consequently of the most value. At least ten resonances assigned to the unique pentad sequences, are observed in order: mmmm, mmmr, rmmr, mmrr, mmrm, rmrr, mrmr, rrr, rrrm and mrrm, from low to high field [3, 4, 8].

The ^{13}C-NMR spectrum of crystalline PP shown in **Figure 8.2(b)** contains only three lines which can be identified as methylene, methine and methyl from low to high field by off-resonance decoupling. An amorphous PP exhibits a ^{13}C spectrum which contains not only these three lines but additional resonances in each of the methyl, methane and methylene regions as shown in **Figure 8.2(a)**. The crystalline PP must therefore be characterised by a single type of configurational structure. In this case the crystalline PP structure is predominantly isotactic, thus the three lines in **Figure 8.2(b)** must result from some particular length of meso sequences. This sequence length information is not available from the spectrum of the crystalline polymer, but can be determined from a corresponding spectrum of the amorphous polymer. To do so one must examine the structural symmetry of each carbon atom to the various possible monomer sequences. Randall [9, 10] carried out a detailed study of the PP methyl group in triad and pentad configurational environments. **Figure 8.3** shows the proton magnetic resonance (PMR) spectrum of hot *n*-heptane solution of atactic PP containing up to 40% syndiotactic placement, and which by Natta's definition may be stereoblock [11]. The spectrum is inherently complex, as a first-order theoretical calculation, and this indicated the possibility of at least 15 peaks with considerable overlap between peaks, because differences in chemical shifts are about the same magnitude as the splitting due to spin-spin coupling.

The largest peak, at high field in **Figure 8.3(a)** represents pendant methyls in propylene units. It is characteristically split by the tertiary hydrogen. By area integration, about 20% of the nominal methyl proton peak is due to overlap of absorption from chain methylenes. This overlap is consistent with a reported syndiotactic triplet, two peaks of which are close to A and B in **Figure 8.3(a)** and a third peak which falls with the low field branch of the methyl split [6]. The absence of a strong singlet peak in the methylene range indicate the virtual absences of 'amorphous' polymer in the aPP shown in Figure 8.3(a), which could possibly be due to the head-to-head and tail-to-tail units. The low field peak represents the partial resolution of tertiary protons which are opposite the methyls on the hydrocarbon chain.

Figure 8.3(a) also shows a spectrum for an iPP, >95% isotactic by solubility (<5% soluble in boiling heptane). This spectrum has the same general character as the aPP. The important difference is a marked decrease of peak intensity in the chain methylene region. This decrease is caused by extensive splitting, and the difference in chemical shifts for the non-equivalent methylene hydrogens in isotactic environments. This is in accord with the studies [11] on deuterated polypropylenes, which indicated that much of isotactic methylene absorption is buried beneath the methyl and tertiary hydrogen peaks. The fractional area in the nominal methylene region of the spectrum is thus sensitive to the number of isotactic and syndiotactic diads, and therefore may be used as a measure of PP and linear polyethylene. The low field absorption in **Figure 8.3(b)**, characteristic of aromatic hydrogens, is due to the polymer solvent, diphenyl ether, which was used throughout. Polymer concentrations in solution can be readily calculated from the ratios of peak areas adjusted to the same sensitivity.

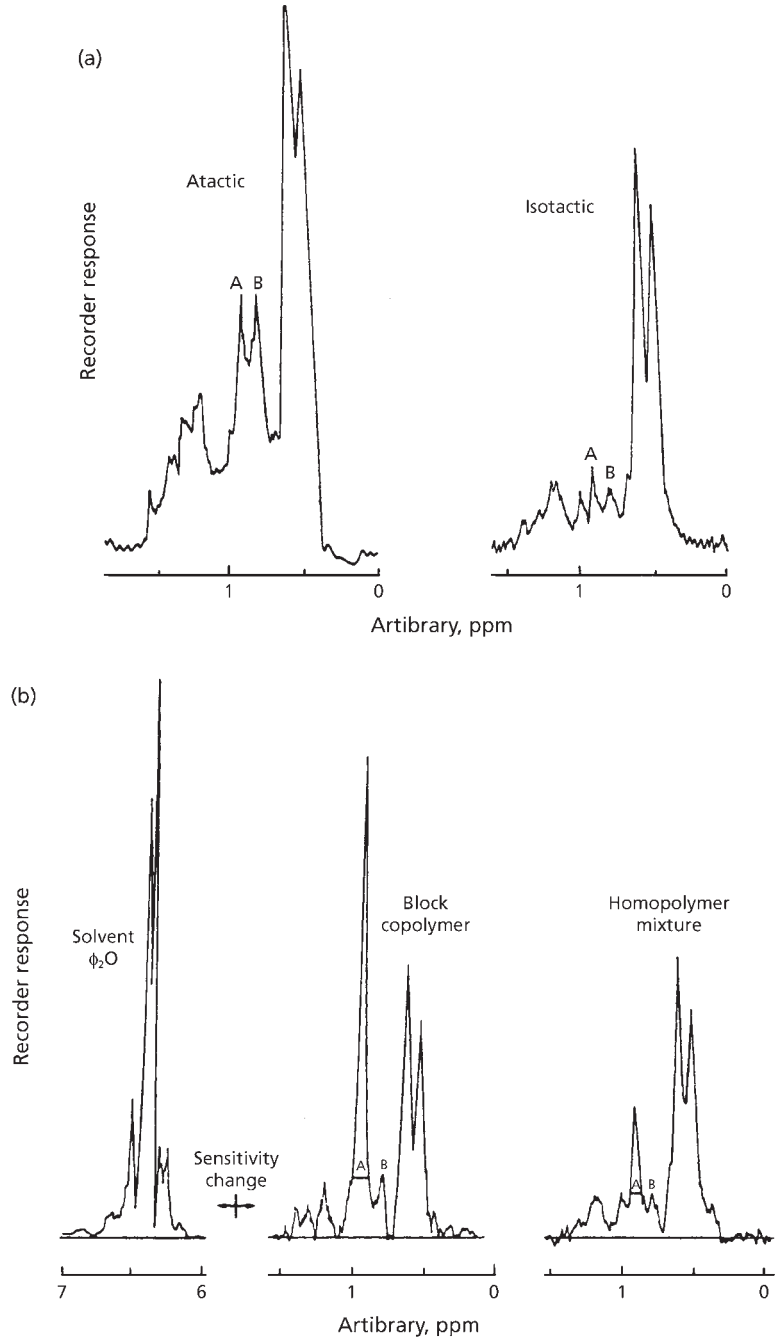

Figure 8.3 PMR spectra of: (a) polypropylenes; (b) ethylene-propylene copolymers. (*Reprinted from J.C. Randall, Journal of Polymer Science, Polymer Physics Edition, 1976,* ***1411****, 2083 [10]*)

The superpositions of spectra that were obtained separately on the homopolymers show the same pattern, with different intensities, as spectra on physical mixtures. The polyethylene absorption falls on the peak marked A of the chain methylene complex in polypropylene. Peak B, also due to chain methylenes in polypropylene, is resolved in both spectra in **Figure 8.3(b)** which also gives the spectrum of an ethylene-propylene block copolymer. The ethylene contribution again falls on peak A.

Various workers have developed analyses for physical mixtures and block copolymers based on the ratio of the incremental methylene area to the total polymer proton absorption. This concept has been tested by Barrall and co-workers [12–13] using PMR analyses on a series of physical mixtures and block copolymers synthesised with ^{14}C-labelled propylene and others with ^{14}C-labelled ethylene. A most important feature of this analysis is that the methylene peaks A and B have virtually the same relative heights in polypropylenes with a variety of tacticities (note **Figure 8.3(a)**). This is also true for PMR spectra given by Satoh and others for a tactic series of PP [14, 15]. This suggests that PMR analyses for ethylene are independent of tacticity, since the area increment of peak A above peak B has been used for analysis.

Quantitative PP tacticities can be estimated by PMR not only for homopolymers (**Figure 8.3 (a)**) but also in the presence of PE and ethylene copolymer blocks. The relative heights of the peaks for secondary and for tertiary hydrogen in **Figure 8.3(b)** indicate that the PP in the copolymer and the physical mixture is dominantly isotactic.

Barrall and co-workers [13] attempted to determine the syndiotactic content of some experimental PP. NMR spectra of samples dissolved in *o*-dichlorobenzene were obtained at 170 °C at 100 ppm. Spectra of syndiotactic and isotactic samples gave the NMR parameters in **Table 8.1**.

Table 8.1 NMR spectra of polypropylene at 170 ºC in *o*-dichlorobenzene syndiotactic and isotactic contents

	Syndiotactic	**Isotactic**
δCH_3	0.835 ppm	0.895 ppm
CH_2	1.075 ppm	1.895 and 1.310 ppm
δCH	1.570 ppm	1.615 ppm
$J_{CH_3\text{-}CH}$	6.0 cps	6.0 cps
$J_{CH\text{-}CH_2}$	6.0 cps	6.0 cps
$J_{H\text{-}H}$ (geminal)	Indeterminate	-14.0 cps

Reproduced with permission from E.M. Barrall II, R.S. Porter and J.F. Johnson, Journal of Applied Polymer Science, 1965, 9, 9, 3061. ©1965, John Wiley and Sons [13]

The reference for the chemical shift measurement was hexamethyl disiloxane. The methylene hydrogens in the isotactic material are nonequivalent - as expected on geometrical grounds. Spectra calculated with the above parameters agreed reasonably well with the observed spectra. High-resolution PMR spectroscopy has been applied to an examination of very highly isotactic, very highly syndiotactic, and stereoblock PP in *o*-dichlorobenzene solutions. Barrall and co-workers discuss the effects of stereoregulation on proton shieldings and some of the complexities of the methylene proton resonances and determine tactic placement contents for several polymers by a method based on the methylene proton resonances. Tactic pair contents were determined for two stereoblock fractions by a method based on the methyl proton resonances. Their results revealed much higher stereoblock characters than those determined for the same fractions from melting data. All the PMR results were in very good accord with the results obtained on several polymers by infrared, x-ray diffraction, and differential thermal analysis.

Stehling [16] defined the stereochemical structure of PP from the PMR spectrum of normal deuterated and epimerised PP.

To determine the isotactic content of PP, Peraldo [17] carried out a normal vibrational infrared analysis. He considered the primary unit as an isolated three-fold helix. From this work and a number of subsequent publications [18-20] it was suggested that the absorptions at 8.57, 10.02 and 11.90 μm were indicative of the helical conformation of the isotactic form. Measurements of the isotactic contents of a series of PP fractions based on these bands were made [20] and compared with results from Flory's melting point theory. Melting points were determined as the point of disappearance of the birefringence on highly annealed samples, all three bands give qualitative agreement with the melting point data, however, only the method based on the 8.57 μm band gives quantitative agreement. Therefore, the method based on this band appears to give a good measure of the isotactic content in PP at least in the 60-100% range.

Burfield and Lo [21] pointed out that although various methods have been developed over the years to measure the stereoregularity of PP [22-24] including: solvent extraction, IR spectrometry, X-ray diffraction, calorimetry and density measurements. All these techniques, provide only an indirect assay of stereoregularity since the parameters are actually measures relating to the crystallinity or conformational arrangement of the PP macromolecule and not tacticity *per se*.

A major breakthrough in PP characterisation was made possible with the application of high resolution ^{1}H and ^{13}C-NMR which allows the absolute determination of tacticity. These methods, which have been comprehensively reviewed [8, 9, 25], are of paramount importance since they permit not only quantification of tacticity but also elucidation of stereo-sequences. However, although NMR characterisation provides

the most fundamental information about stereostructure, secondary methods based on IR spectroscopy or solvent extraction are still very widely employed. The continuing use of these secondary methods is a direct consequence of simplicity, speed, and low equipment cost which are particularly important for routine or screening analysis.

Measurement by IR spectroscopy is potentially promising and semiquantitative evaluations are possible. IR methods suffer from two main drawbacks: the absence of suitable calibration and the problem of thermal history effects. The second limitation is the change induced in the infrared spectrum by thermal history effects. Thus, the IR bonds used to measure isotacticity are actually bonds sensitive to the formation of regular isotactic helices rather than isotacticity itself. As such the IR absorbance will be dependent on pretreatment and annealing which determine the conformation and morphology of the polymer chains.

IR spectroscopy has been widely used in the elucidation of PP stereostructure ever since Natta and co-workers [26-29] first reported the spectrum of the crystalline polymer. Most studies have concentrated on identifying suitable bands to measure tacticity and to correlate with other indices of stereoregularity. The bands apparently associated with isotactic helices absorb at 8.19, 8.56, 10.02, 11.11, 11.89, and 12.36 μm and of these the bands at 11.89 and 10.02 μm have been principally used for the derivation of calibration curves (**Figure 8.4**). Since it is difficult to prepare films of a standard thickness, it is customary to use an internal reference band and the absorptions at 6.85, 8.56, and 10.28 μm have been generally used for this purpose. It is perhaps worth noting that the origin of the reference band at 10.28 μm, which is observable both in the melt of isotactic samples [19, 30] as well as in purely atactic material is disputed [30]. Thus, the band, which has been attributed [30, 31] specifically to the PP head-to-tail sequence of repeating units, has also been associated with the presence of short isotactic helices apparently still present in the melt or atactic material [25].

The earliest study seeking to provide an IR calibration for isotacticity determination appears to be the work of Luongo [19] who indexed the ratio $A_{10.26}/A_{10.05}$ against physical mixtures of supposedly atactic and isotactic polymers. This calibration was later modified by an annealing procedure, initially in air [32] and subsequently under argon [33], the purpose of which was to ensure that all of the isotactic segments were converted to IR active isotactic helices. Hughes [33] suggested that for annealed highly stereoregular PP, the numerical value of the ratio $A_{10.25}/A_{10.26}$ was very close to the isotactic fraction (I). Subsequently, the most extensive studies relating to IR characterisation were carried out by Kissin and co-workers and much of this work has been summarised [24, 34, 35]. Essentially, three indices for measurement of isotacticity were proposed. These included the ratio $A_{10.02}/A_{10.28}$ earlier proposed by Luongo [19], which was now designated as the macrotacticity (M). Two further ratios: $A_{10.28}/A_{14.63}$ [known as the spectral degree of isotacticity (α)] and $A_{11.89}/A_{10.28}$

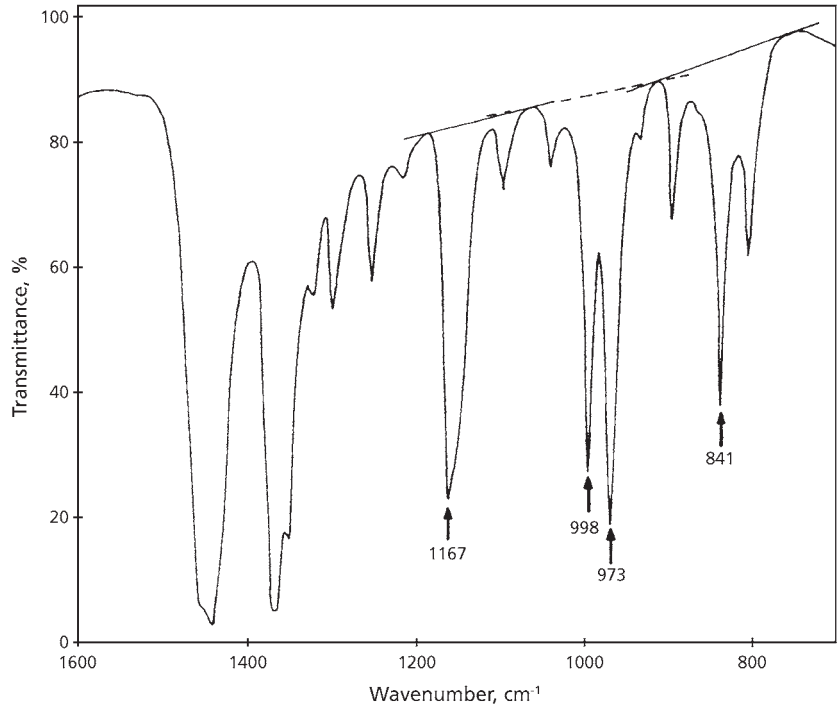

Figure 8.4 IR spectrum of isotactic (*mm* = 0.82) polypropylene in the 1600 cm^{-1} to 700 cm^{-1} region, showing positioning of measurement baselines.
(*Source: Authors own files*)

were also proposed [24]. The significance of utilising three distinct indices lies in the observation that the appearance of these helix bands is sensitive to the length of the isotactic sequences [27]. Thus the critical sequence lengths for the appearance of these bands are: 10.02 μm (11-12 units); 10.28 μm (5 units); 11.89 μm (13-15 units). The advantage claimed for using the 10.28 μm band is its sensitivity to even low levels of isotactic units and its apparent insensitivity to thermal history effects. However, the use of this band is complicated by the uncertainty of the assignment and the reduced sensitivity for highly isotactic polymers.

The quantitative measurements proposed by Kissin and co-workers [34] are based on calibration with supposedly completely isotactic samples and require the assumption that there is a linear relationship between the absorption ratios and isotacticity [36, 34]. Thus, for example, the degree of isotacticity α is given by the relationship [34]:

$$A = (A_{10.28}/A_{6.85}): N$$

N is a normalising factor obtained by calibration with a highly isotactic sample and is sensitive to instrument type. Values of *N* = 0.265 and 0.300 were observed for two different dispersive instruments.

It is quite clear from the previous discussion that none of the numerical values derived from the previous methods can be easily equated to numerical tacticity values determined by more fundamental NMR measurements. Furthermore, there are considerable uncertainties with respect to: sample pretreatment, instrument effects, and calibration standards. In light of these deficiencies Burfield and Lo [21] attempted to establish an empirical method based on an absolute NMR calibration, with standardised sample preparation methods and applicable to a wide range of instrumentation.

Four possible calibration curves of absorption ratio *versus* NMR tacticity were investigated for PP films hot pressed at 120-200 ºC and these are: the absorption at 10.02 μm referenced to bands at 10.28 μm or 8.57 μm and the absorption at 11.89 μm with the same reference bands, i.e., ratios $A_{10.02}/A_{10.28}$, $A_{10.02}/A_{8.57}$, $A_{11.89}/A_{10.28}$ and $A_{11.89}/A_{8.57}$, respectively. Burfield and Lo [21] use the 10.28 μm band as reference providing effective linear calibration curves for both ratios. However, calibrations based on the 8.57 μm reference are curves, the form of which provides rather low sensitivity in the important high isotacticity (mm > 0.8) region. Burfield and Lo [21] consider the 10.28 μm band as the most appropriate reference and consequently data for this band is described, i.e., the ratios $A_{11.89}/A_{10.28}$ (**Figure 8.5**) and $A_{10.02}/A_{10.22}$ (**Figure 8.6**). A further advantage of calibrations involving the 973 cm^{-1} reference is the possibility of representation as the simple linear equation:

$$\text{Absorbance ratio} = m(mn) + c$$

A direct comparison of results obtained by this method with those obtained with Luongo's [19] widely used calibration is shown in **Figure 8.7**. It is apparent that the agreement is rather poor if the % atactic values are compared against the NMR triad readings. However, if Luongo's atactic and isotactic samples are assigned values of *mm* = 0.35 and *mm* = 1.00, respectively, then a good agreement is obtained.

$$\text{Absorption ratio} = m \times 0.35 + c \text{ (for aPP), and Absorption ratio} = m + c \text{ (for iPP)}$$

Syndio and isotacticity studies have been conducted on PP manufactured by various processes. These included metallocene catalysed syndiotactic PP, Ziegler-Natta catalysed iPP and metallocene catalysed iPP [37, 38]. Structural differences between PP homopolymer and PP copolymers and their effect on polymer properties have been discussed [38, 39].

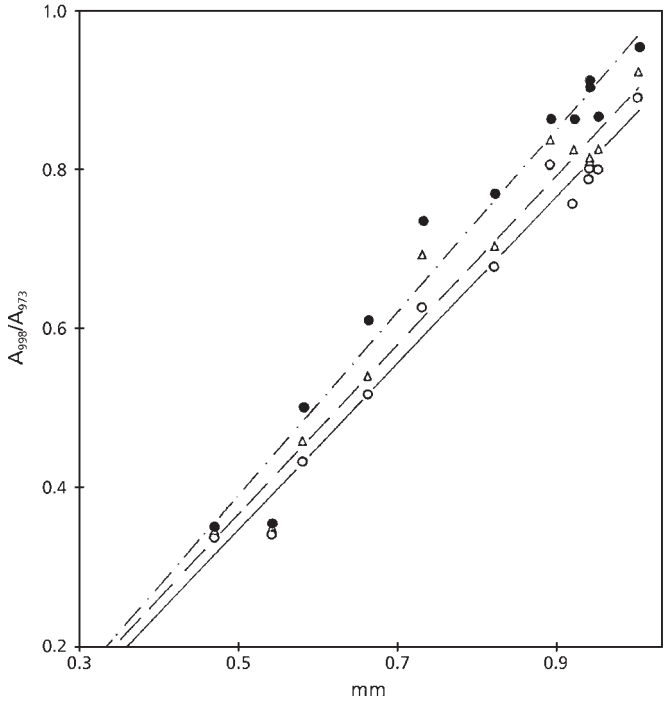

Figure 8.5 Calibration curve for IR absorbance ratio A_{998}/A_{973} *versus* NMR triad isotacticity. (•) High temperature annealed; (o) hot-pressed only; (Δ) ambient temperature annealed. (*Reproduced with permission from D.R. Burfield and P.S.T. Loi, Journal of Applied Polymer Science, 1988,* ***36****, 2, 279. ©1988, John Wiley and Sons [21]*)

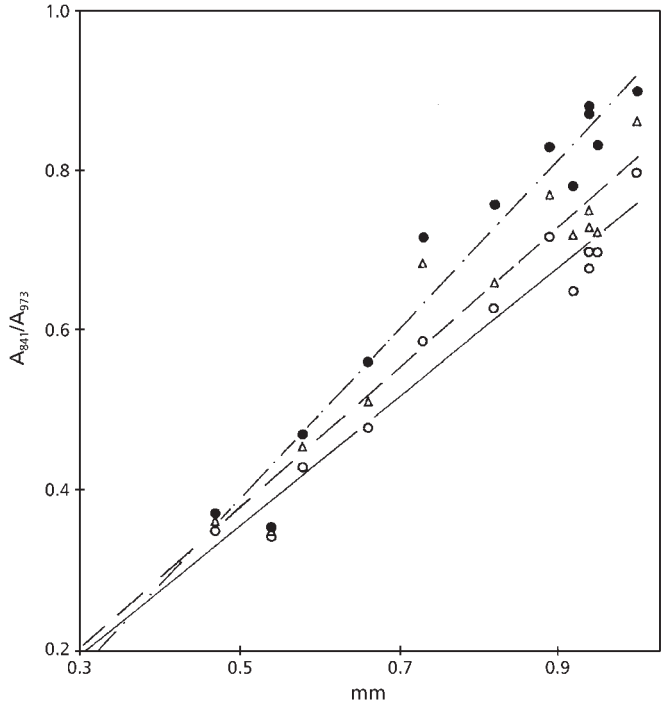

Figure 8.6 Calibration curve for IR absorbance ratio A841/A973 *versus* NMR triad isotacticity. (•) High temperature annealed; (o) hot pressed only; (Δ) ambient temperature annealed. (*Reproduced with permission from D.R. Burfield and P.S.T. Loi, Journal of Applied Polymer Science, 1988,* ***36****, 2, 279. ©1988, John Wiley and Sons [21]*)

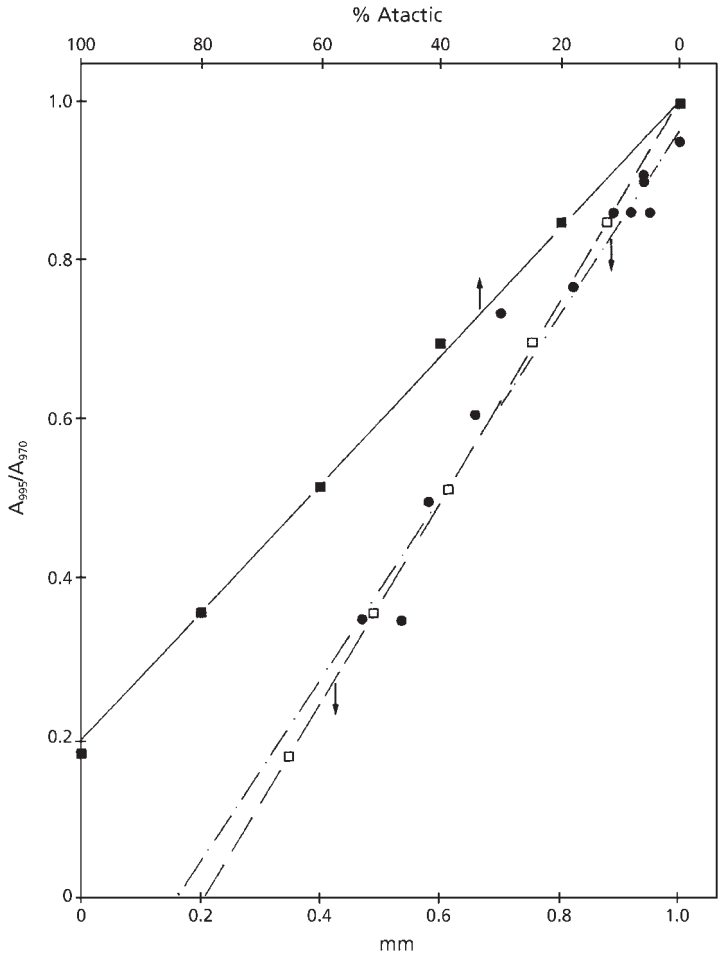

Figure 8.7 Comparison of present calibration data with literature results. (■) Original data from Luongo; (□) Luongo data recalculated using *mm* = 0.35 and *mm* = 1.00 for atactic and isotactic polymers; (•) this work, high temperature annealing. (*Reproduced with permission from D.R. Burfield and P.S.T. Loi, Journal of Applied Polymer Science, 1988, **36**, 2, 279. ©1988, John Wiley and Sons [21]*)

8.2 Tacticity of Syndiotactic Polystyrene

Fully syndiotactic polystyrene is a relatively recent discovery and polymers are now manufactured commercially. Only limited structural information is available [40-47]. It has four main crystalline polymorphic forms: α, β, γ and δ. The attractive and interesting physical characteristics of this polymer can be summarised as follows: (1)

a melting temperature of 270 °C, (2) a fully *trans* planar zig-zag backbone (α and β forms) and (3) the presence of a solid phase transition [40, 42-45].

Because of its inherent backbone stiffness and strong intermolecular interactions, the macroscopic properties such as modulus and strength are expected to exceed those of most polymers, even those of some liquid-crystalline polymers.

A variety of crystal forms have been suggested, including a helical conformation upon crystallisation from dilute solution and an all-*trans* conformation [42] with annealing. The helical phase has been proposed to have a TTGG or $T_3GT_3G^1$ conformation. Reynolds and co-workers [48] were interested in the nature of these crystalline forms and the amorphous state and the transition between them. They used vibrational spectroscopy as the primary characterisation technique. Its sensitivity to local conformation and chain packing changes allows them to observe microstructural changes with annealing, orientation, or solvent treatments and they examined structural differences between samples of different tacticities observed from their IR spectra and evidence is presented for the presence of two different conformational forms and the transition between them caused by thermal treatment or orientation.

The IR spectra of atactic polystyrene (aPS), isotactic polystyrene (iPS), and syndiotactic polystyrene (sPS) are shown in **Figure 8.8**. Large differences in both the IR and Raman data, related to the different chain conformations of these isomers, are observed, especially in the regions of 18.51, 10.33, 11.11, 9.34, and 8.33-7.14 μm.

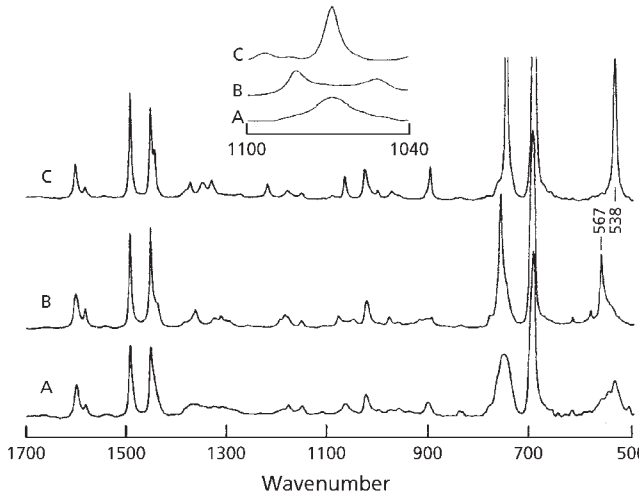

Figure 8.8 Infrared spectra of (A) atactic, (B) isotactic, and (C) syndiotactic polystyrene. (*Reprinted with permission from N.M. Reynolds, J.D. Savage and S.L. Hsu, Macromolecules, 1989,* **22**, *6, 2867. ©1989, ACS [48]*)

Reynolds and co-workers [48] also found that the vibrational spectra can be perturbed significantly by thermal annealing. The spectra obtained for the sPS generally contain bands that are sharp (approximately 6 cm^{-1} in half-width) as compared to the relatively broad features observed for both isotactic or atactic isomers. From the intensity decrease in the helical bands and the corresponding sharpening of the spectroscopic features observed upon annealing, these workers intended to show that annealed sPS is of high crystallinity and has a planar zigzag backbone conformation. One of the primary objectives was to seek explicit evidence of vibrations that can be assigned to the all-*trans* planar zigzag backbone.

In the 18.33-7.14 μm region, a number of conformation-sensitive skeletal vibrations exist. It is also quite likely that these bands are sensitive to chain packing. The IR spectrum of the cast film contains spectroscopic features that disappear when the sample temperature is raised. Some of the weak features (9.27, 9.21, and 9.60 μm) that are hard to observe at room temperature are seen quite clearly at liquid nitrogen temperature, and this is shown in the inset region in **Figure 8.9**. The intensity and position of these weak features are especially sensitive to thermal annealing. One of the more interesting features observed for sPS is the 9.71 μm band. This band, assignable to the combination of CH in-plane bending, CC ring stretching, and CCC

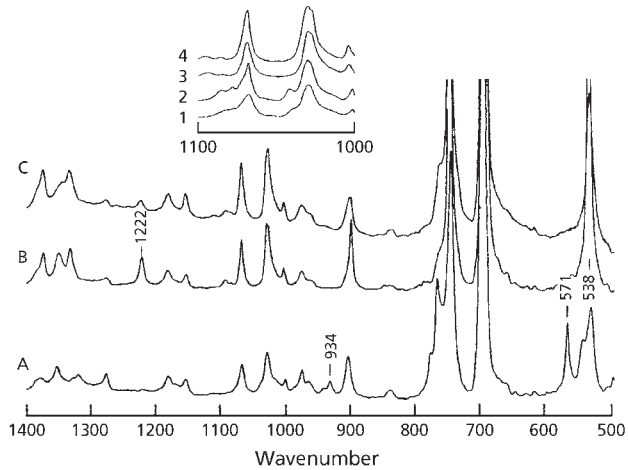

Figure 8.9 Infrared spectra of sPS (A) as cast, (B) after annealing at 295 °C for 0.5 h, and (C) coextruded at 100 °C to a draw ratio of 4; inset region (1) as cast, (2) at liquid nitrogen temperature, (3) annealed at 200 °C for 1 h, and (4) annealed at 200 °C and measured at liquid nitrogen temperature. (*Reprinted with permission from N.M. Reynolds, J.D. Savage and S.L. Hsu, Macromolecules, 1989,* **22***, 6, 2867. ©1989, ACS [48]*)

ring bending vibrations [49], seems to be sensitive to chain packing and clearly splits into two components at 9.71 and 9.72 μm at low temperature. A 9.35 μm band is present as a broad feature in the cast film. However, after annealing, the band sharpens but remains as a singlet even at low temperature. Two bands of medium intensity were observed in this region for iPS (9.50 and 9.23 μm). These bands, seen in the inset region in **Figure 8.8** were assigned previously to ring-backbone and ring CC stretching and to ring stretching and CH in-plane bending, respectively. In that case, they are thought to be associated with the sequence length of preferred conformations in the amorphous phase [49]. Reynolds and co-workers [48] conclude that both of these medium-intensity bands at 9.71 and 9.35 μm in sPS are crystalline in nature. Atactic PS has been shown to possess a significant amount of syndiotactic *trans* isomers [50]. Therefore the spectrum of sPS is expected to be more similar than that of iPS to that of aPS, and this is generally observed.

Reynolds and co-workers [48] assign the two bands at 10.60 and 10.79 μm to the helical conformation found for the cast sample and this is removed by annealing.

In the 500 cm^{-1} region, bands are observed at 17.51, 18.25, and 18.69 μm. After annealing at 200 °C, only a single band at 18.55 μm remains. In iPS a single band at 17.64 μm is observed and is assigned to the υ_{16b} skeletal out-of-plane mode of the aromatic ring [50, 51]. The sPS spectra in this region are consistent with studies of PS model compounds in which a 18.52 μm band is observed when at least four backbone carbons atoms are in a *trans* conformation, whereas a band at 18.05 μm is assigned to a second conformation containing gauche isomers [51]. Thus the 18.55 μm band of sPS is consistent with a syndiotactic all-*trans* structure, while the cast film exhibits a 18.25 μm band, indicating the presence of gauche conformers. Atactic PS exhibits a broad band at 18.48 μm, suggesting a broad conformation distribution. As shown in Figure 8.9, extrusion of a cast film at 100 °C produces spectral changes similar to those observed on annealing.

The drawing process would also transform the helical form present in the cast film to the more extended all-planar zigzag form, and this is observed. Bandwidths are broader for this oriented sample than for the annealed film, indicating that the thermal treatment produced greater structural regularity than extruding the sample to a draw ratio of four.

In conclusion, it is believed that IR spectra of sPS obtained under different crystallisation and thermal conditions are characteristic of the overall structural regularity and the specific chain conformations present. Spectra of samples cast from dilute solution are consistent with previous studies, suggesting a helical conformation. Heat treatment causes a transition to an all-*trans* phase. Long *trans* sequences can only be obtained by annealing or drawing.

More recently, Kellar and co-workers [52] have undertaken a detailed analysis of the Raman spectrum of sPS in the region 16.67 – 11.76 μm. As sPS exhibits considerable polymorphism, spectra of various preparations including melt-crystallised sPS, solvent crystallised sPS and quenched glassy materials, were studied. Peaks are assigned to conformational changes and sequences. The V_1 vibration of the phenyl ring (ring breathing mode) was shown to manifest itself through the presence of two peaks resulting from local conformational changes in the alkyl backbone. The peak centred at 12.94 μm is assigned to an all-*trans* backbone sequence whereas the higher frequency feature at 12.53 μm is attributed to mixed *trans*/gauche transformations.

Comparison with aPS is made. Study of the cross section of a compressed moulded plaque exhibiting a skin/core structure revealed the continuous way the structure varied with changing crystallinity. The various physical forms of sPS and the routes for interchange amongst them are shown diagramatically.

Analysis of the Raman data obtained by Keller and co-workers [52] and published literature enabled them to almost completely assign all the spectral features in this region of the sPS spectrum. The assignments are given in **Table 8.2**, using both Wilson and Hertzberg nomenclature, but in this discussion only the Wilson format is used. Six fundamental vibrational modes can be identified, υ_1, υ_{6b}, υ_{11}, υ_{10a}, υ_4, and β_{as} (CH_2) (by Wilson nomenclature). The first two are derived from in-plane vibrations of the phenyl ring and the rest from out of plane modes or backbone motions shown in **Figure 8.10**.

The spectral profile of the two polymers is very similar differing only with respect to the position and relative intensity of the peaks corresponding to the ν_1 vibration. It has been clearly demonstrated that the highly symmetric nature of the ν_1 vibration is sensitive to the conformation of the backbone and that of its immediate neighbors. For polystyrene, this is shown by the presence of two strong and highly polarised peaks. Previously published work on model compounds has shown that the lower frequency vibration is due to all-*trans* sequences (α/β crystal polymorphs) while the higher frequency peak results from a mixture of *trans* and gauche states. The latter can therefore be attributed to the amorphous component of sPS provided its position is not shifted to values >800 cm^{-1}, which is observed only when long ttg^+g^+ sequences are present resulting in a crystalline helical structure (γ/δ crystal polymorphs). The lower frequency peak at 770-773 cm^{-1} is observed to grow and narrow into an intense feature upon crystallisation. The presence of two ν_1 peaks for aPS reaffirms previous studies using other methods that there is a significant syndiotactic component present within the atactic polymer.

The continuity of these observed changes was demonstrated through analysis of a glassy skin/crystalline core sample. It has been shown that Raman spectroscopy can

Table 8.2 Vibrational assignments for syndiotactic polystyrene and model compounds within 600-800 cm^{-1} region of Raman spectrum[a]

Herzberg	ν_{18}	?		ν_8		ν_4	ν_2	ν_2		ν_{11a}
Wilson	ν_{6b}	?	$CHCl_3$	ν_4	ν_{10b} + ν_{16b}	ν_{11}	ν_1(tt …)	ν_1(t/g …)	$\beta_{as}(CH_2)$	ν_{10a}
Dimer (meso)[b]	623				740	760		780 (tg^+)		844
Dimer (racemic)[b]	623				740	765 sh	751	791 (g^-g^-)		843
Trimer (isotactic)[b]	623				740	763		787 (tg^+tg^+)		843
Trimer (heterotactic)[b]	623				740	763	750	781 (tg^+(tt), g^-t(tt), g^-tg^-)		843
Trimer (syndiotactic), liquid	623				740	763	763	789 ((tt^+)g^+g^+)		843
Trimer (syndiotactic), crystal	623				740	763	763			845
iPS	623				740	768		789 ($(tg^+)_n$)		844
aPS	623				740	762	763 (ttt?) 797 $((tt))_n$			846
sPS trans (crystal)[c]	622			703	740	756	773	796	811	841
sPS (glass)[c]	622	636		699	741	757	770	798	811	841
sPS, helical (crystal)[c]	622	636	670	702	745	758	772	802	812	840
aPS[c]	622			703	741	756	769	796	813	841

[a] *Note: dimer refers to 2,4-diphenylpentane and trimer refers to 2,4,6-triphenylheptane*

[b] *Data from B. Jasse, R.S. Chao andd J.L. Koenig, Journal of Raman Spectroscopy, 1979, 8, 244.*

[c] *Data obtained by Kellar and co-workers [52]*

ν_{18}, ν_8, ν_4, ν_2, ν_{11} *fundamental vibrational modes. Herzberg nomenclature*

ν_{6b}, ν_4, ν_{10b}, ν_{16b}, ν_{11}, ν_1(tt …), ν_1(t/g …), $\beta_{as}(CH_2)$ *and* ν_{10a} *= fundamental vibrational modes, Wilson Nomenclature.*

? vibrational assignment not made.

On Wilson Nomenclature ν_1, ν_{6b} *– derived from in-plane vibrations of phenyl ring,* ν_{11}, ν_{10a}, ν_4, *and* $\beta_{as}(CH_2)$ *derived from out of plane modes or backbone motions.*

t = trans form polymorph, g = gauche form polymorph

Reprinted with permission from E.J.C. Kellar, C. Galiotis and E.H. Andrews, Macromolecules, 1996, ***29****, 10, 3515. ©1996, ACS [52]*

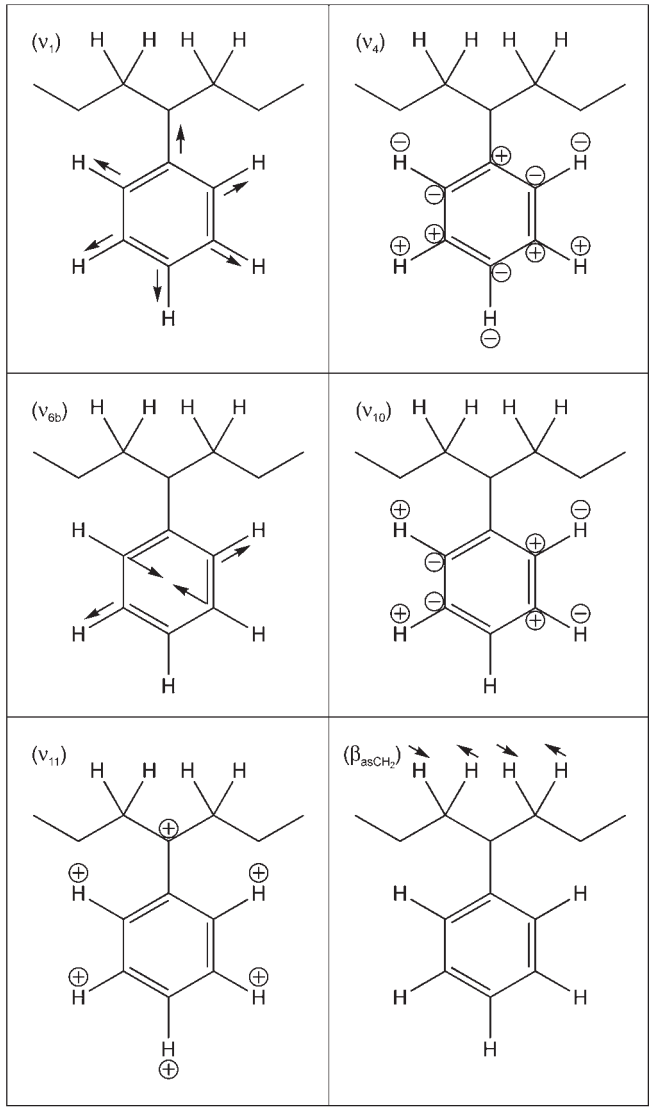

Figure 8.10 Normal vibrational modes of polystyrene present between 600 and 850 cm^{-1}. Symbols θ and ϕ denote motion into and out of the plane of the paper, respectively. (*Reprinted with permission from E.J.C. Kellar, C. Galiotis and E.H. Andrews, Macromolecules, 1996,* ***29****, 10, 3515. ©1996, ACS [52]*)

provide valuable information about the level of crystallinity [53, 54] together with the type of backbone conformation present within sPS samples. Study of a polished cross section by taking spectra at set intervals from skin to core underlines the power of this technique.

Reynolds and Hsu [55] have carried out a normal vibrational analysis of sPS comparing their calculated results with infrared and Raman spectra on drawn fully annealed samples (all-*trans* form). The calculated frequencies agree well with observed bands, and some features such as the 8.18 μm band are identified as being unique to the syndiotactic isomer. Large intensity changes are found for some features upon annealing and drawing, with peaks at 10.60, 10.70 (IR), and 12.5 (Raman) μm disappearing totally with such treatments. These peaks are also found to be absent from the calculated results of crystalline sPS (α/β form), thus providing good evidence that these features are not derived from all-*trans* conformations. A study was carried out by Nyquist and co-workers [56] comparing the vibrational spectra (Raman and IR) for sPS (all-*trans* and helical) with those of iPS, aPS, and toluene. From these comparisons they were able to make partial assignments for both of the sPS polymorphs. Some of the assignments suggested that the crystal structure of the all-*trans* polymorph may not be isomorphous with C_{2v} symmetry. These workers appear to make no distinction between the two known polymorphs which have the all-*trans* conformation. In a paper by Kobayashi and co-workers [57], a variety of techniques were used including Raman and IR spectroscopy to study the differences and transformation between the helical and all-*trans* forms of sPS. By comparing the crystalline samples, they observed a major difference in the 14.28–17.85 μm region of the Raman spectrum. For the all-*trans* material, a strong sharp peak was present at 12.99 μm together with a broad weaker feature at 12.58 μm, but in case of the helical crystal sample the strong broad feature at 12.53 μm now dominated a much weaker peak at 13.00 μm. The sharp 12.99 μm band was attributed to the presence of the all-*trans* conformation and the 12.53 μm feature to the presence of the gauche conformations.

Various other workers [47, 58] have used IR spectroscopy in syndiotactic studies on PS.

Isemura and co-workers [59] carried out stereoregularity studies on PS using pyrolysis-gas chromatography-mass spectrometry (Py-GC-MS). They detected tetramers and pentamers and found that the minimum requirement for a diastereoisomer is the inclusion of more than two asymmetric carbon atoms in the molecule.

Nonobe and co-workers [60] confirmed by the same technique that tetramers and pentamer peaks reflected the original tacticity of the polymer with good reproducibility. Other tacticity studies have been carried out on PS [61-66].

8.3 Tacticity of Polyvinylchloride

The study of stereochemical configuration by ^{13}C-NMR has not been limited to the polyolefins. Schneider and co-workers [67] showed that the absorption around 14.49 µm was proportional to the number of isotactic diads, and in the region of 16.66-15.62 µm to syndiotactic diads.

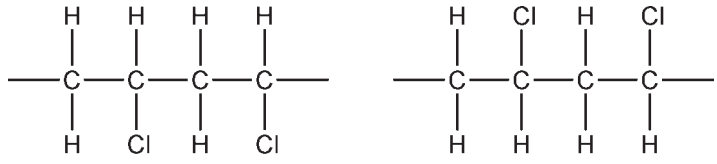

Based on this finding they proposed a method for determining the tacticity of amorphous samples of polyvinylchloride (PVC). As some samples cannot be easily transformed into an amorphous state Schneider and co-workers [68] devised an infrared method of tacticity determination which is independent of the crystallinity of the samples. From the temperature dependence of infrared spectra of PVC samples prepared by different methods, the intensity of the band at 14.40 µm (proportional to the number of isotactic diads in the sample), as well as that of the tacticity-independent C-H stretching band, was found to be independent of the crystallinity of the sample. These lines were applied for the tacticity determination in PVC, measured in the form of potassium bromide pellets. The numerical tacticity value was obtained from the known values of absorbance coefficients of S_{CH} and S_{HH} type C-Cl stretching bands in solution, and from the shape of the spectrum.

Abe and co-workers [69] have investigated the NMR spectra of model compounds of PVC in the hope that these investigations may offer useful information for the analysis of vinyl polymer spectra. They studied the NMR spectra of three stereoisomers of 2,4,6-trichloroheptane as model compounds of PVC:

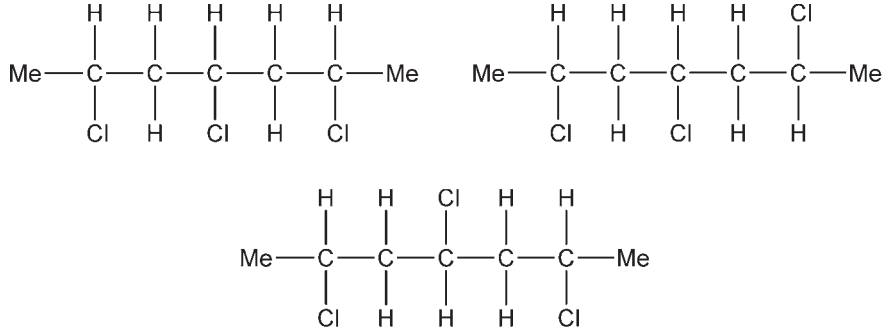

Spectra were observed at 60 and 100 ppm both at room temperature and at high temperatures and spin-decoupling experiments were performed. The difference of the chemical shifts of the two meso methylene protons at 60 ppm was found to be approximately 7 counts per second for the isotactic three unit model while it was approximately 16 counts per second for the isotactic two-unit model or heterotactic three-unit model. The spectra of PVC can be interpreted reasonably on the basis of this result. Observed values of vicinal coupling constants of model compounds were interpreted as the weighted means of those for several conformations, and the stable conformations of the models were determined.

Chemical shifts of PVC and model compounds such as meso- and racemic-2,4-dichloropentane have been measured from NMR spectra [70].

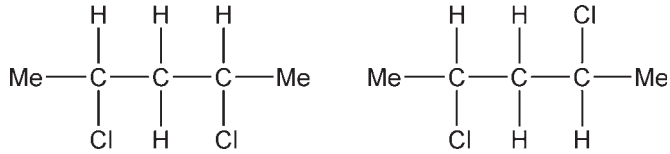

Nakayama and co-workers [71] have carried out a two-dimensional NMR characterisation study of PVC tacticity.

They proposed tetrad assignments of stereosequences in PVC on the basis of the carbon-carbon connectivities revealed on the two-dimensional incredible natural abundance double quantum transfer experiment (2D-INADEQUATE) spectrum. The validity of the proposed assignments was investigated by comparing the relative peak areas observed (based on the assignments by the 2D-INADEQUATE method with those calculated by the Bernoullian propagation model. Further, pentad assignments were provided, from the high-resolution doublet cross peaks in which the connectivities of centred methine carbons in pentads with centred methylene carbons in tetrads appear. Similarly, Bernoullian propagation statistics were used for the confirmation of the pentad assignments.

It is well-known that the polymerisation of vinyl chloride proceeds under the control of the Bernoullian statistical model (selection between meso and racemo). **Table 8.3** shows the comparison of the observed relative areas of methine pentad and methylene peaks with those calculated by Bernoullian propagation statistics. Relative areas of observed peaks are determined by the curve resolution method obtained. The relative areas of observed pentad peaks agree well with those calculated, indicating the validity of their pentad assignments by the method of Dong and co-workers [61]. As for the methylene peaks, observed areas (except peak 6′) agree well with those calculated. Assuming that the resonance of mmrmm overlaps peak 5′, the agreement of the observed and calculated areas of peak 6′ is improved. From the correlation

Table 8.3 Comparison of observed relative areas of methine and methylene peaks with those calculated by Bernoullian propagation statistics

Methine (CH)					Methylene (CH_2)				
Number	Observed pentad		Assignment	Calculated pentad	Number	Observed tetrad	Assignment	Calculated hexad	Calculated tetrad
1	0.07		mrrm	0.06	1′	0.15	rrr		0.16
2	0.15		mrrr	0.15	2′	0.15	rmr		0.14
3	0.08		rrrr	0.09	3′	0.27	mrr		0.27
4	0.07	0.24	Mmrm	0.23	4′	0.11	mmmrm mmmrr	0.05 0.06	0.11
5	0.18		mmrm mmrr		5′	0.14	rmmrm rmmrr	0.06 0.07	0.13
6	0.07	0.26	rmrm rmrm	0.27	6′	0.09	mmrmm mmrmr rmrmr	0.02 0.06 0.03	0.11
7	0.19		rmrr		7′	0.09	mmm	0.02 0.05 0.03	0.10
8	0.05		mmmm	0.04					
9	0.09		mmmr	0.10					
10	0.07		rmmr	0.06					

Reprinted with permission from N. Nakayama, A. Aoki and T. Hayashi, Macromolecules, 1994, 27, 1, 63. ©1994, ACS. [71]

Table 8.4 ^{13}C-NMR chemical shift assignments of PVC in 1,2,4-trichlorobenzene at 90 °C		
Chemical structure	**Chemical shift (ppm)**	**Assignment**
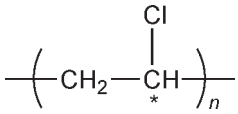	57.11	m<u>rr</u>m
	57.05	m<u>rr</u>r
	56.96	
	56.82	r<u>rr</u>r
	56.47	<u>mmr</u>m
	56.43	m<u>mr</u>m + m<u>mr</u>r
	56.22	r<u>mr</u>m
	56.04	r<u>mr</u>m + r<u>mr</u>r
	55.37	m<u>mm</u>m
	55.23	m<u>m</u>mr
	55.10	r<u>mm</u>r
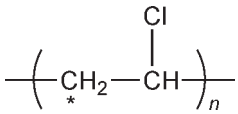	47.73	rrr
	47.29	rmr
	46.82	mrr
	46.27	m<u>mm</u>rm + m<u>mm</u>rr
	46.12	r<u>mm</u>rm + r<u>mm</u>rr + m<u>mrm</u>m
	46.04	m<u>mrm</u>m + r<u>mrm</u>r
	45.47	
	46.32	mmm
	45.18	
Reprinted with permission from N. Nakayama, A. Aoki and T. Hayashi, Macromolecules, 1994, 27, 1, 63. ©1994, ACS. [71]		

between methine peak of rmmr and methylene peak (peak 5′) of rmmrx (x = m or r), this overlap is plausible. It is impossible for the resonances of mmrmr and rmrmr to overlap peak 5′ because this hexad should include the pentad structure, rmmr. Consequently, tactic sequence assignments of PVC are proposed, as shown in **Table 8.4**. In the 1D spectrum of PVC (whole polymer), the peak with the assignment of mmr and mrm by 2D spin-lock relay experiment should be mmmrx (x = m or r) and the overlap of rmmrx (x = m or r) and mrm, respectively.

8.4 Tacticity of Poly(*n*-butyl Methacrylate)

Quinting and Cai [62] carried out high-resolution ^{13}C-NMR and pNMR measurements to determine the tacticity of poly(*n*-butyl methacrylate) (PBMA) with particular focus on the peak assignments for the *n*-butyl side chain. Both free radical and anionic PBMA were examined, with the former being predominantly syndiotactic and the latter isotactic. The pNMR resonances for the *n*-alkyl chain of these polyacrylics show a combination of effects from configurational sensitivity and homonuclear scalar interactions. A combination of *J*-resolved pNMR and proton-^{13}C-heteronuclear correlated 2-dimensional NMR spectra was used to characterise the long-range chemical shift effects due to tacticity.

The *n*-butyl side chain resonances in the high-resolution ^{1}H-NMR spectrum for PBMA at high temperature (100 °C) shows both the expected *J*-couplings from adjacent protons and the previously unreported chemical shift differences from monomer configurational effects. Both free radical and anionic PBMA showed the effect, with the former being predominantly syndiotactic and the latter isotactic. These results suggest that high-temperature and high-resolution ^{13}C- and ^{1}H-NMR spectra provide rich monomer tacticity information, which should often allow expanded use of proton NMR to study the tacticity of complex polymers.

Figure 8.11 shows the ^{13}C-NMR spectrum of syndiotactic PBMA (sample A) obtained at 100 °C in 1,2,4-trichlorobenzene. The resolution in the ^{13}C spectrum is high enough to reveal unexpected splittings of the side-chain methylene C_2' and methyl C_4' peaks. Especially striking is that the relative areas of the three peaks assigned to C_4' seemed to match the relative peak areas for the quaternary carbon: C_2. This observation leads to the suspicion that the splitting is perhaps due to previously unobserved long-range tacticity effects on chemical shift, seen not only in the carbon spectrum but also in the proton spectrum (*vide infra*). The side-chain C_1' and C_3' peaks do not show analogous fine splittings. The carbonyl carbon C_1 region of the spectrum reveals detailed pentad chemical shift sensitivity, while the backbone quaternary carbon C_2 peaks show the relative areas characteristic for a triad distribution. The peaks between 52 and 56 ppm show the diad and tetrad distributions for the β-methylene, C_3. One of the peaks for the methyl carbon (C_4) overlaps with the side-chain methylene C_3' peak, and hence no information could be extracted.

Quinting and Cai [62] determined tacticity through analysis of the carbonyl (C_1), quaternary (C_2), side-chain methylene (C_2'), and methylene (C_4') resonances.

Figure 8.12 shows the ^{13}C spectrum of isotactic PBMA (sample C) obtained at 100 °C in 1,2,4-trichlorobenzene. The quaternary backbone carbon (C_2) resonances of isotactic PBMA were the only peaks intense enough for accurate curve fitting and

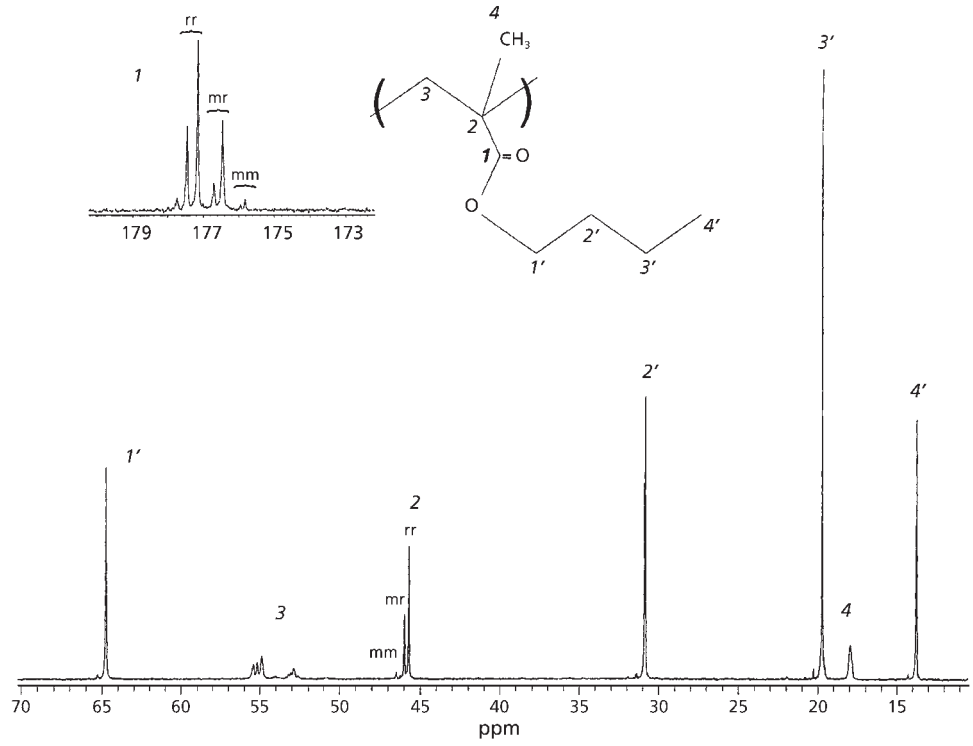

Figure 8.11 ^{13}C-NMR spectrum of syndiotactic PBMA (sample A) in 1,2 4-trichlorobenzene at 100 °C. (*Reprinted with permission from G.R. Quinting and R. Cai, Macromolecules, 1994, 27, 22, 6301. ©1994, ACS [62]*)

tacticity determination. Analysis of the quaternary region gave a P_m value of 0.95. Though the methyl peak (C_4') for the butyl group appeared at first to be a singlet, a close examination revealed shoulders, tentatively attributed to the same long-range effects of tacticity observed for the syndiotactic PBMA sample. The splitting pattern is again analogous to that for the quaternary peak. The farthest downfield and largest of the three paeks corresponds to the mm triad, with the smaller two upfield peaks being the mr and rr peaks, respectively. Deconvolution of the C_4' methyl carbon peaks and subsequent analysis gave a P_m value of 0.95.

Figure 8.13 shows the ^{1}H spectrum of syndiotactic PBMA at 100 °C. Note that the multiplicities for the butyl side chain resonances do not seem consistent with the rules for scalar couplings. For example, the methyl resonances are an apparent quartet instead of the triplet that one expects from scalar coupling to two adjacent and equivalent methylene protons. Further scrutiny reveals that the resonances for

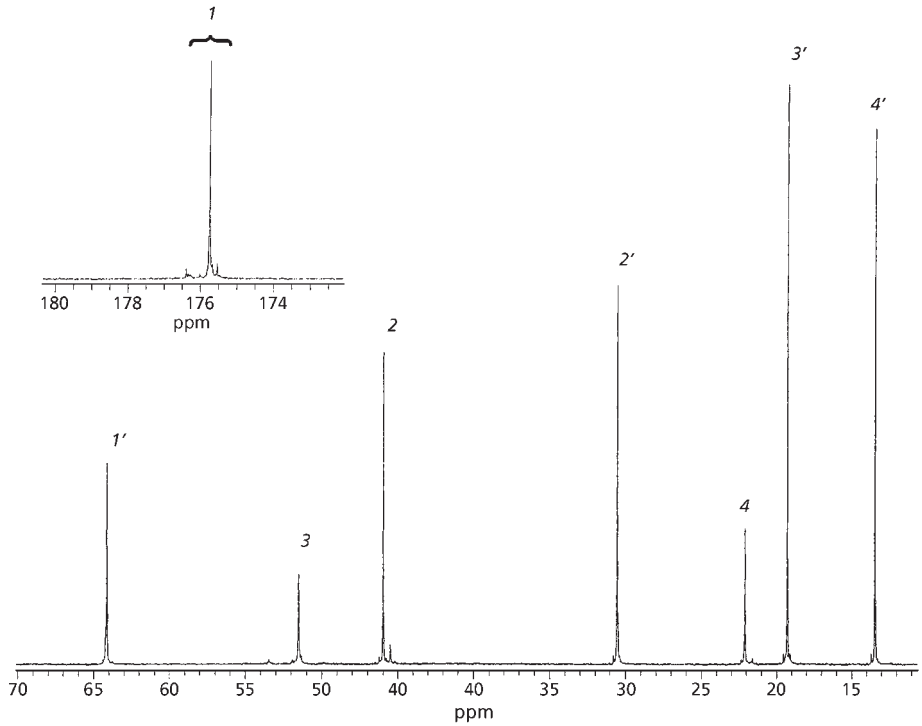

Figure 8.12 ^{13}C-NMR spectrum of isotactic PBMA (sample C) in 1,2,4-trichlorobenzene at 100 °C. (*Reprinted with permission from G.R. Quinting and R. Cai, Macromolecules, 1994, 27, 22, 6301. ©1994, ACS [62]*)

the adjacent methylene protons are an apparent heptet where one expects a hextet. The case is analogous, though less obvious for the two other butyl methylene groups. Curve fitting the butyl methyl 'quartet' gave an area ratio for the two overlapping triplets which closely matches the rr:mr ratio as determined by analysis of the ^{13}C spectrum. Similar ratios were obtained by analysis of the other multiplets.

Figure 8.14 shows the ^{1}H-NMR spectrum of isotactic PBMA at 100 °C. It does not show the 'quartet' for the butyl methyl group (H_4'), which instead seems to be the expected triplet. However, further scrutiny reveals smaller peaks between the peaks of the triplet. The same long-range tacticity effect exists for isotactic PBMA, however, the larger triplet corresponds to the dominant mm triad sequence. The much smaller peaks correspond to the mr sequence.

Ordinarily, it is possible to distinguish between mm/rr and mr/rm triad stereosequences using standard NMR experiments, however, distinction between the resonances of

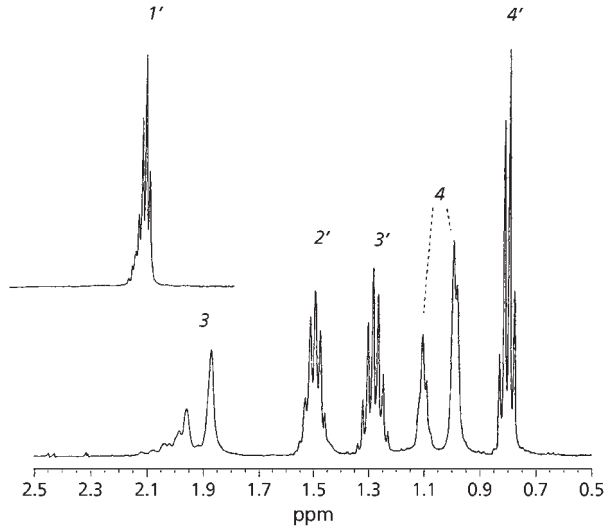

Figure 8.13 ^{1}H-NMR spectrum of syndiotactic PBMA in 1,2,4-trichlorobenzene at 100 °C. (*Reprinted with permission from G.R. Quinting and R. Cai, Macromolecules, 1994, **27**, 22, 6301. ©1994, ACS [62]*)

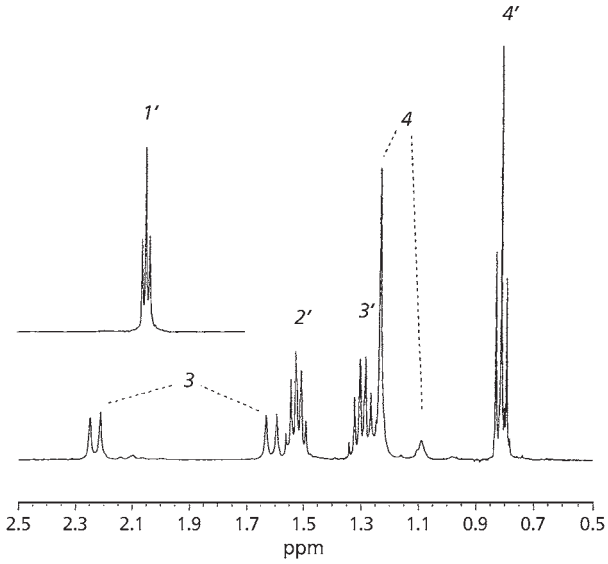

Figure 8.14 ^{1}H-NMR spectrum of isotactic PBMA in 1,2,4-trichlorobenzene at 100 °C. (*Reprinted with permission from G.R. Quinting and R. Cai, Macromolecules, 1994, **27**, 22, 6301. ©1994, ACS [62]*)

mm and rr triads can only be made if a spectrum from a stereoregular polymer of known relative configuration is available.

Triple resonance 3D-NMR techniques combined with isotopic labelling have provided powerful tools for biomolecular structure determination [63-65] which have tremendous potential applications in polymer chemistry.

8.5 Tacticity of Poly(1-chloro-1-fluoroethylene)

Li and Rinaldi [72] and others [73, 74] used a 3D $^{1}H/^{13}C/^{19}F$ triple resonance NMR experiment to unambiguously determine the resonance assignments for mm, mr/rm, and rr triad stereosequences in poly(1-chloro-1-fluoroethylene) (PCFE) without resorting to the preparation of stereoregular polymer with known relative configuration. In a later paper Li and Rinaldi [75] provide a complete description of the technique. Additionally, the significantly better dispersion in 3D-NMR compared to ID- and 2D-NMR was used to resolve additional signals and make unequivocal assignments of the ^{1}H, ^{13}C, and ^{19}F resonances from methylene groups in tetrads and fluorines in pentad sequences.

Figure 8.15 shows the ^{1}H, ^{19}F, and ^{13}C spectra of PCFE. For a fluorine-containing polymer with random stereochemistery, the NMR spectra have enormous complexicity, arising from the various stereosequences found in the polymer as well as from the presence of ^{1}H-^{1}H, ^{19}F-^{1}H, and ^{19}F-^{13}C couplings. **Figure 8.15(a)** shows the ^{1}H spectrum of PCFE with ^{19}F broad band decoupling. Even with the simplification achieved by elimination of ^{19}F-^{1}H couplings, the spectrum is still too complex to interpret because of limited chemical shift dispersion. The ^{13}C spectrum of PCFE with ^{1}H decoupling (**Figure 8.15(b)**) shows two resonances which arise from the quaternary and methylene carbons (the central triplet is $CDCl_3$ solvent peak). When ^{19}F decoupling is applied, the doublet at 108 ppm resulting from the one-bond ^{19}F-^{13}C coupling collapses to a singlet (**Figure 8.15(b)**); the broad peak at about 54 ppm sharpens into two groups of resonances (inset in **Figure 8.15(c)**). Tacticity has only a small influence on the appearance of the methylene resonances in the ^{13}C spectrum and no detectable influence on the $^{13}CF(Cl)$ resonance. In the ^{19}F spectrum of PCFE (**Figure 8.15(d)**), there are three groups of resonances. Cais and Kometani [76] and others [77] originally assigned to rr, mr/rm, and mm in order of increasing field strength, however, no justification for this assignment has been described. Because the ^{19}F chemical shifts are more sensitive to structural differences than are the ^{1}H or ^{13}C chemical shifts, it is possible to obtain ^{1}H and ^{13}C resonance assignments using a 3D $^{1}H/^{13}C/^{19}F$ chemical shift correlation NMR experiment which disperses signals based on the ^{19}F chemical shifts. A 3D-NMR sequence can be adapted for this purpose.

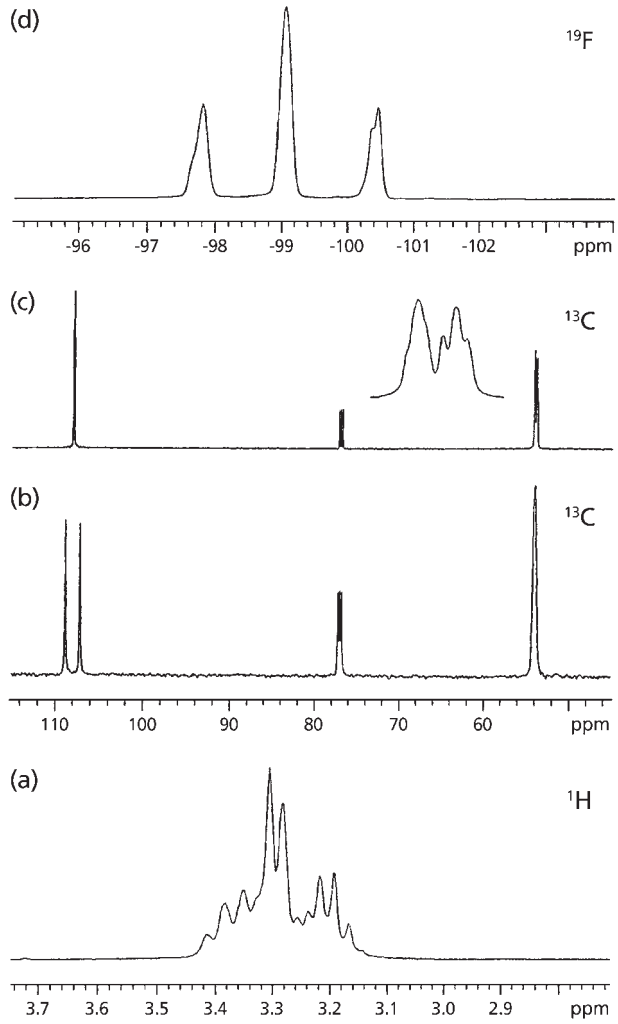

Figure 8.15 1D spectra of PCFE: (a) ^{1}H spectrum with ^{19}F decoupling, (b) ^{13}C spectrum with ^{1}H decoupling, (c) ^{13}C spectrum with ^{1}H and ^{19}F decoupling, and (d) ^{19}F spectrum with ^{1}H decoupling. (*Reprinted with permission from L. Li and P.L. Rinaldi, Macromolecules, 1997, **30**, 3, 520. ©1997, ACS [75]*)

The low resolution ^{1}H/^{13}C/^{19}F/ 3D-NMR spectrum of PCFE is shown in **Figure 8.16**; f_1f_3 (^{1}H-^{13}C correlations) slices at the three different ^{19}F chemical shifts are shown in **Figure 8.16(a)-(c)**, and the relative positions of these slices within the 3D spectrum are schematically illustrated in **Figure 8.16**. At each ^{19}F chemical shift, sets of crosspeaks to at least two different ^{13}C resonances are observed, one for each geminal methylene

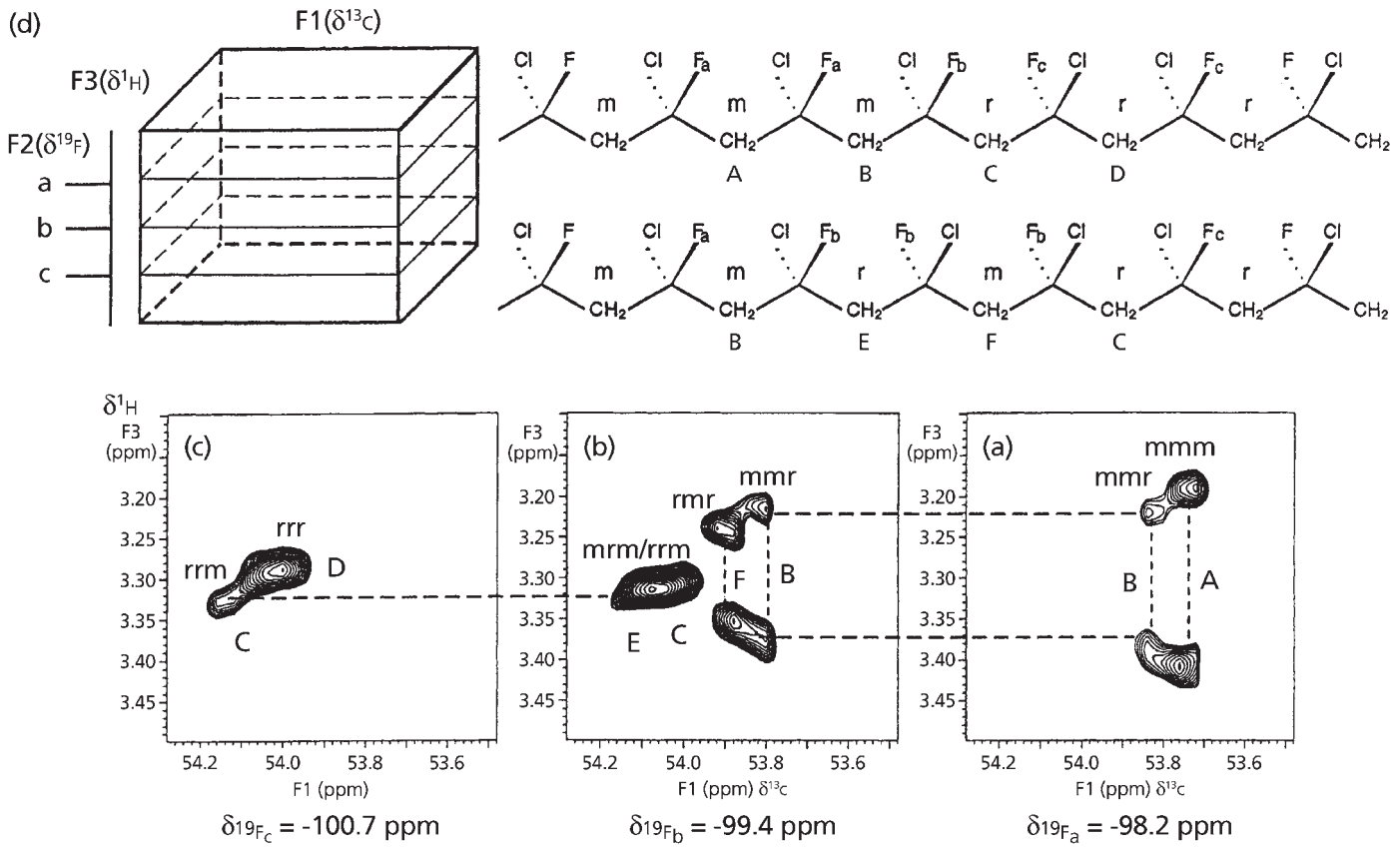

Figure 8.16 $^{1}H/^{13}C/^{19}F$ 3D-NMR spectrum of PCFE with f1f3 slices at different ^{19}F resonance frequencies: (a) $\delta^{19}F$ = -98.2 ppm, (b) $\delta^{19}F$ = -99.4 ppm, (c) $\delta^{19}F$ = -100.7 ppm, (d) Schematic illustration of the 3D spectrum indicating the relative positions of the three slices. (*Reprinted with permission from L. Li and P.L. Rinaldi, Macromolecules, 1997, 30, 3, 520. ©1997, ACS [75]*)

group. Methylene carbons centred in m diads show correlations to the resonances of the two non-equivalent, directly bonded protons (e.g., the A and B pairs of crosspeaks in **Figure 8.16(a)**). The methylene carbons centred in r diads are attached to ^{1}H atoms which are essentially chemically equivalent (although these protons are not rigorously equivalent unless the polymer is syndiotactic, remote stereochemistry has very little influence on the ^{1}H chemical shifts, and separate resonances are not observed in these data) and therefore exhibit a correlation to a single ^{1}H resonance (e.g., crosspeaks C and D in **Figure 8.16**). The fact that methylene protons centred in m diads are non-equivalent was first used by Bovey and Tiers [77] to assign the resonances in the ^{1}H spectrum of polymethyl methacrylate (PMMA). Later, this same characteristic was used in the interpretation of polymer 2D-NMR spectra [78-81].

In the slice at $\delta^{19}F$ = -98.2 ppm (**Figure 8.16(a)**) both carbon resonances from adjacent methylenes show crosspeaks to two proton resonances, therefore, this ^{19}F must be centred in an mm triad (type a fluorines in the structures in **Figure 8.16**). In the slice at $\delta^{19}F$ = -100.7 ppm (**Figure 8.16(c)**), both methylene carbon resonances show crosspeaks to single proton resonances, therefore, this ^{19}F must be centred in an rr triad (type c fluorines). In the slice at $\delta^{19}F$ = -99.4 ppm (**Figure 8.16(b)**), one methylene carbon resonance shows a crosspeak to a single proton resonance and the second methylene carbon resonance shows a crosspeak to two proton resonances, therefore, the fluorines having this shift must be centred in mr/rm triads, the $^{1}H/^{13}C/^{19}F$ 3D-NMR spectrum clearly shows four sets of crosspeaks from several possible tetrad structures (B, C, E and F in **Figure 8.16(b)**).

Once the triad stereosequences are determined from examination of single slices, the relative stereochemistry of adjacent diads in the chain can be determined by looking for identical C-H crosspeaks in different ^{19}F slices. For example, in **Figure 8.16(a)**, the A pair of crosspeaks do not occur in the other two slices; therefore, type A methylenes only show crosspeaks to ^{19}F atoms in mm.

Although heteronuclear 3D-NMR experiments are typically performed in conjunction with isotopic labelling, Li and Rinaldi [72] clearly demonstrate that useful data can be obtained without isotopic labelling, especially when high abundance, NMR active isotopes such as ^{19}F are present in the molecule. By taking advantage of the sensitivity of the ^{19}F chemical shift to structural variations, ^{1}H and ^{13}C resonance assignments can be determined through a $^{1}H/^{13}C/^{19}F$ 3D-NMR correlation experiment. This information could not be obtained from 1D- or 2D-NMR experiments. By dispersing resonances into three dimensions, it is possible to resolve numerous methylene resonances, where only a single signal is detected in the 1D-NMR spectrum. Once these resonances are resolved, the unique ability of 3D-NMR experiments to simultaneously relate the shifts of three coupled nuclei provides unequivocal assignments for the resonances of different stereosequences. While the results described in this paper [72] rely on the presence of ^{19}F as the third nucleus in a fluoropolymer, similar results could be obtained from other NMR active nuclei such as ^{31}P.

8.5.1 Stereoregularity of Polymethyl Methacrylate

Py-GC-MS has also been applied in a study of the stereoregularity of PMMA [82]. In this method the assocuiated diastereomeric tetramers were identified by a directly coupled Py-GC-MS set up.

Figure 8.17 shows a typical pyrogram of PMMA (S-2) at 500 °C obtained by FID. The main peak is due to the monomer (about 96%) because PMMA is easily depolymerised at elevated temperatures. On the pyrogram recorded with higher sensitivity, however, one can clearly recognise the tetramers (about 0.1%) and even the pentamers (about 0.03%) as well as the dimers and the trimers. Among these fragment clusters, the tetramers and the pentamers should contain at least two (m and r) and four (mm, mr, rm and rr) diastereoisomers since they have two and three asymmetric centres in the molecules, respectively. Then, the chemical structures of the diastereoisomers in the tetramer region were estimated from electroionisation (EI) and chemical ionisation (CI) mass spectra of the tetramers obtained by Py-GC-MS in comparison with those of the dimers and the trimers.

Figure 8.18 shows the mass spectra for the dimers (a) and (b) and the trimer. In the corresponding CI spectra, we can clearly observe $[M + 1]^+$ at $m/z = 201$ for both dimers and at $m/z = 301$ for the trimer. The trimer structure is confirmed as that shown in **Figure**

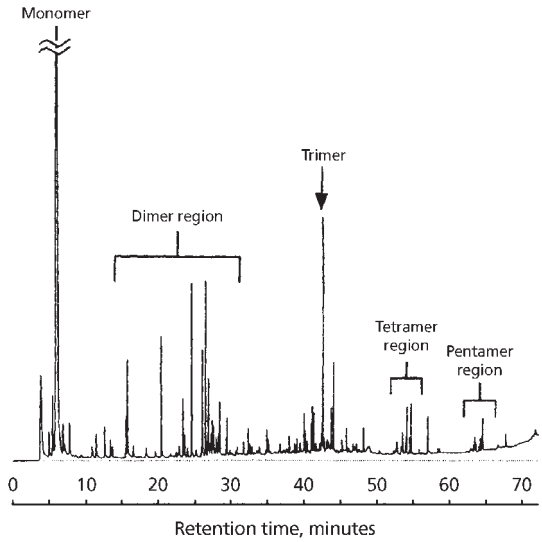

Figure 8.17 Pyrogram of S-2 at 500 °C observed by FID. (*Reprinted with permission from L. Li and P.L. Rinaldi, Macromolecules, 1997, **30**, 3, 520. ©1997, ACS [75]*)

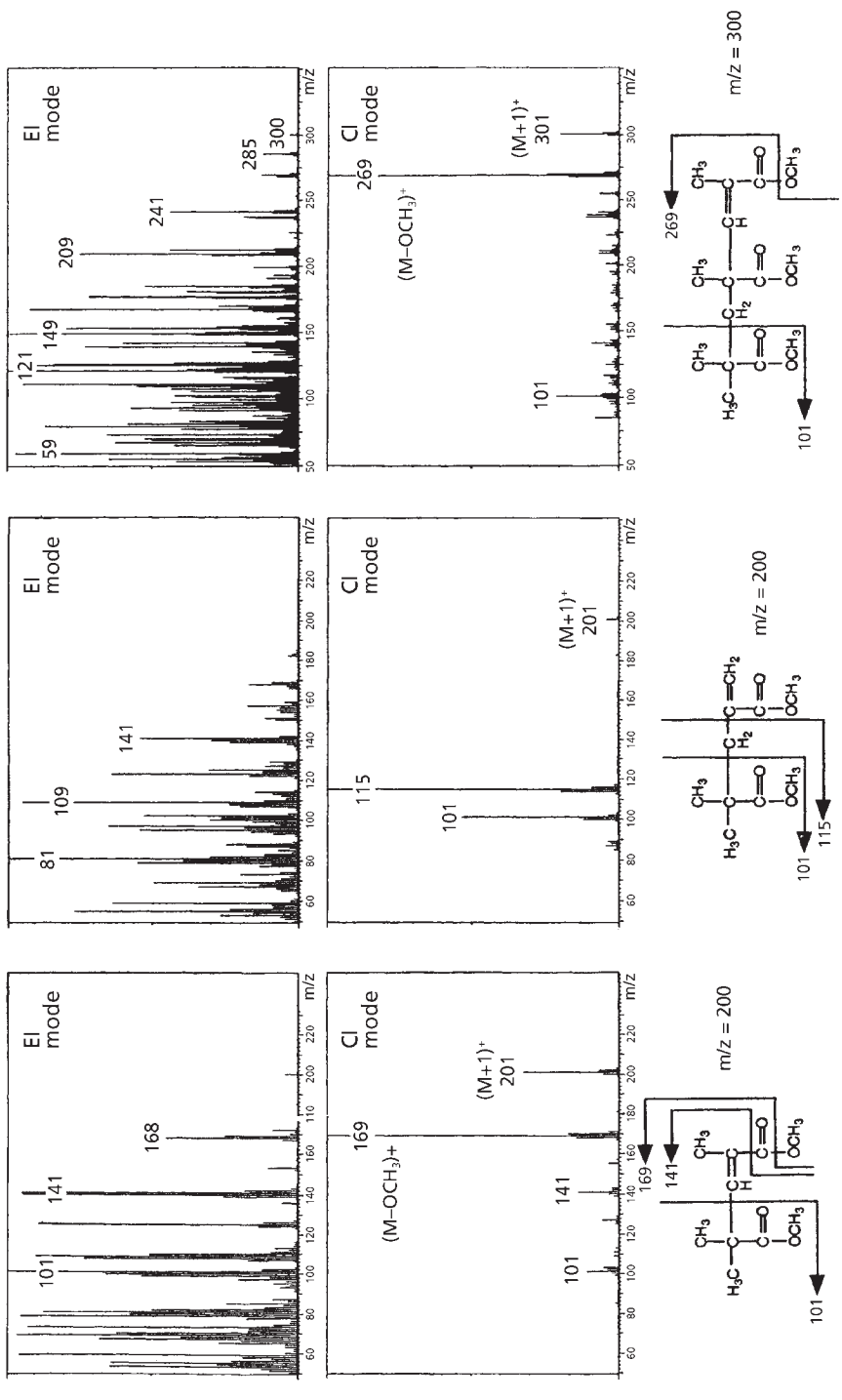

Figure 8.18 EI and CI mass spectra of dimers and trimer and their expected structures. (*Reprinted with permission from L. Li and P.L. Rinaldi, Macromolecules, 1997, **30**, 3, 520. ©1997, ACS [75]*)

8.18 on the basis of the formation mechanism shown in **Scheme 8.1**. Also, the main dimer structures with MW = 200 should be those shown in **Figure 8.18**. Furthermore, according to the characteristic fragments, especially the prominent $[M - OCH_3]^+$ peak observed as the base peak in the CI mass spectra, we can estimate that the dimer (a) and the trimer should have the same terminals illustrated at the bottom of the figure.

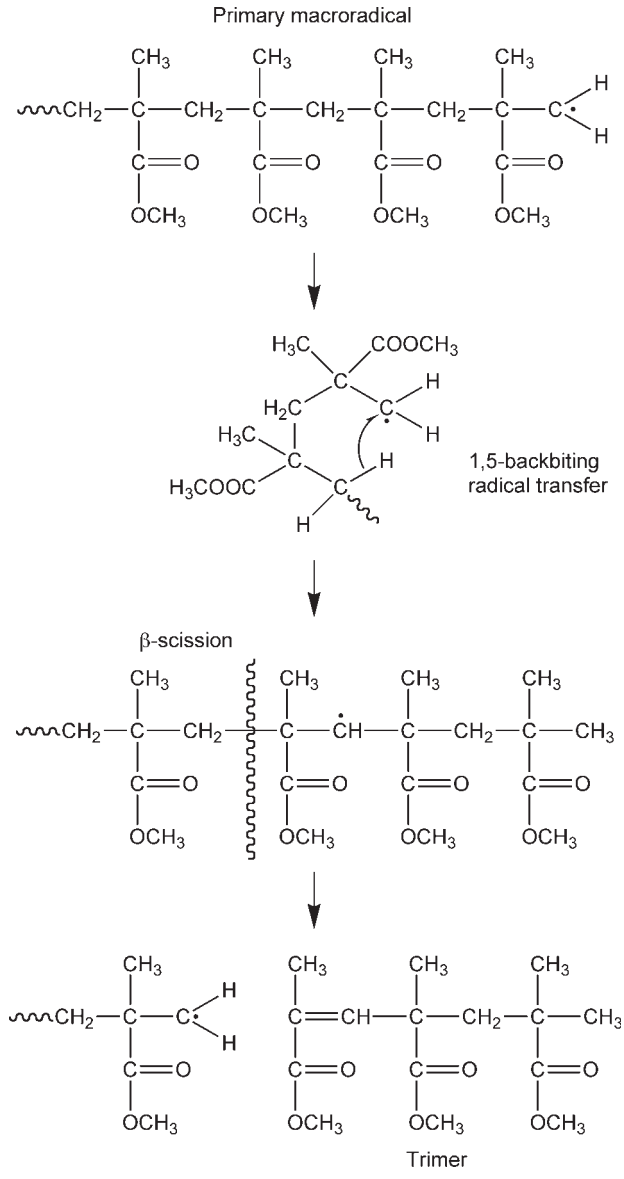

Scheme 8.1

Figure 8.19 shows the El and CI spectra corresponding to the two strong peaks for tetramer A at approximately 45 minutes and tetramer B at about 46 minutes in the pyrogram. Although the expected quasi-molecular ions are not observed even in the CI spectra, the common ions at *m/z* = 369 can be attributed to $[M - OCH_3]^+$. Thus, both A and B should have the same molecular weight (MW = 400). Furthermore, in the El spectra, the tetramer A shows a fairly strong peak at *m/z* = 301, while B exhibits a prominent peak at *m/z* = 315. The possible bond cleavages are shown at the bottom of **Figure 8.18** with the possible structures for the isomers. In this case, the relationship

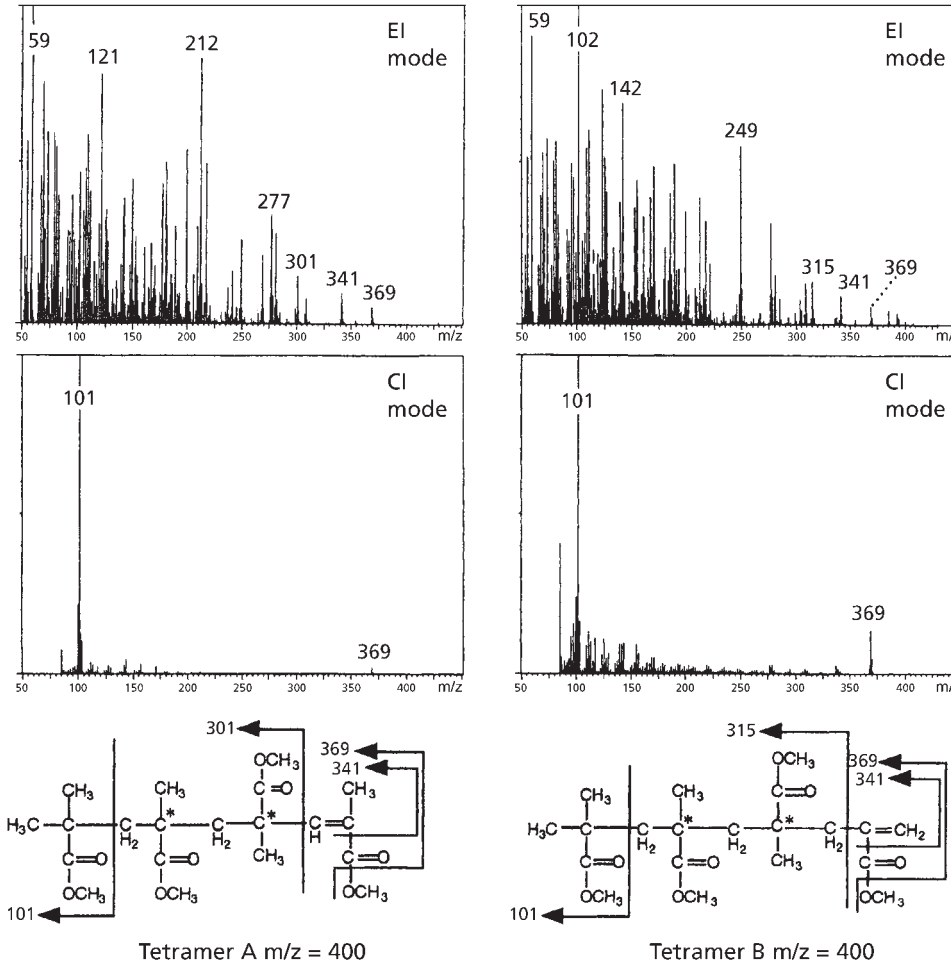

Figure 8.19 El and CI mass spectra of tetramers and their expected structures. (*Reprinted with permission from L. Li and P.L. Rinaldi, Macromolecules, 1997, **30**, 3, 520. ©1997, ACS [75]*)

between the retention times and the position of the double bonds for the tetramers is also consistent with that for the dimers. Additionally the small satellite peaks (A′ and B′) appearing at a little smaller retention times than those of the main tetramers (A and B) observed in the expanded pyrogram showed exactly the same mass spectra for A and A′ and for B and B′, suggesting that they are stereoisomers, respectively.

The reason why the main trimer peak consists of only one component is easily explained by **Scheme 8.1**, where the trimer is exclusively formed through 1,5-radical transfer of the primary macroradical (II) at the fifth methylene carbon followed by β-scission, since 1,5-radical transfer of the primary macroradical (II) at the fifth methyl carbon followed by β-scission yields only a dimer at best. When double back-biting occurs through 1,5- and then 5,9-radical transfers of the primary macroradical (II)

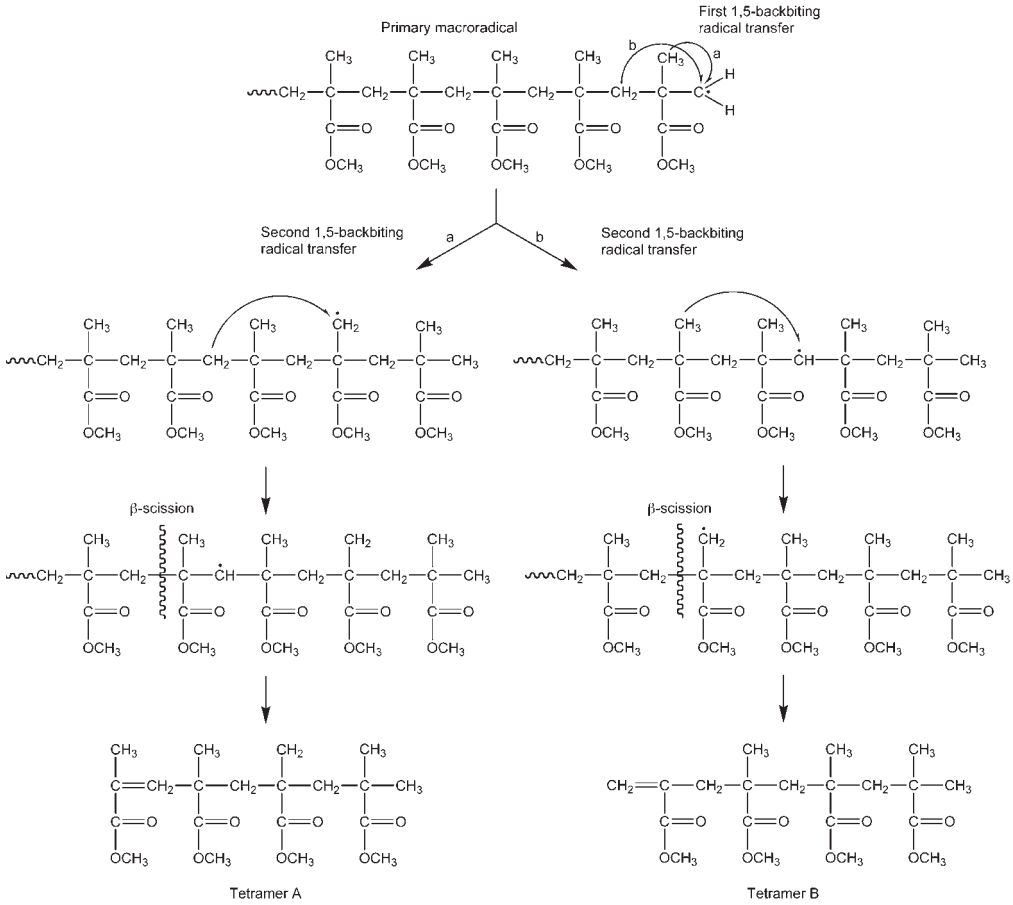

Scheme 8.2

at the fifth and the ninth methylene carbons, the pentamers consisting of only one chemical structure are formed in a similar manner as the trimer formation although they comprise the associated diastereoisomers (**Scheme 8.1**). On the other hand, in the tetramers, two kinds of position isomers [A (or A′) and B (or B′)] can be formed depending on the paths of the double back-bitings followed by β-scission as shown in **Scheme 8.2**. In path (a), the first back-biting occurs at the fifth methyl carbon of the primary macroradical (II) and the second 1,5-radical transfer at the seventh methylene carbon followed by β-scission to yield the tetramer A (or A′), while in path (b), the first back-biting occurs at the fifth methylene carbon and the second 1,5-radical transfer does at the ninth methyl carbon followed by β-scission to yield the tetramer B (or B′). In both paths, there is no chance for the thermal isomerisation since the associated

Table 8.5 Stereospecificity studies on acrylates and methacrylates

Polymer	Comments	Reference
Polymethylmethacrylate	Measurement of isotactic triads, tetrad, pentad and hexad resonances conformation tacticity	[94-96, 97-99, 106, 108]
Polymethylacrylate	Measurement of tetrad configurations of triad, tetrad and pentad configurations	[100]
Polyalkylmethacrylates	Measurement of tacticity	[101]
Polyallylmethacrylate	Measurement of tacticity and sequence length	[102]
Methylacrylate-butadiene	Measurement of isotactic configuration	[103]
Methylmethacrylate-butadiene	Measurement of triad and pentad configuration	[93]
Styrene-methylmethacrylate	Measurement of diad, triad and pentad configurations	[94]
Methyl α-chloro acrylate-methylmethacrylate	Measurement of diad configurations and mean sequence length	[95]
Polymethylacrylate	Measurement of tacticity	[97]
Polyacrylic acid	Measurement of tacticity	[96]
Polymethacrylic acid	Measurement of tacticity	[98]
Diphenylethylene – methyl acrylate	Measurement of tacticity	[99]

Source: Author's own files

radical transfers always occur only at methyl and methylene carbons. In the cases of the thermal degradation of PP and PS, however, the corresponding double back-bitings followed by β-scission to yield their tetramers occur mostly at asymmetric methine carbons resulting in some thermal isomerisation [83, 84].

The diad tacticity determined from the relative peak intensities of the diastereomeric tetramers in the programs was consistent with that obtained by pNMR, suggesting that no appreciable thermal isomerisation occurred during the pyrolysis. The thermal degradation mechanisms yield the diastereomeric tetramers from PMMA without isomerisation and this opens up, the possibility of estimating the triad tacticity of PMMA from the distribution of diastereomeric pentamers.

NMR spectroscopy has been applied to stereospecific studies on 9-fluorenyl methacrylate [85], PMMA [86-88], PBMA [62], poly-naphthyl methacrylate [89], polyacrylic acid [90], polychlorophenolmethacrylate [91-82], poly(2,3-epoxypropylmethacrylate) [92] and polyacrylates [93]. Other work on acrylates and methacrylates is reviewed in **Table 8.5**.

8.6 Tacticity of Polypropylene Oxide

Several attempts have been made to determine the distribution of structural and steric irregularities in polypropylene oxide (PPO), synthesised by partial hydrolysates of some metal alkyls (bisdimethylaluminium oxide dioxane complex) or Pruitt-Baggett type catalysts. For this purpose optical activity measurements [100-104], degradation techniques [101, 102, 105, 106] and NMR techniques [103, 107-110] were used. Information obtained from these studies have been taken as evidence to support or to refute the theories on the nature of catalysts and on the mechanism of stereoregular polymerisation [102-104]. However, the conclusion drawn from the observed sequence concentrations were not justified since PPO obtained from the above systems was a sum of polymers differing in structural regularities [108]. To overcome this difficulty, convenient experimental techniques to separate PPO into fractions differing in melting points have been described [111, 112].

Uryu and Alyürük [113] have shown that PPO can be fractionally crystallised from dilute isooctane solutions, into fractions differing in stereoregularity. They also present some experimental data on the ^{13}C-NMR spectra of these fractions.

Fractionation was achieved by crystallisation from 2 litres of isooctane solution (1 g/l) at 27 ^{o}C by lowering the temperature incrementally to 0 ^{o}C. At each precipitation step the temperature of the system, T_p, was kept constant for 48 hours prior to isolation of the precipitated polymer. The supernatant was filtered through a glass-wool pad.

Table 8.6 Fractionation from isooctane of K-polymer from P_3 for sample of polypropylene oxide

Fraction	T_p (°C)	T_m*[a] (°C)	%Wt	$M_\upsilon \times 10^{-5}$	% Crystallinity
$P_3 - K_1$	45	73	4	0.79	38.7
$P_3 - K_2$	40	-	28	0.74	-
$P_3 - K_3$	35	66	20	0.38	49.6
$P_3 - K_4$	30	-	2	0.45	-
$P_3 - K_5$	25	-	15	0.47	-
$P_3 - K_6$	20	-	13	0.25	-
$P_3 - K_7$	10	48	2	0.13	-
$P_3 - K_8$	0	-	16	0.12	-

[a] *DSC data*

T_m: bulk melting temperature measured by DSC*

Reproduced with permission from N. Uryu and K. Alyürük, Journal of Polymer Science Part A: Polymer Chemistry, 1989, 27, 5, 1749. ©1989 [113]

During the filtration precautions were taken to keep the temperature at T_p. K polymers are insoluble in isooctane, D polymers are soluble in isooctane.

The precipitate was collected and dissolved in benzene and filtered. Prior to freeze drying (except for a small portion of the solution, which was reserved for ^{13}C-NMR characterisation), antioxidant was added. Although each fraction should be defined by a temperature range, lying between the initial temperature of the solution T_i and T_p since the upper limit T_i of each fraction coincides with the crystallisation temperature T_p of the preceeding fraction, only T_p values are given in **Table 8.6** which shows typical results obtained in a fractionation of PPO.

^{13}C-NMR spectra of P_1-K fractions (K polymers insoluble in isooctane) show an increased number of absorption peaks as the crystallisation temperature of the preceeding fraction (T_p) or the bulk melting temperature (T_m*) decreases (**Figure 8.20**). Corresponding fractions from different samples, (i.e., fractions obtained from polymers of different origins at the same T_p) yield almost identical spectra (**Figure 8.22**). ^{13}C-NMR spectra of the main chain carbon atoms of the PPO have been extensively studied and the line assignments were made [103, 108-110] for most of the absorptions arising from structural and steric isomers of the repeat units. Coexistence of both structural and steric isomers did not permit [100]

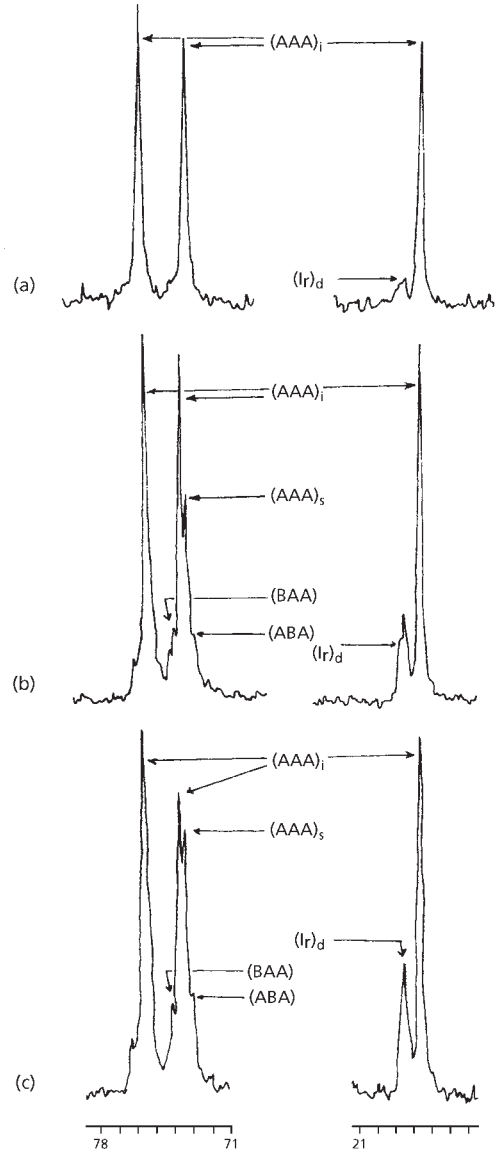

Figure 8.20 ^{13}C-NMR spectra of K Fractions (10 insoluble in isooctane) of Polymer P_1. (a) P_1-K_1, (b) P_1-K_4, (c) P_1-K_6. $(AAA)_i$: structurally regular triad of isotactic dyads (or triads); $(AAA)_s$: structurally regular triad of syndiotactic dyads; (BAA) and (ABA): structurally irregular triads; $(I_r)_d$: structurally and/or sterically irregular isomers. Line assignments of methylene and methine carbon atoms are made after Oguni and co-workers [130]. (*Reprinted with permission from N. Uryu and K. Alyürük, Journal of Polymer Science Part A: Polymer Chemistry, 1989, 27, 5, 1749. ©1989, John Wiley and Sons [113]*)

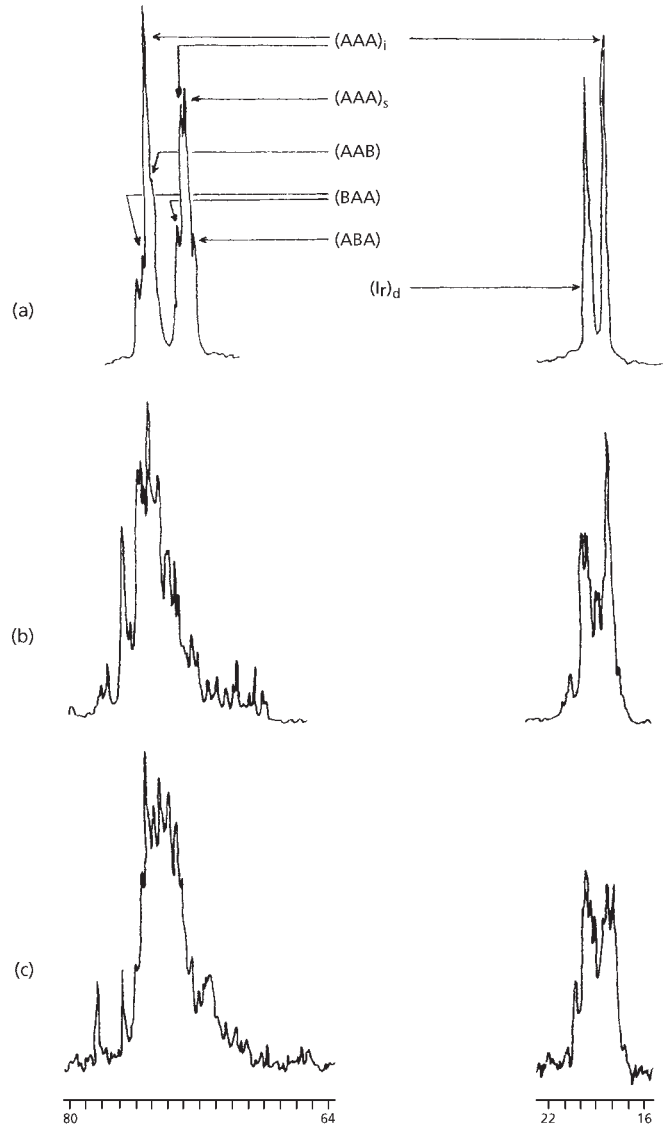

Figure 8.21 ^{13}C-NMR spectra of D-fractions (i.e., insoluble in isooctane) of polymer P_1: (a) $P_1 - D_1$, (b) P_1:- D_3, (c) $P_1 - D_5$. (*Reprinted with permission from N. Uryu and K. Alyürük, Journal of Polymer Science Part A: Polymer Chemistry, 1989, 27, 5, 1749. ©1989, John Wiley and Sons [113]*)

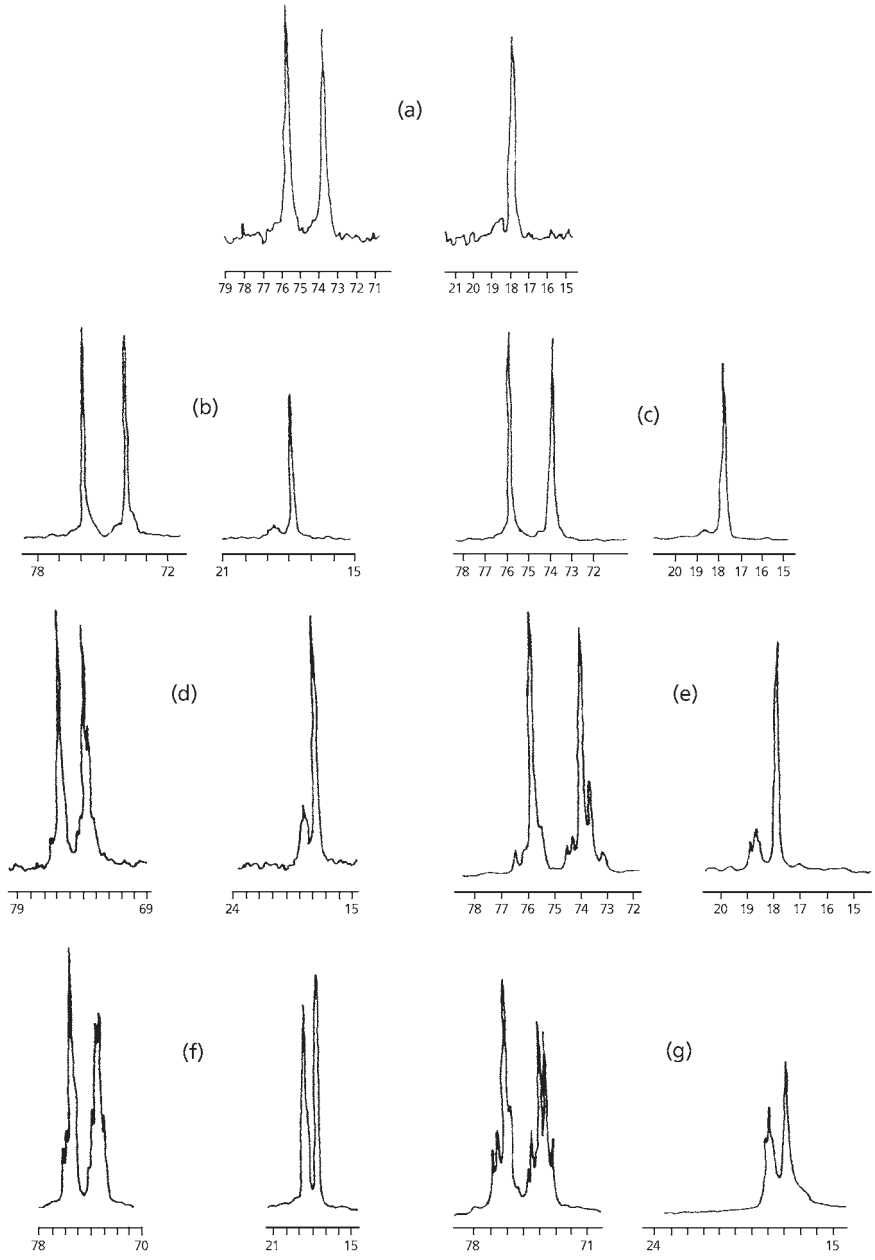

Figure 8.22 Comparison of ^{13}C-NMR spectra of different origin K-polymer fractions, which were precipitated at same T_p. (a) P_1 –K_1 (T_p.= 318 K), (b) P_2 –K_1 (T_p.= 318 K), (c) P_3 –K_1 (T_p.= 318 K), (d) P_1 – K_4 (T_p. = 293 K), (e) P_2 – K_7 (T_p. = 293 K), (f) and (g) D_1 fractions of P_1 and P_2, respectively, both are soluble at 273 K. (*Reprinted with permission from N. Uryu and K. Alyürük, Journal of Polymer Science Part A: Polymer Chemistry, 1989, 27, 5, 1749. ©1989, John Wiley and Sons [113]*)

a quantitative analysis of the sequence concentrations from the data obtained in this work. On the other hand, it is qualitatively apparent that both structural and steric irregularities increase in concentrationsas T_p decreases.

In contrast to Schaefer [108] who concluded that 'the detectable structural and steric information was not transmitted to the side groups of PPO,' absorptions due to the methyl groups showed splitting into mainly two peaks at 17.8 and 18.6 ppm (see **Table 8.7**). Apparently, the peak at 18.6 ppm envelops both of the absorptions due to steric and structural isomers. In fact the spectra of P_2-K_7 (where a 25 MHz spectrometer instead of a 20.1 MHz one was used) (**Figure 8.22(e)**) and some D-fractions showed a further splitting of this peak (**Figures 8.21 and 8.22**). Therefore, in the **Figures 8.20 and 8.21**, the peak appearing at 18.6 ppm was assigned to structurally and/or sterically irregular isomers. Concentrations of the irregular isomers were calculated both from the ^{13}C-NMR data, *N;* and assuming that, they occur randomly along the chain from the Flory's formula [114], N_F.

$$1/T_m^* - 1/T_m^0 = (-R/\Delta H_u)\ln N_F$$

Table 8.7 ^{13}C-NMR data for methyl peaks in polypropylene oxide

Sample	Chemical shift (ppm)	Intensity	Peak Area	N	NF
$P_1 - K_1$	18.7 17.8	- 17.5	- -	- -	0.12
$P_1 - K_3$	18.7 17.8	2.0 11.3	7.4 23.2	0.24	0.20
$P_1 - K_4$	18.7 17.8	4.9 19.5	14.5 38.0	0.28	0.20
$P_1 - K_6$	18.6 17.8	7.0 19.0	17.2 36.6	0.32	0.31
$P_1 - D_1$	18.6 17.8	15.5 17.8	43.7 41.2	0.51	Noncrystalline

N: Concentration of irregular polymers from ^{13}C-NMR

N_F: Concentration of randomly occurring polymers along the chain/Flory formula

K polymers are insoluable in isooctane, D polymers are soluble in isooctane.

The N_F concentrations given in Table 8.6 were calculated by taking the literature values of T_m and ΔH_u as 355 K and 8360 J/repeat unit [115].

Not only increased concentrations of steric and structural isomers, but also chain ends and the presence of cyclic oligomers [112] account for the extremely complex spectra obtained for P_1 - D_3 and P_1 – D_5 fractions (**Figure 8.21**).

Uryu and Alyürük [113] concluded that both structural (head-to-head and tail-to-tail linkages) and steric (syndiotactic dyads) irregularities occur in otherwise isotactic chains and their abundance apparently increased as the melting point and the chain length of the fractions decreased. Various other workers have discussed the application of ^{13}C-NMR spectroscopy to tacticity studies on PPO [103, 116-119].

8.7 Tacticity of Polymethylacrylonitrile

Dong and co-workers [61] derived the configurational assignments of polymethacrylonitrile (PMAN) from double-quantum-filtered phase-sensitive ^{1}H homonuclear shift-correlation and proton-detected ^{1}H-^{13}C heteronuclear shift-correlation NMR spectroscopies. The overlapping peaks for different tacticities in the 1D spectrum have been separated and assigned by 2D methods. Assignments to the methylene region of the ^{1}H and ^{13}C spectra have been made to hexad and tetrad levels, respectively.

Table 8.8 Tacticity Assignments for the Methylene Region of the 1D ^{13}C Spectrum

			Resonance intensity		
Chemical shift, ppm	Assignment of carbon			Calculation[a]	
	This work	Literature	Observed	Dong and co-workers [66]	Literature
45.8-46.7	mrm	mmm	0.109	0.098	0.067
46.7-47.6	mmm + rrm	mrm + mmr	0.333	0.353	0.384
47.6-48.7	rrr + mmr	rrm + rmr	0.400	0.405	0.430
48.7-49.6	rmr	rrr	0.158	0.143	0.210

[a] *Calculated for a Bernoullin distribution with a single statistical parameter P_m = 0.406.*

Reproduced with permission from L. Dong, D.J.T. Hill, J.H. O'Donnell and A.K. Whittaker, Macromolecules, 1994, 27, 7, 1830. ©1994, ACS [61]

Tacticity sequence assignments based on the 1D ^{13}C-NMR spectra of PMAN have previously been made by other authors. In the methylene region, the four peaks were assigned by these authors, from high to low field, to mrm, mmm + rrm, rrr +mmr and rmr tetrads, respectively. **Table 8.8** shows the assignments based on the work of Dong and co-workers [61] and those proposed by the previous workers. The resonance intensities of the four peaks have been calculated by Dong and co-workers [61] using the Bernoullian distribution for their assignments of these peaks and for the assignments proposed by the previous authors. **Table 8.8** also shows the calculated resonance intensities of the four peaks and those determined from the experimental measurements of Dong and co-workers [61]. It is evident that the experimental and calculated resonance intensities show close agreement for their assignments of these peaks and that the previous assignments of the peaks in the methylene region of the ^{13}C-NMR spectra reported in the literature are invalid.

8.8 Tacticity of Other Miscellaneous Polymers

Tacticity studies have been conducted on poly(3-methyl-1-butene) [120], poly(*p*-isopropyl-α-methyl styrene) [121], α-methyl styrene [122], polytetrafluoroethylene [123], polyacrylic acid [124], polymethylvinyl ethers [125], polyacrylonitrile [126, 127], polyvinyltrifluoro acetate [128], polyvinyl alcohol and its ethers [129, 130], isobutene-maleic anhydride [111], isobutene dimethyl fumerate [131], isobutene dimethyl maleate [131], polyacrylonitrile [127], ethylene – vinyl acetate [132-135], polyalkyl vinyl ethers [136, 137], ethyl-2-chloroacetate [133], poly-*trans*-1,3-pentadiene [138], isotactic-1-butene – propylene [139], butadiene – propylene [140], polybutene [141], polychloroprene [142], ethylene – vinyl chloride [143], chlorinated polyethylene [144, 145], poly-α-methyl styrene [146], styrene acrylic acid [147], α-methyl styrene – methacylonitrile [148], styrene acrylonitrile [149], styrene isobutene [150], poly(*p*-fluoro-α-methyl styrene) [151], polyarylamide-6 [152], PP – polyamide-6 [152], polystyrene oxide [153], polybutene [154], atraconic anhydride – *p*-chlorostyrene [155], styrene – maleic anhydride [156, 157], ethylene – vinyl acetate [158], polymethyl vinyl ether [159], propene – carbon monoxide [160], methyl(3,3,3-trifluoropropyl)siloxane [161], poly(diallyldimethyl ammonium chloride) [162], polypropene [163, 164], polyepichlorohydrin [165], maleic anhydride-*p*-chlorostyrene [166], polymethacrylonitrile [167] and polyvinyl acetate [168].

Kumpanenko and Chukanov [169] have reviewed factors which influence the dependence of intensities and widths of regularity bonds in the IR spectra of polymers on the lengths of regular segments in the polymer. Cheng [170], has described a stereochemical probability model for the treatment of stereoregular polymers.

References

1. G. Natta and F. Danusso, *Journal of Polymer Science*, 1959, **34**, 127, 3.

2. F.A. Bovey, *Polymer Conformation and Configuration*, Academic Press, New York, NY, USA, 1969, p.8.

3. J.C. Randall, *Journal of Polymer Science: Polymer Physics Edition*, 1974, **12**, 4, 703,

4. A. Zambelli, P. Locatelli, G. Bajo and F. A. Bovey, *Macromolecules*, 1975, **8**, 5, 687.

5. F.C. Stehling and J.R. Knox, *Macromolecules*, 1975, **8**, 5, 595.

6. J. Schaefer and D.F.S. Natusch, *Macromolecules*, 1972, **5**, 4, 416.

7. D.E. Axelson, L. Mandelkern and G.C. Levy, *Macromolecules*, 1977, **10**, 3, 557.

8. A. Provasoli and D.R. Ferro, *Macromolecules*, 1977, **10**, 4, 874.

9. J.C. Randall in *Carbon 13-NMR Polymer Science*, Ed., W.M. Pasika, ACS Symposium Series No.103, ACS, Washington, DC, USA, 1979.

10. J.C. Randall, *Journal of Polymer Science: Polymer Physics Edition*, 1976, **14**, 11, 2083.

11. R.S. Porter, *Journal of Polymer Science Part A-1: Polymer Chemistry,* 1966, **41**, 59, 189.

12. E.M. Barrall II, R.S. Porter and J.F. Johnson in *Proceedings of the* ACS *Division of Polymer Chemistry 148th National Meeting*, Chicago, IL, USA, 1964.

13. Edward M. Barrall II, Roger S. Porter and Julian F. Johnson, *Journal of Applied Polymer Science*, 1965, **9**, 9, 3061.

14. S. Satoh, R. Chûjô, T. Ozeki and E. Nagai, *Journal of Polymer Science*, 1962, **62**, 164, 510.

15. G.A. Reilly, Shell Chemical Company, Emeryville, CA, USA, private communication, 1964.

16. F.C. Stehling, *Journal of Polymer Science Part A: General Papers*, 1964, **2**, 4, 1815.

17. M. Peraldo, *Gazzetta Chemica Italiana*, 1959, **89**, 798.

18. M.P. McDonald and I.M. Ward, *Polymer*, 1961, **2**, 341.

19. J. P. Luongo, *Journal of Applied Polymer Science*, 1960, **3**, 9, 302.

20. C.Y. Liang and F.G. Pearson, *Journal of Molecular Spectroscopy*, 1960, **5**, 1-6, 290.

21. D.R. Burfield and P.S.T. Lo, *Journal of Applied Polymer Science*, 1988, **36**, 2, 279.

22. J. Boor, Jr., *Ziegler-Natta Catalysts and Polymerisations*, Academic Press, New York, NY, USA, 1979, Chapter 3.

23. D.R. Burfield and P.S.T. Loi in *Catalytic Polymerization of Olefins*, Eds., T. Keii and K. Soga, Kodansha, Tokyo, Japan, 1986, p.387-406.

24. Y.V. Kissin, *Isospecific Polymerization of Olefins with Heterogenous Ziegler-Natta Catalysts*, Springer Verlag, New York, NY, USA, p.229-249.

25. F.A. Bovey, *High Resolution NMR of Macromolecules*, Academic Press, New York, NY, USA, 1972.

26. H.J. Harwood in *Preparation and Properties of Stereoregular Polymers*, Eds., R.W. Lenz and F. Ciardelli, D Riedel Publishing Company, Boston, MA, USA, 1978, Chapters 15 and 16.

27. J.L. Koenig, *Chemical Microstructure of Polymer Chains*, John Wiley, New York, NY, USA, 1980.

28. J.C. Randall, *Polymer Sequence Determination*: *Carbon-13 NMR Method*, Academic Press, New York, NY, USA, 1977.

29. G. Natta, P. Pino, P. Corradini, F. Danusso, E. Mantica, G. Mazzanti and G. Moraglio, *Journal of the American Chemical Society*, 1955, **77**, 6, 1708.

30. H. Tadokoro, M. Kobayashi, M. Ukita, K. Yasufuku, S. Murahashi and T. Torii, *Journal of Chemical Physics*, 1965, **42**, 4, 1432.

31. G. Natta, A. Valvassori, F. Ciampelli and G. Mazzanti, *Journal of Polymer Science Part A: General Papers,* 1965, **3**, 1, 1.

32. J.J. Brader, *Journal of Applied Polymer Science*, 1960, **3**, 9, 370.

33. R.H. Hughes, *Journal of Applied Polymer Science*, 1969, **13**, 3, 417.

34. Y.V. Kissin, V.I. Tsvetkova and N.M. Chirkov, *European Polymer Journal*, 1972, **8**, 4, 529.

35. Y.V. Kissin, *Advances in Polymer Science*, 1975, **14**, 91.

36. Y.V. Kissin, V.I. Tsvetkova and N.M. Chirkov, *Doklady Akademii Nauk SSSR*, 1963, **152**, 1162.

37. D. Choi and J.L. White, *Polymer Engineering and Science*, 2004, **44**, 2, 210.

38. B.P. Garcia, *Revista de Plasticos Modernos*, 2002, **83**, 549, 296.

39. X. Zhang, H. Chen, Z. Zhou, B. Huang, Z. Wang, M. Jiang and Y. Yang, *Macromolecular Chemistry and Physics*, 1994, **195**, 3, 1063.

40. N. Ishihara, T. Seimiya, M. Kuramoto, and M. Uoi, *Macromolecules*, 1986, **19**, 9, 2464.

41. A. Zambelli, P. Longo, C. Pellecchia and A. Grassi, *Macromolecules*, 1987, **20**, 8, 2035.

42. M. Kobayashi, T. Nakaoki and M. Uoi, *Polymer Preprints Japan*, 1988, **37**, 432.

43. O. Greis, T. Asano, J. Xu and J. Petermann, *Zeitschrift für Kristallographie*, 1988, **182**, 58.

44. A. Immirzi, F. de Candia, P. Iannelli, A. Zambelli and V. Vittoria, *Die Makromolekulare Chemie, Rapid Communication*, 1988, **9**, 11, 761.

45. V. Vittoria, F. de Candia, P. Iannelli and A. Immirzi, *Die Makromolekulare Chemie, Rapid Communication*, 1988, **9**, 11, 765.

46. N. Ishihara, M. Kuramoto and M. Uoi, *Macromolecules*, 1988, **21**, 12, 3356.

47. R.A. Nyquist, *Applied Specroscopy*, 1989, **43**, 3, 440.

49. P.C. Painter and J.L. Koenig, *Journal of Polymer Science: Polymer Physics Edition*, 1977, **15**, 11, 1885.

50. B. Jasse, R.S. Chao and J.L. Koenig, *Journal of Raman Spectroscopy*, 1979, **8**, 5, 244.

48. B. Jasse and L. Monnerie, *Journal of Molecular Structure*, 1977, **39**, 2, 165.

51. N.M. Reynolds, J.D. Savage and S.L. Hsu, *Macromolecules*, 1989, **22**, 6, 2867.

52. E.J.C. Kellar, C. Galiotis and E.H. Andrews, *Macromolecules*, 1996, **29**, 10, 3515.

53. G. Guerra, V.M. Vitagliano, C. De Rosa, V. Petraccone and P. Corradini, *Macromolecules*, 1990, **23**, 5, 1539.

54. P. Corradini and G. Guerra, *Advances in Polymer Science*, 1992, **100**, 183.

55. N.M. Reynolds and S.L. Hsu, *Macromolecules*, 1990, **23**, 14, 3463.

56. R.A. Nyquist, C.L. Putzig, M.A. Leugers, R.D. McLachlan and B. Thill, *Applied Specroscopy*, 1992, **46**, 6, 981.

57. M. Kobayashi, T. Nakaoki and N. Ishihara, *Macromolecules*, 1989, **22**, 11, 4377.

58. G. Conti, E. Santoro, L. Resconi and G. Zerbi, *Microchimica Acta*, 1987, **1**, 1-6, 297.

59. T. Isemura, Y. Jitsugiri and S. Yonemori, *Journal of Analytical and Applied Pyrolysis*, 1995, **33**, 103.

60. T. Nonobe, H. Ohtani, T. Usami, T. Mori, H. Fukumori, Y. Hirata and S. Tsuge, *Journal of Analytical and Applied Pyrolysis*, 1995, **33**, 121.

61. L. Dong, D.J.T. Hill, J.H. O'Donnell and A.K. Whittaker, *Macromolecules*, 1994, **27**, 7, 1830.

62. G.R. Quinting and R. Cai, *Macromolecules*, 1994, **27**, 22, 6301.

63. C. Griesinger, O.W. Sorensen and R.R. Ernst, *Journal of Magnetic Resonance*, 1989, **84**, 1, 14.

64. G.M. Clore and A.M. Gronenborn, *Progress in Nuclear Magnetic Resonance Spectroscopy*, 1991, **23**, 1, 43.

65. *Two-Dimensional Nuclear Magnetic Resonance Spectroscopy: Applications for Chemists and Biochemists*, Eds., W.R. Croasmun and R.M.K. Carlson, VCH Publishers, New York, NY, USA, 1994.

66. J. Cavanagh, W.J. Fairbrother, A.G. Palmer III and N. Skelton, *Protein NMR Spectroscopy, Principles and Practice*, Academic Press, New York, NY, USA, 1996.

67. B. Schneider, J. Storr, D. Daskoulova, M. Kolinsky, S. Sykora and D.Lim in *Proceedings of the International Symposium on Macromolecular Chemistry*, Prague, 1965.

68. B. Schneider, J. Štokr, M. Kolínský, M. Ryska and D. Lím, *Journal of Polymer Science Part A-1: Polymer Chemistry,* 1967, **5**, 8, 2013.

69. Y. Abe, M. Tasumi, T. Shimanouchi, S. Satoh and R. Chûjô, *Journal of Polymer Science Part A-1: Polymer Chemistry,* 1966, **4**, 6, 1413.

70. E. Ando, A. Nishoika and S. Wanatabe, *Polymer Journal (Japan)*, 1972, **3**, 3, 403.

71. N. Nakayama, A. Aoki and T. Hayashi, *Macromolecules*, 1994, **27**, 1, 63.

73. P.L. Rinaldi, L. Li, D.R. Hensley, D.G. Ray and H.J. Harwood, *Macromolecular Symposia*, 1994, **86**, 15.

74. P.L. Rinaldi, L. Li, D.G. Ray, G.S. Hafvann, H.T. Wong and H.J. Harwood in *Multidimensional Spectroscopy of Polymers*, Eds., M.W. Urban and T. Provder, ACS Symposium Series, No.598, ACS, Washington, DC, USA, 1995, p.213.

72. L. Li and P.L. Rinaldi, *Macromolecules*, 1996, **29**, 13, 4808.

75. L. Li and P.L. Rinaldi, *Macromolecules*, 1997, **30**, 3, 520.

76. R.E. Cais and J.M. Kometani in *NMR and Macromolecules*, Ed., J.C. Randall, ACS Symposium Series No.247, ACS, Washington, DC, USA, 1984, p.153.

77. F.A. Bovey and G.V.D. Tiers, *Journal of Polymer Science Part A-1: Polymer Chemistry,* 1960, **44**, 143, 173.

78. F.C. Schilling, F.A. Bovey, M.D. Bruch and S.A. Kozlowski, *Macromolecules*, 1985, **18**, 7, 1418.

79. M.W. Crowther, N.M. Szeverenyi and G.C. Levy, *Macromolecules*, 1986, **19**, 5, 1333.

80. M.W. Crowther, N.M. Szeverenyi and G.C. Levy, *Macromolecules*, 1986, **19**, 5, 1333.

81. G. Moad, E. Rizzardo, D.H. Solomon, S.R. Johns and R.I. Willing, *Macromolecules*, 1986, **19**, 10, 2494.

82. W-G. Hiller, H. Pasch and I.V. Lampe, *Macromolecular Chemistry and Physics*, 1991, **192**, 6, 1431.

83. T-M. Wu, T-F. Yin and S-F. Hsu, *Journal of Macromolecular Science B: Physics*, 2004, **43**, 2, 329.

84. O. Tarallo and V. Petraccone, *Macromolecular Chemistry and Physics*, 2004, **205**, 10, 1351.

85. H. Ishizawa, T. Nakano, T. Yade, M. Tsuji, O. Nakagawa and T. Yamaguchi, *Journal of Polymer Science Part A: Polymer Chemistry*, 2004, **42**, 18, 4656.

86. W. Jiang, W. Yang, X. Zeng and S. Fu, *Journal of Polymer Science Part A: Polymer Chemistry*, 2004, **42**, 3, 733.

87. T. Kawamura, N. Toshima and K. Matsuzaki, *Die Makromolekulare Chemie, Rapid Communications*, 1993, **14**, 11, 719.

88. T. Kawamura, N. Toshima and K. Matsuzaki, *Macromolecular Chemistry and Physics*, 1994, **195**, 7, 2667.

89. T. Nonobe, S. Tsuge, H. Ohtani, T. Kitayama and K. Hatada, *Macromolecules*, 1997, **30**, 17, 4891.

90. A. Spyros, P. Dais and F. Heatley, *Macromolecular Chemistry and Physics*, 1994, **195**, 9, 3271.

91. M. Suchopárek, J. Spevácek and B. Masar, *Polymer*, 1994, **35**, 16, 3389.

92. P.K. Dhal, G.N. Babu and A. Steigel, *Polymer*, 1989, **30**, 8, 1530.

93. J. R. Ebdon, *Journal of Macromolecular Science A*, 1974, **8**, 2, 417.

94. B. Ibrahim, A.R. Katritzky, A. Smith and D.E. Weiss, *Journal of the Chemical Society, Perkin Transactions 2*, 1974, **13**, 1537.

95. G. Heublein, W. Freitag and H. Schuetz, *Faserforschung und Textiltechnik*, 1975, 498.

96. G. Smets and W. Van Humbeeck, *Journal of Polymer: General Papers,* 1963, **1**, 4, 1227.

97a. M.M. Kusakov, A.Y. Koshevnick, L.I. Mekenetskaya, L.M. Shulipine, Y.B. Amerik and L.K. Golova, *Vyskomolekulyarnye Soedineniya Seria B*, 1973, **15**, 3, 150.

97b. D. Strasilla and E. Klesper, *Journal of Polymer Science: Polymer Letters Edition,* 1977, **15**, 4, 199.

98a. T. Suzuki and H.J. Harwood, ACS, Division of Polymer Chemistry Preprints, 1975, **16**, 1, 638.

98b. N.N. Aylward, *Journal of Polymer Science Part A-1: Polymer Chemistry*, 1970, **8**, 2, 319.

99a. J. Spevácek and B. Schneider, *Die Makromolekulare Chemie,* 1975, **176**, 3, 729.

99b. K. Ito and Y. Yamashita, *Journal of Polymer Science Part A-1: Polymer Chemistry*, 1966, **4**, 3, 631.

100a. K. Matsuzaki, T. Kanai, T. Kawamura, S. Matsumoto and T. Uryu, *Journal of Polymer Science: Polymer Chemistry Edition,* 1973, **11**, 5, 961.

100b. C.C. Price and R. Spector, *Journal of the American Chemical Society*, 1965, **87**, 9, 2069.

101a. K. Hatada, K. Ohta, Y. Okamoto, T. Kitayama, Y. Umemura and H. Yuki, *Journal of Polymer Science: Polymer Letters Edition,* 1976, **14**, 9, 531.

101b. C.C. Price, R. Spector and A.L. Tumolo, *Journal of Polymer Science Part A-1: Polymer Chemistry*, 1967, **5**, 2, 407.

102a. G. Heublein, R. Boerner and H. Schnetz, *Faserforschung und Textiltechnik*, 1978, **29**, 317. [*Chemical Abstracts*, 1978, **88**, 191695c]

102b. C.C. Price, M.K. Akkapeddi, B.T. DeBona, B.C. Furie, *Journal of the American Chemical Society*, 1972, **94**, 11, 3964.

103a. T. Suzuki, K. Mitani, Y. Takegami, J. Furukawa, E. Kobayashi and Y. Arai, *Polymer Journal Japan*, 1974, **6**, 6, 496.

103b. T. Uryu, H. Shimazu and K. Matsuzaki *Journal of Polymer Science: Polymer Letters Edition,* 1973, **11**, 4, 275.

104. N. Oguni, S. Watanabe, M. Maki and H. Tani, *Macromolecules*, 1973, **6**, 2, 195.

105. C.C. Price and A.L. Tumolo, *Journal of Polymer Science Part A-1: Polymer Chemistry*, 1967, **5**, 1, 175.

106. E.J. Vandenberg, *Journal of Polymer Science Part A-1: Polymer Chemistry*, 1969, **7**, 2, 525.

107. H. Tani, N. Oguni and S. Watanabe, *Journal of Polymer Science Part B: Polymer Letters*, 1968, **6**, 8, 577.

108. J. Schaefer, *Macromolecules*, 1969, **2**, 5, 533.

109. N. Oguni, K. Lee and H. Tani, *Macromolecules*, 1972, **5**, 6, 819.

110. N. Oguni, S. Shinohora and K. Lee, *Polymer Journal*, 1979, **11**, 10, 755.

111. C. Booth, W.C.E. Higginson and E. Powell, *Polymer*, 1964, **5**, 479.

112. K. Alyürük, T. Özden and N. Colak, *Polymer*, 1986, **27**, 12, 2009.

113. N. Uryu and K. Alyürük, *Journal of Polymer Science Part A: Polymer Chemistry*, 1989, **27**, 5, 1749.

114. P.J. Flory, *Transactions of the Faraday Society*, 1955, **51**, 848.

115. C. Booth, C.J. Devoy, D.V. Dodgson and I.H. Hillier, *Journal of Polymer Science Part A-2: Polymer Physics*, 1970, **8**, 4, 519.

116. E. Chiellini, P. Salvadori, M. Osgan and P. Pino, *Journal of Polymer Science Part A-1: Polymer Chemistry*, 1970, **8**, 6, 1589.

117. W. Lapeyre, H. Cheradame, N. Spassky and P.J. Sigwalt, *Journal de Chimie Physique et de Physico-Chimie de Biologique*, 1973, **70**, 838.

118. J. Schaefer, *Macromolecules*, 1972, **5**, 5, 590.

119. K. Miura, T. Kitayama, K. Hatada and T. Nagata, *Polymer Journal*, 1993, **25**, 697.

120. Y.B. Kissin, Y.Y. Gol'dfarb, Y.V. Novoderzhkin and B.A. Krentsel, *Vyskomolekulyarnye Soedineniya Seria B*, 1976, **18**, 3, 167.

121. J. Leonard and S.L. Malhotra, *Journal of Polymer Science: Polymer Chemistry Edition,* 1974, **12**, 10, 2391.

122. D.H. Richards and R.L. Williams, *Journal of Polymer Science: Polymer Chemistry Edition,* 1973, **11**, 1, 89.

123. G.V.D. Tiers and F.A. Bovey, *Journal of Polymer Science Part A: General Papers*, 1963, **1**, 3, 833.

124. G. Smets and W. Humbrecks, *Journal of Polymer Science Part A: General Papers*, 1964, **1**, 4, 1901.

125. S. Brownstein and D.M. Wiles, *Journal of Polymer Science Part A: General Papers*, 1964, **2**, 4, 1901.

126. M. Murano and R. Yamadera, *Journal of Polymer Science Part A-1: Polymer Chemistry*, 1967, **5**, 8, 1855.

127. K. Matsuzaki, M. Okada and T. Uryu, *Journal of Polymer Science Part A-1: Polymer Chemistry*, 1971, **9**, 6, 1701.

128. K. Fujii, S. Brownstein and A.M. Eastham, *Journal of Polymer Science Part A-1: Polymer Chemistry*, 1968, **6**, 8, 2387.

129. W. Cooper, F. R. Johnston and G. Vaughan, *Journal of Polymer Science Part A: General Papers*, 1963, **1**, 5, 1509.

130. K. Fujii, T. Mochizuki, S. Imoto, J. Ukida and M. Matsumoto, *Journal of Polymer Science Part A: General Papers*, 1964, **2**, 5, 2327.

131. M.J. Huchatathorn and M.J. Brock, *Journal of Polymer Science: Polymer Chemistry Edition*, 1975, **13**, 4, 945.

132. B. Ibrahim, A.R. Katritzky, A. Smith and D.E. Weiss, *Journal of the Chemical Society, Perkin Transactions 2*, 1974, **13**, 1537.

133. F. Keller, *Plaste und Kautschuk*, 1975, **22**, 1, 8.

134. T.K. Wu, D.W. Ovenall and G.S. Reddy, *Journal of Polymer Science: Polymer Physics Edition*, 1974, **12**, 5, 901.

135. M. Delfini, A. L. Segre and F. Conti, *Macromolecules*, 1973, **6**, 3, 456.

136. K. Matsuzaki, H. Ito, T. Kawamura and T. Uryu, *Journal of Polymer Science: Polymer Chemistry Edition*, 1973, **11**, 5, 971.

137. K. Matsuzaki, S. Okuzono, T. Kanai, *Journal of Polymer Science: Polymer Chemistry Edition*, 1979, **17**, 11, 3447.

138. K-F. Elgert and W. Ritter, *Die Makromolekulare Chemie,* 1976, **177**, 7, 2021.

139. J.C. Randall, *Macromolecules*, 1978, **11**, 3, 592.

140. C.J. Carman, *Macromolecules*, 1974, **7**, 6, 789.

141. M. Mauzac, J.P. Vairon and P. Sigwalt, *Polymer*, 1977, **18**, 11, 1193.

142. T. Okada and T. Ikushige, *Journal of Polymer Science: Polymer Chemistry Edition*, 1976, **14**, 8, 2059.

143. T.K. Wu, *Macromolecules*, 1973, **6**, 5, 737.

144. I.A. Abu-Isa, *Journal of Polymer Science Part A-1: Polymer Chemistry*, 1972, **10**, 3, 881.

145. I.A. Abu-Isa and M.E. Myers, Jr., *Journal of Polymer Science Part A-1: Polymer Chemistry*, 1973, **11**, 9, 225.

146. K.F. Elgart, H.J. Cantow and B. Stutzel, *Fresenius' Zeitschrift für Analytische Chemie International Edition*, 1973, **12**, 427.

147. K. Yokota and T. Hirabayashi, *Journal of Polymer Science: Polymer Chemistry Edition*, 1976, **14**, 1, 57.

148. K-F. Elgert and B. Stützel, *Polymer*, 1975, **16**, 10, 758.

149. B. Sandner, F. Keller and H. Roth, *Faserforschung und Textiltechnik*, 1975, **26**, 278.

150. Y. Yamashita, M. Yoshida, J. Kawasc, and K. Ito, *Chemical Abstracts*, 1974, **84**, 60070s.

151. W. Regel, L. Westfelt and H.J. Cantow, *Angewandte Chemie International Edition*, 1973, **12**, 5, 434.

152. C. Laurens, R. Ober, C. Creton and L. Léger, *Macromolecules*, 2004, **37**, 18, 6806.

153. M. Sepulchre, A. Kassamaly, M. Moreau and N. Spassky, *Macromolecular Chemistry and Physics*, 1988, **189**, 10, 2485.

154. M.A. Gomez, G. Ellis and C. Marco, *Revista de Plasticos Modernos*, 2002, **83**, 552, 582.

155. P.G. Brown and K. Fujimori, *Polymer Bulletin*, 1993, **30**, 6, 641.

156. G.R. Butler, C.H. Do and M.G. Zerner, *Journal of Macromolecular Science A,* 1989, **26**, 8, 1115.

157. P.G. Brown and K. Fujimori, *European Polmer Journal*, 1994, **30**, 10, 1097.

158. E. Tart, G. Wood, D. Wernsman, U. Sangwatanaroj, C. Howe, Q. Zhou, S. Zhang and A. E. Tonelli, *Macromolecules*, 1993, **26**, 16, 4283.

159. T. Kawamura, N. Toshima, K. Matsuzaki, K. Okuyama and T. Uryu, *Die Makromolekulare Chemie, Rapid Communication*, 1994, **15**, 10, 157.

160. S. Bronio, G. Consiglio, R. Hutter, A. Batistini and U.W. Suter, *Macromolecules*, 1994, **27**, 16, 4436.

161. C-M. Kuo, J.C. Saam and R.B. Taylor, *Polymer Intenational*, 1994, **33**, 2, 187.

162. T.C. Masterman, N.R. Dando, D.G. Weaver and D. Seyferth, *Journal of Polymer Science Part B: Polymer Physics*, 1994, **32**, 13, 2263.

163. T. Kanezaki, K. Kume, K. Sato and T. Asakura, *Polymer*, 1993, **34**, 14, 3129.

164. V. Busico, P. Corradini, R. De Biasio, L. Landriani and A.L. Segre, *Macromolecules*, 1994, **27**, 16, 4521.

165. K.R. Lindfors, S. Pan and P. Dreyfuss, *Macromolecules*, 1993, **26**, 11, 2919.

166. P.G. Brown and K. Fujimori, *Polymer Bulletin*, 1992, **29**, 1-2, 85.

167. T. Kawamura, N. Toshima and K. Matsuzaki, *Macromolecular Chemistry and Physics*, 1994, **195**, 10, 3343.

168. A. Abe and N. Nishoika, *Kobunshi Kagaku*, 1972, 29, 326, 448.

169. I.V. Kumpanenko and N.V. Chukanov, *Tenbir-Texte Phys*, 1986, **9**, 92.

170. H.N. Cheng, *Macromolecular Theory and Simulations*, 1994, **3**, 6, 979.

9 Regioisomerism

As well as stereoisomerism and geometrical isomerism, polymers and copolymers can exhibit a third form of isomerism known as regioisomerism. Head-to-head, head-to-tail and tail-to-head isomerism is well known in the case of simple organic compounds, thus, a dimer of styrene monomer can exist in three different structural forms.

9.1 Polypropylene Homopolymer

For isotactic polypropylene, as shown in structure 9.2, six different placements are possible when considering triads. ^{13}C-NMR spectroscopy can be used to determine isolated head-to-head and tail-to-tail units in polypropylene (PP). Polypropylenes produced using vanadyl catalysts possessed the normal head-to-tail structure [1]. More detailed examination, however shows that the amorphous fractions isolated from these PP do show (IR) absorption at 13.3 μm pointing to the presence of methylene sequences of two units, which can only mean tail-to-tail arrangement of propylene units does occur. A very small absorption peak at 13.3 μm was also found in the spectrum of the crystalline fractions. Polypropylenes prepared with catalysts based on VCl_3 show only the normal head-to-tail arrangement in both amorphous and crystalline fractions, as do polymers prepared from $TiCl_3$ catalyst. The amount of propylene units coupled tail-to-tail was estimated to range from 5 to 15% for the amorphous and from 1 to 5% for the crystalline fractions.

The amount of propylene units in tail-to-tail arrangement was calculated from spectra of thin films by comparing the ratio of the absorbances at 13.60 μm and 8.65 μm in the spectrum of hydrogenated natural rubber. This implies the assumption that the absorbance per CH_2 group is the same at 13.30 μm for $(CH_2)_2$ sequences as at 13.60 μm for $(CH_2)_3$ sequences.

The differences in amount of tail-to-tail coupled units between crystalline and amorphous fractions are to be expected, since every head-to-head and tail-to-tail configuration disturbs the regularity of the isotactic chain. In the PP every tail-to-tail configuration must necessarily be accompanied by a head-to-head coupling.

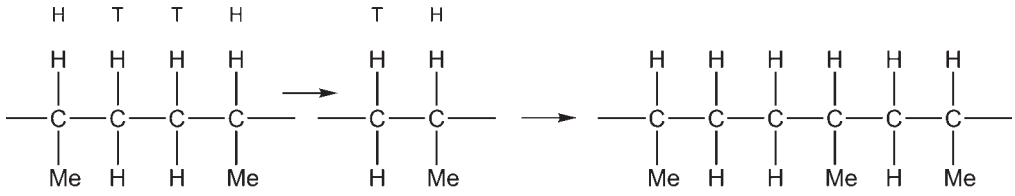

(1)

(2)
Tail to tail – Head to tail

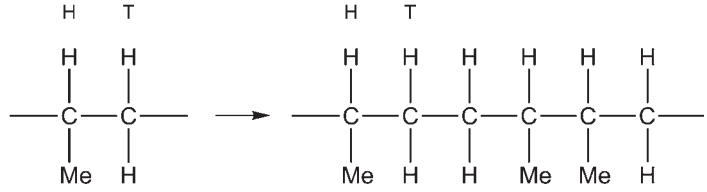

(3)
Tail to tail – Head to head

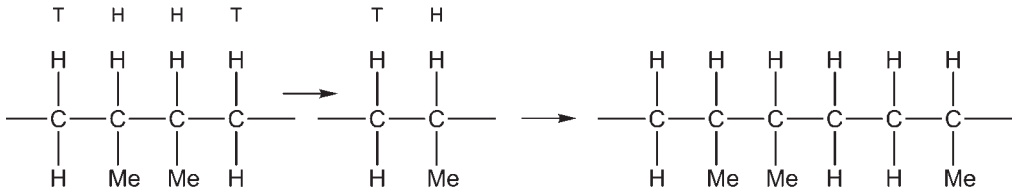

(4)

(5)
Head to head – tail to tail

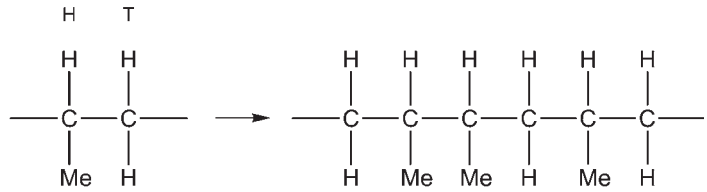

(6)
Head to head – tail to head

This would be expected to show up in an absorption peak at 8.8 to 9.0 μm characteristic of the structure:

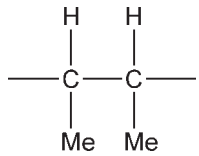

which is also found in hydrogenated poly-2,3,-dimethylbutadiene, used as a model compound and in alternating copolymers of ethylene and butene-2 [2]. In the PP examined by Van Schooten and Mostert [3] and in ethylene-propylene copolymers, they did indeed find an absorption band near 9.0 μm, although, unlike Van Schooten and co-workers [3] (see above) it is much less sharp than in the model compound.

All spectra containing the 13.3 μm peak show a further small band at 10.9 μm which is also found in the spectrum of poly-2,3-dimethylbutadiene. To summarise, the IR spectrum of amorphous PP prepared using vanadyl catalysts in addition to normal head-to-tail structures -CH CH_3-CH_2-CH CH_3-CH_2- shows the following features:

Absorption	Characteristic of	also found in
13.3 μm * tail to tail	methylene sequences of two units, i.e. tail to tail arrangement of propylene units	polybutene-2 ethylene alternating polymer

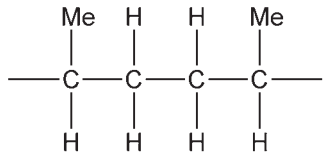

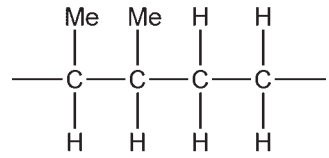

ethylene-propylene copolymer (tail to tail)

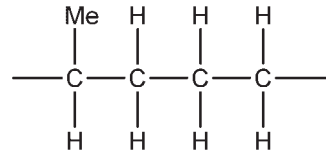

in polypropylene every tail to tail coupling accompanied by head to head coupling

9.0 μm head to head

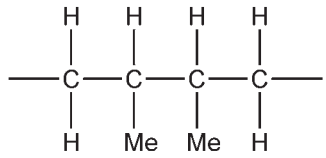

polybutene-2 ethylene alternating copolymer

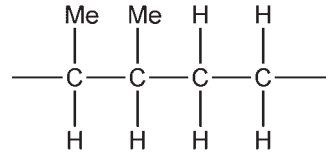

hydrogenated 2,3 dimethylbutadiene

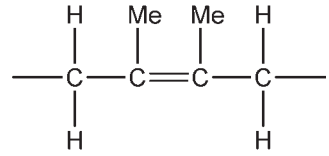

ethylene-propylene copolymer (head to head

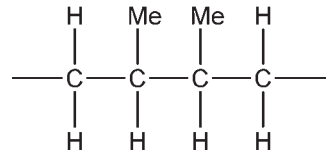

* All ethylene propylene and PP polymers showing an absorbance at 13.3 μm also show small absorbance at 10.9 μm which is also found in poly 2,3-dimethylbutadiene.

9.2 Polypropylene-1-Ethylene Copolymer

Ethylene-propylene copolymers can contain up to four types of sequence distribution of monomeric units. These are propylene-propylene (head-to-tail and head-to-head), ethylene-propylene and ethylene to ethylene:

(1) 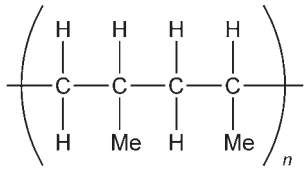

Head to tail isotactic

(2) 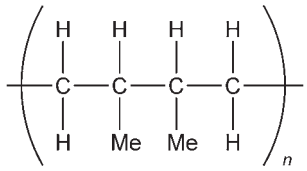

Head to tail isotactic

(3) 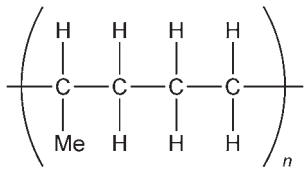

Ethylene-propylene

(4) 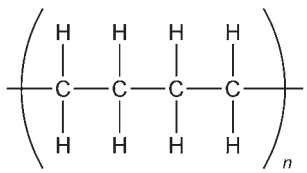

Ethylene-ethylene

In addition, other stereochemical placements could occur, e.g., syndiotactic head-to-tail and head-to-head polypropylene units:

(5) 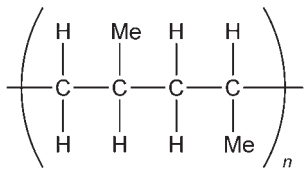

Head to tail syndiotactic

(6) 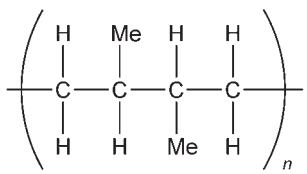

Head to head syndiotactic

Sequences 1-4 depicted in structure 9.5 and their average sequence lengths of both monomer units, can be measured by the Tanaka and Hatada [4] method. Measurements were made at 15.1 MHz. Assignments of the signals were carried out by using the method of Grant and Paul [5], and also by comparing the spectra with those of squalane, hydrogenated natural rubber, polyethylene and atactic polypropylene. The accuracy and the precision of intensity measurements, that is the deviation from the theoretical values and the scatter of the measurements, respectively, were checked for the spectra of squalane and hydrogenated natural rubber, and were shown to be at most 12% for most of the signals.

IR spectroscopy also provides information on regioisomerism in ethylene propylene copolymers. The fact that the polypropylenes prepared with $VOCl_{3-}$ or $VO(OR)_{3-}$ containing catalysts show tail-to-tail arrangement means that tail-to-tail coupling of propylene units may also occur in the ethylene-propylene copolymers. However, because the content of $(CH_2)_2$ sequences in the copolymers is much higher than in the PP prepared with the same catalysts, a large part of these sequences most likely stems from isolated ethylene units between two head-to-head oriented propylene units, their relative amount depending on the ratio of reaction rates of formation of the sequences.

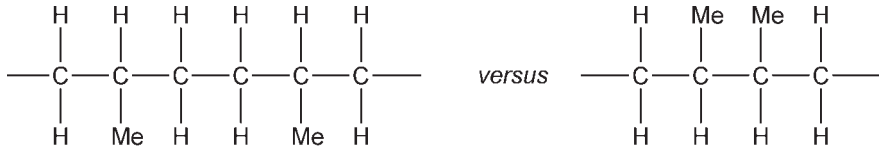

An absorption at 13.3 μm which is characteristic of methylene sequences of two units is characteristic of a tail-to-tail configuration of ethylene and propylene units. This absorption is also found in polybutene-2-ethylene copolymer:

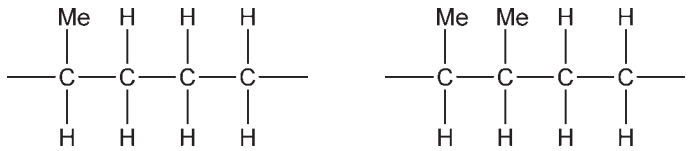

An absorption of 9.0 μm which is characteristic of a head-to-head configuration of the polypropylene units, i.e.,

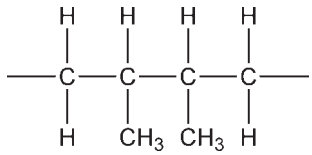

Is found in amorphous ethylene-propylene alternating copolymers and in polybutene-2-ethylene alternating copolymer and in hydrogenated poly 2,3-dimethyl butadiene:

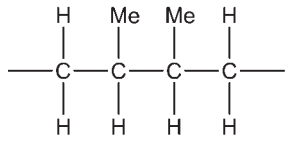

Ethylene-propylene copolymer (head to head)

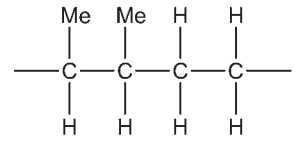

Polybutene-1-ethylene alternating copolymer

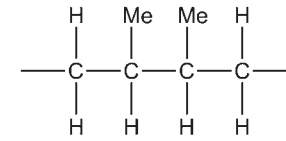

Hydrogenated poly-2,3-dimethyl butadiene

9.3 Polybutadiene-1-Ethylene Copolymer

The infrared spectrum of amorphous alternating polybutene-1-ethylene copolymer shows absorptions at 13.3 μm, characteristic of methylene sequences of two units and at 9 μm characteristic of the structure:

An absorption at 10.8 μm, also found in hydrogenated poly 2,3-dimethyl-butadiene confirms the above structure.

9.4 Poly-2,3-dimethyl Butadiene

Hydrogenated poly 2,3-dimethyl butadiene has a strong IR absorption at 9.0 μm confirming a head-to-head configuration of two propylene units in the hydrogenated polymer:

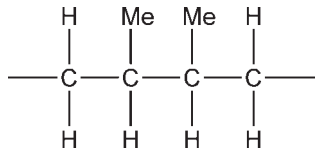

and the following structure for the unhydrogenated polymer:

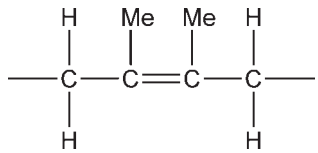

9.5 Polybutadiene

In the case of dimers many regioisometric configurations are possible. Polybutadiene unsaturation occurs in three forms: *trans*-1,4, *cis*-1,4 and vinyl-1,2:

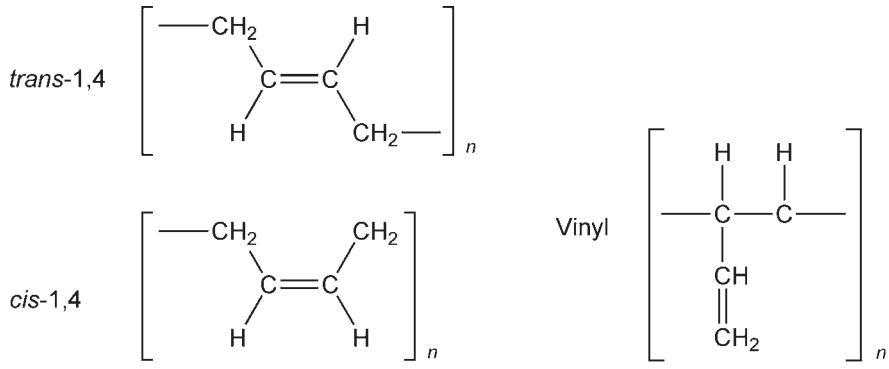

No opportunity for regioisomerism exists in the *cis* and *trans* -1,4 configurations but it does in the case of the vinyl-1,2 unsaturation:

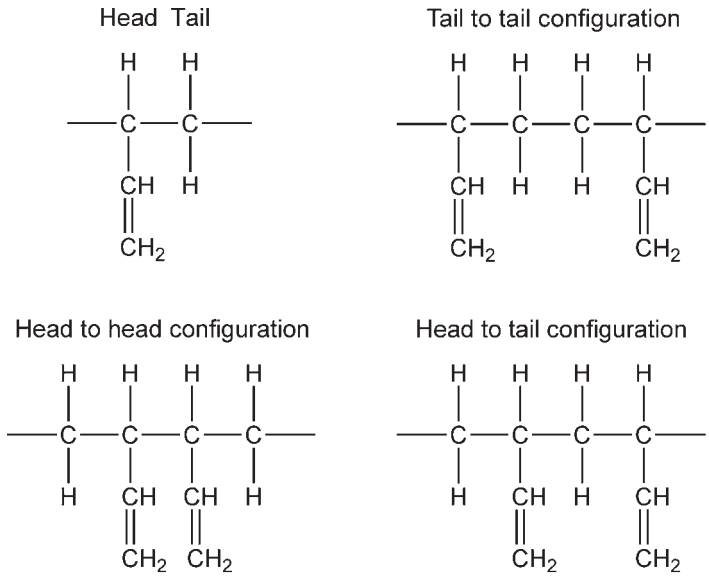

9.6 Polyisoprene

Due to the methyl group, opportunities for regioisomerism exists for all four types of unsaturation present in polyisoprene:

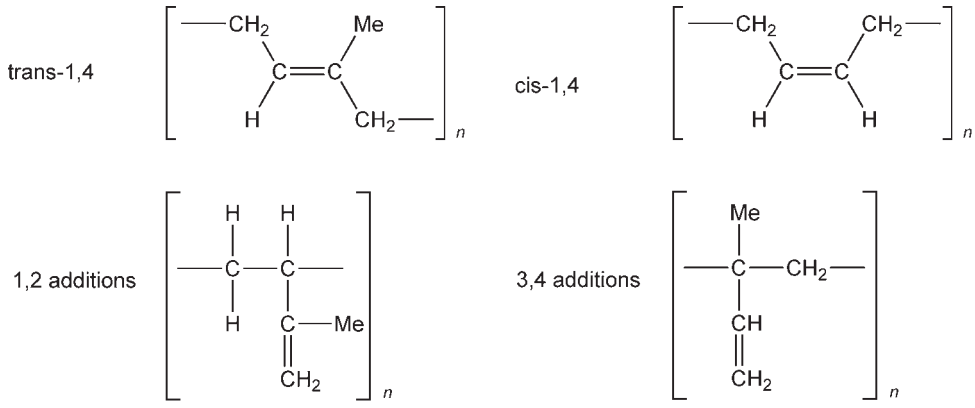

1) Regioisomerism in *trans*-1,4 polyisoprene:

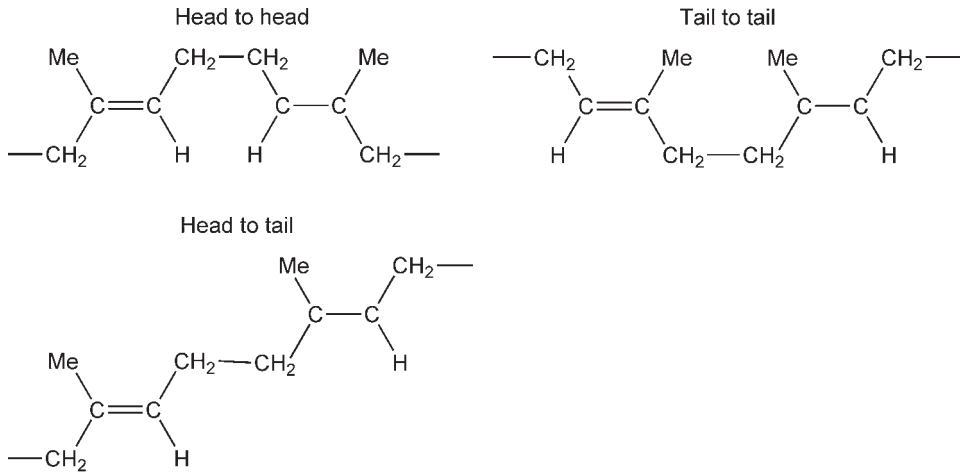

2) Regioisomerism in *cis*-1,4 polyisoprene:

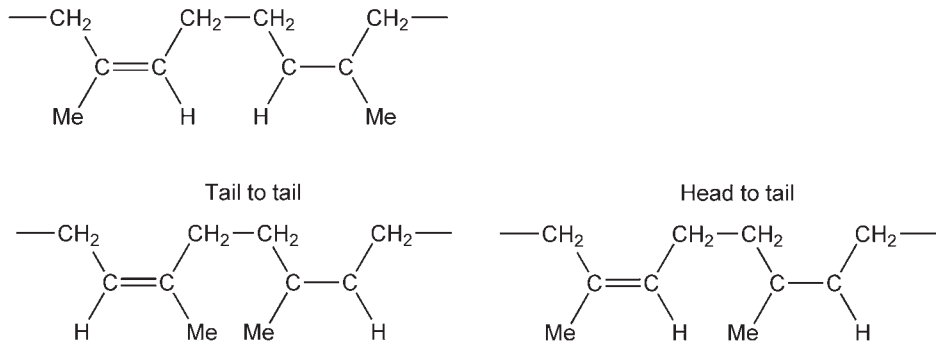

3) Regioisomerism in 1,2 polyisoprene:

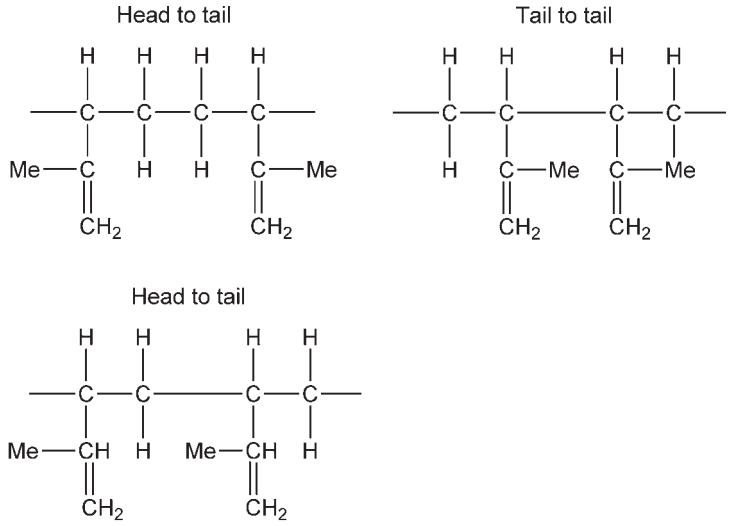

4) Regioisomerism in 3,4 polyisoprene:

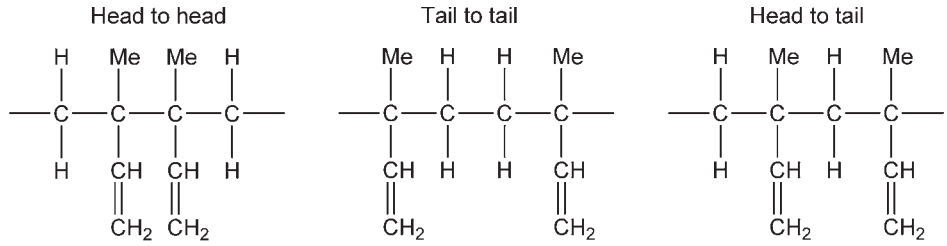

9.7 Polypropylene Glycols

Ozonisation followed by lithium aluminium hydride reduction to oxyalkylene groups has been used to study the occurrence of regioisomerism in polypropylene glycol. Adopting the following nomenclature for propylene glycol:

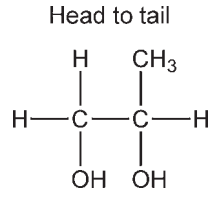

then the following three sequences are possible in PPG:

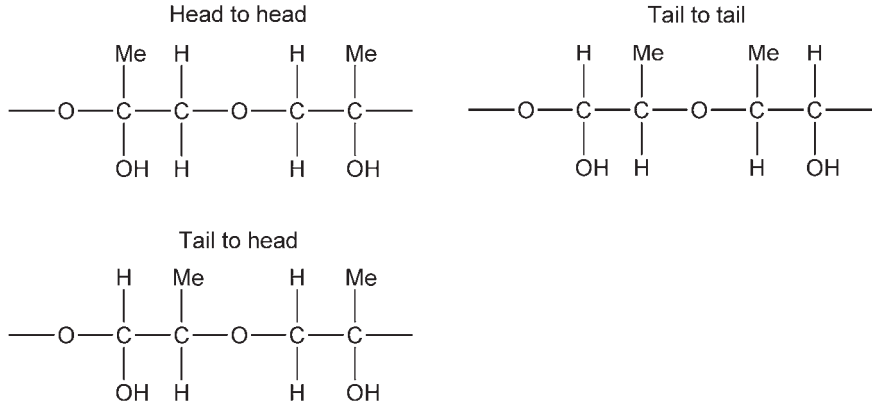

If these sequences occurred consecutively in PPG then it would have the structure:

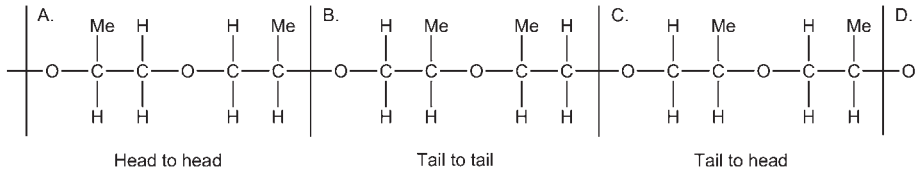

Upon ozonolysis, fission occurs at points A, B, C and D to produce aldehydic and ketonic groups:

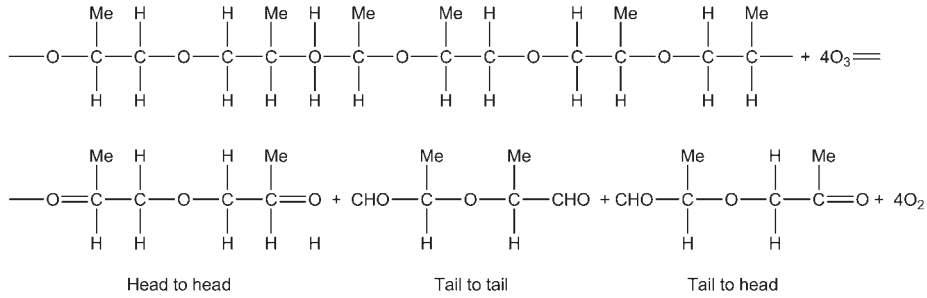

Upon reduction with lithium and aluminium hydride the following diglycols are produced:

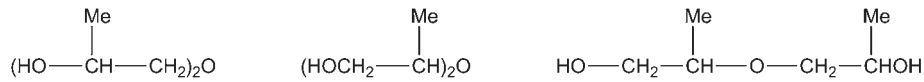

Secondary propylene glycol (head to head)

Primary propylene glycol (tail to tail)

Primary - secondary propylene glycol (tail to head)

From the relative amounts of these three glycols produced, determined by gas chromatography, the amounts of head-to-head, tail-to-tail and tail-to-head configurations can be deduced. Note that the di-primary propylene glycol occurs in two optically active forms, l (a) and (b):

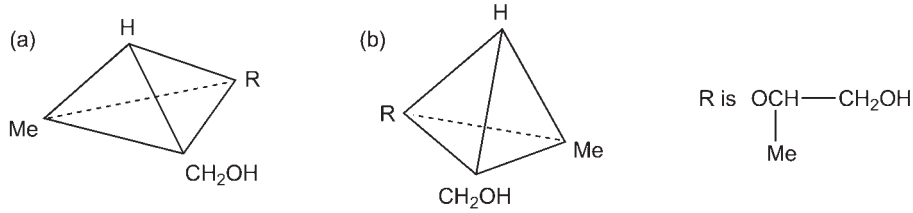

9.8 Polyepichlorohydrin

Epichlorohydrin (ECH) is a cyclic triad:

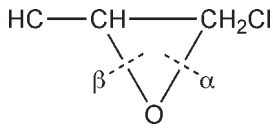

With one oxygen atom, one methine carbon atom with a chloromethylene substituent, and a methylene carbon atom. Because the methine carbon atom has four different substituents, i.e., O, CH_3, CH_2 and CH_2Cl, the monomer exists in both *R* and *S* configurations and can be resolved into pure stereoisomers [6].

The ring-opening polymerisation of ECH can produce polyepichlorohydrin (PECH), -[-O-CH(CH_2Cl)-CH_2-]-$_n$, with a broad range of microstructures that depend on the mode of ring-opening promoted by the initiator and the optical purity of the monomer. In all cases, each of the backbone carbon atoms of PECH is adjacent to an oxygen atom and the chemical shifts observed in their NMR spectra are shifted accordingly. There are two carbon-oxygen (C-O) bonds in the monomer. The sequence in which the C-O bond (β or α in the diagram) above cleaves during polymerisation determines whether the resulting PECH will have a regular head-to-tail structure, a regular head-to-head, tail-to-tail structure, or a more random structure. The head is represented as the -OCH(CH_2Cl)- end of the repeat unit, and the tail is represented as the -CH_2- end of the repeat unit. Polymerisation of a racemic monomer in a regular head-to-tail manner potentially results in PECH with the different stereochemical triads shown in **Figure 9.1**. In practice only the isotactic crystalline polymer has been prepared. Lindfors and co-workers [7] studied a crystalline PECH which had a regular (head-to-tail) isotactic structure with an excess, indicated by its optical

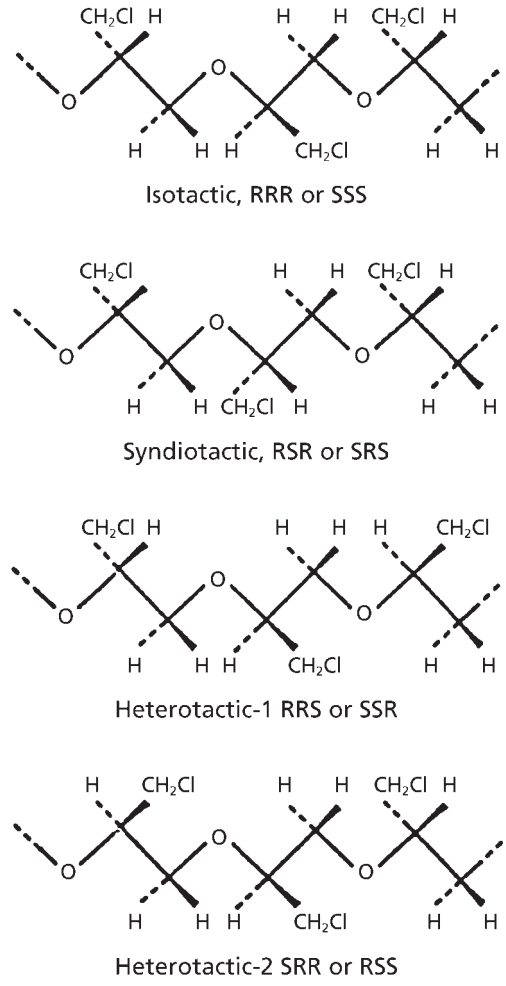

Figure 9.1 Different stereochemical triads of H-T PECH. (*From Author's own files*)

activity, of either -*RRR*- or -*SSS*- polymer chains. Regular *RRR* ... or *SSS*... chains result in identical NMR spectra. This type of isomerism has been studied previously and was not studied further by Lindfors and co-workers [7]. The crystalline polymer was used as an aid for making assignments of regiosequence resonances in the NMR spectra of the amorphous cationic polymer.

If during the ring-opening polymerisation both C-O bonds in ECH are subject to random cleavage, four regiosequence triads are possible for PECH. These are illustrated in **Figure 9.2**. The regular H-T structural sequence results in the regiosequence triad 1.

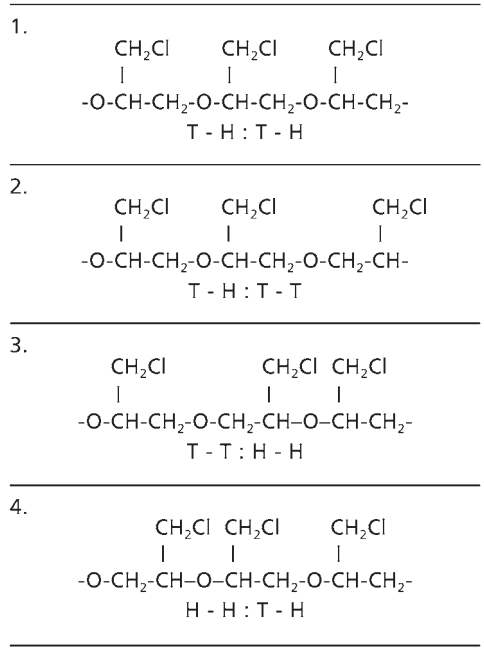

Figure 9.2 Possible regiosequence triads of PECH. (*Reprinted with permission from K.R. Lindfors, S. Pan and P. Dreyfuss, Macromolecules, 1993, 26, 11, 2919. ©1993, ACS [7]*)

For simplicity and clarity of labelling, Lindfors and co-workers [7] focused on the central monomer unit of the triad and the two adjacent carbon atoms, and have therefore called triad 1 T-H:T-H. That is regular H-T structural sequence leads to a T-H:T-H regiosequence triad. If during polymerisation, a single, isolated monomer reversal occurs, three additional regiosequence triads result. These are shown in Figure 9.2 as 2-4 or T-H:T-T, T-T:H-H, and H-H:T-H, respectively. The sequences were obtained by reversing the third (right) monomer unit for 2, the second (middle) monomer unit for 3, and the first (left) monomer unit for 4. By use of the techniques described next, NMR assignments for each of these triads were made and the concentration of each triad was determined. This information permits the first calculation directly from NMR data of the percentage of reversed (H-H, T-T) units, in an irregular PECH.

This 2D-NMR method is capable of analysing PECH to ascertain its regiosequence distribution. It consists of taking its heteroonuclear chemical shift correlation spectroscopy (THCSC) spectrum, integrating the peaks corresponding to the

regiosequence triads, and calculating the dyad concentrations using first-order Markovian statistics. Assignments of both the proton and carbon chemical shifts for the four possible regiosequence triads were made. Proton chemical shifts have not been reported previously. From integration of the peaks in the THCSCH spectrum, the concentration of each regiosequence in a cationic PEC was calculated. When these experimental triads were tested by first-order Markovian statistics, a fit was found for a polymer with short blocks of four to five monomer units resulting from β-cleavage of the ECH (H-T PECH) and the rest of the monomer units from α-cleavage of the ECH (H-H, T-T PECH). The cationic PECH was found to be ~63% H-T and ~37% H-H, T-T.

To reach these conclusions a variety of one-dimensional and 2D-NMR spectra of a cationic PECH were obtained and analysed. Similar spectra of a crystalline PECH aided in the analysis and simplified assignment of some peaks. The distorsionless enhancement by polarisation experiment provided information for CH, CH_2 and CH_2Cl peak identification. ^{13}C spectroscopy allowed basic assignment of the four regiosequence triads in cationic PECH. From two-dimensional *J*-resolved experiments, the heteronuclear coupling constants ($J_{C\text{-}H}$) and homonuclear coupling constants ($J_{H\text{-}H}$) were determined and proton chemical shifts were assigned for different regiosequences. From the THCSCH experiment, absolute proton assignments were correlated with their respective ^{13}C assignments. Chemical shifts and coupling constants for cationic PECH derived from the proton decoupled ^{13}C-NMR spectrum, and heteronuclear 2D *J*-resolved spectroscopy were in good agreement.

9.9 Other Polymers

Regioisomerism is also exhibited by other polymers including polyvinylidene fluoride, polyvinylidene chloride (PVDC) [8-11], polydienes and polyvinyl acetate [12, 13]. Head-to-tail and tail-to-tail sequences have been determined in PVDC [8-12] and polyvinyl acetate [12, 13, 14].

Gadda and co-workers [15] have used ^{1}H-NMR, ^{13}C-NMR, ^{19}F-NMR and ^{29}Si-NMR in the study of regioregularity in cyclotrisiloxane based polymers such as phenyl(3-trifluoromethylcyclotrisiloxone). They showed a high degree of regularity in which the trifluoromethyl electron withdrawing groups enhance stereoregularity. Hugger and co-workers [16] have discussed regiorandom and regioregular forms of poly(3-hexyl-thiophene). Wang and co-workers [17] have also discussed regioregularity in regioregular poly(3-dodecylthiophene). Tonzola and co-workers [18] characterised regioregular polymers containing bis(phenylquinoline) and regioregular dialkyl bithiophene utilising ^{1}H-NMR Fourier Transform IR spectroscopy and thermometric techniques.

References

1. J. van Schooten, E.W. Duck and R. Berkenbosch, *Polymer*, 1961, **2**, 357.
2. G. Natta, G. Dall'Asta, G. Mazzanti and F. Ciampelli, *Kolloid Zeitschrift*, 1962, **182**, 50.
3. J. van Schooten and S. Mostert, *Polymer*, 1963, **4**, 135.
4. Y. Tanaka and K. Hatada, *Journal of Polymer Science: Polymer Chemistry Edition*, 1973, **11**, 8, 2057.
5. D.M. Grant and E.G. Paul, *Journal of the American Chemical Society*, 1964, **86**, 15, 2984.
6. M.P. Dreyfuss in *Proceedings of the 8th Central Regional Meeting of the American Chemical Society*, Akron, OH, USA, 1976.
7. K.R. Lindfors, S. Pan and P. Dreyfuss, *Macromolecules*, 1993, **26**, 11, 2919.
8. F.A. Bovey , F.C. Schilling, T.K. Kwei and H.L. Frisch, *Macromolecules*, 1977, **10**, 3, 559.
9. K. Okuda, *Journal of Polymer Science Part A: General Papers*, 1964, **2**, 4, 1749.
10. R. Chûjô, S. Satoh and E. Nagai, *Journal of Polymer Science Part A: General Papers*, 1964, **2**, 2, 895.
11. J.L. McClanahan and S.A. Previtera, *Journal of Polymer Science Part A: General Papers*, 1965, **3**, 11, 3919.
12. A. Abe and N. Nishoika, *Kobunshi Kagaku*, 1972, **29**, 326, 402.
13. B. Ibrahim, A.R. Katritzky, A. Smith and D.E. Weiss, *Journal of the Chemical Society, Perkin Transactions 2*, 1974, **13**, 1537.
14. A. Abe and N. Nishoika, *Kobunshi Kagaku*, 1972, **29**, 326, 448.
15. T.M. Gädda, A.K. Nelson and W.P. Weber, *Journal of Polymer Science Part A: Polymer Chemistry*, 2004, **42**, 20, 5235.
16. S. Hugger, R. Thomann, T. Heinzel and T. Thurn-Albrecht, *Colloid and Polymer Science*, 2004, **282**, 8, 932.
17. W. Wang, K.C. Toh and C.W. Tjiu, *Macromolecular Chemistry and Physics*, 2004, **205**, 9, 1269.
18. C.J. Tonzola, M.M. Alam, B.A. Bean and S.A. Jenekhe, *Macromolecules*, 2004, **37**, 10, 3554.

10 Branching

Along with chemical composition, molecular weight, molecular weight distribution and type and amount of gel, branching is considered to be one of the fundamental parameters needed to characterise polymers fully, and this latter property, which is a microstructural feature of the polymer, has very important effects on polymer properties. Changes in branching of a given polymer such as polypropylene lead to changes in its stereochemical configuration and this, in turn, is a fundamental polymer property to formulating both polymer physical characteristics and mechanical behaviour. It is important, therefore, to be able to identify the type and amount of side-group branching in polymers.

Although molecular symmetry is well understood, until the development of proton nuclear magnetic resonance (NMR), and later ^{13}C-NMR, a study of this aspect of polymer structure presented problems. A knowledge of short and long chain branching in polymers and other aspects of polymer structure such as stereochemistry, *cis-trans* structures and regioisomerism supplies not only information about the reaction kinetics, but also about the relationship between polymer chain structure and properties.

10.1 Branching in Polyethylene

Low-density polyethylene (LDPE) has a very complex molecular structure despite the fact that it consists of only one monomeric unit, i.e., ethene. LDPE exhbits a broad molar mass distribution. As a result of intra- and inter-molecular chain transfer reactions, short and long chain branching (LCB) exists [1-4]. Revelation of the chain structure is increasingly recognised as a prerequisite, since the reaction kinetics determine the structure which in turn determines the properties. Thus, knowledge about the structure supplies not only information about the reaction kinetics, but also about the relationship between chain structure and properties. In the case of LDPE the most pronounced chain feature is the long chain branching which can occur in various chain architectures, i.e., comb or random [1, 2, 5, 6]. Revelation of the type as well as the number of long chain branching is still difficult.

10.1.1 Methyl Branching in Polyethylene

Nuclear Magnetic Resonance Spectroscopy

A regression analysis of infrared (IR), differential thermal analysis and X-ray diffraction data by Laiber and co-workers [7] for low-pressure polyethylene showed that, as synthesis conditions varied, the number of methyl groups varied from 0 to 15 per 1000 carbon atoms and the degree of crystallinity varied from 84 to 61%.

Saturated hydrocarbons evolved during electron irradiation of polyethylene (PE) are characteristic of short side-chains in the polymer. Salovey and Pascale [8] showed that a convenient analysis is effected by programmed temperature gas chromatography. In order to minimise the relative concentrations of extraneous hydrocarbons, i.e., those not arising from selective scission of complete side-chains, it is necessary to irradiate at low temperatures and doses. Such analyses of a high-pressure polyethylene indicate that the 20 to 30 methyls per 1000 carbon atoms detected in infrared absorption (low-pressure polyethylenes at least an order of magnitude lower) are probably equal amounts of ethyl and butyl branches. These arise by intramolecular chain transfer during polymerisation. At a dose of 10 Mrad about 1-4% of the alkyl group are removed. Methane is the only hydrocarbon detected on irradiation of polypropylene, indicating little combination of methyl radicals to form ethane during irradiation.

The measurement of the methyl absorption at 1378 cm^{-1} (7.26 μm) in polyethylene can serve as a good estimation of branching. However, interference from the methylene absorption at 1368 cm^{-1} (7.31 μm) makes it difficult to measure the 1368 cm^{-1} (7.31 μm) band, especially in the case of relatively low methyl contents.

Neilson and Holland [9] associate the amorphous phase absorption of polyethylene at 1368 cm^{-1} (7.31 μm) and 1304 cm^{-1} (7.69 μm) with the *trans-trans* conformation of the polymer chain about the methylene group. Therefore, the intensities of these two absorptions are proportional to one another. By placing an annealed film (approximately 0.3 - 0.4 mm) of high-density polyethylene (HDPE) in the reference beam of a double beam spectrometer and a thin, quenched film of the sample in the sample beam, most of the interference at 1368 cm^{-1} (7.31 μm) can be removed. The method has the advantage that it is not necessary to have complete compensation for the 1368 cm^{-1} (7.31 μm) band since a correction for uncompensation at 1378 cm^{-1} (7.25 μm) can be applied based on the intensity of the 1368 cm^{-1} (7.31 μm) absorption.

A calibration for the methyl absorption based on mass spectrometric studies of such gaseous products produced during electron bombardment of polyethylene has demonstrated irradiation-induced detachment of complete alkyl units [10]. In addition to saturated alkanes characteristic of the branches, small quantities of

methane, other paraffins, and olefins were simultaneously evolved. It was suggested that 'extraneous' paraffins result from cleavage of the main chain [10, 11]. Nerheim [12] has described a circular calibrated polymethylene wedge for the compensation of CH_2 interferences in the determination of methyl groups in polyethylene by infrared spectroscopy.

Methyl group content of LDPE has been determined with a standard deviation of 0.8% provided methylene group absorptions were compensated by polyethylene of similar structure [13].

Nishoika and co-workers [14] determined the degree of chain branching in LDPE using proton NMR, Fourier transform (FT) NMR (FT-NMR) at 100 MHz and ^{13}C FT-NMR at 25 MHz with concentrated solutions at approximately 100 °C. The methyl concentrations agreed well with those of infrared based on the absorbance at 1378 cm^{-1} (7.25 μm).

10.1.2 Ethyl and Higher Alkyl Groups Branching in Polyethylene

High-density (low-pressure) polyethylenes are usually linear, although the physical and rheological properties of some HDPE have suggested the presence of long chain branching (butyl and higher groups) at a level one to two orders of magnitude below that found for LDPE prepared by a high-pressure process. A measurement of long chain branching in HDPE has been elusive because of the low concentrations involved [16] and can only be directly provided by high-field, high-sensitivity NMR spectrometers.

HDPE prepared with a Ziegler type, titanium-based catalyst have predominantly *n*-alkyl or saturated end-groups. Those prepared with chromium-based catalysts have a propensity toward more olefinic end-groups. The ratio of olefinic to saturated end-groups for polyethylenes prepared with chromium-based catalysts is approximately unity. The end-group distribution is therefore another structural feature of interest in low-pressure polyethylenes, because it can be related to the catalyst used, and possibly to the extent of long chain branching. It is possible not only to measure by ^{13}C-NMR concentrations of saturated end-groups, but also the olefinic end-groups and, subsequently, an end-group distribution.

By far the most difficult structural measurement is long-chain branching. In LDPE the concentration of long-chain branches is such (<0.5 per 1000 carbons) that characterization through size exclusion chromatography (SEC) in conjunction with either low-angle laser light scattering or intrinsic viscosity measurements becomes feasible [15-18].

When ^{13}C-NMR measurements have been compared to results from polymer solution property measurements, good agreement has been obtained between long chain branching from solution properties with the concentration of branches six carbons long and longer [16, 17]. Unfortunately, these techniques utilising solution properties do not possess sufficient sensitivity to detect long chain branching in a range of 1 in 10,000 carbons, the level suspected in HDPE. The availability of superconducting magnet systems has made measurements of long chain branching by ^{13}C-NMR a reality because of a greatly improved sensitivity. An enhancement by factors between 20 and 30 over conventional NMR spectrometers has been achieved through a combination of higher field strengths, 20 mm probes, and the ability to examine polymer samples in essentially a melt state.

It is easy to predict the ^{13}C-NMR spectrum anticipated for essentially linear polyethylenes containing a small degree of long chain branching. An examination of a ^{13}C-NMR spectrum from a completely linear polyethylene, containing both terminal olefinic and saturated end-groups, shows that only five resonances are produced. A major resonance at 30 ppm arises from equivalent, recurring methylene carbons, designated as '*n*', which are four or more removed from an end-group or a branch. Resonances at 14.1, 22.9 and 32.3 ppm are from carbons 1, 2 and 3, respectively, from the saturated, linear end-group. A final resonance, which is observed at 33.9 ppm, arises from an allylic carbon, designated as 'a', from a terminal olefinic end-group. These resonances, depicted structurally below, are fundamental to the spectra of all polyethylenes:

$$\underset{1}{CH_3} - \underset{2}{CH_2} - \underset{2}{CH_2} - CH_2 - \quad \underset{\text{'n'}}{-(CH_2)_n-} \quad - \underset{\text{'a'}}{CH_2} - CH{=}CH_2$$

An introduction of branching, either long or short, will create additional resonances to those described previously.

From the observed ^{13}C-NMR spectrum of the ethylene-1-octene copolymer, Randall [19, 20] found that the α and β and methane resonances associated with branches of six carbons and longer occur at 34.56, 27.32 and 38.17 ppm, respectively. Thus, in HDPE, where long chain branching is essentially the only type present, ^{13}C-NMR can be used to establish unequivocally the presence of branches six carbons long and longer. If no comonomer has been used during polymerisation, it is very likely that the presence of such resonances will be indicative of true long chain branching. In any event, ^{13}C-NMR can be used to pinpoint the absence of long chain branching and place an upper limit upon the long chain branch concentration whenever branches six carbons and longer are detected.

It can be seen from the previous considerations that ^{13}C-NMR is a highly attractive method for characterising polyethylenes. A serious drawback is not encountered even

though branches six carbons in length and longer are measured collectively. The short branches are generally less than six carbons in length and truly long chain branches tend to predominate. On occasions there may be special exceptions for 'intermediate' branch lengths, so independent rheological measurements should be sought as a matter of course. Nevertheless, ^{13}C-NMR is a direct method, which possesses the required sensitivity to determine long chain branching in HDPE, and provide much information of micro-structural interest.

A study of the products produced upon vacuum radiolysis of ethylene homopolymers and copolymers is another means of obtaining information on branching in these polymers [21]. If a correction is applied, to take into account the fragments arising from scission at chain ends, the remaining products can be quantitatively accounted for as entirely due to scission of side-branches introduced onto the backbone chain by the α-olefin comonomer. The cleavage of branches takes place, for all practical purposes, exclusively at the branch points at which the branches are attached to the backbone chain. The same data, together with similar radiolysis data of poly(3-methyl pentene-1) and poly(4-methyl pentene-1), further showed that all branches cleave with equal efficiency, regardless of their length. Radiolysis does, therefore, provide a reliable and convenient tool for the quantitative characterisation of high-pressure polyethylene with regard to the unique short chain branching (SCB) distribution that is characteristic of each.

Short chain branches can be introduced deliberately in a controlled manner into polyethylenes by copolymerising ethylene with a 1-olefin. The introduction of 1-olefins allows the density to be controlled, and butene-1 and hexene-1 are commonly used for this purpose. Once again, as in the case of the high-pressure process LDPE, ^{13}C-NMR can be used to measure ethyl and butyl branch concentrations independently of the saturated end-groups. This result gives ^{13}C-NMR a distinct advantage over corresponding infrared measurements because the latter technique can only detect methyl groups irrespective of whether the methyl group belongs to a butyl branch or a chain end. ^{13}C-NMR also has a disadvantage in branching measurements because only branches five carbons in length and shorter can be discriminated independently of longer chain branches [19, 22]. Branches of six carbons in length and longer give rise to the same ^{13}C-NMR spectral pattern independently of the chain length. This lack of discrimination among the longer side-chain branches is not a deterring factor, however, in the usefulness of ^{13}C-NMR in a determination of long chain branching.

Bugada and Rudin [23] used ^{13}C-NMR and SEC to determine long chain branching in LDPE.

Pyrolysis – Gas Chromatography

An example of early work on this topic is that of Van Schooten and Evenhuis [24, 25] who applied their pyrolysis (at 500 °C) hydrogenation-gas chromatographic (PHGC) technique to the measurement of short chain branching and structural details of three commercial polyethylene samples, a linear polyethylene, a Ziegler low-pressure polyethylene of density 0.945 and a high-pressure LDPE of density 0.92. Details of the pyrograms are given in **Tables 10.1 and 10.2**. It was observed in **Table 10.2**, that the sizes of the iso-alkane peaks increase strongly with increasing amount of short chain branching, i.e., increase as we go from linear polyethylene to

Table 10.1 Relative sizes of n-alkane peaks in pyrograms of various polyethylenes

Peak ratio	Linear polyethylene	Ziegler polyethylene	High-pressure polyethylene
n-C_4 - *n*-C_7	0.71	0.74	1.38
n-C_5 - *n*-C_7	0.59	0.57	0.75
n-C_6 - *n*-C_7	1.52	1.25	1.28
n-C_8 - *n*-C_7	0.63	0.65	0.68
n-C_9 - *n*-C_7	0.67	0.64	0.72
n-C_{10} - *n*-C_7	1.02	0.91	0.88
n-C_{11} - *n*-C_7	1.00	0.71	0.75

*Reprinted from J. van Schooten and J.K. Evenhuis, Polymer, 1965, **6**, 7, 561. ©1965, Elsevier [24]*

Table 10.2 *Iso*-alkane peaks in polyethylene pyrograms

Sample	*Iso*-alkane peak
Zeigler polyethylene	*i*-C_5, $3MC_5$, ($3MC_6$), ($3MC_7$), $3MC_8$, ($3MC_9$)
High-pressure polyethylene	*i*-C_4, $2C_5$, $2MC_5$, $3MC_5$, $2MC_6$, $3MC_6$, $2MC_7$ - $4MC_7$, $3MC_7$, $2MC_8$, - $4MC_8$, $3MC_8$, $4MC_9$ - $5MC_9$, $2MC_9$, $3MC_9$, $4MC_{10}$ - $5MC_{10}$, $2MC_{10}$ - $4MC_{10}$, $3MC_{10}$

*Reprinted from J. van Schooten and J.K. Evenhuis, Polymer, 1965, **6**, 7, 343. ©1965, Elsevier [24]*

high-pressure polyethylene. None of the *n*-alkane peaks in the Ziegler low-pressure HDPE pyrogram is significantly greater than the corresponding peak in the pyrogram of a linear polyethylene) **Table 10.1**.

The pattern of the increased *iso*-alkane peaks in the Ziegler polyethylene pyrogram strongly suggests that these peaks are mainly due to ethyl side-groups. This is in good agreement with the results of electron irradiation experiments. For the high-pressure polyethylene, Van Schooten and Evenhuis [24, 25] found that the *n*-butane peak of the pyrogram showed a clear increase in size, and the *n*-pentane peak a smaller, although probably significant, increase. The increases in the *n*-butane and *n*-pentane peaks are probably due to *n*-butyl and *n*-pentyl side-groups, respectively, pentyl groups being much less numerous than butyl groups. However, from the pyrograms of the ethylene-butene, ethylene-hexane-1 and ethylene-octene-1 copolymers it is known that *n*-butyl side groups give a 2-methyl C_6 peak which is at least equal to the 3-methyl C_7 peak. In the high-pressure polyethylene pyrogram, however, the 3-methyl C_7 peak, therefore, is probably due to ethyl side-groups. This is in agreement with the sizes of the other 3-methylalkane peaks. It may be concluded that in high-pressure polyethylene the short-chain branches are mainly ethyl and, for a smaller part, *n*-butyl groups, while some *n*-pentyl groups may also be present.

Van Schooten and Evenhuis [24, 25] concluded that the results obtained by PHGC appear to be in good agreement with those obtained by infrared and electron irradiation studies. They showed that the pyrograms of a linear polyethylene contained only very small peaks for branched and cyclic alkanes and very large *n*-alkane peaks. The largest peaks in the pyrogram are those for propane, *n*-hexane, *n*-heptane, *n*-decane and *n*-undecane, indicating important hydrogen exchange reactions followed by scission with the fifth (C_3 and *n*-C_6), ninth (*n*-C_7 and *n*-C_{10}) and thirteenth (*n*-C_{11} and *n*-C_{14}) carbon atoms. Hydrogen transfer with the sixth carbon atom would account for the rather large *n*-C_4 peak (*n*-C_4 and *n*-C_7), but this peak could also be due to intermolecular chain transfer reactions.

Pyrograms were also prepared for a range of polyethylene containing different amounts of short chain branching (see **Table 10.3** for details of samples). Previous work by high-energy electron irradiation and mass spectrometry has shown that the short branches in high-pressure polyethylenes are mainly ethyl and *n*-butyl groups, but other short branches have also been thought to be present.

The pyrograms obtained on these various polymers are shown in **Figures 10.1(a)** and 10.1b (*n*-C_6 peak taken as reference). These pyrograms show marked differences which can be attributed to differences in short chain branching. The small amount of branching in Marlex 5003 and Ziegler polyethylenes is reflected only in the somewhat larger iso-alkane peaks, whereas the *n*-alkane pattern is practically the

Table 10.3 Branching frequency of polyethylenes estimated from pyrogram (branches/1000 carbon atoms, from peak surface ratios)				
Sample	***n*-Butane**	***Iso*-pentane**	**3-methyl pentane**	**3-*n*-pentane**
Marlex 50 (Phillips) very little branching – 1 methyl group/1000 carbon atoms	(I)	(I)	(I)	(I)
Marlex 5003 (Phillips) polyethylene containing a little copolymerised butane-1	0.5	4	2	2
Ziegler low-pressure polyethylene (about 3-6 branches/1000 carbon atoms	0.3	7	5	5
Alkathene 2 (ICI) high-pressure polyethylene (20-30 branches/1000 carbon atoms)	21	19	17	19
Lupolen H (BASF) high-pressure polyethylene (20-30 branches/1000 carbon atoms)	(24)	(24)	(24)	(24)
Reprinted from J. van Schooten and J.K. Evenhuis, Polymer, 1965, 6, 7, 343. ©1965, Elsevier [24]				

same as found for Marlex 50 (low branching). The Alkathene 2 and Lupolen H high-pressure polyethylenes show, on the other hand, larger *n*-butane and *n*-pentane peaks (Figure 10.1). The iso-alkane peaks that show the largest increase (for Alkathene 2 and Lupolen H) are the iso-pentane and 3-methyl alkane peaks (**Figure 10.1(b)**). The results in Figure 10.1b clearly show that the highest amount of branching is present in Lupolen H, the lowest in Marlex 50. Assuming arbitrarily that these polymers, contain 24 and 1 short side chains/1000 carbon atoms, respectively, and that the relative increase of the *n*-butane and the iso-alkane peaks is linearly related to the amount of branching, then the branching frequency of the other three samples can be obtained by interpolation. These values are in good agreement with those found in the literature. From the large increase in the *n*-butane peak and the relatively small

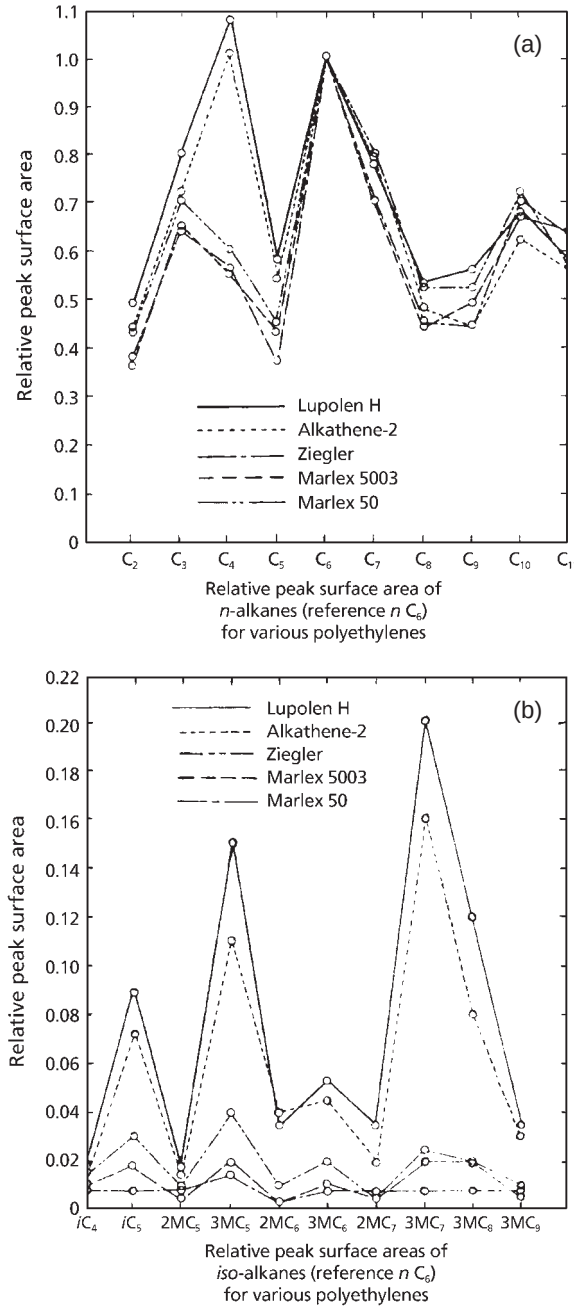

Figure 10.1 Pyrolysis - gas chromatography carbon number distribution (relative peak surface areas of (a) *n*-alkanes, reference *n*-C_6 of various polyethylenes: (b) iso-alkanes, references *n*-C_6 of various polyethylenes. (*Reprinted with permission from J. van Schooten and J.K. Evenhuis, Polymer, 1965, **6**, 7, 343. ©1965, Elsevier [24]*)

increase in the ethane peak it is concluded that the two high-pressure polyethylenes (Alkathene 2 and Lupolen H) contain mainly *n*-butyl side-chains.

PHGC has been used to specifically determine short chain branching in LDPE. Michailov and co-workers [26] identified some of the isoalkane peaks on the hydrogenated pyrograms of LDPE and pointed out that ethyl and butyl branches predominate. Seeger and Barall [13], using ethylene-1-butene and ethylene-1-hexane copolymers as standards, detected about 20 ethyl and 10 *n*-butyl branches per 1000 carbons from the high yields of 3- and 5-methylalkanes. The resolution of the pyrograms, however, was insufficient because of the use of packed columns. Ahlstrom and Liebman [27] demonstrated the presence of ethyl and butyl branches from increases in the size of the 3-methylalkanes and *n*-butane peaks, respectively, although 5-methylalkanes were not resolved.

Later, Mlejnek [28], using a more effective open tubular column and Curie-point pyrolyser, obtained high-resolution pyrograms of PE. On the basis of the relative peak area of isoalkanes, he concluded that the presence of methyl, ethyl, and butyl groups was equally probable in LDPE. In recent work [29-31], glass capillary PHGC was applied to the quantitative analysis of the SCB. Relating the relative peak intensities of characteristic isoalkanes for LDPE to those of reference model co-polymers, they determined methyl, ethyl, and-butyl branch contents in LDPE. Liebman and co-workers [32] reported a comparable study on the SCB in PE by fused-silica capillary PHGC and ^{13}C-NMR spectroscopy. In order to extend the interpretative capabilities of PHGC, a computer simulation method was applied to reproduce the fragmentation pattern of the program of LDPE using the data of known references. They suggested that PHGC can estimate contents of SCB as low as one branch per 10000 CH_2. Recently, Haney and co-workers [33] proposed a new PHGC method at relatively low pyrolysis temperature (360 °C). By this method, enhanced yields of the products pertaining to the branch points were observed on the resulting programs of PE. The observed excess amount of 3-methylpentane from PE was qualitatively attributed to the existence of Willbourn-type branches such as 2-ethylhexyl (branched branch) and 1,3-paired ethyl (pair branch).

However, the existence of amyl branches and branches longer than hexyl, which has been confirmed by ^{13}C-NMR spectroscopy [19, 22, 34-36] has not been clearly characterised by PHGC mainly because of the lack of well-defined model polymers and of insufficient resolution for the associated isoalkanes on the pyrograms. Ohtani and co-workers [37] extended the hydrogenation technique methods for determining the SCB in LDPE - the method was extended up to hexyl branches using a high-resolution fused-silica capillary column and well-characterised model copolymers. Branch content estimated in this way was compared with that obtained by ^{13}C-NMR spectroscopy. In addition, the possible existence of pair and branched branches is also

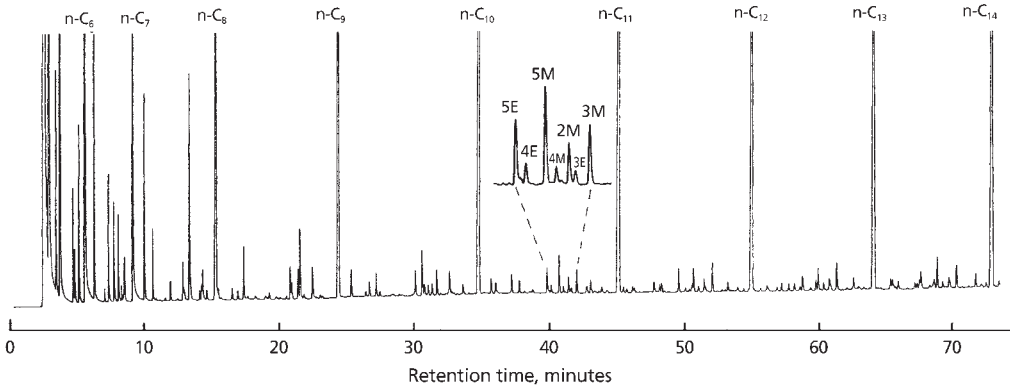

Figure 10.2 A high-resolution pyrogram of LDPE-B at 650 °C: 2M, 2-methyldecane; 3M, 3-methyldecane; 4M, 4-methyldecane; 5M, 5-methyldecane; 3E, 3-ethylnonane; 4E, 4-ethylnonane; 5E, 5-ethylnonane. (*Reprinted with permission from H. Ohtani, S. Tsuge and T. Usami, Macromolecules, 1984, **17**, 12, 2557. ©1984, ACS [37])*

discussed on the basis of theoretical and observed yields for 5-ethylnonane, which is characteristic of the ethyl branch.

Figure 10.2 shows a typical high-resolution hydrogen product pyrogram obtained for a LDPE by use of the fused-silica capillary column. As compared with the previous pyrograms for LDPE [31], drastic improvement in resolution was attained for the isoalkanes which are closely related to the SCB. Although the peak resolution between 2-methyldecane (2M) and 3-ethylnonane (3E) in the C_{11} region was not sufficient with an ordinary glass capillary column, almost complete separation was attained by using the fused-silica column. Thus, the determination of the SCB was carried out on the basis of characteristic peak intensities in the C_{11} region according to the same approach reported previously [33].

Table 10.4 summarises the possible fragmentation products of C_{11} formed from the short-branch structures in the polymer chain provided that any side-chain cleavages do not occur. Each compartment divided by oblique dotted lines depicts the fragments corresponding to each type of branching from C_1 to C_{10}. Branches up to hexyl were taken into consideration except for propyl branches, whose existence in LDPE, if any, is known to be negligibly small.

The most intense peak for amyl was 5-methyldecane (5M), which was also the most intense for butyl, so that the second most intense peak, 4-ethylnonane (4E) was

Table 10.4 Possible fragmentation products of C_{11} from the site of branching in LDPE

Branch type	C_{10}	C_9	C_8	C_7	C_6	C_5	C_4	C_3	C_2	C_1
Scission type	α′	β′	γ′	δ′	ε′	ζ′	η′	θ′	ι′	κ′	
α	n	n	n	n	n	n	n	n	n	n	
β	n	2M	3M	4M	5M	5M	4M	3M	2M		
γ	n	3M	3E	4E	5E	4E	3E	3M			
δ	n	4M	4E	4P	4P	4E	4M				
ε	n	5M	5E	4P	5E	5M					
ζ	n	5M	4E	4E	5M						
η	n	4M	3E	4M							
θ	n	3M	3M								
ι	n	2M									
κ	n										

n: n-undecane
2M: 2-methyldecane
3M: 3-methyldecane
4M 4-methyldecane
5M: 5-methyldecane
3E: 3-ethylnonane
5E: 5-ethylnonane
4P: 4-propyloctane

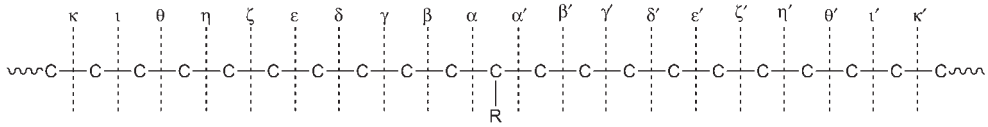

R: short branches

Reprinted with permission from H. Ohtani, S. Tsuge and T. Usami, Macromolecules, 1984, 17, 12, 2557. ©1984, ACS. [37]

allocated for the key peak for amyl instead of 5M. Thus, the correlation factors (*f*) for the content of branches defined previously [31] were first calculated from the corresponding data for the model co-polymers with known branch content:

$$I(\text{key})_{\text{obsd}}\, f = \text{branch number/1000 C} \qquad (10.1)$$

where $I(\text{key})_{\text{obsd}}$ was the relative value when the observed peak intensity of *n*-C_{11} was regarded as $1000(I(n\text{-}C_{11})_{\text{obsd}} = 1000)$.

Table 10.5 summarises the observed $I(\text{key})_{\text{obsd}}$ and the calculated *f* values together with the relative peak intensities of the isoalkanes to the corresponding key peaks.

Table 10.5 Relative peak intensities of isoalkanes to key peak and observed correlation factors (f) for reference copolymer obtained for LDPE

				Relative peak intensities of isoalkanes to key peak[c]							
Reference polymer (A)	**Branch content per 1000 carbon[d]**	**I_{obsd}[a]**	***f*[b]**	**2M**	**3M**	**5M**	**4E**	**4M**	**3E**	**5E**	**4P**
EP	20 methyl	77.3 (2M)	260	1.00	0.46	0.44		0.38			
EB	24 ethyl	55.3 (3M)	430	0.10	1.00	0.093	0.33	0.061	0.36	0.16	0.05
EHX	18 butyl	43.5 (5M)	410	0.24	0.17	1.00	0.035	0.095	0.01	0.33	0.2
EHP	12 amyl	20.5 (4E)	590	0.31	0.30	2.52	1.00	0.18	0.031	0.070	
EO	20 hexyl	51.4 (4M)	390	0.21	0.15	0.15	0.032	1.00	0.20	0.025	

Sample	α-Olefin comonomer	Branch type	Branch content[d]
EP	Propylene	Methyl	20
EB	1-Butene	Ethyl	24
EHX	1-Hexene	Butyl	18
EHP	1-Heptene	Amyl	12
EO	1-Octene	Hexyl	20

a: Key peak intensities relative to peak intensities of $I(n\text{-}C_{11})_{obsd} = 1000$
b: Calculated correlation factor defined by Equation 10.1
c: The underlined values are for key peaks
d: Branch content/1000 C determined by IR spectroscopy

Reprinted with permission from H. Ohtani, S. Tsuge and T. Usami, Macromolecules, 1984, 17, 12, 2557. ©1984, ACS. [37]

Table 10.6 Estimated SCB content in LDPE by PHGC and by ^{13}C-NMR spectroscopy

	Estimated SCB content/1000 carbons[a]						
Sample	**Methyl**	**Ethyl**	**Butyl**	**Amyl**	**Hexyl**	**Longer[b]**	**Total[c]**
LDPE-A	1.3	4.9	8.3	2.3	0.2		17.0
	(0.4)	(6.4)	(7.4)	(2.6)		(2.8)	(19.9)
LDPE-B	1.5	7.2	11.2	2.2	0.3		22.4
	(0.5)	(7.2)	(8.5)	(2.7)		(3.5)	(24.9)
LDPE-C	1.3	4.8	8.6	1.9	0.4		17.0
	(0.5)	(5.4)	(6.4)	(2.2)		(2.4)	(17.3)
LDPE-D	1.0	2.1	4.5	0.6	0.3		8.5
	(0.1)	(2.3)	(2.4)	(0.7)		(1.0)	(6.7)

a: Estimated SCB content by PHGC are given first, and estimated SCB content by ^{13}C-NMR spectroscopy are given in brackets.

b: The longer chain branches are not taken into consideration in the case of PHGC.

c: Content by NMR also involves propyl branch content between 0.2 and 0.5.

Reprinted with permission from H. Ohtani, S. Tsuge and T. Usami, Macromolecules, 1984, 17, 12, 2557. ©1984, ACS. [37]

Table 10.6 summarises the SCB content obtained by this method for the four LDPE along with that found by ^{13}C-NMR spectroscopy. As a whole, the estimated individual short-branch content and the total values are in fairly good agreement with those obtained by ^{13}C-NMR spectroscopy.

Other methods that have been used to determineshort chain branching in polyethylene include SEC – Fourier Transform IR spectroscopy [38, 39], Fourier Transform IR spectroscopy [40-42], SEC – low angle laser light scattering (LALLS) [45] and secondary ion mass spectrometry [47].

10.1.3 Size Exclusion Chromatography and Multiangle Laser Light Scattering (SEC-MALLS)

In addition to those techniques already mentioned SEC-MALLS [43] and SEC with viscometric detection [46] have been used to specifically determine long chain

branching in PE. An example of the latter is the work of Tacx and Tacx [44]. These workers pointed out that the separation of LDPE exclusively according to one molecular parameter (e.g., molar mass, LCB, SCB), without interference of the other parameters, with subsequent characterisation of the fractions according to exclusively another parameter, is nearly impossible. Separation according to SCB is influenced by molar mass and type of SCB. Application of liquid-liquid phase separation results in a separation mainly according to LCB. However, an influence of molar mass cannot be excluded.

Long chain branching causes a decrease in molecular size and hence in the radius of gyration and the hydrodynamic radius, as compared to polymers having a linear structure and having the same molar mass. In principle there is a simple relationship between the ratio of the radii of gyration and the hydrodynamic radii: $g' = g^b$. At constant temperature and one solvent/polymer combination, the *b*-value is mainly dependent on the chain architecture. In the classical approach, determination of *b* as a function of molar mass requires time consuming fractionation with subsequent characterisation of the fractions to determine the hydrodynamic radius and the radius of gyration. Fortunately, by application of SEC in combination with only MALLS and using the universal calibration principle, it appeared possible to determine the *g* and *g'* as a function of the molar mass. Utilisation of this method revealed that LDPE exhibits a continuous decrease with increasing molar mass of the *b*-value from 1.8 to 1.2 for a tubular product, and from 1.5 to 1 for an autoclave product. This was also expected from the polymerisation conditions.

10.2 Branching in Olefin Copolymers

10.2.1 Ethylene-propylene Copolymer

In the preceeding section we discussed the occurrence of butyl and higher alkyl groups formed in side reactions occurring in PE homopolymer.

In this section we discuss the occurrence of side groups in ethylene copolymers ranging from ethylene-propylene to ethylene-octene.

For ethylene-propylene copolymers it is possible to determine the methyl side groups due to propylene units by ^{13}C-NMR.

As shown by a typical example in **Figure 10.3**, each ^{13}C-NMR spectrum was recorded with proton noise-decoupling to remove unwanted ^{13}C-^{1}H scalar couplings. No corrections were made for differential nuclear Overhauser effects (NOE) since constant NOE were assumed [48, 49] in agreement with previous workers [50-53]. Constant

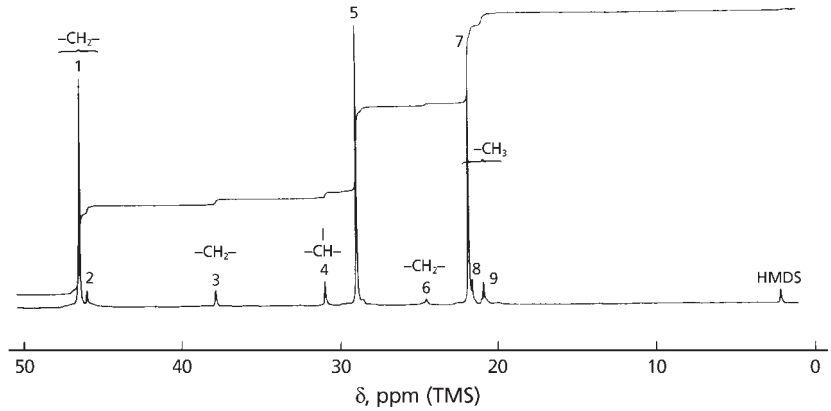

Figure 10.3 A ^{13}C-NMR spectrum at 25.2 MHz and 125 °C of a 97/3 propylene–ethylene copolymer in 1,2,4-trichlorobenzene and perdeuterobenzene. The internal standard copolymer in 1,2,4-trichlorobenzene and perdeuterobenzene. (*Source: Author's own files*)

NOE for all major resonances in low ethylene content ethylene-propylene copolymers have been reported [54].

The ^{13}C-NMR spectrum of an ethylene-propylene copolymer, containing approximately 97% propylene in primarily isotactic sequences, is shown in **Figure 10.3**. The major resonances are numbered consecutively from low to high field. Chemical shift data and assignments are listed in **Table 10.7**. Greek letters are used to distinguish the various methylene carbons and designate the location of the nearest methine carbons.

Paxson and Randall [55] in their method use the reference chemical shift data obtained on a predominantly isotactic polypropylene and on an ethylene-propylene copolymer (97% ethylene). They concluded that the three ethylene-propylene copolymers used in their study (97-99% propylene) contained principally isolated ethylene-ethylene linkages. Knowing the structure of their three ethylene-propylene copolymers, they used the ^{13}C-NMR relative intensities to determine the ethylene-propylene contents and thereby establish reference copolymers for the faster IR method involving measurements at 732 cm^{-1} (13.66 μm). After a detailed analysis of resonances, Paxson and Randall [55] concluded that methine resonances 4 and 5 (**Table 10.7**) gave the best quantitative results to determine the comonomer composition. The composition of the ethylene-propylene copolymers was determined by peak heights using the methine resonances only. In no case was there any evidence for an inclusion of consecutive ethylene units. Thus, composition data from ^{13}C-NMR could now be used to establish an infrared method based on a correlation with the 732 cm^{-1} (13.66 μm) band which is attributed to a rocking mode, *r*, of the methylene trimer, –$(CH_a)_3$–.

Table 10.7 Observed and reference ^{13}C-NMR chemical shifts in ppm for ethylene-propylene copolymers and reference polypropylenes with respect to an internal trimethylsilane standard

Line	Carbon	3/97 E/P	E/P [55]	97/3 E/P	Sequence assignment	Reference crystalline [52]	PP amorphous [52]
1	αα-CH_2	46.4	46.3		PPPP	46.5	47.0-47.5 r 46.5
2	αα-CH_2	46.0	45.8		PPPE		
3	αα-CH_2	37.8	37.8		PPEP		
4	CH	30.9	30.7		PPE		
5	CH	28.8	28.7		PPP	28.5	28.8 mmmm 28.6 mmmr 28.5 rmmr 28.4 mr + rr
6	ββCH_2	24.5	24.4		PPEPP		
7	CH_3	21.8	21.6	P	PPPPP	21.8	21.3-21.8 mm 20.6-21.0 mr 19.9-20.3 rr
8	CH_3	21.6	21.4		PPPE		
9	CH_3	20.9	20.7		PPPEP		
	CH_3		19.8	19.8	EPE		
	CH		33.1	33.1	EPE		
	αCH_2			37.4	EPE		
	βCH_2			27.3	EPE		
	–$(CH_2)_n$–		29.8	29.8	EEE		

E/P: ethylene-propylene

*Reprinted with permission from J.R. Paxson and J.C. Randall, Analytical Chemistry, 1978, **50**, 13, 1777. ©1978, ACS [55]*

Randall [56] has developed a ^{13}C-NMR quantitative method for measuring ethylene-propylene mole fractions and methylene number-average sequence lengths in ethylene-propylene copolymers. He views the polymers as a succession of methylene and methyl branched methine carbons, as opposed to a succession of ethylene and propylene units.

This avoids problems associated with propylene inversion and comonomer sequence assignment. He gives methylene sequence distributions from one to six and larger consecutive methylene carbons for a range of ethylene-propylene copolymers, and uses this to distinguish copolymers which have either random, blocked or alternating comonomer sequences.

10.2.2 Branching in Ethylene – Higher Olefin Copolymers

Nuclear Magnetic Resonance Spectroscopy

Randall [19, 34] obtained ^{13}C-NMR data from both conventional iron magnet spectrometers with field strengths of 23.5 kg and superconducting magnets operating at 47 kg for a homogenous series of six linear ethylene 1-olefin copolymers beginning with 1-propene and ending with 1-octene (see **Figure 10.4**). The side-chain branches

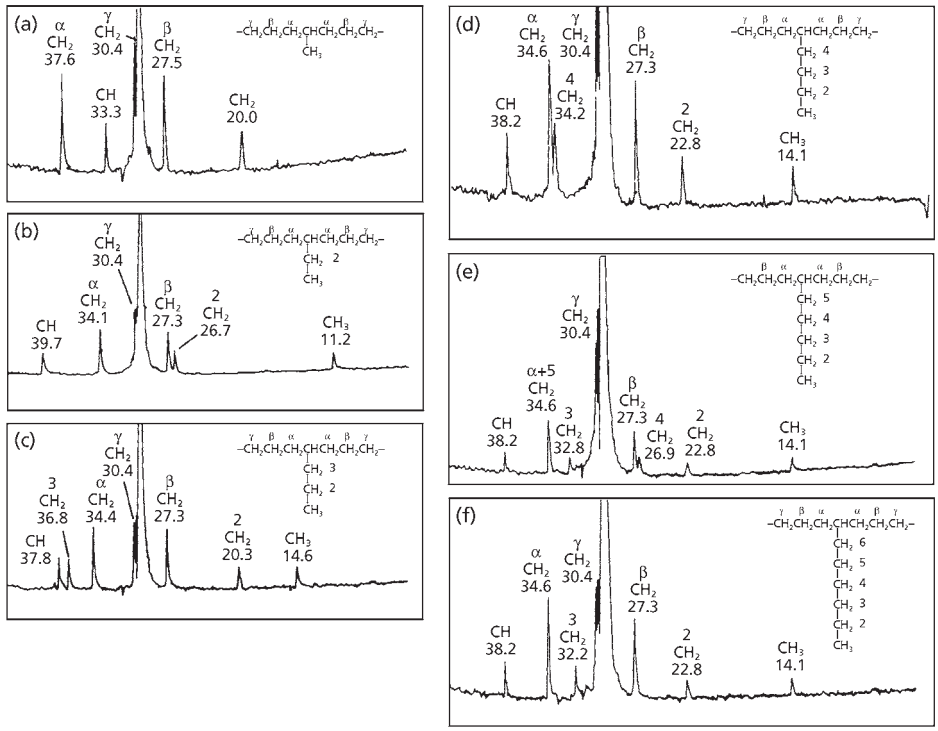

Figure 10.4 ^{13}C-NMR at 25.2 M Hz of (a) an ethylene-1-propene copolymer, (b) an ethylene-butene copolymer, (c) an ethylene-1-pentene copolymer, (d) an ethylene-1-hexene copolymer, (e) an ethylene-1-heptene copolymer and (f) an ethylene-1-octene copolymer. (*Reprinted with permission from J.C. Randall, Journal of Polymer Science: Polymer Physics Edition, 1973,* ***11****, 2, 275. ©1973 John Wiley and Sons [19])*

Table 10.8 Polyethylene backbone and side-chain ^{13}C chemical shifts in ppm from trimethylsilane (±0.1) as a function of branch length (Carbon chemical shifts, which occur near 30.4 ppm, are not given because they are often obscured by the major 30 ppm resonance for the 'n' equivalent, recurring methylene carbons) (solvent: 1,2,4-trichlorobenzene; temperature: 125 °C)

Branch length	Methine			6	5	4	3	2	1
1	33.3	37.6	27.5	20.0					
2	39.7	34.1	27.3	11.2	26.7				
3	37.8	34.4	27.3	14.6	20.3	36.8			
4	38.2	34.6	27.3	14.1	23.4	—	34.2		
5	38.2	34.6	27.3	14.1	22.8	32.8	26.9	34.6	
6	38.2	34.6	27.3	14.1	22.8	32.2	30.4	27.3	34.6

Source: Author's own files

are therefore linear, and progress from one to six carbons in length. Also, the respective 1-olefin concentrations are less than 3%, thus only isolated branches are produced. Unique spectral fingerprints are observed for each branch length. The chemical shifts, which can be predicted with the Grant and Paul parameters [19, 57], are given in **Table 10.8** for this series of model ethylene-1-olefin copolymers. The nomenclature used to designate those polymer backbone and side-chain carbons discriminated by ^{13}C NMR, is as follows:

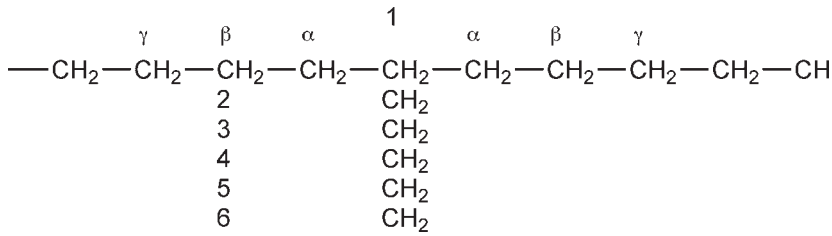

The distinguishable backbone carbons are designated by Greek symbols, while the side-chain carbons are numbered consecutively starting with the methyl group and ending with the methylene carbon bonded to the polymer backbone. The identity of each resonance is indicated in **Figure 10.4**. It should be noticed in **Figure 10.4** that the '6' carbon resonance for the hexyl branch is the same as α, the '5' carbon resonance is the same as β and the '4' carbon resonance is the same as γ. Resonances 1, 2 and 3, likewise, are the same as the end-group resonances observed for linear_polyethylene.

Thus, a six-carbon branch produces the same ^{13}C spectral pattern as any subsequent branch of greater length. ^{13}C-NMR, alone cannot therefore be used to distinguish a linear six-carbon from a branch of some intermediate length or a true long chain branch.

The capability for discerning the length of short chain branches has made ^{13}C-NMR a powerful tool for characterising LDPE produced by free-radical, high-pressure processes. The ^{13}C-NMR spectrum of such a polyethylene is shown in **Figure 10.5**. Others are also present, and Axelson and co-workers, in a comprehensive study [58] have concluded that no unique structure can be used to characterise LDPE. They have found nonlinear short chain branches as well as 1,3 paired ethyl branches. Bovey and co-workers [22] compared the content of branches six carbons and longer in LDPE with the long chain branching results obtained through a combination of gel permeation chromatography (GPC) and intrinsic viscosity. An observed good agreement between the results led to the conclusion that the principal short chain branches contained fewer than six carbons and the six and longer branching content could be related entirely to long chain branching. Others have now reported similar observations in studies where solution methods are combined with ^{13}C-NMR. However, as a result of the possible uncertainty of the branch lengths, associated with the resonances for branches six carbons and longer, ^{13}C-NMR should be used in conjunction with independent methods to establish true long chain branching.

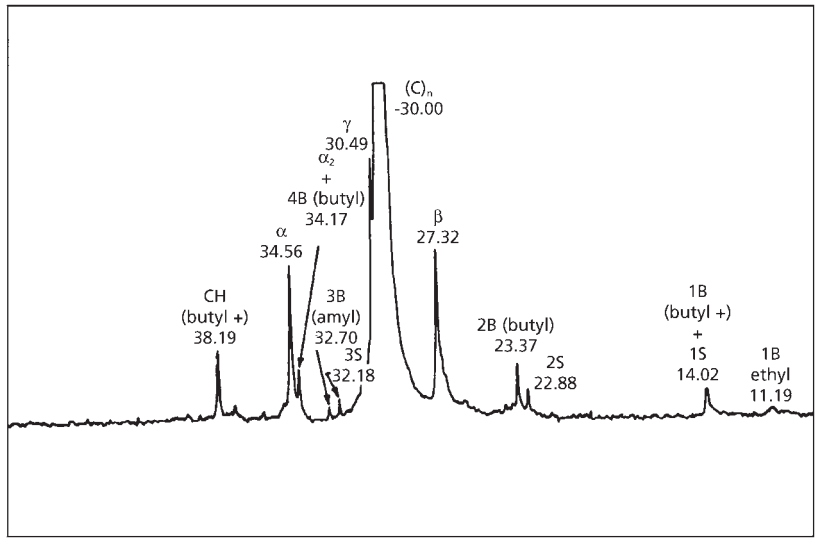

Figure 10.5 ^{13}C spectrum at 25.2MHz of a low density polyethylene from a high-pressure process. (*Reprinted with permission from J.C. Randall, Journal of Polymer Science: Polymer Physics Edition, 1973, **11**, 2, 275. ©1973 John Wiley and Sons[19]*)

De Pooter and co-workers [59] have applied ^{13}C-NMR spectroscopy at sample temperatures of 130 °C to branching studies of copolymers of ethylene with 1-10 mol% of propylene, butane-1, hexane-1, octane-1 and 4-methyl pentene-1. ^{13}C-NMR spectra were recorded with proton noise decoupling to remove unwanted ^{13}C-^{1}H scalar couplings. It was shown that the NOE is nearly full and constant for all carbons in these copolymers.

Delay times between pulses in the pulse FT-NMR method must be five times the longest spin lattice relaxation time (T_1) value for 99% relaxation. Unless five T_l values are allowed between pulses, saturation will occur and the area of the resonance will be attenuated. The methyl carbons in PE generally have the longest T_l values, some of which are as long as 8-10 seconds. Therefore, to be quantitative, a 50 second delay time between pulses would be necessary. Since several thousand scans must be accumulated in order to achieve adequate signal-to-noise, this delay time is not reasonable. An alternate approach for this analysis would be to ignore the methyls and other carbon resonances which have very long relaxation times. The T_l values for the majority of the carbons in the samples are less than 2.0 seconds and, therefore, a delay time of only 10 seconds would be necessary. Since there are several other carbons in the structure to use for quantitative purposes, the methyls and some branch carbons can be neglected without interfering with the quantitative aspects. This has the advantage of shortening the delay time between pulses from 50 to 10 seconds with equivalent accuracy.

The terminology used by De Pooter and co-workers [59] for branching is that commonly accepted, using an octene-1 copolymer as example:

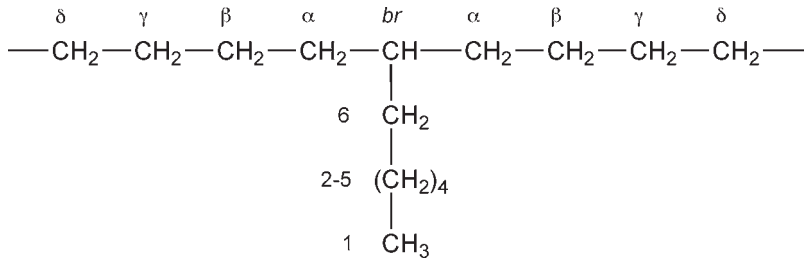

This investigation included the chemical shift assignments (relative to that of the isolated methylene carbons at 30.0 ppm) and a set of experimental conditions for the quantitative analysis of branching in the most commercial types of linear LDPE. The integration limits given in **Table 10.9** not only take into account the isolated branches, but also branches which are separated by one ethylene unit and branches next to each other. These latter two structures occur very infrequently in most commercial products but are significant to the calculations.

Table 10.9 Integration limits for ethylene copolymers*

Copolymer	Area	Region (ppm)	Copolymer	Area	Region (ppm)
Ethene-propene	A	47.5 to 44.5	Ethene-octene-1	A	41.5 to 40.5
	B	39.8 to 36.8		B	40.5 to 39.5
	C	35.5 to 32.5		C	39.5 to 37.0
	C + D + E	35.5 to 25.8		D	Peak at 35.8
	F	25.8 to 23.8		D + E	36.8 to 33.2
	G	22.5 to 18.5		F + G + H	33.2 to 25.5
	H	Peak at 21.6		H	28.5 to 26.5
Ethene-butene-1	A	41.5 to 38.5		I	25.0 to 24.0
	A´	Peak at 39.4		P	24.0 to 22.0
	B	37.8 to 36.8	Ethene-4-methylpentene-1	A	46.5 to 43.5
	C	36.0 to 33.2		B	43.0 to 41.8
	D + E	33.2 to 25.5		C	41.8 to 40.5
	F	25.2 to 24.0		D	37.5 to 34.2
Ethene-hexene-1	A	41.5 to 40.5		E	Peak at 33.7
	B	40.5 to 39.5		F + G	33.2 to 25.2
	C	39.5 to 37.0		G	28.0 to 25.2
	D	Peak at 35.8		H	Peak at 24.1
	D + E	36.8 to 33.2			
	F + G	33.2 to 25.5			
	G	28.5 to 26.5			
	H	24.9 to 24.1			

*Isolated methylene carbons at 30.0 ppm

*Reproduced with permission from M. De Pooter, P.B. Smith, K.K. Dohrer, K.F. Bennett, M.D. Meadows, C.G. Smith, H.P. Schouwenaars and R.A. Geerards, Journal of Applied Polymer Science, 1991, **42**, 2, 399. ©1991, Wiley Interscience [59]*

This analysis method is somewhat time consuming and tedious, but the precision achieved from its detailed approach is excellent. Several sets of precision studies were performed in which one operator performed the analysis at least 10 times on a given sample and also multiple operators performed the analysis to investigate operator bias. The precision data are given in **Table 10.10**. For one operator, the relative standard deviation at the 95% confidence limit (2σ) was between 2.7 and 7%.

Table 10.10 ^{13}C-NMR determination of comonomer incorporation level (mol%)

	EB	E4MP	EH	EO
Freeport	4.86 4.86	3.67 3.79	4.21[a] 4.05[a]	4.92 4.93
Average	4.86	3.73	4.13	4.93
Terneuzen	5.13 5.14 4.95[b]	3.77 3.71 3.54[b]	4.76 4.56 4.43[b]	5.15 4.94 5.04 5.05 5.14 5.00 5.14 5.12 5.16 5.15 5.07[b] 5.07[b] 5.11[b] 5.17[b]
Average	5.07	3.67	4.58	5.09[c]
Midland	4.60 4.90 4.92 4.95 4.96 4.81 4.74 4.61 5.10 4.86	3.82 4.08	4.43 4.75	5.18 5.20
Average	4.85[d]			5.19

[a] Contained approximately 0.8 ethyl branches. This value is not included in the comonomer incorporation.

[b] Operator 2.

[c] The average value for the 14 determinations is 5.09 with a standard deviation of 0.07 (relative precision at 2σ of 2.7%).

[d] The average value for the 10 determinations is 4.85 with a standard deviation of 0.16 (relative precision at 2σ or 6.8%).

EB: Ethene-butene 1 E4MP: Ethene-4-methylpentane-1
EH: Ethene-hexane-1 EO: Ethene-Octene-1

Reprinted with permission from M. De Pooter, P.B. Smith, K.K. Dohrer, K.F. Bennett, M.D. Meadows, C.G. Smith, H.P. Schouwenaars and R.A. Geerards, Journal of Applied Polymer Science, 1991, **42***, 2, 399. ©1991, Wiley Interscience [59]*

Pérez and Vanderhart [60] investigated the morphological partitioning of chain ends and methyl branches in ethylene copolymers by ^{13}C-NMR in the solid state. The PE samples, which were crystallised from the melt, varied in molecular weight, polydispersity, crystallisation rate, and comonomer content. For the limited set of samples considered, the ratio of crystal to overall end concentration is independent of those variables. This ratio takes the values of 0.75 and 0.60 for the methyl and vinyl ends, respectively. When the crystalline fraction of these samples is taken into account, 50-75% of the total saturated ends and 42-63% of the total vinyls reside in the crystal. For an ethylene/propylene copolymer, 21-27% of the methyl branches were determined to be in the crystal. This level of incorporation puts methyl branches in a position intermediate between chain ends and ethyl branches.

Pérez and Vanderhart [60] also studied methyl and vinyl ends (and ethyl branches) in an ethylene-l-butene copolymer of low molecular weight slowly crystallised from the melt. The partitioning of both types of chain ends was established, and the crystalline region was found to contain 57% of the methyl and 46% of the vinyl ends. This polymer contained 2.6 ethyl branches per 1000 carbon atoms. This latter number stands in significant contrast to the corresponding 2-15% values found for vinyls in single-crystal preparations [61-64].

Pyrolysis – Hydrogenation Gas Chromatography

Van Schooten and Evenhuis [25] reported on the application of their PHGC (at 500 °C) - technique to the measurement of short chain branching and structural details in modified PE which contain small amounts of comonomer (about 10% by weight of butene-1, hexane-1, and octene-1). A survey of the isoalkane peaks of the pyrograms of these polymers with their probable assignment is given in **Table 10.11**. The effect of the comonomer on the relative sizes of the *n*-alkane peaks is given in **Table 10.12**. The peaks stemming from the total side group appear to be somewhat increased in intensity (*n*-C_4 peak in the polyethylene-hexane pyrogram, *n*-C_6 peak in polyethylene-octene pyrogram). The polyethylene-octene pyrogram also shows that the peak stemming from the *n*-alkane with one carbon atom less is somewhat enlarged.

This suggests that chain scission may occur both at the α and at the β C—C bond. Only the latter type of scission will produce methyl-substituted iso-alkanes, e.g., after intramolecular hydrogen transfer. A list of iso-alkanes that may be expected to be formed in this way is compared in **Table 10.13** with a list of those that have been found to be significantly increased in size in the copolymer pyrograms.

Table 10.11 Areas of the main iso-alkane peaks in the pyrograms of linear polyethylene, ethylene-butene-1, ethylene-hexene-1 and ethylene-octene-1 copolymers

Component	Peak area in arbitrary units			
	Linear PE	Ethylene-butene-I	Ethylene-hexene-I	Ethylene-octene-I
i-C_4	10	20	<u>37</u>	<u>30</u>
i-C_5	18	<u>47</u>	<u>62</u>	<u>46</u>
2MC	9	14	18	20
$3MC_5$-CyC_5	31	<u>54</u>	46	76
$2MC_6$	14	13	74	22
$3MC_6$	13	33	24	26
$2MC_7$-$4MC_7$	16	17	25	27
$3MC_7$-$3EC_6$	16	<u>67</u>	<u>64</u>	32
$2MC_8$-$4MC_8$-$ECyC_6$	50	44	38	<u>119</u>
$3MC_8$	9	<u>39</u>	12	17
$4MC_9$-$5MC_9$-$4EC_8$	11	21	51	36
i$PCyC_6$-$BuCyC_5$			<u>94</u>	
$2MC_9$-n-$PCyC_6$	40	35	40	65
$3MC_9$	8	<u>27</u>	6	<u>45</u>
$4MC_{10}$-$5MC_{10}$-sec $BuCyC_6$	25	23	<u>67</u>	32
$2MC_{10}$-$4MC_{10}$-n-$BuCyC_6$	33	30	47	<u>102</u>
$3MC_{10}$	15	<u>32</u>	14	34

Underlined figures are for key peaks.

*Reprinted with permission from J. van Schooten and J.K. Evenhuis, Polymer, 1965, **6**, 11, 561. ©1965, Elsevier [25]*

Table 10.12 Relative sizes of *n*-alkane peaks for polyethylene and for ethylene-butene-1, ethylene-hexene-1 and ethylene-octene-1 copolymers

Peak ratio	Marlex 50	Ethylene-butene- 1	Ethylene-hexene-1	Ethylene-octene-1
n-C_4 - *n*-C_7	0.71	0.86	1.15	0.86
n-C_6 - *n*-C_7	0.59	0.69	0.61	<u>0.91</u>
n-C_6 - *n*-C_7	0.52	1.66	1.62	<u>1.88</u>
n-C_8 - *n*-C_7	0.63	0.58	0.66	0.79
n-C_9 - *n*-C_7	0.67	0.63	0.62	0.75
n-C_{10} - *n*-C_7	1.02	0.93	0.99	1.05
n-C_{11} - *n*-C_7	1.00	0.82	0.90	0.92

Underlined figures are for key peaks.

*Reprinted with permission from J. van Schooten and J.K. Evenhuis, Polymer, 1965, **6**, 11, 561. ©1965, John Wiley and Sons [25]*

Table 10.13 Expected and observed increased iso-alkane peaks in copolymer pyrograms

Ethylene-butene-1		Ethylene-hexene-1		Ethylene-octene		Number of backbone C atoms in fragment
Expected	Observed	Expected	Observed	Expected	Observed	
-	-	-	*i*-C_4	-	*i*-C_4	-
-	-	-	*i*-C_5	-	*i*-C_5	-
i-C_5	i-C_5	$2MC_6$	$2MC_6$	$2MC_8$	$2MC_8$	3
$3MC_5$	$3MC_5$	$3MC_7$	$3MC_7$	$3MC_9$	$3MC_9$	4
$3MC_6$	$3MC_6$	$4MC_8$	-	$4MC_{10}$	$4MC_{10}$	5
$3MC_7$	$3MC_7$	$5MC_9$	$5MC_9$	$5MC_{11}$	-	6
$3MC_8$	$3MC_8$	$5MC_{10}$	$5MC_{10}$	$6MC_{12}$	-	7
$3MC_9$	$3MC_9$	$5MC_{11}$	-	$7MC_{13}$	-	8

*Reprinted with permission from J. van Schooten and J.K. Evenhuis, Polymer, 1965, **6**, 11, 561. ©1965, John Wiley and Sons [25]*

Radiolysis – Gas Chromatography

A study of the products produced upon vacuum radiolysis of ethylene homopolymers and copolymers is another means of obtaining information on branching in these polymers [21]. If a correction is applied, to take into account the fragments arising from scission at chain ends, the remaining products can be quantitatively accounted for as entirely due to scission of side-branches introduced onto the backbone chain by the α-olefin comonomer. The cleavage of branches takes place, for all practical purposes, exclusively at the branch points at which the branches are attached to the backbone chain. The same data, together with similar radiolysis data of poly(3-methyl pentene-1) and poly(4-methyl pentene-1), further showed that all branches cleave with equal efficiency, regardless of their length. Radiolysis does, therefore, provide a reliable and convenient tool for the quantitative characterisation of high-pressure polyethylene with regard to the unique short chain branching distribution that is characteristic of each.

The results obtained in a series of irradiations of ethylene-α-olefin copolymers containing about 4 mole% comonomer are shown in **Table 10.14**.

During radiolysis of PE there also takes place a certain amount of random scission at chain ends in addition to the cleavage of branches. The observed extraneous hydrocarbons is derived from scission of stray branches that might have been introduced on the chains by stray impurities during polymerisation, but the fact that one also observes a consistent decrease in the total amount of these extraneous hydrocarbons derived from the homopolymer with an increase in its molecular weight leads to the conclusion that the random scission at chain ends is their main cause. Obviously, then if one makes an appropriate allowance for these radiolysis fragments derived from chain ends, then the only significant paraffin left in the radiolysis products of each copolymer is that corresponding to the branch introduced on the PE backbone by the comonomer.

Since it is generally agreed that high-pressure PE actually contains a variety of short branches, and not just one type of branch, it is obvious that, if one wants to translate the hydrocarbon analysis of its radiolysis products into quantitative branch-type analysis, one will also need accurate information on the relative efficiency of the scission of different branch types. To obtain this information Kamath and Barlow [21] irradiated some additional ethylene α-olefin copolymers, differing significantly in their comonomer content, and the hydrocarbons in their radiolysis products were analysed as before. **Table 10.15** lists these results. The efficiency of scission is calculated from the known comonomer content (methyl group analysis) and the observed G values of the principal hydrocarbons after application of the appropriate correction against the small chain-end fragmentation. It is clear from the data that all branches of up to

Table 10.14 Radiolysis products of ethylene-α-olefin copolymers (^{235}U radiation source)

Copolymers	G value × 10^2*						
	CH_4	C_2H_6	C_3H_{10}	*i*-C_4H_{10}	*n*-C_4H_{10}	*n*-C_5H_{12}	*n*-C_6H_{14}
Ethylene-propylene	1.7	0.1	-	0.03	-	-	-
Ethylene-butene-1	0.2	1.5	0.1	0.1	0.2	0.03	-
Ethylene-pentene-1	0.2	0.3	2.1	0.02	0.05	-	-
Ethylene-hexane-1	0.4	0.3	0.2	0.03	1.2	0.02	-
Ethylene-octene-1	0.2	0.3	0.1	-	0.1	0.1	1.2
Linear polyethylene	0.2	0.3	0.2	0.03	0.06	0.05	-

* G value defined as the number of molecules of the particular product produced per gram of sample per 100 eV of incident radiation dose. This is calculated with 10% accuracy, from the gas chromatographic analysis data of the products, weight of the polymer sample irradiated, and radiation dose to which the sample has been subjected.

*Reprinted with permission from P.M. Kamath and A. Barlow, Journal of Polymer Science Part A-1: Polymer Chemistry, 1967, **5**, 8, 2023. ©1967, John Wiley and Sons [21]*

six carbon atoms or more break off with equal efficiency, and that the branch length *per se* exerts little or no effect on the ease of scission.

Table 10.16 presents results obtained in the radiolysis of high-pressure polyethylenes of various densities. The disparity between the total number of all branches, as determined from the radiolysis data, and the methyl group content, as derived by the infrared method is noteworthy. This may be attributed to the fact that the usual IR method of determining the methyl group content, based on the absorbance of 7.25 μm does not necessarily count all methyl groups. For example, if two methyl groups are attached to one carbon atom, as in polyisobutylene, the characteristic methyl absorption at 7.25 μm splits, giving two bands at 7.20 and 7.40 μm, respectively [65], which consequently are lost in the methyl group determination procedure.

Table 10.15 Efficiency of radiation scission of short branches (G value × 10^2)

Copolymers	CH_3 per 1000						Average G × 10 CH_3 per 1000 CH_4
	CH_2	CH_4	C_2H_6	C_3H_8	*n*-C_4H_{10}	*n*-C_6H_{14}	
Ethylene-propylene	41.9	3.4					0.074
	26.4	1.7					
Ethylene-butene-1	28.7	2.0					0.072
	21.6	1.5					
	4.1	1.1					
Ethylene-pentene-1	25.6		2.1				0.072
	17.1		1.1				
Ethylene-hexene-1	23.5			1.2			0.073
	7.8			0.7			
Ethylene-octene-1	19.1				1.3		0.074
	15.1				1.2		
	11.6				0.9		

*Reprinted with permission from P.M. Kamath and A. Barlow, Journal of Polymer Science Part A-1: Polymer Chemistry, 1967, **5**, 8, 2023. ©1967, John Wiley and Sons [21]*

Table 10.16 Distribution of short-chain branches in high pressure polyethylene (branches per 1000 methylene units)*

Polymer No.	Density (g/cm^3)	-CH_3	-C_2H_5	-C_3H_7	*i*-C_4H_9	-*n*-C_4H_9	-C_5H_{11}	Total branches per 1000 methylene	Methyl group content per 1000 methylene†
A	0.934	2.9	11.8	1.7	0.3	5.9	1.6	24.2	18.8
B	0.929	2.5	15.2	2.1	0.3	8.5	2.0	30.6	24.0
C	0.924	3.8	16.7	2.2	-	9.9	1.8	34.4	30.9

* Calculated from G values of isolated hydrocarbons assuming scission efficiency of 0.073×10^2 per 1000 carbon atoms. As short chain branches outnumber chain ends by 30:1, no correction for the fragmentation products at chain ends was made.

† Determined by infrared analysis.

*Reprinted with permission from P.M. Kamath and A. Barlow, Journal of Polymer Science Part A-1: Polymer Chemistry, 1967, **5**, 8, 2023. ©1967, John Wiley and Sons [21]*

In line with the observations reported by earlier workers, the two most populous branches, according to the radiolysis method, are ethyl and *n*-butyl, which occur in the ratio 2:1, as observed by others [11].

Infrared Spectroscopy

This technique has found a limited application in the determination of 1-10% of branched α-olefins in ethylene copolymers [66].

10.2.3 Branching in Ethylene-propylene Diene Terpolymers

Pyrolysis - gas chromatography (Py-GC) has been used to determine the overall composition of ethylene-propylene-diene terpolymers (EPDM) [67]. In attempting to determine the third component in EPDM, difficulties might be anticipated, since this component is normally present in amounts around 5 wt%. However, dicyclopentadiene was identified in EPDM even when the amount incorporated was very low.

10.3 Branching in 1-polybutene

Whereas in the Py-GC of polyethylene and PE and polypropylene, the splitting up of the main chain is virtually the only result of thermal reaction, the stripping off of side-chains in polybutene-1 is clearly indicated by the nature of the pyrolysis products.

In the case of polybutene-1 a mechanism involving stripping off of side-chains is involved in the formation of ethylene:

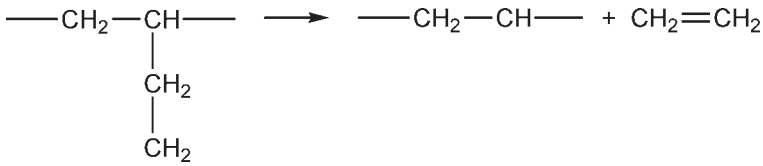

In actual fact a considerable yield of ethylene is obtained from polybutene-1, whereas the production of propylene is much smaller because this can only emanate from the principal chain. The complicated structure of polybutene-1, as compared with the structures of PE and polypropylene, gives rise to the formation of a markedly larger number of structurally isomeric degradation products. Theoretically with a maximum molecular size of C_8, 37 different hydrocarbon decomposition products should be obtainable from polybutene-1 and, in fact, Voigt [68] was able to identify, or indicate the probable existence of 33 compounds for polybutene-1.

10.4 Branching in Polyisoprene

Piskarova and Kartasheva [69] used GPC and light scattering in their studies of branched functions in isoprene synthetic rubber.

10.5 Branching in Polystyrene

SEC combined with viscometry has been used in branching studies on polystyrene (PS) [70]. Papanagopoulas and Dondos characterised branching in PS star polymers by GPC and light scattering [71].

10.6 Branching in Polyvinylchloride

It has been recognised since the work of Cotman [72] that by studying the polyolefin obtained from the reduction of polyvinylchloride (PVC) with lithium aluminium hydride, valuable structural information can be gained concerning the starting molecule. This reduction reaction has been investigated and refined [73] to the point where conditions have been established so that the chlorine may be efficiently removed from the polymer without degradation. The reduced polymer is similar to HDPE in almost all respects [74]. Thus, studies that have been applied to PE may also be applied to reduced PVC. Indeed better qualitative agreement has resulted when γ-ray radiolysis followed by identification of the gaseous hydrocarbons by mass spectrometry used in conjunction with infrared measurements is applied to reduced PVC than when this technique is applied to conventional PE. It was concluded from the large yields of methane relative to butane and ethane that the predominant side-chains along the PVC backbone are mainly one carbon long. It has been demonstrated by ^{13}C-NMR that most of the short branches in PVC are pendent chloromethyl groups [75]. This information was obtained from PVC samples reduced with lithium aluminium hydride and lithium aluminium deuteride, respectively.

Ahlstrom and co-workers [76] applied the techniques of Py-GC and PHGC to the determination of, short-chain branches in PVC and reduced PVC. Their attempts to determine the short-chain branches in PVC by Py-GC were complicated by an inability to separate all the parameters affecting the degradation of the polymer. Not only does degree of branching change the pyrolysis pattern, but so do tacticity and crosslinking [77].

For the pyrolysis of PVC, a ribbon probe was used. On-line hydrogenation of the pyrolysis products was accomplished using hydrogen as the carrier gas with 1% palladium on Chromasorb-P catalyst inserted in the injection port liner. Maximum

Table 10.17 Relative total branch content of HDPE, lithium aluminium hydride - reduced PVC and LDPE	
Sample	**Branched products (%)**
HDPE	12.0
Reduced PVC*	19.0
LDPE	26.0

* Average value

*Reprinted with permission from D.H. Ahlstrom, S.A. Liebman and K.B. Abbas, Journal of Polymer Science, Polymer Chemistry Edition, 1976, **14**, 10, 2479, ©1976, Wiley Interscience [76]*

Table 10.18 Short chain branch content of lithium aluminium hydride reduced PVC		
Sample	***iso*** **C_8- / *n*-C_8-**	**C_{10} (%)**
HDPE	0.1	8.6
Pevikon R341	0.52	7.7
Nordforsk E-80	0.71	7.2
Nordforsk S-80	1.20	7.0
Nordforsk S-54	1.59	6.8
Nordforsk E-54	1.63	6.5
Ravinil R100/650	1.63	6.5
Shinttsu TK1000	1.87	6.3
Low-density polyethylene	1.83*	5.2

*This ratio does not include the C_4 branch content

*Reprinted with permission from D.H. Ahlstrom, S.A. Liebman and K.B. Abbas, Journal of Polymer Science, Polymer Chemistry Edition, 1976, **14**, 10, 2479, ©1976, Wiley Interscience [76]*

triplet formation occurred at C_{14} for LDPE and for reduced PVC and at C_{15} for HDPE. The occurrence of the peak maxima at C_{14} for reduced PVC indicates that the total branch content is higher than that of HDPE. However, aside from the C_{14}/C_{15} peak maxima difference, the pyrolysis pattern for even the most highly

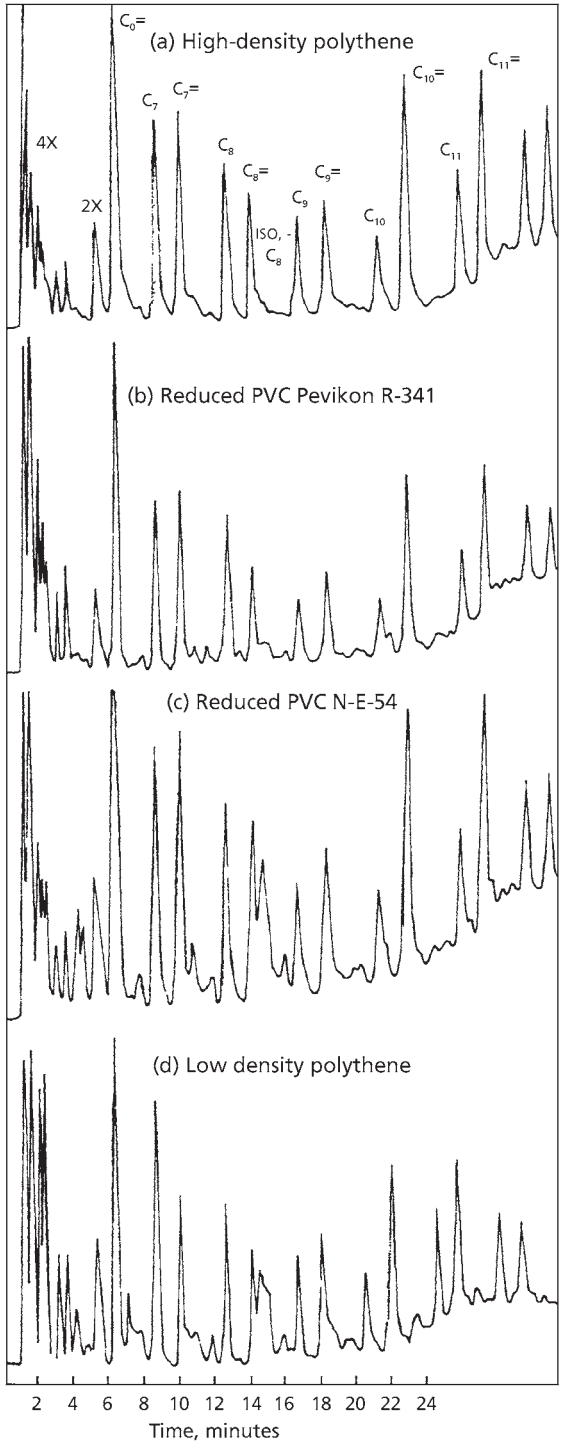

Figure 10.6 Pyrolysis of polyethylenes and reduced PVC (a) high-density polyethylene; (b) reduced PVC Pevikon-R-341; (c) reduced PVC N-E-54; (d) low-density polyethylene Durapak column fragments C_1-C_{11}. (*Reprinted with permission from D.H. Ahlstrom, S.A. Liebman and K.B. Abbås, Journal of Polymer Science: Polymer Chemistry Edition, 1976,* ***14****, 10, 2479. © 1976, John Wiley and Sons [76]*)

branched PVC resembles HDPE more than LDPE. These data indicate that the type of short-chain branch in PVC is qualitatively more like that of HDPE, but that the sequence length between branch sites is shorter in LDPE and PVC. Since LDPE contains a large amount of ethyl and butyl branches, and PVC and HDPE contain mainly methyl and some ethyl branches, this qualitative resemblance would be expected. A relative measure of the total amount of short chain branches for these polymers can be obtained by calculating the percentage of branched products formed (**Table 10.17**).

More information about the specific type of short-chain branch in PVC can be found from an examination of the C_1-C_{11} hydrocarbons (**Figure 10.6**). Here quantitative differences, between the reduced PVC become more apparent. The most obvious differences occur in the amounts of *iso*-C_7 and *iso*-C_8 products formed, which indicate differences in the total branch content. As the amount of short-chain branching (C_{10}) in the reduced PVC increases, there is a decrease in the amount of iso-alkanes formed (**Table 10.18**). The data in **Table 10.18** show small but distinguishable differences in the short-chain branch content of the reduced PVC.

10.7 Branching in Polyvinyl Fluoride

Investigations of the microstructure of polyvinyl fluoride (PVF) by fluorine-NMR have been reported by Weigert [78] and Bruch and co-workers [79]. Weigart studied a laboratory sample at 100 °C in dimethyl-d_6 sulfoxide. The broadband proton-decoupled fluorine-NMR spectrum at 94.1 MHz showed two groups of peaks. The major group, in the region -178 to -182 ppm, was assigned to head-to-tail monomer units, while the minor group, in the region -189 to -197 ppm, was assigned to tail-to-tail monomer units. Peaks within each group were assigned to fluorine atoms from monomer units in different tactic sequences.

Bruch and co-workers [79] studied a commercial sample and also a laboratory-prepared sample containing no monomer reversals. Broadband proton-decoupled fluorine-NMR spectra of solutions in *N*,*N*-dimethylformamide at 130 °C were obtained at 188.2 MHz. A two-dimensional *J*-correlated NMR experiment enabled definitive assignments of the individual peaks to different tactic sequences to be made.

Ovenall and Uschold [80] examined samples of PVF by ^{19}F-NMR at 376.5 MHz and proton NMR at 400 MHz as solutions in *N*-methylpyrrolidone and as swollen gels in dimethyl-d_6 sulfoxide (me_2 50-d_6). Weak peaks in the fluorine-NMR spectra have been assigned to CH_2CH_2F end groups and to tertiary fluorine atoms at branch points. A differential decoupling experiment, in which the proton spectrum was observed with

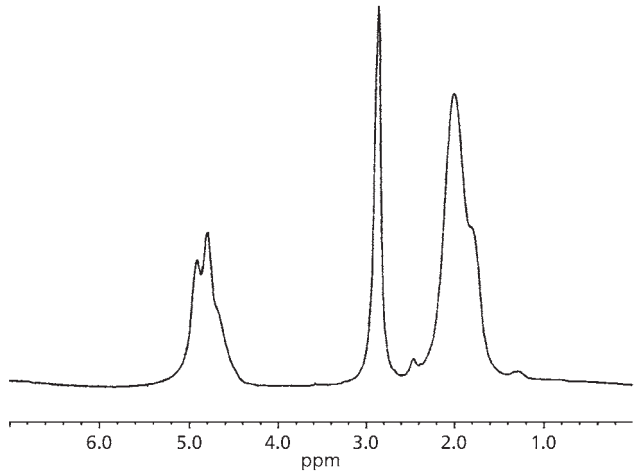

Figure 10.7 400 MHz proton NMR spectrum of polyvinylfluoride. (*Reprinted with permission from D.W. Ovenall and R.E. Uschold, Macromolecules, 1991,* ***24****, 11, 3235. ©1991, ACS [80]*)

and without selective irradiation of the weak fluorine peaks, permitted resonances of protons in the CH_2CH_2F end groups to be observed selectively. Pressure and temperature conditions used for polymer synthesis were found to influence branching but not the number of monomer reversals in the chain leading to head-to-head units. Monomer reversals account for about 13% of the vinyl fluoride in the polymer. Chain branching varies from about one branch every 80 monomer units to one branch every 200 monomer units depending on reactor conditions. Low polymerisation temperature and high pressure yield the most linear polymers. Melting point and heat of fusion measured by differential scanning calorimetry increase with the linearity of the product.

The 400-MHz proton NMR spectrum of a PVF sample swollen in Me_2SO-d_6 is shown in **Figure 10.7**. The features around 4.8 ppm are assigned to CHF protons and the features around 2.0 ppm to CH_2 protons. The feature at 2.9 ppm is from adventitious water. It was hoped it would be possible to identify in the proton spectrum weak peaks from the branched structures detected by fluorine-NMR. However, the proton spectrum was too broad for this to be done directly. Attempts at improving the resolution by Gaussian to Lorentzian resolution enhancement were unsuccessful. A weak peak visible at about 1.2 ppm may be due to methyl protons in end groups with structures $CHFCH_3$, originating from hydrogen abstraction by growing polymer chains ending in reversed monomer units.

For detecting the resonances of hydrogen atoms in chain ends and near branch points, the differential selective fluorine irradiation experiment was used to link the two spectra via H-F couplings:

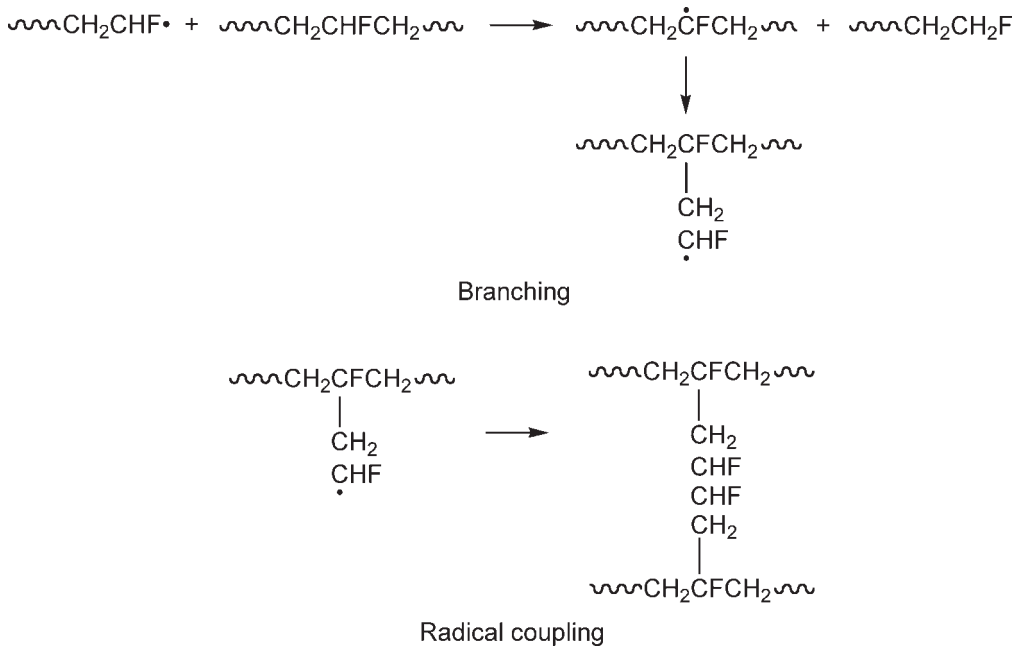

Irradiation of a particular fluorine peak should result in narrowing of the resonances of any protons coupled to the corresponding fluorine atom. These will then appear in a differential mode as sharpened features with the original broad peaks subtracted. The experiment was tested by irradiating one of the major fluorine resonances and gave a positive response. When both fluorine irradiation frequencies were in an empty part of the spectrum, little or no response was given in the proton spectrum, even at the positions of the major peaks. **Figure 10.8** shows the differential proton spectrum obtained when the fluorine NMR spectrum was irradiated at -220 ppm, corresponding to the weak CH_2F resonances. A positive response from the CH_2F protons is seen at 4.5 ppm. No distinct peak is visible at this point in the normal proton spectrum. A weaker response from the CH_2 protons in the CH_2CH_2F end groups is seen at 2.0 ppm. No responses were obtained in the proton spectrum when the weak features at -147 ppm were irradiated. These are assigned to tertiary fluorine atoms which have the closest hydrogen atoms three bonds away, and the H-F couplings are presumably too weak to give a detectable response.

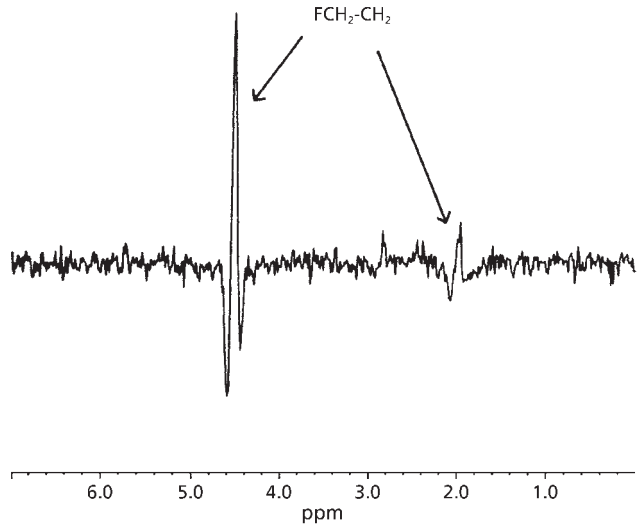

Figure 10.8 400 MHz proton NMR spectrum of polyvinylfluoride with differential fluorine decoupling at -220 ppm. (*Reprinted with permission from D.W. Ovenall and R.E. Uschold, Macromolecules, 1991, **24**, 11, 3235. © 1991, ACS [80]*)

10.8 Branching in Polysaccharide Biopolymers

Yu and Rollings [81, 82] applied a low-angle laser light scattering detector (LALLS) used with SEC (SEC/LALLS) for the determination of molecular weight, molecular weight distribution (MWD), and degree of branching of polysaccharide biopolymers in 0.5 N sodium hydroxide solution. Data from both detectors (differential refractive index and LALLS) are used to calculate the absolute molecular weight at each point in a sample chromatogram. The correct average molecular weight and MWD can be obtained without calibration methods used in conventional SEC. As a consequence of this technique, Mark-Houwink coefficients were predicted from a single broad-distribution, homopolymer without recourse to time-consuming fractionation methods. Moreover, the hydrodynamic volume separation mechanism of SEC can be exploited with the SEC/LALLS method to gain information about polymer branching. SEC/LALLS has been used to obtain data about the branching parameters g_v and g_M for samples of amylose, amylopectin, starch, and glycogen. For three homopolymers (amylose, amylopectin, and glycogen), branching frequency (as measured by chemical means), and the branching parameters *(g_v* and *g_M)* are inversely related. This trend is consistent with theoretical predictions. For starch, a nonhomogeneous branching distribution is observed as a function of molecular weight.

Matsuzaki and co-workers [83] also presented the quantitative branching characterisation of polysaccharide via SEC and LALLS detection from both theoretical arguments as well as direct experimental evidence. The two measurable branching parameters $g_{v(m)}$ $[= (M/([\bar{M}]_n)_m)_v]$ and $g_{v(m)}$ $[= (M/([\bar{M}]_{w(m)v}]$ of a sample mixture were related theoretically to the mixture's composition. There exists linear relationships between $g_{v(m)}$ and $W_{b,\,v}$ (the mass fraction of branched component in mixture) as well as between $g'^{-1}_{v(m)}$ and $w_{b,\,v}$. The latter correlation was demonstrated experimentally employing a combined SEC/LALLS technique. Excellent agreement was obtained with the theoretical predictions. This polymer branching characterisation method was also applied to study enzymic starch hydrolysates products. The MWD and branching distribution have been obtained.

10.9 Branching in Miscellaneous Polymers

Other polymers on which branching studies have been conducted include ethylene-propylene copolymers, polypropylene oxide [84-86], polyalkylvinyl esters [87, 88-92], PVC [93-97], ethylene-2 chloroacrylate copolymers [98], ethylene glycidyl-acrylate copolymers [99], poly-*trans*,1,3-pentadiene [93], poly-ε-caprolactone [94], polytetra-methylene oxide [95], copoly-2-vinyl-naphthalene methylmaleate [96], 2-vinyl naphthalene-4,4-methacrylate [96], polymethylmethacrylate [97], poly *tert*-butyl acrylate [97] and polychloroprene [100].

References

1. R. Kuhn, H. Krömer and G. Roßmanith, *Die Angewandte Makromolekulare Chemie*, 1974, **40**, 1, 361.

2. R. Kuhn and H. Krömer, *Colloid and Polymer Science*, 1982, **260**, 12, 1083.

3. G. Luft, R. Kämpf and H. Seidl, *Die Angewandte Makromolekulare Chemie*, 1982, **108**, 1, 203.

4. G. Luft, R. Kämpf and H. Seidl, *Die Angewandte Makromolekulare Chemie*, 1983, **111**, 1, 133.

5. E. Nordmeier, U. Lanver and M.D. Lechner, *Macromolecules*, 1990, **23**, 4, 1072.

6. E. Nordmeier, U. Lanver and M.D. Lechner, *Macromolecules*, 1990, **23**, 4, 1077.

7. M. Laiber, H. Opera, M. Toader and V. Liaber, *Revista de Chimie (Bucharest)*, 1977, **28**, 881. [*Chemical Abstracts*, 1978, **88**, 23539p]

8. R. Salovey and J.V. Pascale, *Journal of Polymer Science Part A: General Papers*, 1964, **2**, 5, 2041.

9. J.R. Nielson and R.F. Holland, *Journal of Molecular Spectroscopy*, 1960, **4**, 1-6, 448.

10. D.A. Boyle, W. Simpson and J.D. Waldron, *Polymer*, 1961, **2**, 323.

11. A.H. Willbourn, *Journal of Polymer Science*, 1959, **34**, 127, 569.

12. A.G. Nerheim, *Analytical Chemistry*, 1975, **47**, 7, 1128.

13. M. Seeger and E.M. Barrall II, *Journal of Polymer Science: Polymer Chemistry Edition*, 1975, **13**, 7, 1515.

14. A. Nishioka, I. Ando and J. Matsumoto, *Bunseki Kagaku*, 1977, **26**, 308. [*Chemical Abstracts*, 1977, **87**, 102729h]

15. G. Kraus and C.J. Stacy, *Journal of Polymer Science: Polymer Symposium*, 1973, **43**, 1, 329.

16. G.N. Foster, *Polymer Preprints*, 1970, **20**, 2, 463.

17. A. Barlow, L. Wild and R. Ranganath, *Journal of Applied Polymer Science*, 1977, **21**, 12, 3319.

18. L. Wild, R. Ranganath and A. Barlow, *Journal of Applied Polymer Science*, 1977, **21**, 12, 3331.

19. J.C. Randall, *Journal of Polymer Science: Polymer Physics Edition*, 1973, **11**, 2, 275.

20. J.C. Randall, *Journal of Applied Polymer Science*, 1978, **22**, 2, 285.

21. P.M. Kamath and A. Barlow, *Journal of Polymer Science Part A-1: Polymer Chemistry*, 1967, **5**, 8, 2023.

22. F.A. Bovey, F.C. Schilling, F.L. McCrackin and H.L. Wagner, *Macromolecules*, 1976, **9**, 1, 76.

23. D.C. Bugada and A. Rudin, *European Polymer Journal*, 1987, **23**, 11, 847.

24. J. van Schooten and J.K. Evenhuis, *Polymer*, 1965, **6**, 7, 343.

25. J. van Schooten and J.K. Evenhuis, *Polymer*, 1965, **6**, 11, 561.

26. L. Michajlov, P. Zugenmaier and H-J. Cantow, *Polymer*, 1968, **9**, 325.

27. D.H. Ahlstrom, and S.A. Liebman, *Journal of Polymer Science: Polymer Chemistry Edition*, 1976, **14**, 10, 2479.

28. O. Mlejnek, *Journal of Chromatography*, 1980, **191**, 181.

29. Y. Sugimura and S. Tsuge, *Macromolecules*, 1979, **12**, 3, 512.

30. S. Tsuge, Y. Sugimura and T. Nagaya, *Journal of Analytical and Applied Pyrolysis*, 1980, **1**, 3, 221.

31. Y. Sugimura, T. Usami, T. Nagaya and S. Tsuge, *Macromolecules*, 1981, **14**, 6, 1787.

32. S.A. Liebman, D.H. Ahlstrom, W.H. Starnes Jr., and F.C. Schilling, *Journal of Macromolecular Science, Part A: Pure and Applied Chemistry*, 1982, **17**, 6, 935.

33. M.A. Haney, D.W. Johnston and B.H. Clampitt, *Macromolecules*, 1983, **16**, 11, 1775.

34. J.C. Randall, *Journal of Applied Polymer Science*, 1978, **22**, 2, 585.

35. D.E. Axelson, G.C. Levy and L. Mandelkern, *Macromolecules*, 1979, **12**, 1, 41.

36. T. Usami and S. Takayama, *Macromolecules*, 1984, **17**, 9, 1756.

37. H. Ohtani, S. Tsuge and T. Usami, *Macromolecules*, 1984, **17**, 12, 2557.

38. T. Housaki, K. Satoh, K. Nishikida and M. Morimoto, *Die Makromolekulare Chemie, Rapid Communications*, 1988, **9**, 8, 525.

39. J.N. Willis, J.L. Dwyer, X. Liu and W.A. Dark, *ACS Polymeric Materials: Science and Engineering Conference*, 1997, **77**, 27.

40. K. Nishikida, T. Housaki, M. Morimoto and T. Kinoshita, *Journal of Chromatography*, 1990, **517**, 209.

41. J. Blitz in *Crystallization of Polymers*, Ed., M. Dosiere, NATO ASI Series Series C, No.405, 1993, p.375.

42. J. Kong, X. Fan and M. Jia, *Journal of Applied Polymer Science*, 2004, **93**, 6, 2542.

43. B.D. Dickie and R.J. Koopmans, *Journal of Polymer Science Part C: Polymer Letters Edition*, 1990, **28**, 6, 193.

44. W.J. Van Ooij and R.H.G. Brinkhuis, *Surface and Interface Analysis*, 1988, **11**, 8, 430.

45. S. Pang and A. Rudin, *ACS Polymeric Materials: Science and Engineering*, 1991, **65**, 95.

46. F.M. Mirabelle and L. Wild in *Polymer Characterisation: Physical Property, Spectroscopic, and Chromatographic Methods*, Eds., C.D. Craver and T. Provder, Advances in Chemistry Series, No.277, ACS, Washington, DC, USA, 1990, p.23.

47. P. Tacx and J.C.J.F. Tacx, *Polymer*, 1998, **39**, 14, 3109.

48. J. Schaefer and D.F.S. Natusch, *Macromolecules*, 1972, **5**, 4, 416.

49. Y. Inoue, A, Nishioka and R. Chujo, *Journal of Polymer Science: Polymer Physics Edition*, 1973, **11**, 11, 2234.

50. R.S. Porter, S.W. Nicksic and J.F. Johnson, *Analytical Chemistry*, 1963, **35**, 12, 1948.

51. C.E. Wilkes, C.J. Carman and R.A. Harrington, *Journal of Polymer Science:Polymer Symposia*, 1973, **43**, 1, 237.

52. C.J. Carman, R.A. Harrington and C.E. Wilkes, *Macromolecules*, 1973, **10**, 3, 536.

53. G.J. Ray, P.E. Johnson and J.R. Knox, *Macromolecules*, 1977, **10**, 4, 773.

54. J.M. Sanders and R.A. Komoroski, *Macromolecules*, 1977, **10**, 6, 1214.

55. J.R. Paxson and J.C. Randall, *Analytical Chemistry*, 1978, **50**, 13, 1777.

56. J.C. Randall, *Macromolecules*, 1978, **11**, 1, 33.

57. D.M. Grant and E.G. Paul, *Journal of the American Chemical Society*, 1964, **86**, 15, 2984.

58. D.E. Axelson, G.C. Levy and L. Mandelkern, *Macromolecules*, 1979, **12**, 1, 41.

59. M. De Pooter, P.B. Smith, K.K. Dohrer, K.F. Bennett, M.D. Meadows, C.G. Smith, H.P. Schouwenaars and R.A. Geerards, *Journal of Applied Polymer Science*, 1991, **42**, 2, 399.

60. E. Pérez and D.L. Vanderhart, *Journal of Polymer Science Part B: Polymer Physics Edition*, 1987, **25**, 8, 1637.

61. A. Keller and D.J. Priest, *Journal of Macromolecular Science, Part B: Physics*, 1968, **2**, 3, 479.

62. A. Keller and D.J. Priest, *Journal of Polymer Science Part B: Polymer Letters*, 1970, **8**, 13.

63. D.E. Witenhafer and J.L. Koenig, *Journal of Polymer Science Part A-2: Polymer Physics Edition*, 1969, **7**, 7, 1279.

64. J. Runt and I.R. Harrison, *Journal of Polymer Science: Polymer Physics Edition*, 1978, **16**, 2, 375.

65. L.J. Bellamy, *Infrared Spectra of Complex Molecules*, 2nd edition, Wiley, New York, NY, USA, 1958, p. 13.

66. V.L. Khodzhaever, Y.L. Guseva, V.I. Kleiner, V.G. Zaikin, B.A. Krentsel and B.N. Bobrov, *Vysokomolekulyarnye Soedineriya Seriya B*, 1989, **31**, 8, 598.

67. R. Hank, *Rubber Chemistry and Technology*, 1967, **40**, 3, 936.

68. T. Voigt, *Kunststoffe*, 1964, **54**, 2.

69. E.P. Piskareva and G.G. Kartasheva, *International Polymer Science and Technology*, 1988, **15**, 7, T/5.

70. G. Kuo, T. Provder and M.E. Koehler, *ACS Polymeric Materials Science and Engineering*, 1991, **65**, 142.

71. D. Paparagopoulos and A. Dondos, *European Polymer Journal*, 2004, **40**, 10, 2305.

72. J.D. Cotman, *Journal of the American Chemical Society*, 1955, **77**, 10, 2790.

73. M. Carrega, C. Bonnebat and G. Zednik, *Analytical Chemistry*, 1970, **42**, 14, 1807.

74. A.J. de Vries, C. Bonnebat and M. Carrega, *Pure and Applied Chemistry*, 1971, **26**, 26209.

75. F.A. Bovey, K.B. Abbås, F.C. Schilling and W.H. Starnes, *Macromolecules*, 1975, **8**, 4, 437.

76. D.H. Ahlstrom, S.A. Liebman and K.B. Abbås, *Journal of Polymer Science: Polymer Chemistry Edition*, 1976, **14**, 10, 2479.

77. M. Suzuki, S. Tsuge and T. Takeuchi, *Journal of Polymer Science Part A-1: Polymer Chemistry*, 1972, **10**, 4, 1051.

78. F.J. Weigert, *Organic Magnetic Resonance*, 1971, **3**, 373.

79. M.D. Bruch, F.A. Bovey and R.E. Cais, *Macromolecules*, 1984, **17**, 12, 2547.

80. D.W. Ovenall and R.E. Uschold, *Macromolecules*, 1991, **24**, 11, 3235.

81. L-P. Yu and J.E. Rollings, *Journal of Applied Polymer Science*, 1987, **33**, 6, 1909.

82. L-P. Yu and J.E. Rollings, *Journal of Applied Polymer Science*, 1988, **35**, 4, 1085.

83. K. Matsuzaki, S. Okuzono and T. Kanai, *Journal of Polymer Science: Polymer Chemistry Edition*, 1979, **17**, 3447.

84. W. Lapeyre, H. Cheradame, N. Spassky and P. Sigwalt, *Journal de Chimie Physique et de Physico-Chemie de Biologique,* 1973, **70**, 838.

85. T. Uryu, H. Shimazu and K. Matsuzaki, *Journal of Polymer Science: Polymer Letters Edition*, 1973, **11**, 4, 275

86. J. Schaefer, *Macromolecules*, 1972, **5**, 5, 590.

87. K. Matsuzaki, H. Ito, T. Kawamura and T. Uryu, *Journal of Polymer Science: Polymer Chemistry Edition*, 1973, **11**, 5, 971.

88. C. Baker, W.F. Maddams, G.S. Park and B. Robertson, *Die Makromolekulare Chemie*, 1973, **165**, 321.

89. J.L. Millan and J.L. De la Pena, *Revista de Plasticos Modernos*, 1973, **26**, 206, 232.

90. T. Kelen, G. Galambos, F. Tüdos and G. Bálint, *European Polymer Journal*, 1969, **5**, 5, 617.

91. E. Bezdadea, D. Braun, E. Buruiana, A. Caraculacu and G. Istrate-Robila, *Die Angewandte Makromolekulare Chemie*, 1974, **37**, 1, 35.

92. E. Schröder and M. Byrdy, *Plaste und Kautsch*, 1977, **24**, 11, 757.

93. K.F. Elgert and W. Ritter, *Die Makromolekulare Chemie*, 1976, **177**, 7, 2021.

94. J. Choi and S-Y. Kwak, *Macromolecules*, 2004, **37**, 10, 3745.

95. D. Husken, J. Krijgsman and R.J. Gaymans, *Polymer*, 2004, **45**, 14, 4837.

96. G. Montaudo, C. Puglisi, D. Vitalini and Y. Morishima, *Journal of Analytical and Applied Pyrolysis*, 1988, **13**, 3, 161.

97. J. Lesec and M. Millequant, *International Journal of Polymer Analysis and Characterisation*, 1996, **2**, 3, 305.

98. F. Keller, *Plaste und Kautsch*, 1975, **22**, 1, 8.

99. F. Keller, G. Findeisen, G. Raetzsch and H. Roth, *Plaste und Kautsch*, 1975, **22**, 9, 722.

100. H. Krämer-Lucas, J. Ramthun and H.W. Lucas, *Die Makromolekulare Chemie - Macromolecular Symposia*, 1992, **61**, 284.

11 Block Copolymers

Water-soluble triblock polymers of polyoxypropylene and polyoxyethylene, the so-called Pluronics, find widespread application as nonionic surface-active agents. Polyoxyalkylene block copolymers, having surfactant properties, have been utilised as lubricants, dispersants, antistatic agents, foam control agents, and solubilisers and in numerous other applications in the areas of pharmaceuticals, cleaning agents, foods, and personal care products [1, 2]. This diversity in applications results from the various possible structural arrangements of polyoxyalkylene block copolymers. In these materials, ethylene oxide (EO) blocks provide hydrophilicity, and propylene oxide (PO) blocks provide the hydrophobicity necessary for surfactancy. The chemical composition distribution can be modified to achieve the desired surfactant performance. Within this context, it is necessary to obtain a complete description of the molecular composition distribution of the individual blocks in the copolymer in order to understand the structure-function relationships of surfactants with respect to physical, rheological, and mechanical properties. It is important to have detailed knowledge about the sequence and distributions of EO and PO blocks, the degree of polymerisation and block size, the identity and structure of particular end groups (initiator and terminator type), and impurities. Detailed reviews of analytical approaches for studying polyoxyalkylene nonionic surfactants have been compiled by Kalinoski [3], Chu [4], Chu and Zhou [5], and Schmitt [6]. These methods include liquid chromatography, infrared spectroscopy, Raman spectroscopy, viscosimetry, calorimetry, and nuclear magnetic spectroscopy (NMR) spectroscopy. In general, these methods yield only an average distribution of specific structural features and are not suitable for the characterisation of the individual components of molecular weight distributions. In recent years, it has been demonstrated that mass spectrometric methods in combination with soft ionisation techniques, which minimise fragmentation during ionisation and thus produce (pseudo-) molecular ions, can provide this information [7]. Within this range of techniques, matrix assisted laser desorption/ionisation (MALDI) mass spectrometry especially has proven its value in providing accurate and detailed molecular weight data on high molecular weight materials [8, 9]. Since its introduction by Tanaka and co-workers [10] and by Karas and Hillenkamp [11], the technique has evolved as one of the most successful volatilisation and ionisation methods for a wide variety of molecules, such as peptides, proteins, oligosaccharides, and synthetic polymers. Several reviews illustrate the continuously growing scope of MALDI applications [8, 12-14].

In many cases, the MALDI ionisation technique is coupled to relatively inexpensive time-of-flight (ToF) mass spectrometers. These systems provide a large mass range over which the samples can be analysed, with high sensitivity, a mass accuracy of typically 0.1%, and oligomeric mass resolution [15]. For example, MALDI-ToF has been successfully used for obtaining molecular weights of segments of synthetic copolymers and weight averages of the molecular weight distributions [16], and for obtaining the detailed description of the individual components of triblock copolymers of polystyrene-block-poly(α-methylstyrene) bv Wilczek-Vera and co-workers [17].

The recent introduction of delayed extraction has extended the performance of MALDI-ToF systems to isotopic resolved measurements for masses up to ~4000 amu with mass accuracies of ~15 ppm [18]. However, for copolymers exhibiting frequent overlap of peaks corresponding to different copolymer compositions, even higher mass resolution is required in order to differentiate between them. In these cases, the mass resolution of MALDI-ToF systems (even with delayed extraction) is insufficient, and the use of Fourier transform ion cyclotron resonance mass spectrometry (FTICR-MS) becomes imperative. Using the standard resolution in the broadband mode of this instrument, isotopically resolved, singly charged polymers in the mass range up to *m/z* ~4500 with mass accuracies better than 20 ppm are measured routinely [19-23]. Changing to the heterodyne mode (high-resolution mode) increases performance easily to mass resolutions > 1,000,000 and mass accuracies < 1 ppm [24]. Such mass accuracies are frequently sufficient for exact elemental determination of the repeating units, terminal groups, and adducts [23]. However, the determination of accurate molecular weight distributions by MALDI-FTICR-MS is complicated by effects leading to a mass-dependent distortion of the measured distributions.

The MALDI process leads to ions with a broad, mass-independent velocity distribution [25]. Consequently, the various components in a polymer sample will enter the trap of the FTICR-MS with different, mass-dependent kinetic energies. As the trapping efficiency is highly dependent on the kinetic energy of the ions, this will obviously lead to mass discriminations in the MALDI experiments [26, 27]. If the MALDI experiments are carried out in an internal source geometry, trapping of higher kinetic energy ions is provided by the use of gated deceleration potentials [28-30]. However, as MALDI ions with higher masses have higher kinetic energies than lighter ones, it takes longer gated trapping times to slow these ions down. Hence, the duration of the gated deceleration potentials determines the mass range over which ions will be efficiently trapped. In the case of external source MALDI, the efficiently trapped mass range is also gate time dependent. Here, the postsource acceleration during the transport of the ions to the ion cyclotron resonance cell induces a mass-dependent flight time between ion formation and trapping and results in a flight-time-induced discrimination [31, 32]. Van Rooij and co-workers [33] demonstrated the utility of MALDI-Fourier Transform-infrared-MS performed on an external source. FTICR-MS

in a method for the treatment of molecular weight distributions measured by MALDI-FTICR-MS to yield the individual block length distributions in a complex Pluronic sample. The constituent monomer units in this block copolymer are small relative to the overall size of the copolymer, which means that overlap between different components of the molecular weight distribution is likely, and high-resolution mass spectrometry is imperative. The Pluronic sample of the type: $HO(C_2H_4O)_x(C_3HO)_Y(C_2H_4O)_3$-H offers a unique possibility to test the corrections on distortions induced by the experimental technique. The block lengths of both constituents are expected to be uncorrelated (random coupling hypothesis). An equal distribution in the block length of one of the constituents for different block lengths of the other constituent would confirm the validity of the corrections.

Van Rooij and co-workers [33] have described a method for the treatment of molecular weight distributions measured by MALDI on an external ion source FTICR-MS to yield the actual molecular weight distribution and, from that, the individual block length distributions. For the first time, detailed and accurate molecular weight data were obtained on a complex sample using this methodology, which independently validates the data provided by the manufacturer. The experimentally verified random coupling hypothesis proves the validity of the methodology.

The weight average number of polypropylene oxide units for the propylene oxide units (i.e., $\bar{n}_w$PO) obtained by this method was found to be 16.55 which was in good agreement with the value of 16.4 supplied by the polymer manufacturer.

Frisch and Xu [34] used ^{1}H-NMR and ^{13}C-NMR to study the effect of solution radical polymerisation of styrene with methacrylic acid in the presence of a homogeneous, high molecular weight ($M_w = 2 \times 10^5$), poly(2-vinylpyridine) template. The presence of the template had little, if any, effect on the molecular weight, composition, or glass transition temperatures of the copolymers but produced copolymers with significantly longer block lengths of both styrene and methacrylic acid repeat units.

Pyrograms will differentiate between random copolymers and block polymers or polymer mixtures [35-38]. Presence of foreign monomer may interrupt chain transfer processes involved in the degradation. Similar products result but their quantities as determined from peak heights are different. Voigt demonstrated that even for closely related polyolefins the pyrograms will distinguish between polyethylene-propylene block and random copolymers of the same composition [36].

Monge and Haddleton [39] reported on the use of on-line NMR in the analysis of poly(*n*-hydroxysuccinamide methacrylate) – *b*-poly(methylmethacrylate AB) type block copolymer.

References

1. R.Priorr in *Surfactants in Consumer Products: Theory, Technology and Application*, Ed., J. Falbe, Springer Verlag, Heidelberg, Germany, 1987, p.5-22.

2. A.J. Ryan and J.L. Stanford, *Comprehensive Polymer Science*, Eds., G. Allen and J.C. Bevington, Pergamon Press, Oxford, UK, 1989, p.427-455.

3. H.T. Kalinoski in *Nonionic Surfactants: Polyoxyalkylene Block Copolymers*, Ed., V.M. Nace, Surfactant Science Series No.60, Marcel Dekker, New York, NY, USA, 1966, p.31-66.

4. B. Chu, *Langmuir*, 1995, **11**, 2, 414.

5. B. Chu and Z. Zhou in *Nonionic Surfactants: Polyoxyalkylene Block Copolymers*, Ed., V.M. Nace, Surfactant Science Series No.60, Marcel Dekker, New York, NY, USA, 1966, p.67-143.

6. *Analysis of Surfactants*, Ed., T.M. Schmitt, Surfactant Science Series No.40, Marcel Dekker, New York, NY, USA, 1992.

7. L.M. Nuwaysir, C.L. Wilkins and W.J. Simonsick, *Journal of American Society of Mass Spectrometry*, 1990, **1**, 1, 66.

8. A.M. Belu, J.M. DeSimone, R.W. Linton, G.W. Lange and R.M. Friedman, *Journal of American Society of Mass Spectrometry*, 1996, **7**, 1, 11.

9. U. Bahr, A. Deppe, M. Karas, F. Hillenkamp and U. Giessmann, *Analytical Chemistry*, 1992, **64**, 22, 2866.

10. K. Tanaka, H. Waki, Y. Ido, S. Akita, Y. Yoshida, T. Yoshida and T. Matsuo, *Rapid Communications in Mass Spectrometry*, 1988, **2**, 8, 151.

11. M. Karas and F. Hillenkamp, *Analytical Chemistry*, 1988, **60**, 20, 2299.

12. F. Hillenkamp, M. Karas, R.C. Beavis and B.T. Chait, *Analytical Chemistry*, 1991, **63**, 24, 1193A.

13. M. Karas, U. Bahr and U. Giessmann, *Mass Spectrometry Reviews*, 1991, **10**, 5, 335.

14. M.V. Buchanan and R.L. Hettich, *Analytical Chemistry*, 1993, **65**, 5, 245A.

15. D.C. Schriemer and L. Li, *Analytical Chemistry*, 1996, **68**, 17, 2721.

16. P.O. Danis and F.J. Huby, *Journal of American Society of Mass Spectrometry*, 1995, **6**, 11, 1112.

17. G. Wilczek-Vera, P.O. Danis and A. Eisenberg, *Macromolecules*, 1996, **29**, 11, 4036.

18. R.D. Edmondson and D.H. Russell, *Journal of American Society of Mass Spectrometry*, 1996, **7**, 10, 995.

19. M.L. Gross and D.L. Rempel, *Science*, 1984, **226**, 4672, 261.

20. F.W. McLafferty, *Accounts of Chemical Research*, 1994, **27**, 11, 379.

21. P.B. O'Connor and F.W. McLafferty, *Journal of the American Chemical Society*, 1996, **117**, 51, 12826.

22. G.J. van Rooij, M.C. Duursma, R.M.A. Heeren, J.J. Boon and C.G. de Koster, *Journal of the American Society of Mass Spectrometry*, 1996, **7**, 5, 449.

23. E.R.E. van der Hage, M.C. Duursma, R.M.A. Heeren, J.J. Boon, M.W.F. Nielen, A.J.M. Weber, C.G. de Koster and N.K. de Vries, *Macromolecules*, 1997, **30**, 15, 4302.

24. G.M. Alber, A.G. Marshall, N.C. Hill, L. Schweikhard and T.L. Ricca, *Review of Scientific Instruments*, 1993, **64**, 7, 1845.

25. R.C. Beavis and B.T. Chait, *Chemical Physics Letters*, 1991, **181**, 5, 479.

26. J.D. Hogan and D.A. Laude, *Analytical Chemistry*, 1992, **64**, 7, 763.

27. S.A. Hofstadler, S.C. Beu, and D.A. Laude, *Analytical Chemistry*, 1993, **65**, 3, 312.

28. M. Dey, J.A. Castoro and C.L. Wilkins, *Analytical Chemistry*, 1995, **67**, 9, 1575.

29. M.L. Easterling, C.C. Pitsenberger, S.S. Kulkarni, P.K. Taylor and I.J. Amster, *International Journal of Mass Spectrometry and Ion Processes*, 1996, **157/158**, 97.

30. S.J. Pastor and C.L. Wilkins, *Journal of American Society of Mass Spectrometry*, 1997, **8**, 3, 225.

31. F.M. White, J.A. Marto and A.G. Marshall, *Rapid Communications in Mass Spectrometry*, 1996, **10**, 14, 1845.

32. P.B. O'Connor, M.C. Duursma, G.J. van Rooij, R.M.A. Heeren and J.J. Boon, *Analytical Chemistry*, 1997, **69**, 14, 2751.

33. G.J. van Rooij, M.C. Duursma, C.G. de Koster, R.M.A. Heeren, J.J. Boon, P.J.W. Schuyl and E.R.E. van der Hage, *Analytical Chemistry*, 1998, **70**, 5, 843.

34. H.L. Frisch and Q. Xu, *Macromolecules*, 1992, **25**, 20, 5145.

35. A. Barlow, R.S. Lehrle and J.C. Robb, *Polymer*, 1961, **2**, 27.

36. J. Voigt, *Kunststoffe*, 1964, **54**, 2.

37. J. Strassburger, G.M. Brauer, M. Tryon and A.F. Forziati, *Analytical Chemistry*, 1960, **32**, 4, 454.

38. K.J. Bombaugh, C.E. Cook and B.H. Clampitt, *Analytical Chemistry*, 1963, **35**, 12, 1834

39. S. Monge and D.M. Haddleton, *European Polymer Journal*, 2004, **40**, 1, 37.

12 Types of Unsaturation

12.1 Unsaturation in Homopolymers

12.1.1 Polybutadiene Unsaturation

Infrared Spectroscopy

Infrared spectroscopy is a very useful technique for the measurement of different types of unsaturation in polymers. Polybutadiene has the following structure:

$$\underset{1}{CH_2} = \underset{2}{CH} - \underset{3}{CH} = \underset{4}{CH_2}$$

Its polymers can contain the following types of unsaturation:

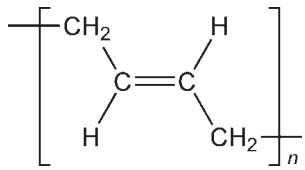

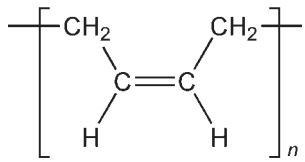

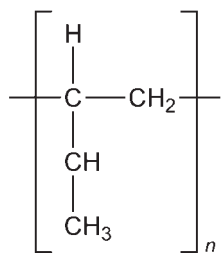

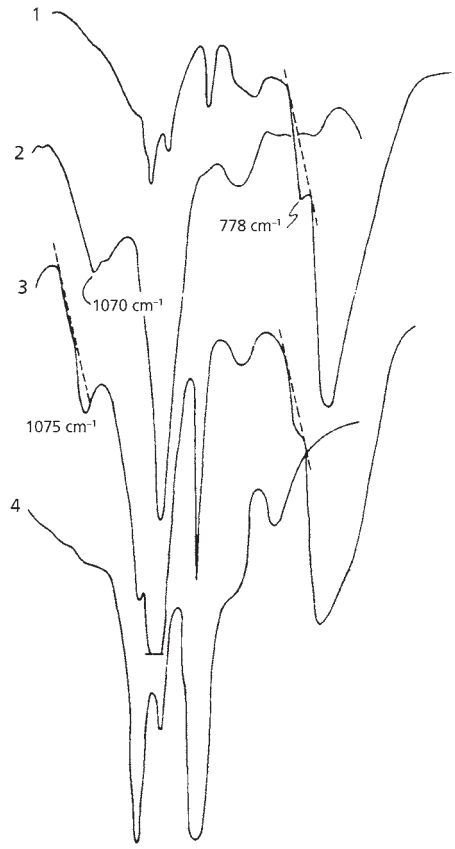

Figure 12.1 Spectra of (1) *cis*-1,4-PBD; (2) *trans*-1,4-PBD; (3) mixed PBD structure; (4) atactic 1,2-PBD. Figures displayed vertically viewing. All samples in carbon disulfide solutions; 2 mm light bath cell with NaCl window. (*Source: Author's own files*)

Fraga [1] has developed an infrared-near-infrared method of analysis of carbon tetrachloride solutions of polybutadienes suitable for the evaluation of *cis*-1,4, 5000-714.2 cm^{-1} (2-14 μm), *trans*-1,4, 9708 cm^{-1} (10.3 μm) and vinyl, 9091 cm^{-1} (11.0 μm) structures. Only polybutadiene is required for calibration purposes. The method is applicable to carbon tetrachloride soluble polybutadienes containing 0-97% *cis*-1,4 structure, 0-70% *trans*-1,4 structure, and 0-90% vinyl structure. Some typical spectra are shown in **Figure 12.1** for a high *cis*-1,4 polybutadiene, and high *trans*-1,4 polybutadiene, and a high 1,2 (atactic) polybutadiene, and other samples of different *cis* and *trans* compositions.

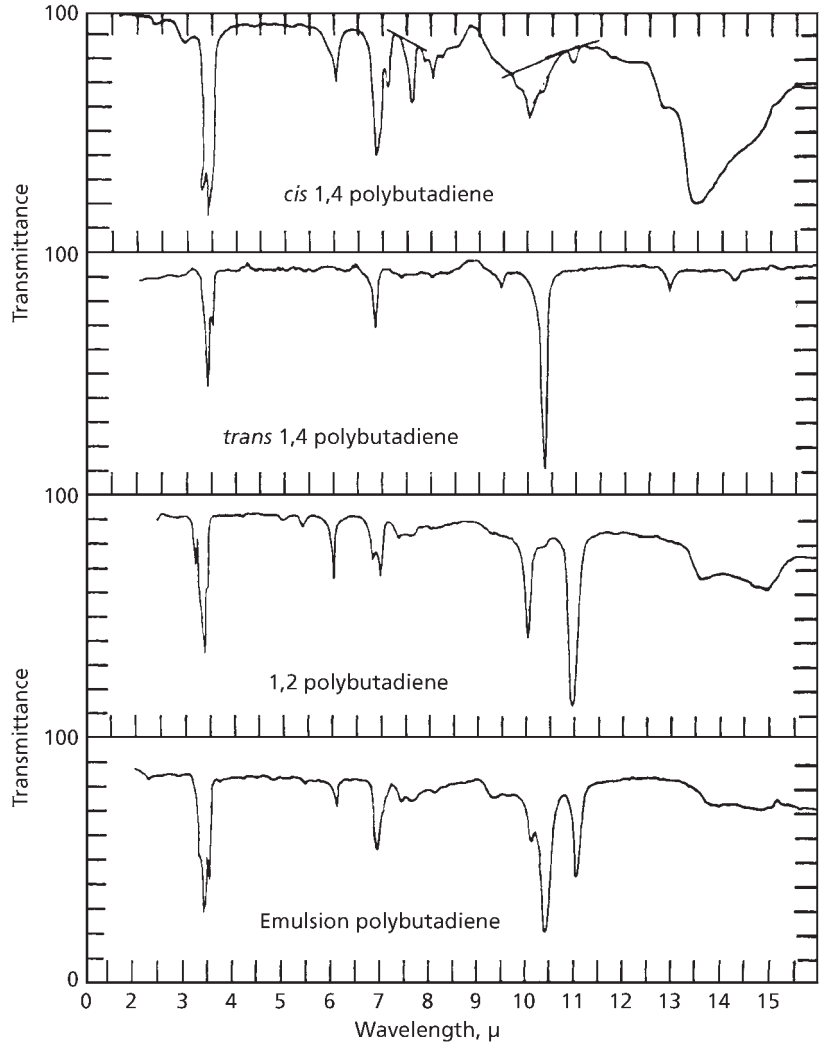

Figure 12.2 Infrared spectra of various kinds of polybutadienes.
(*Source: Author's own files*)

Figure 12.2 shows infrared (IR) spectra of various kinds of polybutadienes [2, 3], which illustrate the usefulness of IR spectroscopy for distinguishing between different types of unsaturation.

Fraga [1] has also described an IR thin film area method for the analysis of styrene-butadiene copolymers. The integrated absorption area between 1515 and 1389 cm^{-1} (6.6 and 7.2 μm) has been found to be essentially proportional to total

bound butadiene, and is independent of the isomeric-type butadiene structure present. This method can be calibrated for bound styrene contents ranging from 25% to 100%.

IR [4-8] and pyrolysis-IR [9] methods have both been tried for determination of the composition of vulcanisates, but both methods have serious disadvantages.

Various workers [10-12] used the aliphatic ^{13}C resonances (assuming Bernoullian statistics) to give indirect information on the relative abundance of the three base units.

Table 12.1 Assignments for the ^{13}C-NMR signals of the olefinic main chain *cis*-1,4 and *trans*-1,4 aarbons in polybutadiene (Polymer E)

Carbon atom	Resonance	Triad assignment	Chemical shift, ppm
–C=C*–	1	vtv	131.79
	2	ctv, ttv	131.35
	3	vcv	130.69
	4	vtt, vtc	130.56
	5	ccv, tcv	130.24
	6	etc, ctt	
	7	vcc, vet	130.08
	8	ttc, ttt	
–*C=C–	9	ctv, ttv	129.88
	10	ccc, tec	129.67
	11	cct, tct	129.48
	12	ccv, tcv	129.34
	13	vtc	128.51
	14	vtt	128.37
	15	vtv	128.23
	16	vcc	128.08
	17	vet	127.90
	18	vcv	127.75

Source: Author's own files

The first method necessitates two independent measurements $^{1}H/^{13}C$-NMR); the second (^{13}C-NMR) is severely hampered by questionable assignments [13, 14] and different compositionally induced diads for the methylene carbons and triads for the methine carbons [12]. Furthermore a T_1 and nuclear Overhauser effects are not necessarily equal for these different signals.

With the previously mentioned assignments of Elgert and co-workers [15] outlined a simple method for measuring the isomeric distribution along the polybutadiene chains. Sequence analysis can therefore be used to quantify the microstructure of polybutadiene.

The assignments for the ^{13}C-NMR signals of the olefinic main chain as 1,4 and *trans* 1,4 carbons in butadiene are given in **Table 12.1**.

Albert [16] has compared determinations of butadiene in high-impact polystyrene by an IR method and by the iodine monochloride method described by Crompton and Reid [17]. The IR method is based on a characteristic absorbance in the IR spectrum associated with the transconfiguration in polybutadiene:

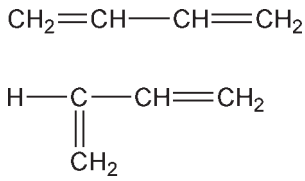

Since different grades of high-impact polystyrene (HIPS) may contain elastomers with different *trans*-butadiene contents, calibration curves based on the standard rubber are not always suitable for analysing these products. The results obtained by the two methods for several high-impact grades are compared in **Table 12.2**. The rubber content of HIPS sample 1 determined by titration is lower than the value obtained by the IR method. This is expected with interpolymerised polymers because of crosslinking, which reduces the unsaturation of the rubber. The other polymers (except sample 3), appear to contain diene 55-type rubber of high (*trans*-butadiene content, since reasonable agreement was obtained between the iodine monochloride and IR methods. HIPS 3 however, must contain a polybutadiene of high *cis*-content to explain the low (1.2%wt) amount of rubber found by the IR method compared to the 9.0% found by the titration method.

More recent studies include the use of near IR spectroscopy to determine *cis* 1,4-, *trans* 1,4- and 1,2-butadiene units in polybutadiene and styrene butadiene copolymers [18] and Fourier transform Raman spectroscopy to determine *cis* 1,4-, *trans* 1,4- and vinyl 1,2 contents of polybutadienes [19-21].

Table 12.2 Rubber content of high-impact polystyrenes (based on polybutadiene)		
Sample	**Polybutadiene, %w (iodine monochloride method)**	**Polybutadiene, %w (IR method)**
Standard: 6.0%w diene 55	6.2	
Standard: 12.0%w diene 55	12.2	
Standard: 15.0%w diene 55	14.8	
High-impact polystyrene 1	8.6	9.7
High-impact polystyrene 2	5.6	5.8
High-impact polystyrene 3	9.0	1.2
High-impact polystyrene 4	11.2	11.4
High-impact polystyrene 5	5.8	5.9
Source: Author's own files		

Nuclear Magnetic Resonance (NMR) Spectroscopy

IR methods rely, more or less, on the availability of isometrically pure reference polymers each containing relatively high concentrations of one of the three kinds of unsaturation units.

Proton NMR spectroscopy, on the other hand does not require pure vinyl 1,2-, *cis* 1,4-, and *trans* 1,4- units. However, except for polymers that contain only two base units, i.e., vinyl 1,2-units and *cis* 1,4 or *trans* 1,4. It is not possible by ^{1}H-NMR to obtain information about the amounts of the three base units that are present in polybutadienes containing significant fractions of all three types of unsaturation [13, 22-24], even when measurements are conducted at 400 MHz.

^{13}C-NMR spectroscopy, on the other hand, offers more information because detailed assignments have been described for the aliphatic [10-13] and olefinic carbons [11-15]. This led Van der Velden and co-workers [25] to attempt a quantitative analysis, excluding the necessity of using model polymers, by measuring 1,2-vinyl/*cis* 1,4 + *trans* 1,4 and the ratio *cis*/*trans* 1,4- via ^{13}C-NMR (aliphatic carbon resonances). The combination of these two techniques results in values for 1,2-vinyl, *cis* 1,4 and *trans* 1,4.

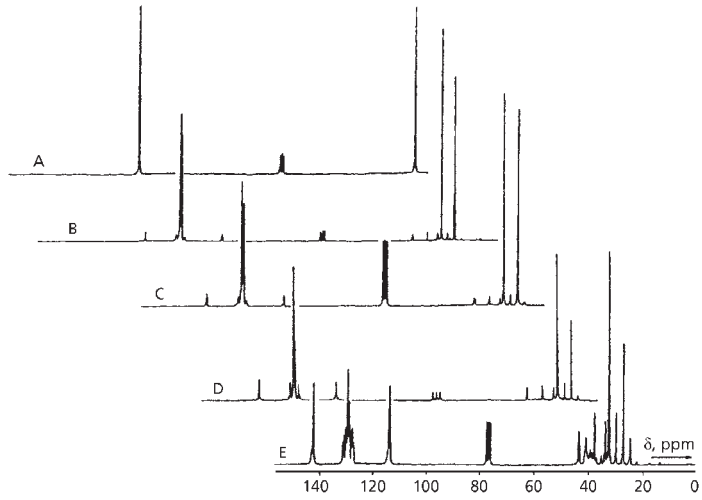

Figure 12.3 NMR spectra of five polybutadienes, *r* of increasing 1,2 vinyl content. (*Reprinted with permission from G. Van der Velden, C. Didden, T. Veermans and J. Beulen, Macromolecules, 1987,* ***20****, 6, 1252. [25]*)

In **Figure 12.3** are shown the ^{13}C-NMR spectra of the five polymers arranged in order of increasing 1,2-vinyl contents. The olefinic region can be subdivided into two parts:

a. The resonances at approximately 114 and 143 ppm have been assigned to the two different vinyl 1,2 carbon atoms, the methylene and methine, surrounded by neighbouring 1,2-vinyl, *cis* 1,4 and *trans* 1,4 units. Besides compositional sequence splittings, configurational splittings (tacticity) also occur. This can be seen in Figure 12.3, especially for polymer E. These deceptively simple ^{13}C-NMR patterns have not been previously analysed [26, 27].

b. The complex resonance pattern between 127-133 ppm, depicted in **Figure 12.4** is due to compositional splittings of the two olefinic carbons in central *cis* 1,4 (c), or *trans* 1,4 (t) units, present in different combinations of homotriads (ccc and ttt), heterotriads (ccv, ttv etc.), and symmetric and non-symmetric isolated triads (tct, vcv, tcv, vet etc.) [11, 12, 15]. When the negligible influence of tacticity effects is ignored, the theoretically expected number of resonances on a triad level is 36, i.e., 2(xcy + xty), x, y = c, t, v. However, the homotriads and the symmetric isolated triads contain two magnetically equivalent carbons, so the number of resonances to be observed cannot exceed 24. Experimentally, 16-18 different carbon resonances are reasonably well resolved (**Figure 12.4**).

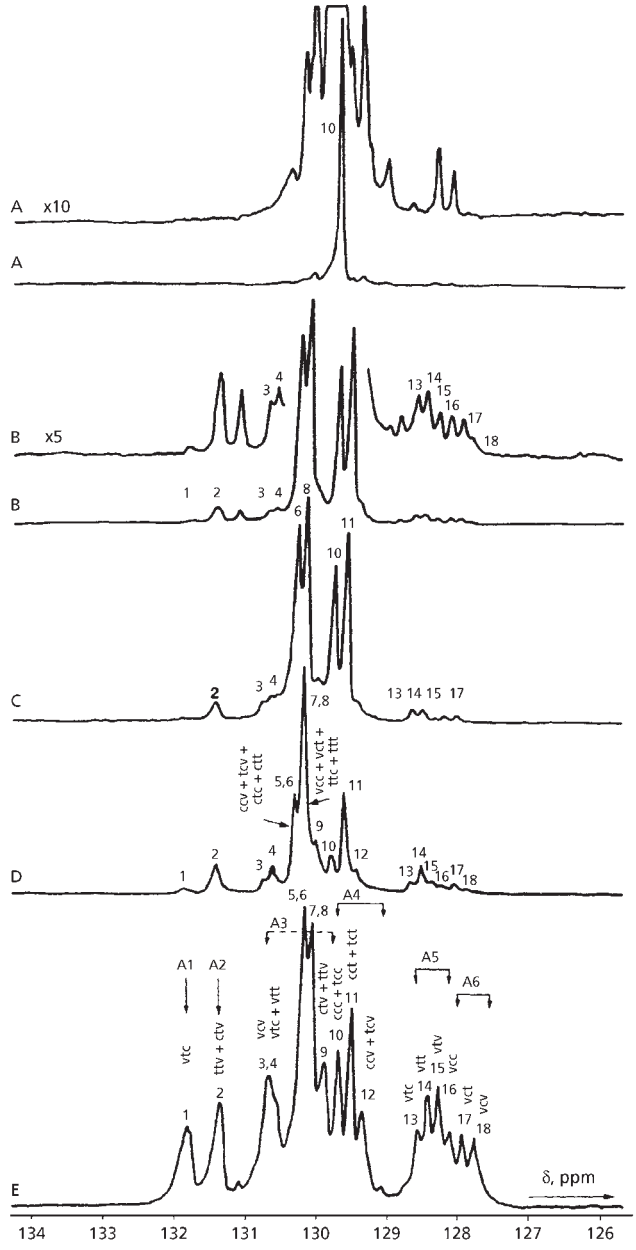

Figure 12.4 ^{13}C-NMR spectra of polybutadienes showing complex resonance patterns between 127 and 133 ppm. Revealing the 16–18 different carbon resonance. (*Reprinted with permission from G. Van der Velden, C. Didden, T. Veermans and J. Beulen, Macromolecules, 1987,* **20***, 6, 1252. ©1987, ACS [25]*)

No new assignments for this spectral region have been accomplished since 1975 [11, 15], therefore der Velden and co-workers [25] used the assignments of Elgert and co-workers [15] in combination with their notation.

It is possible by this technique to quantify small amounts of 1,2-vinyl, and the absence of *trans* 1,4 units. Other workers who have investigated the applications of NMR spectroscopy to the analysis of unsaturation in polybutadiene and styrene-butadiene copolymers include Carlson and Altenau [28], Carlson and co-workers [26], Binder [27], Braun and Canji [29, 30], Hast and Deur-Siftar [31], Silas and co-workers [32], Cornell and Koenig [21], Neto and Di Lauro [33], Clark and Chen [34] and Harwood and Richey [35].

12.1.2 Polyisoprene Unsaturation

Infrared Spectroscopy

Isoprene has the structure:

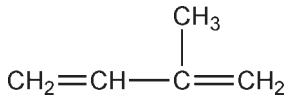

Its polymers can contain the following four types of unsaturation:

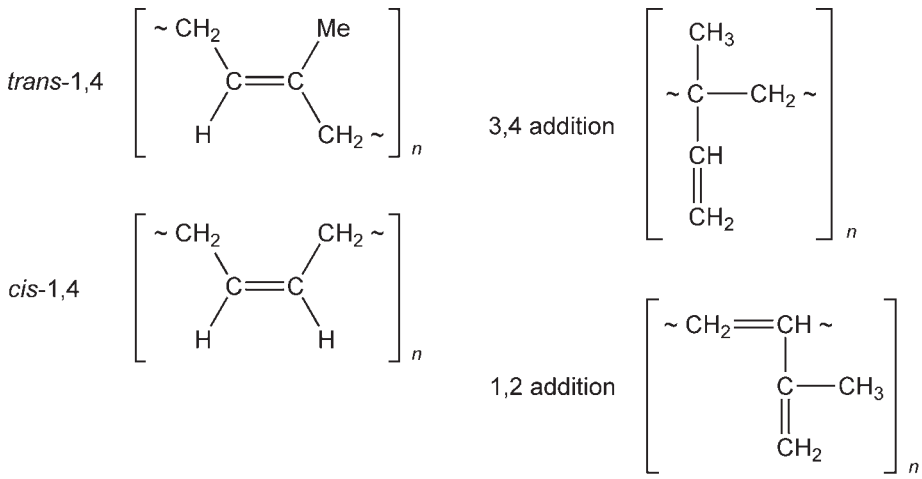

Vodchnal and Kössler [36, 37] have reported an IR method for analysis of polyisoprenes suitable for polymers with a high content of 3,4 addition and relatively small amounts of *cis*-1,4 and *trans*-1,4 structural units.

Absorptivities of the bands which are commonly used for the determination of the amount of 1,4 structural units are about 50 times lower than the absorptivity of the band at 888 cm^{-1} (11.26 μm) which is used for the determination of the amount of 3,4-polyisoprene units. Therefore, in analyses of samples with high content of 3,4-polyisoprene units it is necessary to use two concentrations or two cuvettes with different thicknesses. Application of the 1780 cm^{-1} and 3070 cm^{-1} band (5.62 and 3.26 μm) offers the possibility of using only one cuvette and one concentration. The 1780 cm^{-1} and 3070 cm^{-1} (5.62 and 3.26 μm) absorption bands do not overlap with absorption bands of other structural forms, the accuracy of analyses thus being increased. Besides exact determination of the amount of 3,4 structural units it is possible to estimate an approximate amount of 1,4 addition from the 840 cm^{-1}, 572 cm^{-1} and 600 cm^{-1} (11.90, 17.48 and 16.66 μm) absorption bands.

Values of apparent molar absorptivities of 3,4-polyisoprene, *Hevea* and balata in carbon disulfide solutions for the 572 cm^{-1}, 840 cm^{-1}, 888 cm^{-1}, 1780 cm^{-1}, and 3070 cm^{-1} (17.48, 11.90, 11.26, 5.62 and 3.26 μm) absorption bands are summarised in **Table 12.3**.

The results of measurements of the samples in carbon disulfide solutions, obtained using absorptivities from **Table 12.3** are summarised in **Table 12.4**. The cuvettes employed were 2 mm thick, concentration of polymer varied from 0.5 to 3 g in 100 g solution. From the value of absorption at 840 cm^{-1} (11.90 μm) the minimum amount of 1,4 structural units was estimated assuming that all 1,4 units are *cis*. Analysis using the 572 cm^{-1} and 980 cm^{-1} (17.48 and 10.20 μm) bands was inapplicable due to the presence of cyclic structure.

The results of analyses of the samples in potassium bromide pellets are presented in **Table 12.5**. In these analyses it was possible to utilise the 572 cm^{-1} and 600 cm^{-1} (17.48 and 16.66 μm) absorption bands only, for an approximate estimation of the relative abundance of 1,4 structural units.

Fraga and Benson [38] have investigated a thin-film IR method for the analysis of polyisoprene. They emphasise that clear, smooth and uniform films are necessary, and that these can be cast from a toluene solution of the polymer. Film thickness should be maintained to provide between 0.5 and 0.7 absorbance units at the peak near 1370 cm^{-1} (7.3 μm). When good quality films are used the repeatability of the method is excellent. Thinner films will give slightly lower results. Binder [39] found a direct correlation existed between the intensity of the 742 cm^{-1} (13.48 μm) and the percentage net *cis*-1,4 for various high *cis*-1,4 polyisoprenes. Synthetic *cis*-1,4 polyisoprenes prepared with Zeigler catalysts or lithium catalysts contain a small percentage of the 3,4 structure. On the other hand, naturally occurring polyisoprenes such as natural rubber (*Hevea*), gutta percha balata, and chicle consist exclusively of

Table 12.3 Apparent molar absorptivities km for CS_2 solutions (km; mol^{-1}/cm^{-1})

Sample	1,4 units			3,4 units	
	572 cm^{-1} (17.48 μm)	840 cm^{-1} (11.90 μm)	888 cm^{-1} (11.26 μm)	1780 cm^{-1} (5.62 μm)	3070 cm^{-1} (3.26 μm)
Hevea	5.7	16.6	1.72	0	0
Balata	2.7	7.6	0.58	0	0
3,4-Polyisoprene	6.5	0	110	3.46	30.6

*Reprinted with permission from J. Vodchnal and I. Kossler, Collection of Czechoslovak Communications, 1964, **29**, 2428. ©1964, Institute of Organic Chemistry and Biochemistry, Prague [36]*

Table 12.4 Results of analyses using various infrared absorption bands (structure %)

3,4 units				1,4 units
88 cm^{-1}	3070 cm^{-1}	1780 cm^{-1}	Average	840 cm^{-1}
31.6	32.9	-	32	43
37.0	39.0	-	38	42
37.2	40.2	-	39	47
39.0	42.3	-	41	41
—	49.7	51.3	51	_
—	54.6	59.6	58	28

*Reprinted with permission from J. Vodchnal and I. Kossler, Collection of Czechoslovak Communications, 1964, **29**, 2428. ©1964, Institute of Organic Chemistry and Biochemistry, Prague [36]*

Table 12.5 Results of infrared analyses of polyisoprene

cis-1,4 (%)	*trans*-1,4 (%)	3,4%		
		888 cm^{-1} (11.26μm)	3070 cm^{-1} (3.26 μm)	1780 cm^{-1} (5.62 μm)
0	10	-	57	62
60	9	15	11	-
45	17	-	20	-

Reprinted with permission from J. Vodchnal and I. Kossler, Collection of Czechoslovak Communications, 1964, 29, 2428. ©1964, Institute of Organic Chemistry and Biochemistry, Prague [36]

the 1,4 structure. The differences between the thermal and mechanical properties of the natural and synthetic polyisoprenes have been attributed to the amount of *cis*-1,4 units. It is reasonable to expect that the physical properties of polyisoprenes are also affected by the distribution of the isomeric structure units along the polymer chain, as well as the composition of the polymers.

Various IR methods [40-43] have been reported for the analysis of polyisoprene with predominantly *cis*-1,4 and *trans*-1,4 structural units with low amounts of 3,4 addition.

Maynard and Mochel [44] and Ferguson [45] have described IR methods for determining *cis*-1,4, *trans*-1,4,3,4 and 1,2 structures and 1,4 structures in polyisoprene.

Kössler and Vodchnal [46] came to the conclusion that the IR spectra of polymers containing *cis*-1,4, *trans*-1,4 and 3,4 or cyclic structural units are not additively composed of the spectra of stereoregular polymers containing only one of these structures.

It is known that stereoregular *cis*-1,4 polyisoprene (*Hevea*) and stereoregular *trans*-1,4 polyisoprene (balata) have absorption bands at 1130 and 1150 cm^{-1} (8.84 and 8.69 μm), respectively. These workers found that a polymer having a high content of 3,4 structural units, in addition to the 1,4 structural units, has no absorption band at either 1130 or 1150 cm^{-1} (8.84 or 8.69 μm) but does have a band at 1140 cm^{-1} (8.77 μm). They attribute this band to the C–CH_3 vibration of the –C(CH_3)=CH structural unit separated by other structural units. The appearance of the absorption band at 1140 cm^{-1} (8.77 μm) in some synthetic polyisoprenes has been mentioned by Binder [39, 42, 47] with the comment that the origin of this band is not known [39].

A similar phenomenon has been discovered by analysis of a polymer having approximately 20% *trans*-1,4 in addition to about 75% *cis*-1,4 structural units, as estimated by an analysis using the absorption bands at 572 and 980 cm^{-1} (17.48 and 10.20 μm) [47]. The band at 1130 cm^{-1} (8.85 μm) was shifted towards higher values. In a mixture of *Hevea* and balata with the same content of 20% *trans*-1,4 structural units both the 1130 and 1150 cm^{-1} (8.85 and 8.69 μm) bands are quite distinct. The behaviour of the 1130 and 1150 cm^{-1} (8.85 and 8.69 μm*)* bands is in agreement with the finding of Golub [48, 49] who has shown that during the *cis-trans* isomerisation of polyisoprene the 1136 cm^{-1} (8.80 μm) absorption band appears instead of the 1126 cm^{-1} (8.88 μm) band in *cis*-1,4 isomers or the 1149 cm^{-1} (8.70 μm*)* band in *trans*-1,4 isomers. The statement of Maynard and Mochel [50] that the small amount of *trans*-1,4 structural units may be better detected using the band pair near 1307 cm^{-1} (7.65 μm) rather than the bands at 1131 and 1152 cm^{-1} (8.84 and 8.68 μm) is also in good agreement with the findings of Kössler and Vodchnal [46].

As a consequence of these results it is possible to conclude that only polyisoprenes having long sequences of *cis*-1,4 or *trans*-1,4 units have the absorption bands at 1130 and 1150 cm^{-1} (8.85 and 8.69 μm), respectively. It is also evident that the analysis of synthetic polyisoprenes using these absorption bands leads to distorted results. Kossler and Vodchnal [46] obtained better results using the absorption bands at 572, 980 and 888 cm^{-1} (17.48, 10.20 and 11.26 μm) for *cis*-1,4 and *trans*-1,4 and 3,4 polyisoprene structural units, respectively. The use of various combinations of different absorption bands permits one to conclude whether the polymer in question is more of the block copolymer type or a mixture of stereoregular polymers [47-51].

Nuclear Magnetic Resonance

Tanaka and co-workers [52] spectroscopy determined the distribution of *cis*-1,4 and *trans*-1,4 units in 1,4 polyisoprenes by using ^{13}C-NMR spectroscopy, and found that *cis*-1,4 and *trans*-1,4 units are distributed almost randomly along the polymer chain in *cis-trans* isomerised polyisoprenes, and that chicle is a mixture of *cis*-1,4 and *trans*-1,4 polyisoprenes. These workers [53] have also investigated the ^{13}C-NMR spectra of hydrogenated polyisoprenes and determined the distribution of 1,4 and 3,4 units along the polymer chain for *n*-butyl-lithium catalysed polymers, and have confirmed that these units are randomly distributed along the polymer chain. The polymers did not contain appreciable amounts of head-to-head or head-to-tail 1,4 linkages.

The diad distribution of *cis*-1,4 and *trans*-1,4 units in low molecular weight 1,4-polyisoprene has been determined from the ^{13}C-NMR spectra at 77 °C by Morèse-Séguéla and co-workers [54].

Gronski and co-workers [47], Beebe [55], Dalinskaya and co-workers [56] and Duch and Grant [57], used the chemical shift correction parameters for linear alkanes in the aliphatic region of ^{13}C-NMR spectra to determine the relative amounts of 3,4 and *cis*-1,4 units of polyisoprene.

Microstructure studies have been carried out on the cyclic content and *cis-trans* isomer distribution in polyisoprene [58].

12.1.3 Polyethylene Unsaturation

Much useful information regarding the types of unsaturation present in polyethylene can be gained by the application of IR spectroscopy. Polyethylenes can contain various types of unsaturation which are of great importance from the microstructural point of view. These include, external vinylidene, terminal vinyl and internal *cis* and *trans* unsaturation.

In branched polyethylene most of the unsaturation is of the external vinylidene type, whilst *trans* olefinic end groups and terminal vinyl groups are relatively low in concentration. In linear polyethylene most of the unsaturation is terminal vinyl with relatively small amounts of external vinylidene and *trans* olefinic end groups.

The electron irradiation of linear and branched polyethylenes causes a number of molecular rearrangements in the chemical structure of the polymer [59]. In addition to the significant changes in the type and distribution of unsaturated groups an IR comparison of the radiation-induced chemical changes that occur in air and in a vacuum showed that the presence of oxygen has a marked influence on the structural rearrangements that occur on irradiation.

Figure 12.5 shows the IR spectra of the branched polyethylene before and after irradiation in vacuum and air. Strongly absorbing *trans*-type unsaturation (CH=CH) bands at 964 cm^{-1} (10.37 μm) appear in both the vacuum and air-irradiated sample spectra. Vinylidene decay on irradiation is shown by the decrease in the $R_1R_2C{=}CH_2$ band at 888 cm^{-1} (11.26 μm).

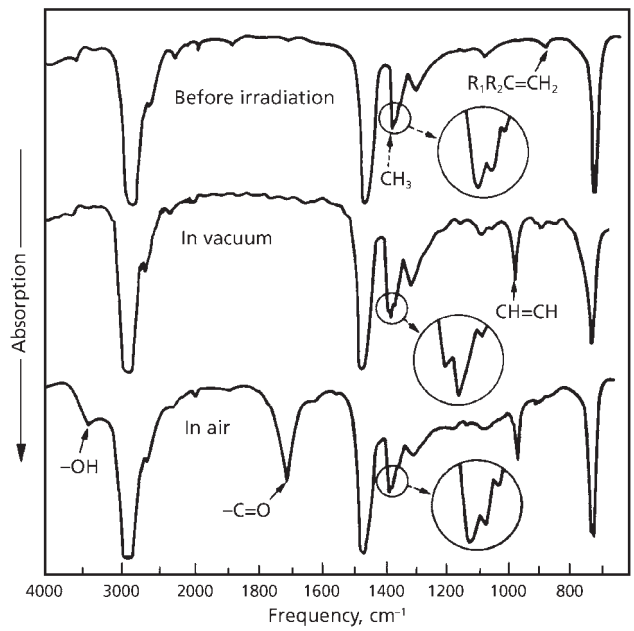

Figure 12.5 The effect of irradiation (500 Mrad) in air and vacuum on branches of polyethylene. (*Reprinted with permission from P.G.M. Van Stratum, J. Dvorako, Journal of Chromatography, 1972, **71**, 1, 9. ©1972, Elsevier [59]*)

Irradiation in vacuum produces a significant decrease in the methyl ($-CH_3$) content (1373 cm^{-1}) (7.28 μm), whereas in the bombardment in air there appears to be only a negligible decrease in $-CH_3$, if any. In addition a comparison of the 720-730 cm^{-1} (13.89-13.70 μm) doublet shows that only the 720 cm^{-1} (13.89 μm) component remains in the spectra of the vacuum sample, whereas there is only a slight decrease of the 730 cm^{-1} (13.69 μm) component in the air-irradiated sample. Additional evidence of structural changes is shown in the spectra of the air-irradiated sample. Here both –OH and C=O bands appear, and there is a general depression of the spectrum background from 1300 to 900 cm^{-1} (7.69 to 11.11 μm).

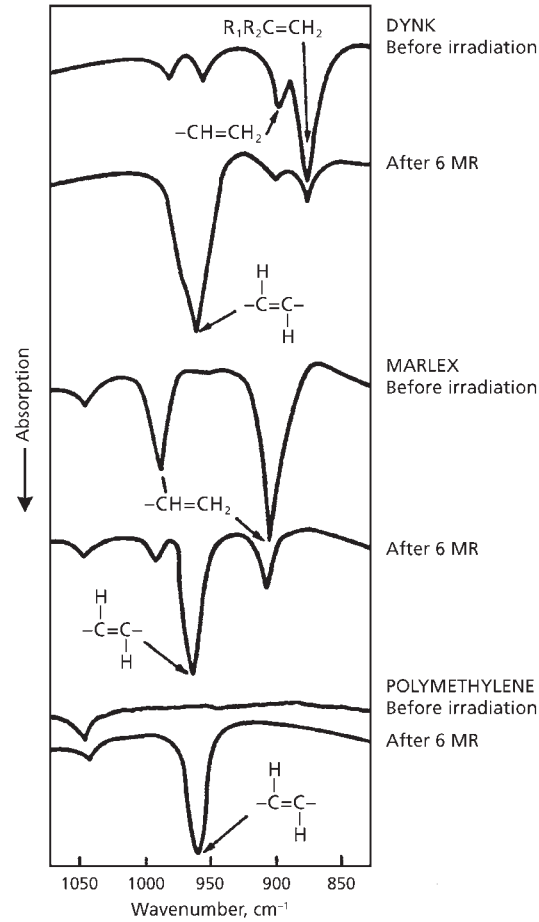

Figure 12.6 Unsaturation region of three polyethylenes before and after irradiation at 6 Mrad. (*Reprinted with permission from P.G.M. Van Stratum, J. Dvorako, Journal of Chromatography, 1972, 71, 1, 9. ©1972, Elsevier [59]*)

Figure 12.6 shows the unsaturation region of the spectra. The top two traces show this region for branched polyethylene before and after 6 Mrad irradiation. The lower traces are those of linear polyethylene before and after similar irradiation. In branched polyethylene before irradiation, most of the unsaturation is of the the external vinylidene type. After a dose of 6 Mrad, *trans*-unsaturation at 964 cm^{-1} (10.73 μm) increases and the vinylidene (at 888 cm^{-1}, 11.26 μm) decreases.

In linear polyethylene almost all the saturation is of the terminal vinyl type ($CH=CH_2$) as shown by the bands at 990 and 910 cm^{-1} (10.10 and 10.99 μm). Here again, after only a 6 Mrad dose, the *trans* groups form rapidly and the vinyl groups at 990 and 910 cm^{-1} (10.10 and 10.99 μm*)* decrease. Because of the rapid increase of *trans* groups during irradiation and the simultaneous decrease of the other unsaturated groups, it might appear that the *trans* groups are being formed from a reaction involving the sacrifice of the other unsaturated groups in the polymer. In order to determine the validity of this observation, Luongo and Salovey [58] exposed to similar doses of irradiation a sample of polymethylene which has no infrared detectable unsaturation or branching. In **Figure 12.6** (lower curves) it is seen that, in polymethylene, the *trans* unsaturation band still forms strongly after irradiation in either air or vacuum. This means that the *trans* groups come from a reaction that is independent of either unsaturation or branching. As for the vinyl and vinylidene decay, although there is no conclusive mechanism to explain their disappearance, they probably become saturated by atomic hydrogen in the system or become crosslinking sites.

Unsaturation in low-density polyethylene has been estimated to ± 0.003 C = $C/10^3$ C atoms by compensating with brominated polymer of the same thickness [60].

Rueda and co-workers [61] have used IR spectroscopy to measure vinyl, vinylidene and internal *cis* or *trans* olefinic end-groups in polyethylene.

Dankovics [62] determined the degree of unsaturation of low-density polyethylene. The total degree of unsaturation in polyethylene was determined by summing the vinyl, vinylene and vinylidene unsaturation derived from the differential IR spectra using an unbrominated polyethylene film as the sample and a brominated film as the reference [61].

Harwood and co-workers [63] used IR spectroscopy to determine vinyl and carbonyl groups in high-density polyethylene.

12.1.4 Polypropylene Unsaturation

The types of unsaturation which can occur in polypropylene are discussed.

Identification of the free radicals produced when polymers are irradiated, normally by gamma-radiation from ^{60}Co or by fast electrons from an electron accelerator tube, can sometimes give vital information regarding structural features, saturated and unsaturated, of the original polymer.

Slovakhotova and co-workers [64] have applied infrared spectroscopy to a study of structural changes in polypropylene in vacuum exposed to fast electrons from an electron accelerator tube (200 kV accelerating field) and with gamma-radiation from ^{60}Co. They found (see previously) the IR spectrum of irradiated polypropylene contains absorption bands in the 1644, 890 and 735-740 – 40 cm^{-1} (6.08, 11.23 and 13.60-13.51 μm) regions. The first two bands correspond to RR′C = CH_2 vinylidene groups and the band in the 2778 – 740 cm^{-1} (3.60-13.51 μm) corresponds region to propyl branches, R-$CH_2CH_2CH_3$. When polypropylene is degraded thermally these groups are formed by disproportionation between free radicals formed by rupture of the polymer backbone. Under the action of ionising radiations the polymer backbone ruptures, with formation of two molecules, with vinylidene and propyl end-groups, at a temperature as low as that of liquid nitrogen, because the corresponding bands are found in the IR spectrum of polypropylene irradiated at -196 °C and measured at -130 °C. When polypropylene is irradiated with dosages greater than 350 Mrad a band appears at (10.99 μm), corresponding to vinyl groups, R – CH = CH_2, i.e., degradation of polypropylene can also involve simultaneous rupture of two C – C bonds in the main and side chains. The strength of the vinyl-group band in the spectrum of irradiated polypropylene is lower than that of the vinylidene group, although the extinction coefficients of these bands are approximately the same.

In the spectrum of amorphous polypropylene irradiated with a dosage of 4000 Mrad at -196 °C and measured at -130 °C, in addition to the band at 1645 cm^{-1} (6.08 μm), a weaker band appears with a maximum near 1667 cm^{-1} (6.00 μm), possibly due to internal bonds:

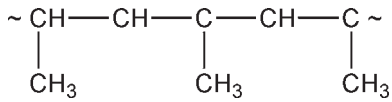

When the spectrum of the specimen is recorded after it is heated to 25 °C this maximum disappears, leaving only a shoulder on the strong band at 6.08 μm. The extinction coefficient [64], of the band at 1667 cm^{-1} (6.00 μm) is less than that of the 1667 cm^{-1} (6.08 μm) band by a factor of 6.7. Supplementary evidence of the formation of internal double bonds in irradiated polypropylene is provided by the presence in the spectrum of bands in the 815 – 855 cm^{-1} (12.27-11.69 μm) region. In this region lie bands due to deformation vibration of CH at double bonds in groups, existing in various conformations [42].

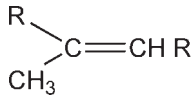

The appearance of bands at 8.15 and 8.55cm^{-1} (12.27 and 11.69 μm) in the spectrum of irradiated polypropylene can be regarded as an indication of the formation of internal double bonds in the polymer.

A study of the electron spin resonance (ESR) spectra of irradiated polypropylene has shown that the alkyl radicals formed during irradiation at -196 °C:

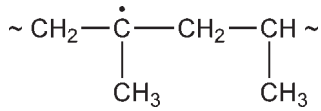

undergo transition to alkyl radicals when the specimen is heated; i.e., on heating, the radical centres migrate to internal double bonds with the formation of stable allyl radicals. Irradiation at room temperature leads immediately to the formation of allyl radicals. It is very probable that the decrease in intensity of the internal double bond valency vibration band at 1677 cm^{-1} (6.00 μm) and the broadening of its maximum after a specimen irradiated at a low temperature is heated to room temperature, is associated with the formation of allyl radicals because interaction of the π-electrons of the double bond with the unpaired electron also lowers the frequency of the double-bond vibration. Comparison of the intensities of the terminal vinyl double-bond bands at 890 and 917 cm^{-1} (11.23 and 10.99 μm) with the band at 1644 cm^{-1} (6.08 μm) in the spectrum of irradiated isotactic polypropylene shows that the intensity of absorption in the 1644 cm^{-1} (6.08 μm) region does not correlate with the intensity of absorption in the 890 cm^{-1} (11.23 μm) regions. Thus, according to the known extinction coefficients for these bands, the ratio of their optical densities should be:

$D_{11.23}/D_{6.08} = 3.7$, $D_{10.99}/D_{6.08} = 3.2$ and $(D_{11.23} + D_{10.99})/D_{6.08} = 3.5$

In the latter case $D_{6.08}$ is the sum of the optical densities of the vinylidene and vinyl absorption bands in this region. An optical density ratio for these bands of approximately this value was found (1.75 to 3.3) for the products of thermal degradation of polypropylene. It is seen that only in the case of amorphous polypropylene irradiated with gamma-radiation from ^{60}Co is the ratio $(D_{11.23} + D_{10.99})/D_{6.08}$ close to the value calculated from the extinction coefficients of these bands. In the spectra of irradiated isotactic polypropylene, however, the intensity of the 1644 cm^{-1} (6.08 μm) band is greater than would be expected if only vibration of terminal double bonds contributes to absorption in this region. This increase in absorption in the 1644 cm^{-1} (6.08 μm) region can be related to absorption by the internal double bond in the allyl radical,

the vibrational frequency of which is lowered by conjugation of the π-electrons of the double bond with the unpaired electron of the radical. In amorphous polypropylene irradiated at room temperature the alkyl radicals can combine rapidly, therefore, there is obviously little formation of allyl radicals. This explains the fact that the ratio of the optical densities of the terminal double bond bands in the 11.10 and 6.08 μm regions is close to the calculated value.

The occurrence of conjugated double bonds in irradiated polypropylene is indicated by the following facts: (1) in the spectra of isotactic polypropylene irradiated with dosages of 2000-4000 Mrad at room temperature there is a band at 1610 cm^{-1} (6.21 μm), which is the region in which polyene bands occur, whereas this band is absent from the spectrum of isotactic polypropylene irradiated with the same dosages at -196 °C; (2) in the electronic spectra of these polypropylene specimens the boundary of continuous absorption is shifted to a region of longer wavelength in comparison with the spectra of polypropylene irradiated with the same dosages at -196 °C.

It has been shown from ESR spectra [65] that when specimens of isotactic polypropylene are heated above 80 °C they contain polyenic free radicals:

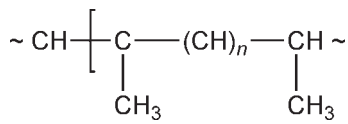

And this also indicates the possibility of migration of double bonds along the polymer chain.

12.2 Unsaturation in Copolymers

12.2.1 Styrene-divinyl Benzene

During the early stages of copolymerisation of styrene and divinylbenzene (DVB), linear and branched primary macromolecules are formed at the DVB repeat units [66-71]. Intermolecular reactions of pendent vinyl groups with growing radicals form crosslinks and lead to the gelation. Intramolecular cyclisations of pendent vinyl groups do not form crosslinks. The extent of reaction at gelation of styrene-DVB copolymers is greater than predicted on the basis of copolymer reactivity ratios. The delay of gelation could be due either to extensive intramolecular cyclisation or to low copolymer reactivity of the second double bond of DVB. The relative contributions of these factors to the delay of gelation could be determined if cyclic structures in the copolymers could be analysed, and if the fraction of pendent vinyl groups could be

analysed accurately enough to determine the reactivity ratios involving the second double bond.

Pendent vinyl groups in styrene-DVB copolymers have been analysed by infrared and Raman spectroscopy [72-83] and by wet chemical methods [71, 82, 84] after extents of reaction varying from before gelation to after nearly complete conversion of monomers. Ford and co-workers [85] report a new analytical approach to the problem. Copolymers of styrene with methane-^{13}C-labelled *p*-DVB were analysed by liquid state and solid state cross-polarisation magic angle spinning (CP-MAS) ^{13}C-NMR methods.

p-DVB, ^{13}C-labelled at the methine carbon of the vinyl group was copolymerised in suspension with styrene at 70, 70 to 95 and 135 to 155 °C using azobisisobutyronitrile as initiator. In this method the number of unreacted vinyl groups in each copolymer was determined by ^{13}C CP-MAS NMR analysis of solid samples, direct polarisation ^{13}C-NMR analysis of deuterochloroform ($CDCl_3$)-swollen gels and bromination. Results from all three methods were found to agree qualitatively.

^{13}C-NMR spectra of the labelled networks were obtained by the direct polarisation, liquid-state method with fully $CDCl_3$-swollen samples, and by the solid-state, CP-MAS method with solid samples. By both methods, the 1% crosslinked samples prepared at 70 and at 95 °C showed a peak at 137 ppm due to the labelled carbon of unpolymerised vinyl groups (**Figure 12.7**). The 137 ppm signal was not seen after further polymerisation of the 1% crosslinked sample at 135-155 °C. Polystyrenes prepared with 10 and 20% of the labeled DVB by the same procedures showed residual vinyl groups both before and after the 135-155 °C post-polymerisation. With the 10 and 20% crosslinked samples only CP-MAS spectra, gave peaks of labelled carbon narrow enough to analyse.

The residual vinyl groups of all labelled samples were analysed quantitatively from peak areas in the NMR spectra by two methods. First, the area of the 137 ppm vinyl peak was compared with the area of all of the aromatic carbon signals in the spectrum due to styrene and DVB carbons in natural abundance. Second, the area of the 137 ppm peak was compared with the area of all of the aliphatic carbon signals in the spectrum, which includes signals from both polymerised labelled carbons of the DVB and from all other aliphatic carbons at natural abundance. It was assumed that all carbon atoms in the sample are equally detectable in each NMR spectrum. Results are shown in Table 12.6. All of the labelled polystyrene networks were also analysed by the bromination of residual vinyl groups.

The ^{13}C-NMR and bromination methods were applied to several commercial crosslinked polystyrenes prepared with unlabelled DVB, which usually consists of a 2:1 *meta*/*para*

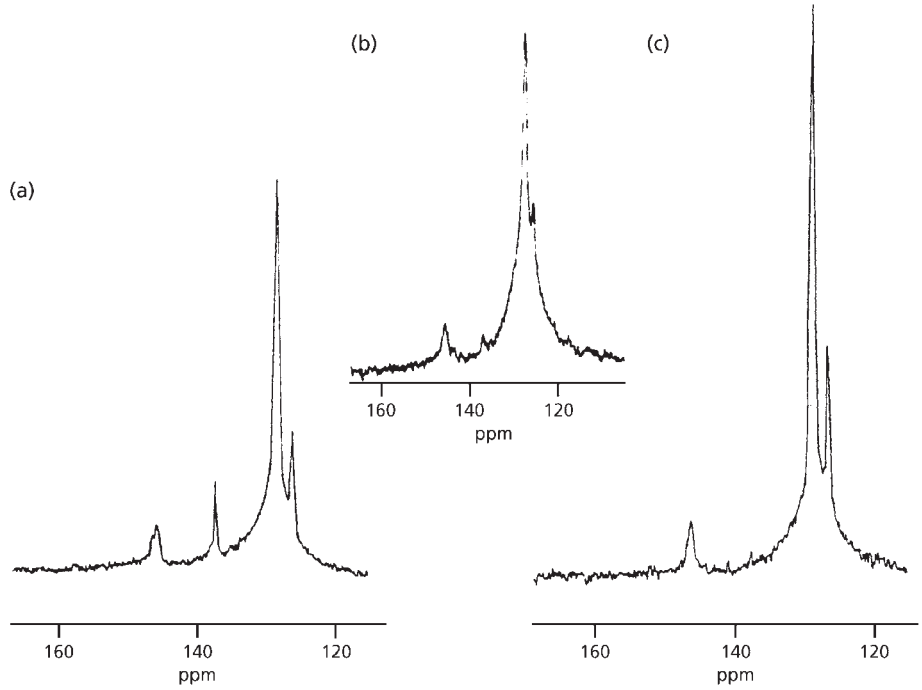

Figure 12.7 Direct polarisation ^{13}C-NMR spectra of $CDCl_3$-swollen polystyrenes crosslinked with 1% of ^{13}C labelled DVB from polymerisations at (a) 70 °C, (b) 95 °C and (c) 155 °C. (*Reprinted with permission from W.T. Ford, M. Periyasamy, S. Mohanraj and F.J. McEnroe, Journal of Polymer Science Part A: Polymer Chemistry Edition, 1989, **27**, 7, 2357. ©1989, John Wiley and Sons [85]*)

mixture of isomers and also contains *meta* and *para*-ethylvinylbenzene. NMR results for 20-80% crosslinked macroporous polymers are shown in **Table 12.6**.

Ford and co-workers [85] concluded that all common styrene-DVB copolymers, containing even as little as 1% DVB, contained unreacted DVB vinyl groups. No method is available yet for accurate, quantitative analysis of residual vinyl groups. Wet chemical methods do not detect vinyl groups in the most hindered parts of the highly crosslinked, heterogenous networks. Infrared and ^{13}C-NMR analyses may contain systematic errors in peak area determinations.

^{1}H-NMR spectroscopy has been used to determine residual vinyl groups in polyDVB [86].

Table 12.6 Fraction of DVB Repeat Units with a Pendent Vinyl Group

DVB (wt%)	Polymerisation temperature	^{13}C CP-MAS[a]		Direct polarisation[b]		
		Vinyl *versus* aliphatic	Vinyl *versus* aromatic	Vinyl *versus* aliphatic	Vinyl *versus* aromatic	Bromine addition[c]
1	70	0.34	0.39	0.54	0.67	0.45 ± 0.10
1	95	0.16	0.16	0.27	0.19	0.13 ± 0.05
1	155	0.00	0.00	0.18	0.17	0.05 ± 0.02
4	95	0.19	0.15			0.10 ± 0.03
10	70	0.21	0.14			0.28 ±0.11
10	155	0.18	0.20			0.18 ± 0.02
20	70	0.28	0.14			0.33 ± 0.05
20	155	0.28	0.19			0.26 ± 0.04
20[d]		0.54	0.39			0.09 ± 0.01
50[e]		0.63	0.47			0.13 ± 0.01
80[f]		0.81	0.51			0.10 ± 0.01

[a] Dry solid samples.
[b] $CDCl_3$-swollen samples.
[c] Average and standard deviation of the three measurements.
[d] Rohm & Haas XAD-1.
[e] Rohm & Haas XAD-2.
[f] Rohm & Haas XAD-4.

Reprinted with permission from M. Periyasamy, W.T. Ford and F.J. McEnroe, Journal of Polymer Science Part A: Polymer Chemistry Edition, 1989, 27, 7, 2357. ©1989, John Wiley and Sons [85]

12.2.2 Polytrimethylolpropane Tri-methacrylate (TRIM)

There are a number of methods for the detection of carbon-carbon double bonds including IR spectroscopy [72, 86-89], Raman spectroscopy [90], and chromatography, together with the formation of Pt(II) complexes [89] and addition of bromine [91, 92]. The high crosslinking density of polyTRIM and its rich IR spectrum make these analyses quite difficult. With the advent of high-resolution solid-state NMR (CP-MAS-NMR), a powerful technique to analyse insoluble polymers has, however, become available. In an unreacted acrylate group, the carbonyl bond is conjugated with a

double bond, which should shift the ^{13}C carbonyl resonance about 10 ppm upfield compared to the reacted units. This has also been used to determine the amount of unreacted units in several different polymers obtained from multi-functional acrylates and methacrylates [93-95] including TRIM [96].

Hjertberg and co-workers [97] used ^{13}C-CP-MAS-^{13}C-NMR to determine the double bonds in TRIM and compared results to the results obtained by standard bromine addition methods. They also examined the possibility of utilising different relaxation parameters obtained by NMR measurements to study the mobility of unreacted units.

A detailed analysis of the cross-polarisation behaviour showed that quantitative results can be obtained. The amount of unreacted units, typically 0-15%, was found to depend on the polymerisation parameters. Conditions favouring mobility, i.e., higher temperatures or increased solvent quality, resulted in lower content of residual double bonds. Bromine addition values are 2-3% higher than the NMR data. The reactivity toward bromine further indicates that the mobility is reasonably high. This has also been confirmed by measurements of the rotating-frame relaxation time constant, T_1 (^{13}C) Most likely, $T_{1\rho}$ is dominated by spin-lattice processes; i.e., it can be interpreted in terms of molecular dynamics. The values obtained for C=O and >C*=CH_2 in unreacted units are about twice that of C=O in reacted units, indicating increased mobility. The reactivity of the remaining double bonds in a radical polymerisation with a chiral monomer was also demonstrated.

The % fraction of unreacted methacrylate groups in TRIM, depend on polymerisation temperature and range from 8.4% at 60 °C to 2.7% at 90 °C.

^{13}C CP-MAS-NMR has also been used in studies on polytetramethylene glycol dimethacrylate [94].

12.2.3 Miscellaneous Copolymers

Pyrolysis – gas chromatography and IR spectroscopy have both been used to determine vinyl groups in ethylene – vinyl acetate copolymers [98]. Electron spin resonance spectroscopy has been applied to studies of unsaturation and other structural features in a wide range of homopolymers including: polyethylene [99-111], polypropylene [112-118], polybutenes [112], polystyrene [119-121], PVC [122, 123], polyvinylidene chloride [124], PMMA [125-133], polyethylene glycol polycarbonate [134-137], polyacrylic acid [133-136, 138, 139], polyphenylenes [140], polyphenylene oxides [140], polybutadiene [141], conjugated dienes [142-143], polyester resins [144], Cellophane [140, 145] and various copolymers including styrene grafted polypropylene [146], ethylene-acroline [147], butadiene-isobutylene [148], vinyl acetate copolymers [149], vinyl chloride propylene [150], and high-density polyethylene [151].

12.3 Ozonolysis Techniques

The oxidation of double bonds in organic compounds and polymers in a non-aqueous solvent leads to the formation of ozonides which, when acted upon by water, are hydrolysed to carbonyl compounds:

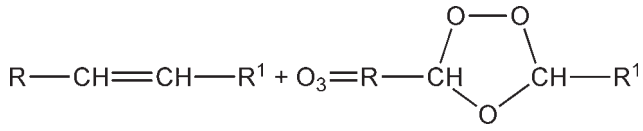

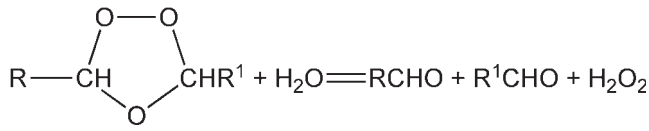

Triphenyl phosphine is frequently used to assist this reaction. Clearly, when applied to complex unsaturated organic molecules or polymers this reaction has great potential for the elucidation of the microstructure of the unsaturation. Examination of the reaction products, for example by conversion of the carbonyl compounds to carboxylates then esters followed by gas chromatography, enables identifications of these products to be made.

An example of the value of the application of this technique to a polymer structural problem is the distinction between polybutadiene made up of consecutive 1,4-1,4 butadiene sequences (**I**), and polybutadiene made up of alternating 1,4 and 1,2 butadiene sequences (**II**), i.e., 1,4-1,2-1,4:

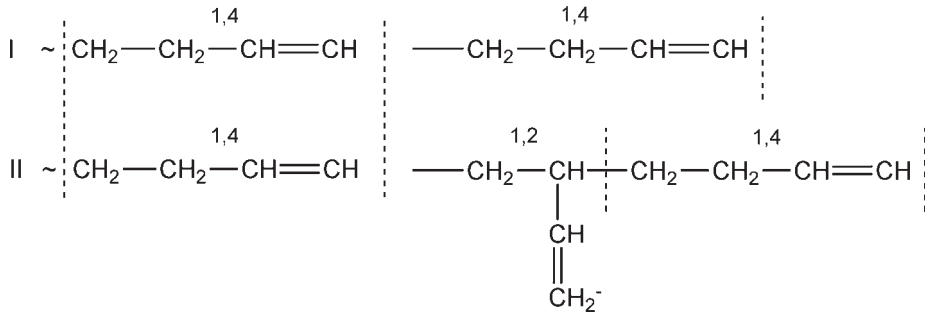

Upon ozonolysis, followed by hydrolysis, 1,4-1,4 sequences produce succinaldehyde (CHO–CH_2–CH_2CHO) and 1,4-1,2-1,4 sequences produce formyl 1,6-hexane-dial.

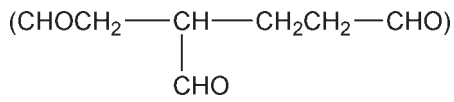

Details of the reactions are given next:

1.4-1.4 Sequences:

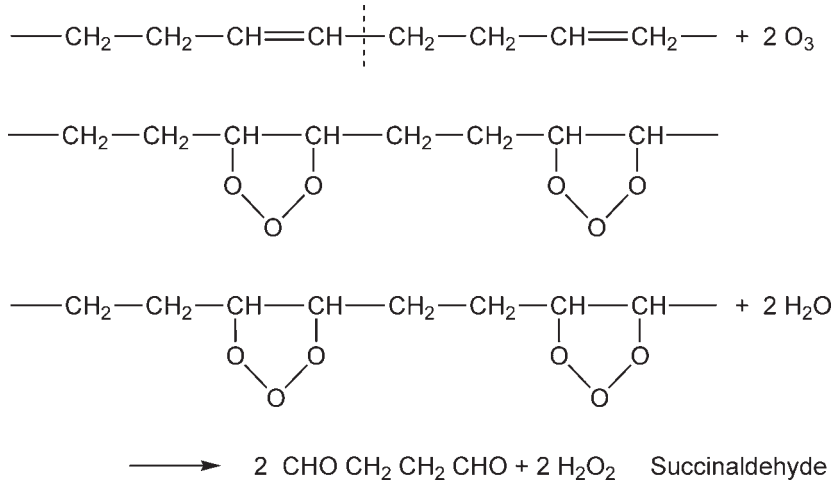

1.4-1.2-1.4 Sequences:

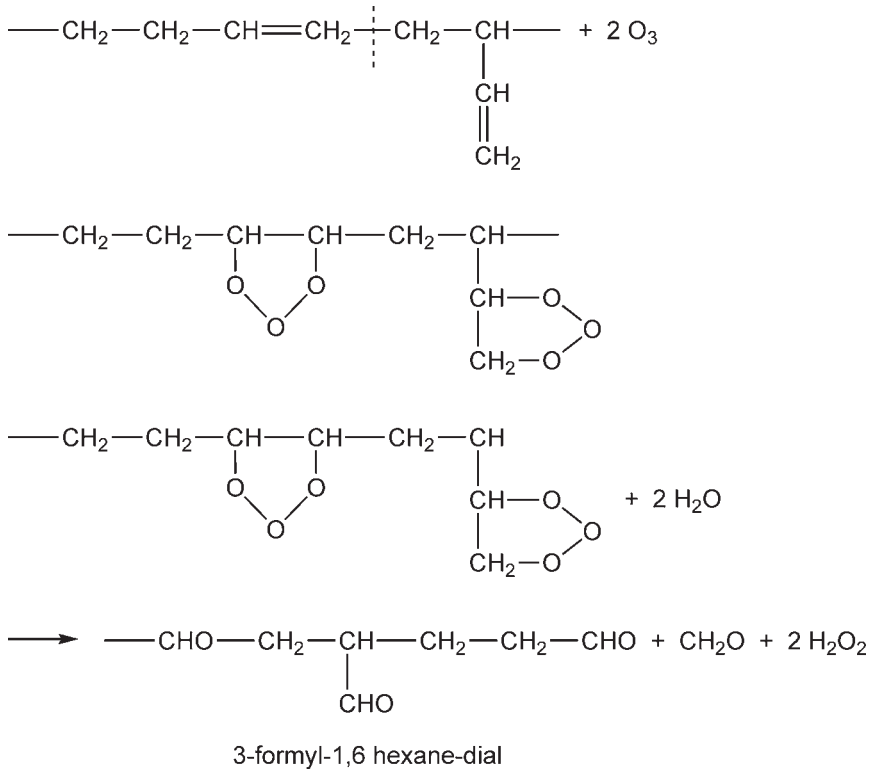

Table 12.7 Microozonolysis of polybutadiene						
Sample	1,4 Vinyl (*cis* + (1,2), *trans*) (%)		Area from GC(%)			
			Succinaldehyde	3-Formyl 1,6-hexanediol	4-Octene 1,8-dial	1,2 units occurring in 1,4-1,2-1,4 sequences
1	98.0	2	50	1	49	0.5
2	89.1	10.9	30	10	60	5
3	89.0	11.0	43	7	50	3
4	81.0	19.0	34	14	52	6
5	76.2	23.8	36	25	39	11
6	71.8	28.2	33	27	40	11
7	69.7	30.3	48	26	26	10
8	67.7	32.3	36	26	38	9
9	64.2	35.8	38	31	31	10
10	62.8	37.2	45	27	28	8
11	50.5	49.5	26	41	33	12
12	56.0	44.0	30	39	31	11
13	26.0	74.0	33	64	3	5
Source: Author's own files						

Analysis of the reaction product for concentrations of succinaldehyde and 3-formyl-1,6-hexane-dial can show whether the polymer is 1,4-1,4 or 1,4-1,2-1,4, or whether it contains both types of sequence.

Various workers [152-157] have applied this technique to the elucidation of the microstructure of polybutadiene. They found that the 3 formyl-1,6-hexane-dial content was directly proportional to the 1,2 (vinyl) content of polymers containing 1,4-1,2-1,4 butadiene sequences.

Polymers having 98% *cis*-1,4 structure, 98% *trans*-1,4 structure and a series of polymers containing from 11% to 75% 1,2 structure were ozonised (**Table 12.7**). The final products obtained from these polymers were succinaldehyde, 3-formyl-l,6 hexane-dial, and 4-octene-1,8-dial. Model compounds were ozonised and the products were ompared with those from the polymers.

Figures 12.8 and 12.9 show chromatographic separation of the ozonolysis products from polybutadienes having different amounts of 1,2 structure, as measured by IR or NMR spectroscopy. **Figure 12.10** shows the relationship of 1,2 content to the amount of 3-formyl-1,6 hexane-dial in the ozonolysis products.

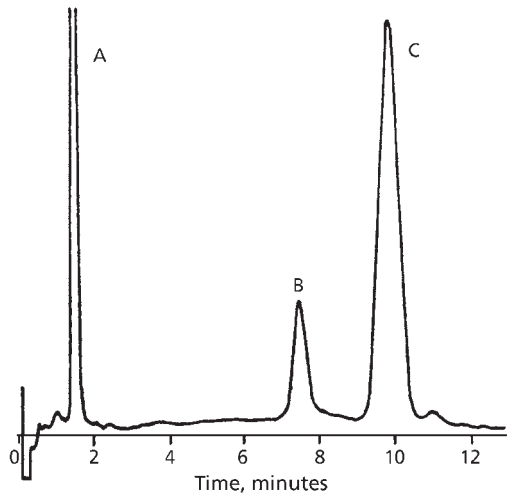

Figure 12.8 Ozonolysis products from butadiene containing 11% vinyl structures: A succinaldehyde; B 3-formyl-l,6-hexanedial; C 4-octene-l,8-dial.
(*Source: Author's own files*)

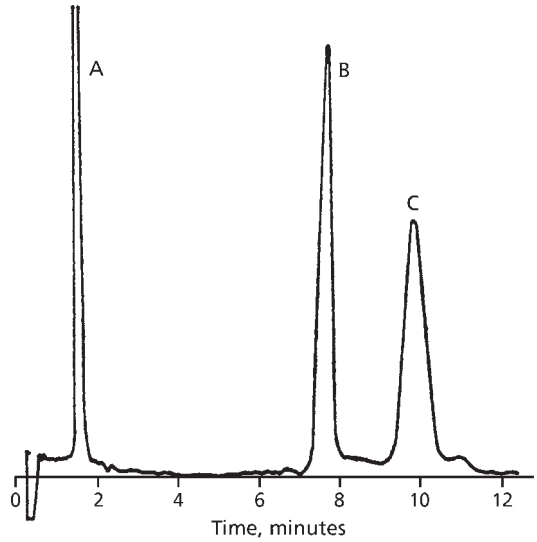

Figure 12.9 Ozonolysis products from polybutadiene containing 37.2% vinyl structure. (*Source: Author's own files*)

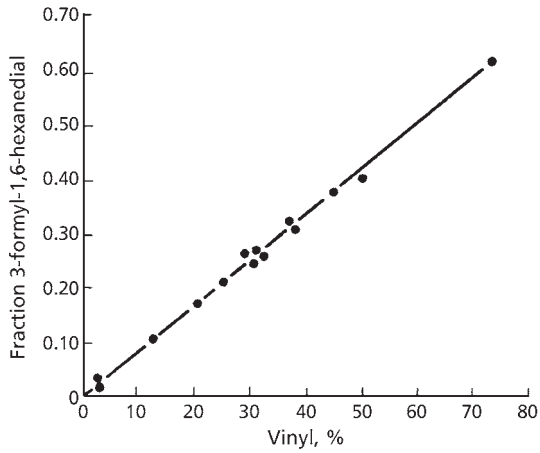

Figure 12.10 Relationship of yield of 3-formyl-1,6-hexanedial from ozonolysis to percentage vinyl structures (from NMR or IR spectra) in polybutadiene. (*Source: Author's own files*)

The amount of 1,4-1,2-1,4 sequences in polybutadienes can be estimated from the amounts of the different ozonolysis products (**Table 12.7**) if one considers the amount of 1,4 structure not detected. (Since the ozonolysis technique cleaves the centre of a butadiene monomer unit, one half of a 1,4 unit remains attached to each end of a block of 1,2 units after ozonolysis. These structures do not elute from the gas chromatographic column.) Using random copolymer probability theory, the maximum amounts of these undetected 1,4 structures can then be calculated.

A further example concerns the application of the ozonolysis technique to butadiene-propylene copolymers [152, 158-160]. Samples of highly alternating copolymers of butadiene and propylene yielded large amounts of 3-methyl-1,6 hexane-dial when submitted to ozonolysis. The ozonolysis product from 4-methyl-cyclohexane:

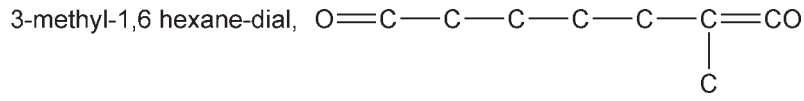

was used as a model compound for this structure. Ozonolysis of these polymers occurs as shown next:

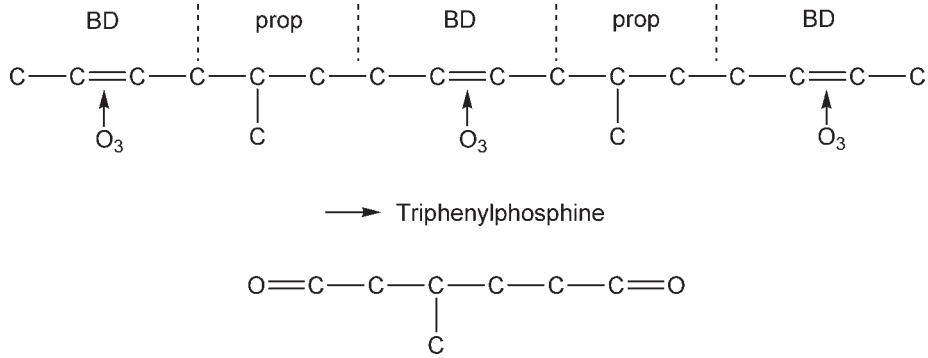

The amount of alternation in these polymers can be determined if the amounts of 1,4 and 1,2 polybutadiene structure and total propylene have been determined by IR or NMR spectroscopy. **Table 12.8** shows results obtained for several butadiene-propylene copolymers having more or less alternating structure. Similar polymers have been analysed by Kawasaki [158] by use of conventional ozonolysis methods with esters as the final products.

The technique has been applied to various other unsaturated polymers. Thus, polyisoprene, having nearly equal 1,4 and 3,4 structures, produced large amounts of levulinaldehyde, succinaldehyde and 2,5 hexanedione, indicating blocks of 1,4 structures in head-tail, tail-tail and head-head configurations.

Table 12.8 A Microozonolysis of butadiene-propylene copolymers								
	1,4 (%) Polybutadiene structure	1,2 (%) Polybutadiene structure	Propylene (mole%)	Area (from gas chromatography) %				
				Succinaldehyde	3-Methyl - 1,6-hexane-dial	3-Formyl 1,6-hexane-dial	4-Octene - 1,8-dial	Alternating butadiene propylene (%)
A	45	5.7	49.3	5	92	1	2	77
B	47.8	2.2	50	11.5	85	0.5	3	71
C	53.1	3.2	43.7	25	61	6	8	48
D	-	-	30	49	38	1	12	33
Source: Author's own files								

Hill and co-workers [160] utilised ozonolysis in their investigation of a butadiene-methyl methacrylate copolymer. The principal products were succinic acid, succindialdehyde and dicarboxylic acids containing several methylmethacrylate residues. The percentage of butadiene (9.2%) recovered as succinic acid and succindialdehyde provided a measure of the 1,4-butadiene-1,4-butadiene linkages in the copolymers, and the percentage of methylmethacrylate units (51%) recovered as trimethyl 2-methyl-butane-1,2,4-tricarboxylate (4) $n = 1$, provided a measure of the methylmethacrylate units in the middle of butadiene-methacrylate-butadiene triads.

Extensive ozonisation followed by lithium aluminium hydride reduction of oxyalkylene groups in polypropylene glycols produces monomeric diglycols as follows:

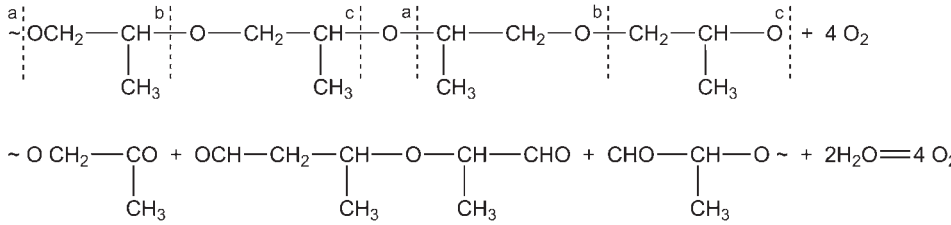

References

1. D.W. Fraga, Emeryville Research Laboratories, Shell Chemical, Emeryville, CA, USA, *Private Communication*.

2. J.L. Binder, *Journal of Polymer Science Part A: General Papers*, 1963, **1**, 42.

3. G. Natta in *Proceedings of 15th Annual Technical Conference of the SPE*, New York, NY, USA, 1959.

4. H. Dinsmore and D. Smith, *Rubber Chemistry and Technology*, 1949, **22**, 2, 572.

5. D.L. Harms, *Analytical Chemistry*, 1953, **25**, 8, 1140.

6. D. Hummel, *Rubber Chemistry and Technology*, 1959, **32**, 3, 854.

7. M. Lerner and R.C. Gilbert, *Analytical Chemistry*, 1964, **36**, 7, 1382.

8. M. Tyron, E. Horowicz and J.J. Mandel, *Journal of Research of the National Bureau of Standards*, 1955, **55**, 219.

9. D.A. MacKillop, *Analytical Chemistry*, 1968, **40**, 3, 607.

10. Y. Alaki, T. Yoshimoto, M. Imanari and M. Takeuchi, *Rubber Chemistry and Technology*, 1973, **46**, 2, 350.

11. A.D.H. Clague, J.A.M. van Broekhoven and L.P. Blaauw, *Macromolecules*, 1974, **7**, 3, 348.

12. P.T. Suman and D.D. Werstler, *Journal of Polymer Science: Polymer Chemistry Edition*, 1975, **13**, 8, 1963,

13. S. Bywater, Y. Firat and P.E. Black, *Journal of Polymer Science: Polymer Chemistry Edition*, 1984, **22**, 3, 669.

14. S. Bywater, *Polymer Communications*, 1983, **24**, 7, 203.

15. K-F. Elgert, G. Quack and B. Stutzel, *Polymer*, 1975, **16**, 3, 154.

16. N.K. Albert, Woodbury Research Laboratory, Shell Chemical Company, Woodbury, USA, *Private Communication*, October 1966.

17. T.R. Crompton and V.W. Reid, *Journal of Polymer Science Part A: General Papers*, 1963, **1**, 1, 347.

18. C.E. Miller, B.E. Eichinger, T.W. Gurley and J.G. Hermiller, *Analytical Chemistry*, 1990, **62**, 17, 1778.

19. H.G.M. Edwards, A.F. Johnson and I.R. Lewis, *Journal of Raman Spectroscopy*, 1993, **24**, 7, 435.

20. R. Hampton, *Rubber Chemistry and Technology*, 1972, **45**, 3, 546.

21. S.W. Cornell and J.L. Koenig, *Macromolecules*, 1969, **2**, 5, 540.

22. H. Harwood, *Rubber Chemistry and Technology*, 1982, **55**, 3, 769.

23. E. Santee, Jr., L. Malotky and M. Morton, *Rubber Chemistry and Technology*, 1973, **46**, 5, 1156.

24. E.R. Santee, Jr., V.D. Mochel and M. Morton, *Journal of Polymer Science: Polymer Letters Edition*, 1973, **11**, 7, 453.

25. G. Van der Velden, C. Didden, T. Veermans and J. Beulen, *Macromolecules*, 1987, **20**, 6, 1252.

26. D.W. Carlson, H.C. Ransaw and A.G. Altenau, *Analytical Chemistry*, 1970, **42**, 11, 1278.

27. J.L. Binder, *Analytical Chemistry*, 1954, **26**, 12, 1877.

28. D.W. Carlson and A.G. Altenau, *Analytical Chemistry*, 1969, **41**, 7, 969.

29. D. Braun and E. Čanji, *Die Angewandte Makromolecular Chemie*, 1973, **33**, 1, 143.

30. D. Braun and E. Čanji, *Die Angewandte Makromolecular Chemie*, 1974, **35**, 1, 27.

31. M. Hast and D. Deur-Šiftar, *Chromatographia*, 1972, **5**, 9, 502.

32. R.S. Silas, J. Yates and V. Thornton, *Analytical Chemistry*, 1959, **31**, 4, 529.

33. N. Neto and C. Di Lauro, *European Polymer Journal*, 1967, **3**, 4, 645.

34. J.K. Clark and H.Y. Chen, *Journal of Polymer Science: Polymer Chemistry Edition*, 1974, **12**, 4, 925.

35. H.J. Harwood and W.M. Ritchey, *Journal of Polymer Science Part B: Polymer Letters Edition*, 1964, **2**, 6, 601.

36. J. Vodchnal and I. Kössler, *Collection of Czechoslovak Communications*, 1964, **29**, 2428.

37. J. Vodchnal and I. Kössler, *Collection of Czechoslovak Communications*, 1964, **29**, 2859.

38. D.W. Fraga and L.H. Benson, Shell Chemical Company Ltd., Torrance, CA, USA, *Private Communication*.

39. J.L. Binder, *Journal of Polymer Science Part A: General Papers*, 1963, **1**, 1, 37.

40. W.S. Richardson and A. Sacher, *Journal of Polymer Science*, 1953, **10**, 4, 353.

41. E.I. Plkovskiu and M. Volkenstein, *Doklady Academii Nauk SSSR*, 1954, **95**, 301.

42. J.L. Binder and H.C. Ransaw, *Analytical Chemistry*, 1957, **29**, 4, 503.

43. P.J. Cornish, *Spectrochimica Acta*, 1959, **15**, 598.

44. J.T. Maynard and W.E. Mochel, *Journal of Polymer Science*, 1954, **13**, 69, 251.

45. R.C. Ferguson, *Analytical Chemistry*, 1964, **36**, 11, 2204.

46. I. Kössler and J. Vodchnal, *Polymer Letters*, 1963, **4**, 415.

47. W. Gronski, N. Murayama, H-J. Cantow and T. Miyamoto, *Polymer*, 1976, **17**, 4, 358.

48. J.L. Binder, *Rubber Chemistry and Technology*, 1962, **35**, 1, 57.

49. M.A. Golub, *Journal of Polymer Science*, 1959, **36**, 130, 523.

50. M.A. Golub, *Journal of Polymer Science*, 1959, **36**, 130, 10.

51. J.T. Maynard and W.E. Mochel, *Journal of Polymer Science*, 1954, **13**, 69, 251.

52. Y. Tanaka, H. Sato and T. Seimiya, *Polymer Journal (Japan)*, 1975, **7**, 2, 264.

53. Y. Tanaka, H. Sato, A. Ogura and I. Nagoya, *Journal of Polymer Science: Polymer Chemistry Edition*, 1976, **14**, 1, 73.

54. B. Morèse-Séguéla, M. St. Jacques, J.M. Renaud and J. Prud'homme, *Macromolecules*, 1977, **10**, 2, 431.

55. D.H. Beebe, *Polymer*, 1978, **19**, 2, 231.

56. E.R. Dalinskaya, A.S. Khachaturov, I.A. Poletayeva and V.A. Kormer, *Makromolekulare Chemie*, 1978, **179**, 2, 409.

57. M.W. Duch and D.M. Grant, *Macromolecules*, 1970, **3**, 2, 165.

58. J.P. Luongo and R.J. Salovey, *Journal of Applied Polymer Science*, 1963, 7, 2307.

59. P.G.M. Van Stratum and J. Dvorák, *Journal of Chromatography*, 1972, **71**, 1, 9.

60. M. Seeger and E. M. Barrall II, *Journal of Polymer Science: Polymer Chemistry Edition*, 1975, **13**, 7, 1515.

61. D.R. Rueda, F.J. Baltá Calleja and A. Hidalgo, *Spectrochimica Acta Part A: Molecular Spectroscopy*, 1974, **30**, 8, 1545.

62. A. Dankovics, *Muanay Gumi*, 1974, **11**, 380. [*Chemical Abstracts*, 82, 86773g.]

63. C.L. Harwood, P.J. Hendra, B.G. Lator, W.F. Maddams and H.A. Willis, *Polymer*, 1988, **29**, 1, 49.

64. N.A. Slovakhotova, Z.F. Il'netheva, L.A. Vasiliev and V.A. Kangin, Karpov Physio-chemical Scientific Research Institute, unpublished work.

65. H. Fischer and K-H. Hellwege, *Journal of Polymer Science*, 1962, **56**, 163, 33.

66. H. Studinger and H. Heuer, *Chemische Berichte*, 1934, **67**, 1174.

67. K. Dusek in *Developments in Polymerisation*, Volume 3, Ed., R.N. Haward, Applied Science Publishers, London, UK, 1982, p.143.

68. K. Dusek and J. Spevácek, *Polymer*, 1980, **21**, 7, 750.

69. K. Dušek, H. Galina and J. Mikeš, *Polymer Bulletin*, 1980, **3**, 2, 19.

70. G. Hild and P. Rempp, *Pure and Applied Chemistry*, 1981, **53**, 8, 1541.

71. G Hild and R. Okasha, *Makromolekulare Chemie*, 1985, **186**, 1, 93.

72. J. Maunsky, J. Klaban and K. Dusek, *Journal of Macromolecular Science and Chemistry*, *Part A: Pure and Applied Chemistry*, 1971, **5**, 6, 1071.

73. G.J. Howard and C.A. Midgley, *Journal of Applied Polymer Science*, 1981, **26**, 11, 3845.

74. G. Popov and G. Schwachula, *Plaste und Kautschuk*, 1981, **28**, 6, 312.

75. A.S. Gozdz and B.N. Kolarz, *Makromolekulare Chemie*, 1979, **180**, 10, 2473.

76. P. Weiss, G. Hild, J. Herz and P. Rempp, *Makromolekulare Chemie*, 1970, **135**, 249.

77. B. Soper, R.N. Haward and E.F.T. White, *Journal of Polymer Science Part A-1: Polymer Chemistry Edition*, 1972, **10**, 9, 2545.

78. R.N. Haward and W. Simpson, *Journal of Polymer Science*, 1955, **18**, 89, 440.

79. M Bartholin, G. Boissier and J. Dubois, *Makromolekulare Chemie*, 1981, **182**, 7, 2075.

80. D-Y.D. Chung, M. Bartholin and A. Guyot, *Die Angewandte Makromolecular Chemie*, 1982, **103**, 1, 109.

81. B. Walczynski, B.N. Kolarz and H. Galina, *Polymer Comunications*, 1985, **26**, 9, 276.

82. D. Kuhnle and W. Fünke, *Makromolekulare Chemie*, 1971, **139**, 255.

83. J. Stokr, B. Schneider, A. Frydrychová and J. Coupek, *Journal of Applied Polymer Science*, 1979, **23**, 12, 3553.

84. J.K. Fink, *Journal of Polymer Science: Polymer Chemistry Edition*, 1981, **19**, 1, 195.

85. W.T. Ford, M. Periyasamy, S. Mohanraj and F.J. McEnroe, *Journal of Polymer Science Part A: Polymer Chemistry Edition*, 1989, **27**, 7, 2357.

86. Y. Nagasaki, H. Ito and T. Tsuruta, *Makromolekulare Chemie*, 1986, **187**, 1, 23.

87. T. Brunelet, M. Bartholin and A. Guyot, *Die Angewandte Makromolecular Chemie*, 1982, **106**, 1, 79.

88. K.A. Kun and R. Kunin, *Journal of Polymer Science Part A-1: Polymer Chemistry*, 1968, **6**, 10, 2689.

89. H.W. Stuurman, J. Köhler, S-O. Jansson and A. Litzén, *Chromatographia*, 1987, **23**, 5, 341.

90. P.P. Wieczorek, B.N. Kolarz and H. Galina, *Die Angewandte Makromolecular Chemie*, 1984, **126**, 39.

91. H. House, *Modern Synthetic Reactions*, 2nd Edition, WA Benjamin Inc., Menlo Park, CA, USA, 1972, p.422.

92. T. Morikawa, *Kagaku Kogaku (Osaka)*, 1967, **41**, 169.

93. R.G. Earnshaw, C.A. Price, J.H. O'Donnell and A.K. Whittaker, *Journal of Applied Polymer Science*, 1986, **32**, 6, 5337.

94. P.E.M. Allen, G.P. Simon, D.R.G. Williams and E.H. Williams, *European Polymer Journal*, 1986, **22**, 7, 549.

95. P.E.M. Allen, G.P. Simon, D.R.G. Williams and E.H. Williams, *Macromolecules*, 1989, **22**, 2, 809.

96. J-E. Rosenberg and P. Flodin, *Macromolecules*, 1986, **19**, 6, 1543.

97. T. Hjertberg, T. Hargitai and P. Reinholdsson, *Macromolecules*, 1990, **23**, 12, 3080.

98. E. Verdu and J. Devasa, *Revista de Plasticos Modernos*, 1989, **58**, 400, 545.

99. H.L. Browning, Jr., H.D. Ackermann and H.W. Patton, *Journal of Polymer Science Part A-1: Polymer Chemistry*, 1966, **4**, 6, 1433.

100. K. Tsuji, *Journal of Polymer Science: Polymer Chemistry Edition*, 1973, **11**, 6, 1407.

101. K. Tsuji, *Journal of Polymer Science: Polymer Chemistry Edition*, 1973, **11**, 2, 467.

102. D. Campbell, K. Araki and D.T. Turner, *Journal of Polymer Science Part A-1: Polymer Chemistry*, 1966, **4**, 10, 2597.

103. D. Campbell and D.T. Turner, *Journal of Polymer Science Part A-1: Polymer Chemistry*, 1967, **5**, 8, 2199.

104. Y. Hama, K. Hosono, Y. Furui and K. Shinohara, *Journal of Polymer Science Part A-1: Polymer Chemistry*, 1971, **9**, 5, 1411.

105. K. Tsuji, T. Seiki and T. Takeshita, *Journal of Polymer Science Part A-1: Polymer Chemistry*, 1972, **10**, 10, 3119.

106. Y. Hori, S. Shimada and H. Kashiwabara, *Polymer*, 1977, **18**, 6, 567.

107. Y. Hori, S. Shimada and H. Kashiwabara, *Polymer*, 1977, **18**, 6, 1143.

108. S-I. Ohnishi, S-I. Sugimoto and I. Nitta, *Journal of Polymer Science Part A: General Papers*, 1963, **1**, 2, 605.

109. K. Soga and T. Keii, *Journal of Polymer Science Part A-1: Polymer Chemistry*, 1966, **4**, 10, 2429.

110. T. Seguchi and N. Tamura, *Journal of Polymer Science: Polymer Chemistry Edition*, 1974, **12**, 8, 1671.

111. T. Seguchi and N. Tamura, *Journal of Polymer Science: Polymer Chemistry Edition*, 1974, **12**, 9, 1953.

112. B.R. Loy, *Journal of Polymer Science Part A: General Papers*, 1963, **1**, 7, 2251.

113. L.A. Wall, *Journal of Polymer Science*, 1955, **17**, 83, 141.

114. T. Buck, Ph.D Thesis, North Western University Microfilm MIC 60-4761, Ann Arbor, MI, USA, 1960.

115. L.J. Forrestal and W.G. Hodgson, *Journal of Polymer Science Part A: General Papers*, 1964, **2**, 3, 1275.

116. S-I. Ohnishi, S-I. Sugimoto and I. Nitta, *Journal of Polymer Science Part A: General Papers*, 1963, **1**, 2, 625.

117. N. Kusumoto, K. Matsumoto and M. Takayanagi, *Journal of Polymer Science Part A-1: Polymer Chemistry*, 1969, **7**, 7, 1773.

118. T. Ooi, M. Shiotsubo, Y. Hama and K. Shinohara, *Polymer*, 1975, **16**, 7, 510.

119. R.E. Florin, L.A. Wall and D.W. Brown, *Journal of Polymer Science Part A: General Papers*, 1963, **1**, 5, 1521.

120. A.T. Bullock, G.G. Cameron and P.M. Smith, *Polymer*, 1973, **14**, 10, 525.

121. R.E. Florin and L.A. Wall, *Journal of Chemical Physics*, 1972, **57**, 4, 1791.

122. I. Ouchi, *Journal of Polymer Science Part A: General Papers*, 1965, 3, 7, 2685.

123. S.A. Liebman, J.F. Reuwer, Jr., K.A. Gollatz and C.D. Nauman, *Journal of Polymer Science Part A-1: Polymer Chemistry*, 1971, **9**, 7, 1823.

124. J.N. Hay, *Journal of Polymer Science Part A-1: Polymer Chemistry*, 1970, **8**, 5, 1201.

125. M.J. Bowden, and J.H. O'Donnell, *Journal of Polymer Science Part A-1: Polymer Chemistry*, 1969, **7**, 7, 1665.

126. Y. Sakai and M. Iwasaki, *Journal of Polymer Science Part A-1: Polymer Chemistry*, 1969, **7**, 7, 1749.

127. J.A. Harris, O. Hinojosa, J.C. Arthur, Jr., *Journal of Polymer Science: Polymer Chemistry Edition*, 1973, **11**, 12, 3215.

128. G. Gueskens and C. David, *Makromolekulare Chemie*, 1973, **165**, 273.

129. H. Yoshioka, H. Matsumoto, S. Uno and F. Higashide, *Journal of Polymer Science: Polymer Chemistry Edition*, 1976, **14**, 6, 1331.

130. M. Sakaguchi, S. Kodama, O. Edlund and J. Sohma, *Journal of Polymer Science: Polymer Letters Edition*, 1974, **12**, 11, 609.

131. A.T. Bullock, G.G. Cameron and J.M. Elsom, *Polymer*, 1974, **15**, 2, 74.

132. R.E. Michel, F.W. Chapman and T.J. Mao, *Journal of Polymer Science Part A-1: Polymer Chemistry*, 1967, **5**, 3, 677.

133. Y. Hama and K. Shinohara, *Journal of Polymer Science Part A-1: Polymer Chemistry*, 1970, **8**, 3, 651.

134. M.R. Clay and A. Charlesby, *European Polymer Journal*, 1975, **11**, 2, 187.

135. J. Placek, F. Szocs and E.J. Borsig, *Journal of Polymer Science: Polymer Chemistry Edition*, 1976, **14**, 6, 1549.

136. Y. Shioji, S-I. Ohnishi and I. Nitta, *Journal of Polymer Science Part A: General Papers*, 1963, **1**, 11, 3373.

137. Y. Hajimoto, N. Tamura and S. Okamoto, *Journal of Polymer Science Part A: General Papers*, 1965, **3**, 1, 255.

138. M. Iwasaki and Y. Sakai, *Journal of Polymer Science Part A-1: Polymer Chemistry*, 1969, **7**, 6, 1537.

139. F.C. Thryion, and M.D. Baijal, *Journal of Polymer Science Part A-1: Polymer Chemistry*, 1968, **6**, 3, 505.

140. N.R. Lerner, *Journal of Polymer Science: Polymer Chemistry Edition*, 1974, **12**, 11, 2477.

141. K. Hiraki, T. Inoue and H. Hirai, *Journal of Polymer Science Part A-1: Polymer Chemistry*, 1970, **8**, 9, 2543.

142. H. Hirai, K. Hiraki, I. Noguchi, T. Inoue, and S. Makishima, *Journal of Polymer Science Part A-1: Polymer Chemistry*, 1970, **8**, 9, 2393.

143. K. Takeda, H. Yoshida, K. Hayashi and S. Okamura, *Journal of Polymer Science Part A-1: Polymer Chemistry*, 1966, **4**, 10, 2710.

144. L. Wichec, *Chemical Analysis (Warsaw)*, 1973, **18**, 853.

145. J.M. Vigneron and A.R. Deschreider, *Lebensmittel-Wissenschaft & Technologie*, 1972, **5**, 6, 198.

146. B. Eda, K. Nunome and M. Iwasaki, *Journal of Polymer Science Part A-1: Polymer Chemistry*, 1970, **8**, 7, 1831.

147. G. Tanaka, *Journal of Polymer Science: Polymer Chemistry Edition*, 1973, **11**, 8, 2069.

148. J. Pilar, L. Toman and M. Marek, *Journal of Polymer Science: Polymer Chemistry Edition*, 1976, **14**, 10, 2399.

149. G. Fleischer, J. Hellebrand and Z. Win, *Naturwissenschaft Reiche*, 1972, **21**, 653.

150. R.D. Athey, *Journal of Polymer Science: Polymer Chemistry Edition*, 1977, **15**, 6, 1517.

151. T. Kawashima, S. Shimada, H. Kashiwabara and J. Sohma, *Polymer Journal*, 1973, **5**, 2, 135.

152. M.J. Hackathorn, and M.J. Brock, *Journal of Polymer Science: Polymer Chemistry Edition*, 1975, **13**, 4, 945.

153. J. Furukawa, K. Haga, E. Kobayashi, Y. Iseda, T. Yoshimoto and K. Sakamoto, *Polymer Journal*, 1971, **2**, 3, 371.

154. R. Hill, J.R. Lewis and J.L. Simonsen, *Transactions of the Faraday Society*, 1939, **35**, 1067.

155. E.N. Alekseeva, *Journal of General Chemistry (USSR)*, 1941, **11**, 353.

156. N. Rabjohn, C.E. Bryan, G.E. Inskeep, H.W. Johnson and J.K. Lawson, *Journal of the American Chemical Society*, 1947, **69**, 2, 314.

157. A.I. Yakubehik, A.J. Spaaskova, A.G. Zak and I.D. Shotatskaya, *Zhurnal Obshchei Khimii*, 1958, **28**, 3080.

158. A. Kawasaki in *Proceedings of the 27th Autumn Meeting of the Japan Chemical Society*, Preprints, 1972, **2**, 20.

159. M.J. Hackathorn, and M.J. Brock, *Rubber Chemistry and Technology*, 1972, **45**, 5, 1295.

160. R. Hill, J.R. Lewis and J.L. Simonsen, *Transactions of the Faraday Society*, 1939, **35**, 1073.

13 Determination of End-groups

Recent trends in multi- and/or higher functionalisation of polymeric materials require their precise characterisation not only of the main structures but also of microstructure. The chain end characterisation of polymers is regarded as one of the most important and challenging subjects in polymer characterisation. It is known that initiators and chain transfer reagents are often incorporated into the polymer as chain ends, and these features often cause significant changes in the polymer properties. Furthermore, this type of information often provides an extremely important clue to the polymerisation mechanisms. The characterisation of the end groups in polymer samples with large molecular weight (MW), however, is an extremely difficult task because of their very low concentration compared with the main chain.

Since end groups in polymers are generally attributed to an initiator and/or chain transfer and terminating agent incorporated into polymer chains, analysis of end groups is one of the most substantial approaches for assessing the mechanism of polymerisation. Furthermore, the presence or absence of specific end groups often causes significant changes in the polymer properties, and thus precise characterisation has eagerly been sought in recent multifunctionalisation of polymeric materials. The characterisation of end groups in a high molecular weight polymer sample, however, is not an easy task because of their very low relative concentration. However, its sensitivity and resolution as the have not always been adequate for quantitative analysis of end groups in high molecular weight polymers.

The characterisation of polymer chain ends give us valuable clues to clarify the polymerisation mechanisms and to design new polymers with improved properties [1-7].

The recent advent of various analytical techniques has made it possible to carry out the practical studies of the end groups of polymers. The radioactive isotope labelling method has been used over a long period to determine the initiator fragment incorporated at chain ends by measuring the specific activities of radioactive samples prepared with ^{14}C-labelled initiator [4-8]. In recent years, high-field nuclear magnetic resonance (NMR) techniques have been successfully applied to study polymer chain ends [1-7, 9, 10]. A number of reports have been published on the NMR studies of the

end groups of various polymers prepared with the initiators isotopically enriched with NMR-active nuclei such as ^{13}C, ^{2}H, ^{19}F, and ^{15}N [2, 5, 6, 11, 12]. In contrast, Hatada and co-workers polymerised totally deuterated methyl methacrylate (MMA) monomer with nondeuterated initiator to determine the content of the initiator fragments incorporated in the polymer chain by ^{1}H-NMR and discussed the mechanism of polymerisation in detail [13-16].

On the other hand, owing to recent developments in highly specific pyrolysis devices, highly efficient separation columns for gas chromatography (GC), and specific identification of the peaks in the pyrograms by GC - mass spectrometry (GC-MS), pyrolysis-GC (Py-GC) has become a powerful tool for the structural characterisation of polymeric materials. Particularly, Py-GC is noted as an extremely sensitive technique as well as a simple and rapid one.

13.1 Polypropylene Oxide

Heatley and co-workers [17] and others [18-27] have described methods for the qualitative and quantitative characterisation of saturated and unsaturated end-groups in anionically polymerised polypropylene oxide (PPO) using ^{1}H- and ^{13}C-NMR at temperatures between 0 and 80 °C using different types and concentrations of initiator.

The main features of the mechanism of the anionic polymerisation of PPO have been well established by ^{13}C-NMR [28, 29]. Propagation proceeds principally by epoxide ring opening via anionic attack at the secondary ring carbon, giving regular head-to-tail monomer enchainment:

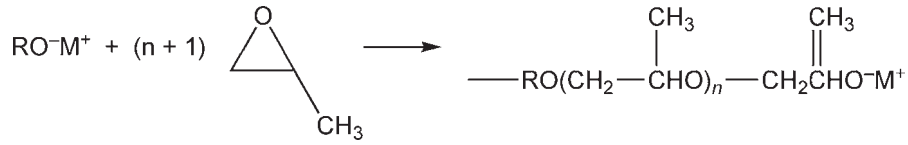

The stereochemistry of the polymer from optically inactive monomer is random and the chains terminate in secondary alcohol groups. About 2.5% of the additions occur by attack at the tertiary carbon [29], giving a small proportion of head-to-head and tail-to-tail monomer placements.

It has also been established [30] that the proton abstraction reaction occurs, leading to the initiation of a new chain via the allyl alcoholate, as well as continued growth of the original chain, since alcohol and alkoxide groups are rapidly equilibrated:

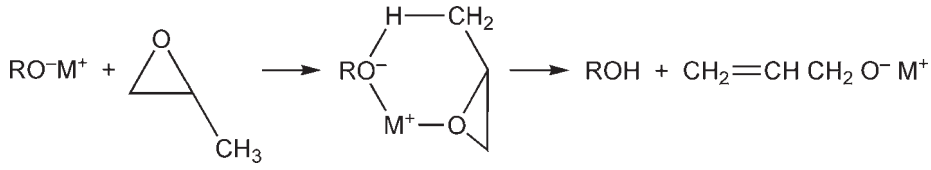

Since new chains are initiated throughout the reaction, the abstraction reaction leads to a broadened molecular weight distribution and a lower average molecular weight than would be expected from the ratio of monomer to initial alkoxide concentrations. Furthermore, the allyl ether may undergo base-catalysed isomerisation to a propenyl ether [30]:

Below are quoted two examples of end-groups as they occur in polymers:

Polyethylene glycols:

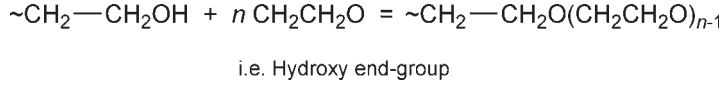

Polyvinyl chloride:

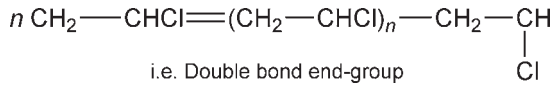

The end-groups, a hydroxy and a double bond, respectively, are a structural feature of the polymer and, as such, it may be important to identify and determine these groups. Various techniques have been used to determine end-groups. Obviously these methods must be highly sensitive as, particularly with high molecular weight polymers, the percentage of end-groups is very low. Thus if 1 mole (62 g) of diethylene glycol is reacted with 20 moles (880 g) of ethylene oxide according to the following equation, then the molecular weight of the product is 62 + 880 = 942.

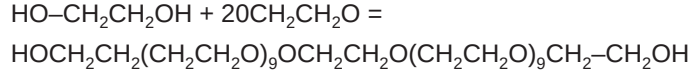

Thus two hydroxy end-groups (34 g) occur per 997 g of polymer, i.e., 3.4% hydroxy group. Similarly if 100 moles of ethylene oxide reacted with 1 mol of diethylene glycol then the final product would have a hydroxy end-group content of 0.76%. One of the uses to which end-group analysis can be put is the determination of molecular weight.

Thus if a polyethylene glycol - ethylene oxide condensate was found to contain 0.3% hydroxy end-groups:

$$HOCH_2CH_2OH + nCH_2CH_2O =$$
$$HO(O\ CH_2CH_2CH_2)_{n/2-1} - O - CH_2CH_2O(CH_2\text{-}\ CH_2O)_{n/2-1}OH$$

$$\text{Percentage hydroxyl} = \frac{2\times 17}{62 + n\times 44} = 0.3$$

$$n = \frac{3400 - 18.6}{132} = 255$$

Molecular weight of polymer is:

$$HO(OCH_2CH_2)_{n/2-1}\ OCH_2CH_2O(CH_2CH_2O)_{n/2-1}\ OH$$
$$= HO(OCH_2CH_2)_{126.5}\ OCH_2CH_2O(CH_2CH_2O)_{126.5}\ OH$$
$$= 11{,}226$$

Using a matrix-assisted laser desorption/ionisation (MALDI) technique with an ion-source Fourier-Transform mass spectrometer, van Rooji and co-workers [28] carried out high-resolution end-group analysis of polyethylene glycols (PEG).

Jackson and co-workers [26] used MALDI combined with collision induced dissociation (CID) using a time of flight instrument to achieve a similar result.

13.2 Polystyrene

^{1}H-NMR has been applied to the end group analysis of polystyrenes (PS) formed by utilising the totally deuterated monomer technique [27, 31]. In addition, ^{13}C-NMR has been used to characterise phenolic end groups in PS prepared by cationic polymerisation in the presence of alkylphenols [32]. Moreover, the initiator-derived residues in polystyrenes prepared by using ^{13}C-labelled initiators have been identified and quantified by ^{13}C-NMR even in high molecular weight polymers [33-37]. This technique was also successfully used to evaluate the role of initiator-derived functionalities in polystyrenes for the thermal degradation [36, 37].

Another technique that has been applied to end-group studies in polystyrene in Py-GC [38, 39, 40]. Thus, Ito and co-workers [39] applied this technique to the determination of end-groups in PS polymerised anionically with *n*-butyl lithium as the initiator. Polymers with molecular weights between 1000 and several million were included in this study.

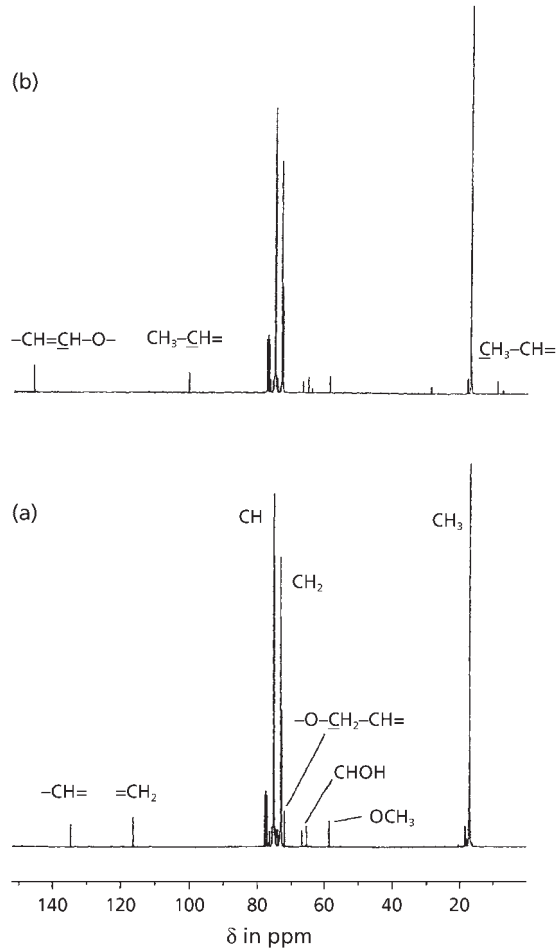

Figure 13.1 ^{13}C-NMR spectrum of polystyrene.
(*Reprinted with permission from Y. Ito, H. Ohtani, S. Ueda, Y. Nakashima and S. Tsuge, Journal of Polymer Science Part A: Polymer Chemistry, 1994,* **32**, *2, 383. ©1994, John Wiley and Sons [39]*)

Figure 13.1 shows the ^{13}C-NMR spectrum of the PS sample immediately after preparation and again after heating at 100 °C for 595 hours. The intense resonances from main-chain carbon nuclei at $\delta \approx 18$ (CH_3), 73 (CH_2) and 76 (CH) were unaffected by heating the polymer, but there were significant changes among the minor peaks. In addition to OCH_3 and CHOH carbon resonances from initiator and secondary alcohol end-groups, respectively, the spectrum of the sample immediately after preparation

Figure 13.1(**a**) shows resonances from an olefinic CH_2 carbon at δ = 116.4, an olefinic CH carbon at δ = 134.7 and a CH_2O carbon at δ = 71.9, all of equal intensity. These three resonances are consistent with assignment to an allyl ether end-group [26]. On heating (**Figure 13.1**(**b**)), these peaks disappear and are quantitatively replaced by two olefinic CH carbon peaks at δ = 100.4 and 145.8 and a CH_3 carbon peak at δ = 9.0 attributable to a propenyl ether end-group [17]. Smaller peaks of unknown origin also appeared at δ ≈ 8, 29 and 65.

Figure 13.2 shows the ^{1}H-NMR spectra of the same PS samples as in **Figure 13.1**. As well as main-chain protons at δ = 0.9 (CH_3) and 3.1-3.5 (CHO + CH_2O), the olefinic protons of the allyl group were evident in the spectrum of the sample immediately after isolation as multiplets in the region δ = 4.3 to 5.8. Using the labelling scheme:

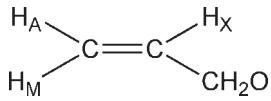

together with the fact that *trans* three-bond H— H spin-spin coupling constants are larger than *cis* [27], the chemical shifts and coupling constants were assigned as δ_A = 4.99, δ_M = 5.08, δ_x = 5.70, J_{AM} = 1.5 Hz, J_{AX} = 10.5 Hz and J_{MX} = 17.5 Hz. The CH_2O protons resonated at δ = 3.82, with a doublet splitting of 5.5 Hz from coupling to H_x. After heating (**Figure 13.2**(**b**)), the propenyl olefinic protons appeared at δ = 4.21 ($CH_3C\underline{H}$=) and 5.81 (=C$\underline{H}$O–), with a mutual coupling constant of 6.2 Hz, while the propenyl methyl protons appeared at δ = 1.42 with a coupling constant of 6.5 Hz to the adjacent olefinic proton. It is noteworthy that although the propenyl group may exist in *cis* or *trans* forms, only one set of propenyl peaks appeared in both ^{1}H and ^{13}C spectra, indicating that only one stereoisomer was produced. From the magnitude of the olefinic coupling constant [33], it was concluded that it was the *cis* isomer which was formed. The relative time-scales of the polymerisation stage (2 hours) and the isomerisation stage (595 hours) indicate that the isomerisation reaction is some two orders of magnitude slower than the polymerisation reaction.

It is also worth noting that in $CDCl_3$ solvent, the propenyl peaks were only observed in freshly prepared solutions. After storage at room temperature for two days, the peaks disappeared due to hydrolysis by trace acid impurities, producing propanal and a-CH_2OH end-group.

The spectra in **Figure 13.2** show two further small peaks of equal intensity, a sharp triplet at δ = 3.00 and a broad multiplet at δ = 3.72. On comparison of the spectra of samples of different molecular weight, the relative intensities of these peaks were found to vary systematically with molecular weight, and the peaks were therefore associated with end-groups. To determine the origin of these peaks, a series of ^{13}C

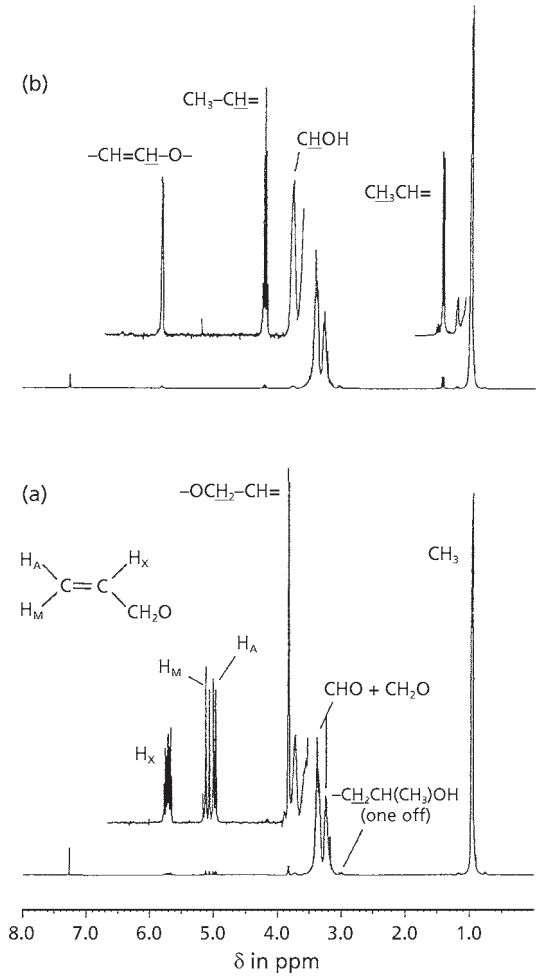

Figure 13.2 ^{1}H-NMR spectrum of polystyrene.
(*Reprinted with permission from Y. Ito, H. Ohtani, S. Ueda, Y. Nakashima and S. Tsuge, Journal of Polymer Science Part A: Polymer Chemistry, 1994,* **32**, *2, 383. ©1994, John Wiley and Sons [39]*)

spectra were recorded with low-power continuous-wave ^{1}H decoupling at various frequencies in the region δ = 3 to 4 in the proton spectrum. These spectra showed that placing the decoupler frequency on the small proton resonance at δ = 372 gave maximum decoupling of the terminal $\underline{C}H(CH_3)OH$ carbon resonances, and this peak was therefore assigned to the CHOH proton. ^{1}H-^{1}H homonuclear spin-decoupling

experiments then showed that the triplet at δ = 3.00 arose from one of the non equivalent protons in the adjacent CH_2 group. Both peaks are sufficiently well resolved at 300 MHz to be of use in the quantitative characterisation of chain length.

Pyrolysis at 600 °C produced 22 different compounds, four being derived from *n*-butyl groups and four from *n*-butyl groups plus a styrene unit (see **Table 13.1**).

Based on these results, M_n values could be estimated using relative molar intensities of these nine characteristic peaks (i = 1-9) against those of the major peaks (i = 1-22). In this case, minor peaks other than i = 1-22 were ignored because the total relative intensity of these peaks was less than a few percent. Since the degree of polymerisation (D_p) of the PS sample is defined as the number of styrene units per end group, the D_p value can be calculated by the following equation:

$$D_p = \frac{\sum_{i=1}^{i=22}\left(I_i \times M_i / n_i\right)}{\sum_{i=1}^{i=9}\left(I_i / n_i\right)}$$

where I_i is the intensity of peak i in the pyrogram of a PS sample having one *n*-butyl end group, m_i is the number of styrene units in the i component, and n_i is the molar sensitivity correction factor of the i component for FID response, i.e., the effective carbon number for the i component.

Of the various pyrolysis products produced one in particular, peak 8 (C_4H_9-$CH_2C(Ph)=CH_2$) (2-phenyl heptane) was the most characteristic of nine products mentioned previously and gave a linear relationship between M_n and the relative intensity of this peak to the total intensity of all 22 peaks in the program.

Li and Renaldi [41] used 3-dimensional NMR to determine the chain-end structure of ^{13}C-labelled PS.

Ghosh and co-workers [42] have carried out end-group analysis of persulfate initiated PS using a dye partition and a dye interaction technique. Sulfate and hydroxyl end-groups are generally found to be incorporated in the polymer to an average total of 1.5 to 2.5 end-groups per polymer chain.

Banthia and co-workers [43] determined sulfate, sulfonate and iso-thioronium salt end-groups in PS by the dye-partition technique. Polymer polarity did not affect the results of the end-group determination. Nitrile groups incorporated in PS by

Table 13.1 Peak assignment in the program of PS						
Peak Number	Structure of pyrolysate	Structure of end-group	Styrene unit (m)	Carbon number (C)	Aliphatic C=C Bond (μm)	Effective Carbon number (n)*
1	$CH_3CH{=}CH_2$	From C_4H_9–	0	3	1	2.9
2	$CH_3CH_2CH_3$		0	3	0	3.0
3	$CH_3CH_2CH{=}\ CH_2$		0	4	1	3.9
4	$CH_3CH_2CH_2CH_3$		0	4	0	4.0
5	$CH_3CH_2CH_2CH_2CH_3$	$-C_4H_9-(CH_2-\underset{\displaystyle Ph}{\underset{\vert}{CH}}-)$	0	5	0	5.0
6	$CH_3CH_2C(Ph){=}CH_2$		1	10	1	9.9
7	C_4H_9-$CH_2CH_2(Ph)$		1	12	0	12.0
8	C_4H_9-$CH_2C(Ph){=}CH_2$		1	13	1	12.9
9	C_4H_9-$CH{=}C(Ph)$ CH_3		1	13	1	12.9

*Reprinted with permission from Y. Ito, H. Ohtani, S. Ueda, Y. Nakashima and S. Tsuge, Journal of Polymer Science Part A: Polymer Chemistry, 1994, **32**, 2, 383. ©1994, John Wiley and Sons [39]*

initiation or copolymerisation have been detected and estimated by dye-partition techniques after reduction to amino groups with lithium aluminium hydride in tetrahydrofuran [44].

13.3 Polyethylene

High-density polyethylene (HDPE) prepared with Ziegler-based catalysts have predominantly *n*-alkyl or saturated end-groups. Those prepared with chromium-based catalysts have a propensity towards more olefinic end-groups. The ratio of olefinic to saturated end-groups for polyethylenes (PE) prepared with chromium-based catalysts is approximately unity.

The end-group distribution is therefore another structural feature of interest in low pressure polyolefins because it can be related to the type of catalyst used, and possibly to the extent of long chain branching. It is possible not only to measure by ^{13}C-NMR concentrations of saturated end-groups, but also of the olefinic end-groups and subsequently an end-group distribution. Pérez and Vanderhart [45] have described a ^{13}C-NMR method for the determination of chain-ends and branches in crystalline and non-crystalline regions in PE. A high proportion of these units resided in the crystalline phase.

Hammond and co-workers [46] conducted an IR study of bond rupture of carbonyl and vinyl groups formed during plastic deformation of HDPE.

The relationship between end-group concentration and the time lapse between deformation and spectroscopic examination was investigated. There is no significant time dependence for vinyl group concentration, whereas the carbonyl group concentration shows a slight increase with time. The carbonyl peak centred at 1742 cm^{-1} reaches a maximum intensity after 48-72 hours. The vinyl out-of-phase deformation band at 909 cm^{-1} was used to measure vinyl end-groups. **Figure 13.3** shows the time dependence of this peak for two randomly selected draw ratios.

The effect of temperature was examined over the range 7-60 °C; the lower limit is set by the increasing brittleness of the polymer as it is cooled, fracture occurring before yield is reached. The results, presented in **Figure 13.4**, show that the concentration of vinyl and carbonyl groups, for a given draw ratio, decreases with increasing temperature.

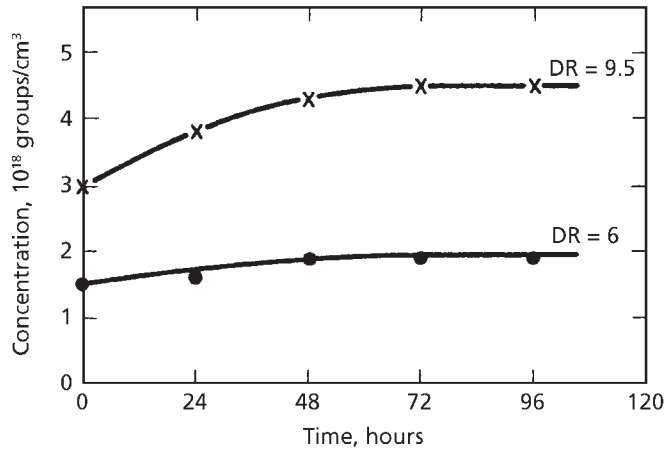

Figure 13.3 Time dependence of vinyl deformation band at 909 cm^{-1} on draw ratio. (*Reprinted with permission from C.L. Hammond, P.J. Hendra, B.G. Lator, W.F. Maddams and H.A. Willis, Polymer, 1988,* ***29****, 1, 49. ©1988, Elsevier [46])*

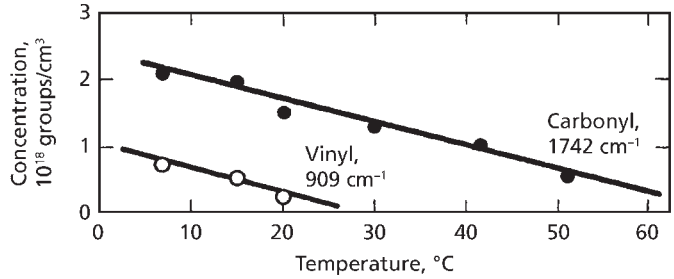

Figure 13.4 Decrease of concentration of vinyl and carbonyl groups in polyethylene on draw ratio. (*Reprinted with permission from C.L. Hammond, P.J. Hendra, B.G. Lator, W.F. Maddams and H.A. Willis, Polymer, 1988,* ***29****, 1, 49. ©1988, Elsevier [46])*

13.4 Polyethylene Terephthalate

Van Houwelingen [47] has used coulometric bromination to determine vinyl ester end-groups in polyethylene terephthalate (PET) formed by thermal chain scission:

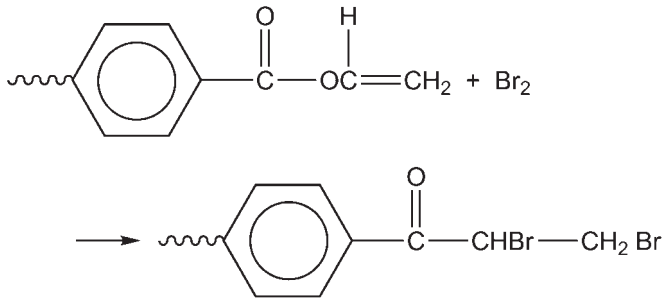

The constant-current generation of bromine is carried out in a medium of dichloroacetic acid, water, potassium bromide and mercury(II)chloride. To this medium, the polymer, previously dissolved in hexafluoroisopropanol and diluted with anhydrous dichloroacetic acid, is added and bromine is generated. The end of the reaction is detected biamperometrically. The suitability of this method was tested against methyl vinyl terephthalate:

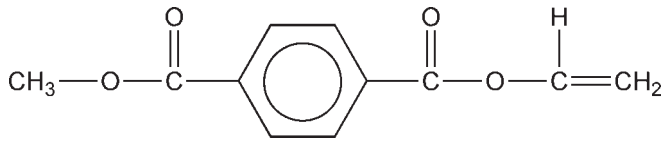

Additions of 14.2 and 1.0 µmol of methyl vinyl terephthalate (corresponding to 30 and 2 mmol of vinyl ester end-groups per kilogram of polymer) were recovered quantitatively (recoveries of 99.8 and 98.5%, respectively).

Nissen and co-workers [48] have described an ultraviolet (UV) spectroscopic method for carboxyl end-groups in PET. Hydrazinolysis led to formation of terephthalomonohydrazide from carboxylated terephthalyl residues to provide a selective analysis for carboxyl groups via UV absorbance at 240 nm.

Other techniques that have been applied to end-group analysis of PET include ^{1}H-NMR, gel permeation chromatography – MALDI-ToF mass spectrometry [49] and MALDI-ToF combined with CID [26].

13.5 Polyisobuylene

In their analysis of ^{1}H-NMR spectra of various end functionalised polyisobutylenes (PIB). Si and Kennedy [50] covered inductive effects (due to *tert*-chlorine-ended PIB), magnetic anisotropic effects (due to olefin groups and phenyl rings) and allylic coupling (due to olefinic end-groups):

I Chlorine-ended PIB

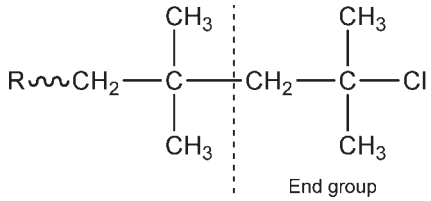

II Olefinic-ended PIB

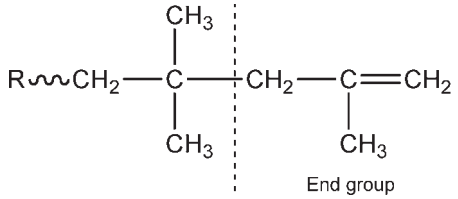

III Hydrogenated PIB

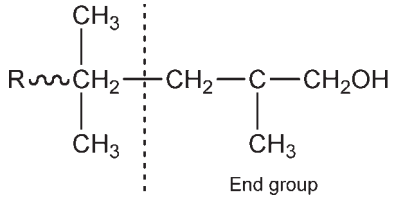

13.5.1 Tert-chlorine Terminated Polyisobutylene

Figure 13.5 shows the $-CH_3$ and $-CH_2-$ proton region of the ^{1}H-NMR spectrum of chlorine-ended PIB (Structure I above). The terminal chlorines exert a strong electron withdrawing effect on the neighbouring – CH_3 and $-CH_2-$ groups and shift the resonances of these groups downfield. The proton resonances of 'normal' $-CH_3$ and $-CH_2-$ groups in PIB appear at 1.09 and 1.40 ppm, respectively, whereas those of the first isobutylene unit adjacent to the *tert*-Cl appear at 1.67 and 1.95 ppm (i.e.,

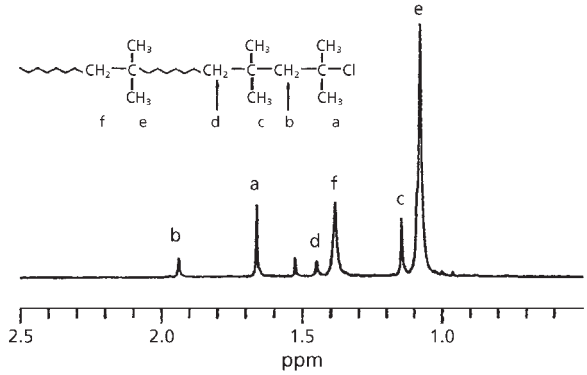

Figure 13.5 CH_3 and CH_2 proton region of 1H-NMR spectrum of chlorine ended PIB. (*Reprinted with permission from J. Si, J.P. Kennedy, Journal of Polymer Science Part A: Polymer Chemistry, 1994, 32, 11, 2011. ©1994, John Wiley and Sons [49])*

they show a downshift of 0.57 and 0.55 ppm), and those of the second isobutylene unit from the *tert*-Cl appear at 1.16 and 1.46 ppm (i.e., with a downshift of 0.07 and 0.06 ppm). The very small shoulder on the downfield side of peak e in **Figure 13.5** (visible by enlargement) indicates that the third isobutylene unit is also subject to the inductive effect by the terminal chlorine. With decreasing molecular weights (down to M_n = 480), the resonances of the CH_3– and –CH_2- groups of the third isobutylene unit separate with downfield shifts of 0.01 and 0.01 ppm, respectively, in respect to their normal position. That indicates that the inductive effect due to the chloride end-group can be transmitted up to 6 σ-bonds along the PIB chain.

13.5.2 Olefin-Terminated Polyisobutylene

Anisotropic Effect

Figure 13.6 shows the ^{1}H-NMR spectrum of **II**. The 'normal' –CH_3 and –CH_2– groups of PIB appear essentially at the same position as in **I** (i.e., at 1.09 and 1.40 ppm). Similarly, the first isobutylene unit adjacent to the double bond shows the –CH_3 and –CH_2– proton resonances at 1.77 and 1.98 ppm (i.e., with down shifts of 0.68 and 0.58 ppm), respectively. In contrast to the first isobutylene unit, the -CH_3 and –CH_2– groups of the second isobutylene unit away from the exo double bond appear at 1.01 and 1.36 ppm, i.e., show *upfield* shifts of 0.08 and 0.04 ppm, respectively. This type of shifting (i.e., first isobutylene unit downfield, the second isobutylene unit

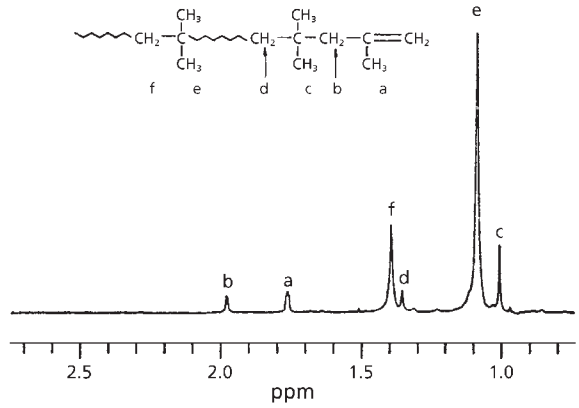

Figure 13.6 NMR spectrum of olefin end PIB.
(*Reprinted with permission from J. Si, J.P. Kennedy, Journal of Polymer Science Part A: Polymer Chemistry, 1994, 32, 11, 2011. ©1994, John Wiley and Sons [49]*)

upfield), is most likely due to shielding anisotropy due to unsaturation [51, 52]. After hydroboration and oxidation the unsaturation disappears and the resonances of the first and second isobutylene units shift back to their usual positions.

13.5.3 Hydroxyl-Terminated Polyisobutylene

In the ^{1}H-NMR spectrum of hydroxyl terminated PIB the (see structure **III** previously) the eight peak pattern in the 3.22-3.48 ppm range is clearly due to the AB part of a typical ABX system. This splitting pattern is most likely due to prochirality: the two protons (g_1 and g_2) in the $-CH_2OH$ group are magnetically nonequivalent, as they are part of a prochiral $-CH_2-$ group:

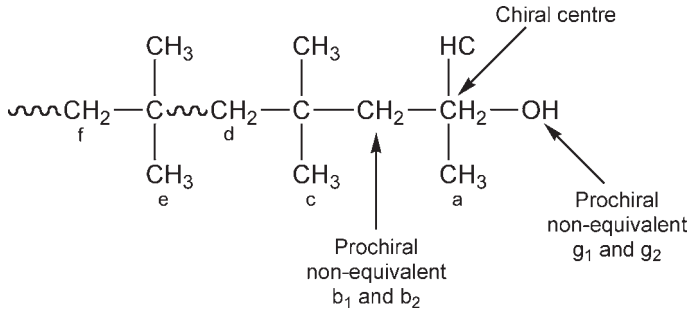

Manaft and co-workers [53] observed ^{1}H-NMR signals for olefinic end-groups, $-CH_2C(CH_3)=CH_2$, $CH=C(Me)_2$, and $-CH_2C-(CH_2)CH_2-$ in high molecular weight PIB.

13.6 Polymethylmethacrylate

Between 1989 and 1997, Ohtani and co-workers [38, 54-60] published a series of papers on the application of Py-GC to the determination of end-groups in polymethylmethacrylate (PMMA).

In earlier work Ohtani and co-workers [54] identified end-groups in PMMA by high resolution Py-GC.

Minor peaks in the chromatogram were associated with end-groups derived from benzoyl peroxide polymerisation initiator or dodecane thiol chain transfer agent reactions. End-group data were related to molecular weight data.

Ohtani and co-workers [58] used Py-GC at 700 °C to determine the end-groups in PMMA macromonomers and their prepolymers which had been synthesised radically in the presence of azobis(isobutyronitrile) (AIBN) as initiator and mercaptoacetic acid (MCAA) or mercaptopropionic acid (MPA) as chain transfer reagent.

Because one of the end groups in most of the PMMA examined in this study should have either a sulfur atom or a cyano group, the Py-GC system is equipped with a simultaneous multidetection system. A flame ionisation detector (FID), was always used in conjunction with either a sulfur-selective flame photometric detector (FPD) or a nitrogen-phosphorus detector (NPD).

In the method developed by Ohtani and co-workers [58] simultaneous-multidetection systems were quantitatively applied to the analysis of end groups. The simultaneous pyrograms of PMMA taken by FID and NPD in the presence of benzothiophene as an internal standard are used for the selective determination of the sulfur-containing chain ends. On the other hand, the simultaneous programs taken by FID and NPD are interpreted in terms of the AIBN residues incorporated into the polymer chains. They compared the results observed by simultaneous multidetection Py-GC with those estimated by size exclusion chromatography (SEC) and kinetic data for the polymerisation.

According to the mechanism of the radical polymerisation which is initiated by AIBN followed by the chain transfer reactions with either MCAA or MPA, most of the resulting prepolymers should be terminated by the corresponding carboxylic residues as follows:

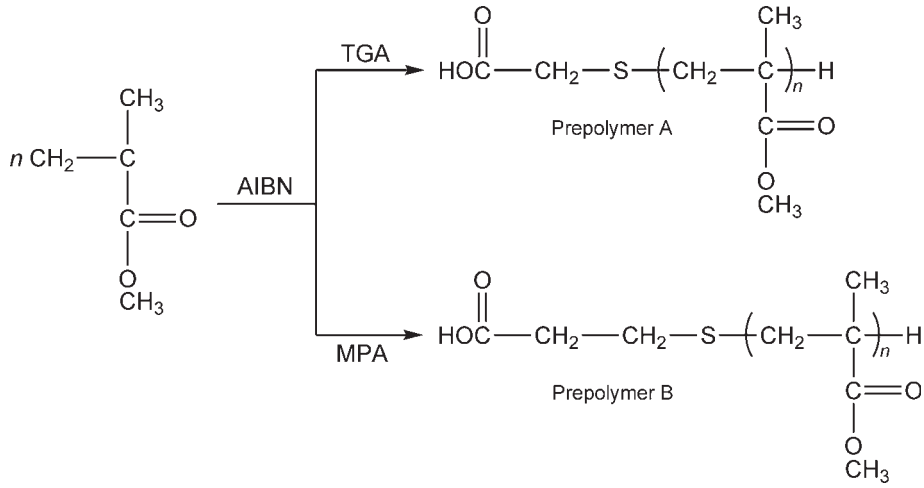

Judging from the big differences in chain-transfer constants, chain transfer reactions with AIBN, monomer, and solvent (benzene) can be regarded negligible in the polymerisation in the presence of either MCAA or MPA. However, the following polymer having the terminal AIBN residue should also be formed depending on the relative feed of AIBN:

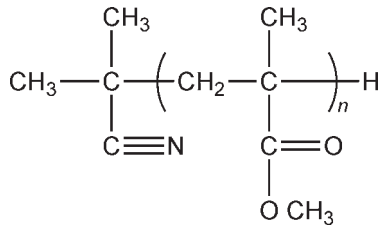

In addition, recombination of disproportionation termination reactions might yield other polymers having different combinations of terminals.

Purified prepolymer-As were converted to the corresponding macromonomers by the reaction of the end carboxylic groups with glycidyl methacrylate in xylene at 140 °C for 6 hours in the presence of the small amount of hydroquinone and *N*,*N*-dimethyllaurylamine as follows:

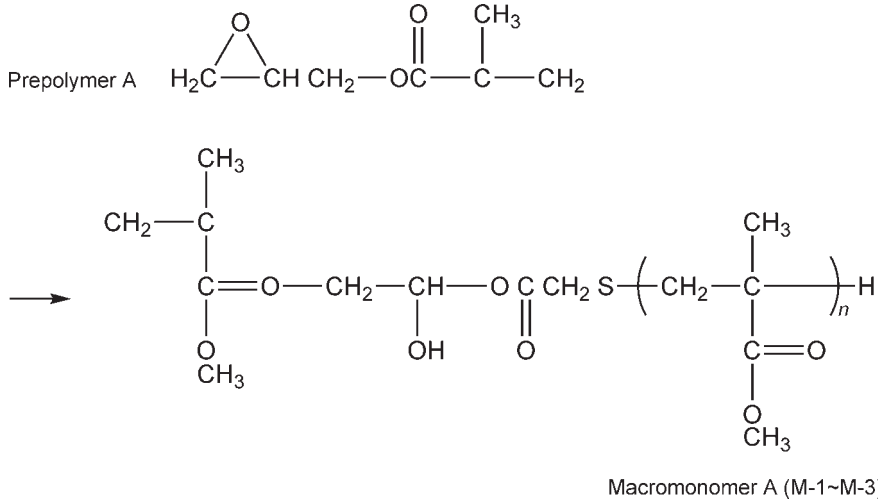

A typical programs of a prepolymers prepared in the presence of MCAA or MPA as a chain transfer reagent is illustrated in **Figure 13.7**, where benzothiophene was used as a common internal standard for FPD and FID. PMMA has a tendency to depolymerise mostly into the MMA monomer at elevated temperatures; therefore, the MMA monomer is the main pyrolysate (more than 70% of the total peak intensities except for the internal standard) on the pyrograms observed by FID. However, the sulfur-containing products characteristic of the MCAA or MPA-chain-end residues are difficult to detect via FID, because even the outstanding peaks observed at retention time up to 10 minutes are mostly assigned to hydrocarbons by GC-MS. On the other hand, only sulfur-containing products formed from the end-group moiety of the MCAA or MPA residues along with the internal standard were detected on the pyrograms observed by FPD. The main component of the MMA monomer is not observed at all because it contains no sulfur atoms. Therefore in order to quantitate the yields of sulfur-containing compounds on the FPD pyrogram relative to the MMA-related products on the FID program, benzothiophene was used as the correlating internal standard because the peak due to this compound was observed by both FPD and FID detectors.

The pyrograms observed by FID for the prepolymers synthesised in the presence of MCAA and MPA were almost identical. However, when comparing the corresponding pyrograms detected by FPD, a fairly strong peak due to CH_3-CH_2SH was characteristic of the various prepolymers examined.

Table 13.2 summarises the characteristic pyrolysates that were observed on the pyrograms and identified by GC-MS. They are the MMA backbone-related products (peaks 1-24) and the AIBN-related ones (peaks B-K) which are also observed in the NPD programs. AIBN-related peak D was used to normalise the MMA backbone related peaks because it was observed as a moderately strong, isolated peak.

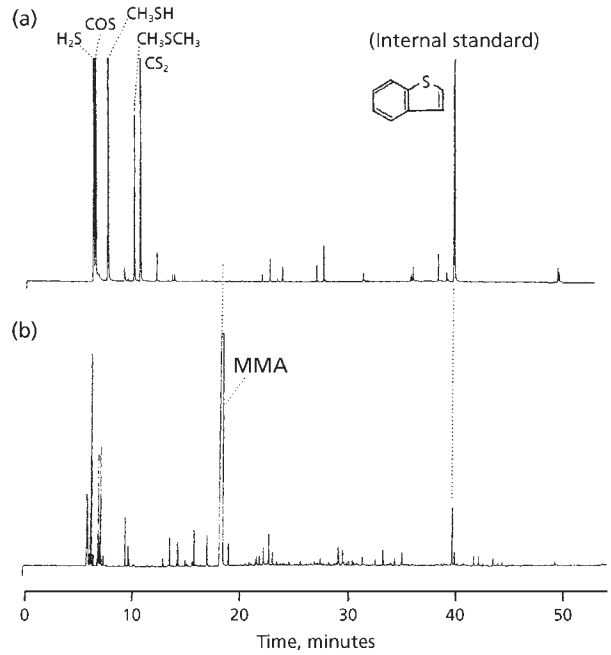

Figure 13.7 Pyrogram of PMMA prepared in the presence of MCAA or MPA chain transfer agents. (*Reprinted with permission from H.Ohtani, Y.F. Luo, Y. Nakashima, Y, Tsukahara and S. Tsuges, Analytical Chemistry, 1994,* **66**, *13, 1438. ©1994, ACS [58]*)

In summary, these results demonstrated that pyrolysis with simultaneous multidetection GC is an effective technique for the chain end analysis of PMMA macromonomers and their prepolymers synthesised via radical polymerisation. In this method, minute amounts of heteroatom-containing end groups in PMMA are determined using the ratios between heteroatom-containing fragments and backbone MMA related products, which are simultaneously detected by the heteroatom-selective detector and by FID, respectively. An appropriate internal standard is used to correlate the simultaneously observed pyrograms.

In further work Ohtani and co-workers [59] characterised branched alkyl end groups of PMMA polymerised radically with 2,2′-azobis(2,4,4-trimethylpentane) (ABTMP) or benzoyl peroxide (BPO) as an initiator by Py-GC. On the resulting pyrogram at 540 °C, characteristic products formed from the end group moiety due to the initiator, such as isobutane, isobutene, and so on, were clearly separated from those from the main chain. Then number-average molecular weight (M_n) of PMMA was determined by the

Table 13.2 Assignment of peaks reflecting chain end AIBN residue in the pyrogram of PMMA		
Peak code	**Molecular weight**	**Structure**
B	67	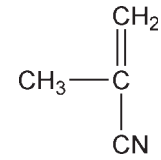
C	69	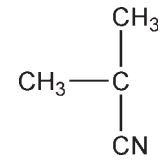
D	123	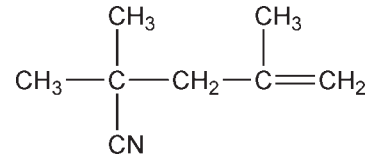
E	125	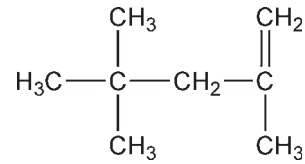
F	136	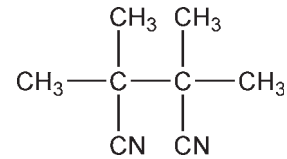
G	155	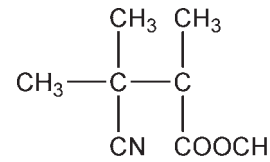
H	169	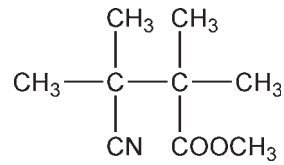

I	169	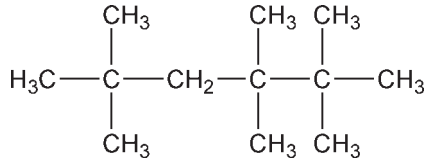
J	167	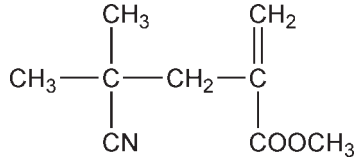
K	183	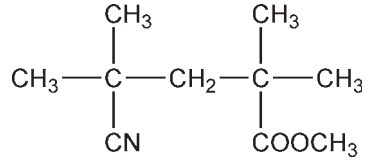
*Reprinted with permission from H.Ohtani, Y.F. Luo, Y. Nakashima, Y, Tsukahara and S. Tsuge, Analytical Chemistry, 1994, **66**, 13, 1438. ©1994, ACS [58]*		

ratio of the relative intensity of these peaks due to the end group and the main chain. After simple correction using a reference PMMA sample having different end groups, M_n values estimated by Py-GC agreed well with those obtained by SEC. Furthermore, determination of end-groups well supported the assumption that disproportionation was dominant in termination in this polymerisation system of MMA.

Figure 13.8 shows pyrograms of (a) PMMA ($M_n = 2.78 \times 10^3$) initiated by ABTMP and (b) the reference PMMA sample initiated by BPO. Since PMMA has a tendency to depolymerise mostly into the original monomer at elevated temperatures, the main pyrolysis product is MMA monomer (approximately 95%). In addition, dimer peaks and a trimer peak are observed in the pyrograms. Furthermore, many minor components are also observed as well-separated peaks. Among these, the five peaks A, C, D, F, and G are observed only in pyrogram a (**Figure 13.8**). This result indicates that these components arise from the end moiety originating from ABTMP initiator. Additionally, peak 6 in **Figure 13.8(a)** should be mostly attributed to one of the initiator related products although it is also observed in the pyrogram of the BPO initiator reference polymer shown in **Figure 13.8(b)** even with weaker intensity. Actually the relative intensity of peak B on the pyrogram on a polymer sample of $M_n = 2.78 \times 10^3$ proved to be much larger than that of a similarly initiated polymer of much lower molecular weight ($M_n = 4 \times 10^5$).

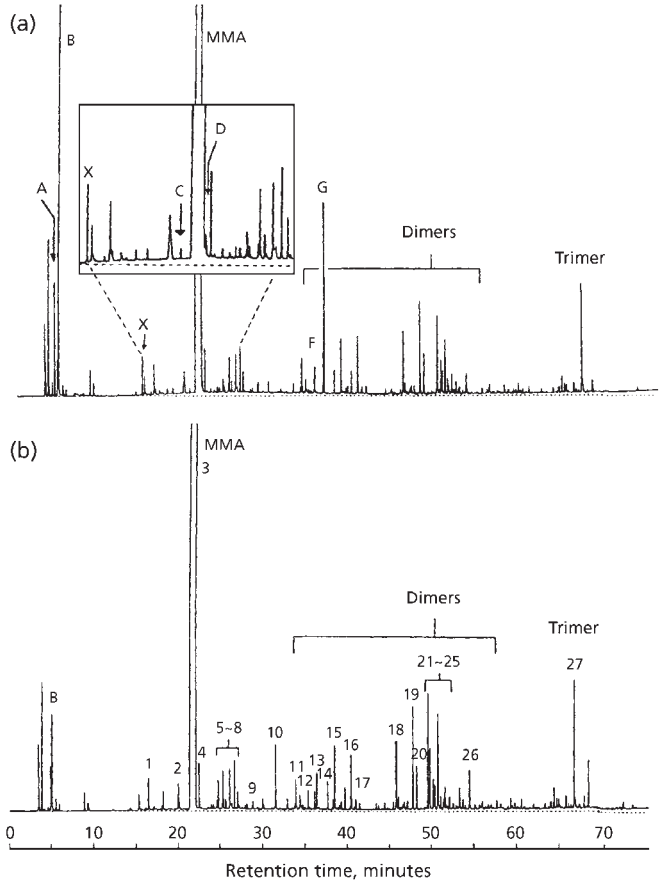

Figure 13.8 Pyrograms of (a) PMMA initiated with ABTMB and (b) PMMA initiated with BPO. (*Reprinted with permission from H. Ohtani, Y. Ito, S. Tsuge, S. Wakabayashi, J-I. Atarashi and T. Kawamura, Macromolecules, 1996, 29, 13, 4516. ©1996, ACS [59]*)

These peaks observed in **Figure 13.8(a)** (the ABTMP initiator) identified by Py-GC-MS are summarised in **Table 13.3,** while the assignment of the other peaks observed in **Figure 13.8(a) and 13.8(b)** is shown in **Table 13.4**. The peaks listed in **Table 13.3** can be mostly attributed to the initiator-related fragments formed from the end group moiety of PMMA obtained with ABTMP.

Number average molecular weights measured by this Py-GC method and SEC are in fairly good agreement and this strongly supports the validity of the assumption implicit in this method concerned with the termination mechanisms exclusively through disproportionation.

Table 13.3 Assignment of peaks concerned with the initiator observed in the pyrograms

Peak	Chemical structure	MMA units	End-group units[a]	ECN[b]	Source
A	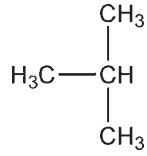	0	0.5	4.0	End moiety
B	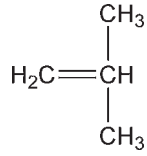	0	0.5	3.9	End moiety and main chain
C	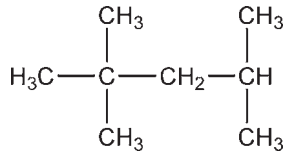	0	1.0	8.0	Remaining initiator fragment
D	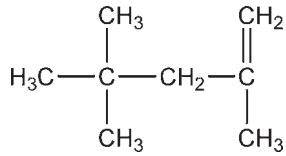	0	1.0	7.9	Remaining initiator fragment
Ec	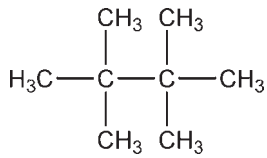	0	1.0	8.0	Initiator
F	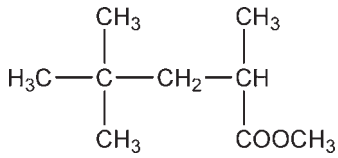	1	0.5	7.75	End moiety
G	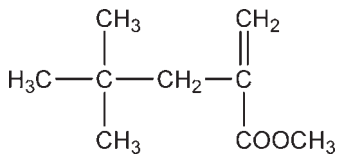	1	0.5	7.65	End moiety

Table 13.3 *Continued*

Peak	Chemical structure	MMA units	End-group units[a]	ECN[b]	Source
H[c]	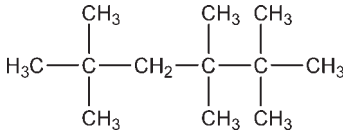	0	1.5	12.0	Initiator
I	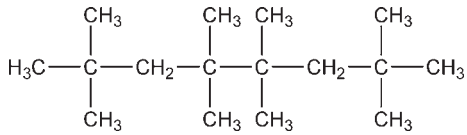	0	2.0	16.0	Initiator

a: End group unit; C_8 = 1.0

b: ECN: effective carbon number

c: Observed only in the pyrogram of the intact initiator.

Reprinted with permission from Y. Ito, S. Tsuge, H. Ohtani, S. Wakabayashi, J-I. Atarashi and T. Kawamura, Macromolecules, 1996, 29, 13, 4516. ©1996, ACS [59]

Ohtani and co-workers [60] determined by Py–GC end groups in anionically-polymerised standard PMMA in the range of number-average molecular weights 20,000 to 1,300,000 with narrow molecular weight distributions. The characteristic fragments reflecting the end groups on the pyrogram of the PMMA were identified by comparison with those of a radically polymerised PMMA, together with the mass spectra of the characteristic peaks on the resulting pyrograms taken by a GC-MS spectrometer system. Concentrations of the end groups determined from their relative peak intensities were interpreted in terms of M_n and then compared with their reference values from the manufacturers and those estimated by proton NMR. By this method, direct determination of the end-groups was possible even for PMMA with M_n about 1,000,000 without using any standard polymer samples.

The anionically polymerised standard PMMA and the radically polymerised PMMA with BPO as an initiator have common backbone structures but have different end-group structures. Therefore, by comparing the pyrograms for the two types of PMMA, the characteristic peaks reflecting the end-groups in the standard PMMA might be estimated. Since PMMA has a tendency to depolymerise, the main pyrolysis product on the pyrograms (about 95%) is the MMA monomer. In addition, various minor

Table 13.4 Assignment of Common Peaks Concerned with the Main Chain of PMMA

Peak	MW	Chemical structure	MMA units	ECN[a]
1	88	$CH_3CH_2COOCH_3$	1	2.75
2	102	$CH_3CH(CH_3)COOCH_3$	1	3.75
3	100	$CH_2=C(CH_3)COOCH_3$ (monomer)	1	3.65
4	116	$C_6H_{12}O_2$	1	4.75
5	92	$PhCH_3$[b]	0	7.00
6	116	$C_6H_{12}O_2$	1	4.75
7	114	$C_6H_{10}O_2$	1	4.65
8	114	$C_6H_{10}O_2$	1	4.65
9	114	$C_6H_{10}O_2$	1	4.65
10	104	$PhCH=CH_2$[b]	0	7.90
11	142	$C_8H_{14}O_2$	2	6.65
12	140	$C_8H_{12}O_2$	2	6.65
13	156	$C_9H_{16}O_2$	2	7.65
14	140	$C_8H_{12}O_2$	2	6.65
15	140	$C_8H_{12}O_2$	2	6.65
16	158	$C_9H_{18}O_2$	2	7.65
17	158	$CH_3OCOCH=CHCH_2COOCH_3$	2	4.40
18	186	$C_9H_{14}O_4$	2	6.40
19	200	$C_{10}H_{16}O_4$	2	7.40
20	186	$C_9H_{14}O_6$	2	6.40
21	200	$C_{10}H_{16}O_4$	2	7.40
22	200	$C_{10}H_{16}O_4$	2	7.40
23	200	$C_{10}H_{16}O_4$	2	7.40
24	214	$C_{11}H_{18}O_4$	2	8.40
25	214	$C_{11}H_{18}O_4$	2	8.40
26	190	$PhCH_2CH=C(CH_3)COOCH_3$[b]	1	10.65
27	300	$C_{15}H_{24}O_6$ (trimer)	3	11.25

[a] ECN: Effective carbon number

[b] These peaks are only characteristics of PMMA initiated by BPO.

*Reprinted with permission from Y. Ito, S. Tsuge, H. Ohtani, S. Wakabayashi, J-I. Atarashi and T. Kawamura, Macromolecules, 1996, **29**, 13, 4516. ©1996, ACS [59]*

Table 13.5 Assignment of peaks concerned with the end groups observed in the pyrograms along with that of MMA monomer			
Peak	**MW**	**Chemical structure**	**ECN**
MMA monomer	100	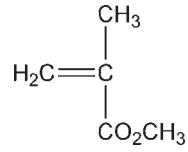	3.65
A	120	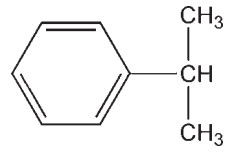	9.0
B	118	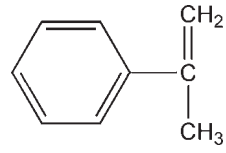	8.9
C	134	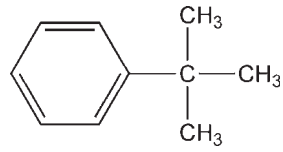	10.0
D	132	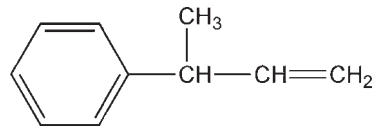	9.9
E	174	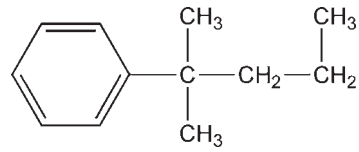	12.9
F	206	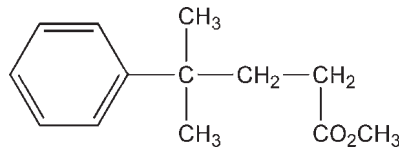	11.75
G	218	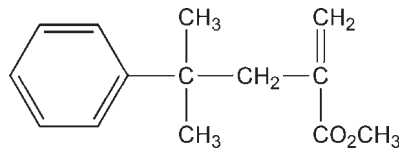	12.65
*Reprinted with permission from H. Ohtani, Y. Takehana and S. Tsuge, Macromolecules, 1997, **30**, 9, 2542. ©1997, ACS [60]*			

products including MMA dimers and trimers are also observed. However, the peaks of larger products than trimers were negligibly small even under high-temperature GC conditions with the oven temperature up to around 400 °C. This fact suggests that almost all the PMMA chains are reflected in the observed pyrograms as the peaks up to trimers. From detailed comparison of these pyrograms, the characteristic peaks (A–G; **Table 13.5**), proved to be observed only in the pyrogram of the polymer with M_n = 20,200. Moreover, among the pyrograms for polymers with M_n 20,200 to 1,330,000, the relative intensities of peaks A-G monotonously decreased with the rise of M_n. These data suggest that the characteristic peaks (**Table 13.5**) are originated from the anionic initiator residue incorporated into the polymer chain.

The structures of these peaks reflecting the chain end were identified mostly by GC-MS. From the observed mass spectra, the relatively abundant peaks of A and B can be assigned as cumene and α-methylstyrene, respectively. These data strongly suggest that these standard polymers contained an amyl end-group at one end of the polymer.

Thus estimated M_n values by Py-GC and ^{1}H-NMR are compared with the reference values from the manufacturer in **Table 13.6**. Data obtained by both Py-GC and

Table 13.6 Number average molecular weight of PMMA calculated from end-group analysis by Py-GC and ^{1}H-NMR

Sample	Number average molecular weight (M_n)		
	Reference[a]	Py-GC	^{1}H-NMR
S-I	20,200	21,400	27,000
S-II	33,900	35,500	35,700
S-III	66,200	70,200	67,200
S-IV	91,400	103,000	98,700
S-V	296,000	317,000[b]	(213,000)
S-VI	797,000	731,000[c]	
S-VII	1,330,000	1,160,000	

[a] Reference M_n specified by the manufacturer
[b] CV = 1.4% for five measurements
[c] CV = 4.1% for five measurements
CV: Coefficient of variance

*Reprinted with permission from H. Ohtani, Y. Takehana and S. Tsuge, Macromolecules, 1997, **30**, 9, 2542. ©1997, ACS [60]*

^{1}H-NMR are in fairly good agreement with the reference values for lower molecular weight samples (S-I to S-IV). However, considering the signal to noise (S/N) ratio for the observed ^{1}H-NMR spectra under the given spectral condition of 500 scans with a 2 second pulse delay, the estimation of M_n was limited to less than 3 x 10^5 or so even by the 500 MHz ^{1}H-NMR used in this work. In order to estimate the higher M_n values by NMR, a much higher number of scans should be needed to enhance the S/N ratio. Moreover, since the T_1 values for the end groups are generally larger than those for the main chains such as OCH_3, a much longer pulse delay time might be required to fulfill the sufficiently quantitative conditions for the measurement. On the other hand, **Figure 13.9** shows a typical ^{1}H-NMR spectrum for a PMMA sample (S-I; M_n = 20,200). On the expanded partial spectrum (× 100) around 7.1-7.4 ppm, three phenyl-proton peaks reflecting the cumyl chain ends are observed. Since the intensity ratio of these three peaks is about 2:2:1, may correspond to the proton number of *o*-, *m*- and *p*- positions in the phenyl ring, respectively. On the other hand, the methoxy proton peak at about 3.6 ppm can be used as the key peak reflecting the backbone of the polymer chain. Using these peak intensities, M_n, of a given PMMA sample can be estimated.

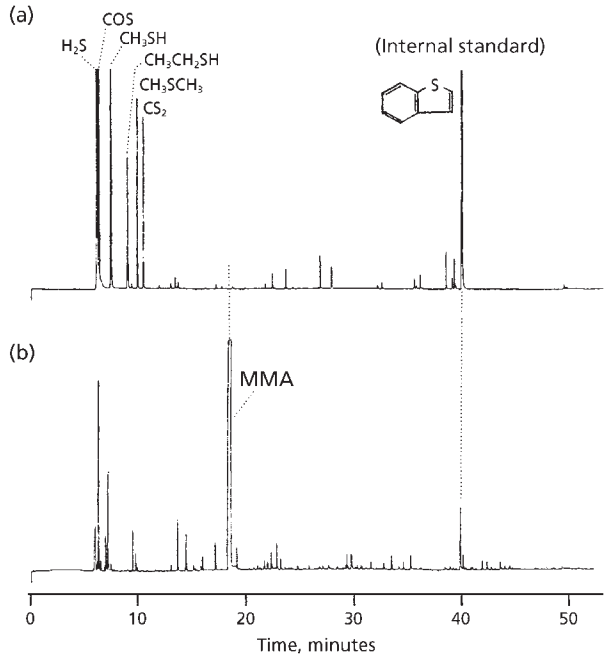

Figure 13.9 NMR spectrum of PMMA.
(*Reprinted with permission from H. Ohtani, Y. Takehara and S. Tsuge, Macromolecules, 1997, **30**, 9, 2542. ©1997, ACS [59]*)

This method is capable of precisely quantifying cumyl end-groups in anionically polymerised PMMA even for the samples with M_n = 10^6, which were difficult to analyse even by NMR. For these PMMA, moreover, it was not necessary to take into account any contribution of the side reaction products. M_n values for the PMMA samples can be directly estimated by the relative peak intensities between MMA formed from the polymer main chains through almost quantitative depolymerisation and the characteristic products of the end groups on the observed pyrograms after making molar sensitivity corrections for those products. Consequently, this technique belongs to one of the absolute methods for determining M_n without using any standard polymer samples with known M_n, provided that all the characteristic products of the end groups are to be quantitatively assigned against those from the main chain for given linear polymeric systems.

13.6.1 MALDI-ToF-MS

MALDI-ToF (CID) MS has been used to obtain information on the end-groups and other structural features in polyalkylmethacrylates [61].

13.6.2 Dye Partition Methods

This technique is best illustrated by an example concerning the determination of end-groups in persulfate-initiated PMMA [42, 62]. Sulfate and other anioic sulfoxy end-groups were determined by shaking a chloroform solution of the polymer with aqueous methylene blue reagent. The greater the anionic content, the more the methylene blue phase is decolorised. The blue colour is evaluated spectrophotometrically at 660 nm. The quantity of anionic sulfoxy end-group present in the polymer is obtained by comparing the experimental optical density values with a calibration curve of pure sodium lauryl sulfate obtained by following a similar procedure.

Results obtained by Ghosh and co-workers [42, 63] in end-group analyses of PMMA indicate that all the polymer samples exhibit a positive response to methylene blue reagent in the dye partition test, indicating the presence of at least some sulfate (OSO_3^-) end-groups.

Maiti and Saha [64] have described a dye partition technique [65-67] utilising disulfine blue for the qualitative detection and, in some cases, the determination of amino end-groups in the free radical polymerisation of PMMA. They found only 0.01-0.62 amino end-groups per chain in PMMA made by amino-azo-bisbutyronitrile system, whereas in polymer made by the titanous chloride and acidic hydroxylamine systems they found 1.10-1.90 amino end-groups per chain.

Ghosh and co-workers [42, 68] have also described a dye partition method for the determination of hydroxyl end-groups in PMMA samples prepared in aqueous media with the use of hydrogen peroxide as the photo-initiator. In this method the dried polymers were treated with chlorosulfonic acid under suitable conditions whereby the hydroxyl end-groups present in them were transformed to sulfate end-groups. Spectrophotometric analyses of sulfate end-groups in the treated polymers was carried out by the application of the dye-partition technique, and thus a measure of hydroxyl end-groups in the original polymers was obtained (average 1 hydroxy end-group per polymer chain).

Saha and co-workers [69] and Palit [65, 66] have developed a dye-partition method for the determination of halogen atoms in copolymers of styrene, MMA, methylacrylate, or vinyl acetate with a chlorine-bearing monomer such as allyl chloride and tetrachloroethylene. The quaternised copolymers were quaternised with pyridine, then precipitated with petroleum ether or alcohol and further purified by repeated precipitation from their benzene solutions with a mixture of alcohol and petroleum ether as the non-solvent. The polymers which were finally precipitated were then washed with petroleum ether and dried in air. The test for quaternary halide groups in polymers was carried out with a reagent consisting of disulfine blue dissolved in 0.01 M hydrochloric acid and the colour evaluated spectrophotometrically at 630 nm. Saha and co-workers [69] and Palit [65, 66] found that there may be some uncertainty in the quantitative aspects of this method.

13.7 Terminal Epoxides

Goddu and Delker [70] have reported that terminal epoxides exhibit sharp absorbances relatively free of spectral interferences in the near IR at 4532 and 6060 cm^{-1} (2.2 and 1.65 μm). These absorptions result from overtones and/or combinations of fundamental vibrations found in the mid-infrared. Using a dispersive infrared spectrometer, Dannenburg [71] conducted a study of epoxides in solution. Sensitivity was restricted by the capabilities of instrumentation available at that time. These investigations were limited to epoxide resins with an equivalent weight less than 1000 g resin/g-eq epoxy. Concentration levels for these resins exceeded 1.0 eq/l.

Paputa and co-workers [72] used a near Fourier Transform IR (FTIR) spectrometry to achieve improved sensitivity over previous near IR techniques. A mercury-cadmium-telluride detector has sufficient sensitivity in the 4600-4500 cm^{-1} region to monitor the epoxide response at the 4532 cm^{-1} combination with an adequate S/N ratio. Co-addition of the interferograms can further diminish the inherent detector noise. Data manipulation routines can isolate the epoxide band from neighbouring absorption bands to facilitate direct numeric integration. With these methods they studied

solutions of resins with epoxide equivalent weights greater than 1000 g resin/g-eq epoxy at concentration levels of meq/l.

The 4532 cm^{-1} combination tone is reasonably free of interferences and can be used to measure oxirane ring concentrations for epoxy coating resin systems during synthesis and crosslinking. With the use of low S/N FTIR supported by computer data manipulation, chloroform solutions of five commercially available resins were analysed for epoxide equivalent weight and correlated with results obtained by perchloric acid titrations. The near infrared technique displays linearity for epoxy concentrations of 3.6-20.7 meq/l. Similar results were obtained via a serial concentration study, indicating that the technique is not strongly affected by matrix effects.

A comparison of terminal epoxide determinations by the near IR method and by standard perchloric acid titration showed that the near IR method is much less subject to interference by solvents and reagents than is titration.

13.8 Poly(2,6-dimethyl 1,4 Phenylene Oxide)

^{13}C-NMR has been proven to be very useful in identifying repeat unit 1, end groups 2 and 3, and units 5-9 in this polymer (**Chart 1**). However, due to the insensitivity of the ^{13}C nucleus for NMR studies and the low concentration of most of these units, it is still impractical to use it as a routine and reliable analytical tool to determine the concentration of these units.

Since most of the trace structural units in PPO resin contain labile phenolic hydroxyl groups, it was thought by Chan and co-workers [73] that these functional groups could serve as a handle for attaching a more sensitive NMR nucleus which would give stronger and well-separated signals for the different structural units. The particular nucleus that they have studied was phosphorus, because it is 377 times more sensitive than carbon [74]. Phosphorus has a large range of chemical shift, ~700 ppm, which ensures a good separation of signals of the ^{31}P nuclei in different environments. Furthermore, it is well-known that derivatisation of a phenolic group with phosphorus halides is quantitative and rapid. This is very significant in order to ensure reliable quantitative results. Finally there are no interfering phosphorus atoms within the PPO resin which simplifies the assignment of the spectra. Diphenyl chlorophosphate has been used previously to derivatise PPO hydroxyl groups, with some success in differentiating the various hydroxyls groups using ^{31}P-NMR.

Brevard and Granger [74] carried out a quantitative analysis on three different samples which can be identified as follows: (A) PPO resin, (B) PPO and PS alloy blend (1:1, *w/w*; PPO/PS), (C) PPO and high impact polystyrene (HIPS) alloy blend (1:1, *w/w*; PPO/HIPS). Results are summarised in **Table 13.7**.

Chart 1

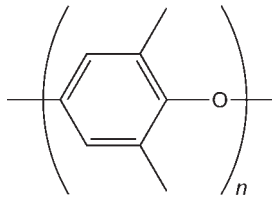

1

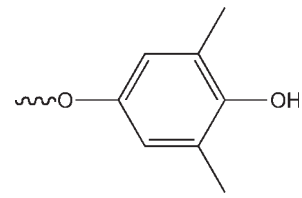

2

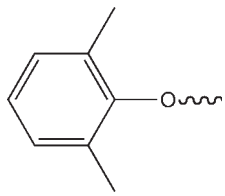

3

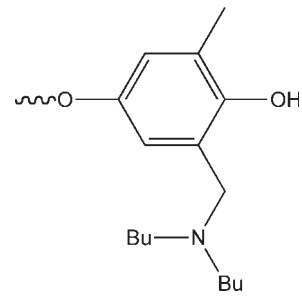

4

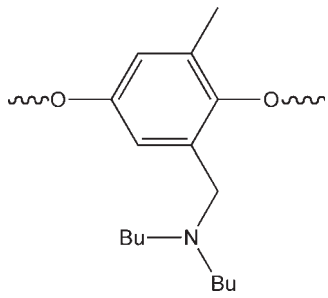

5

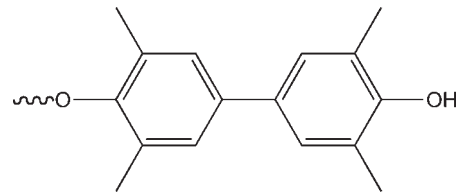

6

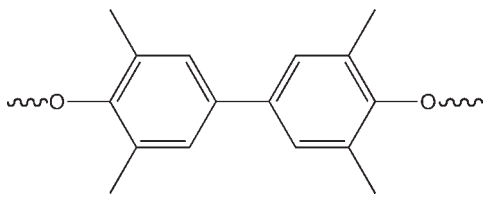

7

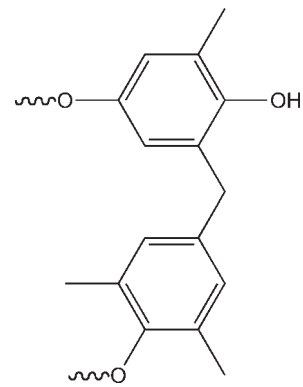

8

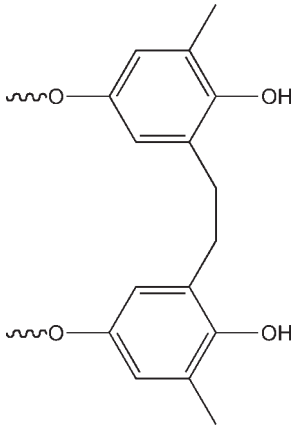

9

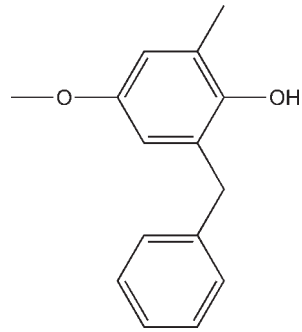

20

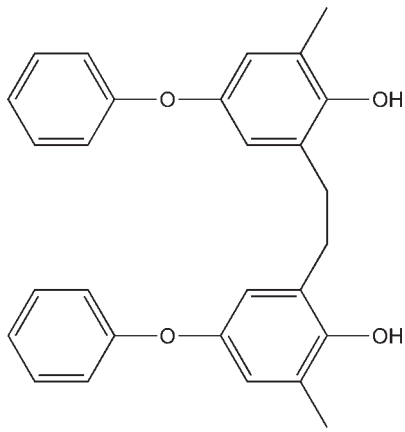

21

On the basis of this technique, they were able to obtain the hydroxyl concentration of normal phenolic ends 2, phenolic ends 4, and phenolic groups on the backbone 8 or 9, as well as the number-average molecular weight of the polymers.

Hydroxy contents obtained by this method agree well with those obtained by IR spectroscopy.

Table 13.7 Results of ^{31}P quantitative analyses obtained for three PPO resins using 1,3,2-dioxaphosphat-amyl chloride 9 as the derivatising reagent

	(A) PPO resin[a]	(B) PPO/PS[a]	(C) PPO/HIPS[a]
(1) % of OH on normal phenolic end	0.087	0.045	0.042
(2) % of OH of phenolic end 4	0.039	Not detected	Not detected
(3) % of OH on backbone phenolic group	Not detected	0.011	0.010
(4) % of total OH groups	0.126	0.056	0.052
(5) % N on phenolic end	0.034	Not detected	Not detected
(6) M_n[b]	13400	18700	20200

[a] Percentage values are expressed as w/w.
[b] M_n of the PPO in the blend is based on the % wt of PPO.
Reprinted from C. Brevard and P. Granger, Handbook of High Resolution Multinuclear NMR, John Wiley & Sons, New York, 1981, NY, USA, p.102. [74]

13.9 Miscellaneous End-groups

Van Rooij and co-workers [25] performed MALDI on an external ion source Fourier transform ion cyclotron resonance mass spectrometer equipped with a 7-T superconducting magnet to analyse end groups of synthetic polymers in the mass range from 500 to 5000 μm. Native, perdeutero methylated, propylated, and acetylated PEG and polyvinyl pyrrolidone with unknown end-group elemental composition were investigated in the mass range up to 5000 μm by using a 2,5-dihydroxybenzoic acid matrix. A small electrospray setup was used for the deposition of the samples. Two methods to process data were evaluated for the determination of end groups from the measured masses of the component molecules in the molecular weight ranges: a regression method and an averaging method. The averaging method is demonstrated to allow end-group mass determinations with an accuracy within 3 μm for the molecular weight range from 500 to 1400 and within 20 μm for the molecular weight range from 3400 to 5000. This is sufficient to identify the elemental composition of end groups in unknown polymer samples.

Mori [75] characterised the end-groups of polyethylene sebacate as a function of molecular size by derivatisation of the hydroxyl and carboxyl groups with 3,5 dinitro

Table 13.8 Miscellaneous methods for determination of end-groups in polymers PMMA (a) $M_n = 2.78 \times 0.03$				
Polymer or Copolymer	**End-Group**	**Method of Analysis**	**Comments**	**Ref.**
Carboxy and hydroxyl terminated polybutadiene	-	IR spectroscopy	Carboxyl/ hydroxyl equivalent weights	[76]
Styrene – acrylonitrile oligomers	Acrylonitrile	IR spectroscopy	Acrylonitrile determined	[77]
Butadiene - isoprene	Terminal hydroxyl	IR spectroscopy	Hydroxy determined	[78]
Miscellaneous	Miscellaneous	Near IR spectroscopy	-	[79]
PVC	Unsaturated end-groups	FT-NMR	End-groups contained allylic groups	[80]
Polyvinylfluoride	CH_2CH_2F	^{19}F-NMR	-	[81]
Polyphenylene-glycidyl ether	End-groups	^{13}C-NMR	-	[77, 82]
Natural rubber	Vinyl	^{13}C-NMR	-	[83]
Poly 2,6-dimethyl 1,4-phenylene ether	End groups	^{13}C-NMR	-	[84]
Polyacrylamide	End groups	MALDI-ToF-MS	-	[85]
Polyaninline	End groups	MS	-	[86]
Polystyrene sulfonic acid	End groups	MALDI-ToF-MS	-	[87]
Polycarbonates	Terminal hydroxy	Spectro-photometry of ceric ammonium nitrate comple	-	[88]
Polycarbonates	Terminal end-groups	Reactive pyrolysis - GC	-	[89, 90]
Hydroxy terminated polybutadiene	Hydroxy end-groups	Ozonisation - SEC	-	[91]

Table 13.8 *Continued*				
Polymer or Copolymer	**End-Group**	**Method of Analysis**	**Comments**	**Ref.**
Oligooxyethylene	End-groups	SEC	Effect of end-group and solvent in SEC	[92]
Poly-*m*-phenylene isophthalate	Carboxy	Potentiometric titration using alcoholic potassium hydroxide	-	[93]
Review of methods of end-group analysis	-	-	-	[94]
Polyfluroinated polyethers	End-groups	Laser desorption/ ionisation MS with multiphoton ionisation (MALDI)	End-group sequence distribution	[95]
Polyvinylpyrrolidone	End-groups	MALDI-FT-MS	-	[25]
Source: Author's own files				

benzoyl chloride and *o*-(*p*-nitrobenzyl)*N*,*N*′-diidopropyliso urea, respectively, and analyses of the derivatised polymers by SEC with IR detection. Methods for the determination of end-groups in other polymers are reviewed in **Table 13.8**.

References

1. J.C. Bevington, J.R. Ebdon, T.N. Huckerby and N.W.E. Hutton, *Polymer*, 1982, **23**, 2, 163.

2. J.C. Bevington, T.N. Huckerby and N.W.E. Hutton, *European Polymer Journal*, 1982, **18**, 11, 963.

3. B.K. Hunter, E. Redler, K.E. Russell, W.G. Schnarr and S.L. Thompson, *Journal of Polymer Science: Polymer Chemistry Edition*, 1983, **21**, 2, 435.

4. J.C. Bevington, J.R. Ebdon and T.N. Huckerby, *European Polymer Journal*, 1985, **21**, 8, 685.

5. P. Locatelli, M.C. Sacchi, I. Tritto and F. Forlini, *Macromolecules*, 1990, **23**, 8, 2406.

6. K. Hatada, K. Ute and M. Kashiyama, *Polymer Journal*, 1990, **22**, 10, 853.

7. J. Bevington, J.R. Ebdon and T.N. Huckerby in *NMR Spectroscopy of Polymers*, Ed., R.N. Ibblet, Blackie Academic and Professional, Glasgow, UK, 1993, p.80-121.

8. C.A. Barson, J.C. Bevington and S.W. Breuer, *European Polymer Journal*, 1989, **25**, 3, 259.

9. D.E. Axelson and K.E. Russell, *Progress in Polymer Science*, 1985, **11**, 3, 221.

10. T. Kashiwagi, A. Inaba, J.E. Brown, K. Hatada, T. Kitayama and E. Masuda, *Macromolecules*, 1986, **19**, 8, 2160.

11. G. Moad, E. Rizzardo, D.H. Solomon, S.R. Johns and R.I. Willing, *Die Makromolekulare Chemie, Rapid Communications*, 1984, **5**, 12, 793.

12. J. Devaux, D. Daoust, R. Legras, J.M. Dereppe and E. Nield, *Polymer*, 1989, **30**, 1, 161.

13. K. Hatada, T. Kitayama, K. Fujikawa, K. Ohta and H. Yuki, *Polymer Bulletin*, 1978, **1**, 2, 103.

14. K. Hatada, T. Kitayama and H. Yuki, *Die Makromolekulare Chemie, Rapid Communications*, 1980, **1**, 1, 51.

15. K. Ute, T. Kitayama and H. Koichi, *Polymer Journal*, 1986, **18**, 3, 249.

16. K. Hatada, T. Kitayama and E. Masuda, *Polymer Journal*, 1986, **18**, 5, 395.

17. F. Heatley, J-F. Ding, G. Yu, C. Booth and T.G. Blease, *Die Makromolekulare Chemie, Rapid Communications*, 1993, **14**, 12, 819.

18. J. Plucinski, R. Janik and H. Malyschok, *Przemysel Chemiczny*, 1981, **60**, 210.

19. F. Heatley, G. Yu, W-B. Sun, E.J. Pywell, R.H. Mobbs and C. Booth, *European Polymer Journal*, 1990, **26**, 5, 583.

20. F. Heatley, G. Yu, M.D. Draper and C. Booth, *European Polymer Journal*, 1991, **27**, 6, 471.

21. F. Heatley, G. Yu, C. Booth and T.G. Blease, *European Polymer Journal*, 1991, **27**, 7, 573.

22. S. Dickson, G. Yu, F. Heatley and C. Booth, *European Polymer Journal*, 1993, **29**, 2-3, 281.

23. E. Breitmeier and W. Voelter, *Carbon-13 NMR Spectroscopy*, 3rd Edition, VCH Verlagsgesellschaft, Weinheim, Germany, 1987, p.192-194.

24. R.K. Harris, *Nuclear Magnetic Resonance Spectroscopy: A Physicochemical View*, Pitman, London, UK, 1983, p.221.

25. G.J. van Rooij, M.C. Duursma, R.M.A. Heeren, J.J. Boon and C.G. de Koster, *Journal of the American Society for Mass Spectrometry*, 1996, **7**, 5, 449.

26. A.T. Jackson, H.T. Yates, J.H. Scrivens, G. Critchley, J. Brown, M.R. Green and R.H. Bateman, *Rapid Communications Mass Spectrometry*, 1996, **10**, 13, 1668.

27. K. Hatada, T. Kitayama and H. Yuki, *Polymer Bulletin*, 1980, **2**, 1, 15.

28. F.C. Schilling and A.E. Tonelli, *Macromolecules*, 1986, **19**, 5, 1337.

29. F. Heatley, Y. Luo, J. Ding, R.H. Mobbs and C. Booth, *Macromolecules*, 1988, **21**, 9, 2713.

30. S.D. Gagnon in *Encyclopedia of Polymer Science and Engineering*, 2nd Edition, Volume 6, Eds., H.F. Mark, N. Bikales, C.G. Overberger, G. Menges and J.I. Kroschwitz Wiley Interscience, New York, NY, USA, 1987, p.273.

31. K. Hatada, T. Kitayama and F. Masuda, *Polymer Journal*, 1985, **17**, 8, 985.

32. B.K. Hunter, E. Redler, K.E. Russell, W.G. Schnarr and S.L. Thompson, *Journal of Polymer Science Part A: Polymer Chemistry*, 1989, **27**, 12, 3915.

33. G. Moad, D.H. Solomon, S.R. Johns and R.I. Willing, *Macromolecules*, 1982, **15**, 4, 1188.

34. G. Moad, D.H. Solomon, S.R. Johns and R.I. Willing, *Macromolecules*, 1984, **17**, 5, 1094.

35. A. Zambelli, P. Longo, C. Pellecchia and A. Grassi, *Macromolecules*, 1987, **20**, 8, 2035.

36. G. Moad, D.H. Solomon and R.I. Willing, *Macromolecules*, 1988, **21**, 3, 855.

37. J. Krstina, G. Moad and D.H. Solomon, *European Polymer Journal*, 1989, **25**, 7-8, 767.

38. H. Ohtani, S. Ueda, Y. Tsukahara, C. Watanabe and S. Tsuge, *Journal of Analytical Applied Pyrolysis*, 1993, **25**, 1.

39. Y. Ito, H. Ohtani, S. Ueda, Y. Nakashima and S. Tsuge, *Journal of Polymer Science Part A: Polymer Chemistry*, 1994, **32**, 2, 383.

40. G. Montaudo, *Trends in Polymer Science*, 1996, 481.

41. L. Li and P.L. Rinaldi, *Macromolecules*, 1997, **30**, 3, 520.

42. P.Ghosh, S.C. Chradha, A.R. Mukherjee and S.R. Palit, *Journal of Polymer Science: Part A General Papers*, A2, 1964, **2**, 10, 4433.

43. A.K. Banthia, B.M. Mandal and S.R. Palit, *Journal of Polymer Science: Polymer Chemistry Edition*, 1977, **15**, 4, 945.

44. C. Kanjial, B.C. Mitra and S.R. Palit, *Die Makromolekulare Chemie*, 1977, **178**, 6, 1707.

45. E. Pérez and D.L. Vanderhart, *Journal of Polymer Science Part B: Polymer Physics*, 1987, **25**, 8, 1637.

46. C.L. Hammond, P.J. Hendra, B.G. Lator, W.F. Maddams and H.A. Willis, *Polymer*, 1988, **29**, 1, 49.

47. G. D. B. van Houwelingen, *Analyst*, 1981, **106**, 1267, 1057.

48. D. Nissen, V. Rossbach and H. Zahn, *Journal of Applied Polymer Science*, 1974, **18**, 7, 1953.

49. D. Tillier, H. Lefebvre, M. Tessier, J-C. Blais and A. Fradet, *Macromolecular Chemistry and Physics*, 2004, **205**, 5, 581.

50. J. Si and J.P. Kennedy, *Journal of Polymer Science Part A: Polymer Chemistry*, 1994, **32**, 11, 2011.

51. T.I. Atta-ur-Rahman, *Nuclear Magnetic Resonance*, Springer Verlag, 1986, p.18-86.

52. D.E. Leyden and R.H. Cox, *Analytical Applications of NMR*, John Wiley & Sons, New York, NY, USA, 1977, p.115-185.

53. S.L. Manaft, J.D. Ingham and J.A. Miller, Jr., *Organic Magnetic Resonance*, 1977, **10**, 1, 198.

54. H. Ohtani, S. Ishiguro, M. Tanaka and S. Tsuge, *Polymer Journal*, 1989, **21**, 1, 41.

55. H. Ohtani, M. Tanaka and S. Tsuge, *Journal of Analytical Applied Pyrolysis*, 1989, **15**, 167.

56. H. Ohtani, M. Tanaka and S. Tsuge, *Bulletin of the Chemical Society of Japan*, 1990, **63**, 4, 1196.

57. Y. Tsukahara, Y. Nakanishi, Y. Yamashita, H. Ohtani, Y. Nakashima, Y.F. Luo, T. Ando and S. Tsuge, *Macromolecules*, 1991, **24**, 9, 2493.

58. H. Ohtani, Y.F. Luo, Y. Nakashima, Y. Tsukahara and S. Tsuge, *Analytical Chemistry*, 1994, **66**, 13, 1438.

59. H. Ohtani, Y. Ito, S. Tsuge, S. Wakabayashi, J-I. Atarashi and T. Kawamura, *Macromolecules*, 1996, **29**, 13, 4516.

60. H. Ohtani, Y. Takehara and S. Tsuge, *Macromolecules*, 1997, **30**, 9, 2542.

61. A.T. Jackson, H.T. Yates, J.H. Scrivens, M.R. Green and R.H. Bateman, *Journal of the American Society for Mass Spectrometry*, 1997, **8**, 12, 1206.

62. S.R. Palit and P. Ghosh, *Microchemical Journal, Symposium Series*, 1961, **2**, 663.

63. P. Ghosh, A.R. Mukherjee and S.R. Palit, *Journal of Polymer Science Part A: General Papers*, 1964, **2**, 6, 2807.

64. S. Maiti and M.K. Saha, *Journal of Polymer Science Part A-1: Polymer Chemistry Edition*, 1967, **5**, 2, 151.

65. S.R. Palit, *Die Makromolekulare Chemie*, 1960, **36**, 1, 89.

66. S.R. Palit, *Die Makromolekulare Chemie*, 1960, **38**, 1, 96.

67. S. Maiti, A. Ghosh and M.K. Saha, *Nature*, 1966, **210**, 5035, 513.

68. P. Ghosh, P.K. Sengupta and A. Pramanik, *Journal of Polymer Science Part A: General Papers*, 1965, **3**, 5, 1725.

69. M.K. Saha, P. Ghosh and S.R. Palit, *Journal of Polymer Science Part A: General Papers*, 1964, **2**, 3, 1365.

70. R.F. Goddu and D.A. Delker, *Analytical Chemistry*, 1958, **30**, 12, 2013.

71. H. Dannenburg, *SPE Transactions*, 1963, **3**, 78.

72. M.C. Paputa Peck, R.O. Carter III, and S.B.A. Qaderi, *Journal of Applied Polymer Science*, 1987, **33**, 1, 77.

73. K.P. Chan, D.S. Argyropoulos, D.M. White, G.W. Yeager and A.S. Hay, *Macromolecules*, 1994, **27**, 22, 6371.

74. C. Brevard and P. Granger, *Handbook of High Resolution Multinuclear NMR*, John Wiley and Sons, New York, NY, USA, 1981, p.102.

75. S. Mori, *Analytical Chemistry*, 1986, **189**, 17.

76. J. Law, *Journal of Polymer Science Part A: General Papers*, 1971, **9**, 589.

77. C. Tsvetanov, I. Panayotov and B. Erussalimsky, *European Polymer Journal*, 1974, **10**, 7, 557.

78. V.I. Valnev, R.A. Shiykher, T.S. Dmitrieva and I.B. Tsvetovskii, *Zhurnal Analiticheskoi Khimii*, 1975, **30**, 1235. [*Chemical Abstracts*, 1975, **83**, 131156d]

79. R.B. Roy and C.J. Kradjel, *Journal of Polymer Science Part A: Polymer Chemistry Edition*, 1988, **26**, 1733.

80. A. Garaculacu and E.C. Bezdadea, *Journal of Polymer Science: Polymer Chemistry Edition*, 1977, **15**, 3, 611.

81. D.W. Ovenall and R.E. Uschold, *Macromolecules*, 1991, **24**, 11, 3235.

82. J.C. Ronda, A. Serra, A. Mantecón and V. Cádiz, *Macromolecular Chemistry and Physics*, 1994, **195**, 10, 3445.

83. D.W. Patterson and J.L. Koenig, *Applied Spectroscopy*, 1987, **41**, 3, 441.

84. T. Usami, F. Keitoku, H. Ohtani and S. Tsuge, *Polymer*, 1992, **33**, 14, 3024.

85. A. Favier, C. Ladavière, M-T. Charreyre and C. Pichot, *Macromolecules*, 2004, **37**, 6, 2026.

86. A.R. Dolan and T.D. Wood, *Synthetic Metals*, 2004, **143**, 2, 243.

87. P.O. Danis, D.E. Karr, F. Mayer, A. Holle and C.H. Watson, *Organic Mass Spectrometry*, 1992, **27**, 7, 843.

88. M.A. Motorina, L.S. Kalinina and E.I. Metelkina, *Plasticheskie Massy*, 1973, **6**, 74.

89. Y. Ishida, S. Kawaguchi, Y. Ito, S. Tsuge and H. Ohtani, *Journal of Analytical Applied Pyrolysis*, 1997, **40-41**, 321.

90. H. Ohtani, Y. Ito, H. Ogasawara, C. Kawaguchi and S. Sage in *Proceedings of the International Symposium of Chromatography*, 35th Annual Research Group, Liquid Chromatography, Japan, World Scientific, Singapore, 1985, p.813-820.

91. M. Ramarao, K.J. Scariah, P.V. Ravindran, G. Chandrasekharan, S. Alwan and K.S. Sastri, *Journal of Applied Polymer Science*, 1993, **49**, 3, 435.

92. J.R. Craven, H. Tyrer, S.P.L. Li, C. Booth and D. Jackson, *Journal of Chromatography*, 1987, **387**, 233.

93. L.N. Kreshboo, L.N. Shvelsovr and E.A. Emelin, *Soviet Plastics*, 1968, **10**, 53. [*Chemical Abstracts*, 1969, **70**, 21345q]

94. G. Montaudo, *Trends in Polymer Science*, 1996, 481.

95. M.S. de Vries and H.E. Hunziker, *Applied Surface Science*, 1996, **106**, 466.

Abbreviations

^{13}C-NMR	Carbon-13 nuclear magnetic resonance
1D	One-dimensional
^{1}H-NMR	Hydrogen-1 nuclear magnetic resonance
2D	Two-dimensional
2M	2-Methyldecane
3D	Three-dimensional
3E	3-Ethylnonane
4E	4-Ethylnonane
5M	5-Methyldecane
A/B	Acrylonitrile-butyl acrylate
A/E	Acrylonitrile-ethyl methacrylate
A/M	Acrylonitrile-methyl acrylate
AA	Adipic acid
ABTMP	2,2′-Azobis(2,4,4-trimethylpentane)
AIBN	Azobis(isobutyronitrile)
amu	Atomic mass unit
AN	Acrylonitrile
aPP	Atactic polypropylene
aPS	Atactic polystyrene
BD	Butadiene
BDO	1,4-Butanediol
BPO	Benzoyl peroxide
$CDCl_3$	Deuterochloroform
CDS	Chemical Data Systems Instruments
CI	Chemical ionisation
CID	Collision induced dissociation
CMA	Acryloyloxyethyltrimethyl ammonium chloride

CMM	Oyloxyethyltrimethylammonium chloride
COSY	**Co**rrelation **s**pectroscop**y**
CPE	Chlorinated polyethylene(s)
CP-MAS	Cross-polarisation magic angle spinning
cPy-GC	Capillary column pyrolysis – gas chromatography
CV	Coefficient of variance
CVA	Cyano-vinyl-acetate
DEPT	Distortionless enhancement by polarisation transfer spectroscopy
DMSO	Dimethylsulfoxide
DMSO-D_6	Duterated dimethylsulfoxide
DMSO-D_6-$CDCl_3$	Duterated dimethylsulfoxide-duterated chloroform
DN	Dinitriles
DO	1,3-Dioxolane
DSC	Differential scanning calorimetry
DTG	Diphthalic dianhydride
DVB	Divinylbenzene
E	Ethylene
ECH	Epichlorohydrin
ECN	Effective carbon number
EGA	Evolved gas analysis
EI	Electroionisation
EMA	Ethylmethacrylate
EMA-CO	Ethylene-methylacrylate copolymer
EO	Ethylene oxide
E-P	Ethylene-propylene
EPDM	Ethylene-propylene-diene terpolymers
ESR	Electron spin resonance
EST	Ethylstyrene
E-V	Ethylene-vinyl chloride
EVE	The triad of two ethylene and one vinyl chloride
EVM	Errors in variables model
EVV	The triad of one ethylene and two vinyl chloride
FFAP	Type of column for chromatography
FID	Flame ionisation detector/detection

FPD	Flame photometric detector/detection
FT	Fourier transform
FTICR-MS	Fourier transform ion cyclotron resonance mass spectrometry
FT-IR	Fourier-Transform infrared spectroscopy
FT-NMR	Fourier transform – nuclear magnetic resonance
GC	Gas chromatography
GC-FID	Gas chromatography with flame ionisation detection
GC-IR	Gas chromatography – infrared spectroscopy
GC-MS	Gas chromatography – mass spectroscopy
GC-TC	Gas chromatography with thermal conductivity detection
GLC	Gas-liquid chromatography
GPC	Gel permeation chromatography
HDO	1,6-Hexanediol
HDPE	High-density polyethylene
HIPS	High-impact polystyrene
HPLC	High-performance liquid chromatography
id	Internal diameter
iPP	Isotactic polypropylene
iPS	Isotactic polystyrene
IR	Infrared
KOH	Potassium hydroxide
LALLS	Low angle laser light scattering
LC	Liquid chromatography
LDPE	Low-density polyethylene(s)
$LiAlH_4$	Lithium aluminium hydride
MA	Methylacrylate
MAA	Methacrylonitrile
MA-co-NVC	Methyl acrylate-*co*-*N*-vinyl carbazole
MALDI	Matrix assisted laser desorption/ionisation
MALDI-ToF	Matrix assisted laser desorption/ionisation – time-of-flight
MALLS	Multiangle laser light scattering
MAN	Methacrylonitrile(s)
MCAA	Mercaptoacetic acid
MDI	4,4′-Methylene-bis(phenyl isocyanate)

Me_2SO-d_6	Dimethyl-d_6-sulfoxide
MMA	Methylmethacrylate
MMA-S	Methyl methacrylate-styrene
MMA-α-MS	Methyl methacrylate-α-methylstyrene
M_n	Number average molecular weight
MPA	Mercaptopropionic acid
MS	Mass spectroscopy
MSM	Methacrylate-styrene-methacrylate
MSt-DVB	Chloromethylstyrene - divinylbenzene
M_w	Molecular weight
MW	Molecular weight
MWD	Molecular weight distribution
NASL	Number-average sequence length
n-BA	*N*-Butyl acrylate
NBR	Acrylonitrile-butadiene rubber
NMR	Nuclear magnetic resonance
NOE	Nuclear Overhauser effects
NPD	Nitrogen-phosphorus detector/detection
NVC	*N*-vinyl carbazole
P(4-MS)	Poly(4-methyl-styrene)
P(α-MS)	Poly(α-methylstyrene)
PA	Polyamide(s)
PAANA	Sodium polyacrylate copolymer
PAI	Poly(amide-imides)
PAM	Polyacrylamide
PAN	Polyacrylonitrile
PBA	Polybutylacrylate
PBD	Polybutadiene
PBMA	Poly(*n*-butyl methacrylate)
PCFE	Poly(1-chloro-1-fluoroethylene)
pCVA	Polycyano-vinyl acetate
PDMSO	Polydimethylsiloxane
PE	Polyethylene
PECH	Polyepichlorohydrin

PEG	Polyethylene glycol
PET	Polyethylene terephthalate
PHGC	Pyrolysis hydrogenation - gas chromatographic
PI	Polyimide(s)
PIB	Polyisobutylene(s)
PIF_1	4,4′-Diamino diphenyl methane
PIF_2	Fluorinated polyimide
pMA	Polymethacrylate
PMAN	Polymethacrylonitrile
PMMA	Polymethylmethacrylate
PMR	Proton magnetic resonance
PO	Propylene oxide
POM	Polyoxymethylene
PP	Polypropylene(s)
PPG	Polypropylene glycol(s)
ppm	Parts per million
PPO	Polypropylene oxide
PS	Polystyrene(s)
PU	Polyurethane(s)
PVC	Polyvinyl chloride
PVDC	Polyvinylidene chloride
PVF	Polyvinyl fluoride
Py	Pyrolysis
Py-EGA-IR	Pyrolysis – evolved gas analysis – infrared spectroscopy
Py-GC	Pyrolysis – gas chromatography
Py-GC-MS	Pyrolysis – gas chromatography – mass spectroscopy
Py-GC-NMR	Pyrolysis – gas chromatography – nuclear magnetic resonance
Py-MS	Pyrolysis – mass spectroscopy
RGC	Reaction gas chromatography
RIS	Rotational isomeric state model
RSD	Relative standard deviation
S/N	Signal to noise ratio
S-AA	Styrene-adipic acid
SEC	Size exclusion chromatography

S-EMA	Styrene-ethylmethacrylate
SIMS	Time-of-flight secondary ion mass spectrometry
SMAN	Styrene-methacrylonitrile
S-MMA	Styrene-methylmethacrylate
SMS	Styrene-methacrylate-styrene
sPP	Syndiotactic polypropylene
sPS	Syndiotactic polystyrene
ST-Cl-MSt-DVB	Styrene - chloromethylstyrene - divinylbenzene
ST-DVB	Styrene-divinylbenzene
STY	Styrene
TFAA	Trifluoroacetic anhydride
TFMA	Trifluoromethacrylic acid
TGA	Thermogravimetric analysis
THCSCH	Two-dimensional heteronuclear chemical shift correlation
TIC	Total ion chromatograms
TMP	2,2,6,6-Tetramethylpiperidine
TMS	Tetramethylsilane
TOC	1,3,6-Trioxocane
ToF	Time-of-flight
ToF-MS	Time-of-flight mass spectroscopy
ToF-SIMS	Secondary ion mass spectrometry
ToF-SIMS	Time-of-flight secondary ion mass spectrometry
TPI	*Trans*-1,4-polyisoprene
TRIM	Trimethylolpropane tri-methacrylate
TVA	Thermal volatilisation analysis
UV	Ultraviolet
V	Vinyl chloride
VCN	Vinylidene cyanide
VVV	The triad of three vinyl chlorides

Subject Index

A

Acrylate and methacrylate copolymers, 252
  Ethylmethacrylate - methyl methacrylate, 255
  Methyl acrylate-*N*-vinyl carbazole, 252
Acrylonitrile and methacrylonitrile containing copolymers, 234
  Acrylonitrile-butyl acrylate, 242
  Acrylonitrile-ethylmethacrylate, 234
  Acrylonitrile methyl acrylate, 238
  Acrylonitrile-methyl methacrylate, 245
  Methacrylonitrile - vinylidene cyanide and cyano-vinyl acetate - vinylidene cyanide, 250
  Methacrylonitrile-methyl methacrylate, 234
Acrylonitrile-butadiene rubbers, 46
Alkali fusion, 128
Anisotropic effect, 484
Atomic emission spectrometry, 74

B

Bernoulli model, 256
Bernoullian propagation statistics, 329 330 434
Block copolymers, 425
Branching, 381 382 383
Butadiene-methylmethacrylate, 229
Butadiene-propylene, 203
Butene-propylene, 194
Butadiene-propylene microzonolysis copolymers, 204

C

Calibration, 382
Calibration principle, 395
Calorimetry, 425
Chemical data systems instruments, 3
Chemical ionisation mass spectrum, 78

Chlorinated polyethylene, 104
Chlorinated polyethylene pyrolysis, 107
Chloromethylated styrene - divinylbenzene copolymers pyrogram, 40 41
Chromatography, 376
Chemical ionisation - mass spectroscopy survey scan, 78 79 80
^{13}C-NMR polypropylene spectroscopy, 311
^{13}C-NMR polystyrene spectrum, 475
^{13}C-NMR spectra, 198 207-210 226 227 232 245 252 258 274 311 312 333 346-350 353 379 396 437 438 450 451 475
^{13}C-NMR spectrometers, 144
^{13}C-NMR spectroscopy, 142 145 150 155 157 158 190-198 205 206 212 216 234 249 256 257 259 276 277 281 309 310 315 328 331 332 351 352 365 379 381 383-385 390 394 395 397-401 403 404 411 427 434-436 443 450 472 474 480 501
Combustion furnace pyrolyser, 4
Copolymer applications, 30
Copolymerisation, 41 179 237 241 242 265 449 480
Copolymers, 116 117 453
  Ethylene - carbon monoxide, 116
  Ethylene-vinyl cyclohexane, 116
  Sequencing, 179
  Styrene maleic anhydride,
Copolymers, unsaturation, 453 449
  Polytrimethylolpropane tri-methacrylate, 452
  Styrene-divinyl benzene, 449
Curie point filament pyrolyser technique, 7 8
Curie point pyrolyser, 5
Cyano-vinyl acetate - vinylidene cyanide, 250

D

Depolymerisation, 14 28 139 141
DEPT spectroscopy, 201
Differential thermal analysis, 382
Dye partition method, 499 500
Dimethyl butadiene, 371

E

End-groups, determination of, 471
Electron spin resonance spectra, 449
Ethylene branching, 398
Ethylene-1-butene, 190
Ethylene-1-hexene, 191
Ethylene-methyl acrylate, 199

Ethylene oxide containing copolymers, 266
  Ethylene oxide - *p*-phenylene vinylene, 276
  Ethylene oxide - propylene oxide, 269
  Polyacetal - ethylene oxide, 266
Ethylene-propylene copolymer, 180 395
Ethylene-propylene copolymer gas chromatograms, 13
Ethylene-propylene diene terpolymers branching, 410
Ethylene-vinyl acetate, 230
Ethylene-vinyl chloride, 201
Ethylmethacrylate - methyl methacrylate, 255

F

Filament pyrolyser, 5
Filament pyrolysis - gas chromatogram of polyvinyl chloride, 6
Fingerprinting, 1 3
Flame ionisation detector, 217 488 489
Flame photometric detector, 486
^{19}F-NMR, 379
Fourier-Transform infrared spectroscopy, 63 64 74 84 109 110 394 500
Fourier-Transform - mass spectrometer, 3 77 474
Fourier-Transform infrared spectra, 229
  Polymethylmethacrylate, 66

G

Gas chromatograms, 1 4 11 77 126 133 140 170 216
Gas chromatography, 1 99 125 160 376 382 454 472
Gas-liquid chromatography, 172 181
Gas chromatography - infrared spectroscopy, 64
Gas chromatography - mass spectroscopy, 46 64 133 472 488 497
Gel permeation chromatography, 150 153 155 156 184 205 400
  Chromatogram, 158
  Curve, 157 159

H

High-performance liquid chromatography, 205
^{1}H-NMR spectroscopy, 205 206 211 222 267 379 427 436 451 472 474 482 486 497
^{1}H-NMR polystyrene spectrum, 477
^{1}H-NMR spectra, 207 212 223-225 236 332 334 335 476 483-485 498
Homopolymers, 99 116 139 179 243 244 252 267 272 318
  Pyrolysis - gas chromatography, 31
  Sequencing, 139 172 173

Homopolymers, unsaturated, 431
  Polybutadiene, 431
  Polyethylene, 443
  Polyisoprene, 439
  Polypropylene, 446
Hydrogenated nitrile-butadiene rubber, 51 52 53 55
Hydrogenation, 47 48 49 50 53 56
Hydrolysis gas chromatography, 126
  Saponification methods, 126
  Zeisel procedures, 126

I

Infrared spectroscopy, 40 47 63 64 184 286 315 316 370 383 410 425 431 433 435 439 443 446 452 503
Infrared spectroscopy interface, 64
Infrared spectra, 163 186-188 202 321 323 353 367 371 435 442 444 447
Infrared techniques, 500 501

L

Laser mass spectrometry, 94
Laser pyrolysis, 9
Lewis-Mayo copolymerisation model, 251
Liquid chromatography, 425

M

Mass spectrometer, 77
Mass spectroscopy, 63 99 125 153
Matrix-assisted laser desorption/ionisation mass spectrometry, 425
Matrix-assisted laser desorption/ionisation technique, 474
Matrix-assisted laser desorption - time-of-flight mass spectroscopy, 426 499 504
Methacrylonitrile - methyl methacrylate, 234
Methacrylonitrile - vinylidene cyanide, 250
Methyl acrylate - *N*-vinyl carbazole, 252
Methyl branching in polyethylene, 382
Methylmethacrylate-α-trifluoro-methacrylic acid, 222
Microozonolysis, 460
  of polybutadiene, 161 456

N

Natural rubber, 56 148 365 370
Nitrile-butadiene rubber, 49 50
Nitrogen-phosphorus detector, 486

NMR spectroscopy, 40 49 77 125 153 160 163 181 189 192 209 211 221 226 255 265 267 276 283 318 339 346 378 381 382 398 425 427 436 439 443 452 453 457 459 471 499
NMR spectra, 201 206 213-215 243 314 328 329 332 336 376 377 450 498
NMR spectrometers, 3 384
NMR tacticity, 318
Nuclear overhauser effect, 310 395
Pyrolysis FT-IR spectra, of Nylons 65

O

Olefin branching copolymers, 395
  Branching in ethylene - higher olefin copolymers, 398
  Ethylene-branching in propylene diene teropolymers, 410
  Ethylene-propylene copolymer, 395
Olefinic copolymers, 180 205
  Butadiene-propylene, 203
  Butene-propylene, 194
  Ethylene-1-butene, 190
  Ethylene-1-hexene, 191
  Ethylene-methyl acrylate, 199
  Ethylene propylene, 180
  Ethylene-vinyl chloride, 121
  Tacticity, 353
Ozonolysis, 155 156-158 160 162 163 203 205 454 457 458 459
Ozonolysis - gel permeation chromatography technique, 155 159 205

P

Poly(1-chloro-1-fluoroethylene) tacticity, 336
Polyacetal - ethylene oxide, 266
Polyacrylamide, 81 255
Polyacrylates, 99 100
Polybutadiene, 276 372
Polybutadiene-1-ethylene copolymer, 371
Polybutene branching, 410
Polybutadiene microozonolysis, 161
Polybutadiene sequencing, 154
Polybutadiene unsaturation, 431
Polybutylacrylates, 99 100 101 102
Polydimethylsiloxane sequences, 167 170
Polyepichlorohydrin, 376
Polyethylene branching, 381
  Ethyl and higher alkyl groups branching in polyethylene, 383
  Methyl branching in polyethylene, 382

Polyethylene sequencing, 139
Polyethylene unsaturation, 443
Polyisoprene, 372
  Branching, 411
  Sequences, 148
  Unsaturation, 439
Polymers, 7
  branching, 418
Polymerisation, 154 234 265 278 286 305 329 376 377 378 382 395 407 471 472 491 499
Polymethylacrylonitrile tacticity, 352
Polymethylmethacrylate copolymers 68 71 72
  FT-IR spectra of, 66
  Stereoregularity, 340
Poly(*n*-butyl methacrylate) tacticity, 332
Polyolefin pyrolysis, 183
Polypropylacrylate, 99 100 101
Polypropylene-1-ethylene copolymer, 369
Polypropylene gas chromatograms
Polypropylene glycol, 374
Polypropylene glycol sequences, 170
Polypropylene homopolymer, 365
Polypropylene oxide tacticity, 346
Polypropylene sequences, 141
Polypropylene tacticity, 306
Polypropylene unsaturation, 446
Polypyrrol, 112
Polysaccharide biopolymers branching, 417
Polystyrene branching, 411
Polystyrene sequences, 151
Polysulfide polymers pyrograms, 27
Polytrimethylolpropane tri-methacrylate, 452
Polyurethane, 78
Polyurethane sequences, 163
Polyvinylchloride branching, 411
Polyvinylchloride pyrolysis, 17
Polyvinylchloride sequences, 172
Polyvinylchloride tacticity, 328
Polyvinyl fluoride branching, 414
Postpyrolysis derivatisation, 125 133
Prepyrolysis derivatisation, 125 133 134
Propylene butadiene-microzonolysis copolymers, 204
Proton magnetic resonance spectra, 312-314
Proton magnetic resonance spectroscopy, 46 181 231 315
Pulse pyrolysis, 3

Pyrogram of chlorinated polyethylene polymers, 106
Pyrograms, 3
Pyrolysis, 1 7 8 11 17 20 28 32 36 38 63 68 69 94 105 109 110 116 134 135 140 141 181 184 216 262 263 267 268 281 413 434
Pyrolysis applications, 1 17
  Determination of degree of cure of rubber, 17 18 19
  Polyacrylates, 19
  Polybutadiene, 19
  Polyethelene oxide, 21
  Polymethacrylates, 19
  Polypropylene, 17
  Polysulfides, 21
  Silicon containing polymers, 30
Pyrolysis hydrogenation-gas chromatography technique, 386 390
Pyrolysis-derivatisation, 125 133
Pyrolysis equipment, 1
Pyrolysis-evolved gas analysis - infrared, 68 74
Pyrolysis FT-IR, 64 67
  Applications, 67
  Instrumentation, 67
  Of polystyrene, 64 65
  Spectra, 64
Pyrolysis - gas chromatography, 1 3 17 30 33 38 40 45 47 50 55 56 63 64 77 116 133 134 148 182 218 221 264 265 267 268 276 283 386 389 410 411 453 472 486 489 491 494 497
Pyrolysis - gas chromatography - FT-IR, 63
Pyrolysis - gas chromatography - infrared spectroscopy, 74
Pyrolysis - gas chromatography - mass spectrometry, 99 101 105 108 109 115 117 216 220 222 327 340 492
Pyrolysis - gas chromatography of polymethylmethacrylate, 19
Pyrolysis - gas chromatography - NMR spectroscopy, 74
Pyrolysis - gas chromatography of Nylon 6, 2
Pyrolysis - gas chromatography of Nylon 6/12, 2
Pyrolysis - gas chromatography of Nylon 6/T, 2
Pyrolysis - gas chromatography of Nylon 12, 2
Pyrolysis - hydrogenation gas chromatography, 404
Pyrolysis instrument, 3
Pyrolysis - liquid trapping system, 33
Pyrolysis - mass spectrometry, 40 77 91 92 94
Pyrolysis of polyethylene, 4
Pyrolysis product identity, 3
Pyrolysis of polyvinylchloride, 66
Pyrolysis, 1 99
Pyrolysis, types of
  Combustion furnace pyrolyser, 4

Curie point pyrolyser, 5
Filament pyrolyser, 5
Laser pyrolyser, 9
Pyroprobe 120, 4
Pyroprobe 1000, 3
Pyroprobe 2000, 3

R

Radical chain mechanism, 140
Radiolysis ñ gas chromatography, 128 407
Raman spectra, 327
Raman spectroscopy, 172 324 425
Random scission, 11 14
Reaction gas chromatography, 125
Regioisomerism, 307 365 372-374 379

S

Saponification methods, 126
Sequences in miscellaneous copolymers, 286
^{29}Si-NMR, 379
Size exclusion chromatography, 383 486 492
Size exclusion chromatography - Multi-angle laser light scattering, 394
Static secondary ion mass spectrometry, 151
Styrene - chloromethylstyrene - divinylbenzene copolymer programs, 42
Stereoisomerism, 305 365
Styrene acrylate and styrene acrylic acid, 206
Styrene-based polymers, 45
Styrene-butadiene, 205
Styrene copolymers, 38 205
Butadiene-methylmethacrylate, 229
Methylmethacrylate-α-trifluoro-methacrylic acid, 222
Styrene acrylate and styrene acrylic acid, 206
Styrene-butadiene, 205
Styrene-methacrylate copolymers, 221
Styrene-methacrylonitrile, 226
Styrene-methyl acrylate, 211
Styrene-methyl methacrylate, 213
Styrene-n-butyl acrylate, 216
Styrene-divinyl benzene, 43 44 45 449
Styrene-methacrylate copolymers, 221
Styrene-methacrylonitrile, 226
Styrene-methyl acrylate, 211
Styrene-methyl methacrylate, 213

Styrene-*n*-butyl acrylate, 216
Syndiotactic tacticity of polystyrene, 320

T

Tacticity, 305 315 327 329
Terminal epoxides, 500
Time-of-flight secondary ion mass spectrometry, 164 168 283 426

U

Ultraviolet spectroscopy, 286 482
Unsaturation types, 1 431 433 446

V

Vinyl acetate copolymers, 230
  Ethylene-vinyl acetate, 230
  Vinyl acetate-methyl acrylate, 231
Vinyl chloride - vinylidene chloride, 262
Viscosimetry, 425

X

X-Ray diffraction, 315 382

Z

Zeisel procedures, 126